

USAAMRDL-TR-74-97C

AD A032129



**HEAVY LIFT HELICOPTER - CARGO HANDLING ATC PROGRAM**

**VOLUME III - Results of Tests, Inspections, and Evaluations**

Boeing Vertol Company  
A Division of the Boeing Company  
Philadelphia, Pa. 19142

October 1976

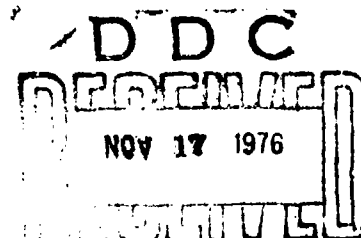
Final Report for Period June 1971 - June 1974

Approved for public release;  
distribution unlimited.

Prepared for

U. S. ARMY AVIATION SYSTEMS COMMAND  
P. O. Box 209  
St. Louis, Mo. 63166

EUSTIS DIRECTORATE  
U. S. ARMY AIR MOBILITY RESEARCH AND DEVELOPMENT LABORATORY  
Fort Eustis, Va. 23604



### EUSTIS DIRECTORATE POSITION STATEMENT

This report was prepared by the Boeing Company, Vertol Division, under the terms of Contract DAAJ01-71-C-0840(P6A). The report documents the results of tests, inspections and evaluations for advance technology components of the Heavy Lift Helicopter Cargo Handling System. Major system elements included herein are the hoist drives, the winch assemblies, load isolators, tension members, signal conduct or subsystem, cargo couplings and system controls.

Approximately 95% of all program objectives were achieved by the designs. The system as designed, with minor modifications, is suitable for installation in a prototype aircraft.

This Directorate concurs with the conclusions presented herein.

The technical monitor for this effort was Mr. Jules A. Vichness, project office, Systems Support Division.

#### DISCLAIMERS

The findings in this report are not to be construed as an official Department of the Army position unless so designated by other authorized documents.

When Government drawings, specifications, or other data are used for any purpose other than in connection with a definitely related Government procurement operation, the United States Government thereby incurs no responsibility nor any obligation whatsoever; and the fact that the Government may have formulated, furnished, or in any way supplied the said drawings, specifications, or other data is not to be regarded by implication or otherwise as in any manner licensing the holder or any other person or corporation, or conveying any rights or permission, to manufacture, use, or sell any patented invention that may in any way be related thereto.

Trade names cited in this report do not constitute an official endorsement or approval of the use of such commercial hardware or software.

#### DISPOSITION INSTRUCTIONS

Destroy this report when no longer needed. Do not return it to the originator.

SECURITY CLASSIFICATION OF THIS PAGE (When Data Entered)

next  
race

UNCLASSIFIED

SECURITY CLASSIFICATION OF THIS PAGE(When Data Entered)

20. Abstract (continued)

achieved by design, fabrication, and testing of specific ATC hardware in three critical air vehicle subsystems:

- a. Rotor/Drive System
- b. Flight Control System
- c. Cargo Handling System

cont.

→ The HLH Cargo Handling system tested and evaluated herein consists of: tandem pneumatically driven hoists which provide high speed inflight stability for externally slung cargo, with pitch attitude control and a long reach cargo acquisition and delivery capability; a visual augmentation system to assist the load controlling crewman in acquiring cargo under conditions of darkness and visual obscuration, and a static electricity discharge system to protect ground cargo handlers from shock hazards.

Volume III contains descriptions and results of: design support and development tests, which assisted in finalizing and substantiating the designs for the cargo handling components; the integrated test rig program, which demonstrated feasibility and achievement of design, functional, performance and reliability characteristics; and the disassembly and teardown inspection of selected components utilized on the integrated test rig.

✓

DISTRIBUTION AVAILABILITY CODES		
Dist.	AVAIL.	NOG. or SPECIAL
A		

UNCLASSIFIED

SECURITY CLASSIFICATION OF THIS PAGE(When Data Entered)



## SUMMARY

This report presents a formal documentation of the efforts and results of the cargo handling system segment of the Heavy Lift Helicopter (HLH) Advanced Technology Component (ATC) development program.

Purposes of the HLH ATC were to minimize technical, cost, and schedule risks associated with future HLH system research, development, test and evaluation (RDT&E), and production programs. This was achieved by design, fabrication, and testing of specific ATC hardware in three critical air vehicle subsystems:

- a. Rotor/Drive System
- b. Flight Control System
- c. Cargo Handling System

This report covers only the cargo handling system and consists of three volumes:

### Volume I:

- Part 1 - Detail Design (including design layouts)
- Part 2 - Structural Design and Weights Analysis
- Part 3 - Static and Dynamic Load Analysis

### Volume II - Fabrication of Test Hardware and Fixtures (Integrated Test Rig)

### Volume III - Results of Tests, Inspections, and Evaluations

Volume III contains descriptions and results of: design support and development tests, which assisted in finalizing and substantiating the designs for the cargo handling components; the integrated test rig program, which demonstrated feasibility and achievement of design, functional, performance and reliability characteristics; and the disassembly and teardown inspection of selected components utilized on the integrated test rig.

## TABLE OF CONTENTS

	<u>Page</u>
SUMMARY . . . . .	3
LIST OF ILLUSTRATIONS . . . . .	5
LIST OF TABLES . . . . .	16
INTRODUCTION . . . . .	21
DESIGN SUPPORT AND DEVELOPMENT TESTS . . . . .	22
Hoist Assembly . . . . .	22
Pneumatic Hoist Drive Unit . . . . .	49
Load Isolator . . . . .	126
Span Positioning (Traverse) System . . . . .	163
Cable Cutter . . . . .	167
Tension Member . . . . .	170
Cargo Coupling . . . . .	335
Signal Conductor Reeling Mechanism . . . . .	371
Controls and Display System . . . . .	395
Visual Augmentation System . . . . .	411
Static Electricity Discharge System . . . . .	413
INTEGRATED TEST RIG DEMONSTRATION . . . . .	420
TEARDOWN INSPECTION AND RESULTS . . . . .	457
CONCLUSIONS . . . . .	489
RECOMMENDATIONS . . . . .	490
REFERENCES . . . . .	493

## LIST OF ILLUSTRATIONS

<u>Figure</u>	<u>Page</u>
1 Drum Thickness Test Fixture . . . . .	23
2 Drum Deflection Test Results . . . . .	24
3 Drum Groove Wear Rate . . . . .	26
4 Hoist Drum Ultimate Load Test Rig . . . . .	28
5 Hoist Development Test Rig . . . . .	29
6 Drive Torque Curve for 50% Load Condition . . .	33
7 Drive Torque Curve for 100% Load Condition . .	34
8 Drive Torque Curve for 125% Load Condition . .	35
9 Load vs. Deflection Curves - Fwd Side Frame 30° Fwd Cable Angle - Steps T-U . . . . .	42
10 Cable Stretch for 30° Fwd Cable Angles . . . .	43
11 Cable Stretch for 40° Aft Cable Angles . . . .	44
12 Damage to Hoist and Load Isolator after Cable Cutting Test . . . . .	47
13 Torque Performance, Partial Admission, 7.0-in-dia Turbine . . . . .	51
14 Torque Performance, Full Admission, 7.0 -in-dia Turbine . . . . .	52
15 Torque Performance, Full Admission, 7.0 -in-dia Turbine . . . . .	53
16 Output Power, Full Admission, 7.0-in-dia Turbine . . . . .	54
17 Output Power, Full Admission, 4.4-in-dia Turbine . . . . .	55
18 Unloaded Turbine Reversal, 4.4-in-dia Turbine Driving . . . . .	57

# LIST OF ILLUSTRATIONS

<u>Figure</u>		<u>Page</u>
19	Unloaded Turbine Hoisting, 4.4-in-dia Turbine Driving . . . . .	58
20	Unloaded Turbine Reversal, Output Power, 7.7-in-dia Turbine . . . . .	59
21	Unloaded Turbine Reversal, Output Power, 4.4-in-dia Turbine . . . . .	60
22	Unloaded Turbine Reversal . . . . .	62
23	Unloaded Turbine Accelerations . . . . .	63
24	Turbine Windage . . . . .	65
25	Turbine Windage, Full Admission . . . . .	66
26	Turbine Windage, Partial Admission, Valves Open . . . . .	67
27	Turbine Windage, 7.0-in-dia Turbine, Partial Admission . . . . .	68
28	Turbine Windage, 7.0-in-dia Turbine, Partial Admission, Various Inlet Air Pressures. . . . .	69
29	Turbine Windage, 7.0-in-dia Turbine, Full Admission, Various Inlet Air Pressures . . . . .	70
30	Results of Windage Reduction Efforts, 7.0-in-dia Turbine, Full Admission . . . . .	71
31	Turbine Windage, 7.0-in-dia Shrouded Turbine. . . . .	73
32	Comparison of Shrouded and Unshrouded Windage, 4.4-in-dia Turbine, Full Admission . . . . .	74
33	Turbine Windage, 4.4-in-dia Turbine, Full Admission . . . . .	75
34	Turbine Windage, 4.4-in-dia Turbine, Full Admission, 1/16 Inch Vane/Turbine Clearance . . . . .	76

# LIST OF ILLUSTRATIONS

<u>Figure</u>		<u>Page</u>
35	Turbine Windage, 4.4-in-dia Turbine, Full Admission, 3/16 Inch Vane/Turbine Clearance . . .	77
36	Predicted ATM Windage . . . . .	78
37	Net Windage and Friction Horsepower . . . . .	79
38	Improved Turbine Performance . . . . .	81
39	Response Time, 4.4-in-dia Turbine . . . . .	82
40	Gearbox Friction Horsepower . . . . .	83
41	Gearbox Friction Log Horsepower . . . . .	84
42	Thermal Tests, 4.4 -in-dia Turbine, Valves Open .	86
43	Thermal Tests, 4.4 -in-dia Turbine, Valves Closed	87
44	Stalled Turbine Thermal Tests, 4.4-in-dia Turbine	88
45	Test Cell Layout - Dual Hoist Drives . . . . .	91
46	Hoist Drive Test Rig No. 1 . . . . .	92
47	Hoist Drive Test Rig No. 2 . . . . .	93
48	ATM Hoisting Turbine Performance, Torque Vs. Speed.	94
49	Redesigned ATM Turbine Performance, Torque Vs. Speed	100
50	Turbine Performance, Hoisting, 50 PSIA . . . . .	110
51	Turbine Performance, Reversing, 50 PSIA . . . . .	111
52	Turbine Performance, Hoisting, 60 PSIA . . . . .	112
53	Turbine Performance, Reversing, 60 PSIA . . . . .	113
54	High-Speed Gearbox Jackshaft . . . . .	125

## LIST OF ILLUSTRATIONS

<u>Figure</u>	<u>Page</u>
55 Failed Two-Piece Jackshaft . . . . .	125
56 Load Isolator Mounting Fixture . . . . .	128
57 Isolator Load/Deflection at Ambient (75°F) . . . . .	134
58 Isolator Fluid Pressure/Deflection . . . . .	135
59 Friction Values during Vibration Tests . . . . .	138
60 Isolator Equivalent Spring Rates - Modified Unit . . . . .	139
61 Isolator Static Load/Deflection . . . . .	140
62 Isolator Load/Deflection at -32°F . . . . .	143
63 Isolator Load/Deflection at +127°F . . . . .	145
64 Isolator Gland Assembly After Leakage . . . . .	148
65 Typical Vibration Test Oscillogram Displays . . . . .	152
66 Load Cell Sealing . . . . .	153
67 Limit Load and Proof Pressure Tests . . . . .	155
68 Ultimate Load Test . . . . .	156
69 Load Isolator Installation Geometry . . . . .	159
70 Equivalent Load/Deflection at Cable . . . . .	161
71 Hydraulic Loading Fixture . . . . .	164
72 Loading Fixture for Duty Cycle Test . . . . .	166
73 Cutting Knife Penetrating Anvil 0.43 Inch . . . . .	169
74 400X - Photomicrograph - Fissures in .4 Mil Nickel-Boron Coating on .105 inch Carbon Steel Wire After Drawing to .0345 inch Diameter. . . . .	173

# LIST OF ILLUSTRATIONS

<u>Figure</u>		<u>Page</u>
75	Corrosion at Pinholes in Pre-drawn Nickel-Boron Coating . . . . .	174
76	Zinc/Nickel-Boron Coating Condition During Wire Drawing Process . . . . .	175
77	Aluminum/Epoxy Termination Specimen (DuPont) . .	180
78	Kevlar 49 Termination . . . . .	181
79	Fatigue Test Machine for Bend Tests of 1/8-in Fiber Bundles (Prodesco) . . . . .	182
80	Kevlar 49 and Kevlar 29 Load Versus Bend-Over-Drum Stress Cycles . . . . .	187
81	Kevlar 49, 1/2-Inch, 3-Strand Rope Specimen After Tensile/Ultimate Test . . . . .	191
82	Candidate Wire-Rope Constructions and Materials .	195
83	Comparison of Right-and Left-Lay Rope Torques . .	198
84	Comparison of Theoretical and Actual Values of Torque Required to Produce Rotation of the Load-Equalizer Bar with Left-and Right-Lay Cables . .	199
85	Typical Tension/Elongation Characteristics of Galvanized 0.78-in 36X7 Lang-Lay Wire Rope . . . .	209
86	Typical Tension/Elongation Characteristics of 0.78-in Galvanized 6X36 Lang-Lay Wire Rope . . . .	202
87	Typical Tension/Elongation Characteristics of 0.78-in Bright 6X36 Lang-Lay Wire Rope . . . . .	203
88	Typical Tension/Elongation Characteristics of 0.78-in 17-7 PH 6X36 Lang-Lay Wire Rope . . . . .	204
89	Typical Tension/Elongation Characteristics of 0.78-in 18-2 Mn 6X36 Lang-Lay Wire Rope . . . . .	205

# LIST OF ILLUSTRATIONS

<u>Figure</u>		<u>Page</u>
90	Tension/Elongation Characteristics of 36x7, 0.78-Inch-Diameter Cable . . . . .	207
91	Tension/Torque Characteristics of 0.78-Inch-Diameter, Galvanized, 36x7 Lang-Lay Cable . . . . .	209
92	Layout of Bend-Over-Drum Fatigue Machine With a Typical Cable Specimen . . . . .	211
93	Location of Wire Breakage During Bend-Over-Drum Fatigue Tests . . . . .	213
94	Breaking Strength of Cable Specimens . . . . .	216
95	Comparison of Drum Groove Configurations - Cable Design Support Test and HLH Design . . . . .	217
96	Apparent Cable Wear After 10,800 Load Cycles . . . . .	218
97	Tension-Over-Drum Test Rig for Ultimate Load Test of .78-Inch-Diameter Cable Wrapped 180° Over a 20/1 Grooved Drum . . . . .	219
98	Breaking Strengths, Pure Tension and Tension-Over-Drum Tests . . . . .	220
99	Typical AISI 4130 Fitting After Being Swaged onto a 36x7 Cable . . . . .	240
100	Comparison of Swaging Penetration . . . . .	245
101	Shank Geometries Showing How Change in Nose Taper Allowed for Shorter Shank Length While Maintaining the Same Effective Swage Length . . . . .	248
102	Left-Lay Specimen Showing Cable "Center Break" . . . . .	250
103	Typical Swage Fittings and 0.70-Inch-Diameter Cable After Cable Center Breaks . . . . .	253
104	Cut Through Swaged Shank Specimen: A-3/VI - 0.70-Inch Cable, $R_A = 10.5\%$ . . . . .	253



## LIST OF ILLUSTRATIONS

<u>Figure</u>		<u>Page</u>
105	Sectioned Swage - End Fitting Showing Reduced Swaging Penetration . . . . .	279
106	Equalizer-Bar Fittings Before and After Swaging on 0.70-Inch, Right-Lay, 36x7 Cable . . . . .	259
107	X-Ray of End Fitting Specimen F-4 After Swaging .	260
108	X-Ray of End Fitting Specimen D-1 Showing Reduced Swage Penetration (Bulge) at Center Location . .	261
109	X-Ray of End Fitting Specimen A-7 After Progressive Swaging . . . . .	263
110	X-Ray of End Fitting Specimen A-8-1 and -2 After Swaging with $R_A$ 's = 20.6 and 25.4% . . . . .	264
111	X-Ray of Overswaged End Fittings with Cable Failure at Fitting Nose . . . . .	266
112	Sketch of Equalizer-Bar Threaded-Eye Configuration	268
113	Sketch of Single-Point Adapter Threaded-Eye Configuration . . . . .	268
114	Differential Heat-Treatment Setup . . . . .	271
115	Eye Section - Failure Modes . . . . .	271
116	Typical Eye-Splice Test Specimen . . . . .	274
117	Splice I Using Two Sleeves and a Cap . . . . .	276
118	Splice II Using One Sleeve and a Cap . . . . .	276
119	Distortion of Cable After Swaging of Sleeves . .	277
120	Failure of Eye Splice Using Standard Sleeves . .	277
121	Eye-Splice Sleeves Designed to Prevent Cable Distortion Upon Swaging . . . . .	278

## LIST OF ILLUSTRATIONS

<u>Figure</u>		<u>Page</u>
122	Comparison of Commercial and New Sleeve Configuration . . . . .	279
123	Eye-Splice Specimen B-2 Using Cylindrical Sleeves (cold rolled steel), 4-and 6-Inch Sleeve Lengths, 10-Inch Loop Length, and 3/4-Inch MacWhyte Thimble . . . . .	281
124	Center Break of Eye-Splice Specimen B-2, Two Inches from the 6-Inch Sleeve . . . . .	282
125	Center Section of Eye-Splice Specimen, B-2/IV, Two 0.70-Inch Cables, $R_A = 11.9\%$ . . . . .	283
126	Section Views of Specimen E-3 Which Ruptured at 62,300 lb (Eye-Splice, Swaged Dual Hole Sleeve, P/N SK301-11561-6). . . . .	284
127	End of Drum Button After Cable Pull Out . . . . .	289
128	Edge and Face Views of SK301-11561 End Fittings and Bushings for Tension Members . . . . .	291
129	Array of Fittings After Test . . . . .	293
130	Extensometer Attached to Cable During Tension/Elongation Measurements . . . . .	293
131	Tension/Elongation Characteristics of Right-Lay, 36x7 Cable (Specimen D-1) . . . . .	295
132	Tension/Elongation Characteristics of Left-Lay, 36x7 Cable (Specimen D-2) . . . . .	296
133	Tension/Torque Characteristics of Right-Lay, 36x7 Cable (Specimen D-1, Run 1). . . . .	298
134	Tension/Torque Characteristics of Right-Lay, 36x7 Cable (Specimen D-1, Run 10) . . . . .	299
135	Tension/Torque Characteristics of Left-Lay, 36x7 Cable (Specimen D-2, Run 1) . . . . .	300

# LIST OF ILLUSTRATIONS

<u>Figure</u>		<u>Page</u>
136	Tension/Torque Characteristics of Left-Lay, 36x7 Cable (Specimen D-2, Run 10) . . . . .	301
137	Tension/Torque Characteristics of Right-Lay, 36x7 Cable (Specimen D-3, Run 10) . . . . .	302
138	Layout of Tension/Bending Fatigue Machine and a Typical Specimen . . . . .	306
139	Machine Used for Development Tension and Bend- Over-Drum Fatigue Tests . . . . .	307
140	Hoist Drum Groove Configuration Using 0.70-Inch- Diameter, 36x7 Cable . . . . .	307
141	Specimens G-1 and G-2 After 3200 Fatigue Cycles but Before Salt-Fog Exposure . . . . .	312
142	Salt-Fog Exposure Specimens After 120 Hours . . .	313
143	Salt-Fog Exposure Specimens After 240 Hours . . .	314
144	Tension-Over-Drum Ultimate Test Rig - 0.70-Inch, 36x7 Cable and ATC Fittings . . . . .	322
145	Eye-Splice Sleeve Failure of Specimen E-3 at 62,300 lb . . . . .	328
146	Cable Lubricant Migration After 5400 Load Cycles	330
147	Sheave Groove After Tension-Over-Drum Testing . .	330
148	Photographs of MS21241 Bearings After Repeated Testing . . . . .	332
149	Coupling Device Test Specimen . . . . .	340
150	Schematic of Load Beam Latch Sensing Mechanism .	341
151	Coupling Retaining Nut Redesign . . . . .	356
152	Load Deflection Curve . . . . .	358

# LIST OF ILLUSTRATIONS

<u>Figure</u>		<u>Page</u>
153	Torque on Two Swivels . . . . .	359
154	48-Hour Humidity Cycle . . . . .	363
155	Failed Cargo Coupling . . . . .	368
156	Coupling Modifications . . . . .	370
157	Reeling Mechanism Test Stand . . . . .	372
158	Reeling Mechanism Response with Overhead Pulley .	373
159	Reeling Mechanism Response without Overhead Pulley	374
160	Reeling Mechanism Response without Excess Oil . .	375
161	Reeling Mechanism Response Corrected for Static Friction . . . . .	376
162	Shock Test Position . . . . .	402
163	Integrated Test Rig . . . . .	421
164	Synchronous Lift of 4000- and 6800-lb Loads . .	426
165	Control Room View of 32,000-lb Load Used in Synchronous Hoisting Tests . . . . .	427
166	Container Handling Device SK24955 . . . . .	428
167	Release of the 1000-lb Load from Coupling Assembly. . . . .	432
168	Demonstration Test of HLH/ATC Two-Point Suspen- sion with MILVAN and Container Handling Device - Test Load 58,544 Pounds . . . . .	440
169	Instrumentation and Rigging Used for Weighing Ballasted MILVAN . . . . .	441
170	Single-Point Adapter and 58,559-lb Test Load (58,520 Design) . . . . .	444
171	Hoisting the 58,559-lb Test Load Used for Single-Point Demonstration Cycles . . . . .	445

# LIST OF ILLUSTRATIONS

<u>Figure</u>		<u>Page</u>
172	Maximum Static Load Demonstration. . . . .	446
173	Hoist Drive Unit, S/N 001 . . . . .	459
174	Two Cracks Radiating From Electron Beam Weld from Shaft to Lightening Holes . . . . .	460
175	Hoist Drive S/N 2 Turbine Wheel. . . . .	462
176	Hoist Drive S/N 2 Reversing Turbine Nozzle . . . .	463
177	Articulating Duct. . . . .	465
178	Hoist S/N 103 - Right-Hand Drum Parts Stackup with Broken Thrust Washer. . . . .	466
179	Hoist S/N 103 - Left and Right Sun Gears with Wear and Discoloration on LH Part . . . . .	467
180	Location of Damaged Bearing . . . . .	470
181	Spalled Bearing - Damaged Inner Races. . . . .	471
182	Location of Cracks in Ball Grooves . . . . .	473
183	Hoist Drums, S/N 104. . . . .	474
184	Single-Point Adapter Cables . . . . .	477
185	SCRM S/N 1 Gearbox and Geartrain. . . . .	482
186	Sheared SCRM Splined Shaft . . . . .	483
187	SCRM S/N 2 Gearbox and Geartrain. . . . .	485
188	Extensive Flaking of Sheave Bearing Teflon Lining. . . . .	487

## LIST OF TABLES

<u>Table</u>		<u>Page</u>
1	Conditions for Hoist Operational Tests . . . .	31
2	Sample Test Results and Hoist Efficiencies . .	32
3	Drum Lateral Static Load Test Conditions . . .	39
4	Drum Longitudinal Static Load Test Conditions .	40
5	Static Brake Loading Schedule . . . . .	102
6	Command Speeds . . . . .	104
7	Command Speeds . . . . .	105
8	Command Speeds . . . . .	106
9	Command Speeds . . . . .	106
10	Turbine System Test Results . . . . .	107
11	Turbine Performance Test - Requirements . . .	108
12	Turbine Performance Test - Requirements . . .	109
13	Command Speeds . . . . .	114
14	Command Speeds . . . . .	115
15	Dual Mode Control - Test Results . . . . .	116
16	Command Speeds . . . . .	117
17	Synchronization Test - Test Results . . . . .	118
18	Command Speeds . . . . .	119
19	Command Speeds . . . . .	119
20	Command Speeds . . . . .	120
21	Schedule of Dimensional Measurements . . . . .	131

# LIST OF TABLES

<u>Table</u>		<u>Page</u>
22	Load Sensor Calibration . . . . .	132
23	Load Sensor Calibration . . . . .	133
24	Load/Deflection Values - 75°F . . . . .	136
25	Comparison of Static and Dynamic Characteristics	141
26	Test Plan Vibration Spectrum Requirement . . .	146
27	Vibration Testing Completed . . . . .	149
28	Revised Test Plan Vibration Spectrum . . . . .	150
29	Load Isolator Geometry Ratios . . . . .	160
30	Summary of Nickel-Boron Coating Evaluation . .	177
31	Average Tensile Properties of Kevlar 49 Fiber Bundles . . . . .	183
32	Tensile Properties of Fiber Bundles Cemented to Aluminum Tabs . . . . .	184
33	Rupture Load of Kevlar 49 Fiber Bundles with End Terminations . . . . .	186
34	Yarn Ultraviolet Exposure Tests . . . . .	189
35	Comparison of Ultraviolet Loss in 1/8-in Fiber Bundles and 1/2-in, 3-Strand Cable Constructed of Kevlar 49. . . . .	190
36	Abrasion Test of Kevlar 49, Nylon, and Dacron 1/2-Inch Ropes . . . . .	192
37	Size/Weight Projection of Kevlar 49 HLH/ATC Tension Members . . . . .	193
38	Elastic Modulus and Torque Characteristics of Cable Test Specimens . . . . .	206
39	Effect of Repeated Loading on 36x7 Cable, 0.78-Inch Diameter . . . . .	208

# LIST OF TABLES

<u>Table</u>		<u>Page</u>
40	Fatigue Loading Program . . . . .	212
41	Results of Single-Wire Tests . . . . .	213
42	Construction Details for Electrogalvanized 36x7 Lang-Lay Wire Cable (0.78-in-dia). . . . .	225
43	HLH/ATC Characteristics of .78-Inch-Diameter Cable from Preliminary Design Tests . . . . .	226
44	Planned Tension Member Design Development Tests - Evaluation of End Fittings and 0.70-Inch- Diameter, 36x7 Cable . . . . .	232
45	Development Cable - 0.70-Inch-Diameter, 36x7 Construction Characteristics . . . . .	235
46	Tension Member End Fitting Configurations and Design Criteria . . . . .	239
47	Swaged Shank End Fitting Development - Tests with 0.78-Inch-Diameter Design Support Test Cable(a). . . . .	243
48	Swaged Shank Fitting Development for 0.70-Inch- Diameter Cable . . . . .	249
49	0.70-Inch Cable Failure Characteristics . . . . .	251
50	Test Results - Swaged Shank End Fittings Used in Development Tests . . . . .	254
51	Supplementary Swaged Shank Development Tests - 0.70-in. 36x7 Cable . . . . .	267
52	Test Specimen Failing Loads and Calculations of Strengths of Similar Fittings with Minimum Hardness . . . . .	272
53	Eye-Splice Development Tests for 0.70-Inch- Diameter Cable . . . . .	286



# LIST OF TABLES

<u>Table</u>		<u>Page</u>
54	Results of Hoist Drum-Button Development Tests .	288
55	Results of Tension/Elongation and Tension/Torque Tests. . . . .	303
56	Cargo System/Tension Member Design Spectrum Loading . . . . .	308
57	Results of Fatigue Tests - Cyclic Tension and Bend-Over-Drum . . . . .	311
58	Results of Endurance Limit Fatigue Tests for F Specimens. . . . .	317
59	Results of Internal Examination of Tension/Bend-Over-Drum Fatigue Specimens . . . . .	318
60	Results of Internal Examination of Tension/Bend-Over-Drum Fatigue Specimen F-2 . . . . .	319
61	Cable Elongation Due to Fatigue Testing . . . . .	320
62	Tension-Over-Drum Test Criteria. . . . .	324
63	Summary of Tension-Over-Drum Test Results . . . . .	325
64	Tension-Over-Drum Cable Strength Losses . . . . .	326
65	Summary - New 0.78-Inch, 36x7 Test Data . . . . .	333
66	Maximum Trail Angle for 40-Lb Weight Release . . . . .	348
67	Results for Single Solenoid Release Mode . . . . .	349
68	Ground Release Knob Mode with 40-Lb Shackle on Load Beam . . . . .	350
69	Results of 45° Trail Angle Release . . . . .	352
70	Results of 33°, 40°, and 45° Trail Angle Releases . . . . .	354
71	Mechanical Shock Test . . . . .	367

# LIST OF TABLES

<u>Table</u>		<u>Page</u>
72	Signal Conductor Reel Runaway Speeds . . . . .	379
73	Measured Cable Tensions - Stalled Operation . .	380
74	Driving Conditions - Normal Duty Cycle Test . .	382
75	Pressure and Temperature Conditions - Normal Duty Cycle Test . . . . .	382
76	Normal Duty Cycles . . . . .	383
77	Test Data for Transient Operation . . . . .	386
78	Results of Hook Release Test . . . . .	387
79	Endurance Test Operating Cycle . . . . .	388
80	Time Allocation - Endurance Test . . . . .	388
81	Matrix of Cargo Handling System, Integrated- Test-Rig Test Requirements and Periods of Testing. . . . .	425
82	Maximum Measured Tension Member Velocities-FPM .	430
83	Cable Payout Limits . . . . .	435
84	Two-Point Suspension Demonstration Consisting of Eight Endurance Cycle Elements . . . . .	442
85	Single-Point Suspension Demonstration Consisting of Eight Basic Endurance Cycle Elements. . . . .	447
86	Cable Diameter Measurements Following Demonstration Tests and Coupling Failure . . . . .	478

## INTRODUCTION

Final cargo handling ATC hardware designs were based in part on the results of design support, development, and, later, demonstration on an integrated test rig. This document presents the results of these tests and a teardown inspection of selected components used in the design demonstration.

This document is subdivided into sections which cover; component testing performed on each of the major cargo handling ATC elements, the integrated test rig program, and finally the teardown inspections. In general, each test is presented separately as a requirement or objective followed by the test procedure employed and the results obtained.

## DESIGN SUPPORT AND DEVELOPMENT TESTS

### HOIST ASSEMBLY

#### DESIGN SUPPORT TESTS

Tests were conducted during the design phase to establish or substantiate those areas of the hoist design which were not amenable to accurate analysis. These tests consisted of:

1. Drum wall thickness test to establish the minimum acceptable material gauge.
2. Drum wear test to establish the operational compatibility of the hoist drum material and the cable.
3. Ultimate load test of the hoist drum and support structure.

#### Drum Wall Thickness Test

In order to ensure the lightest weight (minimum thickness) drum, the hoist vendor, Western Gear, subjected a sample drum to design loads and measured deflections and stresses. The arrangement of the test specimen and the fixture is shown in Figure 1. The tests were conducted with three different wall thicknesses. Deflection data was plotted against drum wall thickness as shown in Figure 2. The curves show the maximum diametrical deflection that was measured when the load was applied through three wraps of cable. The maximum diametrical drum deflection considered acceptable for the support spline is .028 inch.

Testing was continued until the maximum deflection measured for a 25,000-pound load was .019 inch. Since the accuracy of the locating and measuring instrumentation allowed errors as high as .004 inch, the resulting .023-inch deflection (.019 + .004) represents a margin of 20 percent under the .028-inch deflection limit.

Results of the drum deflection test established a drum wall thickness of 0.34 inch as the minimum gauge to ensure that diametrical deflections will not prevent the correct functioning of the support spline assembly.



Figure 1. Drum Thickness Test Fixture.

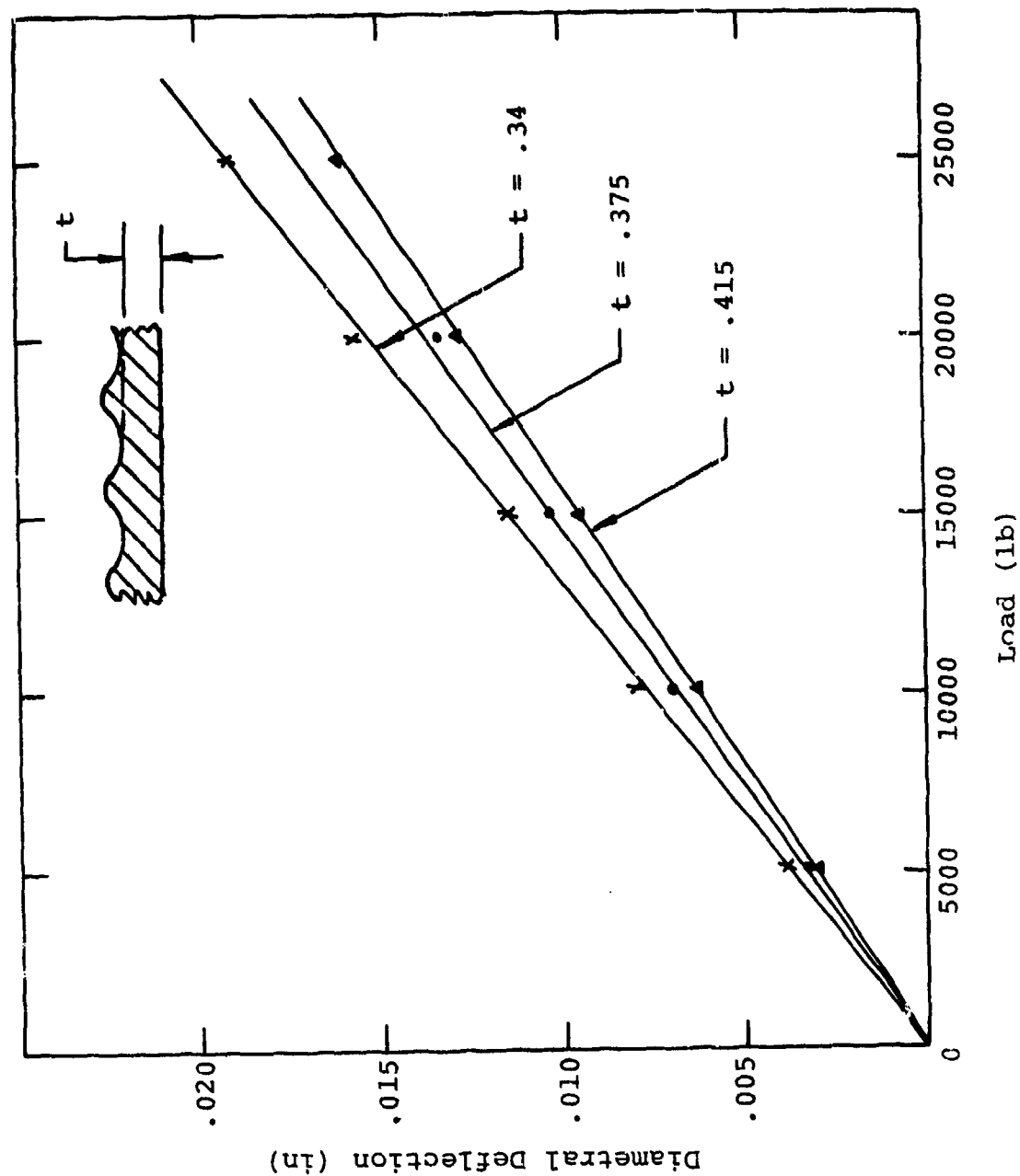


Figure 2. Drum Deflection Test Results.

### Drum Wear Test

Drum wear is principally caused by the cable sliding over the drum when the cable is stretched by the lifting of a load or when it reverts to its original length after the load is removed. A formula was developed to convert the total required life of the hoist with the projected load spectrum into a total sliding distance at each of the various load levels in the load spectrum and to convert this into a number of cycles for reciprocating a test drum segment with a cable under load. The basic formula made a number of assumptions, including the number of wraps required to dissipate the load and the frequency of operation at a certain cable length. The cable sliding spectrum evolved is:

<u>Cable Tension - Lb</u>	<u>Cable Travel - In.</u>
10,000	80
20,000	850
25,000	150

A specimen configured to represent a portion of the drum groove, of similar material and finish, was reciprocated by a hydraulic cylinder in accordance with the above spectrum with a cable of similar construction to the final ATC design configuration lying in the groove. The amount of groove wear was measured at the end of each loading increment.

The test resulted in a wear rate as shown on Figure 3. The rate of wear was maximum at the highest load, as expected, due not only to the high load, but also to the trapping of drum particles between the cable strands. This condition would be less severe in normal service since a normal hoisting operation would cause some or all of these particles to fall out.

The test indicated a maximum drum wear of .006 inches under the severe test criteria. This magnitude of wear will not affect the operation of the drum and was therefore acceptable. No significant wear to the cable was found.

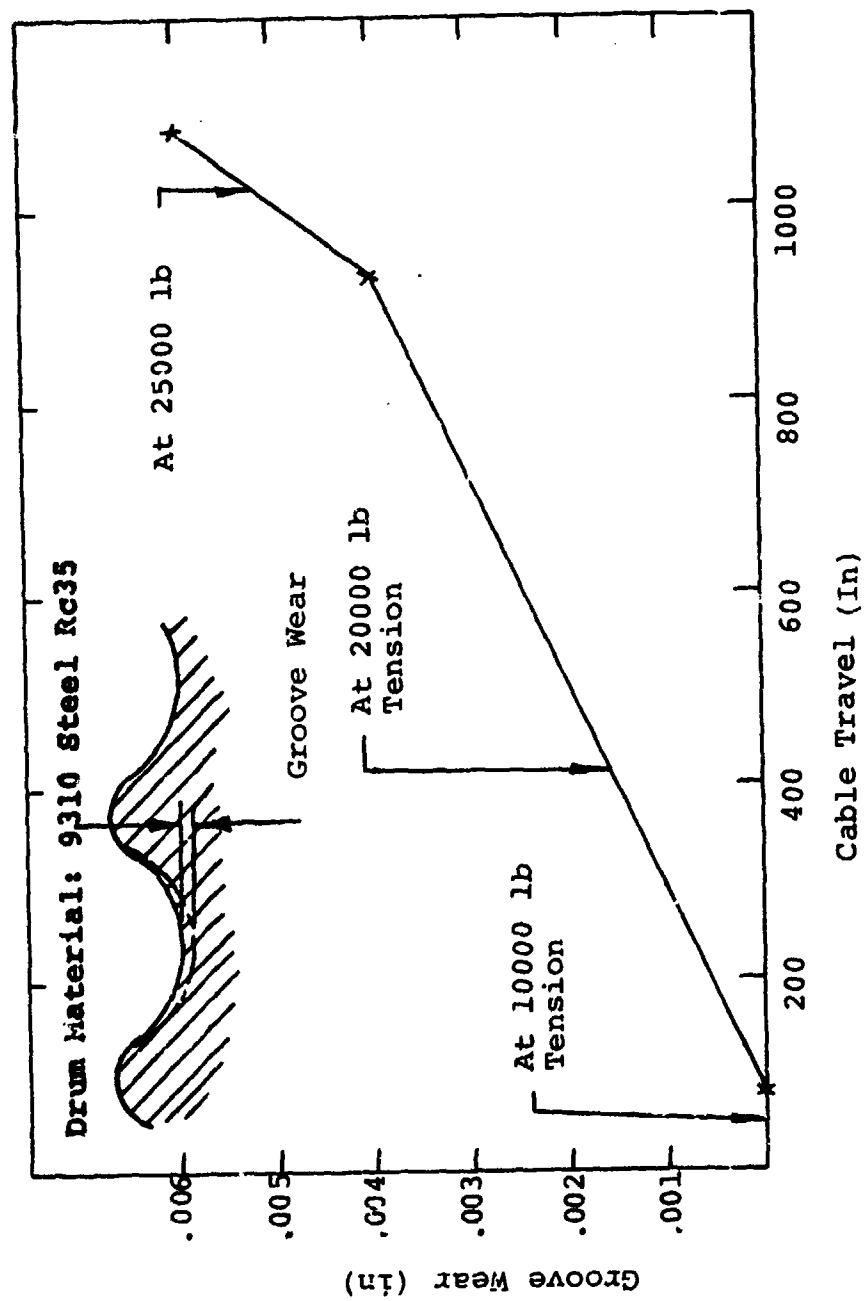


Figure 3. Drum Groove Wear Rate.



### Hoist Drum Ultimate Load Test

An ultimate load test was conducted on a section of drum complete with linear ball spline and center support structure. The objective of this test was to substantiate the strength of the linear ball spline design. The drum section and the center support structure were mounted on a test rig as shown on Figure 4. Approximately eight wraps of cable were wound on the drum. The center support was restrained to prevent rotation, and tension equivalent to the designed ultimate load was applied to the cable. Inspection of the drum and center support structure after the test revealed heavy brinnelling of the spline ball grooves. There was no permanent deformation of the drum or the support structure, and no failures of the support balls. The brinnelling of the spline ball grooves at the limit load had been measured previously and was found to be within acceptable limits. This test confirmed the suitability of the spline design.

### DESIGN DEVELOPMENT TESTS

Three phases of development testing were conducted on the hoist:

1. Phase I involved all dynamic operations of the hoist assembly.
2. Phase II involved a demonstration of the static strength of the drum and consisted of loading at maximum cable angles.
3. Phase III involved the performance of the cable anti-backlash system.

### Phase I - Dynamic Operations of Hoist

#### Objectives

1. To demonstrate that the hoist will operate at the design loads and speeds.
2. To establish the efficiency of the gearing at each load and speed.
3. To demonstrate the operations of the cable drum limit switches.

#### Procedure

With the test and slave hoists mounted on the test fixture, as shown in Figure 5, the test cables were installed between the two hoists. The torque measuring device was mounted to the input of the test hoist.

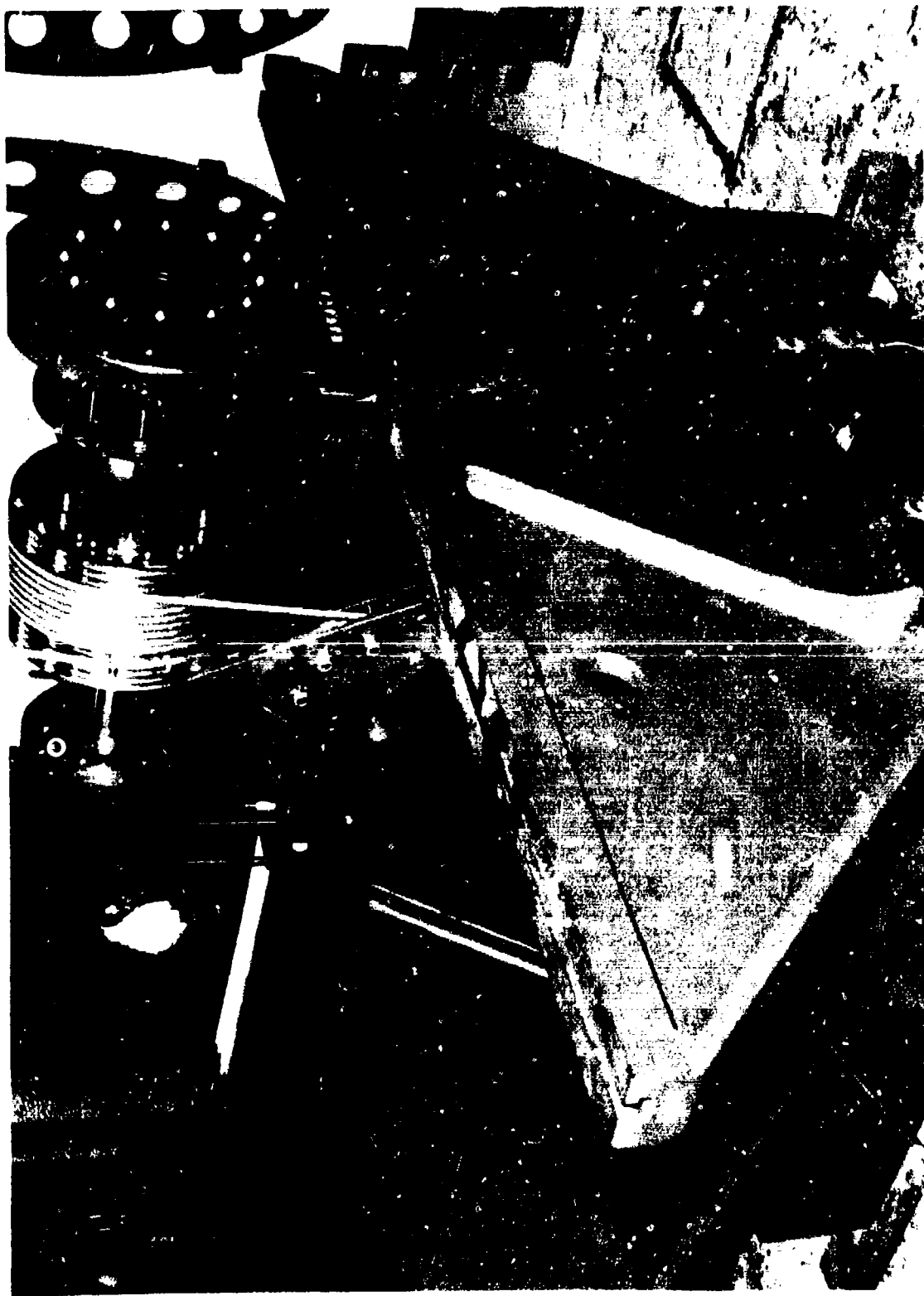


Figure 4. Hoist Drum Ultimate Load Test Rig

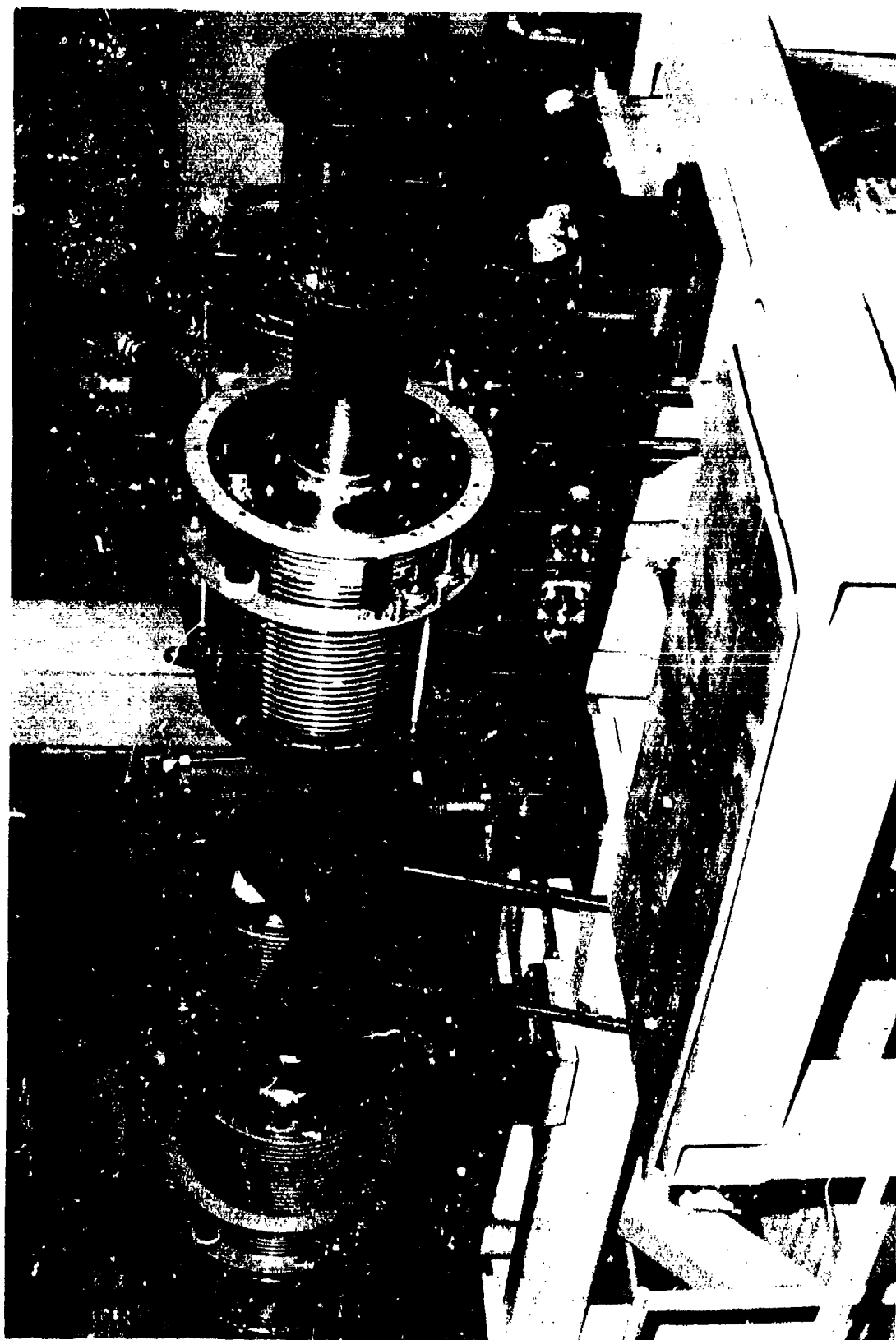


Figure 5. Hoist Development Test Rig.

The required hydraulic motor-pump was mounted to each hoist. Thermocouples were attached to the sump areas of the bevel drive assemblies on each hoist. The drum limit switches were installed and adjusted.

The hoist was then operated at the loads and speeds noted in Table 1 for the required number of cycles for each sequence. Cable loads and speed, input torque, and bevel gear drive temperatures were recorded.

### Results

The test hoist completed and met all the operational requirements of the Phase I tests.

Hoist serial number 102 was used as the test hoist and serial number 101 was used as the slave hoist.

The two test cables used were special. Each cable was provided with the same configuration anchor fitting at each end. The anchor fittings conform to the HLH/ATC tension member assembly hoist drum buttons per SK301-11561-4 and -5. The cables were 158.5 feet long and designated as serial numbers 1.

Sample test data is presented in Table 2 and Figures 6, 7, and 8. The total cable loads shown in the Table are based on the combined average loads for the two cables during each sequence.

The gear drive temperatures during operation were considered normal for the type of testing performed. The planetary drive temperatures were monitored by touch and did not indicate temperatures above 120°F.

The temperatures recorded before the start of testing were above the ambient. This was due to the operation required to establish the speed and load for each test sequence.

The testing proved that the hoists are capable of continuous operation in excess of five cycles at the 125% load condition of sequences "I" and "J" without problems.

The total cable loads were held on the high side of the values called for in Table I. This was due to the fact that the two cable loads could not be held constant, and therefore it was difficult determining the average cable loads during testing.

TABLE 1. CONDITIONS FOR HOIST OPERATIONAL TESTS.						
No. of Cycles	(1)		Cable Direction	Cable Dis- placement (ft) ±1%	(2) (3)	
	Sequence				Cable Loads (lb) +5%	Cable Speed (ft/min) +5%
5	A	Deploy Out	100	100	0	120
	B	Reel In	100	100	0	120
5	C	Deploy Out	100	100	8,400	105
	D	Reel In	100	100	8,400	105
5	E	Deploy Out	100	100	16,800	90
	F	Reel In	100	100	16,800	90
5	G	Deploy Out	100	100	33,600	60
	H	Reel In	100	100	33,600	60
5	I	Deploy Out	100	100	42,000	45
	J	Reel In	100	100	42,000	45
<b>Notes</b> (1) Each sequence represents ½ cycle. (2) Cable loads are the sum of both cable loads. (3) These values were not required for the initial and final 15 feet of cable travel.						

TABLE 2. SAMPLE TEST RESULTS AND HOIST EFFICIENCIES.

Sequence	Load Condition &	Total Cable Load (lb)	Input Torque 100% Eff. (in-lb)	Motor Press. (PSI)	Motor Speed (RPM)	Actual Motor Torque (in-lb)	Efficiency (%)
F	50	17,640	503.941	2,350	6,016.76	535.5	94.11
H	100	33,648	961.258	3,150	4,011.18	1,027.0	93.60
J	125	42,852	1,224.199	2,600	3,008.38	1,330.5	92.01
J	125	42,864	1,224.542	2,600	3,008.38	1,330.5	92.04
J	125	43,104	1,231.398	2,625	3,008.38	1,357.5	90.71
J	125	43,116	1,231.741	2,625	3,008.38	1,357.5	90.74
H	100	33,837 Average	966.659	-	4,011.18	1,019.673 Average	94.80

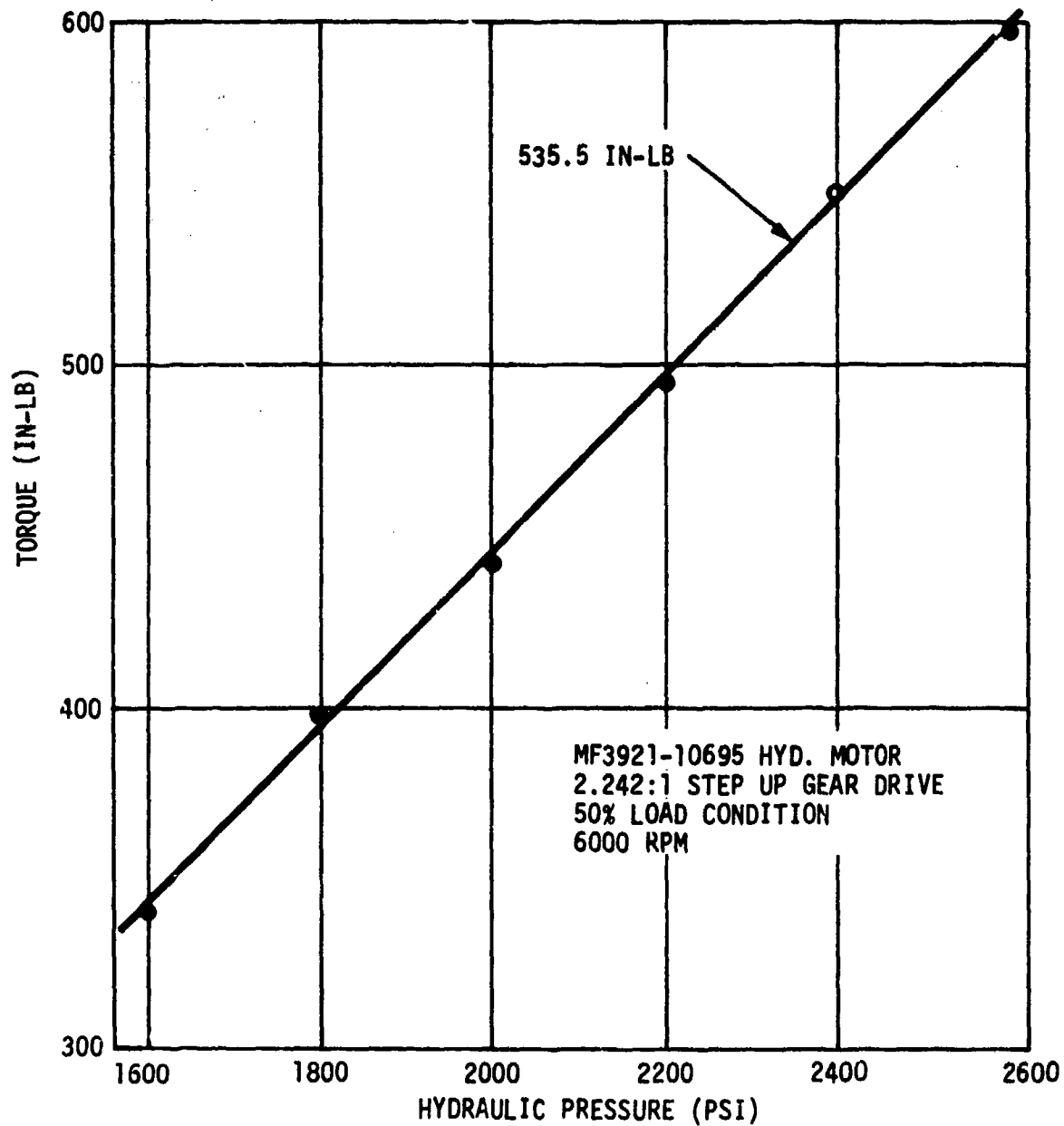


Figure 6. Drive Torque Curve for 50% Load Condition.

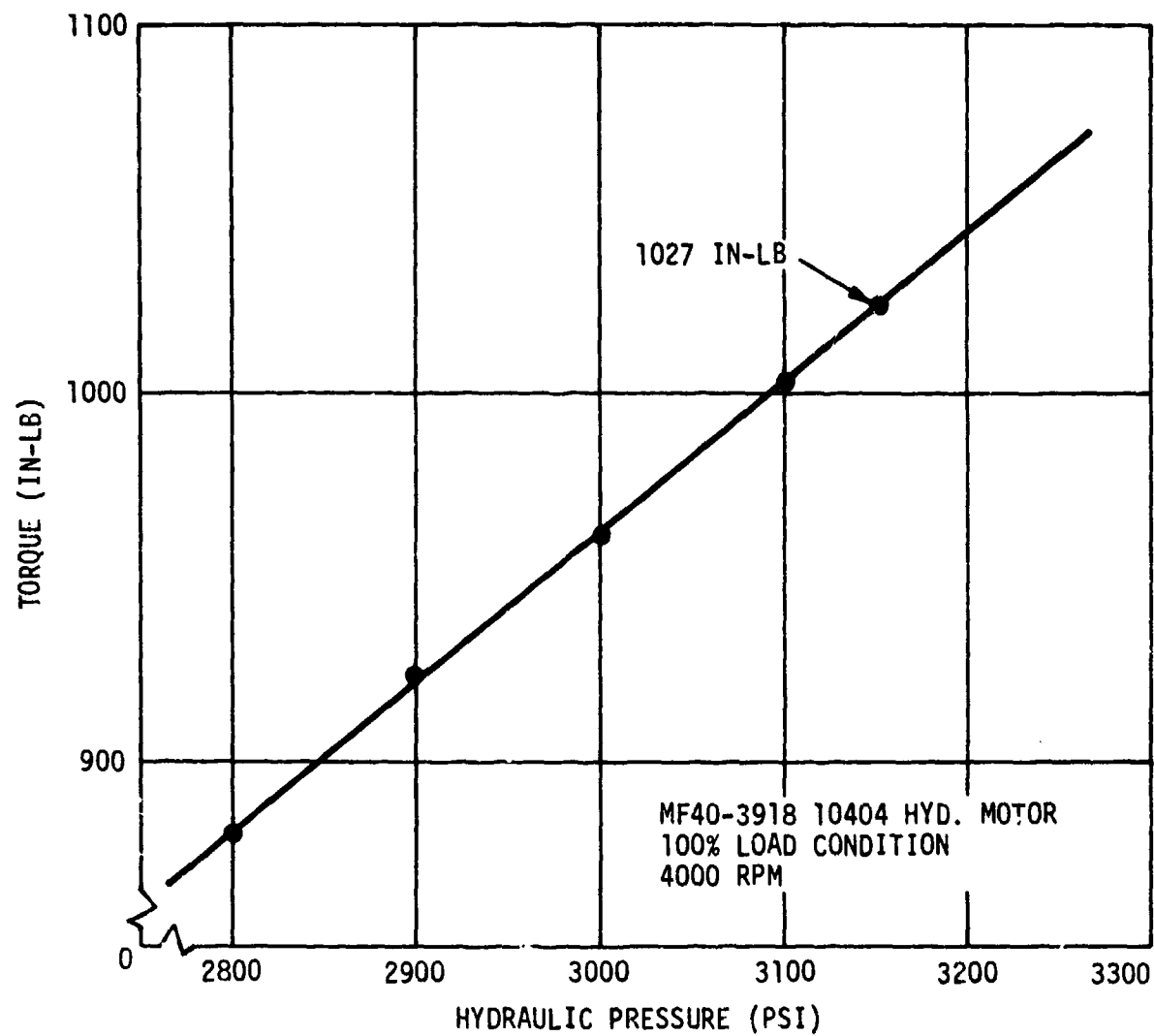


Figure 7. Drive Torque Curve for 100% Load Condition.



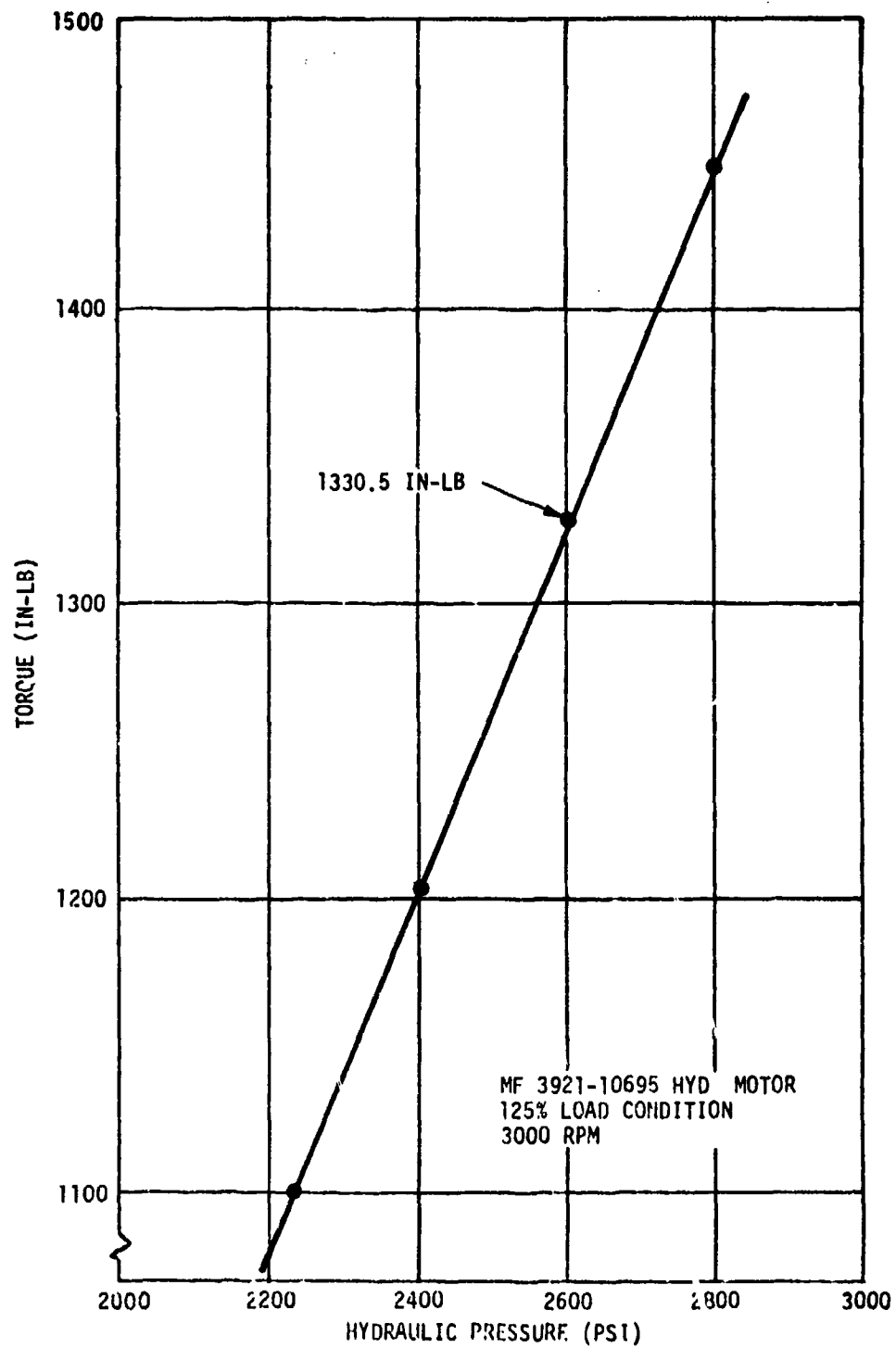


Figure 8. Drive Torque Curve for 125% Load Condition.

Dummy isolators were used during testing to position the hoist isolator arms in a position equivalent to the maximum load stroke position of the load isolators.

The load isolators were not used during testing due to the isolator travel or stroke caused by the cable loads. The cables between the test and slave hoists prevented rotation of the drums in the reel-in direction. The input of the hoist, therefore, had to rotate in order to relieve the load in the isolators.

Operation of the cable drum limit switches was checked during the testing of hoists serial numbers 103 and 104. The switches operated satisfactorily during the testing.

A problem was encountered with the cable-deployed-out switch actuator. The force of the plunger spring in the switch caused a heavy force on the actuator button, rubbing it against the drum. After a number of switch actuating cycles, the surface of the button was worn through the electroless nickle plating. Wear in the actuator button did not effect the switch operation and had little effect on the position of the drum.

A small amount of lubricating oil had been expelled from the breathers of the 2nd stage bevel drives after a few cycles of continuous high speed operation. This was more predominate in the RH drives. Churning of the oil and rise in temperature was the primary cause. Once the oil levels were reduced a small amount and the breathers cleaned with solvent, the oil leakage stopped.

Normal operation of the hoist should not cause a loss of lubricant from the bevel gear drives.

The exposed oil seals did not show any evidence of oil leakage.

During the early stages of testing, a bearing failure was experienced on the input shaft of the slave hoist 1st stage bevel drive. The failure occurred in the MRC 204R bearing located at the opposite end of the shaft from the input drive spline. The type of failure indicated that the bearing was subjected to an excessive thrust load. Since the bearing life, based on the radial loads and thrust from the pinion, is in excess of the design life required, the failure had to be caused by an external force. Investigations revealed that the drive shaft between the bevel drive and hydraulic motor was the cause of the failure. The shoulder to shoulder length of the

drive shaft was sufficient to cause an axial interference when the motor was mounted on the hoist, creating the excessive thrust. To avoid future problems, the test drive shaft was roworked by removing approximately .060 inches from one shoulder. The remaining tests were then completed without any further problems.

The torque meter used in the tests gave trouble and did not record the true drive torques delivered to the test hoist. The torque meter operation is based on the reaction torque of the drive system deflecting a beam incorporating strain gages. The drive system is mounted through support bearings and must be free to rotate in order to obtain true torque readings. The problem appeared to be due to the restraint developed in the high pressure hoses connected to the drive motor. The hydraulic hoses were redirected in an attempt to eliminate any possible restraint. The angle ports in the drive motors and the use of step up gear drives in combination with the motors would not permit the hose to be located in the same plane as the axis of the drive system. Input torque readings during the 100% load condition under test sequence "H" appeared to be nearest to the actual torque required to drive the hoist. Using the data on one of the strip charts, the efficiency of the hoist drive system was calculated above 94%.

During the testing, drive pressures were recorded on the strip charts at marked points. This was done for the 50%, 100%, and 125% load conditions. Tests were subsequently conducted on the drive systems in order to plot a pressure/torque curve for each of the load conditions noted above. Using this data and the cable loads at the marked points on the strip charts the efficiencies of the hoist were calculated. Table II shows the efficiencies for the three conditions. The efficiencies were well above the minimum 90% required.

## Phase II - Drum Static Strength Demonstration

### Objectives

1. To establish the structural integrity of the mounting frame assembly.
2. To determine the rate of load dissipation in the cables and the effect of lubrication on this rate.

### Procedure

A heavy coat of grease, used to lubricate the cables was applied to the aft drum cable grooves of the test hoist in the area of the first eight turns from the cable anchor. The grooves of the forward (LH) drum were cleaned with solvent and the grease from the surface of the forward (LH) test cable removed using a damp rag with solvent.

The twin hydraulic cylinders were installed first at the 30° left-hand lateral mounting position and subsequently the 30° right-hand lateral mounting position. With the cylinders in the extended position, the slack was removed from the cables in each loading condition by rotating the input spline of the hoist. The input shaft of the hoist was then locked with a spline lock plate. Equal loads were then applied to the cables at each of the loading positions shown in Table 3.

Frame deflections were measured by dial indicators and recorded for increasing and decreasing loads.

On completion of the left-hand and right-hand lateral pulls the hydraulic cylinders were re-positioned to pull the cable at a 30° forward angle and subsequently a 40° aft angle to the schedule shown in Table 4.

Before completing steps "T" and "U" (Table 4) for the 30° forward cable angles, a 1,000 pound load was applied to each cable. A lateral line was then marked across the wraps of cable on the aft drum as close to the departure point of the cable as possible.

At the end of step "T", with the 100,000 pound total load applied to the cables, a second lateral line was marked across the wraps of cable on the aft drum. This line was placed in the same angular plane from the lateral as the line originally marked with the 1,000 pound load applied. After completing step "U" the distance between the lines was recorded for each wrap of cable on the drum.

The above procedure was repeated for the 40° aft angle pull.

TABLE 3. DRUM LATERAL STATIC LOAD TEST CONDITIONS.			
Step	Cable Angle Position	(1) Cable Loads 1,000 lbs.	Load Increments (1000 lbs)
A	30° LH Lateral  ↓	1	1
B		0 to 50	10
C		50 to 0	10
D		0 to 80	20 up to 60 10 from 60 to 80
E		80 to 0	20
F		0 to 100	20 up to 80 5 from 80 to 100
G		100 to 0	20
H	30° RH Lateral  ↓	1	1
I		0 to 50	10
J		50 to 0	10
K		0 to 80	20 up to 60 10 from 60 to 80
L		80 to 0	20
M		0 to 100	20 up to 80 5 from 80 to 100
N		100 to 0	20
<u>Note:</u>			
(1) Cable loads are the sum of both cable loads.			

TABLE 4. DRUM LONGITUDINAL STATIC LOAD TEST CONDITIONS.			
Step	Cable Angle Position	(1) Cable Loads 1,000 lbs.	Load Increments (1000 lbs)
O	30° Forward  ↓	1	1
P		0 to 50	10
Q		50 to 0	10
R		0 to 80	20 up to 60 10 from 60 to 80
S		80 to 0	20
T		0 to 100	20 up to 80 5 from 80 to 100
U		100 to 0	20
V	40° Aft  ↓	1	1
W		0 to 50	10
X		50 to 0	10
Y		0 to 80	20 up to 60 10 from 60 to 80
Z		80 to 0	20
AA		0 to 100	20 up to 80 5 from 80 to 100
BB		100 to 0	20
<u>Note:</u>			
(1) Cable loads are the sum of both cable loads.			

## Results

The test hoist met all the requirements of the Phase II tests.

The cables used in the Phase II testing conformed to the HLH/ATC tension member assembly requirements with the exception that the lengths were only 40 feet long. The cables used were designated serial number 5.

Inspection of the hoist and test data, after completing the loads for each cable angle position, did not indicate any damage or permanent set in the hoist and its mounting frame. A sample load/deflection curve for the forward side frame is presented in Figure 9.

The indicator readings in the majority of cases did not return to zero at the end of each load cycle. This was due in part to the load hysteresis in the hoist system, the shifting of the hoist at the support roller area, and the permanent deformation of the support rollers in the area of contact with the support blocks. After completing each step, we applied a 500-lb load to each cable and then set the indicators to zero. This eliminated any errors in readings due to a change in the hoist position.

Figures 10 and 11 show the data on the cable stretch on the drum for the 30° forward and 40° aft position loading. Both cables were marked for each of the two cable positions. A board was taped to the roller frames for the marks on one cable and the hold down rollers at the 45° position were used for the marks on the opposite cable. The figures on the subject pages show the locations used in marking the cables. From the data it can be seen that the cables did not move on the drum for the first few wraps from the cable anchor.

From the data detailed on Figure 10 and 11, the coefficient of friction between the cable and the drum has been established as approximately .086 for the unlubricated drum and .067 for the lubricated drum.

There was some pinging noise from the cables at the higher loads. This was more predominate when the cables were loaded against the side load beams during the 30° LH and 30° RH lateral angle testing.

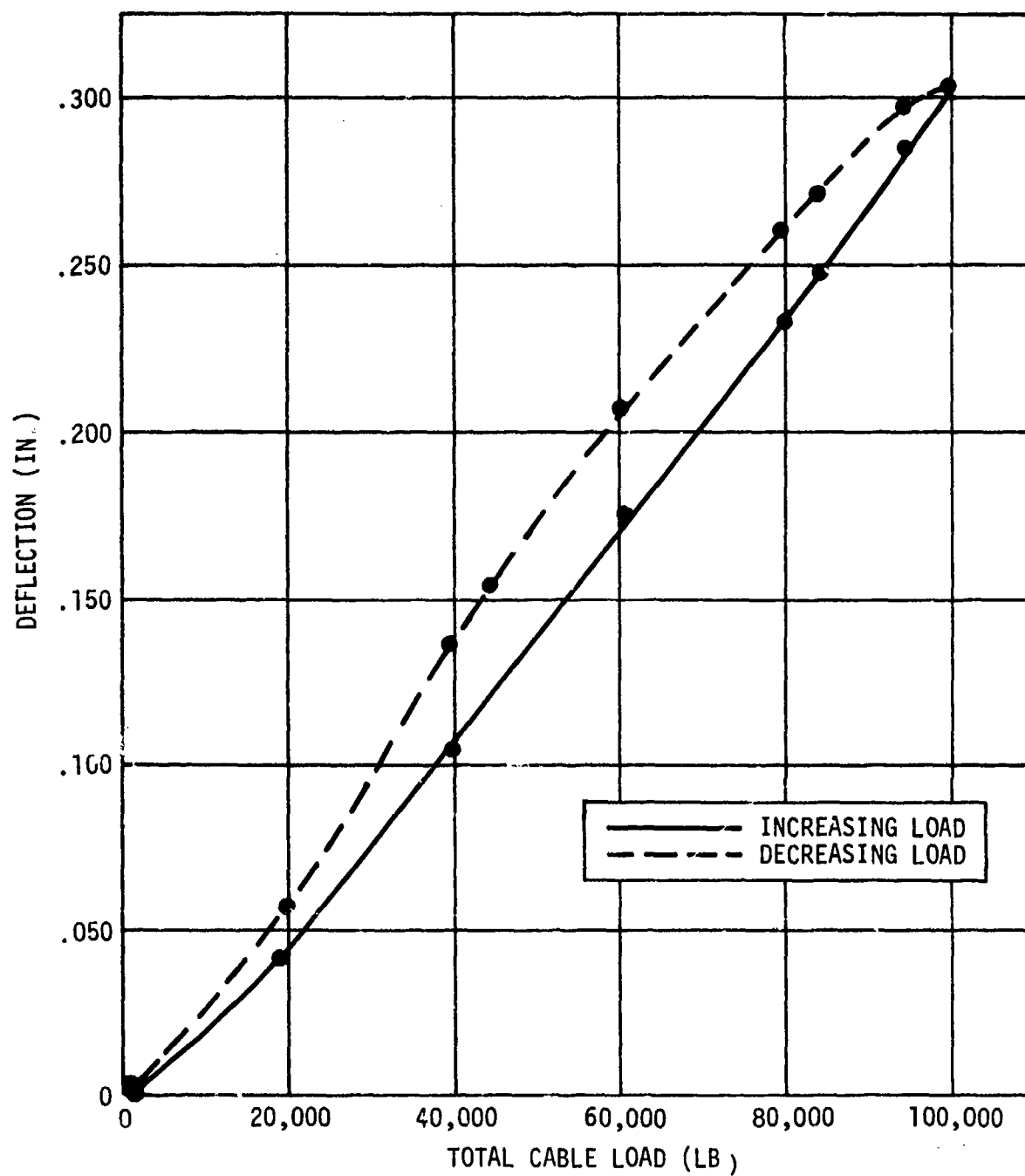
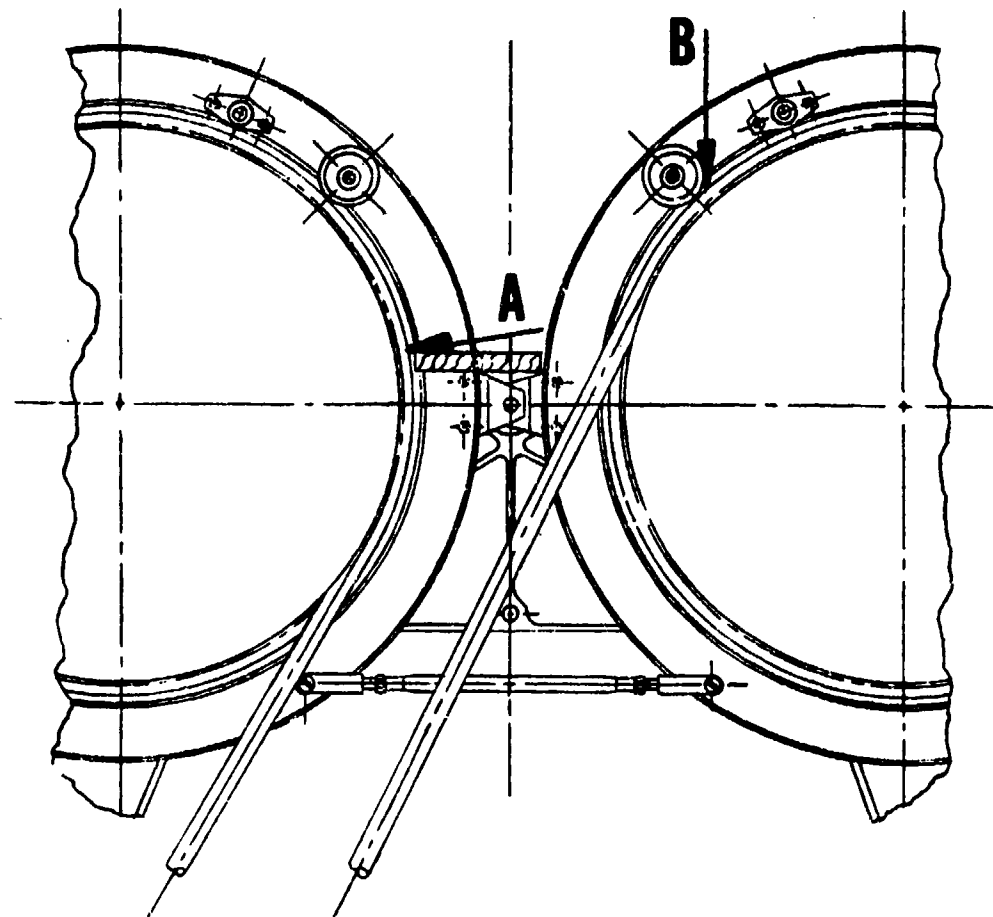


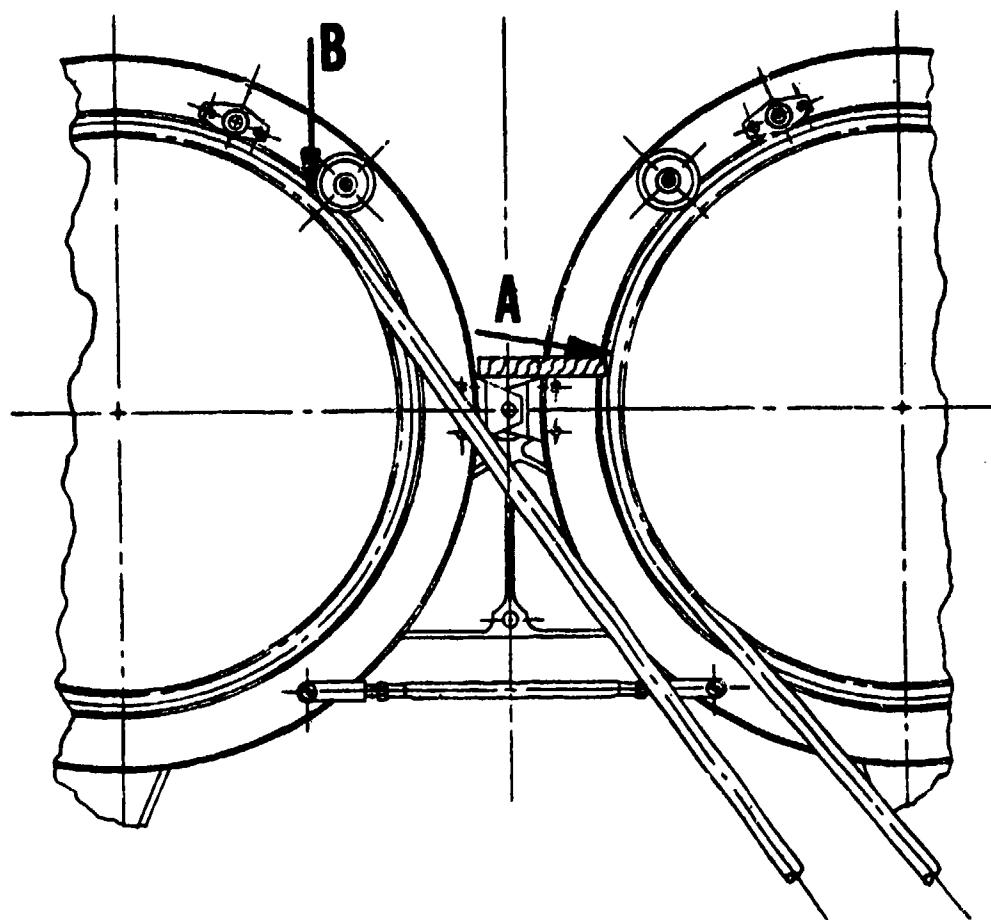
Figure 9. Load vs. Deflection Curves - Fwd Side Frame  
30° Fwd Cable Angle - Steps T - U.





<u>POSITION</u>	<u>LOCATION A</u> FWD. Cable Movement - Inches	<u>LOCATION B</u> AFT Cable Movement - Inches
Payout End	1.40	1.50
1st Wrap	.90	1.00
2nd Wrap	.65	.75
3rd Wrap	.55	.55
4th Wrap	.50	.50
5th Wrap	.50	.50
6th Wrap	.50	.50
Anchor End	.50	.50

Figure 10. Cable Stretch for 30° Fwd Cable Angles.



<u>POSITION</u>	<u>LOCATION A</u> AFT Cable Movement	<u>LOCATION B</u> FWD Cable Movement
Payout End	1.50	1.50
1st Wrap	1.05	1.00
2nd Wrap	.75	.85
3rd Wrap	.60	.70
4th Wrap	.50	.70
5th Wrap	.45	.65
6th Wrap	.45	.65
Anchor End	.45	Cable in Anchor Pocket

Figure 11. Cable Stretch for 40° AFT Cable Angles.

### Phase III - Performance of Cable Anti-Backlash System

#### Objectives

1. To demonstrate that the hold down roller assemblies will retain the cable on the drum when the cable is subjected to a vertical compressive load.
2. To demonstrate that the hold down roller assembly will prevent a severed cable from leaving the drum.
3. To ensure that there will be no substantial damage to the hoist assembly when the cable is cut.
4. Assess the potential for damage to the surrounding structure and the degree of containment necessary.
5. To demonstrate that the severed cable does not jam on the drum and may be readily removed.

#### Compressive Load Test

##### Procedure

With the free end of the cable anchored to the hydraulic cylinder to be used for the cable severing test, the drum was rotated to place a compressive load on the cable.

##### Results

The cable assumed an arc between the drum tangency point and the hydraulic cylinder. The hold down roller successfully retained the stored cable on the drum.

#### Cable Severing Test

##### Procedure

With the hoist input shaft locked, the single cable design load of 16,939 pounds was applied to the free end of one cable. The cable exit angle was essentially vertical. High speed movie cameras were started and then the cable cutter was energized to sever the loaded cable.

## Results

The test cable was retained on the drum by the hold down roller as required. The energy in the cable caused the cable to worm its way down the drum resulting in a small amount of looseness in four wraps of the cable at the anchor end of the drum. The first wrap of cable at the severed end was loose in the area of normal departure of the cable from the drum.

There was no visual damage to the hoist except that caused by the separation of the load isolator. Since the load isolator was not designed for high tension loads, the high energy developed in the system caused the end fitting of the load isolator to be separated from its shaft on the piston rod. This separation permitted the hoist isolator arm to travel beyond its normal retracted position, causing damage to the bevel gear housing, isolator arm lock assembly, and shearing the bolts mounting the isolator arm lock assembly and hoist lifting plate.

A small piece of housing and the isolator arm lock assembly along with the sheared bolt heads were thrown from the hoist. The hoist lifting plate tumbled down in the load isolator area. The largest part thrown from the hoist was the isolator arm lock assembly, which is made of steel and has an approximate weight of .42 pounds. Figure 12 shows the winch and load isolator damage.

Using both charges in the cable cutter caused the cutter housing outside the anvil area to become distorted. This condition prevented the removal of the cutter assembly from the carriage assembly. A small amount of filing was required in the raised areas of the cutter housing in order to remove the cutter assembly. The blade penetrated the anvil approximately  $3/8$  inch. The hoist was operated to remove the cable.



Figure 12. Damage to Hoist and Load Isolator after Cable Cutting Test.

## CONCLUSIONS

The hoist performance through the development test program and operation in the integrated test rig has demonstrated compliance with the strength and functional requirements. The hoist, with modified mounting fittings, is suitable for installation in the prototype HLH.

Damage to the hoist resulting from the Phase III test could be reduced. We recommend that a frangible material, which is economical to replace, be used to absorb the released energy.

## RECOMMENDATIONS

Our recommendations for minor changes to the hoist and further studies to improve the effectiveness of the hoist system are discussed in the concluding section of this volume.

## PNEUMATIC HOIST DRIVE UNIT

### DESIGN SUPPORT TESTS

The purpose of the design support testing was to collect information upon which the subsequent ATM design would be based. Information was collected to determine: the output power of turbines for forward and reverse modes of operation, the power needed to drive a turbine wheel in reverse, ways to reduce this power, the amount of heating which would take place, and the response times of turbines in various configurations.

In order to keep down the costs and the time spent in the design support testing phase, a Sundstrand F-110 jet engine starter was modified to simulate different components of the HLH hoist system for different phases of the test program. This starter consisted of a turbine wheel 7.0 inches in diameter with partial-admission inlet nozzles. The gearbox of the starter unit employs a two-step, jackshaft-type spur gear reduction with a ratio of 16.3:1 with splash lubrication.

The unit was modified by replacing the partial admission inlet with full admission inlet nozzles. For the air turbine motor tests, a 4.4-inch in diameter turbine was acquired from Sundstrand stock and used as the reversing turbine. Further modifications were made on these turbines to reduce wheel drag.

A third turbine, 3.4 inches in diameter, was also used in windage testing. This was also an existing turbine which was used in the auxiliary power unit in the Poseidon Missile.

### ATM Performance

The F-110 starter unit was first tested to determine its performance in the reverse direction. This was done for both the partial admission and full admission nozzle configurations. The 7.0-inch turbine was rotated in the reverse direction with a hydraulic motor coupled through a magnetic clutch. Torque values, obtained with a torque shaft measuring device, were recorded, along with shaft speeds, for various inlet air pressures.

Testing was also done in the full admission configuration to determine the output torque at different speeds of forward rotation for specified air pressures. This was accomplished by applying a specified air pressure and recording the output torque as a function of turbine speed. This was done for both the 7.0-inch and 4.4-inch turbines.

The results for the partial admission case, shown in Figure 13, verify that the torque is a linear function of speed to a good approximation. Figure 14 presents the test data for the full admission case. The data for negative speeds was taken when the inlet air temperature was 60°F; while data for positive speeds was taken when the inlet air temperature was 300°F. The static friction of the turbine and gearbox is responsible for the discontinuity in the curve at zero speed. Figure 15 is corrected for these two factors.

A comparison of Figures 13 and 14 shows that the use of the partial-admission nozzles increases the torque produced for a specified inlet air pressure and turbine speed. While a partial-admission nozzle covers 240° of the arc of admission (66.7%), the nozzle area is larger (1.76 square inches) than the full-admission nozzle (1.60 square inches). This gives a greater recirculating flow and higher output torque.

Figure 16 shows the output power of the 7.0-inch turbine with full admission nozzles. The power output is quite low due to a variety of factors. The turbine wheel used was designed to handle an inlet gas temperature of 3000°F, the tip clearance was quite high (greater than 0.060 inch). This particular wheel had been used previously and was quite pitted and worn. The nozzles were not designed for this turbine. Although they were full admission, they did not extend across the full height of the turbine blades. Consequently, windage losses were expected over the unused part of the blades. Since the windage horsepower increases directly with the cube of the speed, this effect is more important at higher speeds. This explains the more abrupt drop in the power curve for higher speeds of rotation. The fact that the nozzle angle was not correct for this turbine wheel also contributed to the low power output. The combination of these effects forced the efficiency of the turbine down to the 40% range; consequently, the output power was low.

The output power of the 4.4-inch turbine is also effected by the same factors. Figure 17 shows this output power, which is in the linear range at this low rpm.



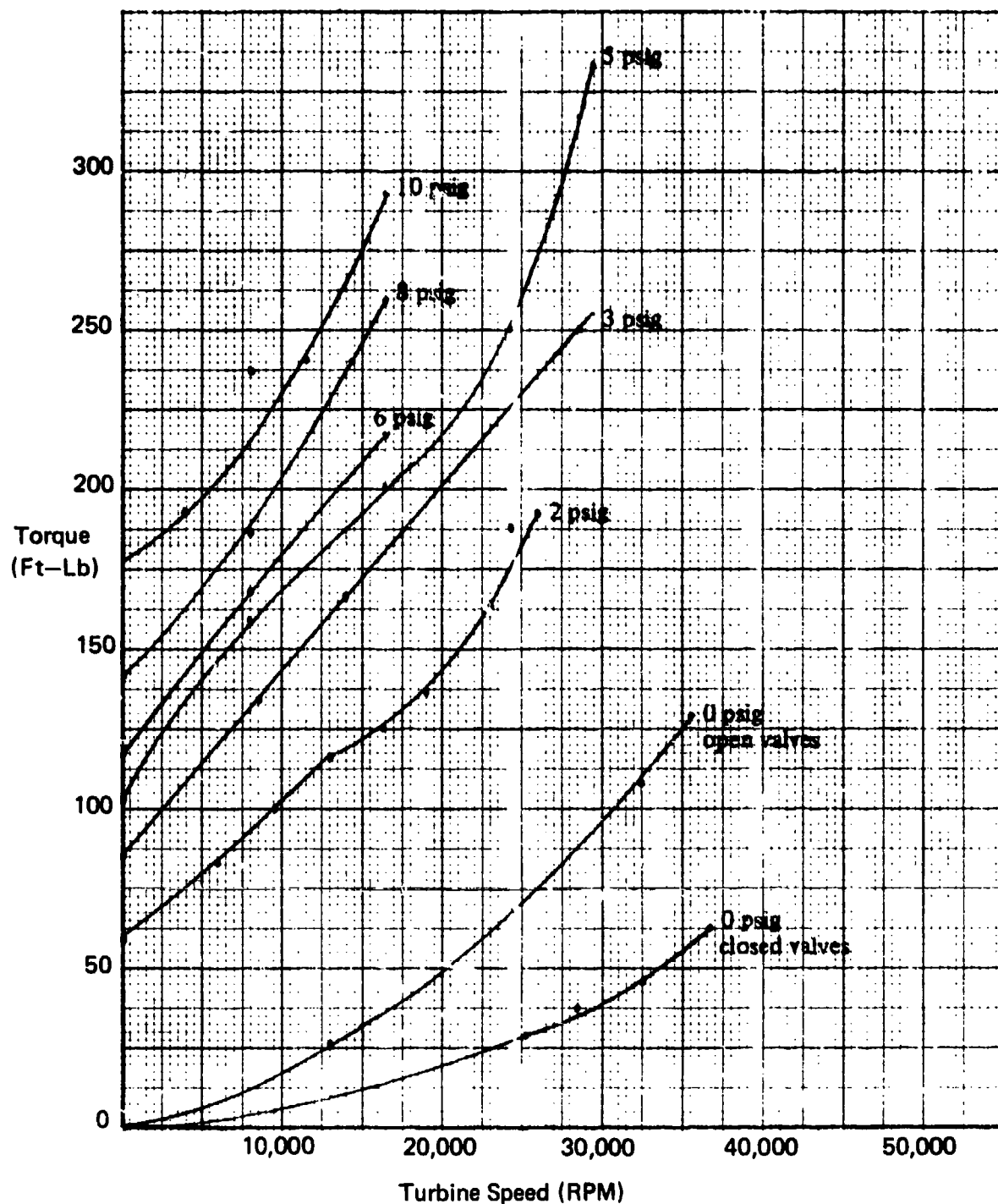


Figure 13. Torque Performance, Partial Admission, 7.0-in-dia Turbine.

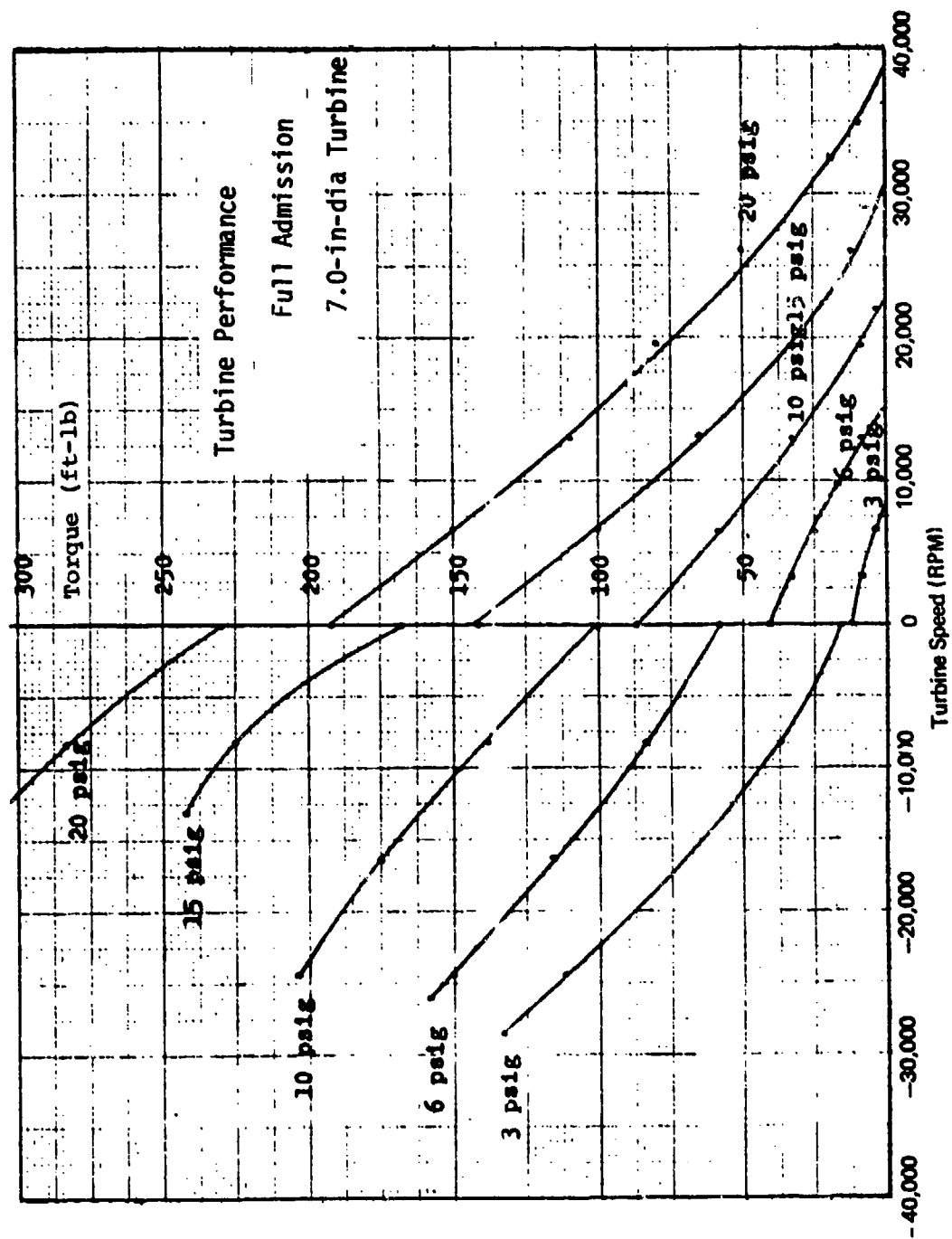


Figure 14. Torque Performance, Full Admission, 7.0-in-dia Turbine.

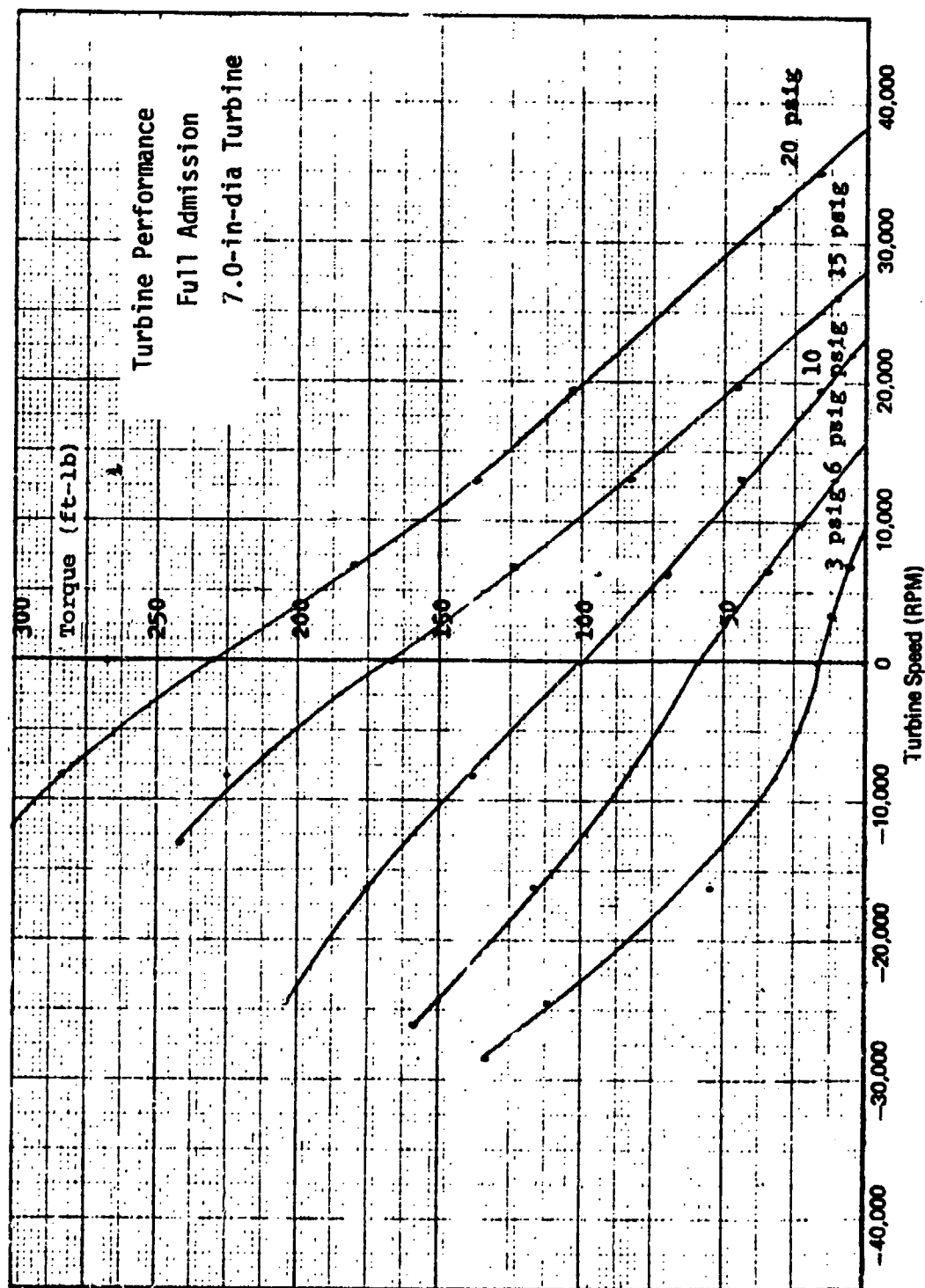


Figure 15. Torque Performance, Full Admission, 7.0-in-dia Turbine.

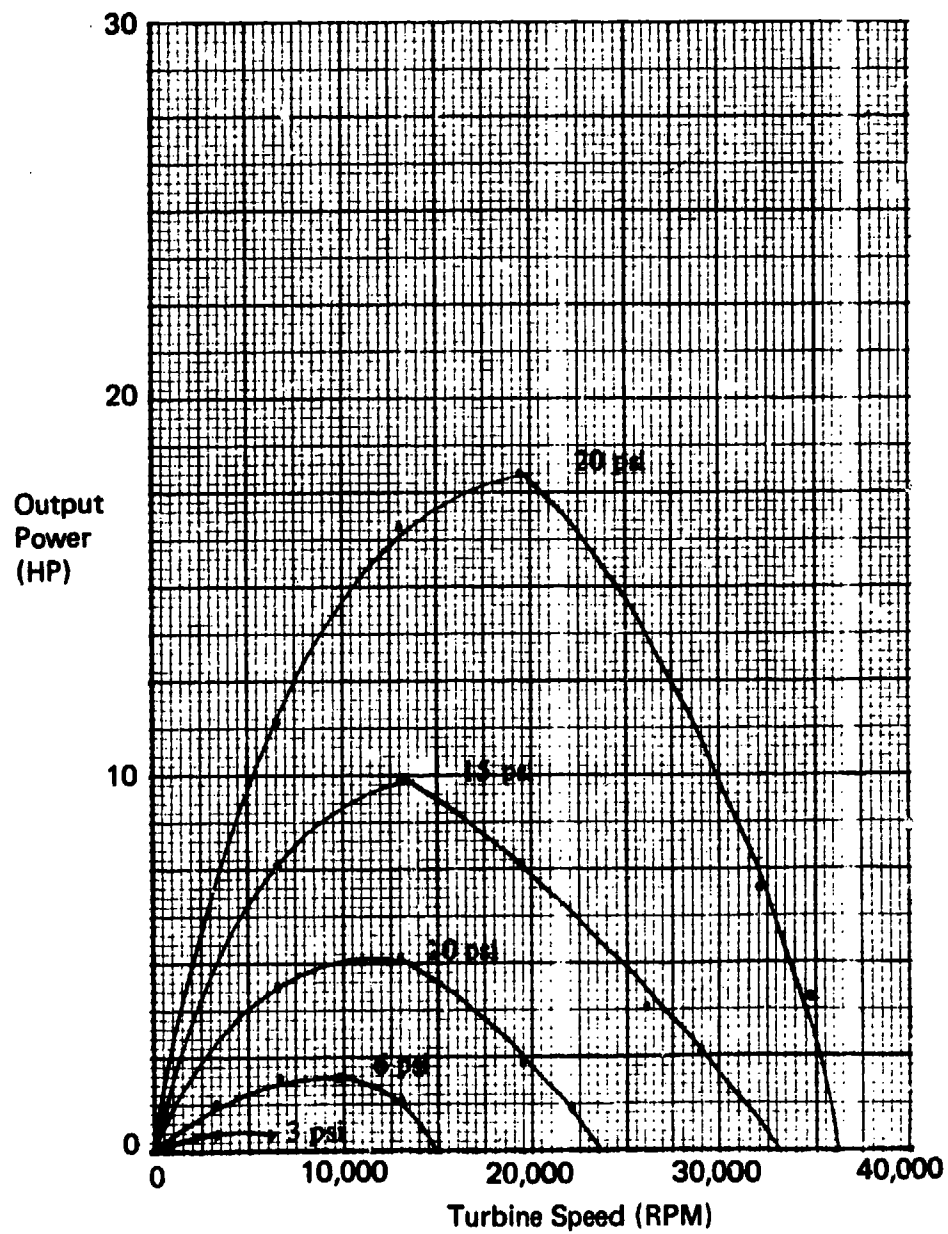


Figure 16. Output Power, Full Admission, 7.0-in-dia Turbine.

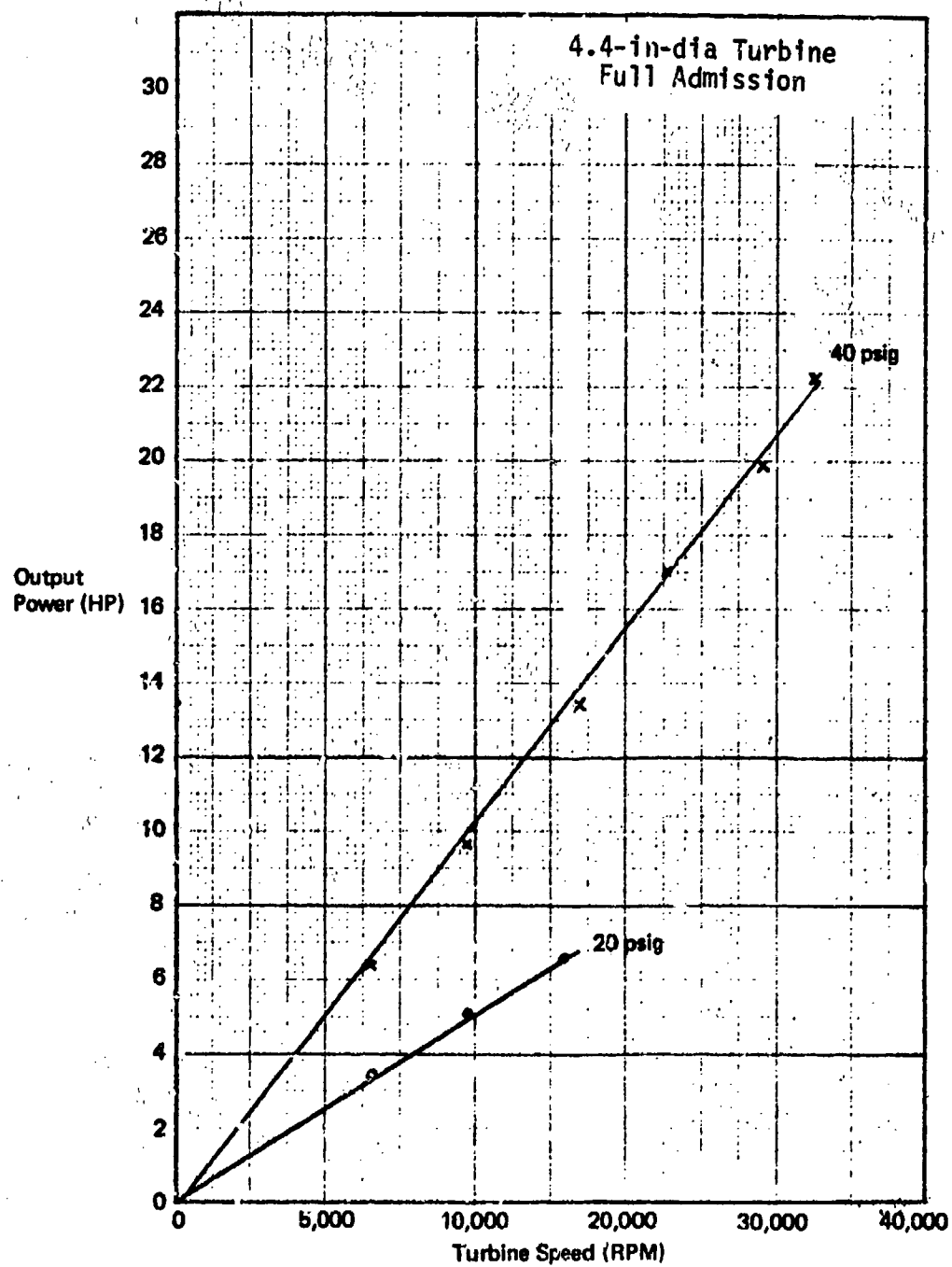


Figure 17. Output Power, Full Admission, 4.4-in-dia Turbine.

### Unloaded Turbine Reversal

The unloaded turbine reversal tests were run after a modification of the original starter unit. A 4.4-inch turbine, representing the reversing wheel, was attached to the same shaft as the 7-inch turbine, which represented the hoisting turbine. The two turbines were equipped with separate, full admission nozzles and were exhausted into a common chamber. A baffle plate was fabricated for the 7.0-inch turbine; and, for subsequent tests, slots were machined in this plate. This plate was installed on the exhaust side of the 7-inch turbine.

Each turbine (hoisting and reversing) was supplied with a separate, independently controlled air line. The turbine output shaft was coupled through a magnetic clutch to an industrial brake.

Tests were run to find the maximum speed which could be attained for a specified inlet pressure (hoisting and reversing) in three modes of operation:

1. No baffle plate
2. Baffle plate installed on the 7.0-inch turbine
3. Slotted baffle plate installed

The results of these tests are shown in Figures 18 and 19. The baffle plate greatly increased the reversing speed which could be attained for a specified reversing air pressure, but it severely limited the forward performance of the hoisting turbine. The addition of slots to the baffle plate helped to bring up the hoisting turbine efficiency but this also decreased the maximum attainable reversing speeds from the levels obtained with the non-slotted baffle plate.

The maximum speed is attained in this test when the output power of the driving turbine equals the windage power of the turbine being driven in reverse. Figures 20 and 21 show the previously obtained output power curves and windage curves. The point of crossing is the maximum speed attainable for a specified inlet air pressure. The actual values for these speeds are also shown. The error shown is due to possible friction horsepower variations caused by variations in oil level.

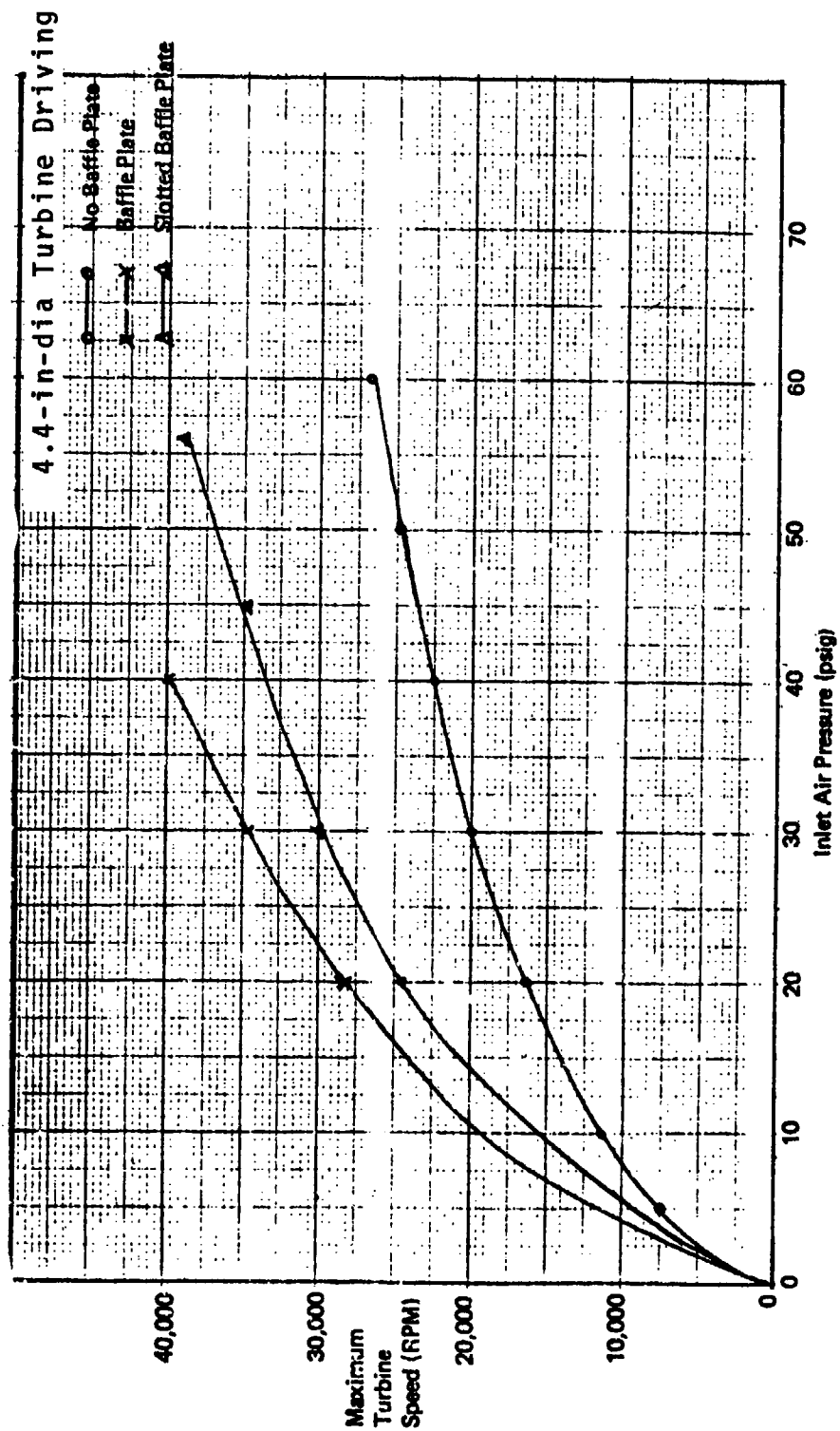


Figure 18. Unloaded Turbine Reversal, 4.4-in-dia Turbine Driving.

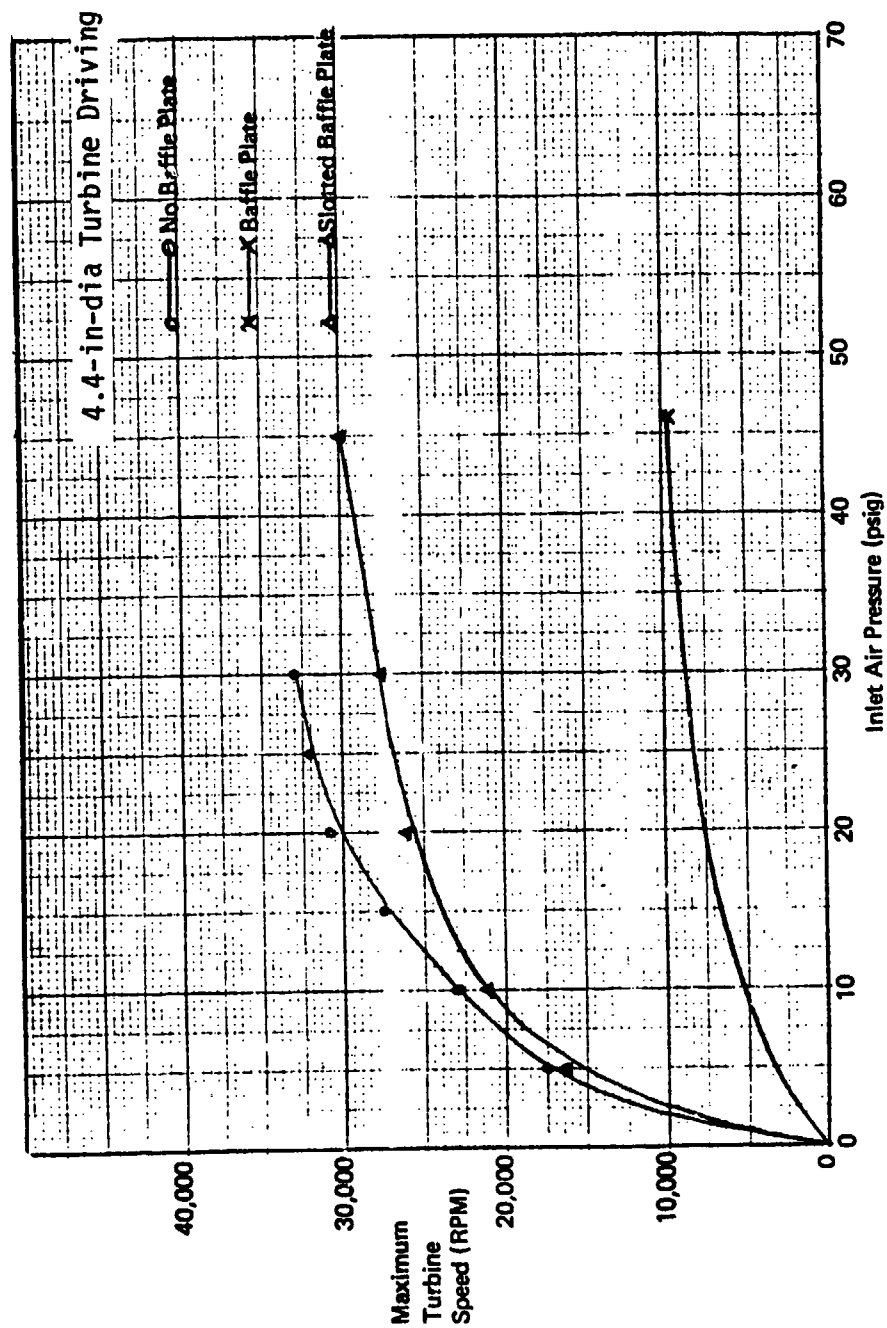


Figure 19. Unloaded Turbine Hoisting, 4.4-in-dia Turbine Driving.



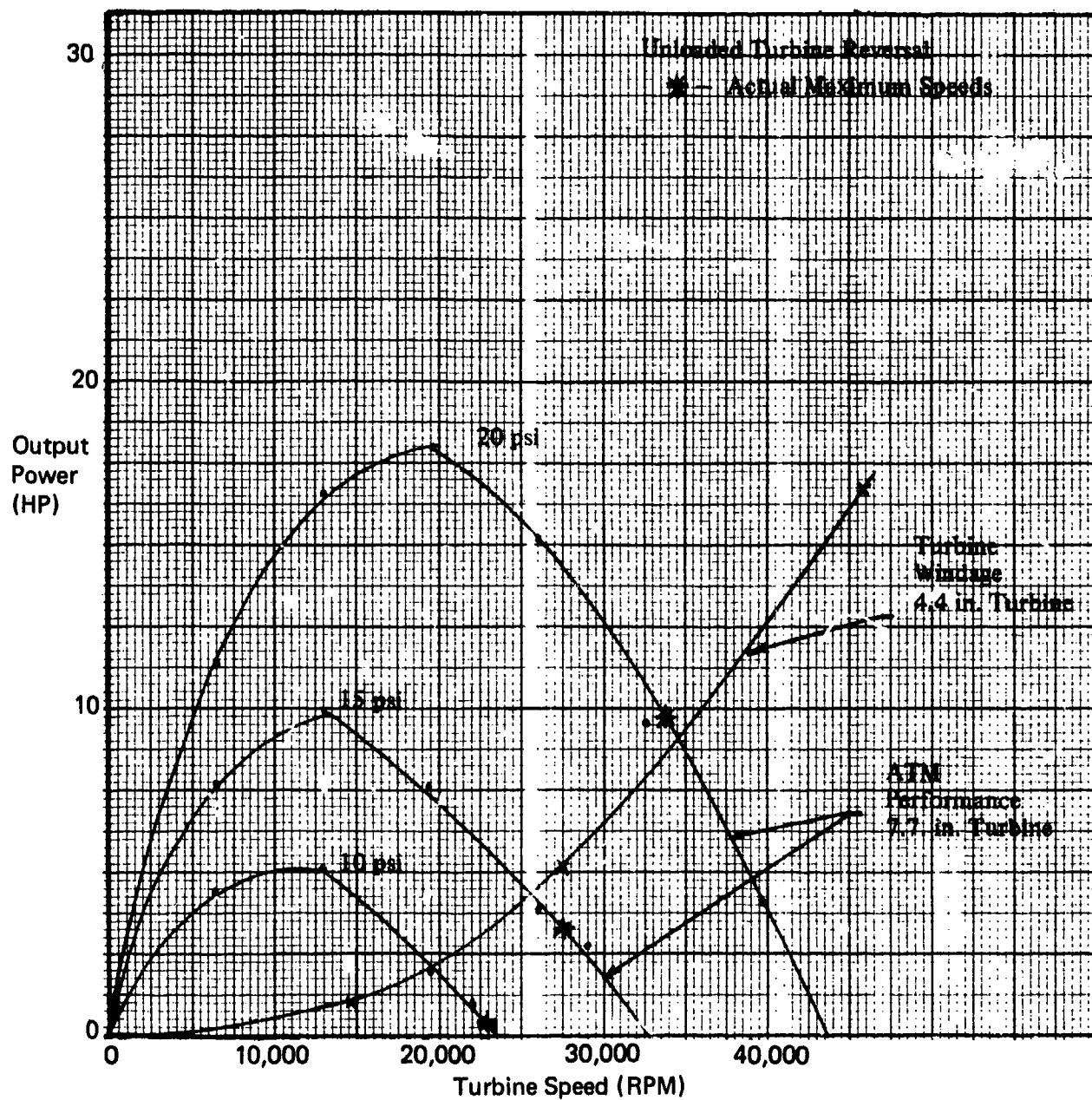


Figure 20. Unloaded Turbine Reversal, Output Power, 7.7-in-dia Turbine.

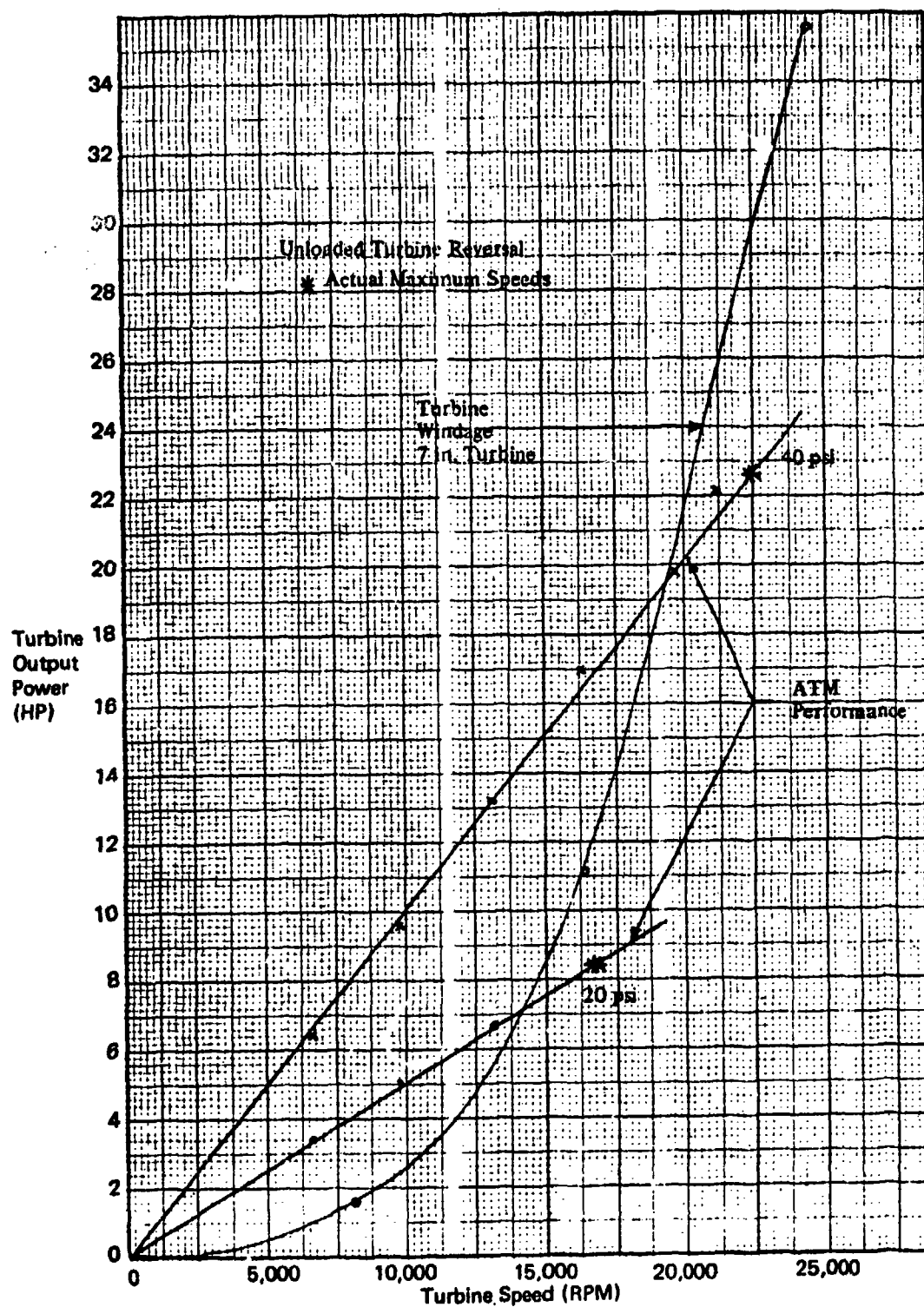


Figure 21. Unloaded Turbine Reversal, Output Power, 4.4-in-dia Turbine.

Tests were run to determine the speed of response for reversal in this configuration. The starter was run first in the forward direction and then reversed. The time to go from full-speed forward to full-speed reverse, shown in Figure 22, is higher than expected in the ATM final design due to the low efficiencies and high inertias of the test turbines. The hoisting air pressure was 45 psig and the reversing air pressure was 48 psig.

Figure 23 shows the speed vs. time curve for the hoisting and reversing turbines starting from rest. The turbine response times are high, again due to the higher inertia and lower efficiency of the test hardware in comparison with the proposed ATM system.

#### Wheel Drag Reduction - 7.0-in-dia Turbine

Theoretically, turbine windage is a function of the speed (N) cubed and the turbine diameter (D) to the fifth power. (Windage HP  $\cong N^3 \times D^5$ ).

The reason for this relationship is that the windage generates a pressure rise which causes a recirculating flow. When the axial turbine is driven backwards, it acts as a compressor and demonstrates similar characteristics.

The energy imparted to the air is directly proportional to  $N^2$ . Also, the amount of recirculating air increases directly with N. The product of energy/lb and recirculation mass in lb/sec yields horsepower.

$$\text{Energy} \cong N^2$$

$$\text{Mass flow} \cong N$$

$$\text{Windage horsepower} \cong N^3$$

If the amount of recirculation is decreased, then the windage horsepower will vary with speed to an exponent less than 3.0.

As diameter increases for a particular rotational speed, the energy imparted to the air is directly proportional to  $D^2$ . The amount of recirculating flow is directly proportional to  $D^3$  because the flow area is increasing as a function of  $D^2$ , and the basic recirculation caused by the increase in tip speed is increasing approximately as a linearly function of D. The product of energy/lb and recirculating mass in lb/sec yields horsepower.

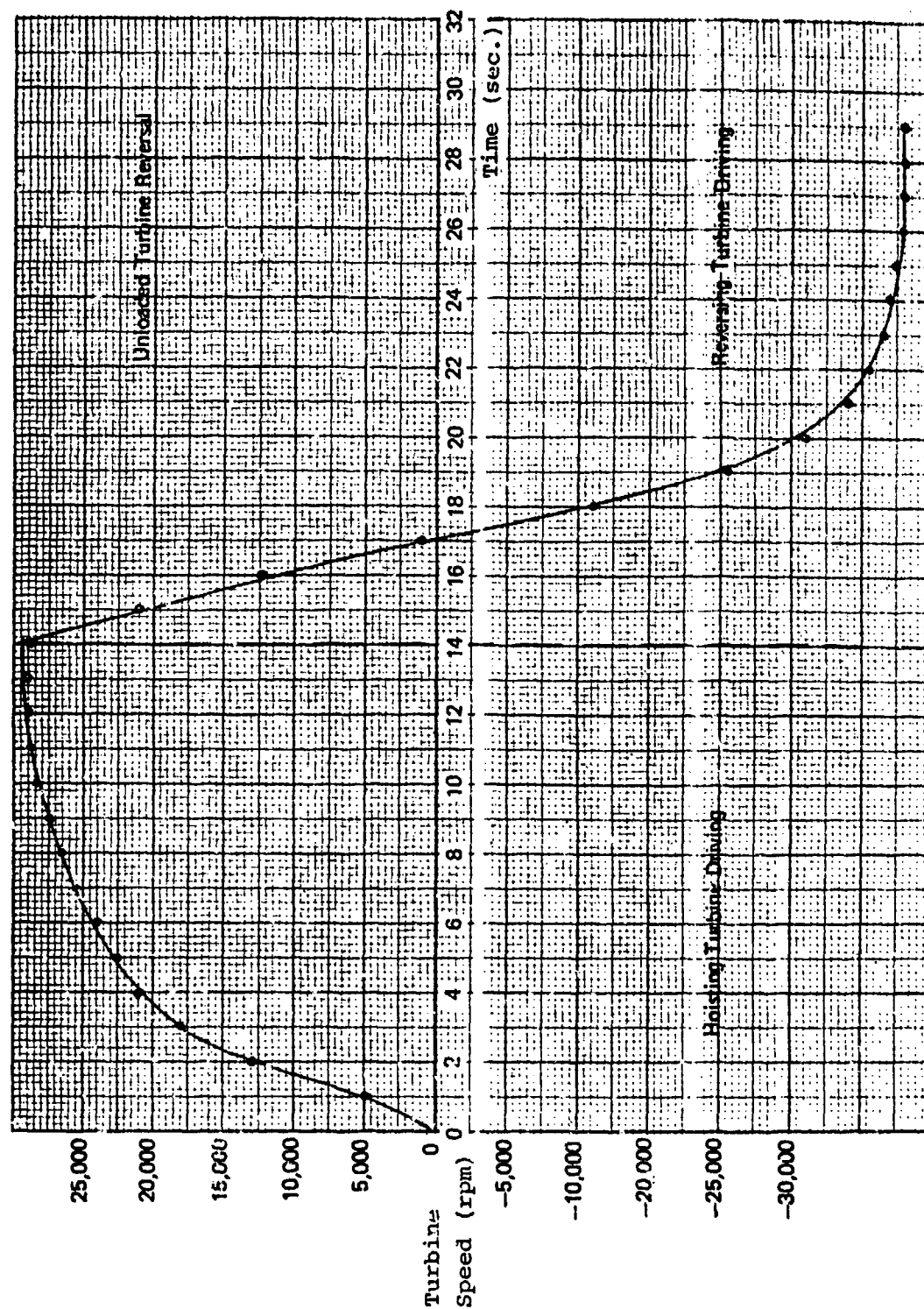


Figure 22. Unloaded Turbine Reversal.

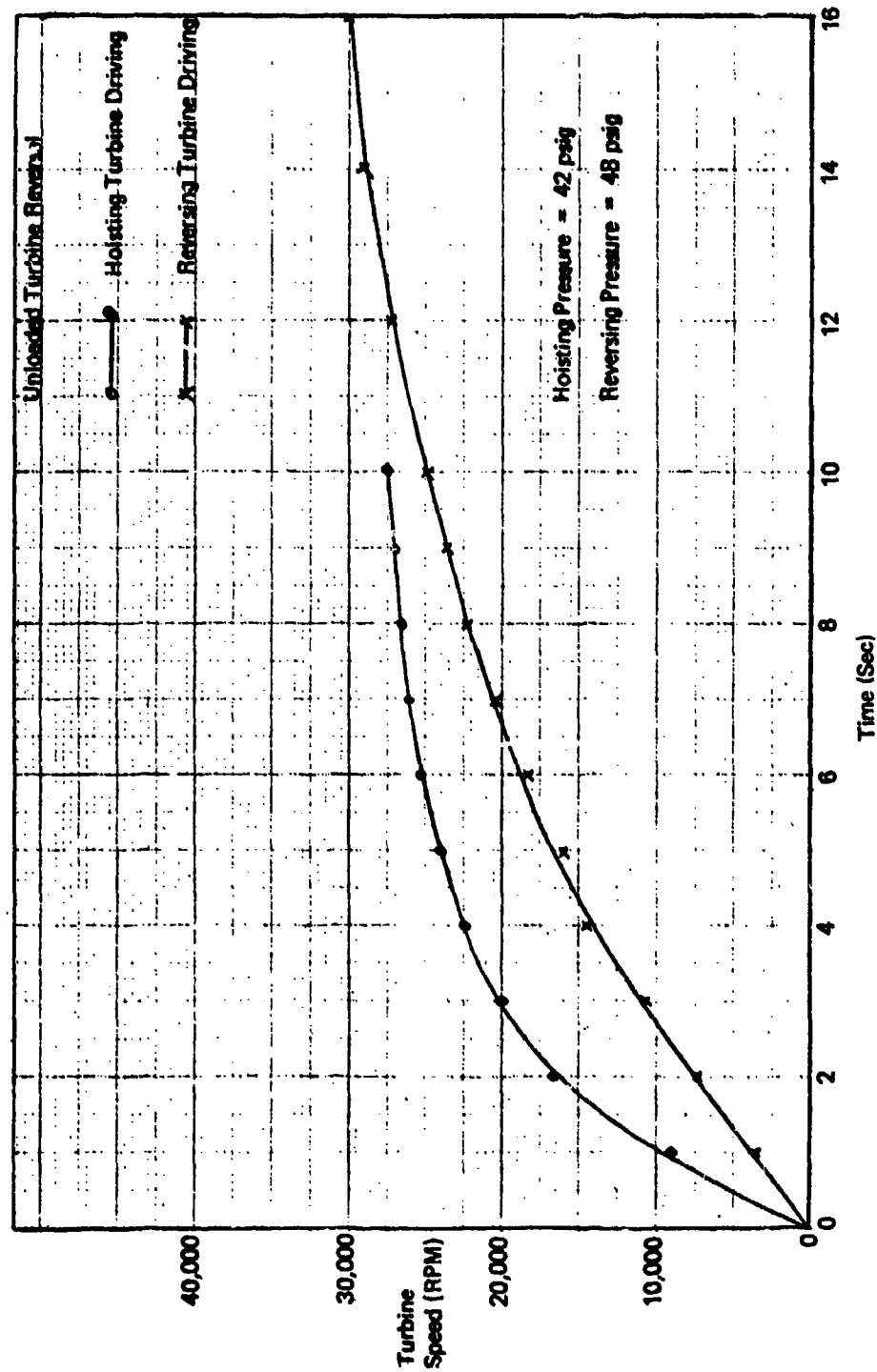


Figure 23. Unloaded Turbine Accelerations.

$$\text{Energy} \approx D^2$$

$$\text{Mass Flow} \approx D^3$$

$$\text{Windage} \approx D^5$$

Again, if the amount of recirculating flow can be reduced or choked off, the variation in windage will be a function of  $D^X$  where X is less than 5.

Tests were run first to verify the theoretical equation derived above. The test unit was coupled directly to an electric motor and values of input torque were taken with a torque shaft. The 7.0-inch and 4.4-inch turbines were run in the reverse direction at various speeds from 0 to 50,000 rpm. The 7.0-inch turbine was run with both full admission and partial admission nozzles. Another turbine, the 3.4-inch turbine used in the Poseidon Missile Auxiliary Power Unit, was also used to further confirm the theoretical equation.

Figures 24 and 25 show the verification of the windage exponent. The slope of the line equals the exponent.

$$\text{Windage} = D^X N^Y$$

Figure 24 shows that x is, in practice, nearly equal to 5.0 and Figure 25 shows that y is also close to its theoretical value of 3.0. These tests were conducted with the inlet valves and the exhaust open to the atmosphere. Figure 26 shows the windage horsepower as a function of the turbine rpm for the 7.0-inch and 3.4-inch (Poseidon) turbines.

Figure 27 shows the windage reduction achieved simply by closing the inlet and exhaust valves for the 7.0-inch turbine. The closing of the valves helped to eliminate the "pumping action" of the turbine and allowed a drop in the windage horsepower to about 40% of that needed with the valves open.

Figures 28 and 29 show the windage horsepower with the partial and full admission nozzles with inlet air pressure applied. Here again, the windage horsepower was higher for the partial admission nozzle at a specified pressure and speed than for the full admission nozzle.

Figure 30 presents the results of an effort to reduce the windage of the 7.0-inch turbine. A shroud band was electron-beam welded on the outer diameter of the turbine.

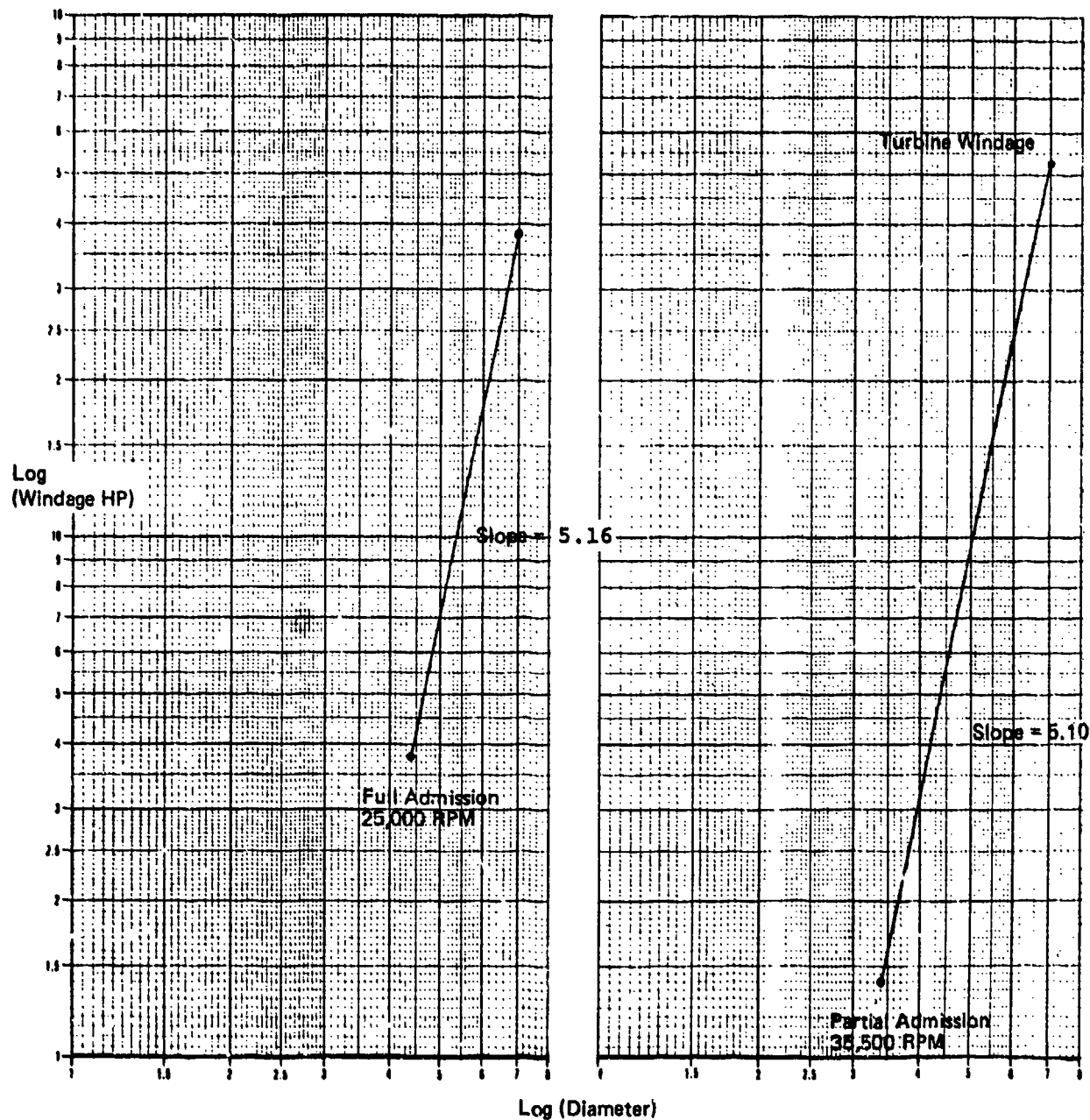


Figure 24. Turbine Windage.

# Turbine Windage - Full Admission

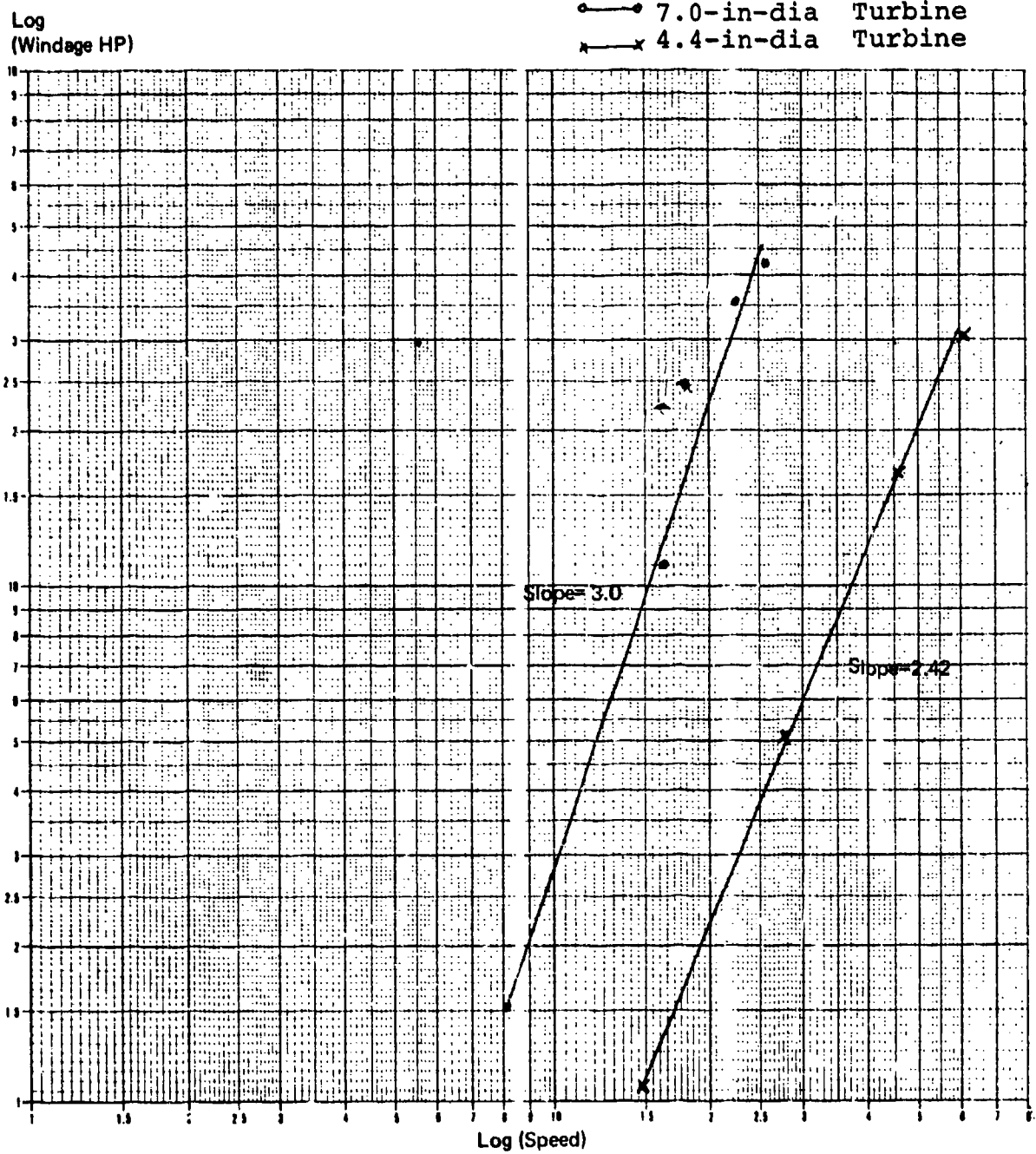


Figure 25. Turbine Windage, Full Admission.



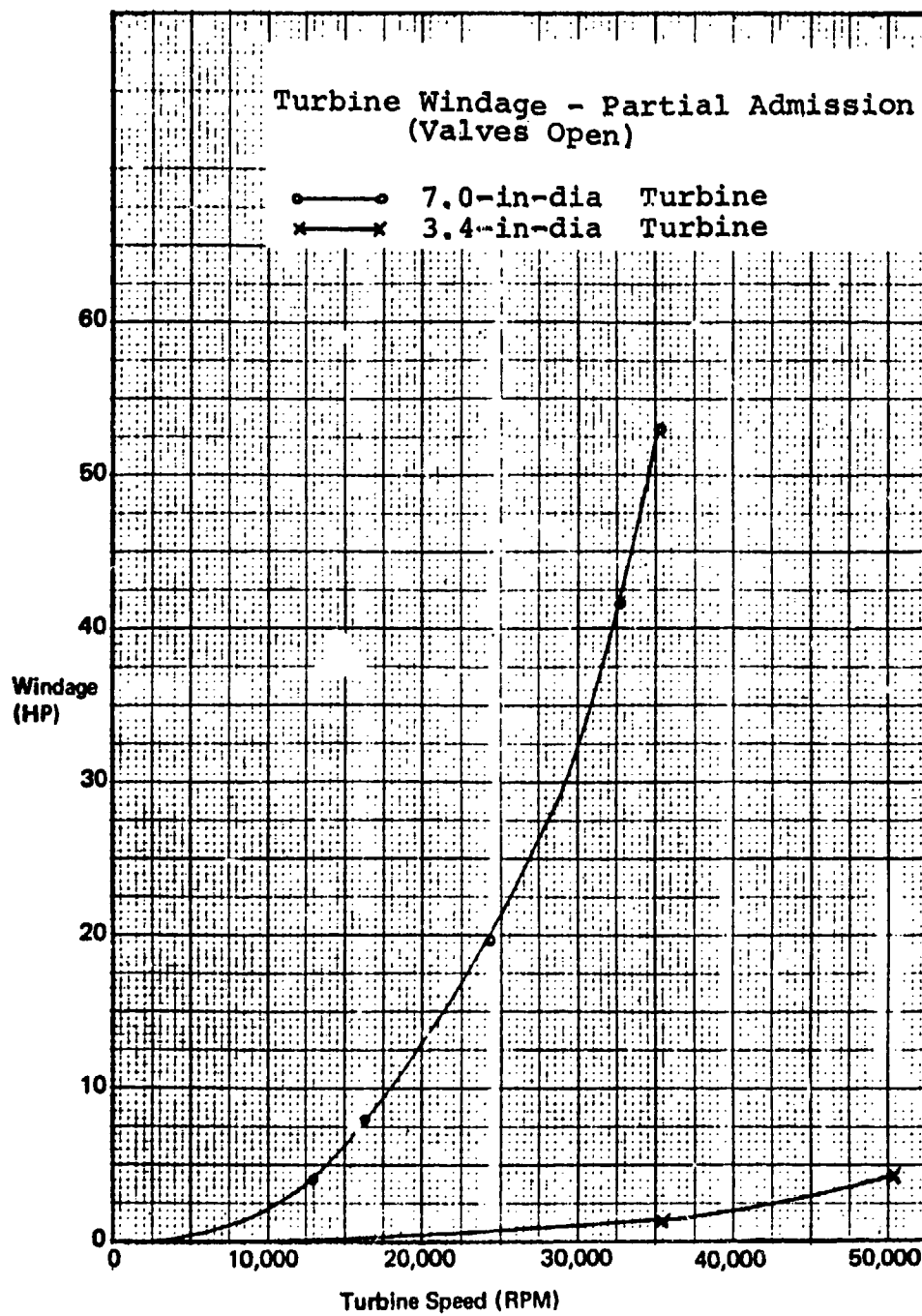


Figure 26. Turbine Windage, Partial Admission, Valves Open.

# Turbine Windage

7.0-in-dia Turbine  
Partial Admission

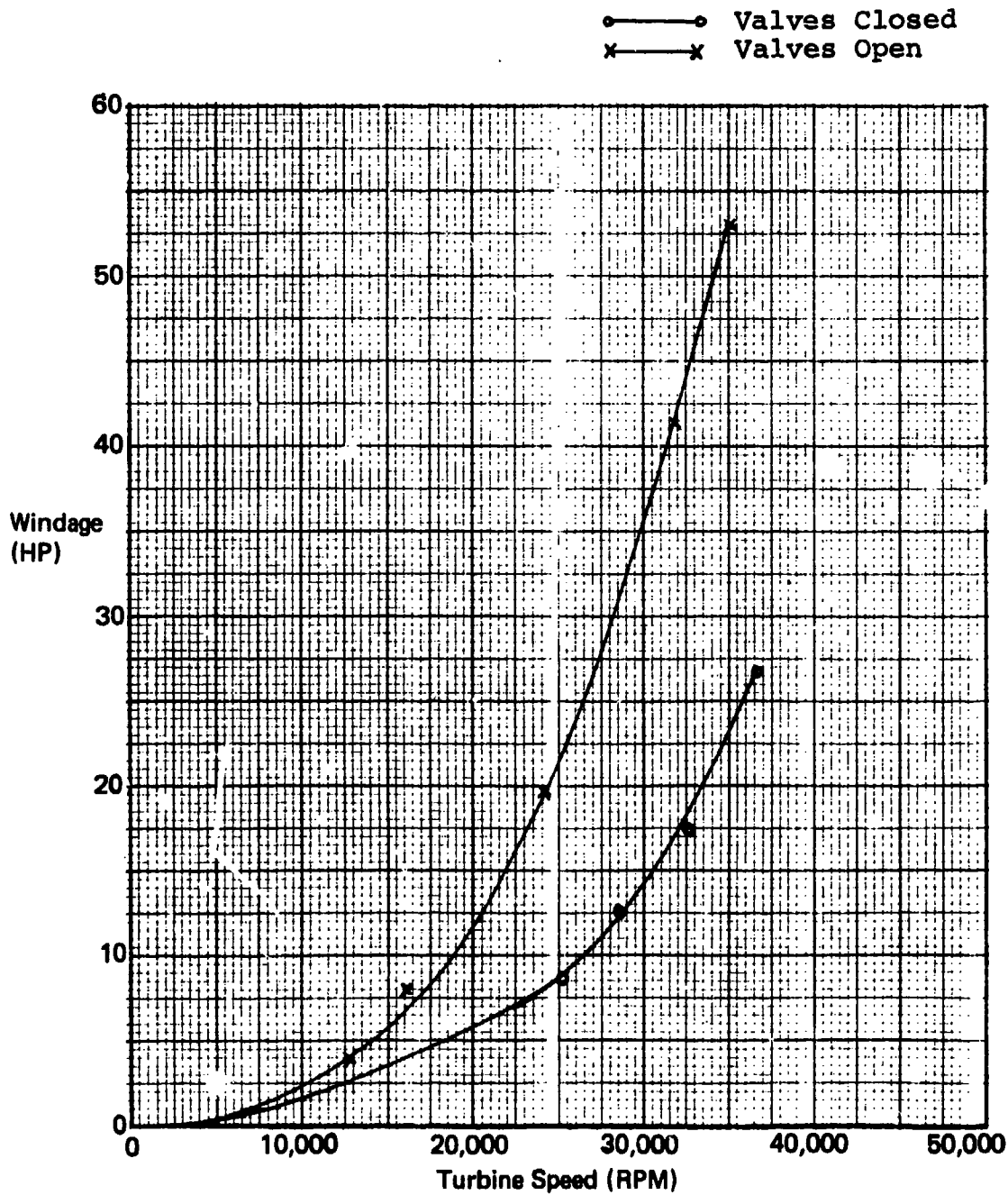


Figure 27. Turbine Windage, 7.0-in-dia Turbine, Partial Admission.

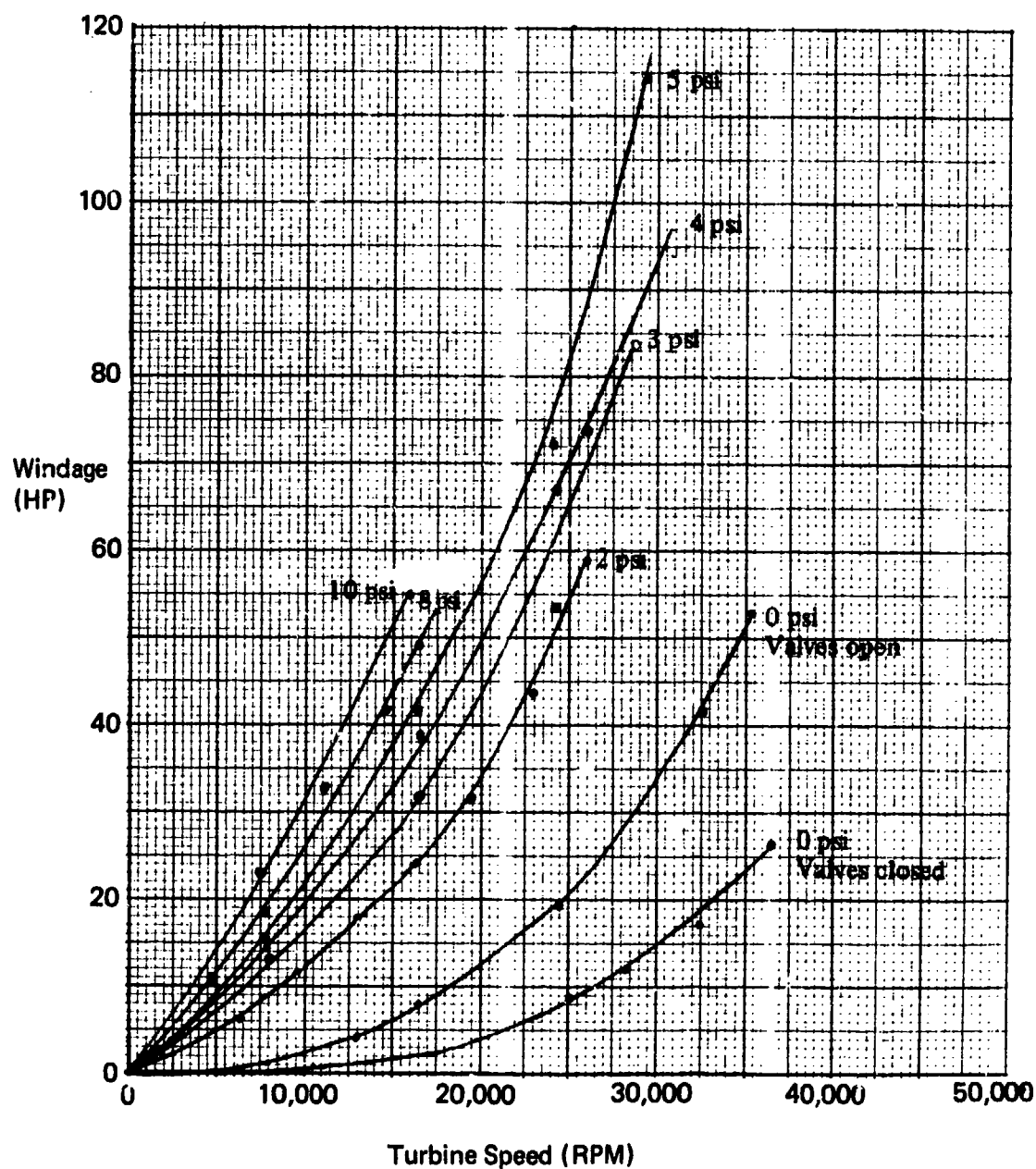


Figure 28, Turbine Windage, 7.0-in-dia Turbine, Partial Admission, Various Inlet Air Pressures.

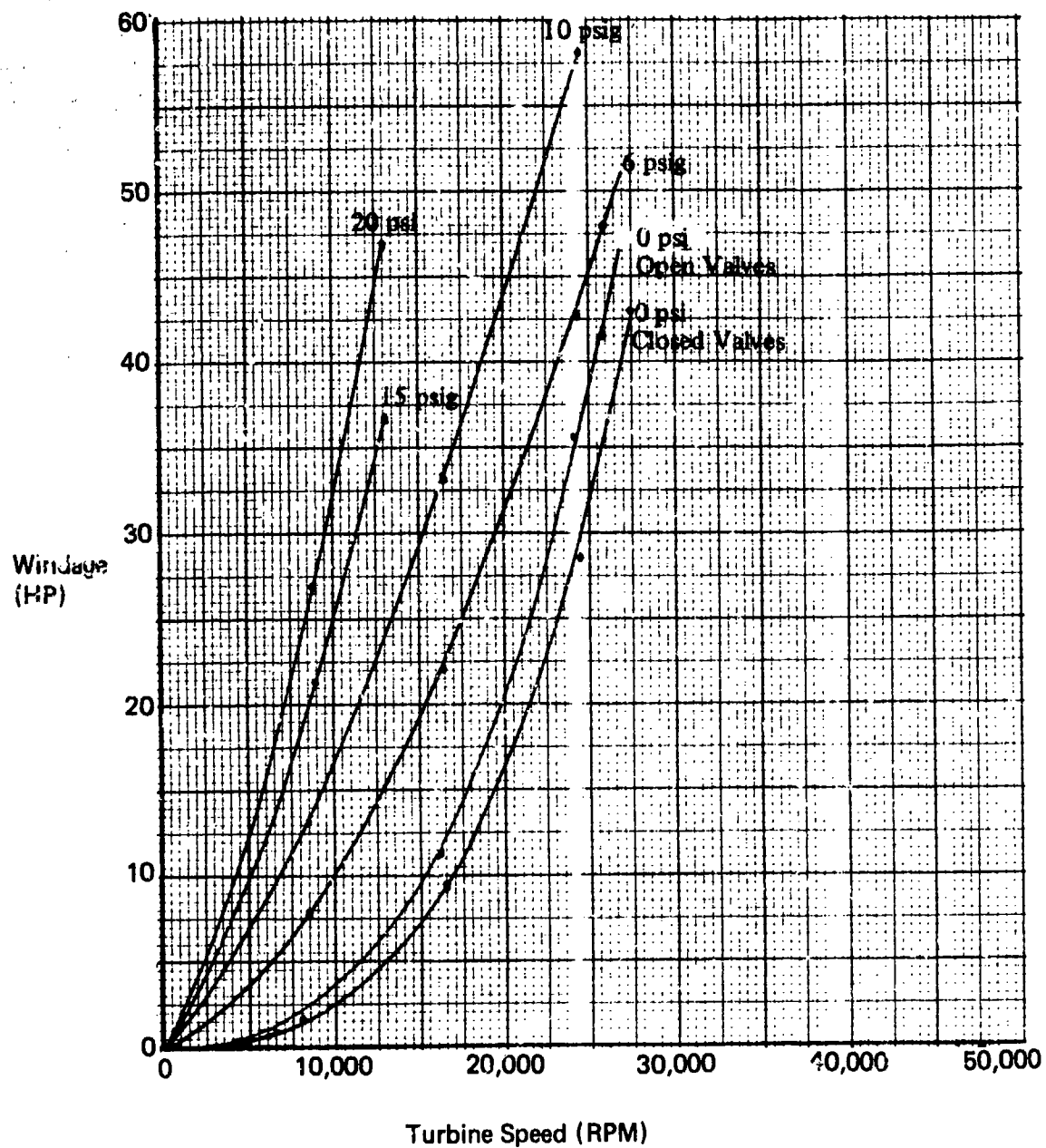


Figure 29. Turbine Windage, 7.0-in-dia Turbine, Full Admission, Various Inlet Air Pressures.

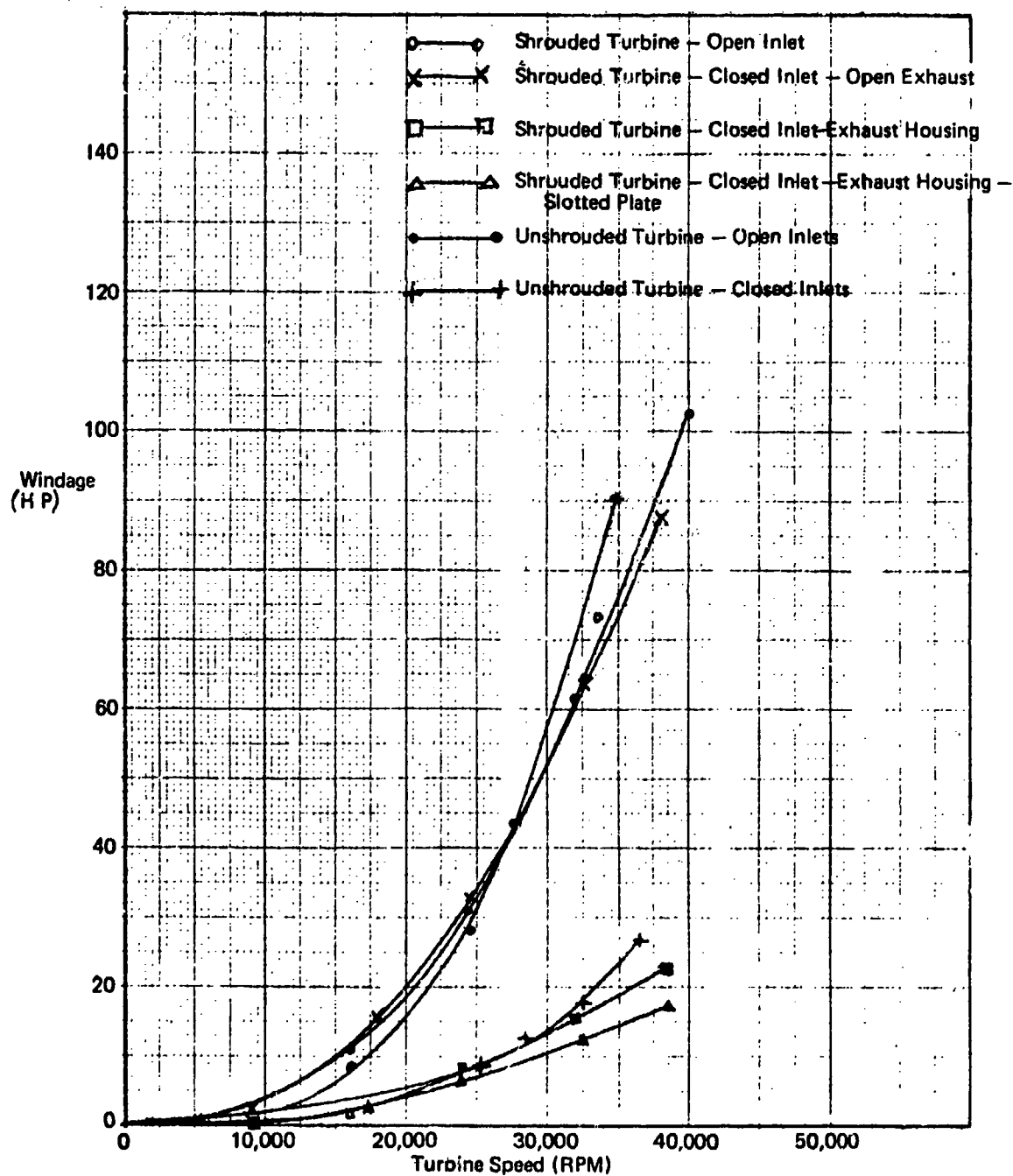


Figure 30. Results of Windage Reduction Efforts, 7.0-in-dia Turbine, Full Admission.

It was expected that this shroud band would reduce the windage by reducing the recirculating flow. Tests were also run with the inlet duct closed, with an exhaust housing blocking the flow in the exhaust duct, and with the slotted plate.

The comparison shows that the shroud band had the effect of slightly increasing the windage at low speeds but slightly reducing the windage at high speeds. The factor that had the greatest effect on turbine windage was the closing of the inlet valves, which reduced the windage by approximately 60%. Further reductions were achieved through the use of the shroud band and the slotted plate.

Figure 31 shows the effect on the exponent of the shrouded turbine with inlet and exhaust ducts closed. The net effect was to reduce the exponent to 2.48.

The windage control testing showed that a significant reduction could be achieved in turbine windage.

#### Wheel Drag Reduction 4.4-in-dia Wheel

Windage reduction tests for the 4.4-inch wheel were similar to those conducted on the 7-inch turbine. Figure 32 shows the comparison of the shrouded and unshrouded windages obtained. As in the 7.0-inch turbine tests, the shroud band had the effect of increasing the windage at lower speeds while decreasing the windage at higher speeds. The exponents, shown in Figure 33, show corresponding decreases for the shrouded turbines.

Tests were run on the 4.4-inch turbine using a plate which reduced the vane-turbine axial clearance to  $1/16$  inch. Tests were also run with  $3/16$ -inch vane-turbine axial clearance. The results, shown in Figures 34 and 35, show that the reduced clearance had little effect on reducing the turbine windage.

The best windage control is to have a shroud band and to have the exhaust duct blocked. Using the resulting value for turbine windage and the results of tests of the gearbox friction present in the test unit, it is possible to predict the windage present in the ATM final design. Figure 36 shows the prediction. The results of the windage control tests for the 4.4-inch shrouded turbine with inlet and exhaust blocked are used. The actual gearbox friction was deducted and the theoretical friction of the final design was added to give the expected net windage and friction horsepower. This power is shown as a function of turbine speed in Figure 37. It should be noted that at maximum reversing speed of 87,200 rpm,

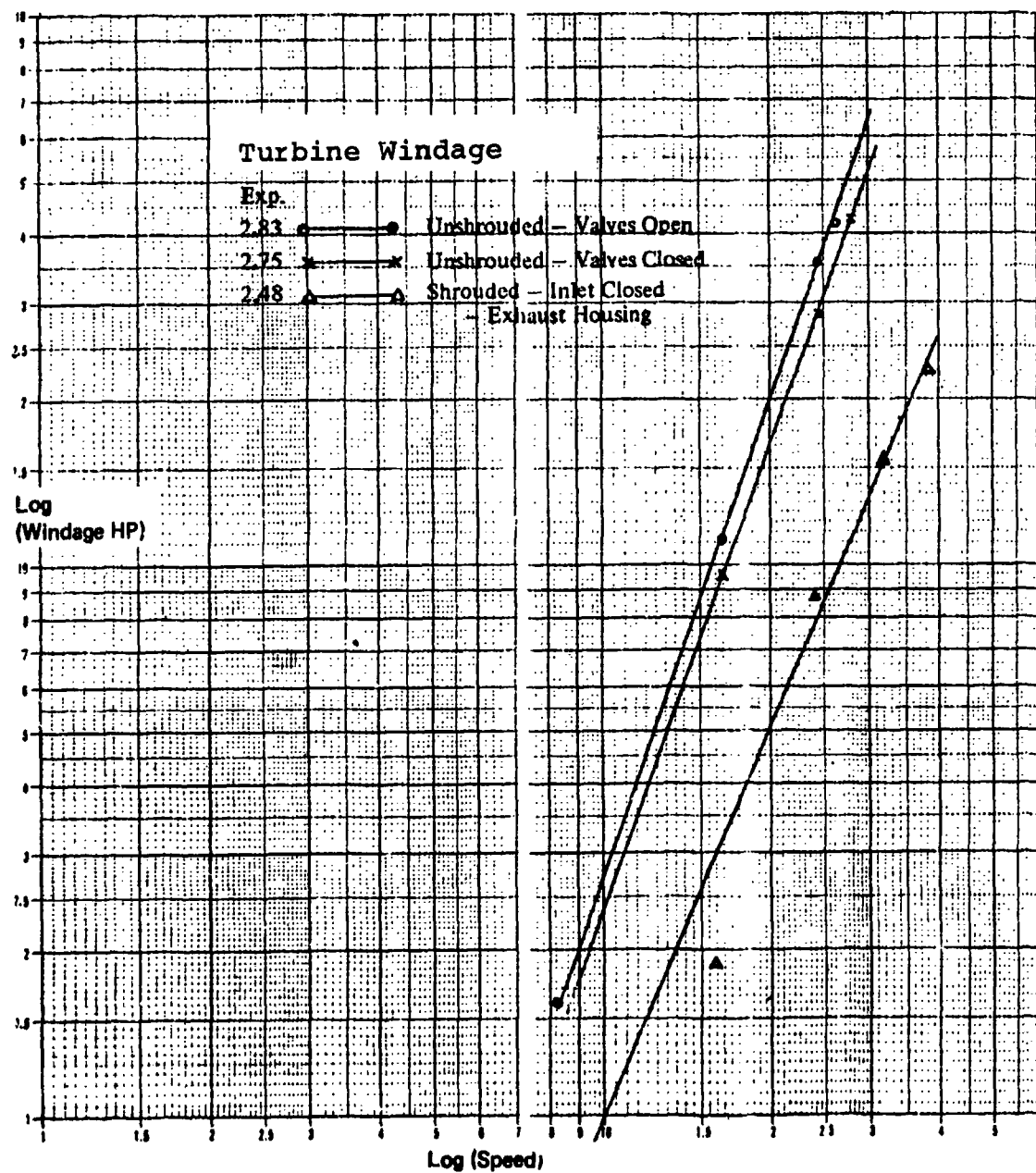


Figure 31. Turbine Windage, 7.0 in-dia Shrouded Turbine.

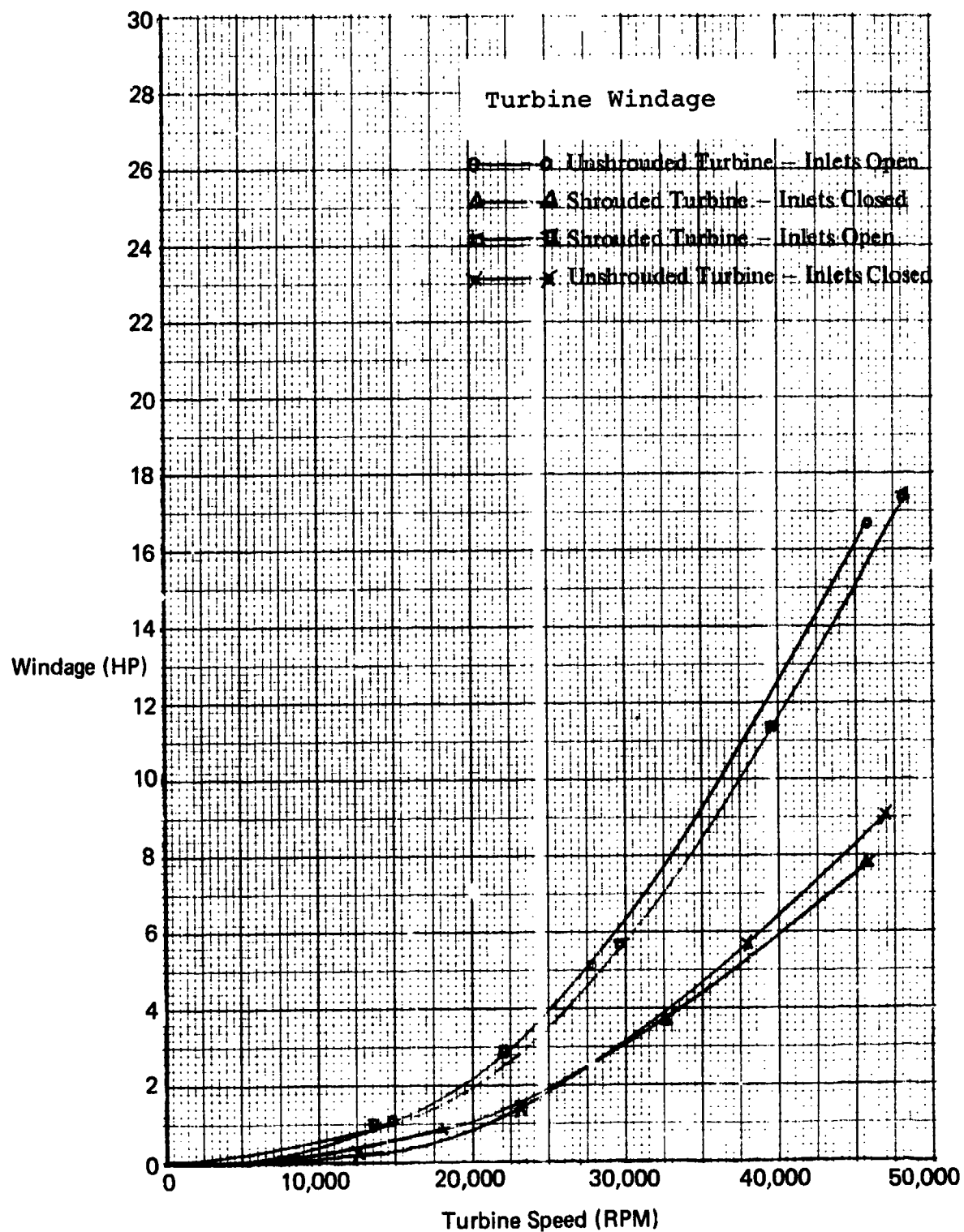


Figure 32. Comparison of Shrouded and Unshrouded Windage, 4.4-in-dia Turbine, Full Admission.



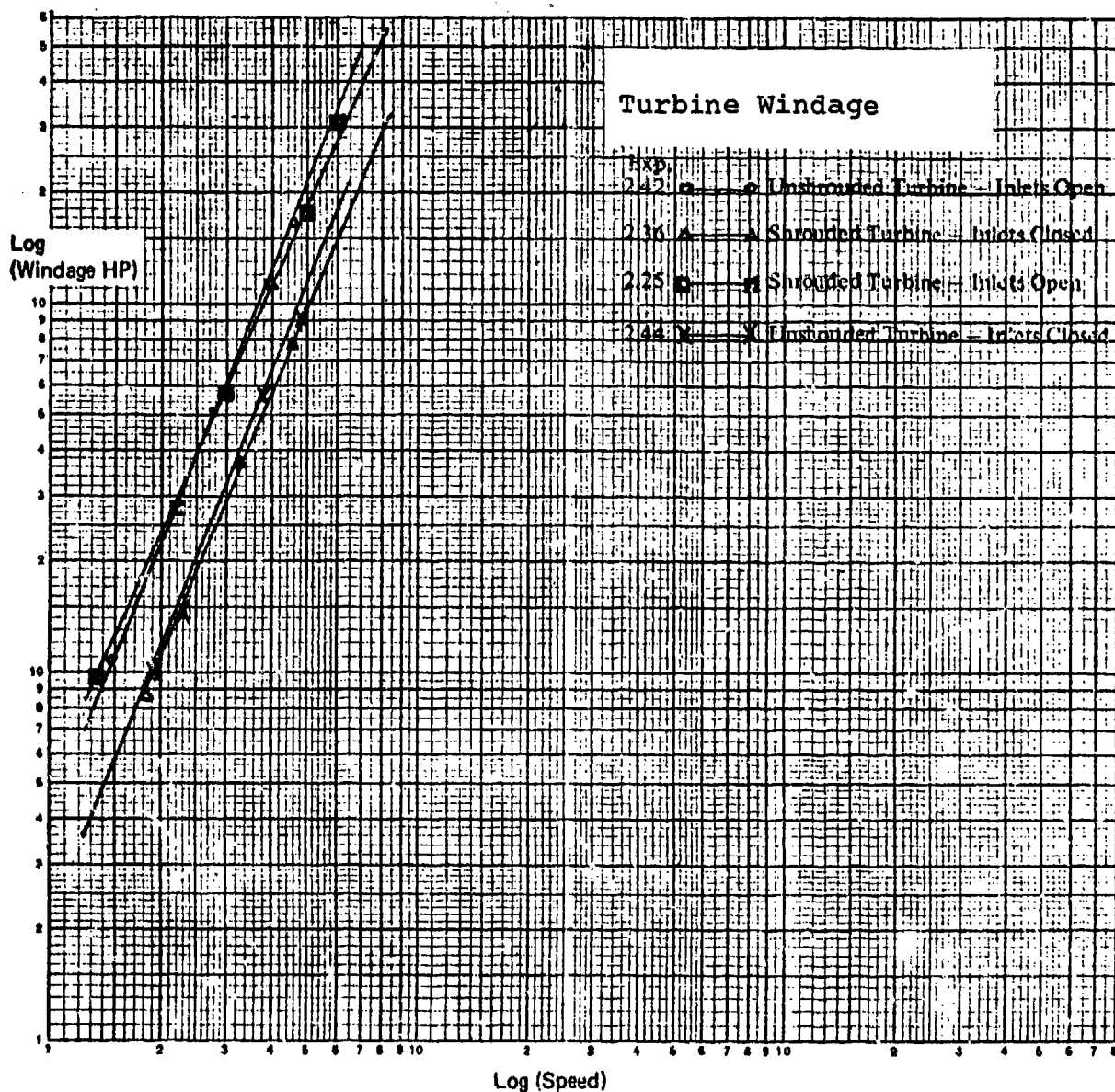


Figure 33. Turbine Windage, 4.4-in-dia Turbine, Full Admission.

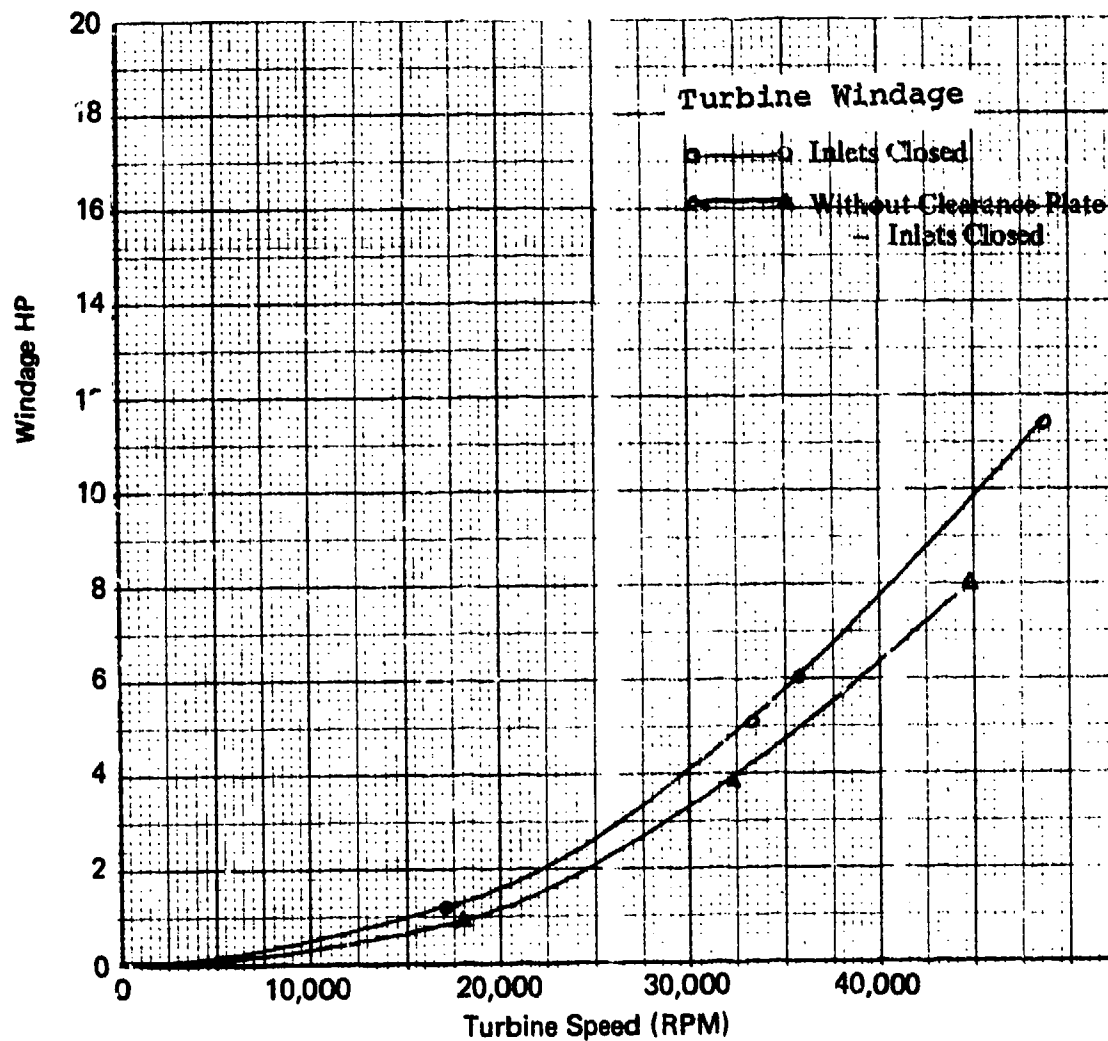


Figure 34. Turbine Windage, 4.4-in-dia Turbine, Full Admission, 1/16 Inch Vane/Turbine Clearance.

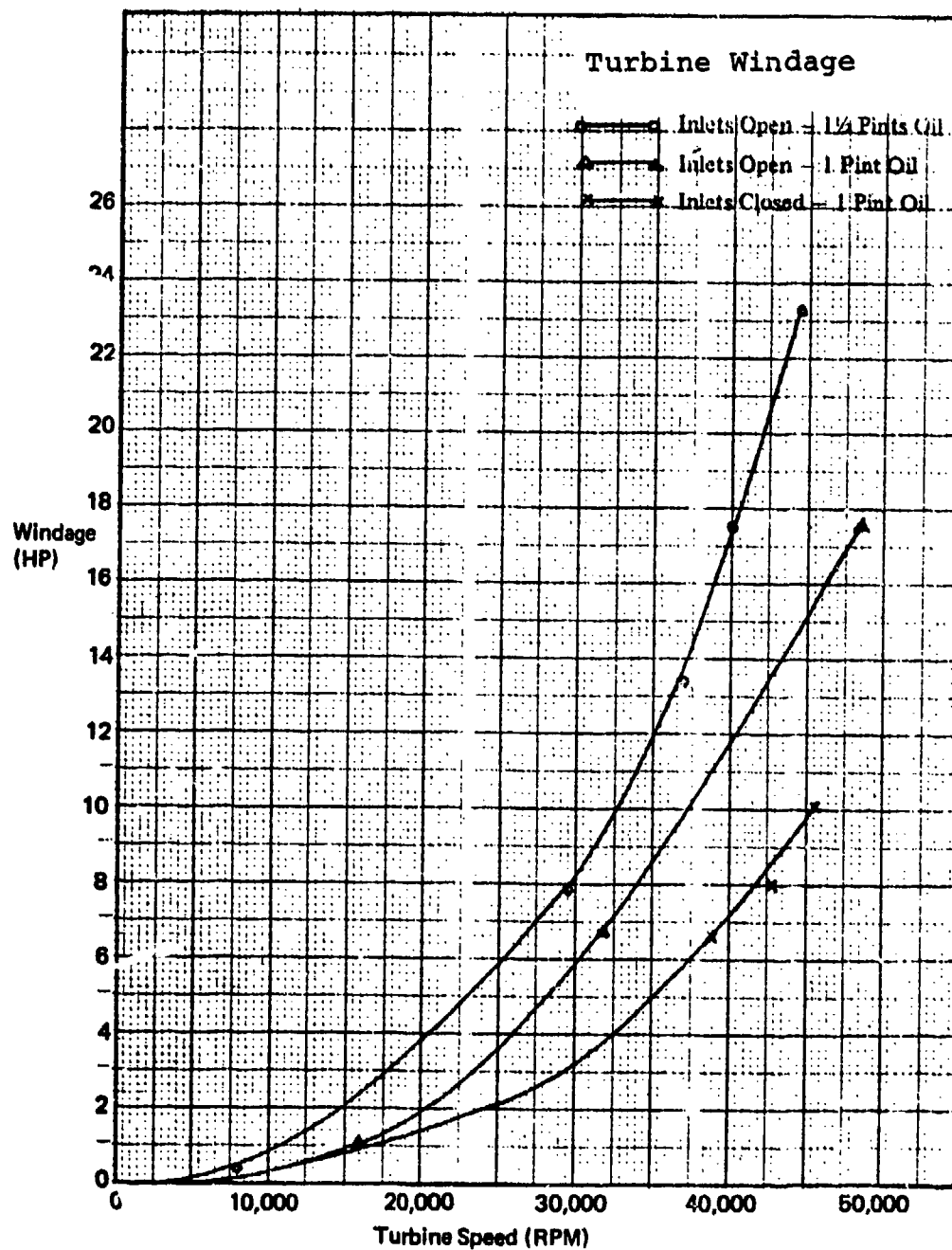


Figure 35. Turbine Windage, 4.4 -in-dia Turbine, Full Admission, 3/16 Inch Vane/Turbine Clearance.

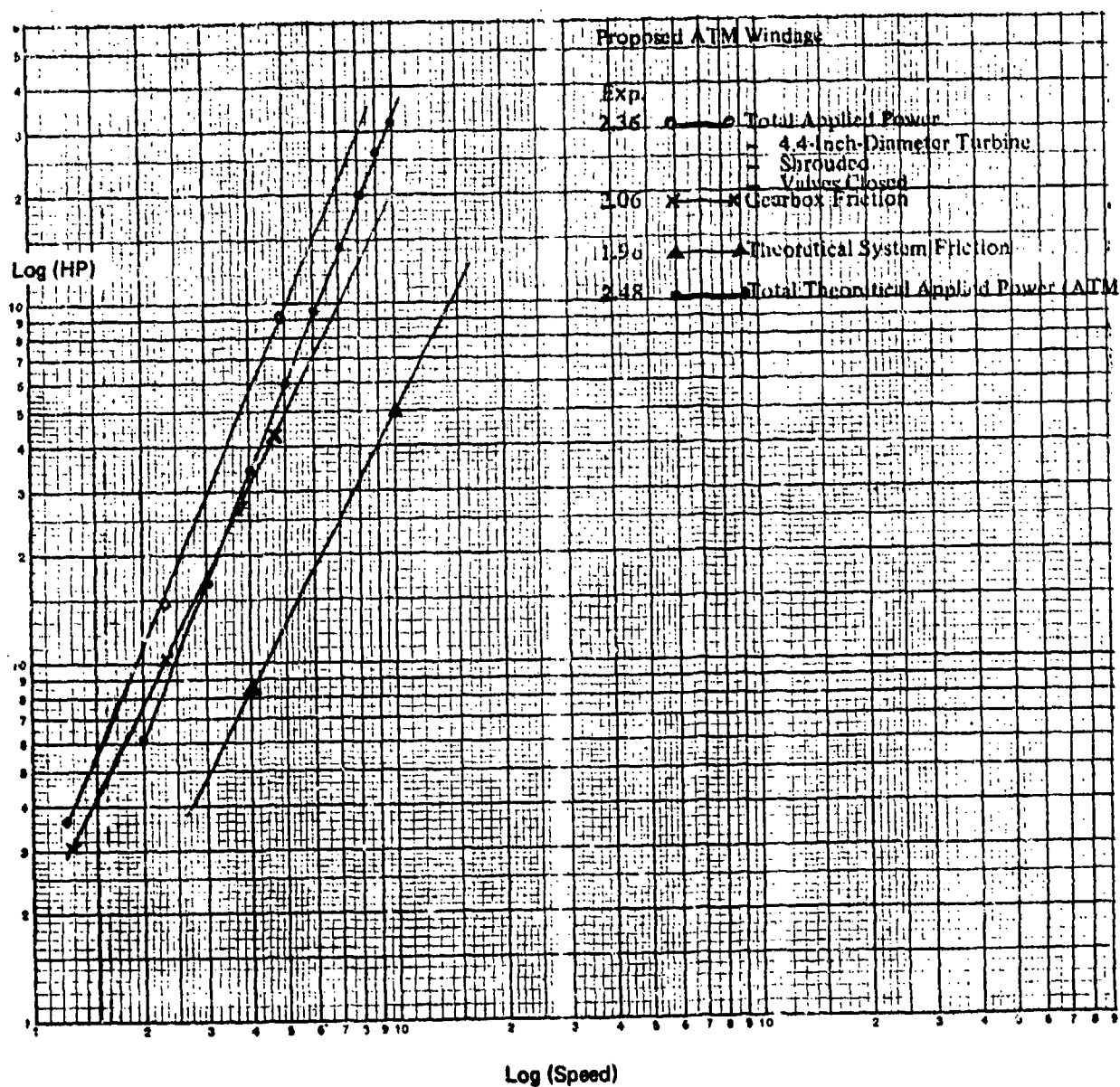


Figure 36. Predicted ATM Windage.

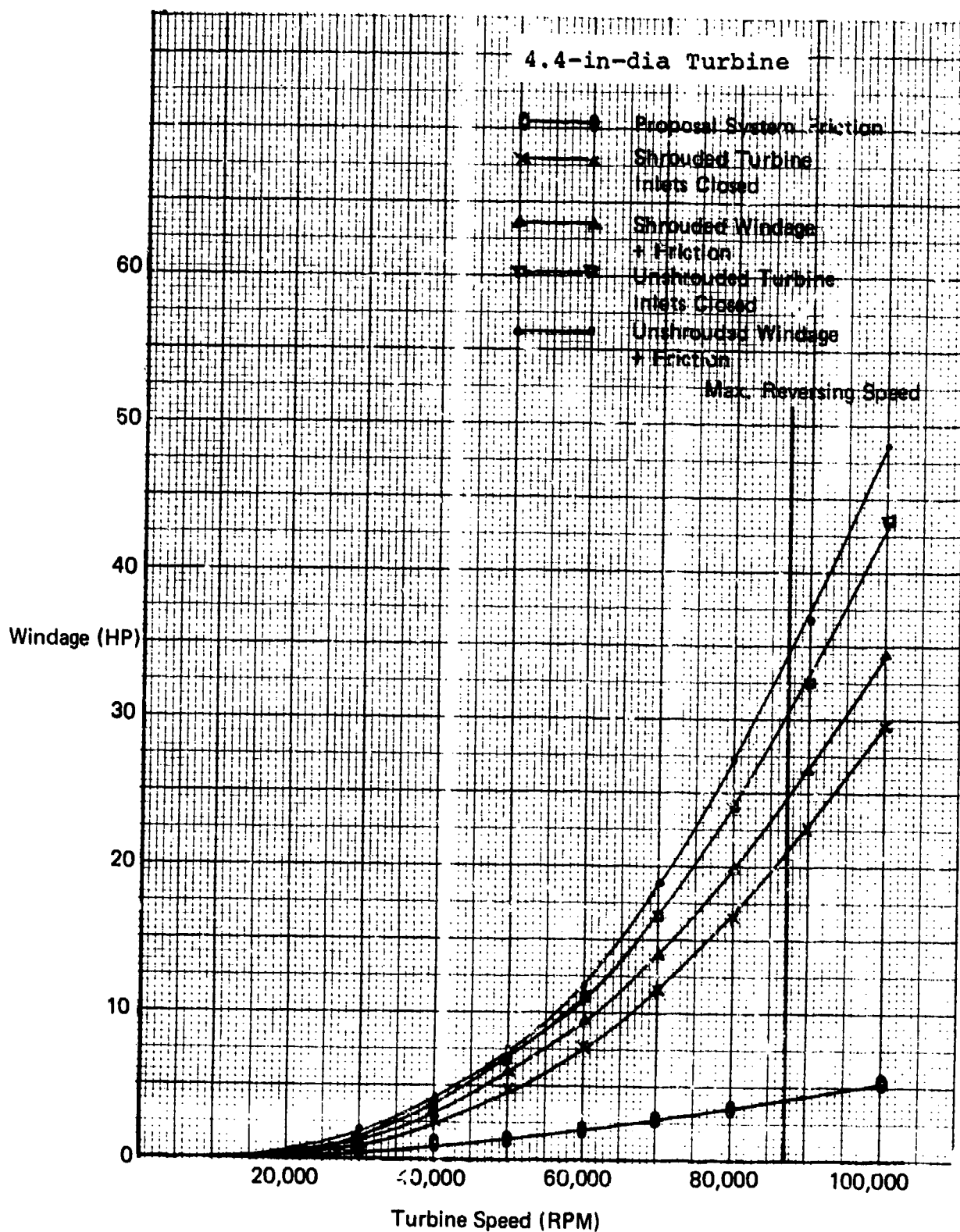


Figure 37. Net Windage and Friction Horsepower.

the net power is approximately 25 horsepower. This value corresponds favorably with the value given in Figure 38 as the improved performance of the 4.4-inch turbine.

#### Turbine Response Characteristics

The 4.4-inch turbine wheel was tested alone to determine the response time of the system. A brake was applied to the turbine shaft to prevent motion until a specified air pressure was reached. At this point, the brake was released and the turbine was allowed to accelerate with no load. The resultant speed vs time curves for different air pressure values are shown in Figure 39.

The response of the test system is slower than what is expected in the final design system. One reason for this is that the 7.0-inch turbine was cut down and machined into a 3-5/8-inch diameter disk. This piece of metal acted as a flywheel, tending to slow the response of the system.

The ATM final design will have a lower inertia and a higher efficiency than that tested. Theoretical calculations show that the proposed air turbine motor will reach design speed in 0.288 seconds.

#### Friction Horsepower Tests

For the friction horsepower tests, the starter unit was driven in reverse in the same manner used in windage testing. In this case, however, both turbines were removed and the test was run on the bare shaft. The shaft was driven in reverse at various speeds and data was taken on the speed and torque for various oil levels in the gearbox. The type of oil used was MIL-L-7808. The results of the tests are shown in Figure 40.

Figure 41 shows the exponents for the different oil levels. The friction horsepower varies as a function of the square of the speed for low levels of oil. As the oil level is increased, the gears start dipping in the oil, which brings the exponent closer to 3.0 (similar to windage).

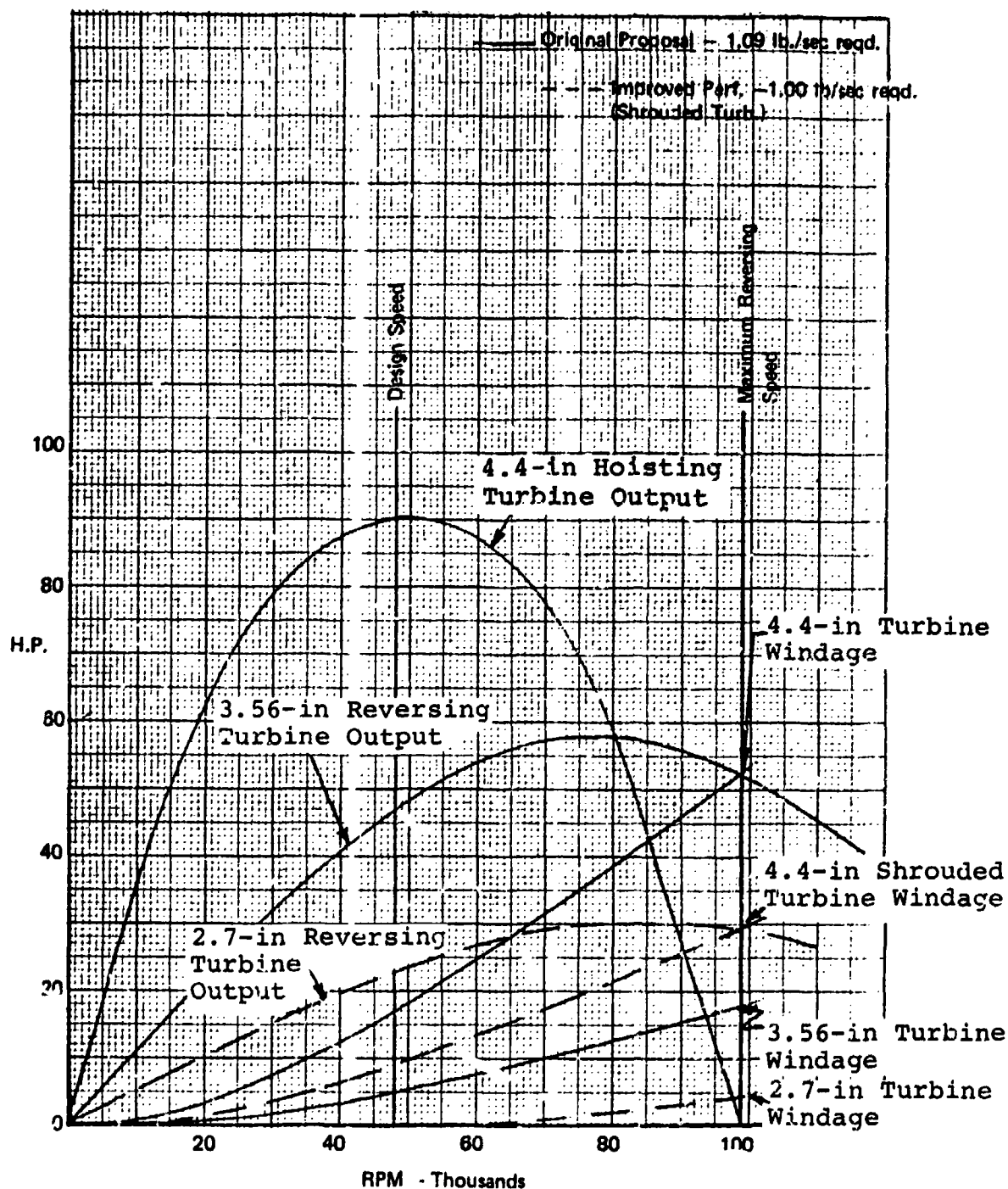


Figure 38. Improved Turbine Performance.

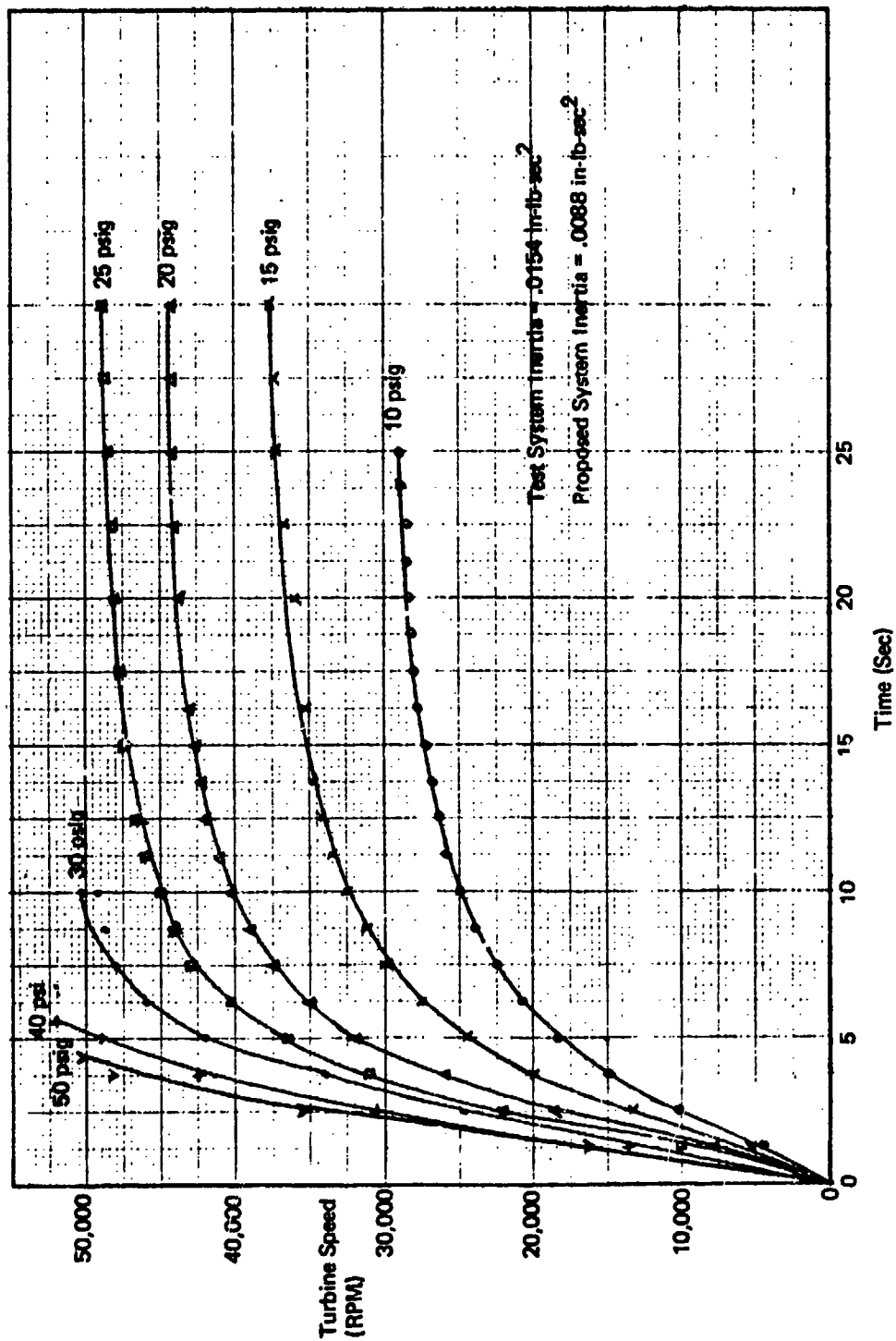


Figure 39. Response Time 4.4-in-dia Turbine.



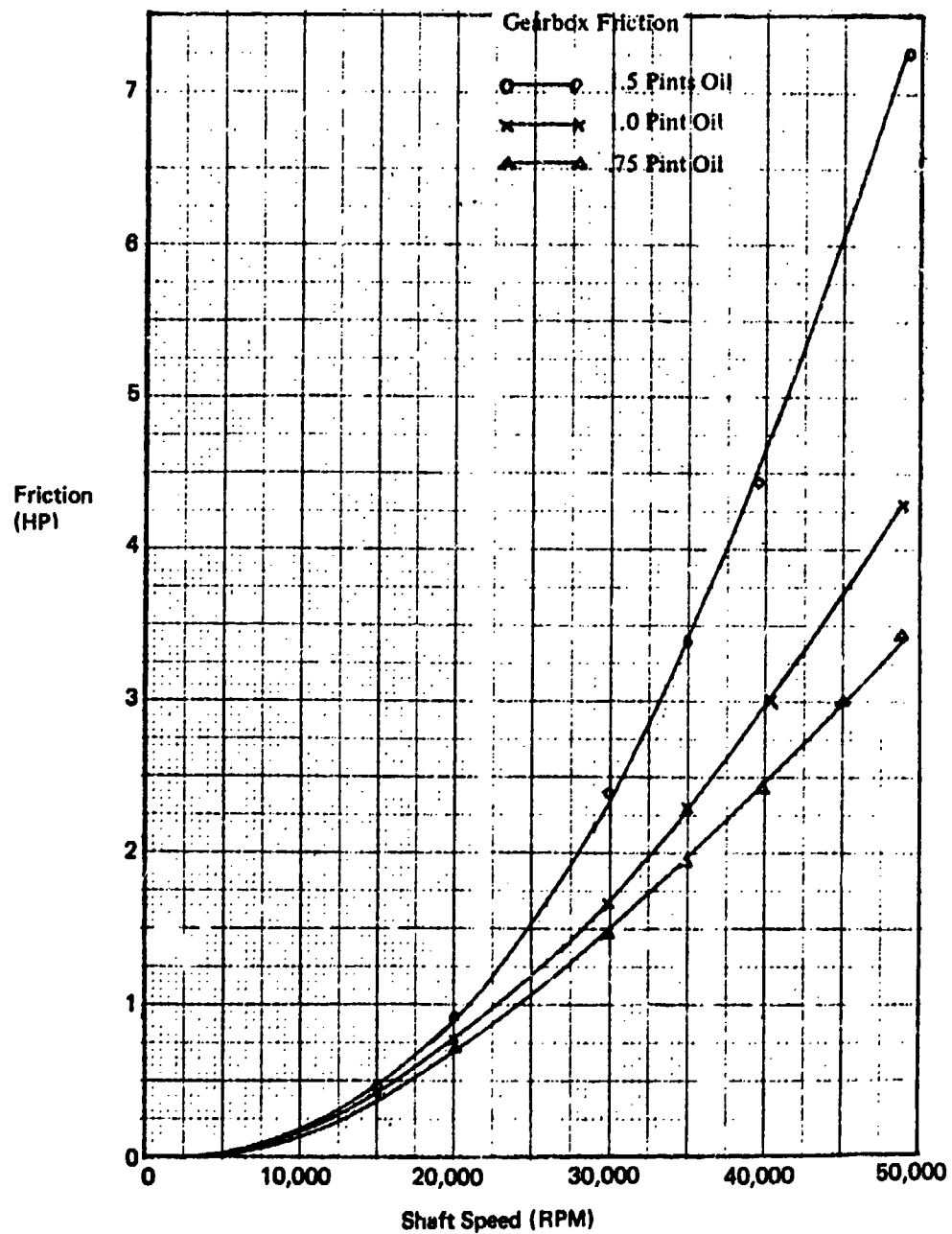


Figure 40. Gearbox Friction Horsepower.

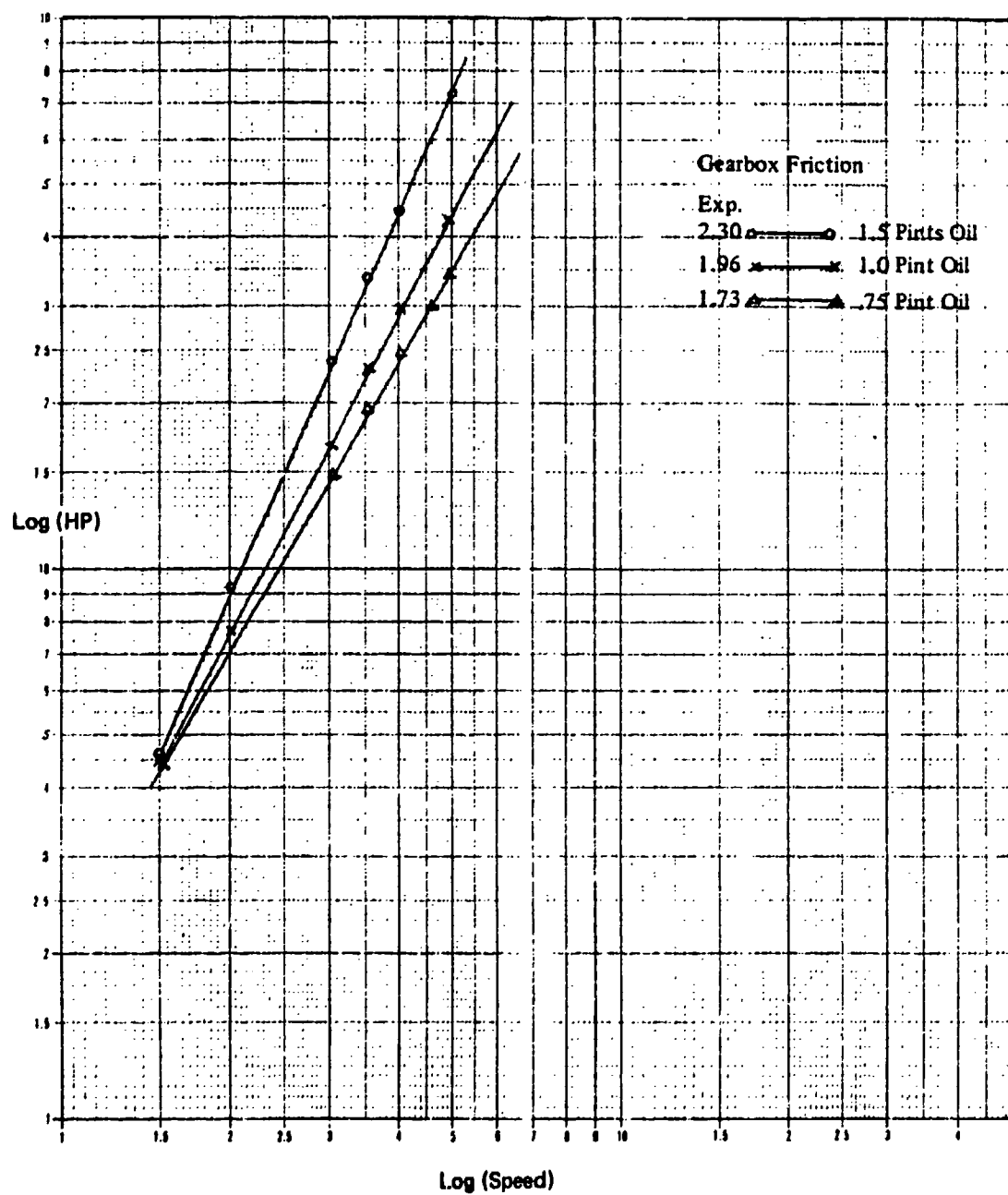


Figure 41. Gearbox Friction Log Horsepower.

### Turbine Heating Characteristics

The 4.4-inch turbine wheel with a shroud band, electron-beam welded to the blade tips, was tested to determine the operational temperatures that could be expected in the ATM final design. The turbine was driven in the reverse direction at 50,000 rpm for a period of 5 minutes. Thermocouples were attached to the hoisting and reversing air inlet ducts, the gearbox, and inside the reversing air inlet duct to sample air temperature. Tests were run with the inlet ducts open and closed. The results of the tests are plotted in Figures 42 and 43.

For a third test, temperature-sensitive paint was applied to the buckets of the turbine wheel. This paint indicated the maximum temperature of the wheel was 550°F for the 50,000 rpm, 5-minute condition.

Although the windage horsepower is greater with the valves open, the temperature does not go as high. This is true because the windage horsepower goes into a smaller volume of air with the valves closed, which results in a higher temperature.

The curves show that the gearbox is quite unresponsive to temperature changes. The gearbox temperature rises more slowly than the others, but it continues to rise after the shutdown time and it is extremely slow in cooling off.

Thermal tests were also run to simulate the thermal response of the ATM to prolonged operation in the stalled condition. A brake was applied to the turbine shaft to prevent motion. Air at up to 300°F was then applied to the inlet duct of the turbine and the gearbox temperature was measured. The applied air temperature and the resulting gearbox temperatures are shown in Figure 44 as a function of time. The test showed that there is no danger of overheating under conditions where rapid command signals prevent the brake from coming on and the load is effectively held in dynamic balance by the stalled turbine.

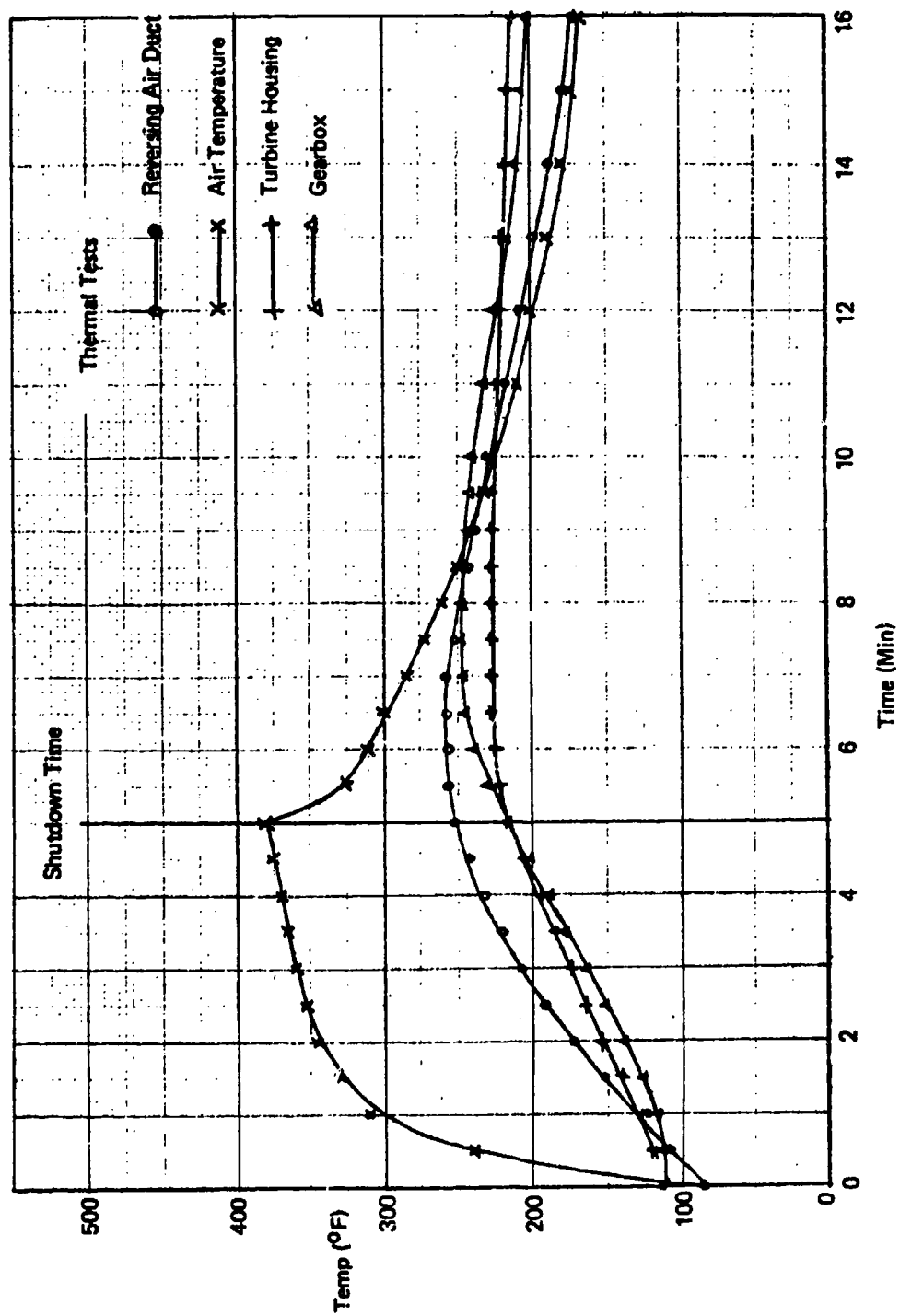


Figure 42. Thermal Tests 4.4-in-dia Turbine, Valves Open.

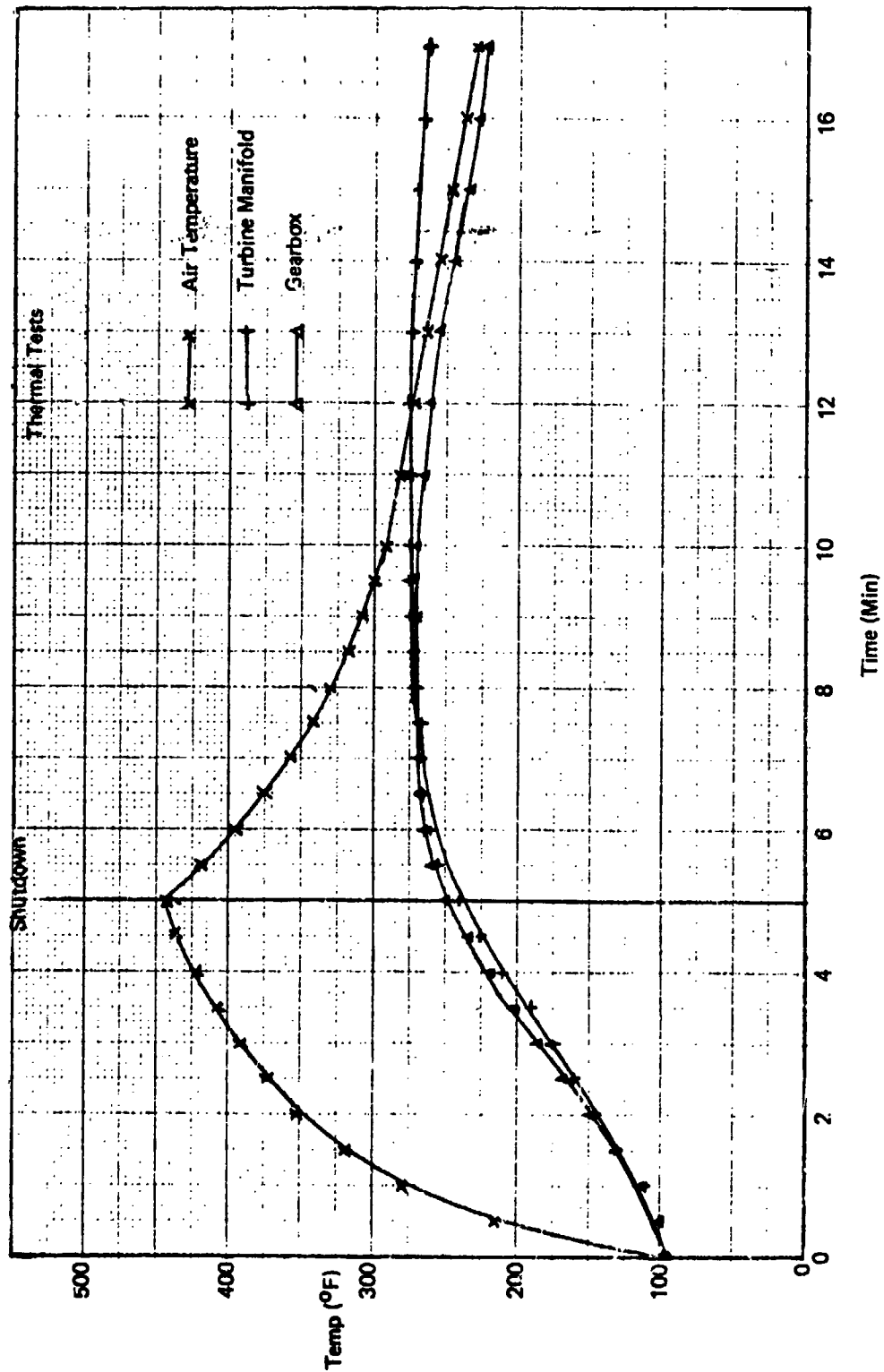


Figure 43. Thermal Tests, 4.4-in-dia Turbine, Valves Closed.

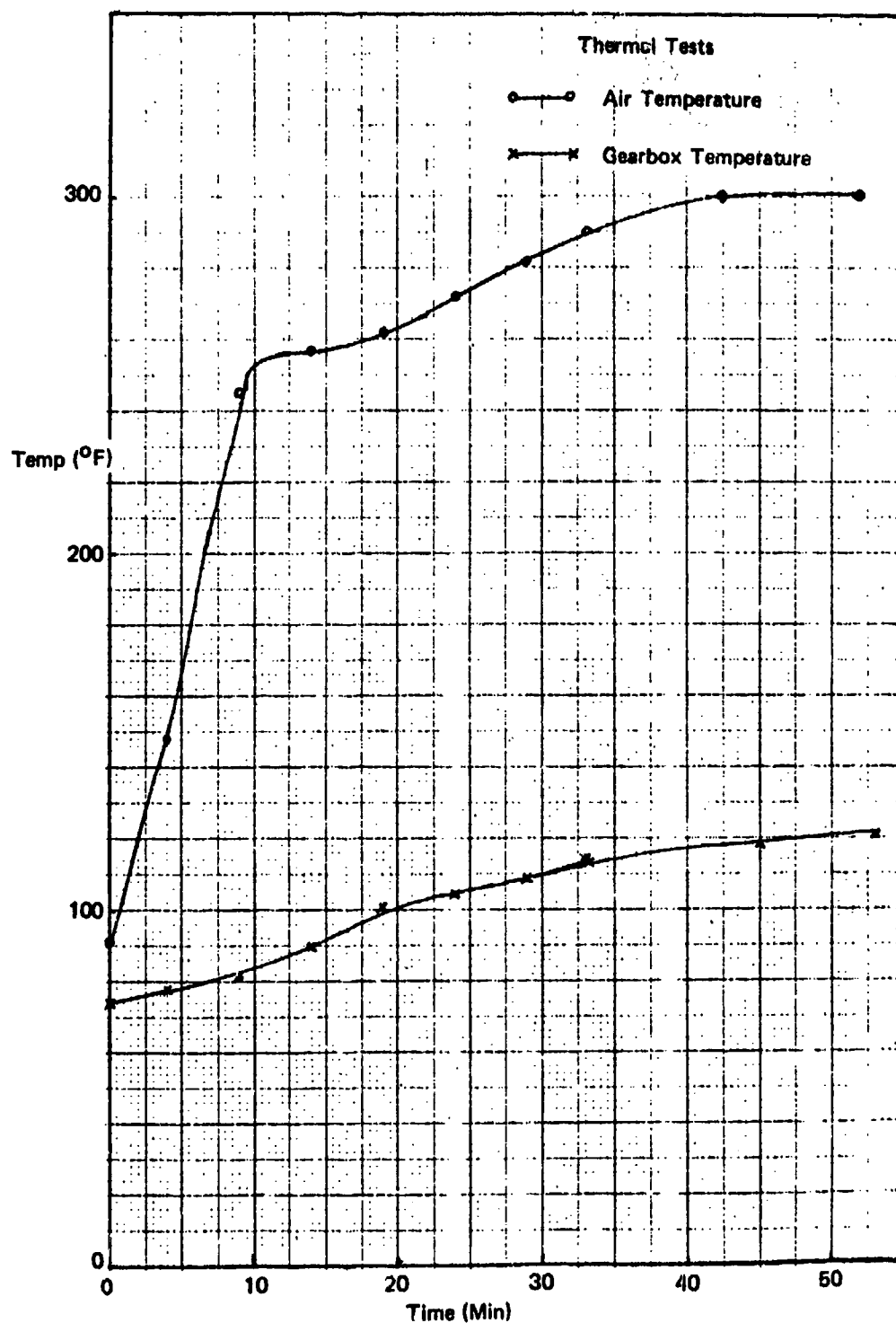


Figure 44. Stalled Turbine Thermal Tests, 4.4-in-dia Turbine.

## DESIGN DEVELOPMENT TESTS - HOIST DRIVE SYSTEM

### Performance Tests - Design Objectives

The design specification for the HLH hoist defines the "design day" conditions as 4,000-foot altitude and 95°F ambient temperature.

The design of the turbine was dictated by the stall torque requirement of 236 ft-lb at the output shaft. Additional design objectives included being able to:

1. Hoist 60% of a 28-ton load at 60 ft/min (94 ft-lb at 4,000 rpm ATM output speed)
2. Hoist an empty hook at 120 ft/min (8,000 rpm ATM output speed)
3. Pay out an empty hook at 120 ft/min (8,000 rpm ATM output speed)

It should be pointed out that the mass flow through the turbine was chosen to meet the stall torque requirements only. The pitch diameter of the hoisting turbine was limited by the design condition of being able to hoist the empty hook at 120 ft/min; therefore, when hoisting 60% of the 28-ton load at 60 ft/min, the mass flow was greater than required. To meet the 60-ft/min requirement, the turbine inlet air flow was throttled to a lower pressure ratio.

The reversing turbine design power was arrived at by estimating the hoisting turbine windage losses when running in reverse. This was based on hoisting turbine windage data obtained from tests with a 4-inch turbine wheel at 40,000 rpm and corrected for gas density speed, pitch diameter, and the ratio of blade height to pitch diameter. The estimated power need was 30 hp at 120-ft/min cable speed.

### Initial Design of Turbines

#### Description

The hoisting turbine was designed as a single-stage, full admission, predominantly impulse turbine with cascade nozzle guide vanes (NGV). Five percent reaction was incorporated in order to reduce the adverse pressure gradients in the rotor blade passages and at the endwall surfaces. This was done in order to improve turbine efficiency.

After the turbine design was completed, an analysis of thermal blade stress revealed that the blade stresses at operating temperatures were unacceptable. The gearbox was redesigned to reduce the gear ratio from 12.375 to 10.9, which decreased the blade stresses to within acceptable limits. To coincide with the gearbox change, the turbine wheel was resized to meet the 236 ft-lb stall torque requirement at sea level.

The reversing turbine was designed with the same philosophy as the hoisting turbine. Although efficiency is not of primary importance, due to the availability of excess air, the turbine was designed with 5% reaction to obtain the stipulated 79% turbine efficiency.

#### Tests Results for Initial Design

Development testing of the ATM was at the "sea level" condition using the facility shown in Figures 45, 46, and 47. In order to compare the design estimates with the actual performance of the ATM, it was necessary to establish requirements at sea level which were equivalent to those at 4000 feet altitude. A stall torque of 205 ft-lb at 4000 feet is equivalent to 236 ft-lb at sea level. In addition, the estimated windage losses of the hoisting turbine increased from 31 hp at 4000 feet to 37 hp at sea level. The runaway speeds (hoisting and reversing) are relatively unaffected by altitude.

Development testing proved the design to be inadequate for the following reasons:

1. The hoisting turbine power was below the design power due to lower than anticipated air flows.
2. The reversing turbine power was below design power.
3. The windage losses of the hoisting turbine were higher than expected.

The actual performance of the hoisting turbine, as compared with the design performance, is shown in Figure 48. The actual performance of the turbine is shown to be deficient in the area of stall torque (236-ft-lb required, 205-ft-lb actual). Measurement of the air flow of the hoisting nozzles showed that the air flow was below design levels. At the design pressure and temperature (45.3 psig at sea level, 414°F) the design air flow was 1.46 lb/sec while the actual air flow was 1.28 lb/sec (corrected for air temperature).



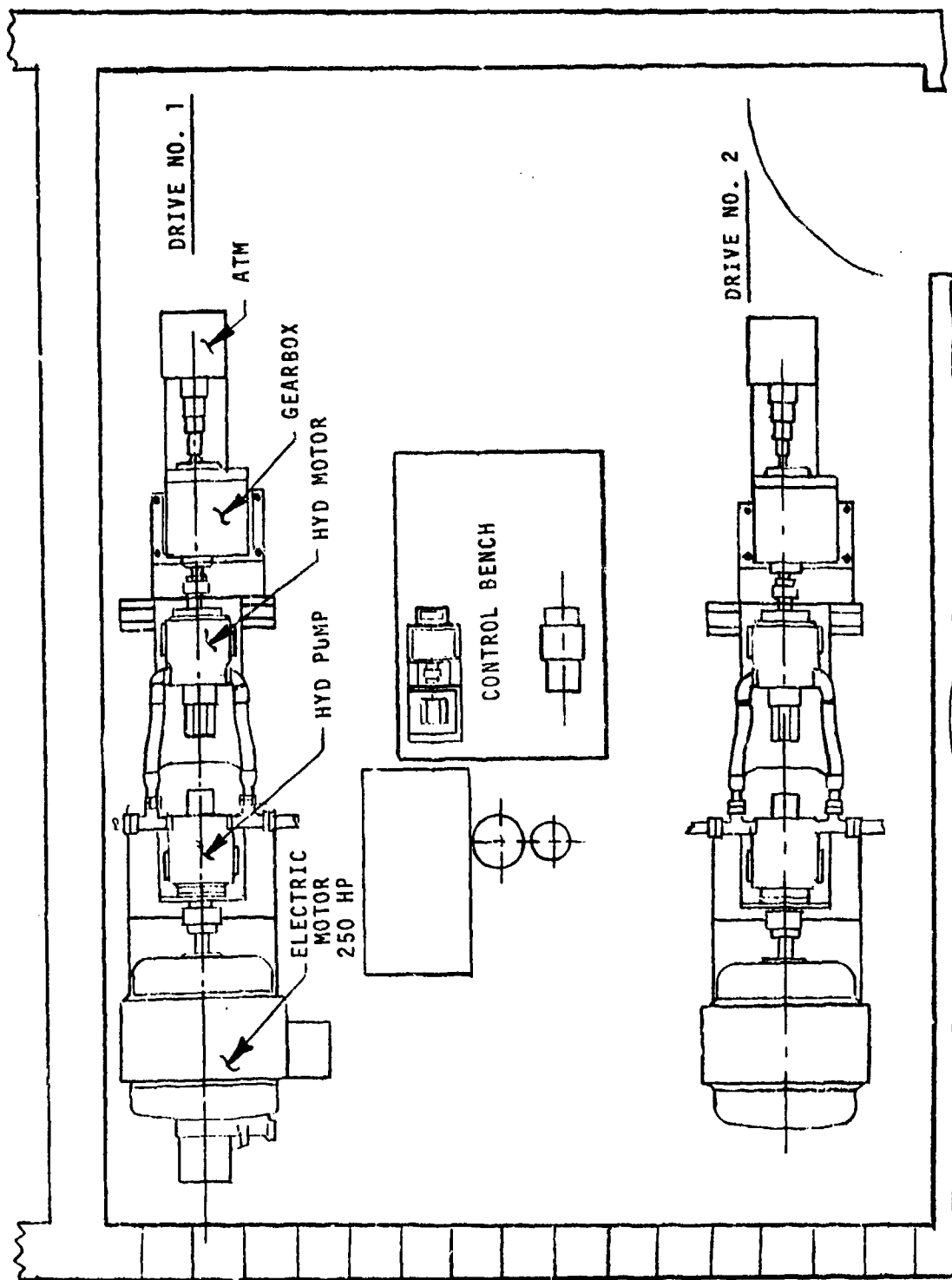


Figure 45. Test Cell Layout - Dual Hoist Drives.



Figure 46. Hoist Drive Test Rig No. 1

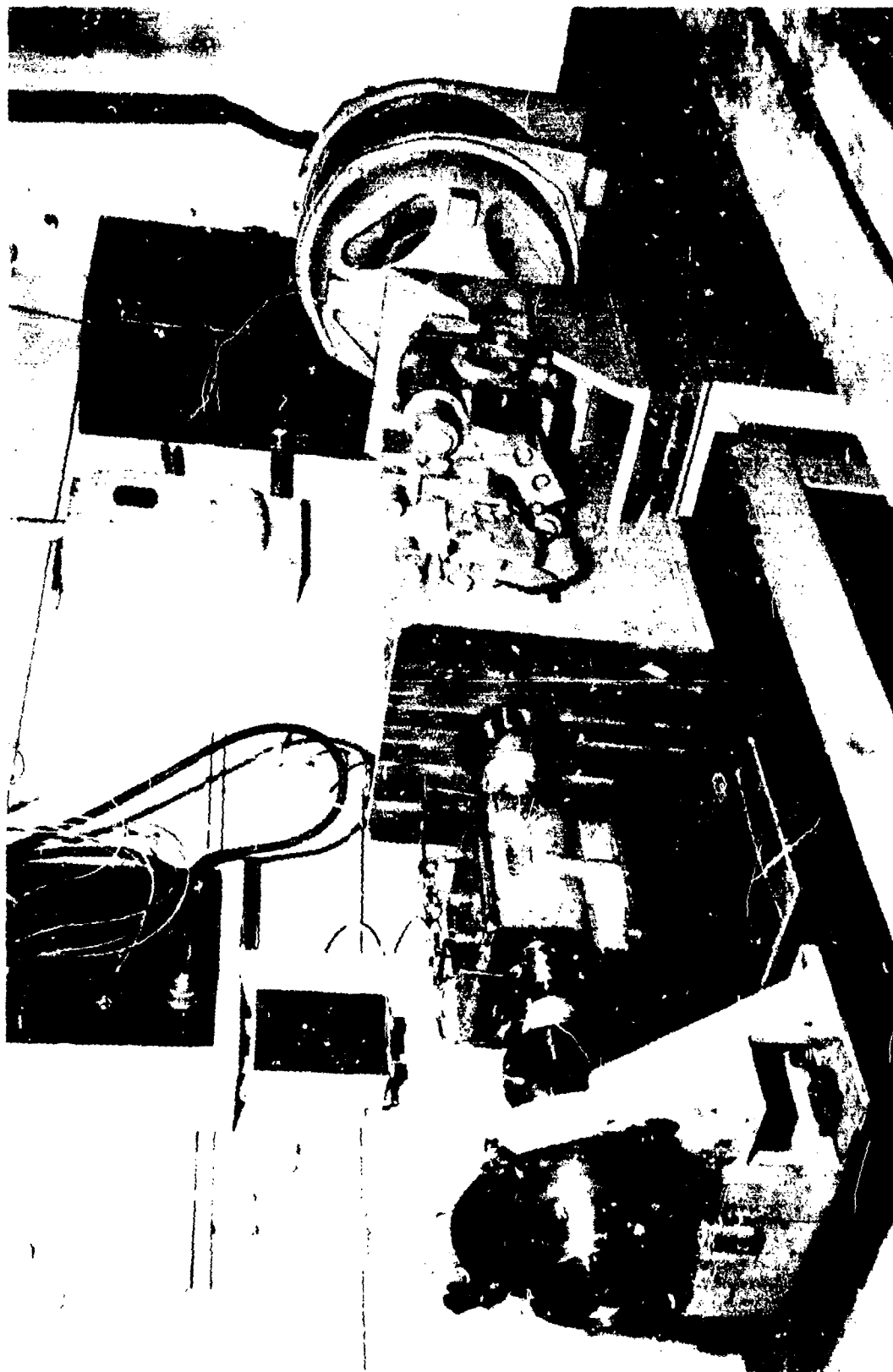


Figure 47. Hoist Drive Test Rig No. 2

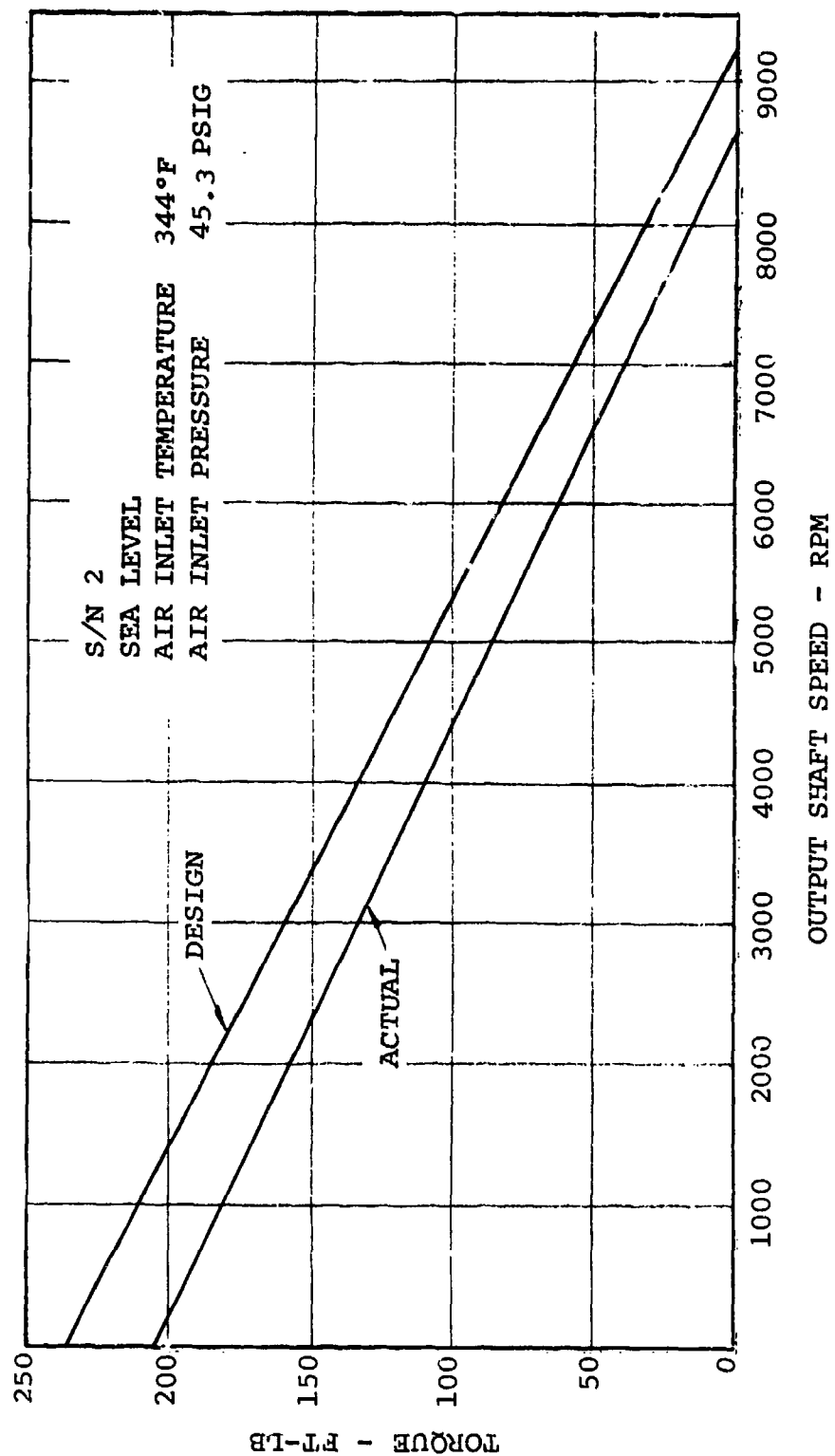


Figure 48. ATM Hoisting Turbine Performance, Torque vs. Speed.

Through calculation of the hoisting turbine efficiencies, it was concluded that the hoisting turbine was also below the design level in efficiency. The peak efficiency of the hoisting turbine was 71% as compared to the design estimate of 79%.

The reversing turbine power also proved to be below the design estimates. The maximum ATM reversing speed attained was 4,200 rpm compared with the design requirement of 8,000 rpm. Output power was below the estimated level of 37 hp. The actual windage at 8,000 rpm was found to be 69 hp instead of the predicted 37 hp.

### Redesigned Turbines

#### Performance Considerations

Hoisting Turbine - The reduced airflow of the original hoisting turbine was attributed to a nozzle flow coefficient of 0.86, as compared with 0.95 used in the design. It is believed that the relatively long, narrow nozzle-flow passages caused boundary layer buildup and reduced the flow coefficient.

A turbine wheel incorporating a small amount of reaction was used in the initial design for efficiency reasons. However, this provided a turbine torque-speed curve somewhat flatter than a pure impulse turbine characteristic, thus tending to reduce stall torque and increase maximum reel-in speed. Generally, an impulse turbine will produce superior stall torque for the same airflow. In order to achieve the stall torque objective, it was decided to provide a redesigned turbine having the following features:

1. The nozzle-flow passages would be relatively short, and fewer passages would be used.
2. The nozzle throat area would be increased to allow increased airflow.
3. An impulse turbine with symmetrical blading would be used to improve stall torque characteristics.

Reversing Turbine - The reversing turbine must provide sufficient power to drive the hoisting turbine backwards at maximum payout speed. This power requirement is composed of the windage hp of the hoisting turbine run backwards and the friction hp of the hoisting/reversing turbine assembly.

Based upon design support testing, the windage and friction value used in the initial design was 37 hp at sea level. The reversing turbine was therefore designed to produce 37 hp at maximum payout speed.

Actual output was 20 hp at approximately 5000 rpm. Analysis indicated that the airflow was low for the nozzle area provided, with only 0.43 lb/sec obtained through a 0.572-sq-in. nozzle throat area. This corresponds to a 0.75 nozzle-flow coefficient as compared to 0.95 used in the design. Overall turbine efficiency at maximum hp was 44%. The poor performance of the turbine nozzle is believed to have been a major cause of the low airflow and also the low efficiency. A flow check of the nozzle, without the turbine installed, did not yield increased flow.

An analysis of the turbine wheel indicated that an increased blade solidity would improve turbine efficiency. This could be best accomplished by widening the blade chord.

The reversing turbine was of the reaction type in order to obtain the maximum hp at a high velocity ratio ( $U/C_o$ ). Maximum hp should have occurred at 8000 rpm (output speed); however, output levelled off at 5000 rpm, indicating insufficient reaction.

It was concluded from analysis that a redesign of the reversing turbine should incorporate the following features:

1. Relatively short nozzle passages. Also, the number of passages should be reduced.
2. Increased nozzle throat area for increased airflow.
3. A turbine wheel with wider blade chord to provide greater turbine solidity.
4. Greatly increased turbine reaction to provide maximum hp at maximum payout speed.

Windage Considerations - A motoring test of the hoisting turbine, driven in the reversing direction, revealed that the windage and friction was 69 hp rather than 37 HP as used in the design. Of the 69 hp, only 8 hp was friction.

A detailed analysis of the windage problem was conducted and it was concluded that possibly the reaction blading, with the flared axial height passage, might be a contributing factor. It was also evident that blade height was a key factor. Turbine windage is a function of blade height to the 1.50 to 2.0 power. From the original design support test data, and comparison with the data obtained from the windage test, it was determined that windage has this relationship with blade height (L):

$$\text{windage hp} = L^{1.8}$$

for two turbines having the same 4.0-inch pitch diameter.

A reduced blade height hoisting turbine therefore seemed very desirable from the standpoint of windage reduction. A number of designs were studied and are discussed below.

#### Analysis of the Redesigned Turbine

Hoisting Turbine - The design objective for the hoisting turbine was twofold:

1. Increase the stall torque to a 241 ft-lb minimum at sea level, corresponding to the original design objective.
2. Reduce the reversing windage hp to permit the reversing turbine to meet the payout speed requirement.

These objectives were achieved by designing an efficient enlarged nozzle and an impulse turbine having reduced blade height. These changes made it necessary to increase the airflow to provide the stall torque while reducing the turbine blade annulus to reduce the windage hp in the reversing direction.

The initial design of the nozzle and turbine used relatively small nozzle and turbine angles: 14° for the nozzle exit, 28.4° at the turbine inlet and 24.8° at the turbine exit. This was done to maximize efficiency. However, the small angles result in greater turbine blade height with correspondingly greater windage. In general, greater torque per unit airflow is obtained with smaller angles due to the increased velocity-turning in the wheel. Due to the great importance of turbine windage, it was decided to increase the angles, permitting larger airflow with reduced blade height.

A number of designs covering nozzle angles from 16° to 24° were analyzed. Generally, the higher angles provide less torque, lower efficiency, and reduced reel-in speed. Assuming a velocity coefficient of 0.95 in the nozzle and 0.90 across the wheel with 1.50-lb/sec flow, the following stall torque estimates were obtained for three nozzle angles, with turbine angles matched for 0° incidence at the rated speed.

<u>*Nozzle Angle</u>	<u>Turbine Angle</u>	<u>Stall Torque</u>
14°	25°	251.
18°	31°	245.
22°	36.9°	234.

\*Above includes 5% allowance for leakage and miscellaneous losses.

At the rated speed of 4,000 rpm, the comparison of torque and efficiency is as follows:

<u>Nozzle Angle</u>	<u>Torque</u>	<u>Efficiency*</u>
14°	144	.735
18°	138.	.705
22°	130.	.665

\*Includes 5% allowance for leakage and other losses.

The higher nozzle and turbine angles will tend to reduce the maximum reel-in speed. A speed margin currently exists, however, at that condition. The 18° nozzle was selected since it provides an optimum trade-off between stall torque, hoisting torque, payout speed and reel-in speed.

The windage losses in a turbine operated in reverse were analyzed and checked by a consulting firm, which searched all available information relative to reverse operating turbines. Two methods were used in arriving at the windage hp values. Both methods estimated the value to be approximately 50 hp at 7500 rpm. Blade length to the 1.8 power was used in calculating windage. This was checked by the consultant using other references.

Turbine blade stresses were calculated at 80,000 psi in tension at the blade root. Using 186,000-psi yield for René 95, a 53% speed margin existed at the yield point. Using 230,000-psi ultimate, a 70% overspeed margin existed to burst.



Reversing Turbine - Based on the hoisting turbine's estimated reverse windage, the reversing turbine must produce 50-55 hp to provide maximum payout speed.

Whereas the hoisting turbine operates at its rated load at 0.414 velocity ratio, the reversing turbine must operate at 0.460 velocity ratio. This is past the efficiency peak for such a small turbine, and a relatively high reaction must be built in.

The design selected had a number of features intended to provide maximum hp at high payout speed. First, the nozzle was designed to converge to the throat with no diverging section. Throat pressure was 32.0 psia. The nozzle was enlarged as much as possible in the space available and passed a maximum flow. Expansion takes place to 20 psia between the throat and the turbine blade inlet, providing a reaction of 5 psi across the turbine. Turbine annulus area was increased from the previous design, as well, to provide maximum flow. A nozzle angle of  $18^\circ$  was selected to retain sufficient air turning at high speeds, thus retaining high speed torque. The nozzle area was changed to 0.84 sq in. Compared to the previous 0.57 sq in.; however, the flow rate was doubled from 0.43 lb/sec to 0.82 lb/sec. Efficiency was expected to increase from 44% to 60%. Provisions were incorporated to rework the throat flow area from 0.84 sq in. to 0.93 sq in. if necessary.

In order to improve the solidity, especially toward the rotor OD, the blade chord was increased from .250 in. to .320 in. The number of blades was reduced from 47 to 43 to provide sufficient spacing between the blades at the root for manufacturing and tooling reasons. The two revisions provided optimum turbine solidity.

#### Test Results of Redesigned Hoisting and Reversing Turbines

The redesigned hoisting and reversing turbines were tested in air turbine motor serial number 3. The actual performance is shown in Figure 49.

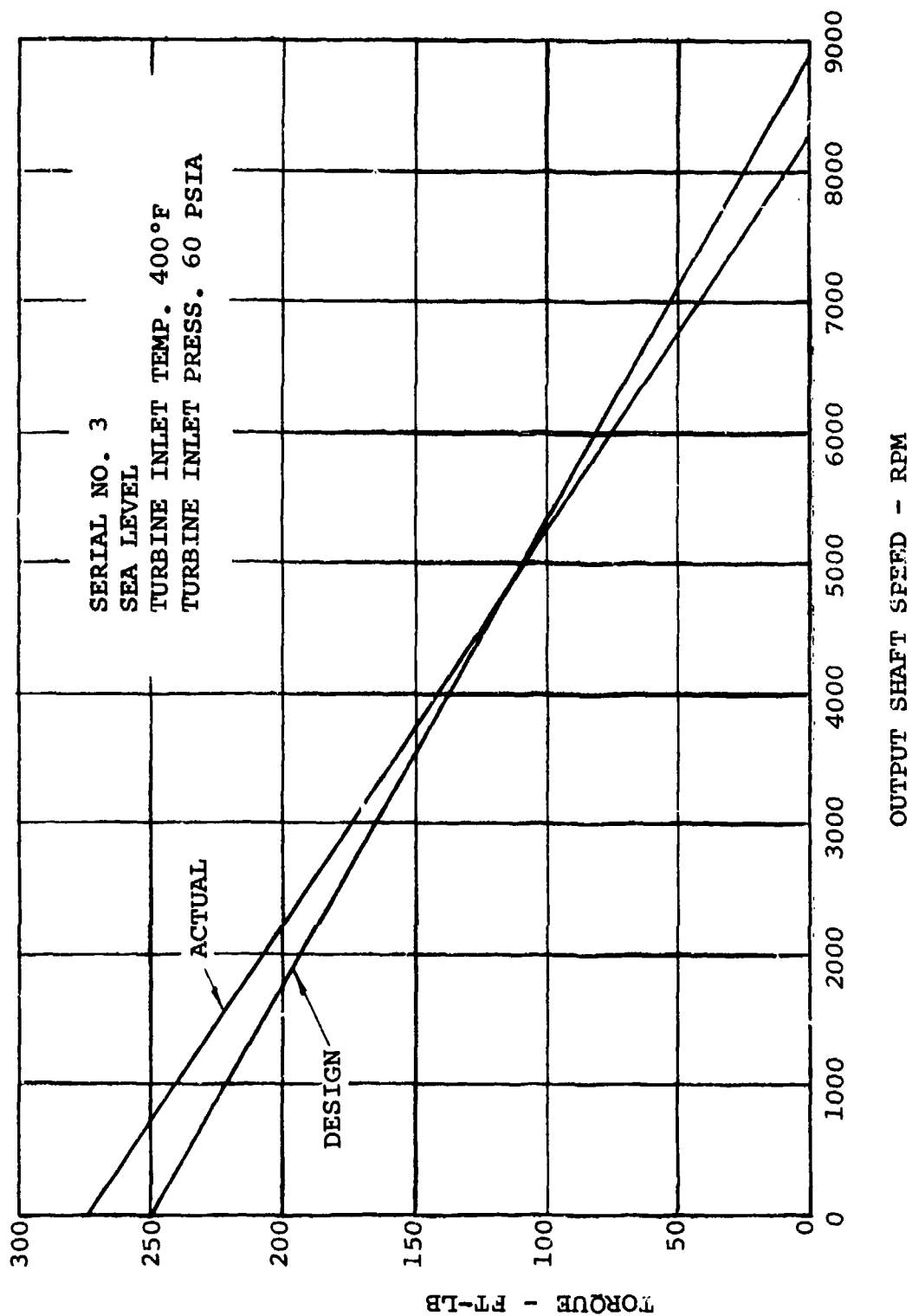


Figure 49. Redesigned ATM Turbine Performance, Torque vs Speed.

The hoisting turbine developed 275 ft-lb of stall torque at sea level conditions. Maximum reel-in speed was 8,250 rpm at no-load. At 4000 rpm, the torque level was 141 ft-lb, corresponding to 107 hp. At this condition, the hoist drive overall efficiency, including ATM, gearbox, and brake, was 71%.

Airflow tests were performed on serial number 3 ATM. The choked condition coefficient (Mach number of air in turbine nozzle thrust equal to one) was 0.766, which resulted in an effective nozzle area of 1.439 sq in. and a 0.95 nozzle coefficient.

A payout speed test was run with the redesigned turbines. The maximum payout speed was 5600 rpm, which is 40% higher than achieved with the original design.

A motoring run, driving the hoisting turbine backwards, revealed that the windage horsepower of the redesigned turbine was nearly double what was anticipated. The explanation for the increase in windage loss in the redesigned turbine is a result of an increase in nozzle area from 1.360 sq in. to 1.51 sq in. Also, the improved nozzle acts as a more efficient diffuser, which results in an increase in the scroll pressure. The wheel, rotating in the reverse direction, pumps air from the root of the blade to the tip by centrifugal force, which results in a pressure increase, forcing the air into the supply scroll. As the pressure in the supply scroll increases, the air returns through the nozzle which creates dynamic braking on the turbine wheel. Two horsepower losses actually occur at the wheel, first, due to the pumping of the air and, second, due to the dynamic braking effect of the air reentering the turbine blade.

### Static Brake Test

#### Objective

The purpose of this initial test was to establish and verify the static holding capacity of the multiple disc plates and to determine whether the spring force selected provided the proper holding torque (under 2.5g's at maximum loading).

#### Test Procedure

The static brake was loaded according to Table 5.

The loading was applied to simulate a maximum payload acting on the hoist drive at 2.5 g's. The brake was checked for slippage at each test condition.

TABLE 5. STATIC BRAKE LOADING SCHEDULE		
Load (ft-lb)	RPM	Time (min)
230	0	2.0
236*	0	2.0
240	0	2.0
245	0	2.0
250	0	2.0
255	0	2.0
260**	0	2.0
*236 ft-lb corresponds to maximum payload with 2.5g acceleration.  **Static proof load.		

Slippage or intermittent shaft rotation was defined as a total rotation greater than 0.20 rev at the output shaft in any one minute time period. After completing the test, the brake housing was removed and an inspection was performed of the braking components. The Table 5 loading program was then repeated a total of ten times. A post-test inspection was performed at the conclusion of all the runs.

### Results

No malfunctions occurred. The system remained at 0 rpm for the entire range of loads applied.

## Initial Brake Interface with the ATM and Control System

### Objective

The purpose of this test was to demonstrate the ability of the brake control system and mechanical actuators to react to a command signal from the hoist control when interfaced with the ATM and the control system.

### Test Procedure (Dynamic Braking)

The air supplied to the braking system during this test was at a temperature of 414°F and a pressure of 60 psia. The operating tolerances were  $\pm 5\%$  of the full scale. The system was then run through a set of procedures according to the commands listed in Table 6. Upon completion of that test, the overspeed control circuitry was tested. In this test, the tachometer in the control unit was fed signals from a signal generator to simulate the signal of a turbine running 220-230% of its design speed. In the mean time, the turbine was running at 20% of its designed maximum speed with a 5- to 10-ft-lb load.

Next, simulate tracking overspeed control circuitry under 5-10 ft-lb load and at 10% of maximum hoisting speed. This system provides brake actuation in the event the control system malfunctions and the actual speed exceeds the command speed. Introduce a 35-40% generator signal to the tachometer and check that the brake goes on and operates satisfactorily. Repeat under two other speed conditions: 15 and 20% actual hoisting speed.

Without actuating brake, load assembly to a proof load of 260 ft-lb to demonstrate gearing integrity.

TABLE 6. COMMAND SPEEDS			
Command Speed Signal*	Direction	Load (ft-lb)	Time At Stabilized Speed (Min.)
5%	Hoisting	0-5	2.0
Stop		0-5	0.5
5%	Reversing	0-5	2.0
Stop		0-5	0.5
10%	Hoisting	0-5	2.0
Stop		0-5	0.5
10%	Reversing	0-5	2.0
Stop		0-5	0.5
20%	Hoisting	15-20	2.0
Stop		15-20	0.5
20%	Reversing	15-20	2.0
Stop		15-20	0.5
30%	Hoisting	15-20	2.0
Stop		15-20	0.5
30%	Reversing	15-20	2.0
Stop		15-20	0.5
40%	Hoisting	25-30	2.0
Stop		25-30	0.5
40%	Reversing	25-30	2.0
Stop		25-30	0.5
50%	Hoisting	25-30	2.0
Stop		25-30	0.5
50%	Reversing	25-30	2.0
Stop		25-30	0.5
*Percent of maximum hoisting speed			

## Results

During the test the brake performed as designed. No malfunctions occurred and all test phases were performed within specification limits. After the overspeed tests, the brake assembly was inspected and no wear was noticed/discovered.

## Turbine System Testing

### Objective

The purpose of this test was to see if the ATM's performance conformed to the design standards in the areas of performance and control response.

### Test Procedure

The air supplied to the turbine was 414°F at 60 psia. Operating tolerances were  $\pm 5\%$  of full scale. Speeds of 10% of design maximum were commanded according to Table 7.

TABLE 7. COMMAND SPEEDS.		
Command Signal	Direction	Time At Stabilized Speed (min)
Desired Speed	Hoisting	2.0
Desired Speed	Reversing	2.0
Stop		2.0

The hoist loading was 94 ft-lb (1.0g design load condition). Loading was applied to simulate a downward force. Next, the Table sequence was repeated at speeds 10% higher than the first time.

Speeds of 100% of design maximum were then commanded in accordance with the Table 8 conditions.

TABLE 8. COMMAND SPEEDS.		
Command Signal	Direction	Time At Stabilized Speed (min)
Desired Speed	Hoisting	2.0
Desired Speed	Reversing	0.3
Desired Speed	Hoisting	0.3
Desired Speed	Reversing	2.0
Stop		1.0

The hoist load was 94 ft-lb (1.0g design load). Loading was applied to simulate a downward force or weight.

Speeds of 10% of design maximum were next commanded in accordance with Table 8 and that series of commands was repeated five times.

Next, a speed of 110% of design maximum was commanded in accordance with Table 9.

TABLE 9. COMMAND SPEEDS.		
Command Signal	Direction	Time At Stabilized Speed (min)
Desired Speed	Hoisting	2.0
Desired Speed	Reversing	2.0
Stop		2.0

The loading was 0-5 ft-lb. The loading, where applied, simulated a downward force. Sequence of Table 9 was repeated, increasing the command signal from 100% of design maximum to 200% in 10% increments.

### Results

No damage was suffered by the system and its operation was not impaired. Speeds recorded were within specification limits and the system reacted to the command signals as specified. Test results are shown in Table 10.



TABLE 10. TURBINE SYSTEM TEST RESULTS

Command Speed % Hoist/ Reverse	Data Point	Output Shaft Torque	Output Shaft Speed	Turbine Inlet Press.	Reverse Scroll Press.	Command Signal	Lube Oil Press.	Lube Oil Temp.
CS	DP	T1 ft-lb	N1 RPM	PTI-1 PSIG	PTI-2 PSIG	CS-1 VDC	PIO-1 PSIG	TIO-1 °F
10H	1	94	.4	15	1	+ .2	3	116
10R	2	94	.4	10.5	1	- .3	3	116
20H	3	92	.8	15.5	1	+ .45	6	134
20R	4	92	.8	9.5	1	- .5	6	148
30H	5	93	1.2	17.5	1	+ .75	8	172
30R	6	94	1.2	10	.5	- .8	8	191
40H	7	94	1.6	19.5	.5	+1.0	12	197
40R	8	94	1.6	9	.5	-1.0	12	196
50H	9	94	2.0	22.5	.5	+1.2		209
50R	10	94	2.0	7.5	.2	-1.3	18	219
60H	11	94	2.4	23	.5	+1.5	22	228
60R	12	88	2.4	6	.2	-1.5	22	237
70H	13	94	2.8	25	1	+1.75	28	247
70R	14	94	2.8	7	0	-1.8	31	209
80H	15	94	3.2	27	1	+2	36	237
80R	16	94	3.2	7	0	-2	36	250
90H	17	94	3.6	29	1	+2.2	42	266
90R	18	94	3.6	7	.1	-2.3	42	280
100H	19	94	4.0	33	1.5	+2.5	50	294
100R	20	94	4.0	7	.1	-2.5	50	303
100H	21	94	4.0	32	2	+2.5	55	237
100R	22	94	4.0	5	.2	-2.5	55	247
100H	23	94	4.1	33	2.0	+2.5	55	255
100R	24	94	4.0	6	.2	-2.5	55	266
100H	25	94	4.0	33	2.0	+2.5	55	266
100R	26	90	3.9	5	0	-2.5	54	275
100H	27	94	4.0	32	2.0	+2.5	51	280
100R	28	94	4.0	6	0	-2.5	51	275
100H	29	94	4.0	32	2.0	+2.5	57	228
100R	30	94	4.1	6	0	-2.5	60	247
100H	31	94	4.0	32	2.0	+2.5	51	247
100R	32	94	4.0	6	0	-2.5	54	266
100H	33	94	4.0	32	2	+2.5	51	272
100R	34	94	4.1	6	0	-2.5	54	280
100H	35	94	4.0	31	1.5	+2.5	49	280
100R	36	94	4.0	6	0	-2.5	51	284
100H	37	94	4.0	32	2	+2.5	54	228
100R	38	94	4.0	6	0	-2.5	58	247
100H	39	94	4.0	32	1.5	+2.5	51	256
100R	40	94	4.0	6	0	-2.5	55	266
110H	41	2.0	4.4	8	1.2	+2.7	75	180
110R	42	2.0	4.4	3	36	-2.8	75	209
120H	43	4.0	4.8	10	1.5	+3	70	250
120R	44	2.0	4.8	4	41	-3.1	75	280
130H	1	4.0	5.2	13	1.5	+3.2	90	191
130R	2	2.0	5.2	5	42	-3.3	88	245
140H	3	4.0	5.6	14	1.5	+3.5	81	294
140R	4	4.0	5.7	5	46	-3.9	88	310
150H	5	1.0	6.0	15	2	+3.7	86	250
160H	6	0	6.4	18	2	+4.0	78	320
170H	7	4.0	6.8	24	3	+4.2	84	250
170R	8	4.0	6.8	34	3	+5.2	84	255

## Turbine Performance Evaluation Test

### Objective

The purpose of this test is to establish the performance of the air turbine motors, both hoisting and reversing, for the complete range of possible working conditions at local standard barometric pressures.

### Test Procedure

The ATM was subjected to the maximum load possible while still maintaining the desired speed with the air inlet conditions listed in Table 11. The ATM was then subjected to the same procedure in the reverse direction. Then the procedure was repeated for the hoisting and reversing directions with the air inlet pressure reducing in increments of 10 psi until the brake piston failed to fully retract.

TABLE 11. TURBINE PERFORMANCE TEST - REQUIREMENTS.

Air Pressure (psia)	Air Temperature (°F)	Output Shaft Speed (rpm)	Direction
60.0	414	8,000	Hoisting
50.0	414	7,000	Hoisting
60.0	414	6,000	Hoisting
60.0	414	5,000	Hoisting
60.0	414	4,000*	Hoisting
60.0	414	3,000	Hoisting
60.0	414	2,000	Hoisting
60.0	414	1,000	Hoisting
60.0	414	0	--

\*Equivalent to 60 fpm hoisting velocity.

The ATM was then subjected to the maximum load attainable while maintaining the desired speed with the air inlet conditions of Table 12, for both the hoisting and reversing directions. The procedure was then repeated using an inlet air temperature of 350°.

TABLE 12. TURBINE PERFORMANCE TEST - REQUIREMENTS.			
Air Pressure (psia)	Air Temperature (°F)	Output Shaft Speed (rpm)	Direction
60.0	375	8,000	Hoisting
60.0	375	4,000	Hoisting
60.0	375	2,000	Hoisting
60.0	375	0	-
50.0	375	8,000	Hoisting
50.0	375	4,000	Hoisting
50.0	375	2,000	Hoisting
50.0	375	0	-
40.0	375	8,000	Hoisting
40.0	375	4,000	Hoisting
40.0	375	2,000	Hoisting
40.0	375	0	-

#### Test Results

The results of the turbine performance test are plotted in Figures 50 through 53. The operation was not impaired during the test and no damage was suffered by the unit. The design objectives for the turbine performance were satisfactorily met with the exception of the maximum reverse payout speed which was limited due to the windage effects of the hoisting turbine.

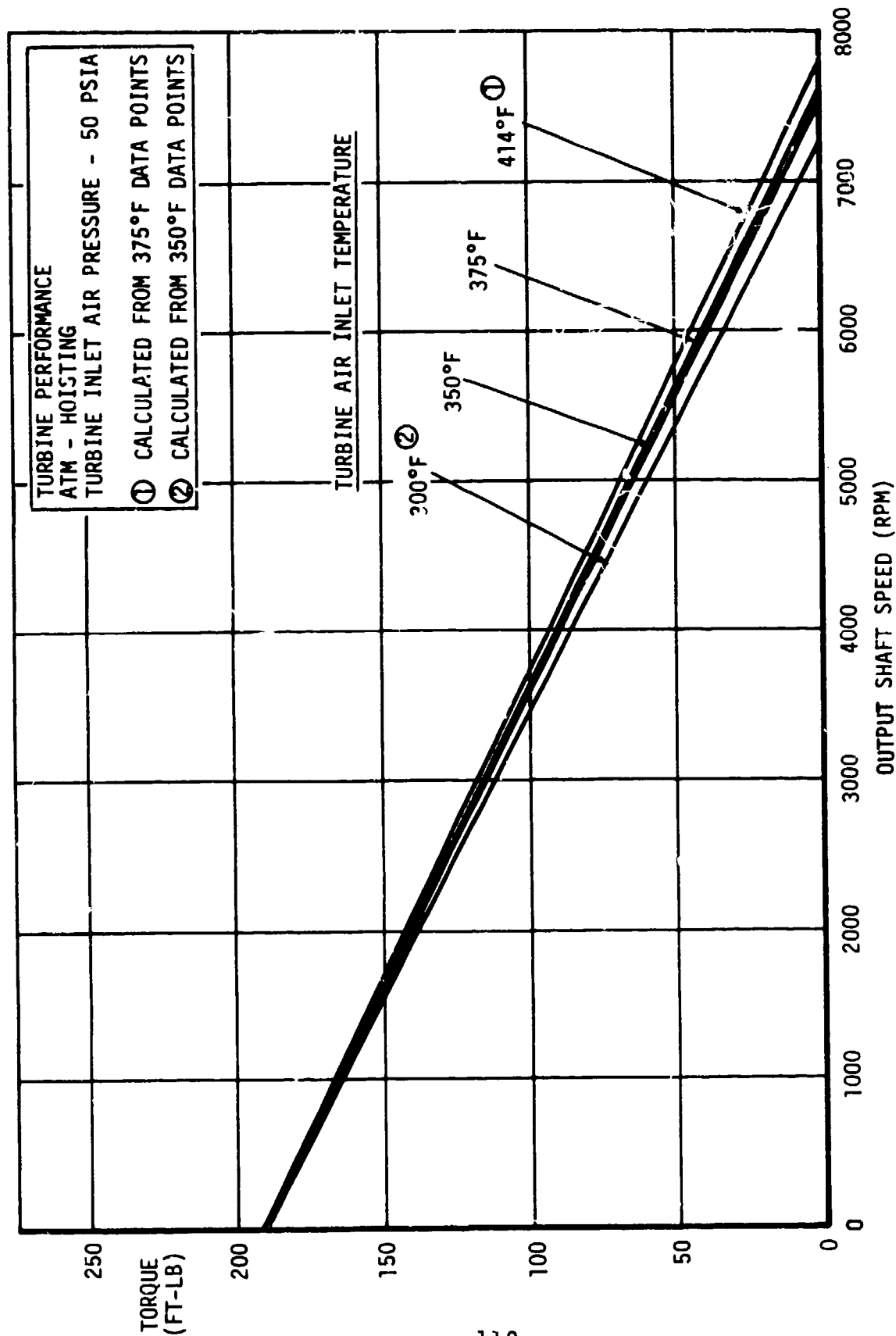


Figure 50. Turbine Performance, Hoisting, 50 PSIA.

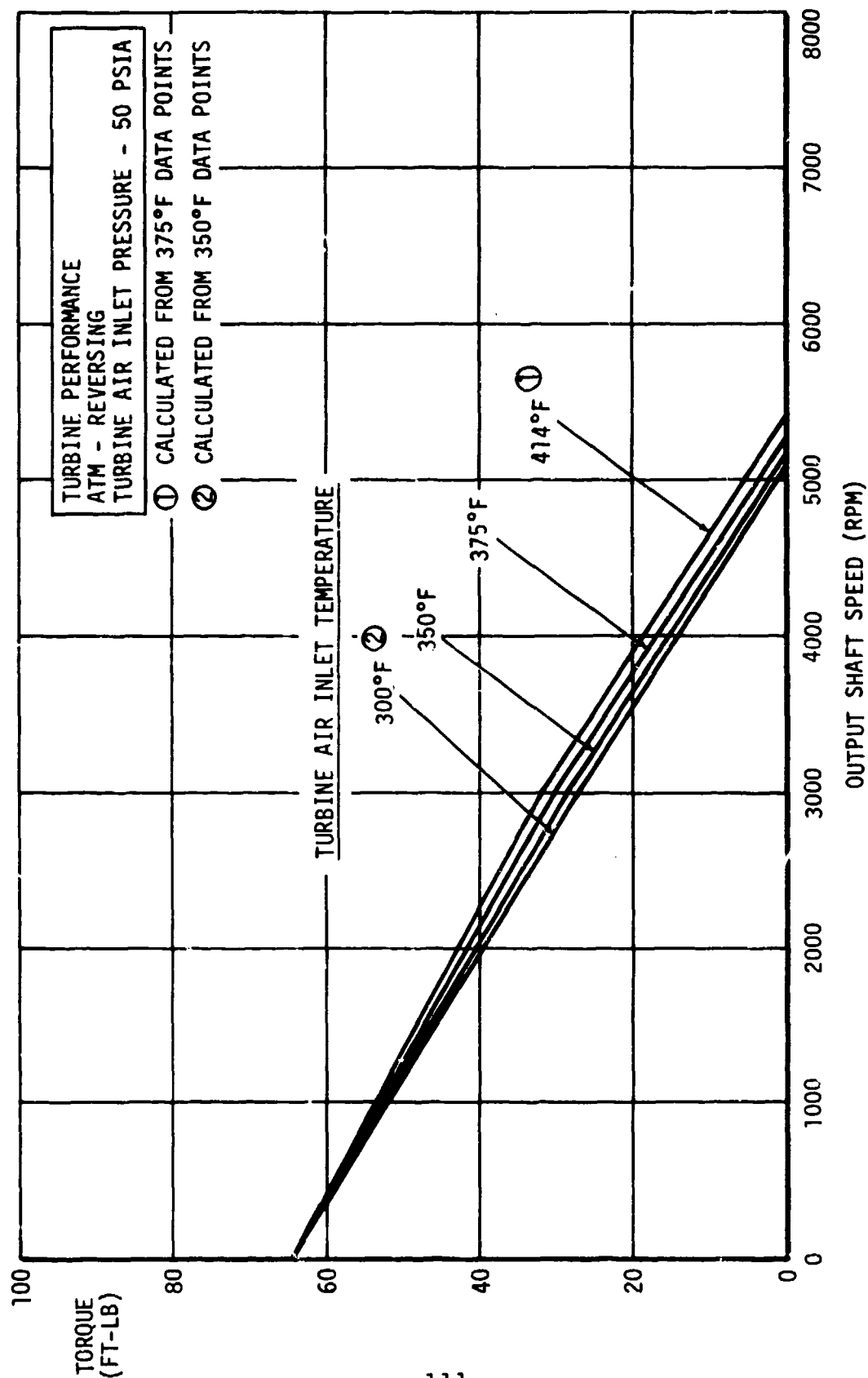


Figure 51. Turbine Performance, Reversing, 50 PSIA.

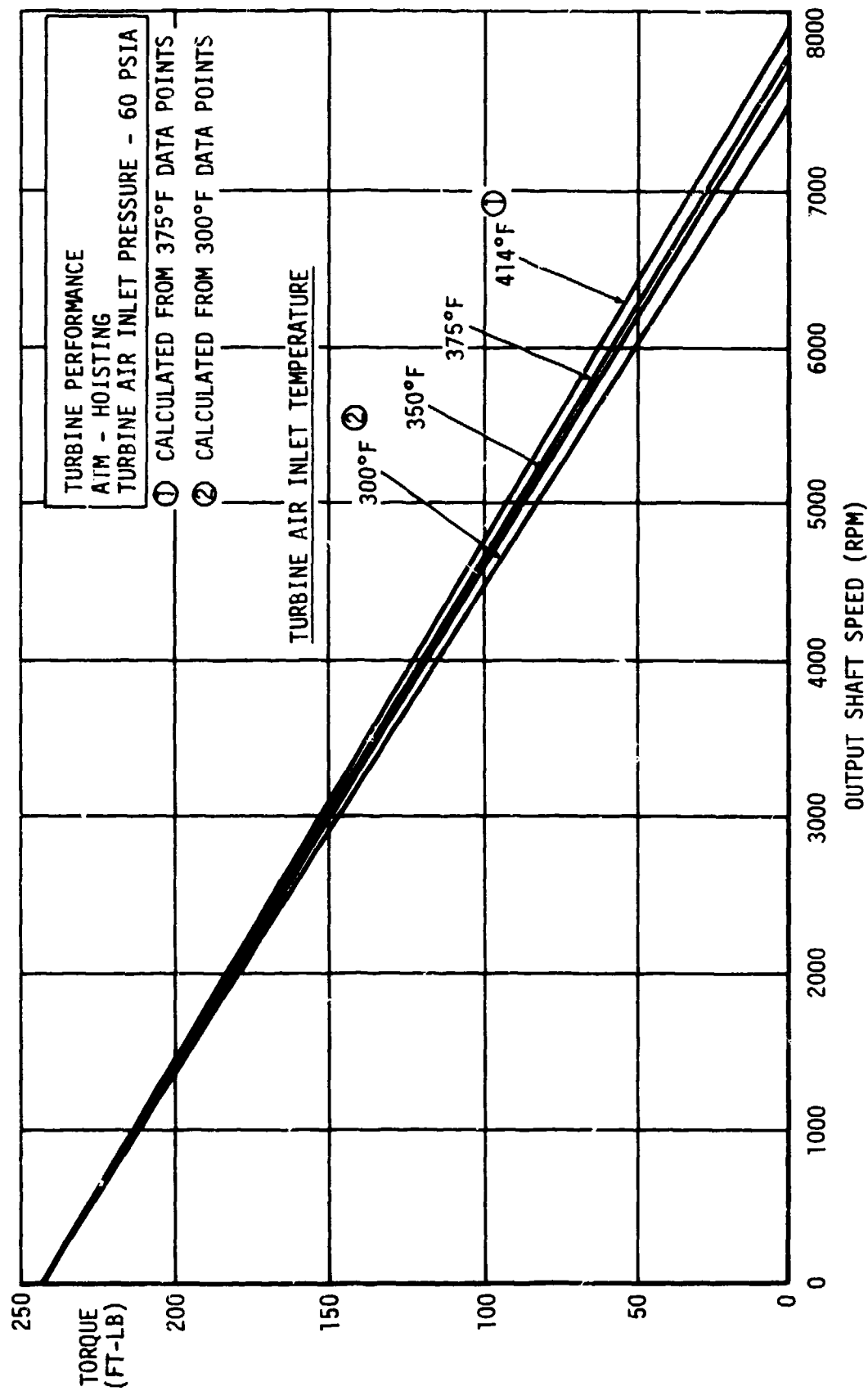


Figure 52. Turbine Performance Hoisting, 60 PSIA.

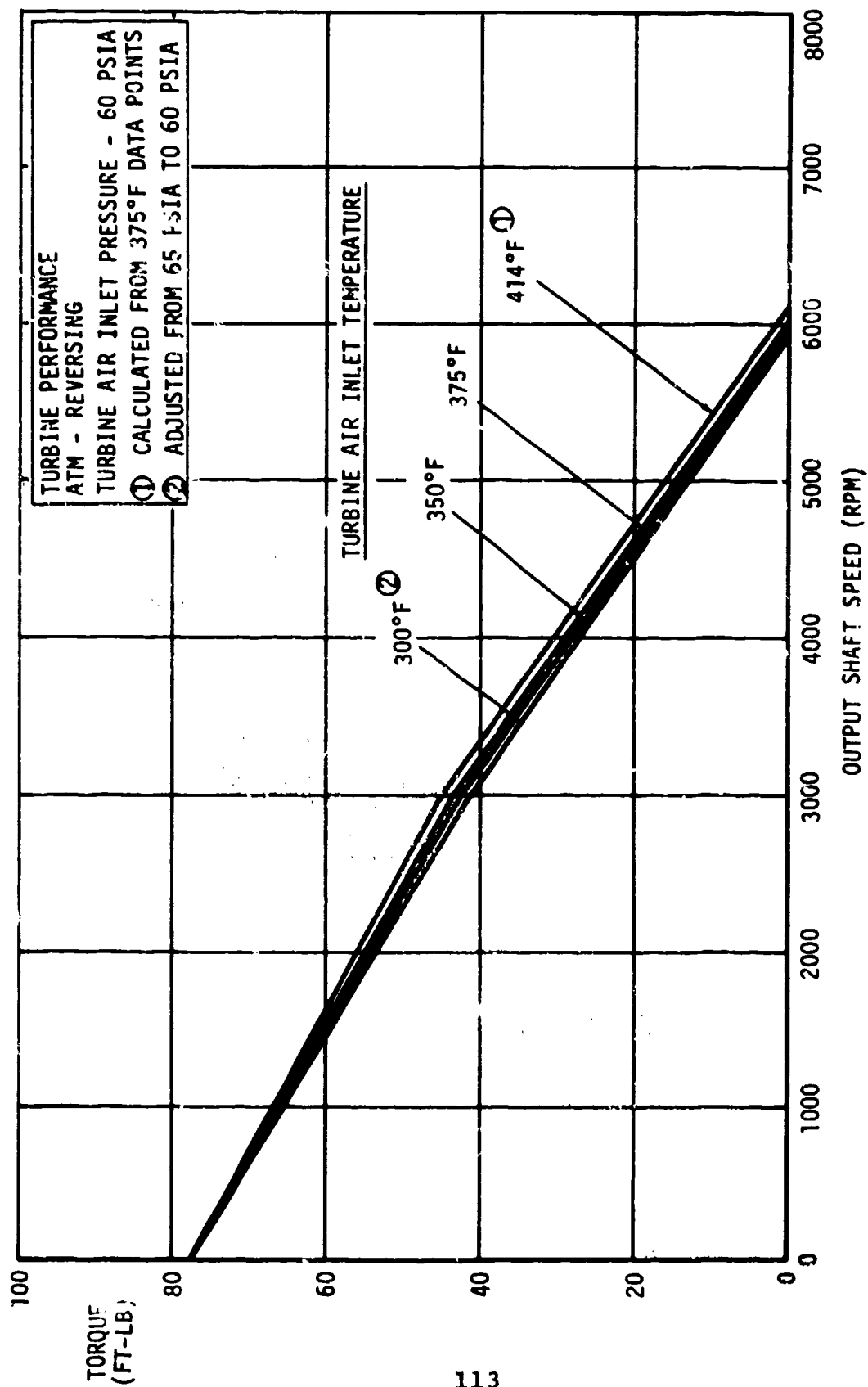


Figure 53. Turbine Performance Reversing, 60 PSIA.

## Emergency Brake Testing - Turbine Overspeed Condition

### Objective

The purpose of this test was to confirm the capability of the static brake to provide an emergency method for stopping the hoist under the most adverse conditions two times.

### Test Procedure

Supply air conditions were: pressure 60 psia, temperature 414°F. Operating tolerances were  $\pm 5\%$  or full scale. Speeds were commanded according to Table 13.

TABLE 13. COMMAND SPEEDS.			
Signal Command ( $\frac{1}{2}$ Design Max)	Direction	Load	Time At Stabilized Speed (min)
100%	Reversing	94 ft-lb	0.5
220%	Reversing	103 ft-lb	--

The load was applied to simulate a downward force or weight. The brake was then applied to stop the turbine. The procedure was repeated a second time. The brake and ATM assembly were then removed and inspected for failure and wear in all sections containing moving parts.

### Results

The static brake successfully performed two overspeed emergency stopping operations. The brake was able to completely stop the ATM and hold the torque. Disassembly did not reveal any wear or damage.



## Dual Mode Control

### Objective

The purpose of this test was to ensure that the two ATM systems could be operated simultaneously but independently.

### Test Procedure

Air supply conditions were: pressure 60 psia, temperature 414°F. Operating tolerances were +5% of full scale. Speeds were commanded according to Table 14.

TABLE 14. COMMAND SPEEDS.							
Command Signal (%)		Direction		Load (ft-lb)		Time At Stabilized Speed (min)	
#1 ATM	#2 ATM	#1 ATM	#2 ATM	#1	#2	#1	#2
50	25	Hoist	Hoist	94	62	1.0	1.0
100	25	Hoist	Reverse	62	62	1.0	1.0
100	75	Hoist	Reverse	62	62	1.0	1.0
Stop							5.0
75	100	Reverse	Reverse	75	75	1.0	1.0
50	75	Reverse	Hoist	75	75	1.0	1.0
50	100	Reverse	Hoist	62	94	1.0	1.0
Stop							5.0
150	100	Hoist	Hoist	0-5	94	1.0	1.0
200	100	Hoist	Reverse	0-5	94	1.0	1.0
200	160	Hoist	Reverse	0-5	0-5	1.0	1.0
Stop							5.0
25	100	Reverse	Reverse	62	94	1.0	1.0
50	100	Reverse	Hoist	62	74	1.0	1.0
Stop							5.0

### Results

The systems were operated simultaneously in accordance with the requirements except that the systems could not attain the desired speed at 200% command signal in the reverse mode, due to hoisting turbine windage losses. This condition was run at the maximum speed attainable. Table 15 details the results of the test.

TABLE 15. DUAL MCDE CONTROL - TEST RESULTS

Lube Oil Pressure PSIG		Lube Oil Temp. °F		Output Shaft Torque ft.-lb		Output Shaft Speed RPM		Turbine Inlet pressure PSIG		Command Speed		Direction	
#1	#2	#1	#2	#1	#2	#1	#2	#1	#2	#1	#2	#1	#2
28	9	80	85	100	61	202	979	24	13	1.2	0.5	H	H
69	8	110	96	65	62	4059	63	27	5	2.4	-0.7	H	R
65	48	135	116	63	61	4060	3037	26	3	2.4	-2.0	H	R
40	76	147	145	83	77	3064	4039	6	4	-2.0	-2.6	R	R
18	40	168	172	92	77	2089	2973	20	6	1.2	-1.9	H	R
17	72	171	183	63	94	2089	4029	16	7	1.2	-2.6	H	R
84	66	205	204	3	94	5983	4060	17	38	3.7	2.7	H	H
79	62	227	213	1	94	8052	3939	34	7	4.9	-2.4	H	R
4	66	187	188	65	93	1087	3927	6	7	-0.7	-2.6	R	R
15	64	191	203	65	96	2010	4015	5	39	-1.3	2.9	R	H

## Synchronization Test

### Objective

The intent of this test was to demonstrate the ability of the hoist control system to respond to a master controller and to maintain synchronization of the hoist couplings.

### Test Procedure

The supply air conditions were: pressure 60 psia, temperature 414°F. Operating tolerances were +5% of full scale. Speeds and loads were in accordance with Table 16. The series of operations was repeated twice.

TABLE 16. COMMAND SPEEDS.					
Command Signal (% Design Maximum)		Direction	Load (ft-lb)		Time At Stabilized Speed (min)
#1 ATM	#2 ATM		#1	#2	
10	10	Hoisting	0-2	0-2	2.0
10	10	Reversing	0-2	0-2	2.0
Stop					1.0
25	25	Hoisting	94	62	2.0
25	25	Reversing	94	62	2.0
Stop					1.0
50	50	Hoisting	62	94	2.0
50	50	Reversing	62	94	2.0
Stop					1.0
75	75	Hoisting	94	62	2.0
75	75	Reversing	94	62	2.0
Stop					1.0
100	100	Hoisting	62	94	2.0
100	100	Reversing	62	94	2.0
Stop					1.0
125	125	Hoisting	47	31	2.0
125	125	Reversing	47	31	2.0
Stop					1.0
150	150	Hoisting	31	47	2.0
150	150	Reversing	31	47	2.0
Stop					1.0

### Results

No malfunctions occurred during the test and synchronization was maintained. In the reversing mode, the windage losses of the hoisting turbine caused a reduction in maximum speed capability. Results of the test are detailed in Table 17.

TABLE 17. SYNCHRONIZATION TEST - TEST RESULTS.

Direction	Command Signal (%)	Output Speed (RPM)	Load		Revolutions		Error (%/100 Ft)
			Fore	Aft	Fore	Aft	
Hoist	5	200	0	0	473	493	4.14
Reverse	5	200	0	0	627	616	1.82
Hoist	25	1000	62	94	2083	2104	.98
Reverse	25	1000	62	94	2198	2214	.72
Hoist	20	2000	94	62	1648	1665	1.04
Reverse	50	2000	94	62	4108	4128	.49
Hoist	75	3000	62	94	6029	6150	1.98
Reverse	75	3000	62	94	6045	6069	.39
Hoist	100	4000	94	62	6659	6685	3.04
Reverse	100	4000	94	62	7903	7930	.34
Hoist	125	5000	31	47	10162	10300	1.36
Reverse	125	5000	31	47	10198	10213	.14
Hoist	150	6000	47	31	12218	12386	1.36
Reverse	150	6000	47	31	7495	7445	.22

## Duty Cycle Testing

### Objective

The purpose of this test was to demonstrate that the hoisting system was able to perform the typical and prescribed cycles of operation.

### Test Procedure

Supply air conditions were: pressure 60 psia, temperature 414°F. Operational tolerances were +5% of full scale. Speed was commanded according to Table 18. The procedure was repeated a total of three times.

TABLE 18. COMMAND SPEEDS.				
Command Signal	Direction	Load (ft-lb)		Time At Stabilized Speed(sec)
		#1 ATM	#2 ATM	
160%	Reversing	0-2	0-2	54.5
Stop				60
100%	Hoisting	94	62	102.5
Stop				60
100%	Reversing	94	62	104.4
Stop				60
160%	Hoisting	0-2	0-2	53
Stop				60
Pause for 10 minutes before repeating cycle.				

Next, hook intermittent vertical placement (beeping) was simulated. The series of operations in Table 19 were repeated a total of four times.

TABLE 19. COMMAND SPEEDS.				
Command Signal	Direction.	Load (ft-lb)		Time At Stabilized Speed (sec)
		#1 ATM	#2 ATM	
25%	Hoisting	79	79	7.0
Stop				3.0
25%	Reversing	79	79	4.0
Stop				3.0
25%	Hoisting	79	79	4.0
Stop				3.0
25%	Reversing	79	79	6.0
Stop				3.0
Pause for 10 minutes before repeating cycle.				

Thermal duty cycling was simulated by commanding speeds shown in Table 20. The procedure was repeated a total of three times.

TABLE 20. COMMAND SPEEDS.			
Command Signal	Direction	Load (ft-lb)	Time At Stabilized Speed(sec)
160%	Reversing	0-2	54.5
Stop			5.0
200%	Hoisting	0-2	53
Stop			5.0
160%	Reversing	0-2	54.5
Stop			15.0
100%	Hoisting	94	102.5
Stop			
Pause for 10 minutes before repeating cycle.			

### Results

The ATM system performed satisfactorily under duty cycle testing without exceeding blade, housing, or lubrication oil temperature limits. A maximum of 160% of maximum hoisting command signal was used in the reversing mode due to the windage losses of the hoisting turbine.

### Environmental Tests

#### High Temperature Test

Test Procedure - Functional Test - With an environmental enclosure around the operational ATM system test setup, 160°F air was supplied to the enclosure. Temperatures were monitored within the enclosure, on the ATM surface, and inside the ATM. When the ATM internal temperature reached 125°F, the chamber was stabilized for one hour. Pneumatic supply temperature was adjusted to 414°F with the modulating valve closed to maintain the ATM at 125°F. The following operational mode tests were conducted twice with performance and temperature data being taken in all modes:

1. Simulated payout with empty hook
2. Simulated hoisting with rated load
3. Simulated lowering with rated load
4. Simulated hoisting with empty hook

Test Procedure - High Temperature Test The ATM was placed in the test chamber in accordance with MIL-STD-810B, Section 3, Paragraph 3.2.2. Chamber temperature was then raised to 120°F and maintained at this temperature for 6 hours. Chamber temperature was next raised to 160°F within a one-hour period and maintained at this temperature for four additional hours. The temperature was then lowered to 120°F within one hour. The 12-hour cycle, from 120°F to 160°F and back to 120°F, was repeated two additional times. At the completion of the three 12-hour temperature cycles, the functional test described above was repeated.

Results No malfunctions occurred as a result of the high temperature test and comparison of the functional test data showed that the system was within specification limits before and after testing. During the high temperature functional test, the ON-OFF valve, P/N EP6003-2012, failed to operate on command until the valve body was tapped lightly. Once the valve was operating, no other malfunctions occurred and the rest of the test was run without incident. The results of the test were within specification limits.

#### Low Temperature Test

Test Procedure - Functional Test With an environmental enclosure around the operational ATM system test setup, CO<sub>2</sub> was supplied to the enclosure. Temperatures were monitored within the enclosure, on the ATM surface, and inside the ATM. When the ATM internal temperature reached -25°F, the chamber was stabilized for 2 hours. The pneumatic air supply was adjusted to approximately 300°F. The following operational mode tests were conducted twice with performance and temperature data being taken in all operational modes:

1. Simulated payout with empty hook
2. Simulated hoisting with rated load
3. Simulated lowering with rated load
4. Simulated hoisting with empty hook

Test Procedure - Low Temperature Test The ATM was placed in the test chamber in accordance with MIL-STD-810B, Section 3, Paragraph 3.2.2. Chamber temperature was then lowered to 10°F (-12°C) and maintained for six hours. Internal chamber temperature was then lowered to -85°F and maintained until the ATM temperature stabilized. The chamber and test item were then returned to ambient conditions and stabilized. The functional test described above was then repeated.

Results - No malfunctions occurred as a result of the cold temperature test, and comparison of the functional tests showed that the system was within specification limits.

During the cold temperature functional test, the ON-OFF valve, P/N EP6003-2012, failed to operate on command until the body was tapped lightly. Once the valve was operating no other malfunctions occurred and the rest of the test was run without incident. The results of the test were within specification limits.

#### Humidity Test

Test Procedure - The test was conducted in accordance with Method 507, Procedure I, of MIL-STD-810B.

The test sample was installed in the test chamber in a manner simulating service usage.

Initially, the chamber temperature was maintained between 68° and 100°F with uncontrolled humidity. During the first 2-hour period, the temperature was gradually raised to 160°F. This temperature was maintained during the next 6-hour period. During the following 16-hour period, the temperature in the chamber was gradually reduced to a temperature between 68°F to 100°F, constituting one cycle. The relative humidity throughout the cycle was 95%. The humidity cycle was repeated to extend the total time of the test to 240-hours (10 cycles).

The velocity of air throughout the test area did not exceed 150 feet per minute. Demineralized water, having a pH value between 6.0 and 7.2 and a temperature of 73°F was used to obtain the desired humidity.

The test sample was not operated or energized during the test.

Test Results - Comparison of operational test data obtained before and after the humidity test established that neither the unit nor its operation were impaired by the humidity test.

#### Salt Fog Test

Test Procedure - The ATM system was cleaned and prepared in accordance with MIL-STD-810B, Method 509, Paragraph 3.1.5. It was then placed in the test chamber in accordance with Section 3, Paragraph 3.2.2 and exposed to salt fog for a period of 48 hours.



The salt solution and internal chamber temperature were maintained as specified in MIL-STD-810B, Method 509.

Test Results - Slight surface corrosion was noted on the exposed weld areas of the hoisting turbine housing, reversing turbine and exhaust housing, lube relief valve housing, tube filter by-pass valve housing, and the internal exhaust vane investment castings. Due to this corrosion, the drawings were changed to incorporate passivation of the housings following welding. Corrosion was also found on 10% of the exposed surface area of the brake output spline. When the unit is mounted to the hoist reduction gearbox, the spline shaft will not be exposed to the atmosphere. Some of the hexagonal head screws were corroded where the cadmium plating was chipped by the installation tools. This corrosion was easily washed off and is considered acceptable. No other visible damage was sustained by the unit.

Comparison of operational test data obtained before and after the salt fog test confirmed that operation of the ATM was not impaired due to the salt fog test.

#### Sand and Dust Test

Test Procedure - The test was conducted in accordance with Method 510, Procedure I, of MIL-STD-810B.

The test assembly was placed in the test chamber and then subjected to the following temperature, air velocity, and dust density test conditions.

<u>Step</u>	<u>Temperature</u>	<u>Air Velocity</u>	<u>Dust Density</u>	<u>Duration</u>
1	+ 77°F	1750 fpm	0.3 gm/ft <sup>3</sup>	6 hours
2	+145°F	300 fpm	None	16 hours

The relative humidity did not exceed 10% at any time during the test. The sand and dust used in the test was of an angular structure, and possessed the characteristics specified in MIL-STD-810B. Upon completion of the test, the test sample was removed from the chamber, stabilized at room temperature conditions, and visually inspected.

Test Results - Comparison of operational test data obtained before and subsequent to the sand and dust test substantiated that operation of the unit was not impaired by the test conditions. During disassembly of the ATM, light surface scratches were found on the plate between the lube pump and scavenge pump, P/N

EP6003-46. These scratches resulted from slight traces of sand, which was introduced through the breather gear port during the sand and dust test. No other damage resulted nor was the unit's operation impaired.

#### HIGH-SPEED GEARBOX JACKSHAFT FAILURE

Following 470 synchronous load cycles on the integrated test rig with a 58,544-pound load, a failure occurred in the aft hoist drive unit. The cause was found to be a failure of a jackshaft in the high-speed gearing of the hoist drive unit. As shown in Figure 54, the jackshaft was constructed of two pieces joined by electron-beam welding. The axial length of contact between the two pieces was 0.35 inch with a weld penetration of 50%. The unwelded portion of contact length was a crack which acted as a stress riser. The part failed because of reverse bending fatigue. Figure 55 illustrates the failed part.

#### Corrective Action

A vendor who was capable of cutting the required gears in a one-piece jackshaft was found. The corrective action consisted of a design change to a one-piece construction and verification of the change by fabrication of replacement hardware which was subsequently installed and tested as part of the system tests on the cargo handling integrated test rig.

#### Test Results

Based on limited testing on the integrated test rig, the one-piece jackshaft was found to be satisfactory.

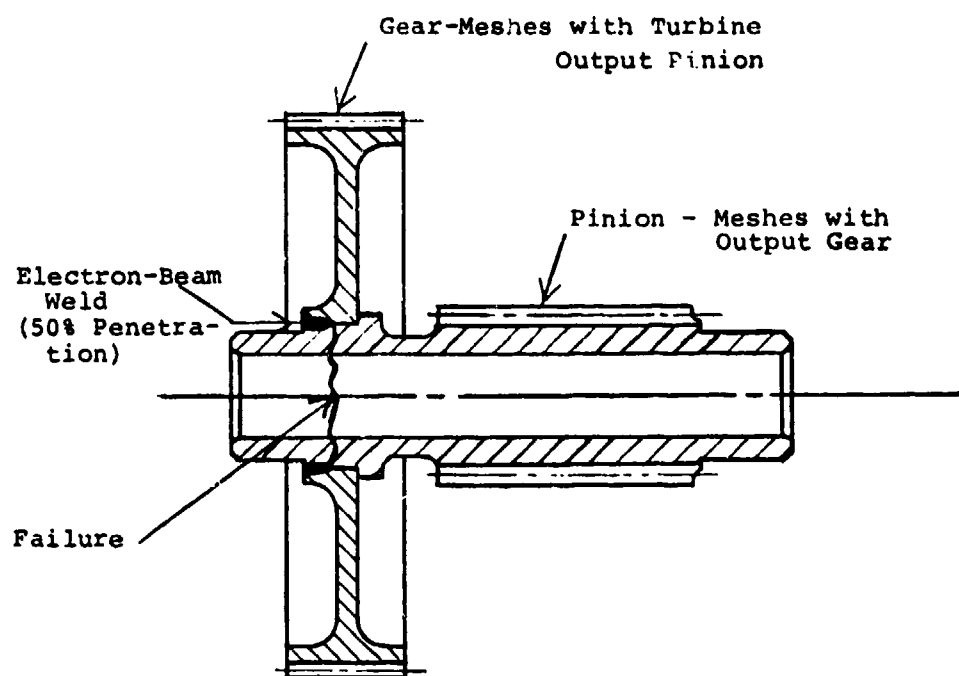


Figure 54. High-Speed Gearbox Jackshaft.

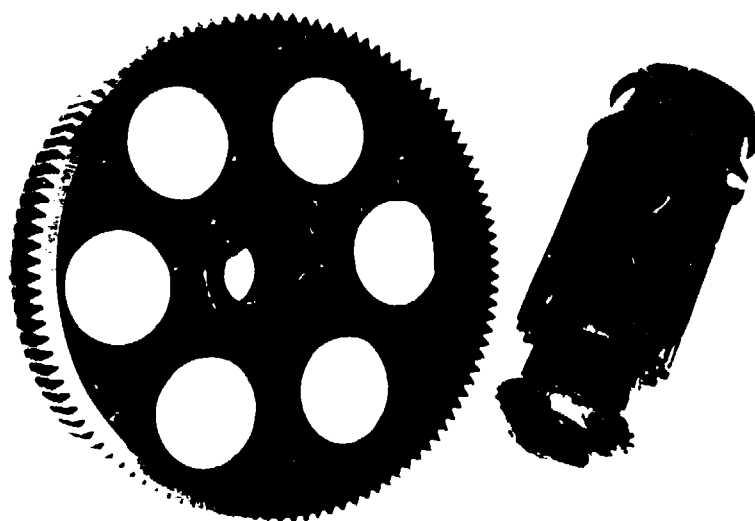


Figure 55. Failed Two-Piece Jackshaft.

## LOAD ISOLATOR

### DESIGN SUPPORT TESTS

No design support tests were performed in conjunction with the development of this component. Design requirements were explicitly defined by preexisting analytical methods and test data from the CH-47 helicopter. Industry confidence was high that the HLH requirements (see Volume I) could be met using any of several methods which involved information proprietary to the vendors.

### DESIGN DEVELOPMENT TESTS

#### Requirements

One load isolator assembly was to be subjected to static strength and frequency response tests to determine the performance characteristics.

#### Test Program

Development tests were planned to accomplish the following:

1. To establish the dynamic characteristics of the isolator.
2. To confirm the static strength of the unit.
3. To investigate gland seal life through vibration testing.

Production and testing were conducted concurrently due to time restrictions. Changes to the isolators found necessary as a result of the test program were incorporated by means of modification kits.

#### Specimen Design Concept

The load isolator consists of a liquid spring, which uses a high-compressibility silicone fluid and a nitrogen charged recuperator chamber. The piston rod terminates in a clevis to allow connection with the hoist planetary reaction arm and includes a load cell for axial load sensing. The cylindrical spring-fluid housing has a self-aligning bearing, installed to suit the hoist mounting provisions, that splits the fluid volume into two inter-connected areas. Below the spring fluid housing is the recuperator chamber.

The recuperator piston has differential areas so that the fluid pressure is approximately twice that of the nitrogen charge. When the liquid spring is fully extended, the recuperation fluid has direct passage to the spring fluid, causing the spring fluid pressure to be a function of the nitrogen pressure. As the nitrogen pressure will not vary with temperature to the same extent as the silicone fluid, the recuperator partially compensates for temperature changes, resulting in the liquid spring having acceptable spring rates over a temperature range of  $-32^{\circ}\text{F}$  to  $127^{\circ}\text{F}$ . Initial movement of the piston rod closes a valve isolating the spring fluid from the recuperator. Maximum fluid pressure at full stroke is approximately 23,000 psi.

The recuperator piston provides a visual indication of the correct fluid volume; a pressure gage indicates the nitrogen pressure. Dry air may be used in lieu of nitrogen to charge the recuperator.

The detail design of the isolator is covered in Volume I of this document.

#### Test Fixture Design

Load deflection tests and structural strength tests were conducted in a 200-ton press manufactured by W.T. Avery, Ltd. A fixture was used to mount the isolator body to the ram of the press. The piston rod was attached to the top beam of the press by a machined fitting. The fixture was designed to permit tie bars to be installed to pre-load the isolator, prior to use in the fatigue test machine. Figure 56 illustrates the fixture arrangement.

Vibration tests were conducted in a 20-ton fatigue test machine designed and manufactured by Dowty Rotol, Ltd.

#### Test Instrumentation

The master load was provided by an Avery 30-ton testing machine certified to grade "A" of British Standard 1610, i.e., accuracy within 1% of the applied load. This load was used to check the load sensor output by comparing the testing machine's reading with the digital voltmeter (DVM) reading. The machine load scale was also used for the static load deflection tests and for the proof pressure tests.

The load sensor was used to provide the load signal during the dynamic load deflection tests.

Deflection was measured by a linear potentiometer in all tests and displayed on the DVM for static tests.

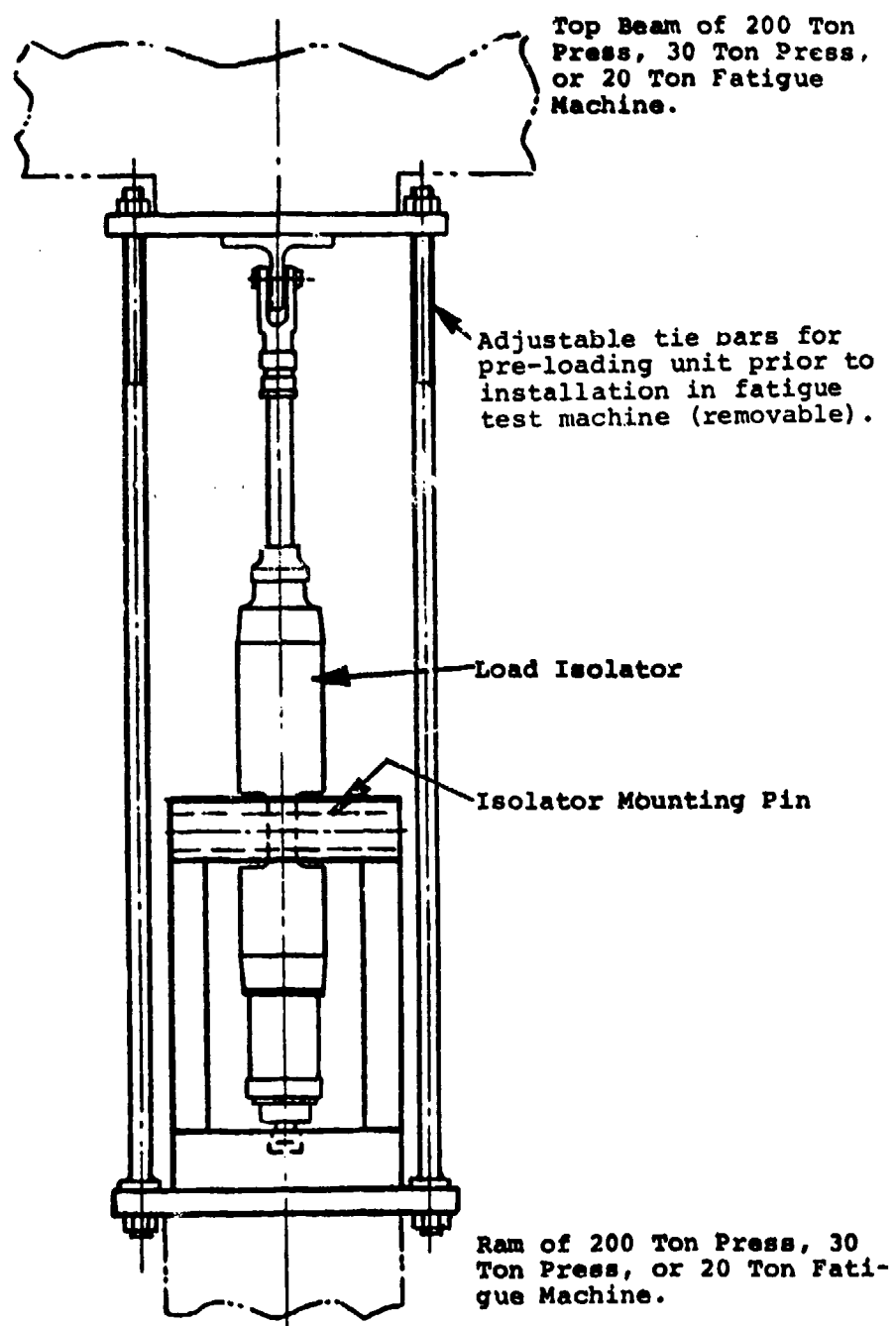


Figure 56. Load Isolator Mounting Fixture.

For the dynamic load deflection tests, the load sensor signal and linear potentiometer signals were applied to an X-Y plotter of suitable response to plot hysteresis loops.

Ultimate loads were applied in a 200-ton testing machine certified to grade "B" of BS 1610, i.e., accuracy to within 2% of applied load.

The 20-ton fatigue machine, used for vibration tests, has a strain sensing load cell providing monitoring to an accuracy to within 0.5% of Lissajou display, combined with a four-decade back-off. Displacement was measured to an accuracy within 1% by an integral displacement transducer.

#### Test Facilities

All facilities used for these tests are owned by the isolator subcontractor, Dowty Rotol, Ltd., of Gloucester, England, and included:

Heat chamber of 180 cubic foot capacity, maximum temperature 120°C (248°F).

Environmental chamber of 330 cubic foot capacity capable of temperatures down to -65°C (-85°F).

67,200-pound hydraulic testing machine made by W.T. Avery, Ltd.

448,000-pound hydraulic testing machine made by W.T. Avery, Ltd.

±45,000-pound fatigue testing machine designed and manufactured by Dowty Rotol, Ltd. This is a closed loop hydraulic servo system with load or displacement control provided by load cell or displacement transducer feedback signals.

#### Test Conditions, Procedures and Results

Unless specified otherwise, testing was conducted at room temperature and pressure. These temperatures were recorded and used in determining the isolator characteristics.

The dynamic characteristics of the isolator, as originally tested, were not within the limits defined in the design specification. In order to reduce the dynamic stiffness, the fluid volume was increased and piston area reduced by revising the piston rod diameter from 1.3125 to 1.25 inches. Since all testing conducted prior to the change was repeated, only the results of the modified isolator tests are reflected here.

### Preliminary Evaluation

Prior to commencing the tests, the dimensions of parts that could be distorted were recorded. These parts were measured after the tests with the results shown on Table 21.

### Load Sensor Check

The objective of the test was to determine that the load sensor output is linearly proportional to the applied load within  $\pm 1.0\%$  up to 50,000 lb.

The tests were conducted on the 67,200-lb testing machine; the load was applied to the sensor in increments of 1,120 lb. During initial checks, a maximum load of only 32,500 lb was attained. These results are shown in Table 22.

Subsequently, at the time of limit load application, the sensor was rechecked to 50,000 lb. The results are shown in Table 23.

The results show that on the initial check all readings were within the  $\pm 1\%$  tolerance band. The subsequent check did exhibit larger errors at the lower loads. At this time, the load cell had been subjected to several extreme temperature exposures that may have influenced the strain gage calibration.

The maximum error of approximately 200 lb at the 2 long ton loads is equivalent to a 0.4% error on full-scale reading and is acceptable for this application. Generally, the error on increasing load was significantly less than on the decreasing load.

### Dynamic Load Deflection Test at Room Temperature

The objective of this test was to establish a load deflection curve for the unit and establish the dynamic friction.

Compression/extension tests were conducted on the 67,200 lb testing machine at a stroking velocity of 1.6 in/sec for 7.3 inches of stroke. Fluid pressure was recorded for one of the cycles. The resulting load/deflection curves for four cycles is shown in Figure 57. The fluid pressure plot is shown in Figure 58. From a curve in Figure 57, the load/deflection values have been determined and are shown in Table 24. From these values, the dynamic friction was established. The dynamic friction, at approximately 5% of the applied load, is well above the specification objective of 2%.



<b>Drawing No.</b>	<b>Description</b>	<b>Dimension No.</b>	<b>Measurement Required</b>	
200646002	Unit	1	Weight when operational	
200646001	Unit	2	Center to center dimension from trunnion to piston rod eye end.	
200646603	Piston Rod	3	Outside dia. 1" from stop shoulder.	
		4	Length from end face to bleeder boss.	
200646600	Cylinder	5	Outside dia. of oil cylinders at approx. mid. position of each.	
		6	Trunnion center to each end.	
200646601	Recuperator Cylinder	7	Outside dia. at approx. mid position.	
200646602	Recuperator Rod	8	Outside dia. at approx. mid position.	
<b>Drawing #</b>	<b>Description</b>	<b>Dim. #</b>	<b>Measurements</b>	
			<b>Before Test</b>	<b>After Test</b>
200646002	Unit Weight	1	45.71	N/A
200646633	Piston Rod	3	1.2488/1.2489	1.2488/1.2488
200646600	Cylinder P.R.End	5	4.148	4.149
200646600	Cylinder Recup.End	5	4.148	4.148
200646601	Recup. Cylinder	7	3.348	3.349
200646602	Recuperator Rod	8	2.3978	2.3977/2.398
Where two dimensions are given, the first is on the centerline of the unit in the bottom view the second dimension being at 90° to the centerline.				
Due to a number of strip and rebuilds, dimensions 2, 4 and 6 were no longer comparable.				

TABLE 22. LOAD SENSOR CALIBRATION.			
Applied Load Long Tons (2,240 lb)	Load Sensor DVM Reading Increasing Load	Load Sensor DVM Reading Decreasing Load	Max. Error % of Applied Load
0	0	0	-
0.5	0.50	0.50	0
1.0	1.00	0.99	1
1.5	1.50	1.50	0
2.0	2.00	2.00	0
2.5	2.49	2.49	0.4
3.0	2.99	2.98	0.7
3.5	3.48	3.48	0.6
4.0	3.98	3.97	0.7
4.5	4.49	4.48	0.4
5.0	4.98	4.98	0.4
5.5	5.47	5.48	0.5
6.0	5.98	5.98	0.3
6.5	6.48	6.48	0.3
7.0	6.99	6.98	0.3
7.5	7.50	7.49	0.1
8.0	8.00	8.00	0
8.5	8.50	8.49	0.1
9.0	8.99	9.00	0.1
9.5	9.50	9.50	0
10.0	10.00	10.01	0.1
10.5	10.50	10.51	0.1
11.0	11.00	11.02	0.2
11.5	11.49	11.51	0.1
12.0	12.00	12.04	0.3
12.5	12.50	12.54	0.3
13.0	13.00	13.07	0.5
13.5	13.50	13.58	0.6
14.0	14.00	14.07	0.5
14.5	14.48	-	0.1

TABLE 23. LOAD SENSOR CALIBRATION.			
Applied Load Long Tons (2,240 lb)	Load Sensor DVM Reading Increasing Load	Load Sensor DVM Reading Decreasing Load	Max. Error % of Applied Load
0	0	0	-
1	0.98	0.95	5.0
2	1.95	1.90	5.0
3	2.96	2.92	2.7
4	3.98	3.94	1.5
5	4.97	4.95	1.0
6	5.95	5.91	1.5
7	6.96	6.93	1.0
8	7.96	7.95	0.6
9	8.98	8.97	0.3
10	9.98	10.01	0.2
11	10.98	10.99	0.2
12	11.99	12.02	0.2
13	12.98	13.04	0.3
14	13.99	14.05	0.4
15	14.99	15.05	0.3
16	15.97	16.08	0.5
17	16.97	17.09	0.5
18	17.96	18.11	0.6
19	18.95	19.10	0.5
20	19.94	20.14	0.7
21	20.92	21.13	0.6
22	21.85	22.10	0.6
22.32	22.17	-	0.7

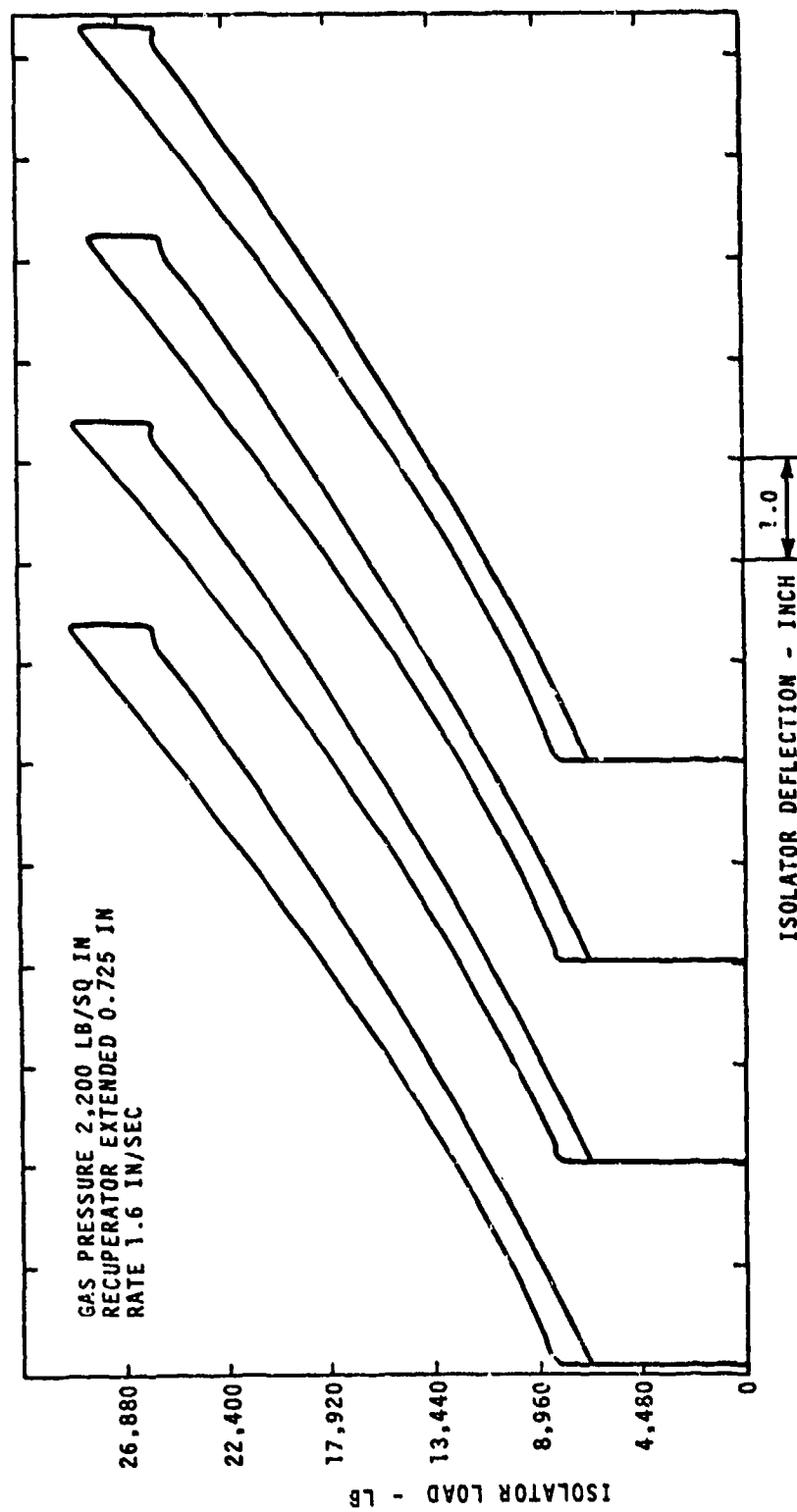


Figure 57. Isolator Load/Deflection at Ambient (75°F).

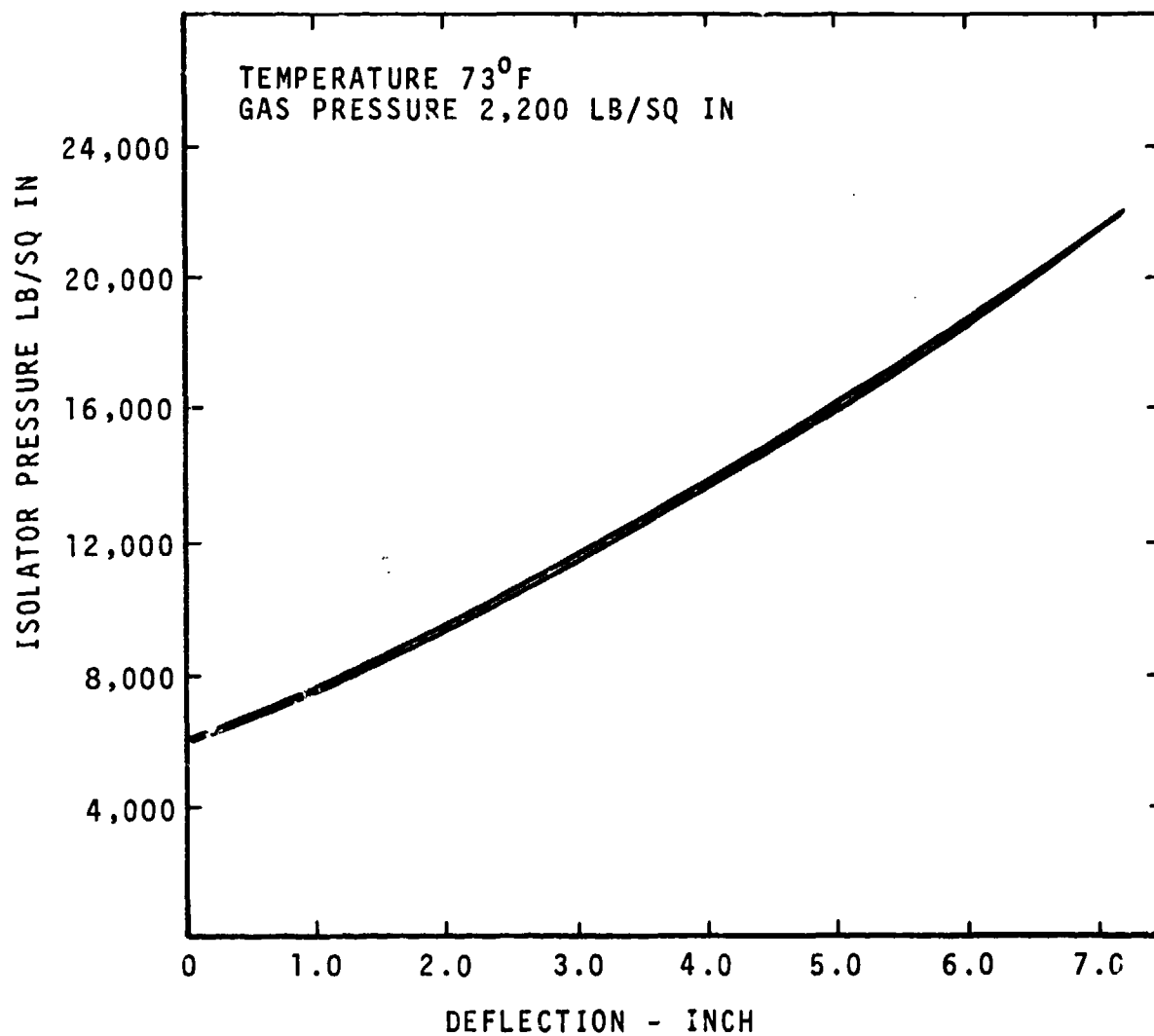


Figure 58. Isolator Fluid Pressure/Deflection.

TABLE 24. LOAD/DEFLECTION VALUES - 75° F.						
Isolator Deflection Inch	Isolator Load (lb)		Friction		Mean Load	
	Increasing Load	Decreasing Load	Mean Load	Lb	% Load	From Pressure Curve, Fig.
0	7,930	6,720	7,325	605	8.26	7,360
1	9,990	8,780	9,385	605	6.45	9,330
2	12,280	11,020	11,650	630	5.41	11,540
3	14,920	13,530	14,225	695	4.89	14,120
4	17,740	16,220	16,980	760	4.48	16,750
5	20,790	18,900	19,845	945	4.76	19,650
6	24,100	21,770	22,935	1,165	5.08	22,830
7	27,550	25,000	26,275	1,275	4.85	26,200
7.3	28,580	25,940	27,260	1,320	4.84	27,250

Friction does decrease with operation and a plot of friction values taken during the vibration testing shows a dynamic friction value of less than 1% of applied load after 20 hours of operation. This friction value curve is shown in Figure 59.

To determine compliance with the specification, the mean load/deflection curve has been used to establish the equivalent spring rate at the tension member. This curve is shown in Figure 60, falling within the boundaries between the 5-foot cable length, 2.0-Hz requirement and the 60-foot cable length, 1.5 Hz requirement. This curve satisfies the requirements of the specification.

#### Static Load Deflection Test at Room Temperature

The objective of this test was to establish the static friction of the unit and derive a static load/deflection curve. The same setup was used as in the previous test; however, the load was applied with a 5-minute dwell at each inch of isolator compression and extension. The resultant load/deflection curve is shown in Figure 61. No high break-out friction occurred. The static friction is small compared with the dynamic friction, so that it is not possible to establish a value for the break-out friction. From the curve, Figure 61, the break-out value is well below the specification objective of 3% of applied load.

The mean load/deflection curve provides the values used in Table 25. In this Table, the values for the dynamic and static curves are compared. The static curve reflects a "softer" spring characteristic than the dynamic curve, establishing a contributing reason why the initial isolator configuration had dynamic characteristics too stiff to meet the specification requirements.

It is recognized that the relationships between static and dynamic load/deflection curves will vary with the speed of load application for the dynamic curves. The rate of load application used during these tests is in the same order as that resulting from the principle vibration frequencies.

#### Dynamic Load/Deflection Test at Low Temperature

The objective of this test was to establish the load deflection curve for the isolator at -25°F.

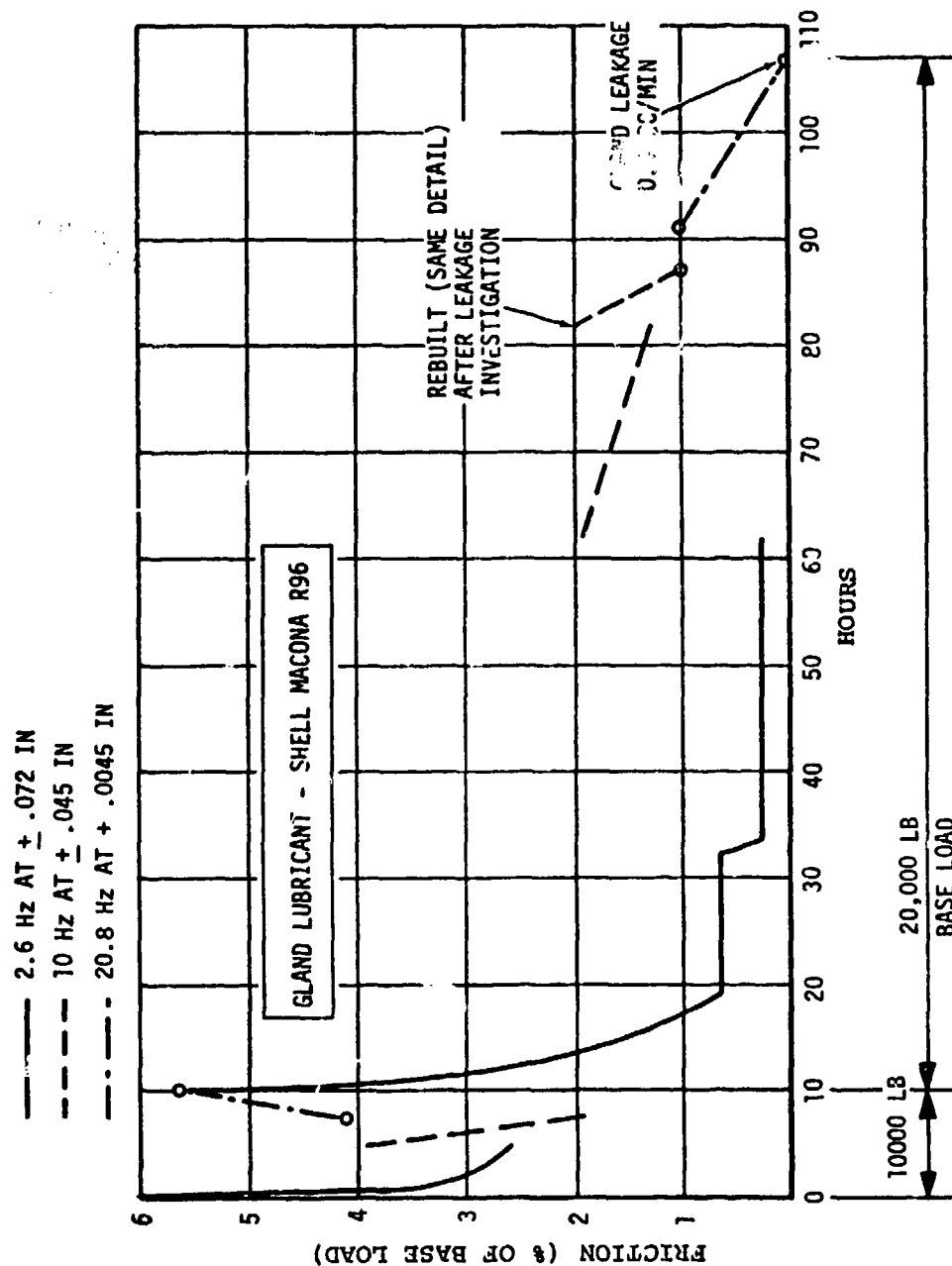


Figure 59. Friction Values during Vibration Tests



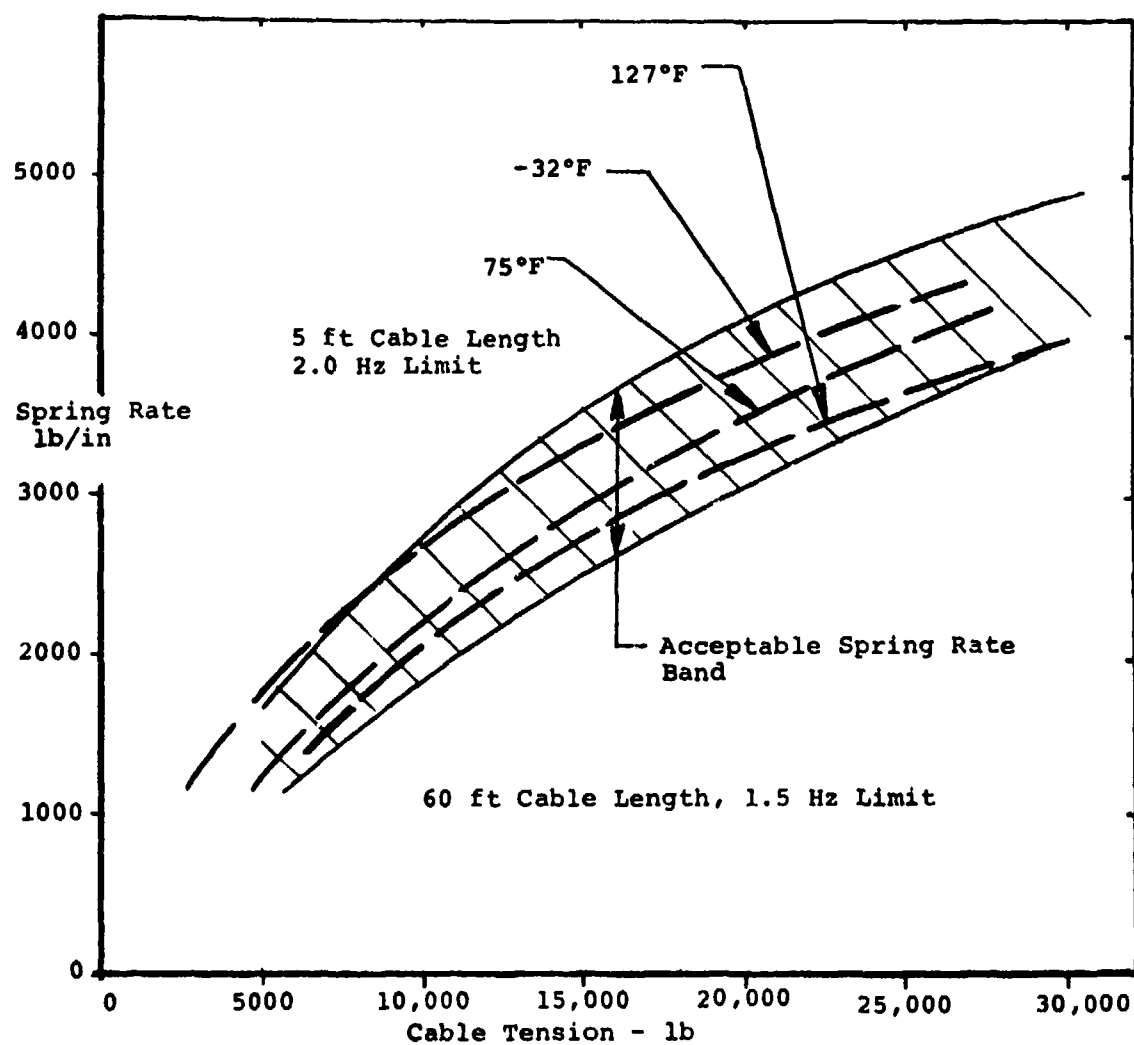


Figure 60. Isolator Equivalent Spring Rates - Modified Unit.

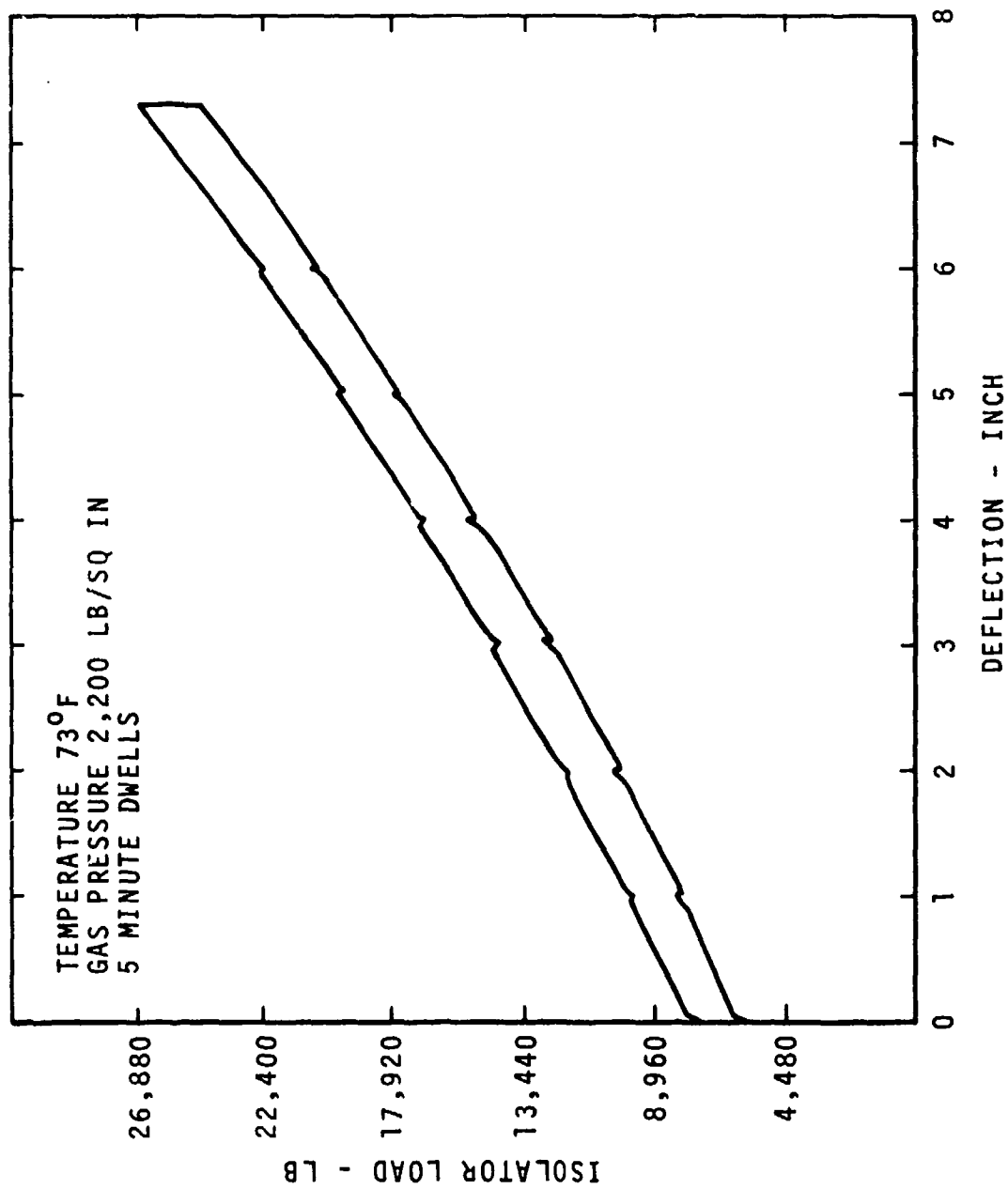


Figure 6l. Isolator Static Load/deflection.

TABLE 25. COMPARISON OF STATIC AND DYNAMIC CHARACTERISTICS.			
Deflection Inch	Dynamic Mean Load At 1.6 In/Sec	Static Mean Load	% Reduction In Stiffness Of Static Values
0	7,325	7,170	2.1
1	9,385	9,000	4.1
2	11,650	11,110	4.6
3	14,225	13,530	4.9
4	16,980	16,000	5.8
5	19,845	18,640	6.1
6	22,935	21,500	6.3
7	26,275	24,640	6.2
7.3	27,260	25,670	5.8

The isolator, assembled in the test fixture, was cold soaked in the environmental chamber at  $-34^{\circ}\text{F}$  for 16 hours. After the cold soak, the fixture with the isolator was transferred to the 67,200-lb testing machine and subjected to six dynamic load/deflection cycles at 1.6 in/sec. The first, third, and fifth cycles were recorded and are shown in Figure 62.

The tests were completed within six minutes of leaving the low temperature chamber, and maximum body temperature during the test was  $-31^{\circ}\text{F}$ .

The mean load/deflection curve of one cycle was used to establish the equivalent spring rate at the tension member. This curve is shown in Figure 60 and falls above the 60-foot cable length 1.5-Hz requirement and below the 5-foot length, 2.0-Hz requirement except for cable tensions below 8,000 lb. This result is considered optimum since any further reduction in stiffness would shift the high temperature curve, as explained below, in the paragraph entitled "Dynamic Load/Deflection Test at High Temperature", below the 60-foot, 1.5-Hz curve.

During the low temperature tests with the isolator as originally configured, some leakage had occurred past the "O" ring seal between the body and gland housing. The "O" ring was replaced and the unit operated satisfactorily. On the subsequent low temperature tests, at the end of the soaking period, the gas pressure was down to 1,000 lb/sq in. with the recuperator piston still almost fully extended. On completing the six load/deflection cycles there was no external leakage. Disassembly of the unit showed the recuperator gas volume to have an oil/gas mixture.

Strip examination showed that the Teflon backing rings and rubber seal had been extruded past the piston lands. Failure of the seal was due to the Teflon backing rings having insufficient strength for the piston design. It was therefore decided to revert back to the original Tufnol backing ring and seal with the inner diameter chamfered at .020 in.  $\times 45^{\circ}$  to provide an outward energizing force.

#### Dynamic Load/Deflection Test at High Temperature

The objective of this test was to establish the dynamic load/deflection curve for the isolator at  $+125^{\circ}\text{F}$ .

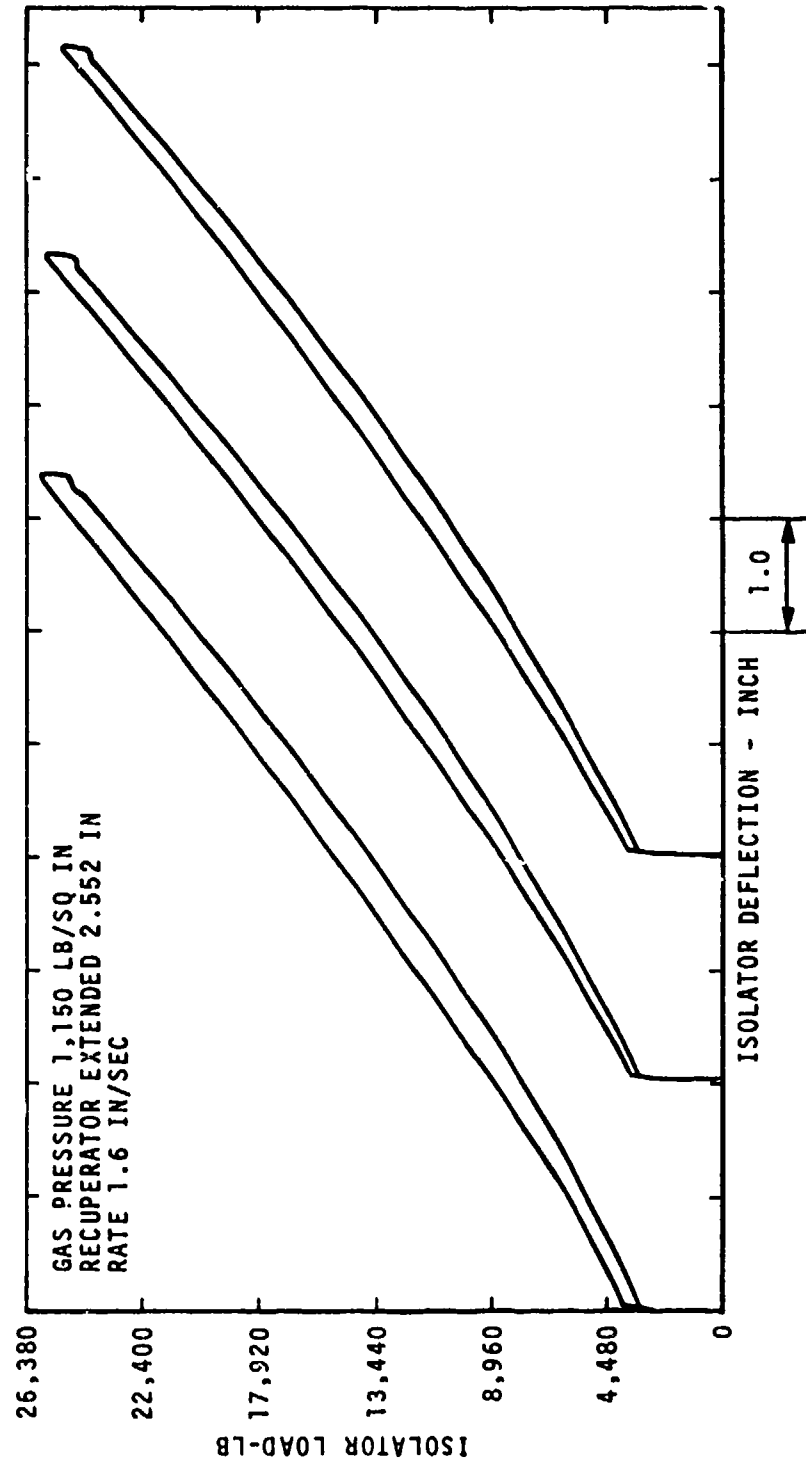


Figure 62. Isolator Load/Deflection at  $-32^{\circ}\text{F}$ .

The isolator and the test fixture were assembled and were heated in the heat chamber for six hours at 134°F. Then, they were transferred to the 67,200-lb testing machine and subjected to six load deflection cycles at 1.6 in/sec. The tests were completed with a minimum body temperature of 127°F. There was no leakage during this test. The first, third, and fifth cycles were recorded and are shown in Figure 63.

The mean load deflection curve of one cycle was used to establish the equivalent spring rate at the tension member. This curve is shown in Figure 60, falling between the 5-foot cable length, 2.0-Hz requirement and the 60-foot length, 1.5-Hz requirement, complying with the specification.

#### Extreme Temperature Tests

The objective of this test was to demonstrate that the isolator's performance will not be impaired after exposure to +160°F and -65°F temperature extremes.

The isolator was soaked at 160°F for six hours in the heat chamber, then soaked at -65°F for 15 hours in the environmental chamber. Upon restabilizing at room temperature, the isolator was subjected to six load/deflection cycles. The resultant curves from these cycles were not significantly different from the curves obtained earlier. These tests show no evidence of damage or malfunctioning. There was no oil or gas leakage throughout the tests.

#### Vibration Tests

The objectives of the vibration tests were to demonstrate the gland life and to establish that the performance at the defined vibration level was within the specification requirements.

Vibration tests had been initiated prior to the configuration change to reduce the piston rod diameter and were continued on the new design.

Testing was conducted on the 45,000-lb fatigue test machine. The isolator body temperature was monitored with thermocouples to control an air blower that limited the maximum body temperature to 122°F.

The test plan required the spectrum of tests shown in Table 26.

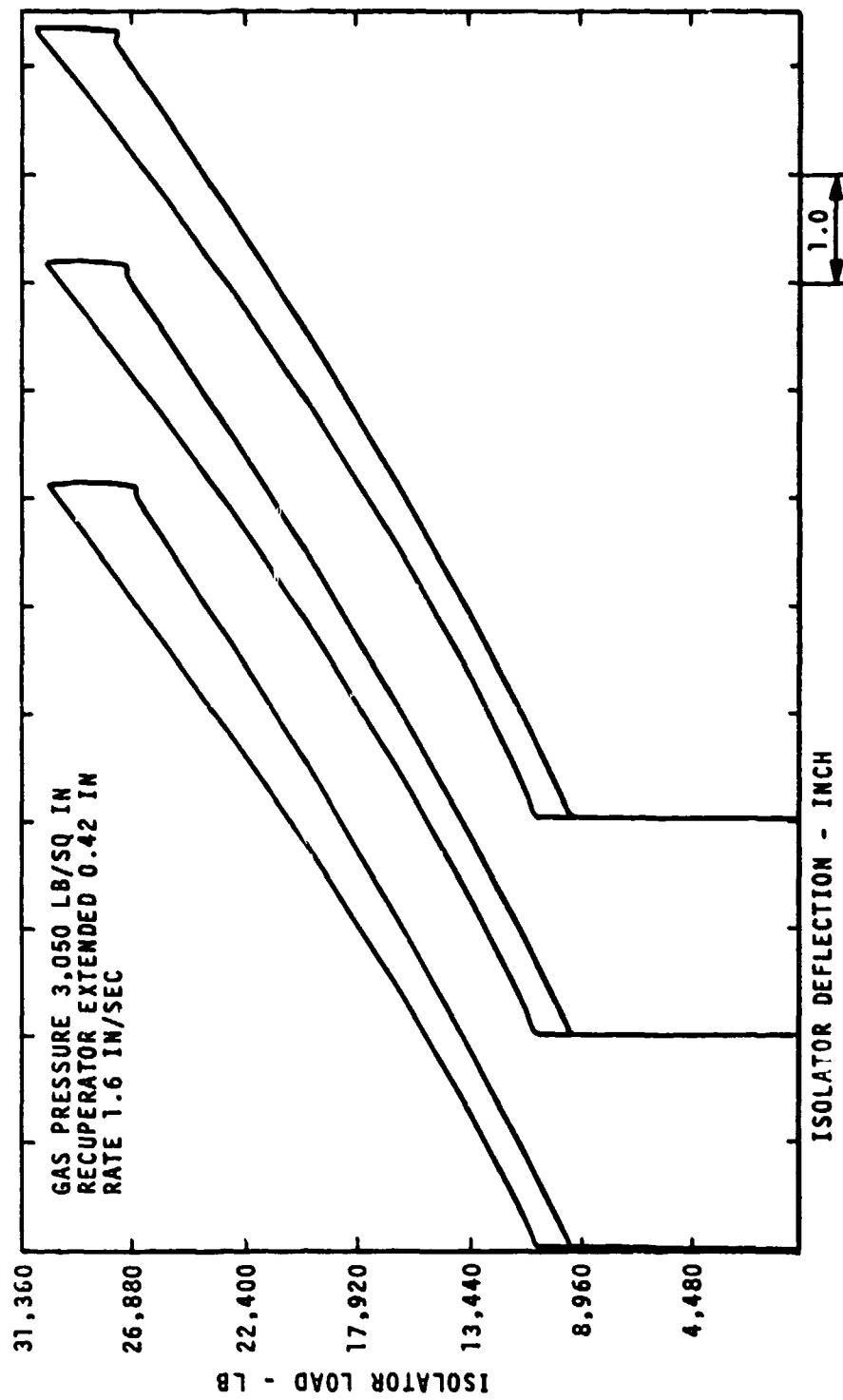


Figure 63. Isolator Load/Deflection At +127°F.

TABLE 26. TEST PLAN VIBRATION SPECTRUM REQUIREMENT.			
Unit Preload lb	Hours	Frequency Hz	Amplitude Inch
10,000	5	2.6	<u>+ .0725</u>
	2½	10.0	<u>+ .045</u>
	2½	20.8	<u>+ .0045</u>
20,000	50	2.6	<u>+ .0725</u>
	25	10.0	<u>+ .045</u>
	25	20.8	<u>+ .0045</u>
25,000	5	2.6	<u>+ .0725</u>
	2½	10.0	<u>+ .045</u>
	2½	20.8	<u>+ .0045</u>



The isolator had completed the 10,000-lb preload test and 12-1/2-hours testing with a 20,000-lb preload at a 2.6-Hz frequency when the test was discontinued because of leakage from the gland. Gland lubricant (Shell EP 140) and silicone fluid (CPT 3801) had leaked from the gland nut threads. The unit was compressed further to regain the 20,000-lb base load and this indicated a fluid loss of approximately 1.4 cubic inches.

A further 2-hours running at 2.6-Hz showed almost no leakage.

A strip examination of the gland assembly showed slight wear in the bore with some glazing (associated with high temperature) at the outboard end (see Figure 64). A dimensional check showed that the gland bore was the same size as the rod diameter.

At this stage of the program, performance calculations showed the spring stiffness at -29°F to be outside the specification limits and therefore not acceptable. In order to reduce the stiffness, it was necessary to reduce the piston rod diameter from 1.3125 inches to 1.250 inches.

After the isolator had been modified and the dynamic load/deflection tests repeated, the unit was again installed in the 45,000-lb fatigue machine.

Prior to commencement of vibration tests, the gland seal lubricant was changed from Shell EP 140 to Shell Macona R96. It was also decided that each hour, longer strokes should be carried out equivalent to one full excursion ( $7 \pm 0.5$  in.).

Table 27 lists the endurance tests that were completed before leakage again stopped the tests.

Records of the Lissajou displays taken during the tests show the friction values to have decreased during the 2.6 Hz and 10 Hz runs but to have increased rapidly during the 20.8 Hz  $\pm .0045$  in. run. The friction values are graphed in Figure 59.



Figure 64 . Isolator Gland Assembly After Leakage

TABLE 27. VIBRATION TESTING COMPLETED.				
Load-lb	Hz	Amplitude	Hours Completed	
10,000	2.6	$\pm .0725$	5	
10,000	10	$\pm .045$	2.5	
10,000	20.8	$\pm .0045$	2.5	
20,000	2.6	$\pm .0725$	51.8	
20,000	10	$\pm .045$	20.15	See Note (1)
20,000	10	$\pm .045$	5	
20,000	20.8	$\pm .0045$	20.75	See Note (2)
<p><u>NOTES:</u></p> <p>(1) Silicone leakage in excess of the 1 cc permitted occurred from the threads of the gland nut. Strip examination showed no obvious damage to the gland but there was no preload between the gland and the rod. The unit was rebuilt to the same design standards and the tests were continued. After filling and inflating there was no leakage.</p> <p>(2) Silicone leakage again occurred, the leakage being approximately 0.5 cc/min. The tests were discontinued due to the continuous change in the displacement position.</p>				

Analysis of the friction curve, Figure 59, shows a marked increase in friction during the test at 20.8 Hz,  $\pm .0045$  in. displacement. It was concluded that at this higher frequency and smaller amplitude, the gland lubricant was not flowing over the piston rod surface, resulting in rapid wear. As this frequency is equivalent to the aircraft 8-per-rev vibration and, in the aircraft, will always be associated with the primary 1-per-rev vibration, the test requirement was modified to superimpose the 20.8-Hz frequency onto the 2.6-Hz frequency. The revised test requirement is shown in Table 28.

Two new gland assemblies were fabricated and installed in a double ended gland development slave rig. One had an inner dynamic seal of rubber/fabric construction similar to the surface used on the basic unit. The other was a molybdenum filled Teflon ring. Both glands completed 12 hours of testing before leakage of the Teflon ring stopped the test. The rubber/fabric seal was also worn so that it was apparent that the test life would not be obtainable.

Another gland design, similar to a type previously developed, was fabricated and installed in the isolator. This was a preloaded Teflon composite design. This design leaked after 26 hours of testing. The failure was due to the deflection of the gland backing ring, causing a deposit of bronze on the piston rod, and inadequate preloading of the sealing elements. A revised design able to overcome these deficiencies appears feasible.

TABLE 28. REVISED TEST PLAN VIBRATION SPECTRUM.			
Unit Preload lb	Hours	Frequency Hz	Amplitude Inch
10,000	7½	2.6	$\pm .0725$
		20.8	$\pm .0045$
	2½	10.0	$\pm .045$
20,000	75	2.6	$\pm .0725$
		20.8	$\pm .0045$
	25	10.0	$\pm .045$
25,000	7½	2.6	$\pm .0725$
		20.8	$\pm .0045$
	2½	10.0	$\pm .045$

A gland assembly, using the same design concept as that originally tested, was installed in the isolator and subjected to the revised vibration spectrum. This gland completed the test's requirements. Leakage occurred when the unit was locked in a loaded condition for 60 hours, 1.2 cubic inches of fluid being lost. No leakage occurred after the tests were resumed. Teardown of the gland after the test showed the seal to be in good condition although the leather anti-extrusion ring was badly worn.

Typical oscillogram records of the Lissajou display are shown in Figure 65.

The major difficulty in obtaining a satisfactory life is the overall gland size restriction imposed by the installation geometry which prevents the use of a gland O.D. to I.D. ratio of the same order as previous designs. Gland failure results in a progressive leakage pattern, apparent by fluid visible on the outside of the isolator piston rod and by the position of the recuperator piston. As shown in Table 27, the unit continued to operate for over 25 hours after initial leakage before the unit became ineffective.

#### Proof Load Test

The objective of this test was to prove the mechanical integrity of the unit at limit load. In this test, the isolator was filled and inflated to 2,230 lb/sq in, and mounted in the 67,200-lb capacity test machine. An end load of 50,000 lb was applied and held for two minutes. During loading and unloading, the load sensor calibration was checked with the results shown in Table 23. There was no permanent distortion of the unit except for a slight indentation of the gland nut outer face caused by the piston rod. Figure 66 shows the affected area.

The isolator was then subjected to five full closure cycles with no leakage.

#### Proof Pressure Test (Liquid Spring)

The objective of this test was to prove the pressure vessel integrity at 1.25 times the maximum fluid pressure.

To over-pressure the unit an aluminum slug was inserted in the oil chamber next to the recuperator. The isolator was then filled and pressurized to 2,230 lb/sq in. From previous load/deflection curves, the end load needed to generate a pressure of 30,900 lb/sq in. was determined

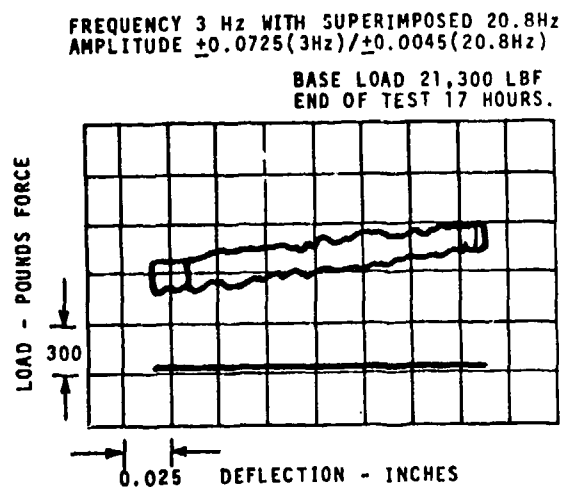
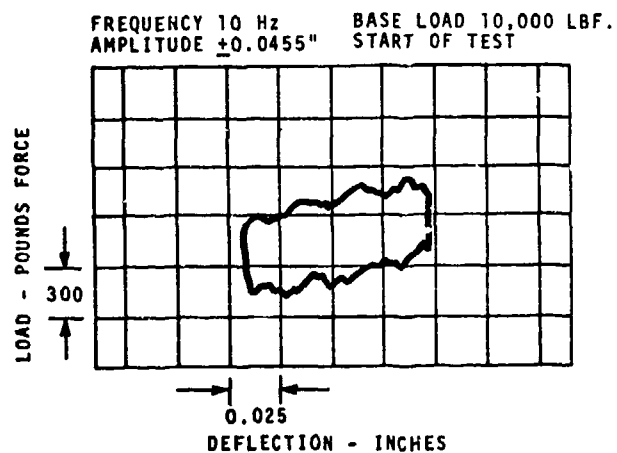
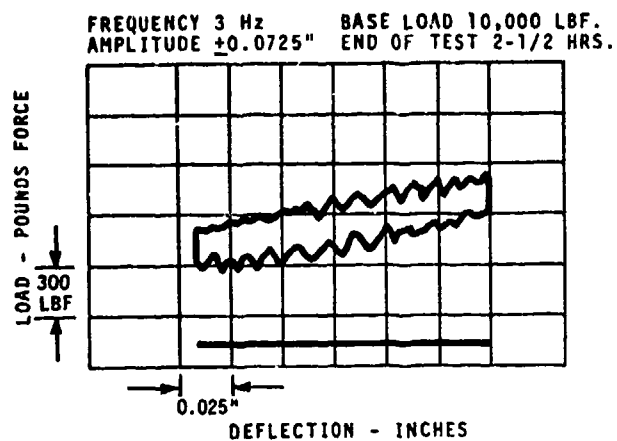


Figure 65. Typical Vibration Test Oscillogram Displays.

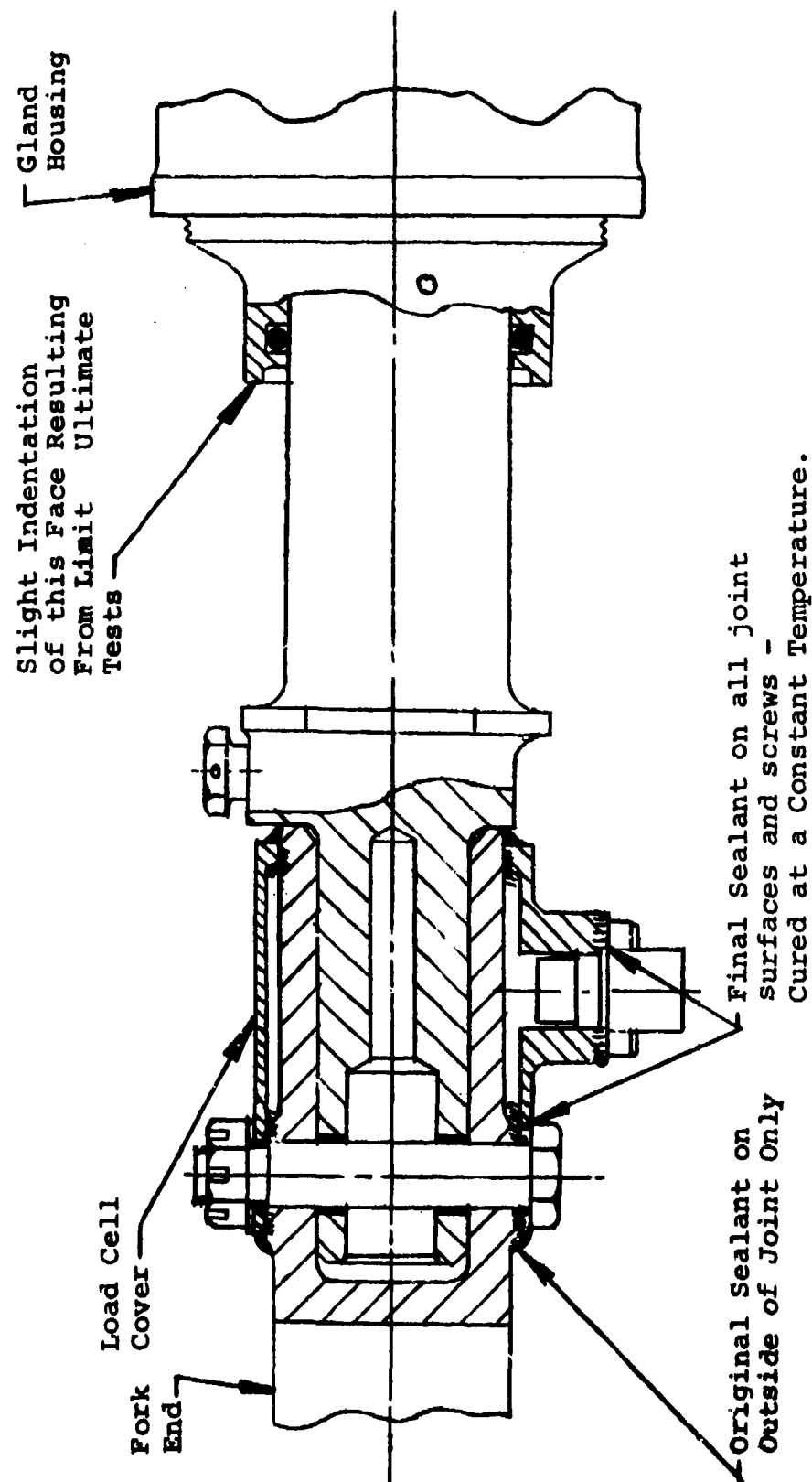


Figure 66. Load Cell Sealing.

38,500 lb. The unit was then loaded in the Avery 57,200 lb testing machine but the piston rod bottomed at 36,200-lb end load. To increase the load before bottoming, the recuperator gas chamber was filled with oil and pressurized to 2,500 lb/sq in.

The proof pressure test was then performed satisfactorily, the 38,500 lb load being obtained at 7.43 inches piston rod stroke. The load/deflection curve is shown in Figure 67.

There was no permanent deformation of the unit or leakage from the isolator.

#### Proof Pressure Test (Recuperator)

The objective of this test was to ensure the integrity of the recuperator at proof pressure.

The recuperator gas volume was filled with oil and pressurized to 3,260 lb/sq in. Pressure was held for two minutes with no visible distortion or leakage.

The isolator was then dismounted and dimensionally checked. Due to the numerous times the unit had been dismantled and reassembled during testing it was impossible to obtain comparable figures for all dimensions recorded prior to the test start. Those dimensions that could be compared are recorded in Table 21.

#### Ultimate Load Test

The objective of this test was to ensure that the unit is capable of accepting the ultimate end load without failure.

After teardown, the unit was reassembled in the normal way except that the recuperator was filled with oil (as a safety measure) and pressurized to 2,000 lb/sq in.

The isolator was installed in the 448,000-lb testing machine and loaded to 75,000 lb. The load was held for 2 minutes. Deflection readings were taken during loading and unloading; these are plotted in Figure 68.

There was no sign of leakage, rupture, or collapse of the unit during this test. There was a slight indentation, approximately .010 in., on the gland nut outer end due to contact with the piston rod shoulder (see Figure 66).



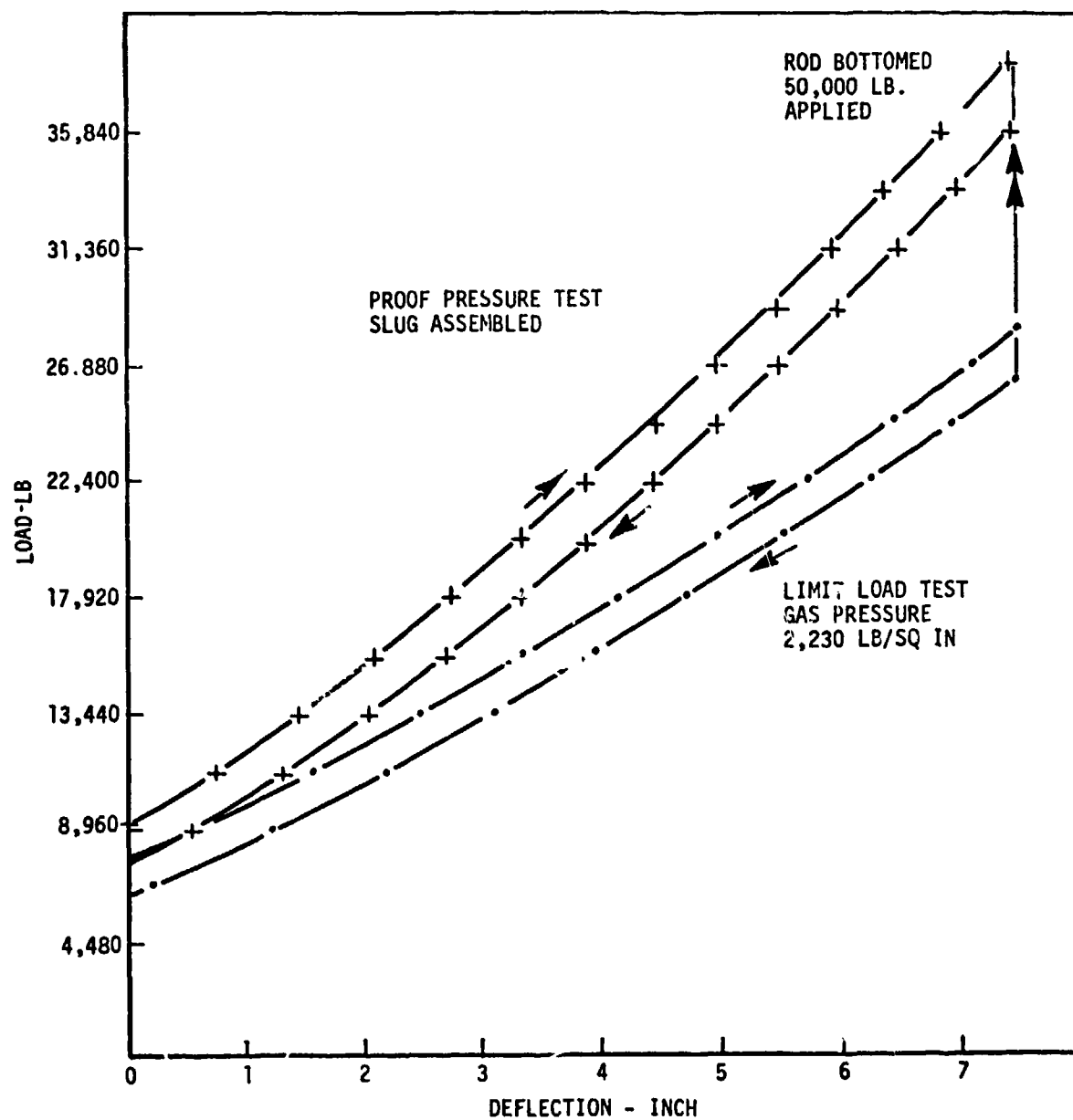


Figure 67. Limit Load and Proof Pressure Tests.

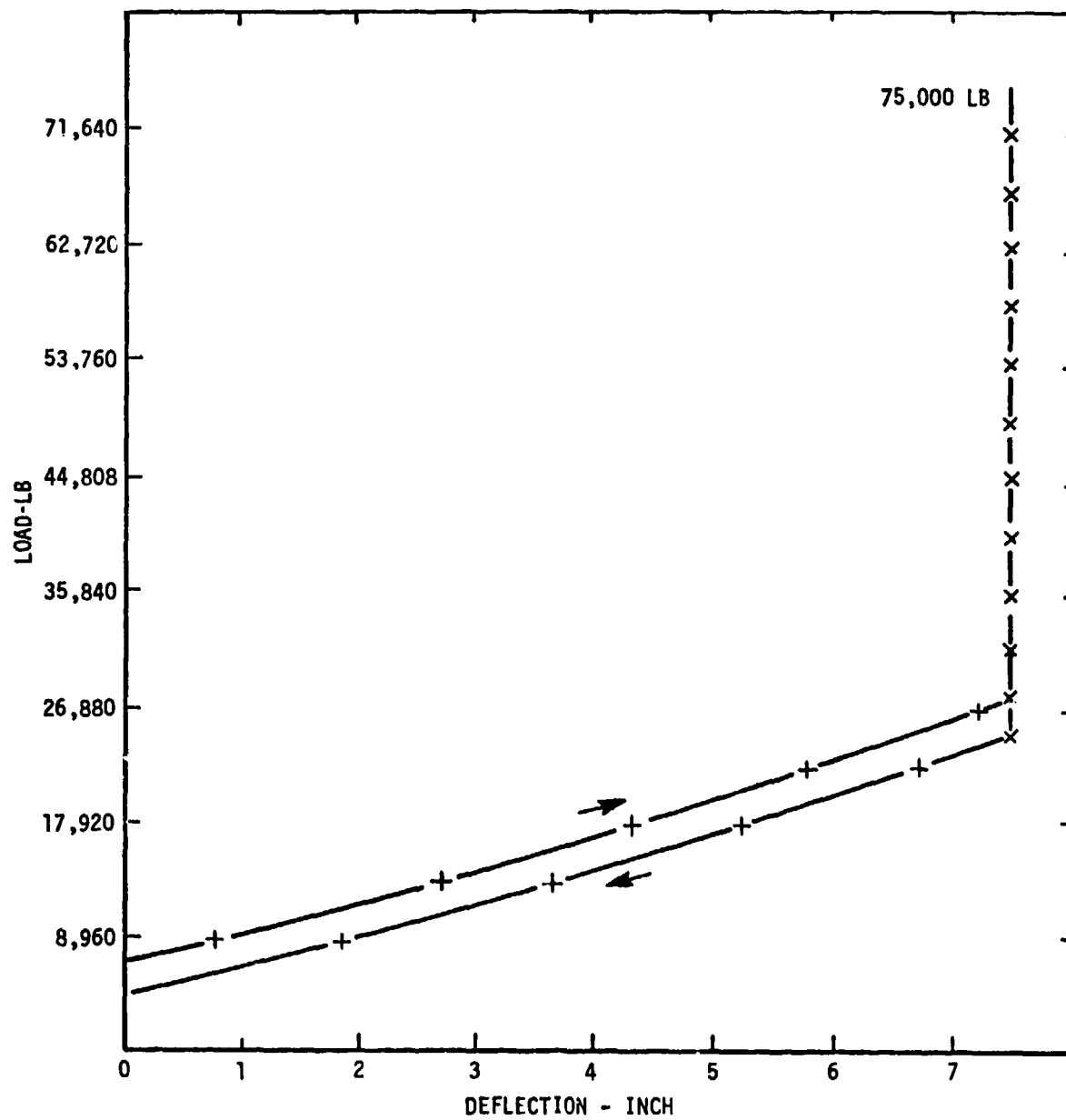


Figure 68. Ultimate Load Test.

### Load Sensor Test to MIL-STD-810B

The load sensor was checked for water leakage in accordance with MIL-STD-810B, Method 512, Procedure I. The test conditions dictated by this procedure are that:

"The temperature of the water shall be  $18^{\circ} +5^{\circ}\text{C}$  ( $64^{\circ}\text{F}$ ) and the temperature of the test item shall be  $27^{\circ} +3^{\circ}\text{C}$  ( $49^{\circ}\text{F}$ ) above the temperature of the water used for the test. The water container shall have sufficient capacity so that the immersion of the test item will not raise the temperature of the water more than  $3^{\circ}\text{C}$  ( $5^{\circ}\text{F}$ )."

The procedure dictated that the test be performed as follows:

"Immerse the test item in the water so that the uppermost point of the test item is  $36 +5 -0$  in. below the surface of the water. The test item shall remain immersed for  $120 +5$  minutes. Upon completion of the test period, remove the test item from the water and wipe the exterior surfaces of the test item dry. Open the test item and examine the interior and contents for evidence of leakage."

Any evidence of leakage constitutes failure.

The first test, on the original sealing, failed. This was thought to be due to the sealant having been applied only on the outsides of the joints as shown in Figure 66.

For the second test, sealant PR1422-2 was applied to the joint faces in addition to the outsides of the joints. But this test also failed, due to seepage through the smaller outer joint because the sealant had cracked.

For the third test, Sealant PR 1422-BT2 was used in the same manner as in the second test. This sealant is more flexible than the PR 1422-2. The unit was placed on a radiator to hasten the curing process, as was done in the second attempt, but it was noticed that this resulted in a buildup of air pressure which forced air bubbles through the outer end joint, creating a leakage path. This was probably the cause of the second test failure also, and therefore, the curing of the sealant must be performed at a constant temperature.

The joint was resealed and cured in a constant temperature, after which the immersion test was performed satisfactorily.

### Data Reduction

Data obtained from the load deflection tests is recorded directly as a load deflection plot as shown in Figures 57, 62, and 63. From these curves, the effective spring rate at the tension member was derived.

### Derivation of Effective Spring Rate at Tension Member

The installation geometry of the load isolator in the hoist assembly is shown in Figure 69. The tension member (cable) has a radius of 9.35 inches, and the relationship between isolator travel, cable travel, and the ratio of cable tension/load isolator force has been calculated and is shown in Table 29.

Using this ratio in conjunction with the mean value of the isolator load deflection curve, a curve of cable tension versus cable movement may be constructed. A curve derived from the room temperature isolator load deflection is shown in Figure 70. The rate of change of this curve when plotted against cable tension results in the cable spring rate curves shown in Figure 60.

### Conclusions

The development tests established that the dynamic characteristics of the isolator are within the defined limits.

The testing confirmed the strength of the unit as a strut up to the ultimate load, and its strength as a pressure vessel up to 1.25 times maximum working pressure.

Vibration testing has shown that the gland life is influenced by the test method. Superimposing the higher frequency, low amplitude movements onto the basic one-per-rev vibration resulted in a considerably improved life. Cylinder fluid pressure also has a very marked influence on gland life; the loading spectrum used for these tests was severe. Service life in an aircraft environment is therefore expected to be extended beyond that demonstrated during the tests. It is concluded that the isolator is suitable for use in the prototype aircraft.

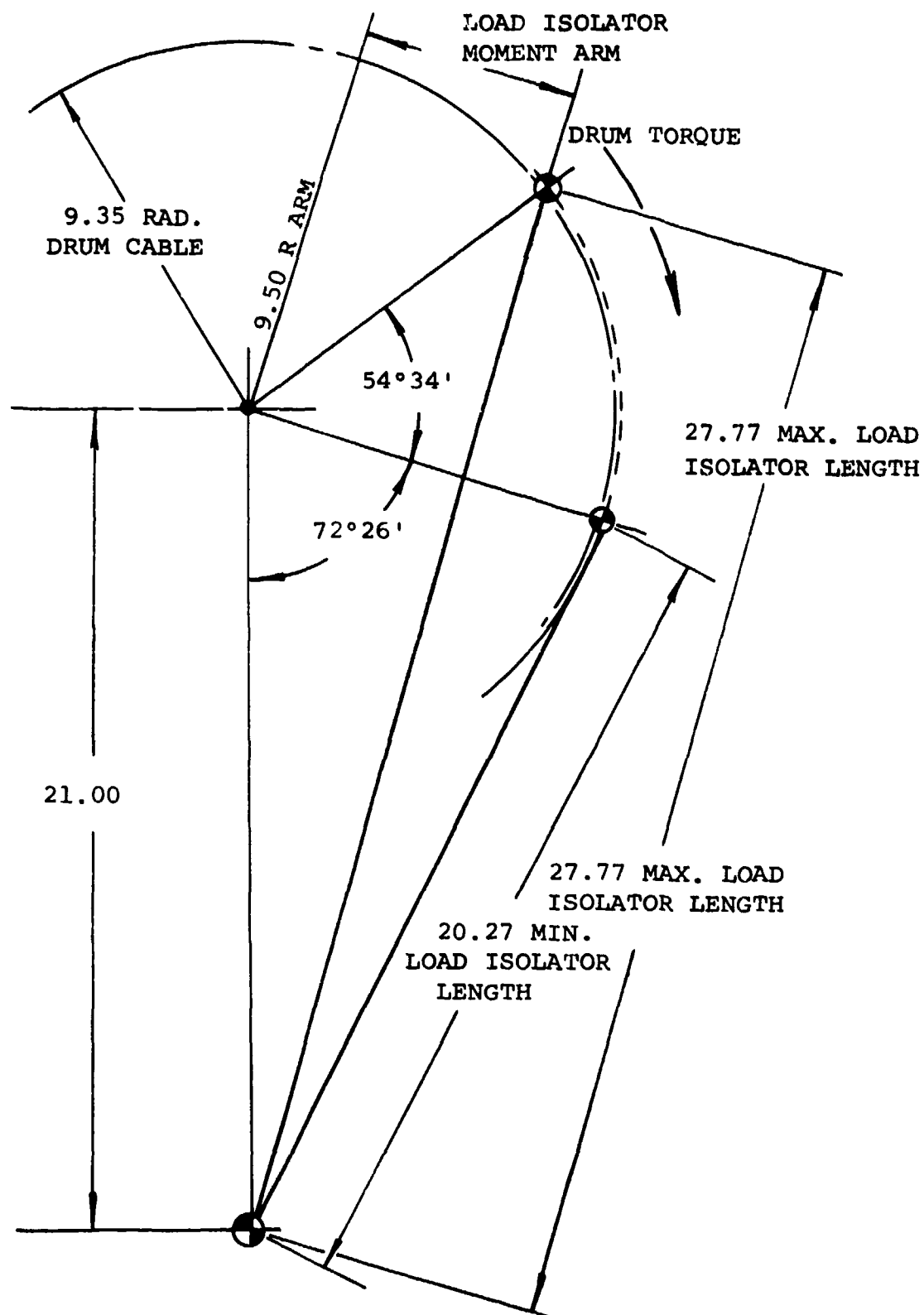


Figure 69. Load Isolator Installation Geometry.

TABLE 29. LOAD ISOLATOR GEOMETRY RATIOS.		
Isolator Stroke Inch	Cable Travel Inch	Ratio Cable Tension Load Isolator Force
0	0	.614
1	1.51	.706
2	2.86	.780
3	4.09	.843
4	5.24	.894
5	6.33	.937
6	7.39	.970
7	8.40	.995
7.5	8.90	1.003

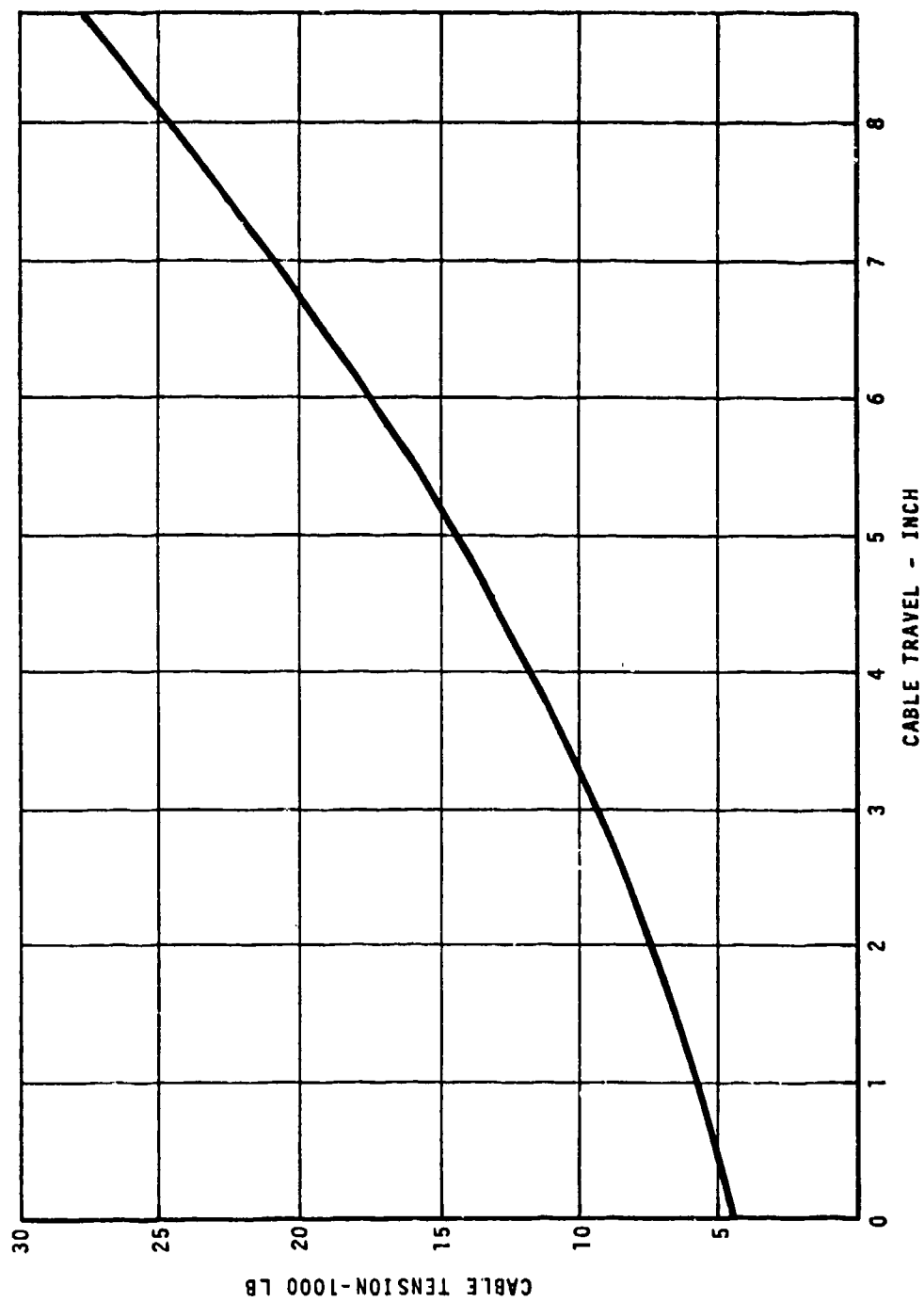


Figure 70. Equivalent Load/Deflection at Cable.

### Recommendations

Due to the limited life of the isolator gland assembly established by the test, it is recommended that further development work be initiated to improve the life of this component. Two approaches should be considered:

1. Continued development of a gland within the existing envelope.
2. Designing an optimum sized gland based on previous experience, and assessing the impact of the enlarged gland housing on the hoist design.

The requirements for the isolator, as established in the specification, should be confirmed by suitable instrumentation in the HLH prototype airframe.



## SPAN POSITIONING (TRAVERSE) SYSTEM

### DESIGN DEVELOPMENT TESTS

#### Description

The span positioning (traverse) system consists of two cable circuits attached to each hoist which, via an arrangement of pulleys, connect to a single electrically powered capstan drum. Rotation of this drum in the clockwise direction moves the hoist in one direction, rotation in the counterclockwise direction moves the hoist in the opposite direction.

The electrically powered capstan drum is based on a standard electric motor used in other cargo handling applications, a conventional gear reduction box, and an external metal drum. Design development testing consisted of verification that the adaptation of these standard elements into one package for this application was done properly and did not create any new problems.

Actual weight of the unit was 14.75 lb, which met the requirement of 15.0 lb or under.

#### Unit Performance Test

This test established that the unit will drive a 2,900-in-lb torque load (967-lb cable tension load) at 4.25 rpm in the clockwise direction and 4.3 rpm in the counterclockwise direction, which met the requirement of 4 rpm in either direction. The test was performed at room temperature using the setup shown in Figure 71. The maximum line to neutral current drains in the clockwise and counterclockwise directions were 1.5 and 1.4 amperes, which met the requirement of 2.0 amperes or less.

#### Manual Input Test

This test established that a 50-in-lb maximum torque applied to the manual input will drive a 2,900-in-lb torque load at the output shaft (967-lb cable tension load). The test was performed at room temperature using the setup shown in Figure 71. The motor remained off during this test. Both the clockwise and counterclockwise directions of drum rotation were checked.

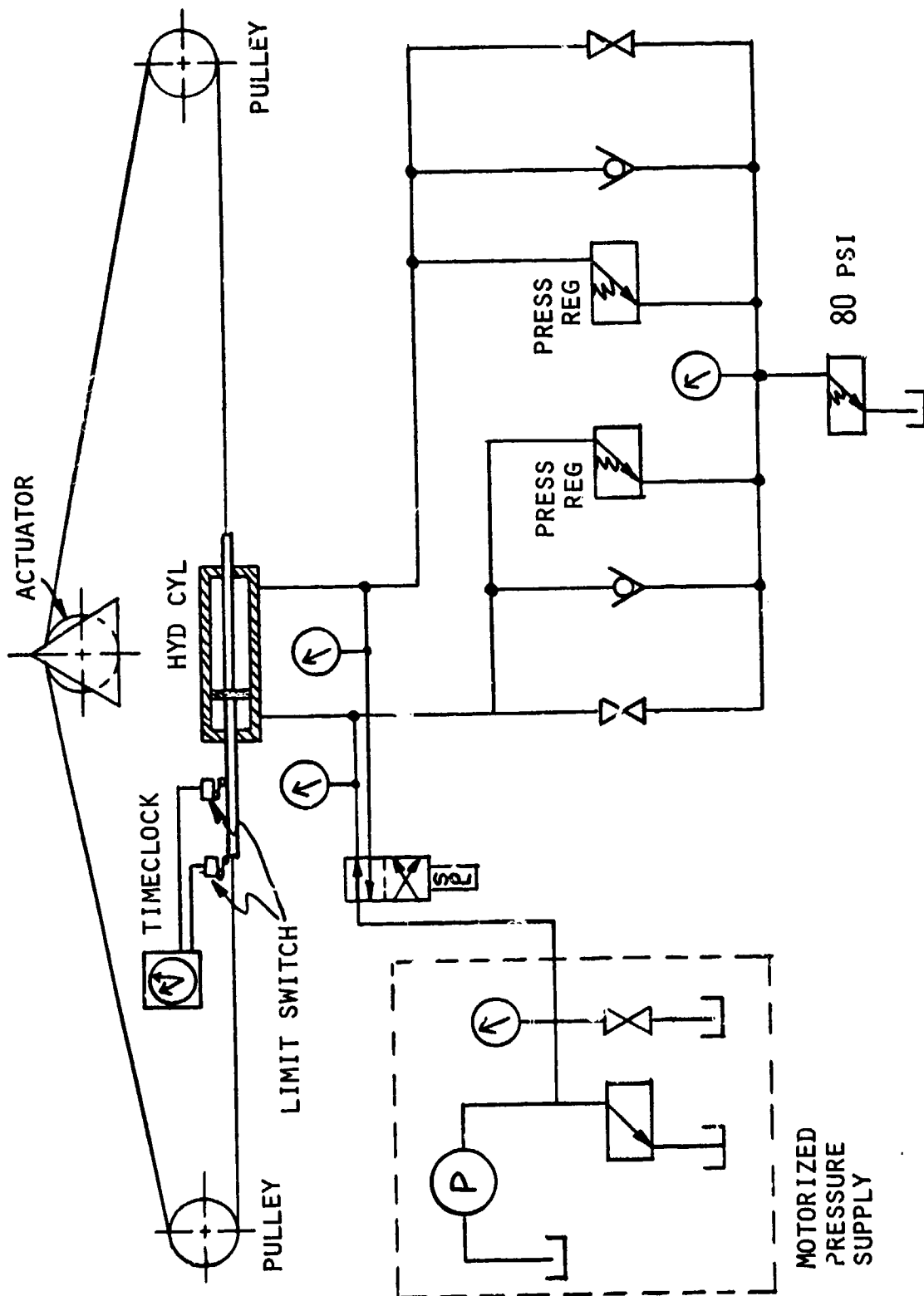


Figure 71. Hydraulic Loading Fixture.

### Holding Torque Test

This test established that the static holding torque of the brake exceeded the requirement of 7,200-in.-lb. This test was performed at room temperature using the setup shown in Figure 71. The motor remained off. A cable tension of 2,400 lb was applied, and it was then verified that the cable drum did not slip. Both the clockwise and counterclockwise directions were checked.

### Duty Cycle Test

The test fixture shown in Figure 72 was utilized for this room temperature test. A torque load of 2,900-in.-lb was applied in both the clockwise and counterclockwise directions. The system was then operated for two hours by repeating the following cycle:

1. 43-second clockwise rotation (60.4-in. cable travel)
2. 48-second counterclockwise rotation (60.4-in. cable travel)
3. 10-minute rest period.

All testing was satisfactorily completed. The unit performance test manual input test, and holding torque test, described above, were repeated satisfactorily to verify that the duty cycle test had not caused any damage to the unit.

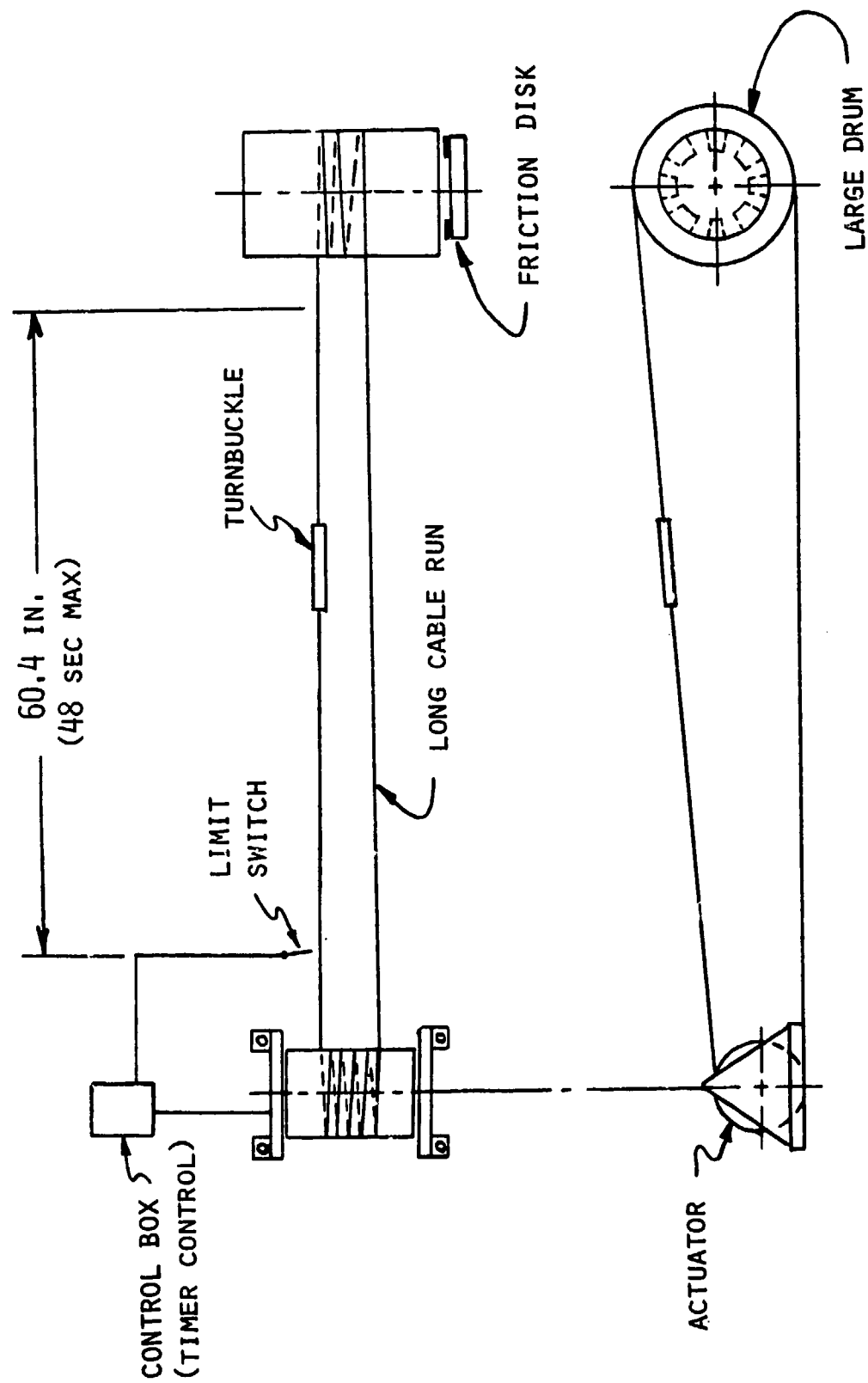


Figure 72. Loading Fixture for Duty Cycle Test.

## CABLE CUTTER

### DESIGN SUPPORT TESTS

Cable cutter development was undertaken by the U.S. Army's Frankford Arsenal. A summary of the results of the Army testing is presented here for completeness.

Preliminary tests were conducted to check the quantity of charge and the operational integrity of the cutter. These tests were conducted at ambient temperature using two charges and a single initiator activated with a 5-ampere current to the initiator bridge wire. Two one-grain WC230 propellant charges sealed in two separate chambers and ignited by separate XM47 electric ignition elements were selected for the final configuration.

### Design Development Tests

A total of 32 test firings were conducted over the temperature range from -65°F to +160°F on the final cutter configuration using samples of the 36 x 7 Heavy Lift Helicopter (HLH) tension member. To simulate the HLH installation, only one of the two available bridge wires in the initiators was activated. (NOTE: The XM47 initiators used contain two bridge wires of 1.1M ohms resistance each.)

A typical test cycle is outlined below:

1. The cutter assembly, including a section of 36 x 7 tension member, was cold soaked at -65°F for 4 hours.
2. The cutter was removed from the cold chamber and mounted in a pipe vise in the test chamber.
3. Test wiring was immediately connected to the cutter. This included a 28-volt DC firing circuit to one XM47 initiator. A second live XM47 initiator was not hooked up. A monitoring circuit which times the actual cable cutting was also hooked up. A chamber pressure sensing device was attached.
4. A 5-amp signal was applied to the initiator.

The results of -65°F firings were:

1. The cable was cut cleanly.
2. The actual time to cut the cable was .002 second with a peak gas pressure of 4,900 to 5,000-psi.

3. The knife was imbedded in anvil 0.125 inch.
4. The anvil, the knife, and the knife piston were all in good shape and were easily dismantled from the body as a unit for visual inspection.
5. The fired initiator had no continuity in either bridge wire.
6. The unconnected initiator was not fired. Each bridge wire of this unit was checked and found to have a 1Mohm resistance.
7. The knife body was hard frame anodized aluminum and showed only scorching from the powder and no apparent metal deterioration.

Testing included a simulation of the worst possible combination of factors which might prevent ignition. These included: cold temperature (-65°F), one failed electrical supply source, one faulty powder charge, and low output on the second electrical supply source. A single charge was used with a dummy installed to simulate the volume of the second charge. Only one initiator was activated with the current limited to 3.75-amperes instead of the normal 5-amperes. The cable was cut cleanly.

To demonstrate cutter integrity in the highest pressure producing conditions, a hot day test was performed. This consisted of presoaking the cutter to a stabilized temperature of +160°F, using two powder charges, and activating both initiators simultaneously. The cutter body remained intact.

No malfunctions or safety hazards were experienced during any of the tests and all cutters remained intact after firing. The estimated probability/reliability of safe functioning based on these firings, was 93% minimum at the 90% confidence level.

The reliability of the cutter initiation system was further demonstrated by testing at Boeing Vertol. The test involved repeatedly applying power to a simulated squib firing circuit using electrical hardware equivalent to that proposed for the HLH prototype. The test required 532 operations of the switch and acceptance criteria required two or fewer failures. The test was completed with no failures.

A further test involving the cable cutter was the Phase III test conducted on a hoist assembly by Western Gear Corporation as part of the hoist development test program. To demonstrate the hoist cable hold-down features, a cable assembled to the hoist was loaded to design load (16,800 lb) and then severed using the cable cutter system. The cable was cut cleanly, with the cutting knife penetrating the anvil 0.43 inch. Figure 73 shows the cutter and anvil after this test. The hold-down system held the severed end of the cable in the drum grooves as desired.

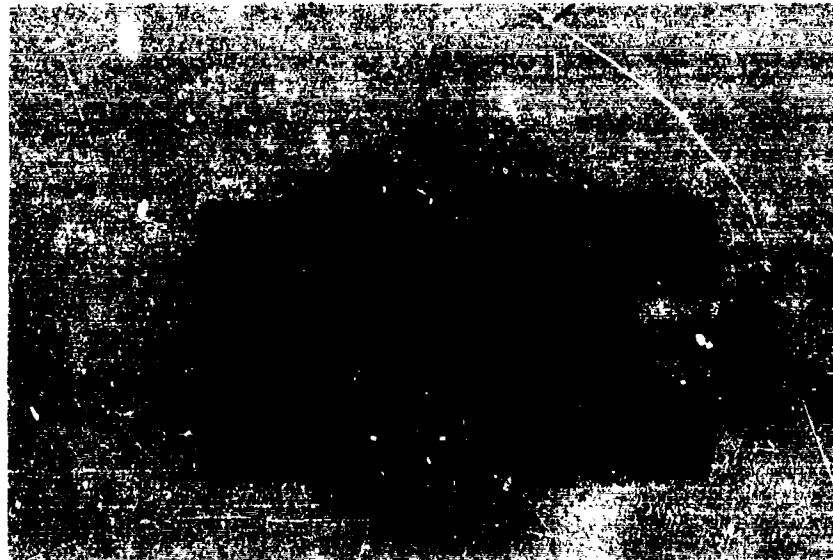


Figure 73. Cutting Knife Penetrating Anvil 0.43 Inch.

## TENSION MEMBER

The tension member testint consisted of design support and design development testing phases for the cable and design development testing for the end fittings.

The design support tests were conducted in order to select a candidate material and construction for development that best fit the ATC criteria and to prove the "paired cable" concept. Design development tests were conducted to develop suitable end fittings and to substantiate the adequacy of a smaller-diameter cable and end fitting designs for both the multi-point and single-point applications.

### DESIGN SUPPORT TESTS

#### Introduction

This section presents the results of design support tests which consisted of the following:

1. Anti-corrosion Feasibility Study
2. Nonmetallic Tension Member Feasibility Study
3. Metallic Tension Member Study

All tests were conducted between January and July 1972. The tests conducted and the results obtained are described and discussed below.

#### Test Objectives and Philosophy

The objective of these tests was to study new technology in materials and constructions not previously used in hoisting tension members and to evaluate them in comparison with the best conventional possibilities. Applicable new technological advances were constrained by the ATC timeframe and manufacturing feasibility.

Particular problems investigated during the course of the work were: inhibiting corrosion of carbon steel wire, and the use of low-density, high-strength fibers.



## Tension Member Anti-Corrosion Feasibility Study

### Nickel-Boron, an Anti-Corrosion Coating Material

The nickel-boron coating is a wear and corrosion-resistant plate of nickel alloy. It may be applied over a range of .1 mil to 10 mils. Its thickness varies less than 5%. Its corrosion resistance is dependent on the coating thickness, and it may be hardened by heat treatment with a 90-minute soak in a temperature range of 300° to 400°C. The coating is hard, tough, refractory. Its lubricity provides excellent resistance to both lubricant and unlubricated wear. The coating reduces the coefficient of friction of steel-on-steel approximately an half. Its surface is wetted by oil but not by water.

The objective of this design support study was to determine the feasibility of using a new electroless nickel-boron coating on high-strength carbon steel wire to resist corrosion and to determine the compatibility of the coating with the processes involved in cold wire drawing and wire rope construction. Another important attribute of the Ni-Bo coating was its abrasion resistance. While this characteristic could also be used to advantage in possibly improving cable life, it was of secondary importance.

### Test Specimen Design

The nickel-boron coating was applied in place of zinc on partially drawn and patented wire before finished drawing was accomplished. The coated wire was then cold reduced by 89% to its final use size and strength with normal drawing procedures. The suitability of the nickel-boron coating after drawing was evaluated by visually inspecting the coating continuity, and by performing physical properties tests and salt-fog exposure tests. The combination of commercially applied zinc over the nickel-boron coating was also evaluated after cold reduction of 91.5%.

The wire used for this study was a typical high-strength carbon steel identified as ACCO-VHS, supplied in a .105-inch diameter (drawn from .281 to .312 inch diameter rod). An intermediate heat treat performed before drawing to .105 inch was followed by patenting (heat treatment to 1,100°F followed by quenching in a lead bath) in preparation for drawing to final size. The coating was applied by dipping in an electroless nickel-boron bath at 90°C. The coating

thickness used for the tests was .4 mils. Prior to subjecting the .105 inch wire to cold reduction, wire physical property, coating adhesion, and corrosion tests were conducted.

Next, the sample wire was drawn using conventional drawing lubricants and processes. The established ground rules eliminated the use of special equipment or lubrication during the final drawing process.

A second series of tests were run with hot dipped zinc applied over the nickel-boron coating. This zinc/nickel-boron coated wire was then cold drawn, and corrosion tests were repeated. The zinc over nickel-boron was introduced to provide a sacrificial (anodic) medium for subsequent evaluation with the high abrasion resistance of the nickel-boron coating.

Corrosion tests were conducted following methods conforming to MIL-STD-810B, Method 509-1-509-4, and Federal Test Method 151a, Method 811.1. A salt-fog chamber was used with a 5% salt solution at 95°F and additional tests were conducted by immersion in an agitated 95°F aqueous solution of 5% salt.

#### Test Results

Drawing of the .4 mils nickel-boron coated wire from .105 to .0345 inch diameter was successful in that it proved the satisfactory adhesion on the nickel-boron to the wire. The continuity of the coating however, was unsatisfactory in that the coating did not flow completely, resulting in fissures in the surface. This surface condition is shown in Figure 74. Corrosion encountered in pinholes in the predrawn coating are shown in Figure 75.

In the second draw, with zinc applied over the nickel-boron coating, the zinc was worked into the fissures in the nickel-boron coating by the first few dies but was peeled off the wire completely by the sixth die. These conditions are illustrated in Figure 76. Post-drawing corrosion tests of samples taken after each die were unsatisfactory.

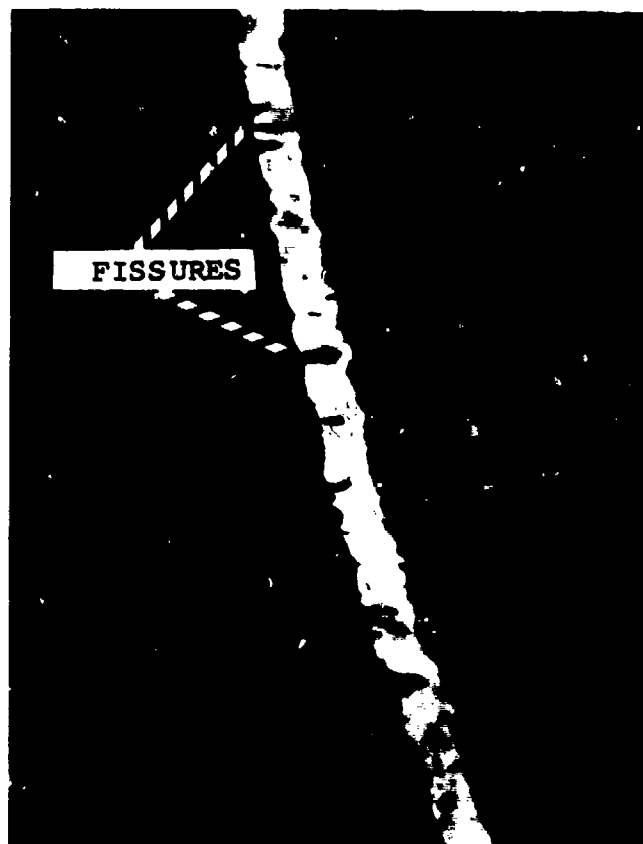
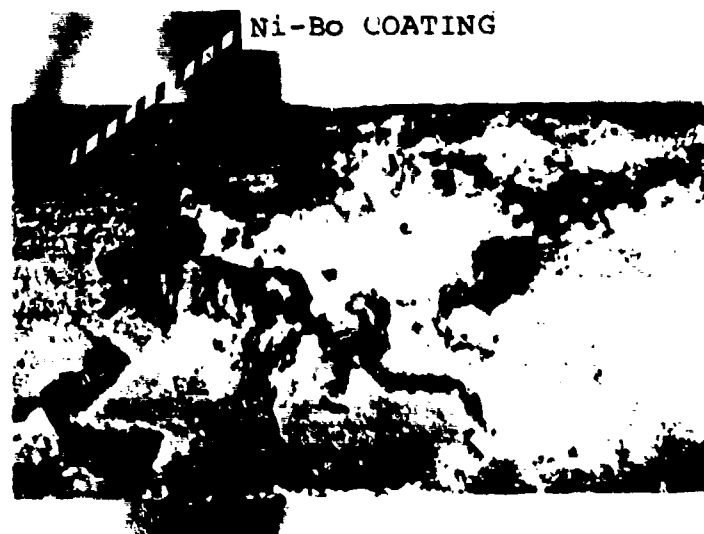


Figure 74. 400X-Photomicrograph - Fissures in .4 mil Nickel-Boron Coating on .105-in Carbon Steel Wire after Drawing to .0345 in-dia.

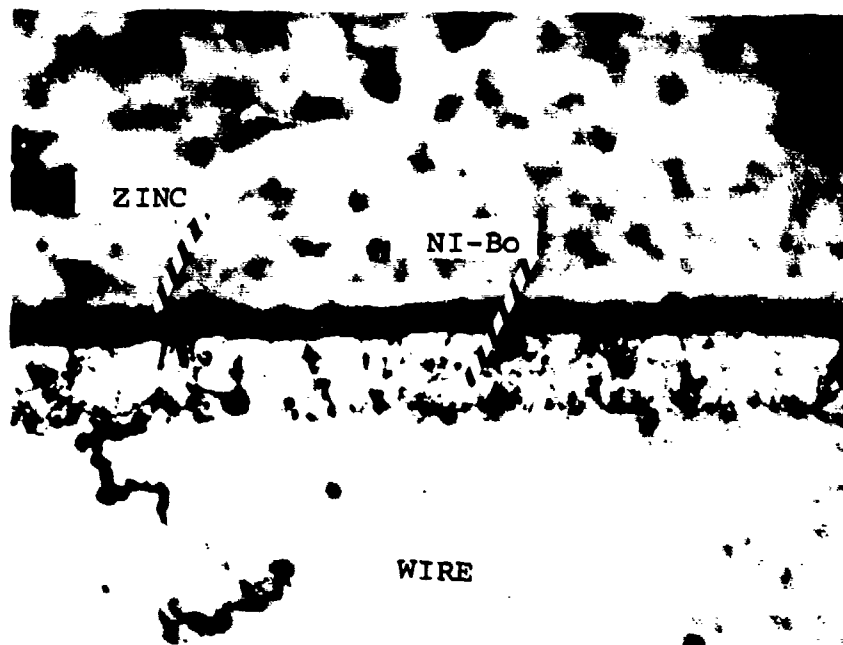


Corrosion resulting from 168 hours of exposure in salt-fog chamber - Nickel-Boron/Carbon Steel "as coated" sample.



Corrosion pit formed beneath pin hole in Nickel-Boron/Carbon Steel, .105-in wire sample before drawing, but after 168 hours of salt-fog exposure..

Figure 75. Corrosion at Pinholes in Pre-drawn Nickel-Boron Coating.



.080-in-dia after 2nd die



.030-in-dia after 8th hole

Figure 76, Zinc/Nickel-Boron Coating Condition During Wire Drawing Process.

Table 30 summarizes these evaluation activities with comments on wire physical properties and the tolerance of the coatings to the drawing process.

The tests proved that:

1. A .1 mil thick zinc coating, applied to the nickel-boron coating after drawing, did not provide adequate corrosion protection.
2. Zinc applied to nickel-boron coated wire by the hot dip process before drawing did not survive the drawing process well enough to provide adequate corrosion protection.

#### Nonmetallic Tension Member Feasibility Study

An investigation was made to determine the feasibility of using nonmetallic fibers such as Kevlar 49 (PRD-49-Type III) and Kevlar 29 (Fiber B) for hoisting tension members in view of their high strength-to-weight ratio characteristics.

#### Test Specimen Design

The test specimens consisted of fiber bundles or "building blocks" of 1/8 inch diameter. Variations in yarn twist, fiber finish, and bundle construction were evaluated to determine their influence on achieving maximum fiber strength. The manufacturer's yarn properties are as follows:

<u>Parameter</u>	<u>Kevlar 49</u>	<u>Kevlar 29</u>
% Elongation at Break	2.1	4.2
Tenacity, Grams/Denier	21	20-22

#### Tests

This feasibility study consisted of two phases of design support tests. The first phase included static and environmental tests; the second, an evaluation of fatigue characteristics and a determination of tensile properties of simple end termination techniques.

TABLE 30. SUMMARY OF NICKEL-BORON COATING EVALUATION.

Test Specimen	Visual Examination	Physical Properties	Corrosion Tests	Remarks on Fabrication Process
Nickel-Boron: "as coated" (.105 wire; .4 mils Ni-Bo)	Gold color, smooth and slippery	No change	Corrosion of wire under Coating at Pinhole Locations	Coating not 100% Continuous. Pinholes noted.
Drawn Ni-Bo Coated Wire (.105 Wire with .4 mils Ni-Bo)	Excellent appearance and lubricious feel. Fissures noted at 400X magnification. Coating not continuous.	Satisfactory as drawn-wire physicals.	Unsatisfactory corrosion resistance.	Drawing process hotter than normal. Vaporized sodium stearate drawing lubricant (soap).
Drawn Zn/Ni-Bo Coated Wire (Hot Dip Zn over .105 Wire with .4 mils Ni-Bo)	Coating removed and wire scratched.	Satisfactory as drawn-wire properties.	Unsatisfactory corrosion resistance.	Zinc was deposited in Ni-Bo Fissures early in draw, but zinc peeled off by sixth die. Normal high temperature drawing lubricants heated beyond burning point caused rapid die wear.
Zn/Ni-Bo Comparison with Electro-galvanized Mill Run Wire. (.040 and .068 inch diam. with .25 mils Post Drawn Zn Coating)	--	--	Combination of drawn Zn/Ni-Bo and electroplate Zn over drawn Ni-Bo were inferior to mill run drawn Zn coated wire.	--

### Elongation, Strength, and Fatigue Tests

Tests included tensile elongation, over-a-drum tensile strength, and bundle fatigue characteristics when bent over a (hoist) drum. Fiber stresses representative of actual conditions were used. Temperature, abrasion, and ultraviolet degradation factors were investigated.

The initial tests involved study and development of the fiber bundle configurations of Kevlar 49 to achieve optimum strength characteristics.

Procedure - In order to establish design criteria for a full-scale tension member, developed strength and losses to be considered in the cable elements were determined by test. One-eighth inch (nominal) diameter yarn bundle "building blocks" were developed from the 380 denier singles yarn by successive additional twisting and plying stages using prescribed total twist levels of 3, 5, and 7 turns per inch (TPI), respectively, in the yarn. Two proprietary yarn finishes, called A and B, applied by the manufacturer were used in tensile tests.

The study plan was to:

1. Select yarn bundle candidates with the best strength properties as determined by static tests.
2. Conduct bend-over-drum fatigue tests at representative tensile and bending stress levels.
3. Design and evaluate two end termination techniques.

New fabrication and test trials were established outside the scope of the original program in order to further explore:

1. Improved bundle efficiency
2. Effect of twist levels
3. Pure tension (tabbed samples without capstans).  
In this regard, two additional elements were introduced for comparative purposes:
  - a. Additional Kevlar 49 yarn bundles were developed producing a higher total denier and a more tightly constructed bundle.



- b. Yarn bundles were developed utilizing another organic fiber, Kevlar 29, having high tensile properties but with greater elongation properties than Kevlar 49.

The tensile sample (tabs), end terminations, and fatigue test machine are shown in Figures 77, 78, and 79.

### Test Results

An analysis of the test indicated a lack of conclusive data to show that the maximum potential of the Kevlar 49 fiber had been realized with the fiber twist level selected. Wide variances between like specimens within a given test lot and between test groupings indicated that variation in individual strand tensions within yarn bundles precluded a maximum strength configuration. Table 31 summarizes the tension, tension-over-drum, and high temperature tests for variations in twist and fiber finish.

Low elongation characteristics of Kevlar 49 (2%) tend to emphasize the difference between individual filament or strand lengths thereby preventing typical compensation for these variations that would contribute toward an "averaging" effect upon length, as would be the inclination of other materials exhibiting greater elongation properties. There was evidence of this effect when comparing test results of percent elongation at rupture load for Kevlar 29 and Kevlar 49. A comparison of tensile strength of reconstructed Kevlar 49 versus Kevlar 29 (Table 32) shows that for Kevlar 29 there was a consistency between specimens with an average rupture load of 1,123 pounds. The reconstructed Kevlar 49 shows considerable variation between specimens in tensile strength with an average rupture load of 1,006 pounds.

Fiber bundles of these materials were produced in all instances under identical procedure and equipment conditions. The higher elongation properties of Kevlar 29 (as given in Table 32) were evidently the significant factor contributing to the difference between the tests.

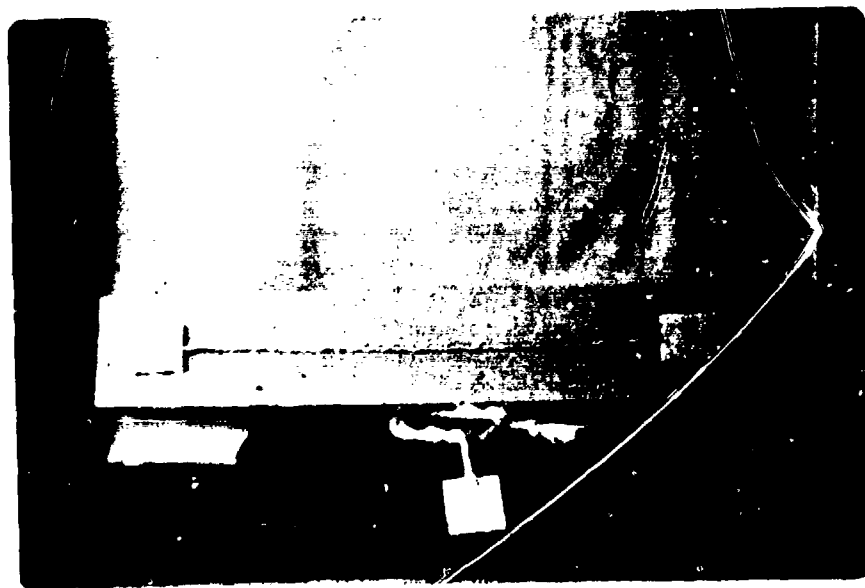
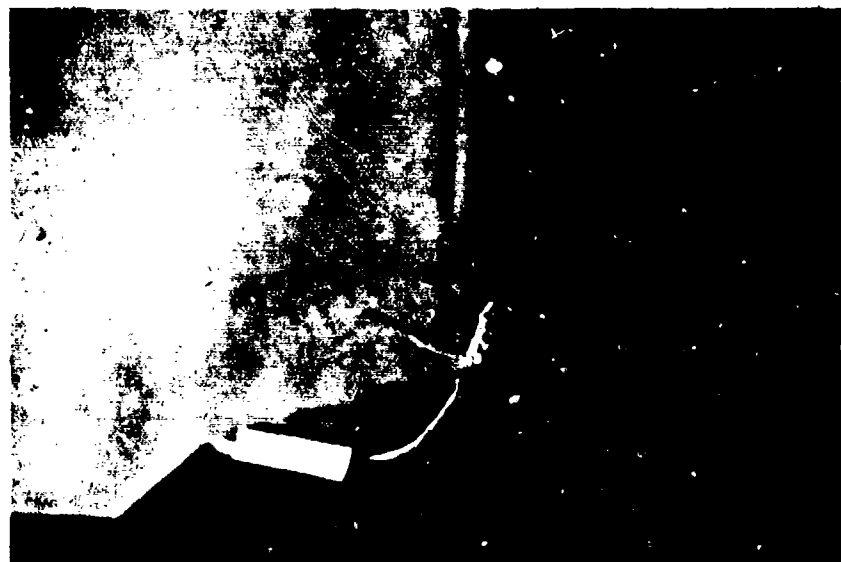
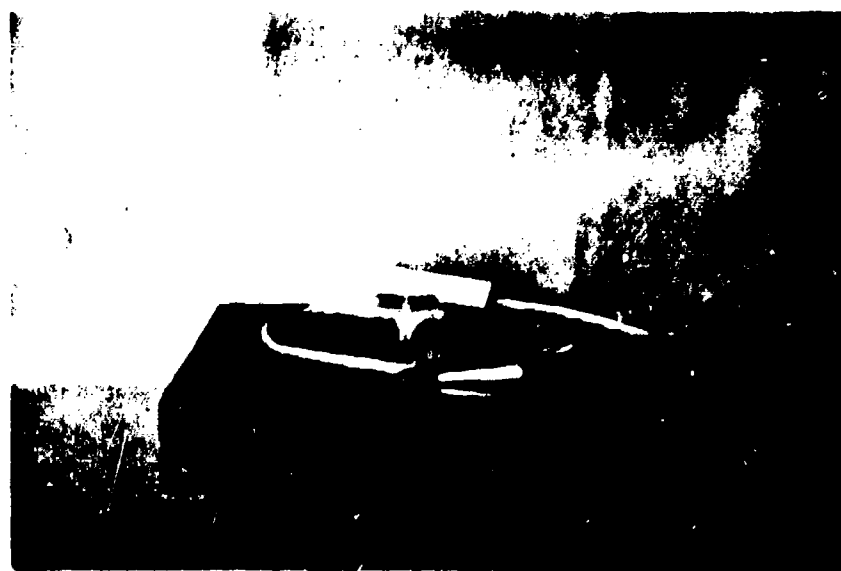


Figure 77. Aluminum/Epoxy Termination Specimen  
(DuPont).



Final cable strands back-braided to form tapered and epoxy termination (Prodesco)



Flared, combed fibers of yarn bundle forming a hollow conical form to accept tapered plug (Prodesco)

Figure 78. Kevlar 49 Termination.

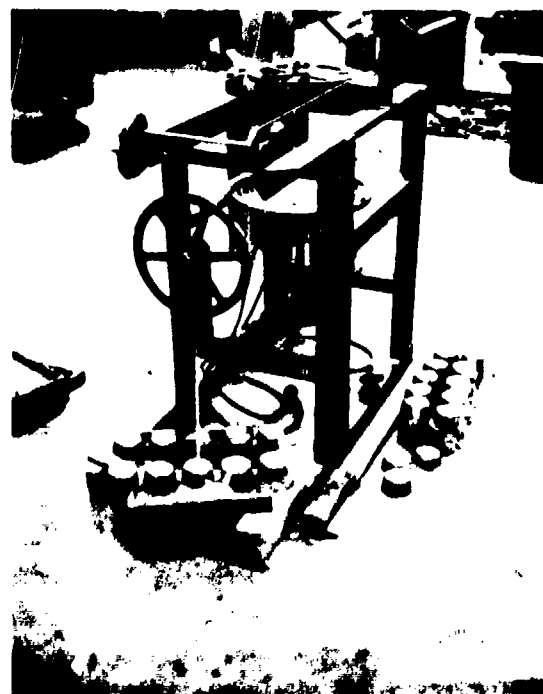
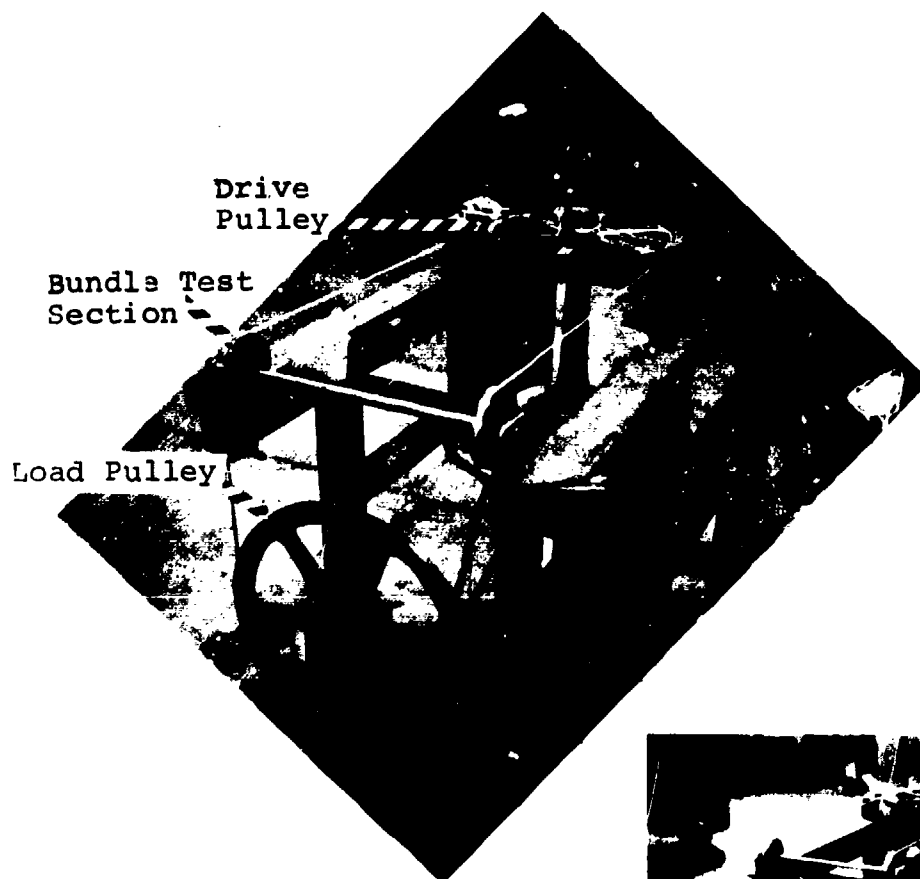


Figure 79. Fatigue Test Machine for Bend Tests of 1/8-in Fiber Bundles (Prodesco).

TABLE 31. AVERAGE TENSILE PROPERTIES OF KEVLAR 49 FIBER BUNDLES.  
(4-ply 6x4 construction, ambient and 160°F after 48 hour soak at 160°F)

<u>AMBIENT</u>		Singles Twist (tpi)	Cables Failed	32:1*		24:1*		15:1*		
Finish	Rupture Elong. (%)			Rupture Load (lbs)	Cables Failed	Rupture Load (lbs)	Cables Failed	Rupture Load (lbs)	Cables Failed	Rupture Load (lbs)
A	3	2	1.5	1270	1	1160	1	1100		
A	5	2.7	1.5	1240	1.7	1270	1.7	1170		
A	7	2.3	2.1	1180	-	----	-	----		
B	3	1.7	1.5	1060	1.3	1110	1.7	1040		
B	5	1	1.4	970	1	830	1	930		
B	7	2.3	1.2	1110	-	----	-	----		
<u>160°F</u>										
Finish	Singles Twist (tpi)	Cables Failed	Rupture Elongation (%)	Rupture Load (lbs)	Strength Loss (%)					
A	3	1.3	2.0	1120	12					
A	5	1.7	1.4	1090	12					
A	7	3.0	1.8	1090	3					
B	3	1.7	1.6	920	13					
B	5	1	1.6	930	4					
B	7	3.7	1.7	1000	10					
*Ratio of jaw diameter to cord diameter.										

TABLE 32. TENSILE PROPERTIES OF FIBER BUNDLES CEMENTED TO ALUMINUM TABS

Material Identification	Specimen	Cables Failed	Rupture Elongation (%)	Rupture Load (lb)	Location of Failure
Kevlar 49, (Singles Twist, 5 tpi), 4-ply 6x4 construction	A	4	1.9	1040	At epoxy
	B*	4	2.2	1140	At epoxy
	C	2	2.3	1040	1/2-inch from epoxy
Kevlar 29, 2-ply, 4x4 construction	A	1	6.7	1120	In gauge length
	B*	1	4.4	1140	At epoxy
	C	1	5.9	1110	At epoxy
Kevlar 49, Reconfigured Structure, 4-ply, 2x4x4 construction	A	1	2.9	1140	In gauge length
	B*	1	2.9	950	In gauge length
	C	1	3.4	930	In gauge length
*These specimens were loaded to 60% of rupture load, relaxed for 15 minutes, then reloaded to rupture.					

In comparing the original Kevlar 49 and reconstructed Kevlar 49 fiber bundles, the tensile test results for these fiber bundles (Table 32) indicated that although the total denier is greater in the reconstructed Kevlar 49, the higher twist employed in these specimens is apparently the factor contributing to their lower tensile strength. Test results obtained with the two end termination techniques are presented in Table 33.

Fatigue-over-drum tests conducted with the Kevlar 49 and Kevlar 49 reconstructed fiber bundles enclosed in a braided nylon jacket (sheath) showed that jacketed Kevlar performed better than its unjacketed counterpart. Comparisons are illustrated by the Figure 80 fatigue curve. The tests conducted at elevated temperatures showed average strength losses of from 3 to 13% after exposure and testing at 160°F. The small sample lots and variability in test results prevents a definite conclusion that the strength loss is completely attributable to the elevated temperature.

Tension-over-drum tests at ambient conditions suggest that somewhat better strengths are realized at the 24:1 D/d ratio than either 32:1 or 15:1. However, due to the prevailing tension unevenness or strand length, and variability within the fiber bundle as previously described, no definite conclusions can be drawn from the data concerning the effect of the fiber bundle, the temperature or the drum diameter on strength.

TABLE 33. RUPTURE LOAD OF KEVLAR 49 FIBER BUNDLES WITH END TERMINATIONS.

Description	Gauge Length (inches)	Rupture Load (lb)	Cables Failed	Location of Failure
Color Coded-Black	11.5	1165	3	One strand within epoxy but outside fitting; other 2 at end fitting
	12	950	3	At end fitting
	10.5	$\frac{1095}{1070}$ Avg.	3	At end fitting
Color Coded-Yellow	7.25	1130	1	Within epoxy but outside end fitting
	9.25	1000	2	At end fitting
	9.25	$\frac{1080}{1080}$ Avg.	3	At epoxy



Original Kevlar 49		Kevlar 29		Reconstructed Kevlar 49	
□	W/O Jacket (4x6x4) 36,480 Denier	◇	W/O Jacket 48,000 Denier	△	W/O Jacket 48,640 Denier
⊠	W/Jacket (4x6x4) 36,480 Denier			⊕	W/Jacket 48,640 Denier

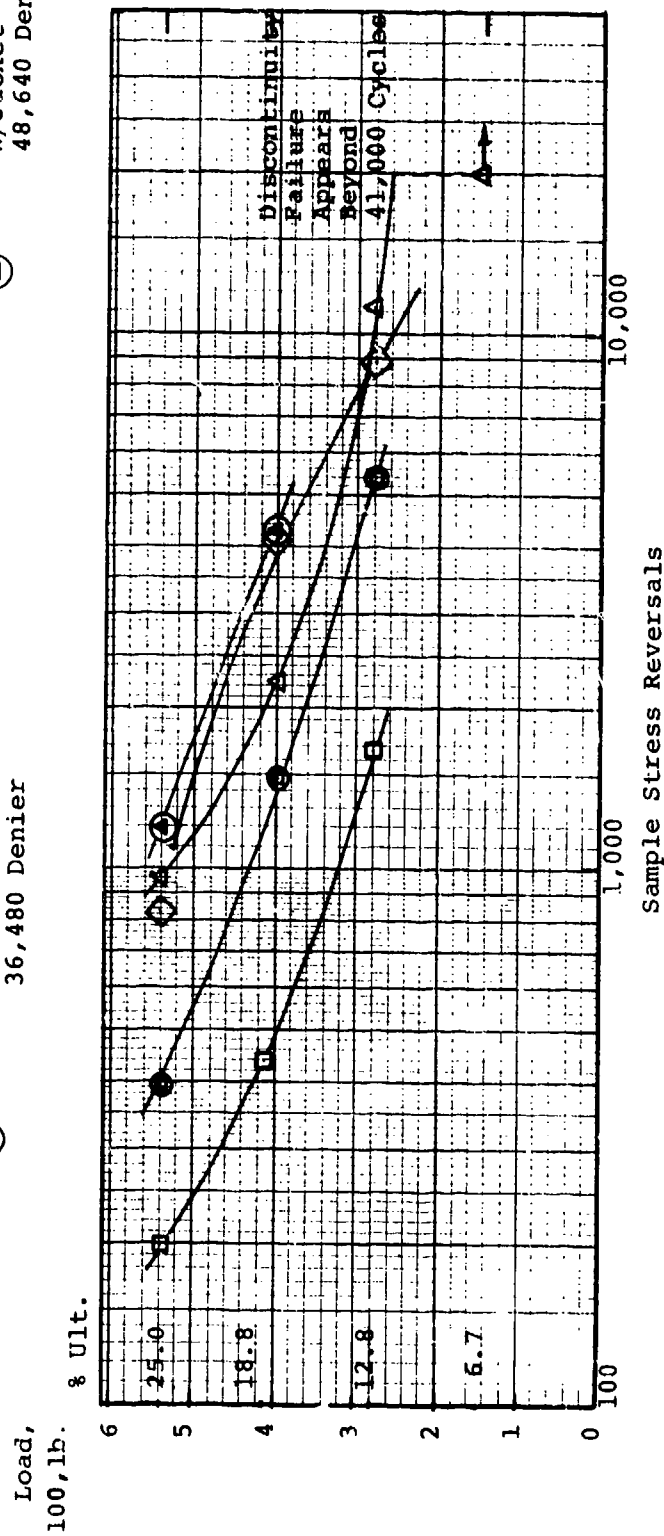


Figure 80. Kevlar 49 and Kevlar 29 Load Versus Bend-Over-Drum Stress Cycles.

### Ultraviolet Stability Tests

Application of Kevlar 49 to tension member design required an evaluation of fiber strength stability under ultraviolet radiation.

This evaluation was accomplished in accelerated exposure tests using Atlas Weather-Ometer and Fade-Ometer equipment, which are standards for the fiber and fabric industry. Test methods followed the practice of the American Association of Textile Chemists and Colourists (AATCC) as covered by AATCC Methods 111A-1968 and 16-1964.

Samples used for the 1/8-inch fiber bundle tests were taken from the 4-ply 6x4-cable produced. Both A and B yarn finishes were evaluated. The comparative data was obtained with DuPont Company furnished material, Kevlar 49, in yarn and 1/2-inch three-strand rope forms as well as Dacron and Nylon yarns.

While strength losses are high in the Kevlar yarn radiation tests, the self-screening properties of the material are evident with fiber buildup where the losses in bundle and rope forms are approximately 1/2 and 1/7, respectively, of the losses encountered in the yarn. Dacron and Nylon losses are shown for comparison in the yarn form, but these materials are essentially transparent and, therefore, not self-screening. Tables 34 and 35 present the results of tests averaged from five samples of each type. A typical 1/2-inch three-strand rope sample after tensile load test is shown in Figure 81.

Further reduction in Kevlar cable strength losses may be achieved by jacketing and other screening methods. No tests were conducted with jacketed configurations.

### Abrasion Tests

The abrasion resistance of a Kevlar 49, 1/2-inch diameter, nonjacketed, three-strand rope was compared to commercial Dacron and Nylon ropes on a 1-1/2-inch hexagonal (section) bar abrading machine. Rope samples were bent over the rotating bar with a tension of 40 pounds. Ropes were dry except for normal fiber finishes.

Tests showed a superiority in the order of 15:1 for the Nylon over the Dacron and Kevlar. See Table 36.

TABLE 34. YARN ULTRAVIOLET (UV) EXPOSURE TESTS.  
(KEVLAR 49 COMPARISON WITH DACRON  
AND NYLON)

Sample Identification & Exposure Time	Denier	Tenacity (gpd)	Break Elong. (%)	Modulus (gpd)	Strength Loss (%)
<b>Kevlar 49 Cord</b>					
<u>380/1/2; Twist</u>					
Control	769	22.31	2.5	887	--
100-hr Fade-Ometer	769	13.10	1.6	848	41
200-hr Fade-Ometer	769	11.86	1.3	994	47
100-hr WOM Dry	769	12.58	1.5	872	44
200-hr WOM Dry	769	10.7	1.3	870	52
100-hr WOM Wet	769	13.09	1.5	864	41
<b>F-68 Dacron</b>					
<u>1300/1/2; Twist</u>					
Control	2880	7.51	19.1	38.9	--
100-hr Fade-Ometer	2897	6.77	17.0	34.6	10
200-hr Fade-Ometer	2880	6.71	16.3	43.1	11
100-hr WOM Dry	2897	4.76	13.7	37.4	37
200-hr WOM Dry	2880	4.27	14.0	36.2	43
100-hr WOM Wet	2897	5.01	13.4	36.8	33
<b>T-728 Nylon</b>					
<u>1260/1/2; Twist</u>					
Control	2810	8.38	27.2	21.7	--
100-hr Fade-Ometer	2802	6.97	23.1	12.1	17
200-hr Fade-Ometer	2800	7.31	23.0	19.1	13
100-hr WOM Dry	2802	7.98	26.2	16.1	5
200-hr WOM Dry	2800	7.64	25.7	17.3	9
100-hr WOM Wet	2802	7.88	30.0	13.2	6

NOTES

WOM: Weather-Ometer  
gpd: grams per denier

TABLE 35. COMPARISON OF ULTRAVIOLET (UV) LOSS IN 1/8-INCH FIBER BUNDLES AND 1/2-INCH, 3-STRAND CABLE CONSTRUCTED OF KEVLAR 49			
Sample Identification	Weight (lb/100 ft)	Strength (lb)	Strength Loss (%)
1/8 Fiber Bundle			
Finish A			
Control	.30	1,322	--
100 hr WOM Dry	----	1,030	22
1/8 Fiber Bundle			
Finish B			
Control	.29	1,220	--
100 hr WOM Dry	----	943	22
1/2 Rope			
Finish B			
Control	7.4	11,400	--
200 hr WOM Dry	----	10,625	7
NC <sup>TES</sup> WOM: Weather-Ometer (Atlas, carbon arc light source)			



Figure 81. Kevlar 49, 1/2-Inch, 3-Strand Rope Specimen  
After Tensile/Ultimate Test.

TABLE 36. ABRASION TEST OF KEVLAR 49, NYLON, AND DACRON 1/2-INCH ROPES		
Specimen Material	Cycles to Failure	
	Sample 1	Sample 2
Kevlar 49	1,200	1,350
Dacron	1,440	1,620
Nylon-1	19,800	19,980
Nylon-2	23,250	22,950

Based on the above, a nylon-jacketed Kevlar cable would have an abrasion resistance advantage over a plain Kevlar cable.

The objective of these tests was to acquire design data from which an HLH/ATC tension member could be configured. Tensile test data now available indicates the types, magnitudes, and trends of strength losses that must be considered in fiber rope design.

### Conclusions

Based strictly on strength characteristics, a Kevlar cable suitable for the ATC tension member application (75,000-pounds cable ultimate with D/d-24/1) could be developed in the range of 1-3/16 to 1-1/2 inches depending upon construction efficiency. These tension member designs would result in an estimated weight saving over the use of steel wire in the tension member in the range of 63 to 40%, respectively. However, in order to fully capitalize on this weight benefit for the present hoist concept, the Kevlar cable must be capable of operating at a lower D/d than now contemplated for the steel cable. The fatigue life of each of the 1/8-inch fiber bundle configurations tested at a D/d of 24/1 was lower than required (10,800 cycles) at the representative fiber bundle design load (25% of ultimate strength). However, the data shows a trend of increased life with larger Kevlar cable sizes (36,480 to 48,600 denier) and with the added protection of an outer abrasive-resistant sleeve. Full scale tests must be done to further define the influence of these factors on Kevlar 49 or Kevlar 29 cable applications.

Strength and weight projections based on tensile test data are summarized in Table 37. Ultraviolet degradation and

TABLE 37. SIZE/WEIGHT PROJECTION OF KEVLAR 49 HLB/ATC TENSION MEMBERS. (6)											
	36 x 7 Base- line Steel Cable	Fiber Bundles				3-Strand Rope			8-Str. Rope		
		Ideal	Test			Ideal	Test		Ideal	Test	
		Tensile Parallel Fibers	Tensile Const. Loss	Const. & TOD Loss	Const., TOD & Temp. Loss	Tensile Parallel Fibers	Tensile Const. Loss	Const., TOD & Temp. Loss	Const., TOD & Temp. Loss	Const., TOD & Temp. Loss	
Ultimate Load lb.	76,100	75,000	75,000	75,000	75,000	75,000	75,000	75,000	75,000	75,000	
Diameter in.	.70	.647	.693	.755	.856	.855	1.37	1.52	1.20		
Conversion Efficiency, %	.82	1.00	.812	.77	.663	1.0	.39	.318	.615		
Weight, lb./100 ft.	96	13.8	14.4	17.9	22	19.2	49.2	60.5	37.6		
Remarks	With Cable Twist Effect	Without Cable Twist Effect Bundle Twist Only				With Cable Twist Effect			8 Par- allel Fiber, Jacketed Strands; Plaited		
See Notes	(1) (5)	(1)	(1) & (3)	(2)	(1)	(1) & (2)	(4)				
NOTES	(1) Test Data, Ambient (2) Pull Test @ 160°F (3) TOD (lumped) Pull Tests 32 & 24/1, D/d (4) Less Strand Jackets (8)	(5) TOD = Tension-Over-Drum (6) Size projections based on measurement test sample diameter d <sub>1</sub> /8 = .10 inches (Fiber Bundles) d <sub>1</sub> /2 = .535 inches (3-Strand Rope)									

abrasion effects are time dependent losses which may be alleviated by jacketing with appropriate synthetic material. Diametral and weight effects of jacketing were not included in the projections. While jacketing will not decrease the PRD weight advantage significantly, it will increase cable diameter; a disadvantage if outside size is a critical factor.

Also, the final cable diameter using a fiber construction will be larger in diameter than now anticipated for a steel cable design, thereby requiring a longer drum or a new hoist configuration.

No significant conclusions can be drawn about the terminal designs used because of the sensitivity of the cable to nonuniform fiber loading within the bundle. Bundle "center breaks" were achieved however, with some tabbed samples and the 1/2-inch rope tensile tests with epoxy terminals, possibly indicating the need for special techniques in terminal fabrication.

Based on the above, it was concluded that the development of a non-metallic tension member configuration with maximum fiber strength utilization, minimum diameter, and an adequate fatigue life is not compatible with the HLH/ATC time frame.

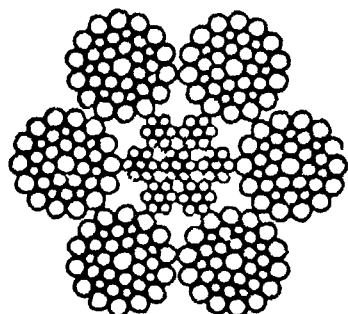
## METALLIC TENSION MEMBER DESIGN SUPPORT TESTS

### Introduction

During preliminary design, emphasis was placed on selecting a tension member material and construction, and verification of the "paired cable" torque balance concept. The materials and constructions evaluated are summarized in Figure 82. Testing consisted of:

1. Paired-cable torsion and rotation demonstration
2. Cable tension/elongation measurements
3. Cable bending fatigue tests
4. Cable tension-over-drum tests
5. Tension/elongation tests of candidate wire materials
6. Torsion tests of candidate wire materials

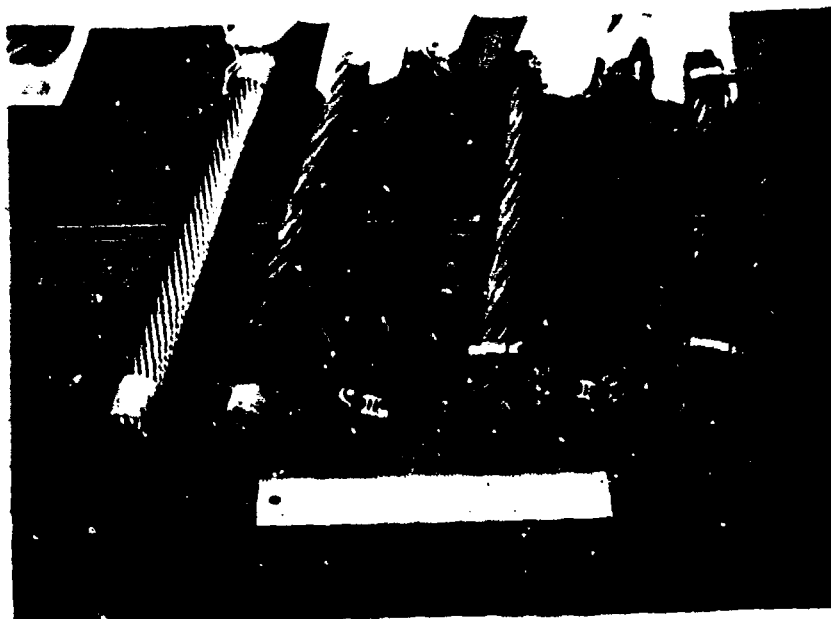




6X36 Warrington-Seale,  
IWRC Construction.



36 x 7 Swaged-Strand Construction.  
(Each of the 36 elements  
is a seven-wire swaged strand.)



.78-INCH DESIGN SUPPORT TEST CABLES (LEFT TO RIGHT):

<u>WIRE TYPE</u>	<u>CABLE CLASSIFICATION</u>	<u>CONSTRUCTION</u>
ELECT. GALV.	36 x 7	LANG LAY
ELECT. GALV.	6 x 36	LANG LAY
BRIGHT CARBON STEEL	6 x 36	LANG LAY
17-7 PH	6 x 36	LANG LAY
BRIGHT CARBON STEEL	6 x 36	REGULAR LAY
18-2 Mn	6 x 36	LANG LAY

Figure 82. Candidate Wire-Rope Constructions and  
Materials.

### Test Specimens

Three cable configurations were used in these design support tests. A 3/4-inch commercial 6X25, filler-wire (FW), fiber-core (FC) wire rope was used for the torsion and rotation tests. The other two cables tested were fabricated specifically for the HLH/ATC development program using wire drawn to 300,000 to 325,000-psi tensile strengths. These wires were used in the construction of 0.78-to 0.79-inch diameter (3/4 inch nominal) cable in 6x36-IWRC and 36x7-Lang lay constructions. Standard petrolatum lubricant was used in the cable fabrication. The 0.78-cable diameter was selected for correlation with available test data on 3/4 (0.79) inch, regular lay, high-strength cable to facilitate the selection of a size for design development, and as a best approximation of a candidate size for the hoist drum preliminary design studies.

### Paired Cable Torque Balance Demonstration Test

Of major significance in the tension member design support tests was the demonstration that the "paired-cable" tension member could be designed as a torque free assembly, showing that it would not tend to wind up on itself under any load or payout condition. To demonstrate the "torque balance" and confirm analysis, a static test was conducted using a representative 8-inch cable separation and full cable payout through the load range to the limit of 125% design load.

To evaluate the manufacturing sensitivity required for paired cables of identical torque characteristics, left and right lay cables were selected at random from available warehouse stock in the size and load range required by the ATC/HLH design.

Two tests were run:

1. To define the tension and torque characteristics of individual left- and right-lay cables.
2. To define the tension and rotation characteristics of a cable pair.

Samples, 15 1/2-ft long of the same 3/4-inch diameter, 6x25-FW, FC cable were loaded in tension to 125% design load, and the torque produced (due to untwisting tendency) was measured.

At maximum applied load (25,000 lb), it was found that each cable, as individually loaded, developed approximately 1,800 inch-pounds with a variation of 18-20 inch-pounds, or approximately 1%.

Figure 83 shows the tension/torque relationship found between the two identical, but opposite lay cables. The data was found to be linear and repeatable. The controlling factors are governed by the relationship

$$M = \frac{E d^2}{L}$$

M = torque  
d = cable diameter  
L = strand lay length

Two 3/4-inch, 6x25-FW FC cables of opposite lay, each 94-feet 6-inches long, were loaded in tension through yokes representing the hoist at one end and the load equalizer bar at the other.

Tests were made with and without a swivel under incremental loading to 50,000 pounds; without a swivel to determine the torque unbalance generated, and with a swivel to measure the resulting degree of rotation. Restoring experiments were run by twisting the pair incrementally to  $\pm 225^\circ$ .

The tests showed that the extremely small differences in torsion of the left and right lay paired-cable system resulted in a nearly perfect torque-balanced assembly.

Rotation experiments with the swivel showed that the twisted pair restoring torque exceed the cable mismatch torque by a factor of 30. The pair returned to an approximate zero position within the frictional limit of the swivel from either direction.

Figure 84 shows the experimental data superimposed on the theoretical curve for the 8-inch test separation. Note that the experimental values go through zero (20 inch-pounds) for this test. A larger torque bias in cable torque will displace the experimental curve along the vertical axis with the vertical position dictated by the direction of the bias (CW or CCW).

Determining the effects of cable length variations was also an objective of this testing since equal cable loading must be maintained. The relative change in length which occurred in the test cable after repeated loading to 125% design load was small. The variation found was attributable to measurable manufacturing differences in the cable fabrication, e.g., cable diameter and lay length, which result in elastic modulus variations.

For the cables tested, the manufacturing variations recorded were:

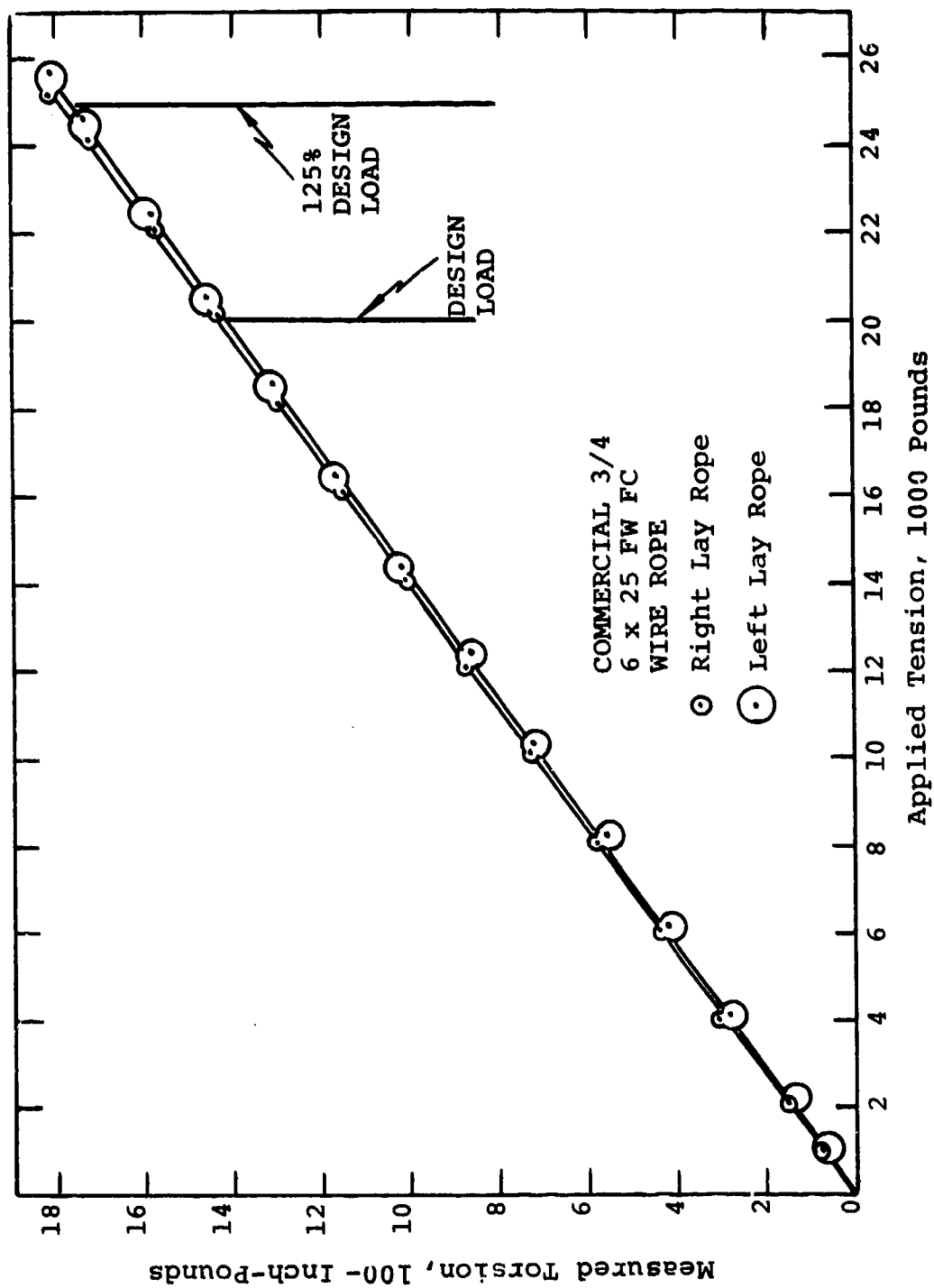


Figure 83. Comparison of Right- and Left-Lay Rope Torques.

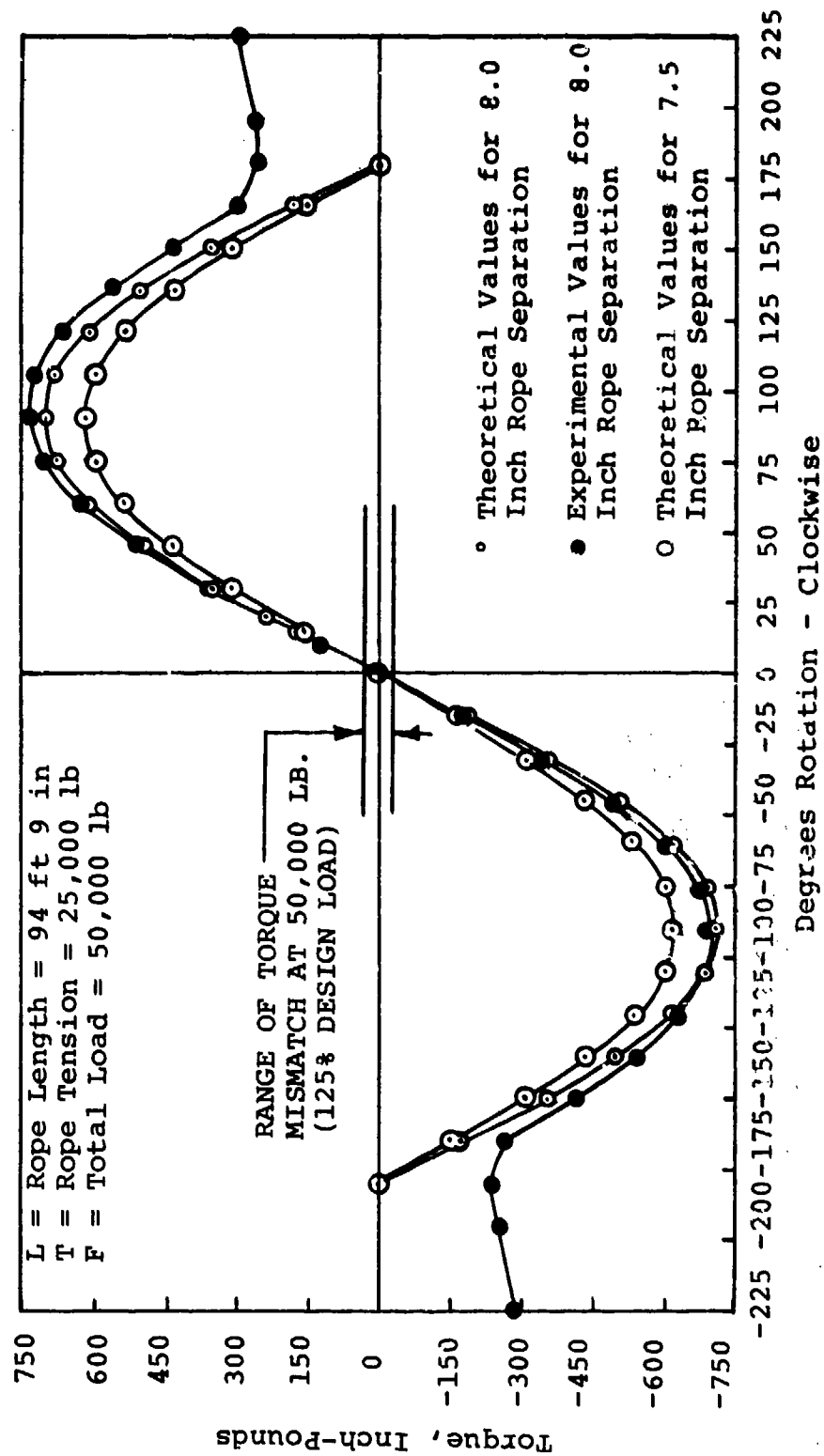


Figure 84. Comparison of Theoretical and Actual Values of Torque Required to Produce Rotation of the Load-Equalizer Bar With Left- and Right-Lay Cables.

	<u>Left Lay</u>	<u>Right Lay</u>
Diameter, inches	0.776	0.798
Lay Length, inches	4.569	4.735

Control of these cable parameters will be required so that the combined effect on elastic elongation within the operating load range may be maintained within approximately 1/2 inch. Constructional stretch will be removed by pre-loading before the final sizing and the attachment of the end fittings.

#### Cable Tension/Elongation Measurements

Each candidate cable construction was subjected to tension/elongation to determine the elastic modulus, proportional limit, and ultimate breaking strength.

The tests were conducted under ambient environmental conditions. To determine the load and elongation characteristics of the cables, each specimen was repeatedly loaded to limit load of 50,000 pounds. Ten loading cycles were used to establish a stable load/elongation curve.

Load/strain curves are presented in Figures 85, 86, 87, 88 and 89 for the 36x7 electro-galvanized 6x36, 17-7 PH, and 18-2Mn (see Figure 82). These plots show cable characteristics such as stress-strain proportionality, change in stiffness upon removal of constructional stretch by repeated loading, and load/unload hysteresis.

In these curves, it is evident that the 36x7 cable construction exhibits more desirable characteristics because of its small constructional stretch. The removal of its stretch in one load cycle, and its linear load/elongation curve from approximately 50% design load (10,000 lb) through design load (20,000 lb) to limit load (50,000 lb). Additional loading was required with the 6x36 cables to achieve stabilization and removal of constructional stretch. This requirement for additional loading is characteristic of the looser construction of the 6x36 cable than for the 36x7 cable.

In Table 38, the tensile modulus and torque developed by each of the cables is shown. In each case, the 36x7 demonstrates the most desirable characteristics. In terms of elongation alone, for 100 feet of cable payout under design load, the 36x7 would stretch approximately 4.8 inches whereas the 6x36 cable would stretch 6.4 inches. The 18-2 Mn cable demonstrated a tensile ultimate load which was too low to warrant further consideration.

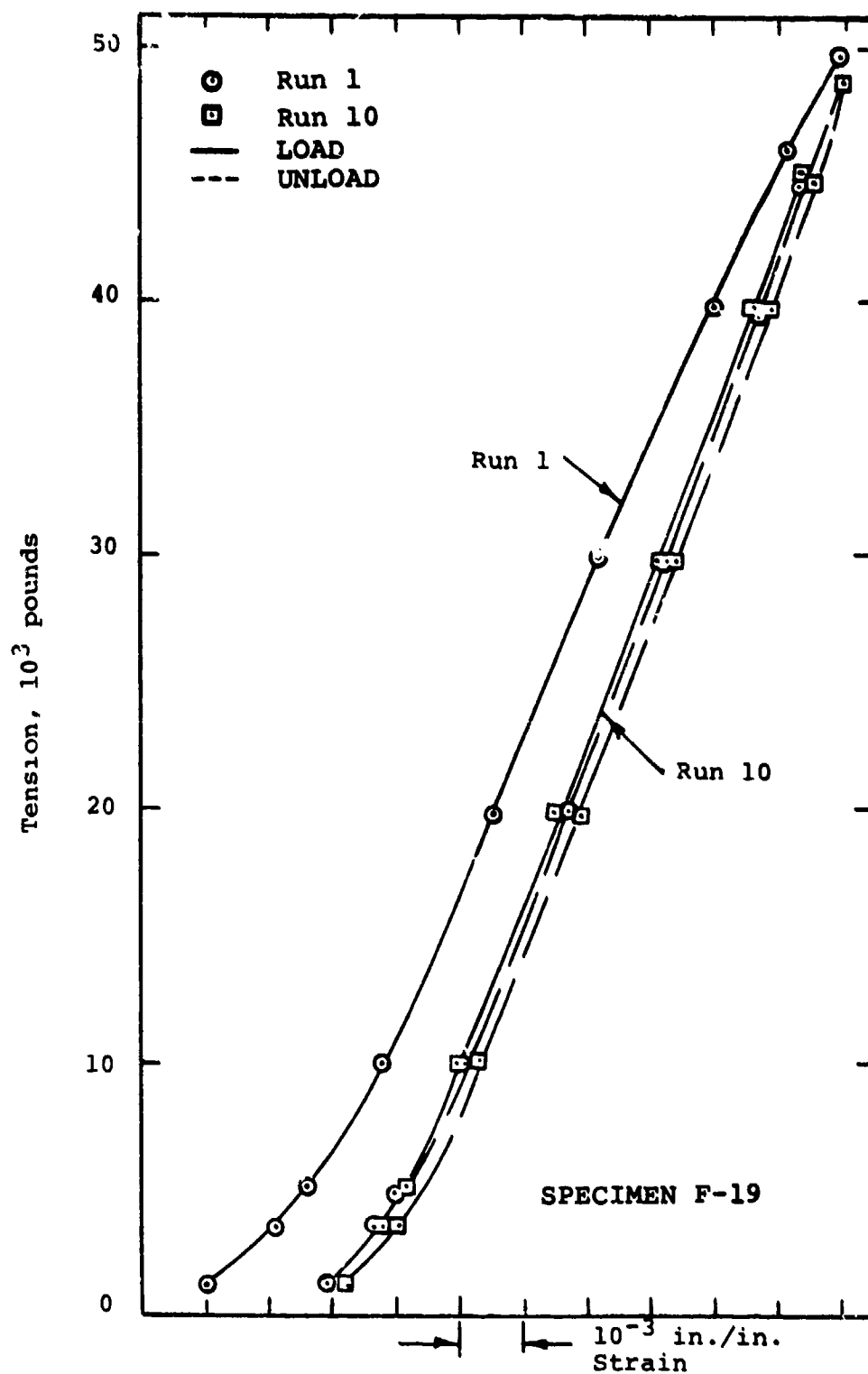
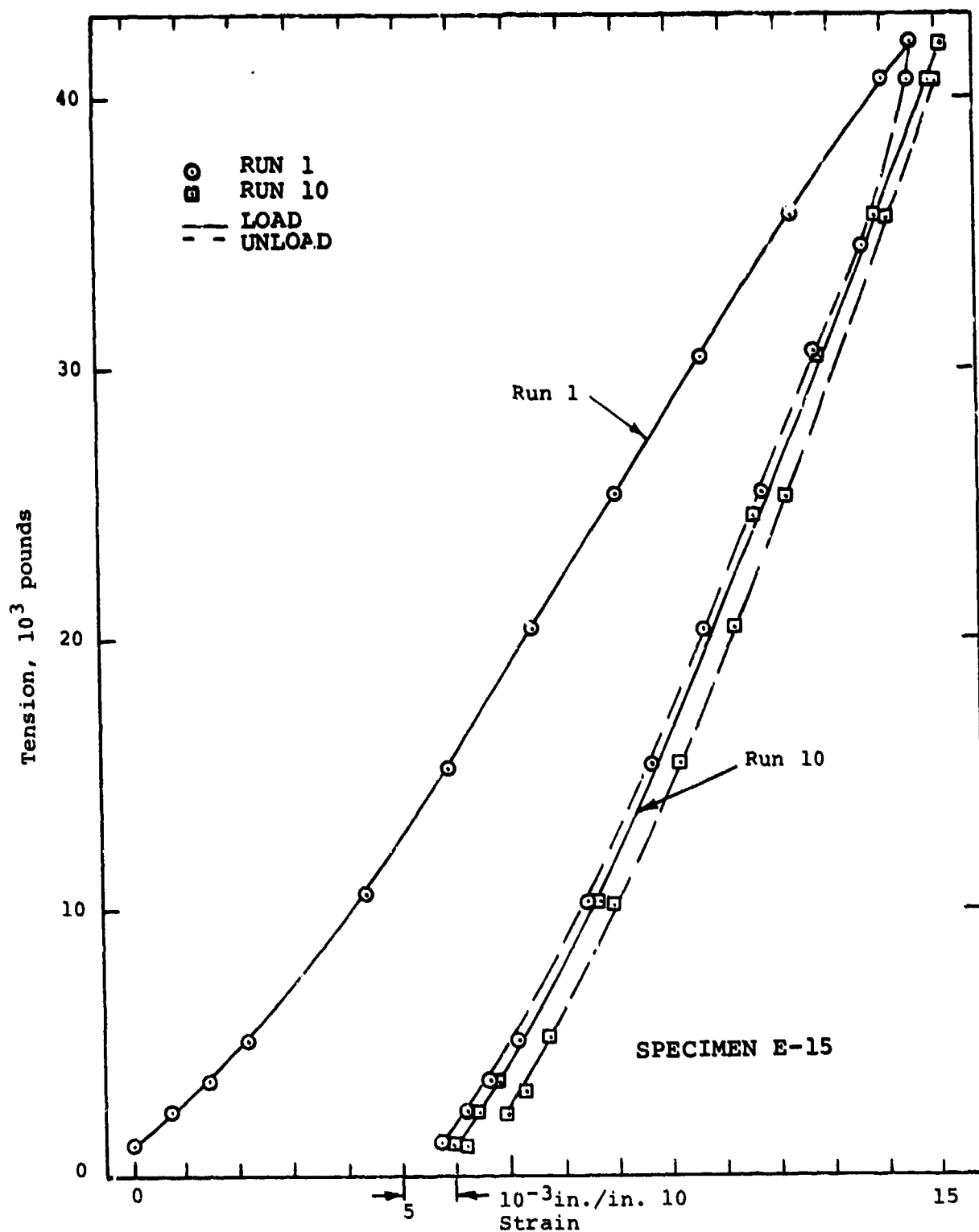


Figure 85. Typical Tension/Elongation Characteristics of Galvanized 0.78-inch 36x7 Lang-Lay Wire-Rope.





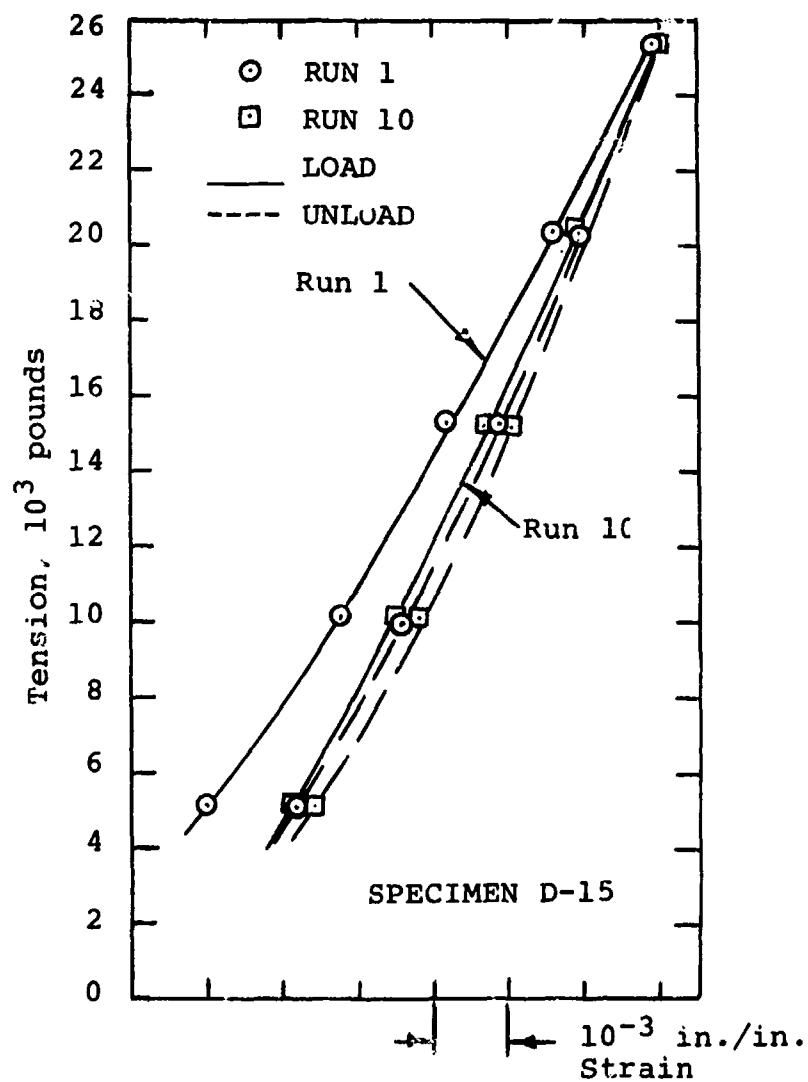


Figure 87. Typical Tension/Elongation Characteristics of 17-7PH 6x36 Lang-Lay Wire-Rope. (0.78-inch-diameter)

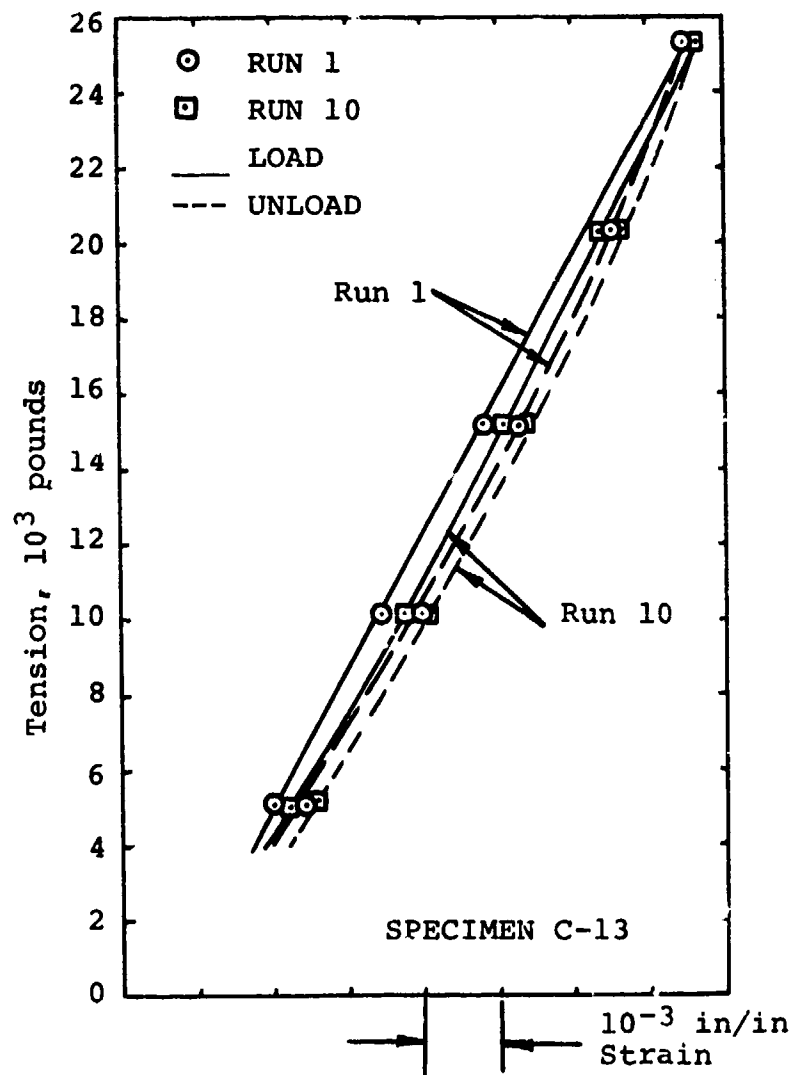


Figure 88. Typical Tension/Elongation Characteristics of 18-2 Mn 6x36 Lang-Lay Wire Rope (0.78-Inch-Diameter)

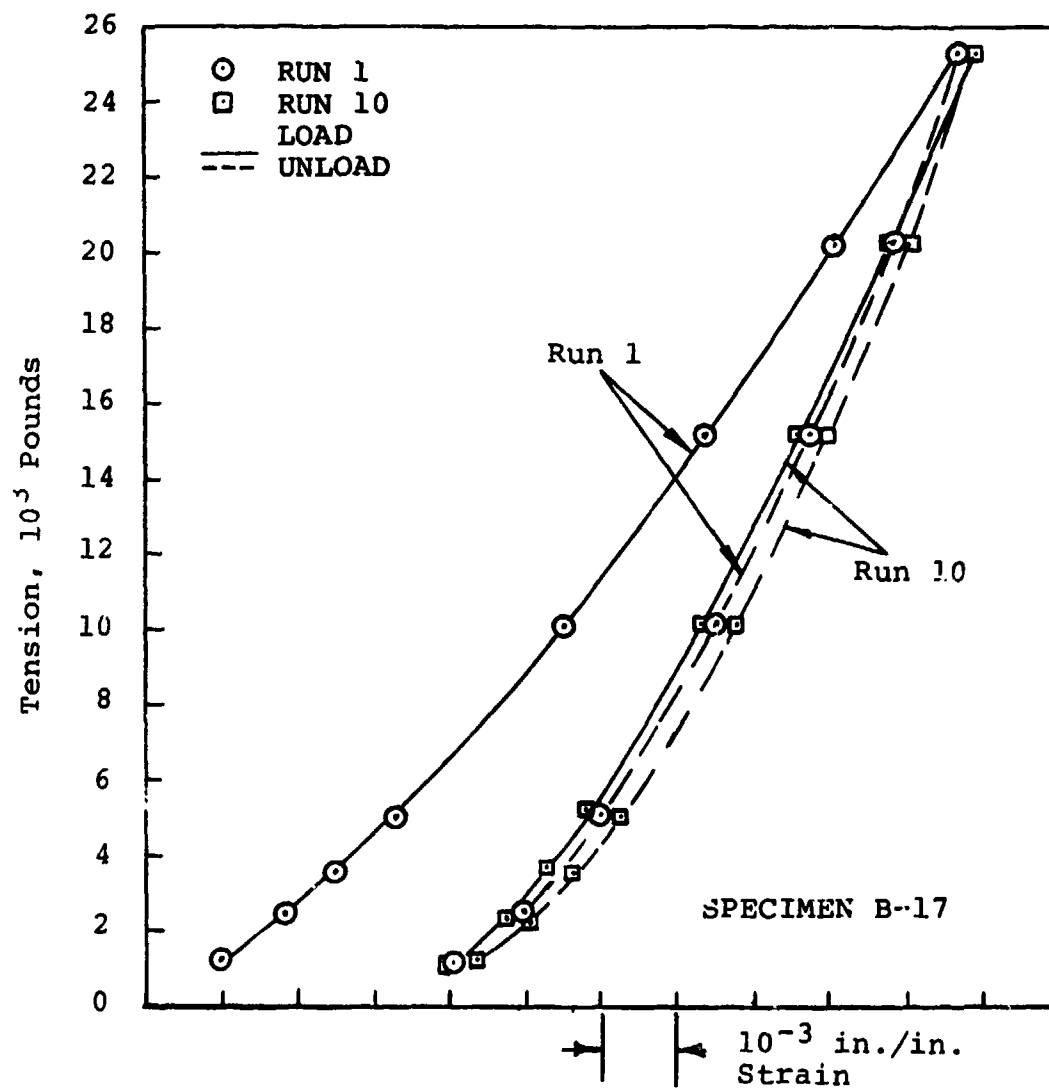


Figure 89. Typical Tension/Elongation Characteristics of Bright 6x36 Lang-Lay Wire Rope (0.78 Inch Diameter).

TABLE 38. ELASTIC MODULUS AND TORQUE CHARACTERISTICS OF CABLE TEST SPECIMENS.		
Rope Type	Rope Modulus At 25,000-lb Tension, 10 <sup>6</sup> psi	Rope Torque At 25,000-lb Tension, in-lb
Bright 6 x 36 Lang-Lay Rope	16.4	2140
18-2 Mn 6 x 36 Lang-Lay Rope	14.7	2070
17-7 PH 6 x 36 Lang-Lay Rope	17.8	2100
Galvanized 6 x 36 Lang-Lay Rope	18.1	2170
Galvanized 36 x 7 Lang-Lay Rope	19.7	1980

Since the .78-inch, 36x7 cable provides more tensile capacity than required, an additional test was conducted to determine whether a smaller diameter cable of the same construction could meet HLH/ATC limit load requirement of 50,000 lb without yield.

At yield, it was assumed that any cable of the same construction would develop a strength proportional to its metallic area and the same average cable stress. Therefore, to establish the yield point of smaller cables, such as .70-inch in diameter cables, the .78-inches, 36x7 test cable must demonstrate a yield point above 62,500 lb.

Such a test was run on a new cable specimen with repeated loadings made to 60,000 and 70,000 lb to stabilize stretch related to the various load levels. Initial loading to 70,000 lb showed linearity between 5,000 and 60,000 lb, and subsequently to 65,000 lb after repeated loading. See Figure 90.

Since diametral yield characteristics were also of interest relative to drum groove fit, cable size measurements were taken during the stabilizing loading. Results are presented in Table 39.

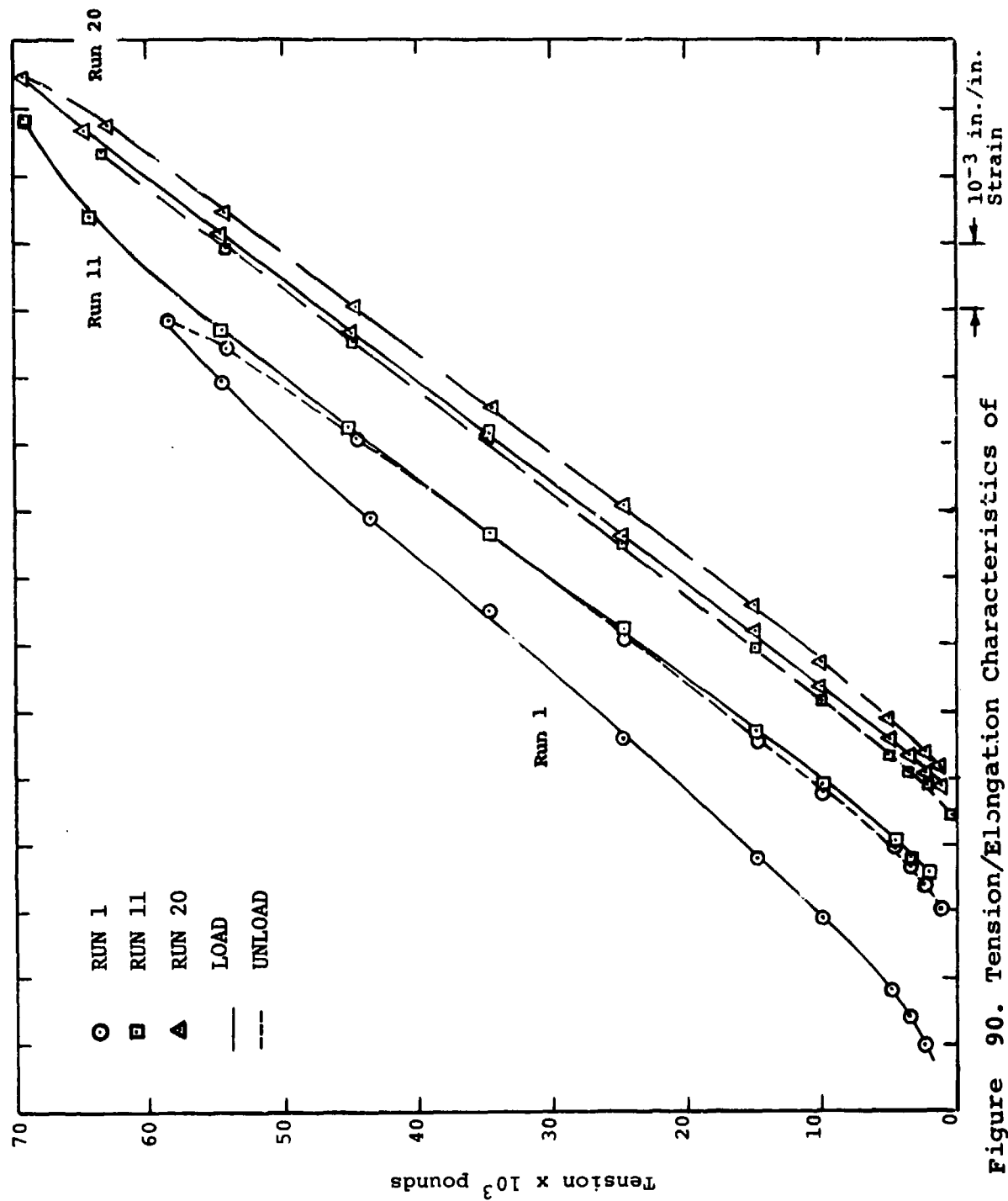


Figure 90. Tension/Elongation Characteristics of 36x7, 0.78-Inch-Diameter Cable.

TABLE 39. EFFECTS OF REPEATED LOADING ON 36x7 CABLE, 0.78-INCH DIAMETER. (Specimen F-27)			
Run	Approximate Tension-Lb.	Diameter In Inches	Reduction Dia/In
1	300	0.790	.000
	24,700	0.775	.015
	34,600	0.773	.017
	58,500	-----	-----
	150	0.778	.012
10	600	0.776	.014
	24,700	0.769	.021
	34,600	0.768	.022
	60,000	-----	-----
	1,200	0.773	.017
11	24,800	0.769	.021
	34,600	0.768	.022
	70,000	-----	-----
	500	0.772	.018
20	1,200	0.772	.018
	24,700	0.766	.024
	34,800	0.766	.024
	70,000	-----	-----
	1,150	0.771	.019

During this tension/elongation experiment, torque values were recorded to approximately 70,000 pounds tension. The tension/torque curve was linear and indicated a torque of approximately 5,400 inch-pounds at 70,000 pounds tension, as shown in Figure 91.

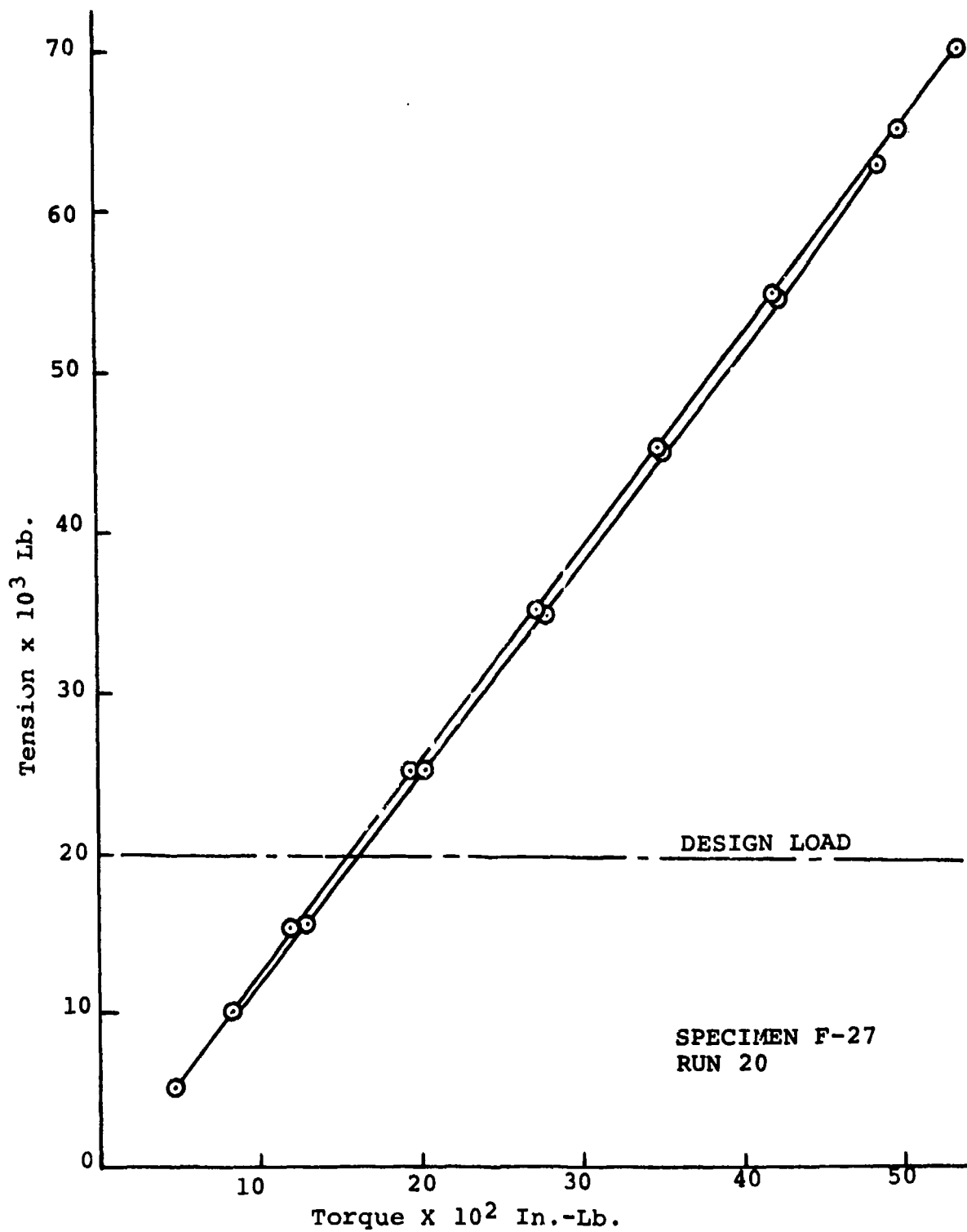


Figure 91. Tension/Torque Characteristics of 0.78-Inch-Diameter, Galvanized, 36X7 Lang-Lay Cable.

### Cable Bending Fatigue

Tests were conducted to determine the fatigue behavior and modes of failure of a cable being bent in a manner simulating the way the cable will be bent on the helicopter hoist.

Two specimens are tested simultaneously, connected together end-to-end on a two sheave machine as shown in Figure 92.

The test sheaves utilized provide a drum pitch diameter to cable diameter ratio of 20:1. Wrap pressure loading was simulated by the use of the groove shape, surface finish, and fit identical to those used on the hoist design. The helix angle provided on the test machine was larger than planned for in the HLH hoist design. This was done to accelerate the wear and scuffing caused by the edge of the drum groove.

The bend-over-drum fatigue tests were conducted under ambient laboratory conditions and without additional cable lubrication.

Fatigue test loading conditions are given in Table 40.

Four specimens of each cable configuration were used for conditions A, B, and D. Condition C was only used on two 36x7 specimens. The spectrum loading (D) was run in ten blocks of 1,080 cycles each. At the end of each 10,800 cycles, the specimens were removed from the fatigue machine and placed in a tensile loading machine to determine the remaining tensile strength (RTS), a measure of the cable's ability to perform its mission if an additional loading cycle were required.

Bend-over-drum fatigue tests established the following:

The electro-galvanized 36x7 cable samples demonstrated that they were superior to all other configurations tested. This result is based on the total number of external and internal wires broken in the cable samples as a result of the 10,800 simulated hoisting cycles. External wire breakage was apparent during and after the test. Internal failures were determined by examination of the cable test sections. On this basis, the cable configurations tested were ranked in the order of fatigue resistance, with number one being the best:



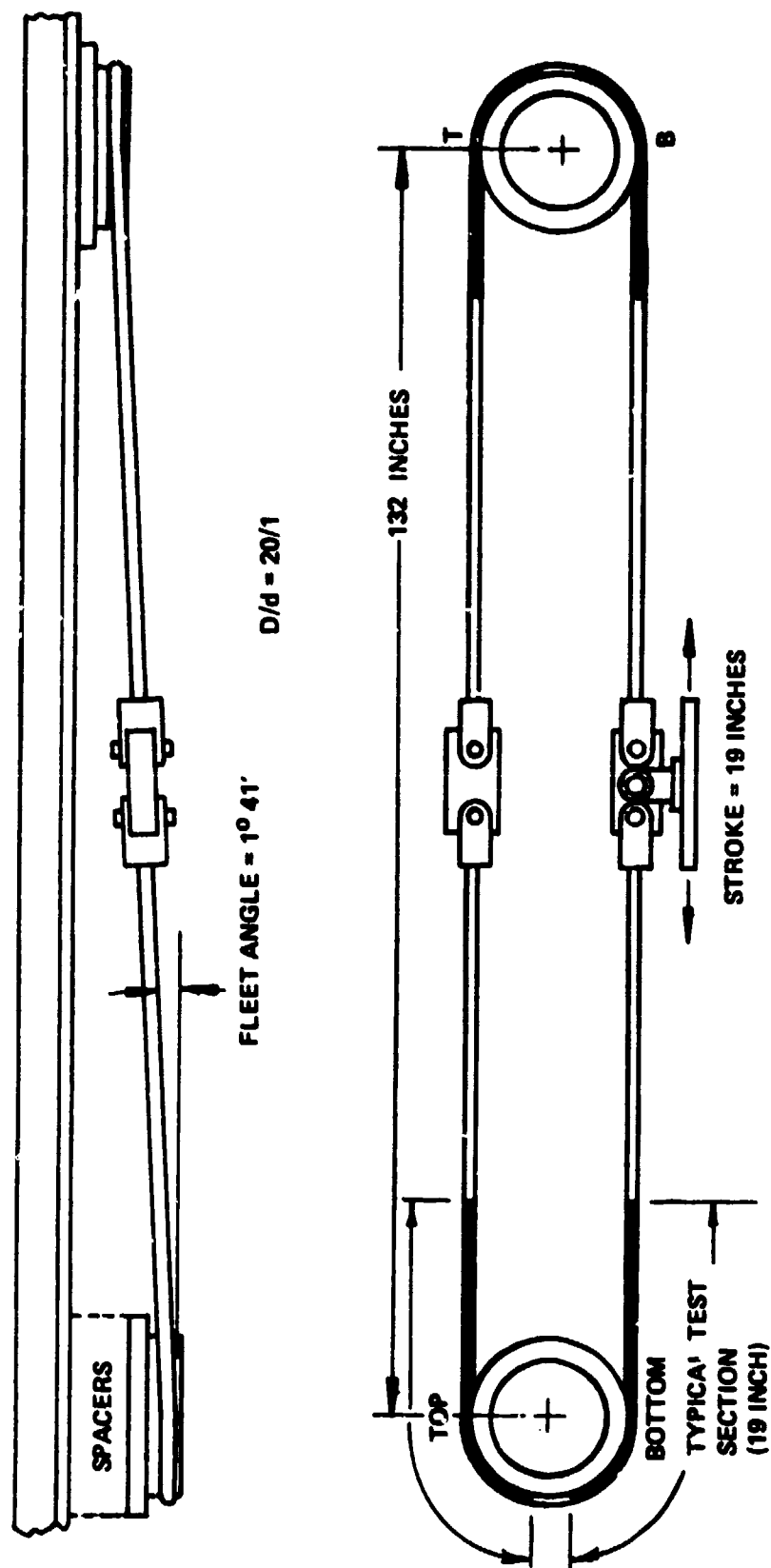


Figure 92. Layout of Bend-Over-Drum Fatigue Machine  
With a typical cable specimen.

TABLE 40. FATIGUE LOADING PROGRAM.					
<u>Constant Loading Fatigue Tests</u>			% Design Load	Test Load	% DBS* (Ult.)
Condition	Loading Time	# of Cycles			
A	Constant	10,800	100	20,000	26
B	Constant	10,800	125	25,000	33
C	Constant	10,800	150	30,000	40
<u>Spectrum Loading Fatigue Tests</u>			% Design Load	Test Load	% DBS (Ult.)
Condition	% of Life	# of Cycles			
D	10	1,080	125	25,000	33.3
	75	8,100	100	20,000	26.7
	10	1,080	50	10,000	13.3
	<u>5</u>	<u>540</u>	25	5,000	6.7
100% Total		10,800 Cycles			
*DBS = Design Breaking Strength.					

1. Electro-galvanized 36x7 Lang-lay
2. Electro-galvanized 6x36 Lang-lay
3. Bright carbon steel 6x36 Lang-lay
4. 17-7 PH stainless steel Lang-lay
5. Bright carbon steel 6x36 regular-lay

From this ranking, it is also apparent that a Lang-lay construction performed better than the regular-lay construction of the same size and strength level. In a direct comparison of electro-galvanized carbon steel and 17-7 PH stainless steel, the coated carbon steel was better, having fewer external and internal wire breaks than the stainless steel.

Typical locations of wire breakage occurring during bend-over-drum fatigue experiments are shown in the cross section of the 6x36 cable in Figure 93.

Location of Breaks  
on Strand Crowns  
in Lang-Lay Rope

Location of Breaks  
in Strand Valley in  
Lang-Lay Rope

Location of Breaks  
on Strand Crowns  
in Regular-Lay Rope

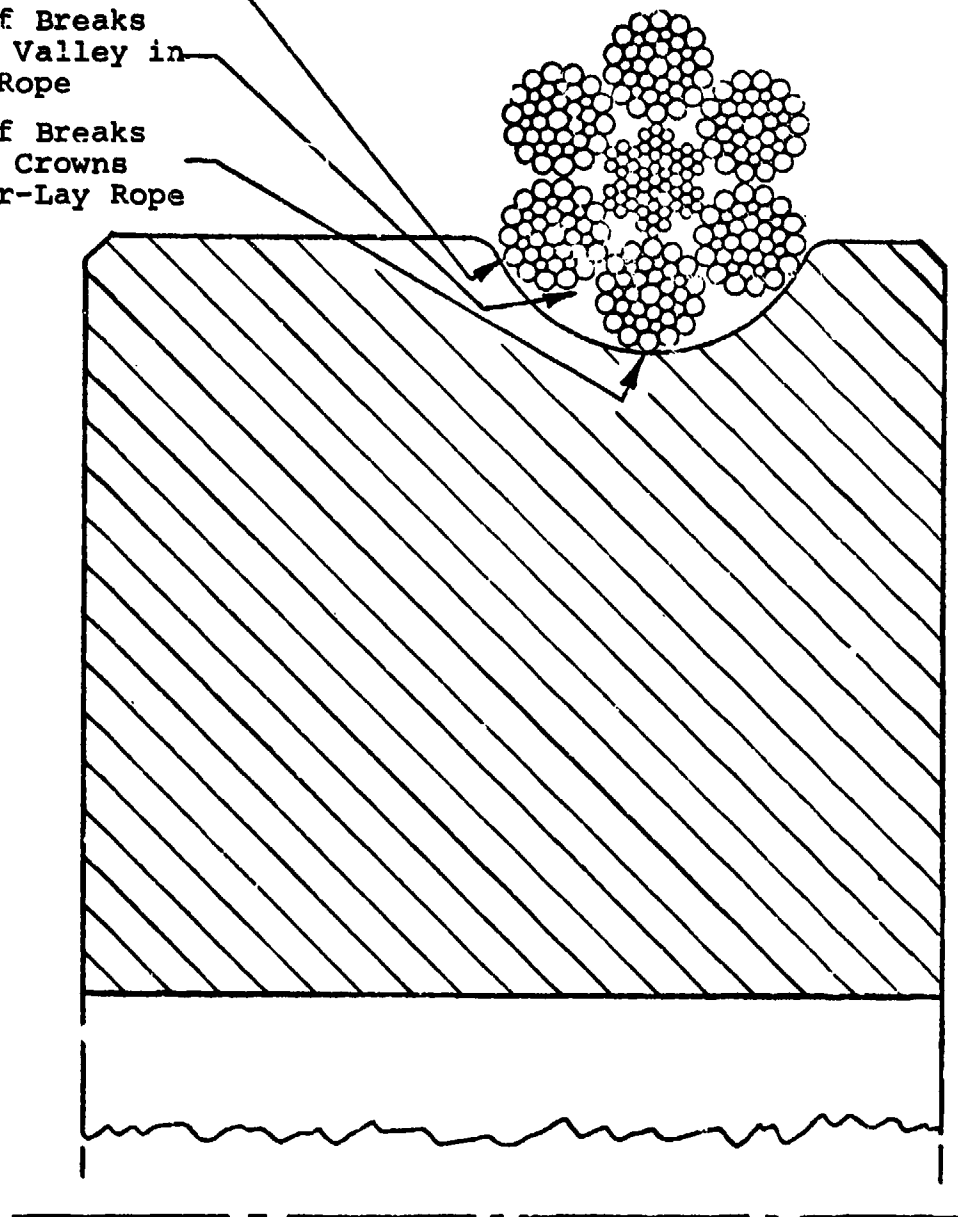


Figure 93. Locations of Wire Breakage During Bend-Over-Drum Fatigue Tests.

### Cable Breaking Strength

The most significant physical characteristics to be determined from the cable test samples were the ultimate tensile (breaking) strength and the tensile strength remaining after fatigue by bending over a drum. The maximum pure tensile breaking loads obtained during the design support tests are listed here:

<u>Maximum Cable Breaking Strength (Lb)</u>	<u>Material/Construction</u>
90,100	Electro-galvanized carbon steel, 36x7 Lang-lay
67,800	Electro-galvanized carbon steel, 6x36 Lang-lay
66,800	Bright carbon steel, 6x36 Lang-lay
66,500	Bright carbon steel, 6x36 regular-lay
61,100	17-7 PH stainless steel, 6x36 Lang-lay
48,000	18-2 Mn stainless steel, 6x36 Lang-lay

The tensile tests also show the superiority of the 36x7 cable over its competitors. The values obtained were relative and not absolute breaking strength, since all but 2 of the 74 cable samples tested failed at their end termination. The two tests that failed in the cable center occurred in cases where fatigue damage was evident.

Based on these results, it was expected that the true tensile strength of each of the cables in the test program would be somewhat higher than that recorded although the true strength was not determinable due to the limitations of end fittings employed. More efficient and possibly specially designed fittings for end terminations would be required to achieve cable "center breaks".

It is interesting to note that in the case of the 36x7 cable, many of the highest test values were obtained on specimens subjected to fatigue testing at 150% design load. Fatigue damage, if any, was therefore not apparent from these tests since local cable damage induced by attachment of end fittings influenced the failing loads of all specimens. Figure 94 shows the relative cable specimen tensile breaking loads obtained with new and fatigue-tested specimens.

Cable fatigue tests were designed to include wear factors more severe than anticipated. The groove shape was designed to maximize drum stiffness and cable support under load (considering cable contraction during load lift). The cable "fleet angle", due to the cable pitch and D/d selected for test, provided a larger helix angle than planned for the HLH/ATC to exaggerate wear. This more severe interface condition also provided a means of determining the influence of cable wear on the fatigue life of each candidate. The test configuration is shown graphically in Figure 95 along with comparative ATC hoist study design parameters.

In general, 6x36 cable wear appeared to be affected by groove geometry and cable construction but cable wear showed little influence on cable fatigue compared with other test factors.

With the 36x7 construction, the wear was negligible (see Figure 96) because of the more continuous surface contact of the cable with the groove shoulder, which reduces the unit contact pressure.

#### Tension-Over-Drum Tests

Tension-over-drum experiments were conducted to determine whether the breaking strength of a new cable is degraded by being pulled while wrapped over a 20/1 D/d hoist drum. These tests were to establish strength losses due to combined tension, bending, and strand-to-strand compression, and the effect of these losses on design requirements.

The test specimens for these experiments were cable sections approximately 10 feet long with standard open spelter (zinc) sockets attached to each end. Each specimen was wrapped around the tensioning sheave and the ends were secured to a strongback. A load was applied until the specimen pulled apart. The machine is shown in Figure 97.

A, Bright 6x36 Regular-Lay	D, 17-7 PH 6x36 Lang-Lay
B, Bright 6x36 Lang-Lay	E, Electro-Galv. 36x7 Lang-Lay
C, 18-2 Mn 6x36 Lang-Lay	F, Electro-Galv. 36x7 Lang-Lay

 36 x 7

### ④ Manufacturer's Test

**NOTE: All cable failures were at end fittings**

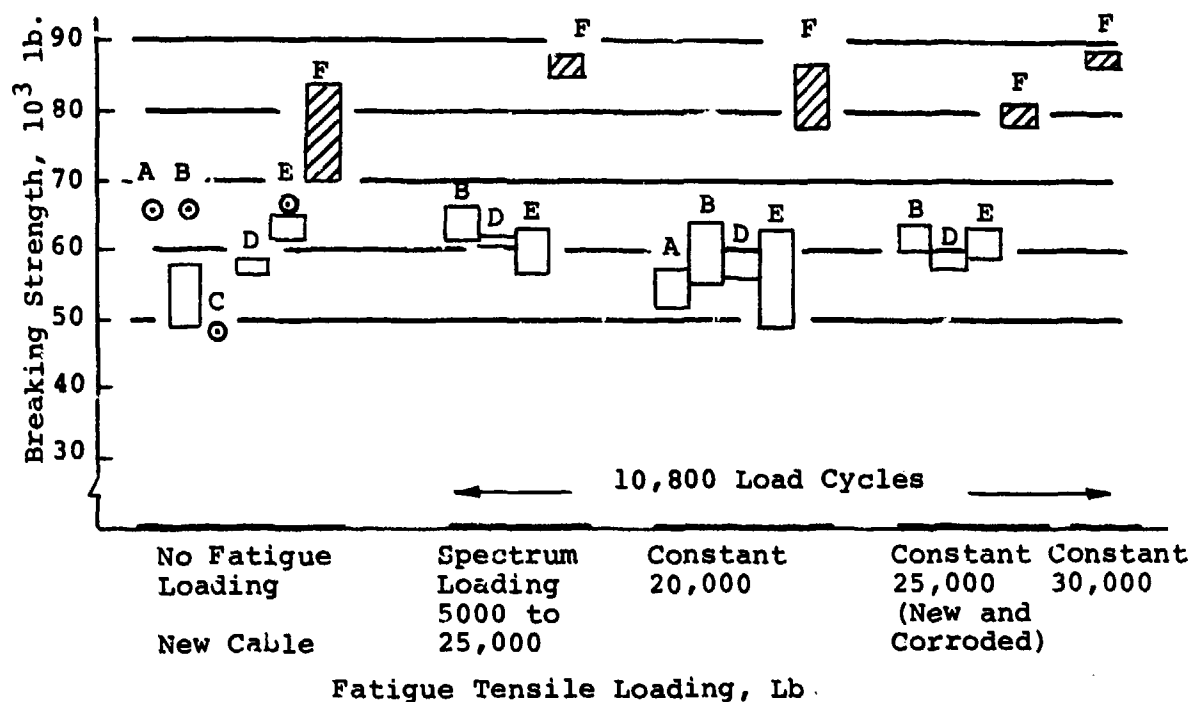
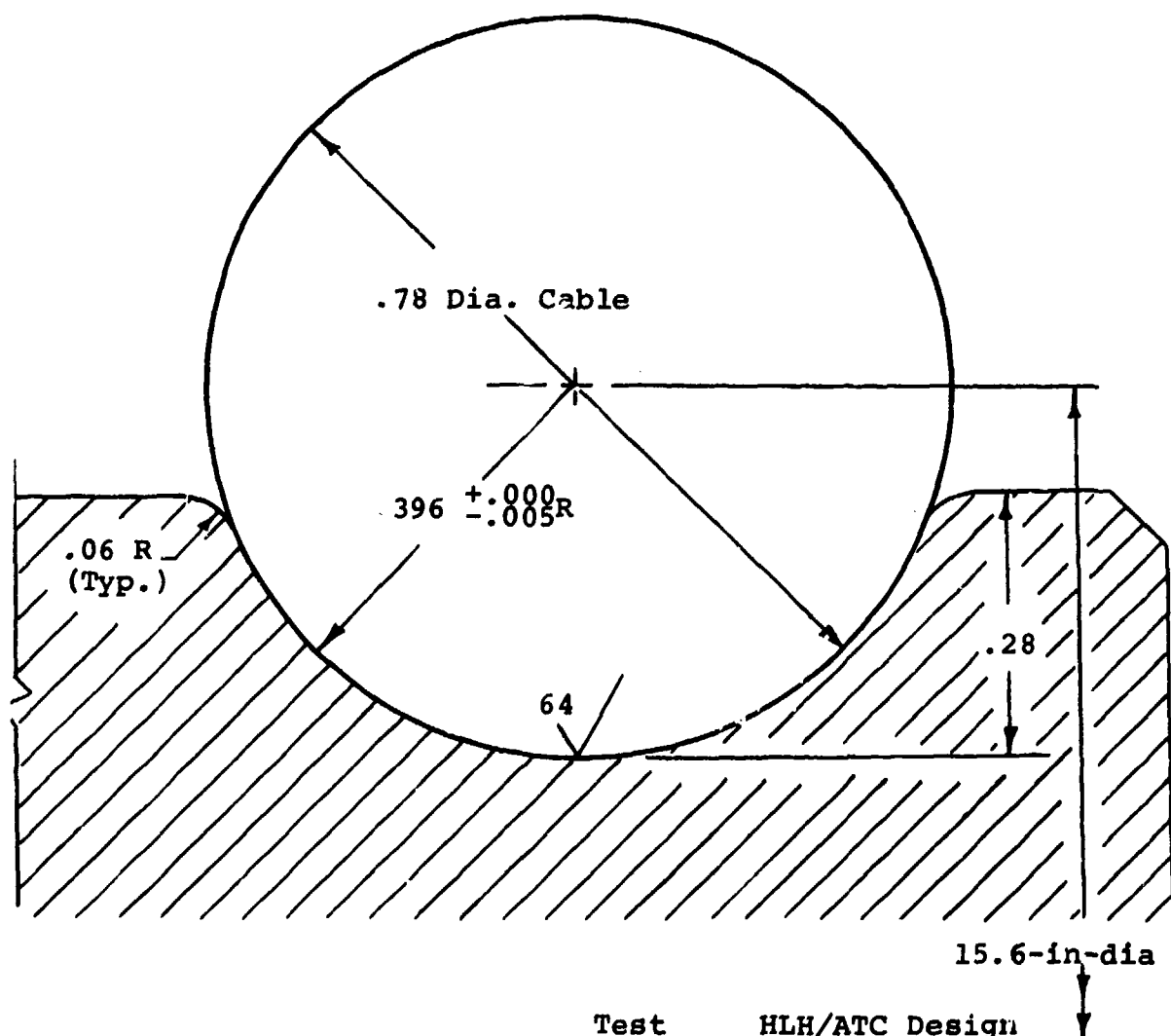


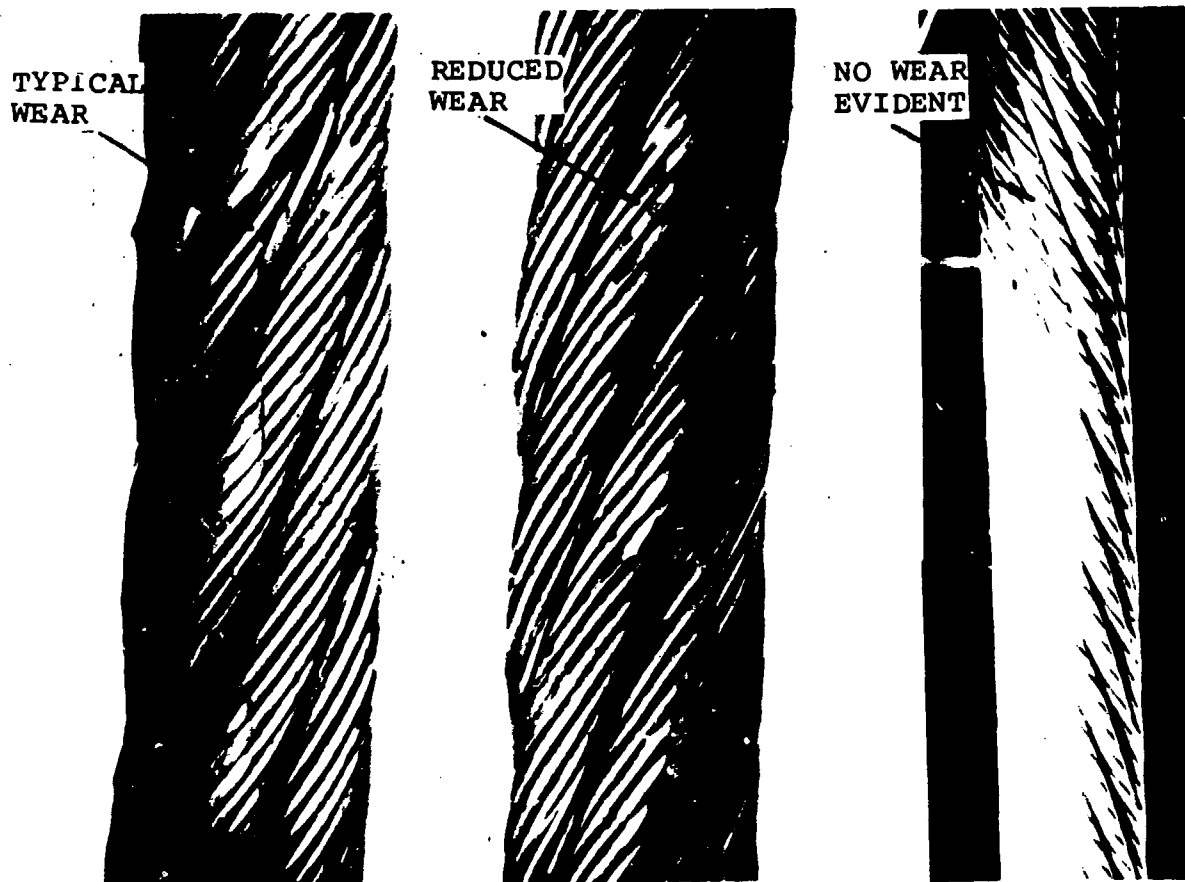
**Figure 94. Breaking Strength of Cable Specimens.**

Material: Mild steel carburized to 0.045 minimum depth,  
case hardened to Rockwell C 58-62.  
(No Surface Coating)



D/d	Test	HLH/ATC Design
Drum Diameter, Inch	20/1	24/1
Groove Helix Angle	15.6	18.75
	1°41'	0°50'

Figure 95. Comparison of Drum Groove Configurations - Cable Design Support Test and HLH Design.



CABLE  
CONSTRUCTION

6x36

6x36

36x7

DRUM GROOVE EDGE  
RADIUS (IN.)

.030

.060

.060

Figure 96. Apparent Cable Wear After 10,800 Load Cycles.



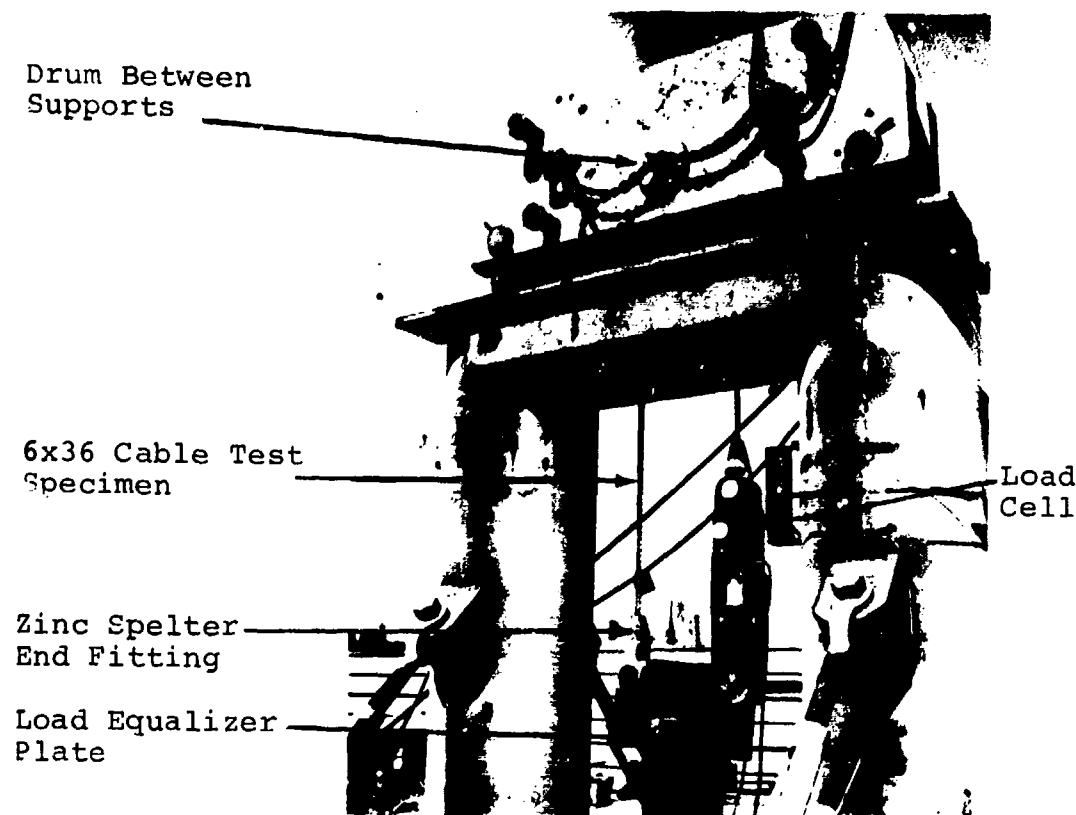


Figure 97. Tension-Over-Drum Test Rig for Ultimate Load Test of .78-Inch Diameter Cable Wrapped 180° Over a 20/1 Grooved Drum.

These tests were conducted with four cable configurations, the 18-2 Mn having been eliminated. In the case of the 17-7 PH, 6x36 cable, failures occurred in the area of the drum groove and this cable demonstrated the smallest variation in the breaking load of the four cable types. In the cases of the galvanized 36x7, the bright and galvanized 6x36 cables, all failures were at one of the sockets with a greater variability in load than shown in the 17-7 PH cable, although within the range of previous pure tension tests. The 36x7 cable again demonstrated significant tensile strength superiority. See Figure 98 for the comparison of the failing loads in pure tensile (straight pull) tests, versus tension over drum tensile strength tests.

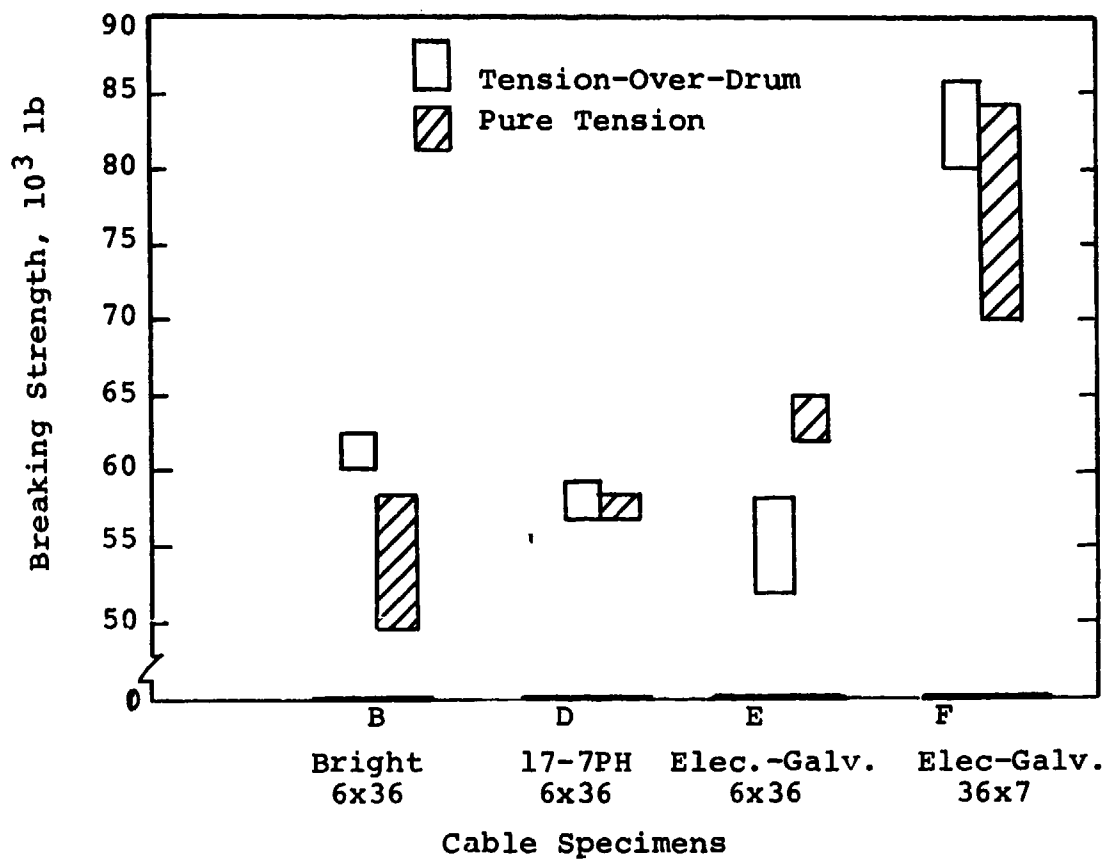


Figure 98. Breaking Strengths, Pure Tension and Tension-Over-Drum Tests.

### Tension/Elongation Tests of Candidate Materials

Tension tests were conducted to determine the ultimate strengths and yield points of the candidate tension-member materials, using samples of wire used in fabricating the outer strands of the test cables - carbon steel, bright and drawn electro-galvanized, stainless steel 17-7 PH and 18-2 Mn.

The tests were conducted at two temperatures, ambient and -65°F. Half of the samples tested were new wires, half were tested after a 48-hour exposure to a salt-fog environment while under a static stress condition (200,000 psi bending) conducive to stress corrosion cracking.

Yield and ultimate tests of representative wire, simultaneously exposed to 200,000 psi bending stress in a corrosive atmosphere at 95°F, showed no degradation of physical properties for the galvanized carbon steel, the 17-7 PH, or the 18-2 Mn stainless steel at ambient temperature. Bright carbon steel showed 6% to 10% reduction in strength in ambient temperature and a reduction of 4% to 8% under a temperature condition of -65°F.

The bright-carbon steel was noticeably affected by the salt-spray exposure, as expected, because of the absence of corrosion resistant coating. All materials exhibited a higher ultimate tensile strength at -65°F than at ambient temperature.

The 18-2 Mn and 17-7 PH stainless steels and the galvanized carbon steel were virtually unaffected by the salt-fog exposure test. The highest average ultimate tensile strength achieved was by the heat-treated 17-7 PH stainless steel exposed to salt-fog and tested at -65°F. The next highest ultimate tensile strength average was the galvanized carbon steel under the same conditions.

### Torsion Tests of Candidate Materials

Torsion tests were conducted on all candidate wire materials as described in Federal Specification QQ-W-470. The torsion test is a standard method used by wire manufacturers to evaluate the ductility and quality of the wire material.

The torsion experiments were conducted using a single-wire torsion machine similar in operation to the machines used by the wire manufacturers and specified in the wire specification. The number of turns to failure are an indicator of the wire ductility and quality. In general,

the higher the number of turns to failure the better the material ductility.

These torsion experiments were conducted both at ambient and low temperature (-65°F) conditions. Half of the specimens of each material were tested at each test temperature in the as-received condition, the remaining specimens of each material were torsion tested at each temperature after exposure to the same stress and corrosion conditions used in the tensile strength evaluation.

As in the tensile tests, the bright carbon steel wire suffered because of the salt-fog exposure prior to testing.

The 18-2 Mn stainless steel exhibited very little ductility during the torsion test. A failure to obtain as-drawn wire from the manufacturer necessitated that wires for torsion testing be removed from a rope. As a result the wires received a degree of cold working during the stranding and preforming operation as well as from the hand straightening which took place upon removal from the rope.

The 17-7 PH stainless steel performed fairly well as far as high-strength-stainless steel is concerned. Stainless steels are known for their inherent lack of ductility at high strength levels. Two data points for the 17-7 PH material were unusually low. These failures were a result of flaws on the surface of the wire, observed under a microscope after failure.

Although the tensile behavior of the galvanized carbon steel was virtually unaffected by the salt-fog exposure, the torsional behavior was affected to a degree. In general, the galvanized carbon steel material performed better than the other materials tested. The results of the tension and torsion tests performed on the wire samples are summarized in Table 41.

The results of the wire tensile and torsion tests revealed the galvanized-carbon steel to be the best material for a corrosion resistant high strength wire-rope application. Its average tensile strength was almost equal with that of the 17-7 PH stainless steel (the highest tested) and its torsional behavior was extremely good even after exposure to salt-fog corrosion testing. The apparent low ductility characteristics of the high strength 17-7 PH may have accounted for its performance in a cable since its ultimate strength and

TABLE 41. RESULTS OF SINGLE-WIRE TESTS.										
Wire Material	Test Temp.	Yield Point 103 psi		UTS, 103 psi		RA (b) Percent		Torsions (c)		
		New	Exp (a)	New	Exp (a)	New	Exp (a)	New	Exp (a)	
Bright Carbon Steel	Ambient	261	255	307	285	44.7	49.0	68	30	
	-65°F	271	272	322	303	47.2	53.8	77	26	
18-2 Mn	Ambient	213	222	284	285	33.8	25.5	5	4	
	-65°F	263	253	326	323	42.4	39.9	4.2	2.8	
17-7 PH (heat-treated)	Ambient	286	284	324	326	49.7	44.8	36	41	
	-65°F	310	314	345	348	45.5	44.2	34	32	
Galvanized Carbon Steel	Ambient	266	261	327	327	45.9	48.5	80	67	
	-65°F	284	280	344	347	46.0	49.7	82	65	
(a) 48-hour salt-fog exposure per FED-STD-151.										
(b) Reduction in area at tensile failure.										
(c) 8-inch gage length for tension, 10-inches for tensile tests.										

fatigue resistance as a cable were lower than those demonstrated by the electrogalvanized carbon steel cable.

#### End Fitting Tests

The cable design support tests utilized commercial swaged and open-spelter(zinc) sockets. Damage resulting from the application of these fittings precluded development of the full cable strengths. Some socketing improvements were implemented that reduced this damage so that adequate strength and efficiency were developed to provide a basis for design projections.

Detailed end fitting development was not carried out as part of the design support testing because a variety of cables were being evaluated. The purpose of these tests was to select one candidate material and construction for detailed development. The development of the three types of end fittings required for each of the cable constructions would have been uneconomical.

#### Conclusions Drawn From Design Support Tests

Tension member design-support testing demonstrated that the 0.78-inch diameter electrogalvanized, 36X7 swaged strand, lang-lay, Warrington-Seale construction exceeds the design performance requirements of the ATC program. The characteristics of the tested 36x7 cable are shown in Table 42. The advantages of this material/construction combination are quantitatively compared in Table 43 and summarized below:

1. Highest tensile strength.
2. Highest strength-to-weight ratio.
3. Highest efficiency.
4. Meets fatigue spectrum loading criteria with acceptable remaining tensile strength. Bending fatigue 150% overload for 10,800 cycles had no perceptible effect on the strength of the cable.
5. Insensitive to drum groove wear due to bending fatigue (including operation at 150% overload).
6. Its material has acceptable corrosion resistance. There was no significant cable degradation due to bending fatigue or salt-fog exposure.

TABLE 42. CONSTRUCTION DETAILS FOR ELECTROGALVANIZED 36 x 7 LANG-LAY WIRE CABLE (0.78 INCH DIAMETER).					
WIRE LOCATION	WIRE DIAMETER, INCH	ULTIMATE TENSILE STRENGTH, 10 <sup>3</sup> PSI	TOTAL NUMBER OF WIRES	WIRE BREAKING LOAD, LB	AGGREGATE WIRE STRENGTH LB
Outer 14 Strands	0.046	309	84	514	43,176
Outer 14 Strands	0.049	314	14	592	8,288
Inner 7 Strands	0.038	330	42	374	15,708
Inner 7 Strands	0.041	322	7	425	2,975
Inner 7 Strands	0.029	348	42	230	9,660
Inner 7 Strands	0.031	350	7	264	1,848
Inner 7 Strands	0.038	330	42	374	15,708
Inner 7 Strands	0.041	322	7	425	2,975
Core Strand	0.056	307	6	756	4,536
Core Strand	0.059	306	1	837	837
Total Aggregate Strength					105,711
Metallic Area = .330 sq. inches					
Measured Weight = 1.219 lb/ft					

TABLE 43. HLH/ATC CHARACTERISTICS OF .78-INCH-DIAMETER CABLE FROM PRELIMINARY DESIGN TESTS.									
Material	Cable Type		Aggregate Strength Lb	Breaking Strength Lb	Cable Efficiency %	Cable Weight Lb/Ft	Strength Lb -Wt / Ft	Modulus E 10 <sup>6</sup> PSI	Cable Torque In/Lb
	①	Construction							
Electro- Galvanized Carbon Steel	36 x 7		105,711	90,100	85.3	1.219	74,100	19.7	1980
Electro- Galvanized Carbon Steel	6 x 36		86,200	67,800	78.5	.997	68,013	18.1	2170
Bright Carbon Steel	6 x 36		84,968	66,800	78.6	1.006	66,385	16.4	2140
Bright Carbon Steel	6 x 36 RL		82,645	66,500	80.5	1.043	63,700	②	②
Stainless 17-7 PH	6 x 36		86,800	61,128	70.5	.966	63,400	17.8	2100
Stainless 18-2 Mn	6 x 36		83,093	48,000	57.7	1.012	47,407	14.7	2070
① All samples are Lang-lay except for regular-lay (RL) shown.									
② Test not conducted.									



7. Its material is insensitive to stress corrosion.
8. Its construction characteristics are desirable:
  - a. It has the highest elastic modulus.
  - b. It develops the lowest torque.
  - c. It exhibits the least permanent elongation or constructional stretch and a proportional limit well above required limit load.

## Tension Member Development Tests

### Introduction

This section presents the results of development tests and the evaluation of the metallic tension member design for the HLH/ATC Cargo Handling System. Tests were conducted between December 1972 and March 1973. Supplemental end fitting tests and evaluation of the 0.78-inch-diameter cable were conducted between May and August 1973.

To evaluate the potential improvement over state-of-the-art configurations and to maximize the strength-to-weight ratio of the cable design, a 0.70-inch-diameter cable was selected for development testing. This selection was based on the desire to use high strength, specially drawn wire that is producible with existing tools. The average wire tensile strength minimum drawing specification was in the range of 340,000 to 350,000 psi. To achieve this high tensile strength and retain wire ductility, the wire was drawn from hot-dipped rather than electrogalvanized material.

### Test Objectives and Philosophy

The objectives of this test program were to develop the cable and end fitting designs, evaluate their performance as tension member assemblies, and to substantiate that the cable and the end fittings meet the requirements of HLH/ATC.

The tests outlined in this program were an extension and expansion of the tests conducted during the design support investigations. They were intended to provide sufficient test data to establish the tension member physical and life characteristics under static and dynamic loads, and simulated hoist system operating conditions. The static test data was to determine:

1. Cable assembly stress/strain characteristics at design limit load
2. Tensile strength
3. Strength degradation (if any) due to bending over a drum, fatigue or corrosion
4. Failure modes

The dynamic tests were to determine compliance with requirements of the tensile strength, bending, wrap pressure loading, and fatigue life under design spectrum loading.

The tests were conducted under the following constraints:

1. A hoist drum simulation was used during both static and fatigue tests.
2. All specimens for fatigue testing were proof-loaded to limit load (67% ultimate) before testing.

#### Specimen and Test Equipment Design

Specimen Design - The evaluated cable assemblies satisfy the multi-point and single-point HLH tension member design requirements stipulated in Boeing Vertol Drawing 301-10253.

Each tension member consists of a pair of opposite (left and right) lay cables and appropriate end fittings for the four interfaces involved. Each test specimen included a .70-inch-diameter cable of Lang-lay construction consisting of 36 swaged strands of seven wires each. The material was galvanized music-wire grade carbon steel. The specimen lengths were either 5 or 12 feet, determined by the specific tests.

Tension member end fitting specimens were made to conform to the interface space limitations and requirements as shown in the following Boeing Vertol drawings:

301-11149 - Interface-Coupling Equalizer Bar  
301-11170 - Interface-Single-Point Adapter  
301-10322 - Interface-Hoist Drum  
301-10271 - Assembly, Sheave Envelope (Coupling Load Beam)

These interfaces required the development of configurations for three end fitting types with limits as follows:

<u>Type</u>	<u>Length</u>
Eye with swaged shank	
Equalizer bar:	7.25 inches, eye to nose length
Adapter:	7.75 inches, eye to nose length
Swaged button	
L.H. Drum:	1.25 inch O.D., 3.0 inches long
R.H. Drum:	1.125 inch O.D., 3.5 inches long
Eye-Splice	
Load Beam:	10 inch loop, 17 inches overall

Standard MS bushings and commercial components were specified by the respective interface drawings.

Test Fixture-Static Strength - Two test fixtures were used for static strength tests. One fixture was used for pure tensile loading of single end fitting cable specimens. The second fixture was used for tensile loading of a single specimen bent over a simulated hoist drum. Loading capacity of these machines was 90,000 pounds and 600,000 pounds, respectively.

Fatigue Test Fixture - A fatigue test fixture was used for applying both cyclic tension and cyclic bending to a pair of test specimens. The specimens were mounted end-to-end over two offset simulated hoist drums, forming an endless loop. The loading capacity of this machine was 140,000 pounds.

Test Instrumentation - Primary instrumentation for all tensile tests described below consisted of a tensile/torsion load cell with strain indicator readout for each load cell circuit. The tensile load cell capacity was 150,000 pounds with a calibrated accuracy of less than 0.5% of full-scale reading. The strain indicator as calibrated at 100,000 pounds had a sensitivity (scale division) of 10 pounds. The torque cell capacity was 300 foot-pounds. Cable measurements were made with a Vernier Caliper.

The calibration of the tension/torque load cell unit is traceable to the National Bureau of Standards.

## Test Methods

### General Test Program

Environmental Conditions - Except as otherwise specified, all testing was conducted at the laboratory's ambient temperature and humidity conditions.

Specimen Preparation - All test specimens prepared for bend-over-drum/tension-tension fatigue testing were proof-loaded to 50,000 pounds (cable-design limit load). End fittings were magnetically inspected prior to test, except as noted.

Test Procedure - Loads were stabilized before instrument data was recorded. Specimen processing and inspection records were maintained, and significant specimen dimensions were recorded before and after test.

Test Program Plan - Table 44 presents a summary of the design development tests planned. For each type of test, the table gives the test specimen configurations, the test conditions, the number of specimens used, and the specific end fitting/cable combinations developed and evaluated during the fatigue tests.

### Design Development Test Program

The tension member design development program reported in this document includes cable and end fitting development, performance, and validation tests.

#### Cable Development

Objective - The tension member development objective was to produce an advanced technology cable with a higher strength-to-weight ratio than commercially available (i.e., smaller diameter, lighter weight), with a finite fatigue life and suitable corrosion protection. The ATC cable was to be fabricated using existing industrial tooling.

To this end, design support tests were conducted to evaluate various materials and cable constructions as potential ATC candidates.

Design Support Test Results - In the design support tests, one configuration of the 0.78-inch diameter cables evaluated exceeded the ATC design performance requirements. This cable was the 36x7 Lang-lay, Warrington-Seale, swaged strand construction using electrogalvanized music-wire carbon steel. Highlights of the 36x7 characteristics demonstrated were:

1. The highest strength-to-weight ratio
2. The highest efficiency
3. No discernible strength loss from bending, fatigue or corrosion (with a  $D/d = 20/1$ ) when evaluated by straight tensile testing.

TABLE 44. PLANNED TENSION MEMBER DESIGN DEVELOPMENT TESTS - EVALUATION OF END FITTINGS AND 0.70-IN-DIA, 36X7 CABLE						
Specimen		End Fitting		Test Conditions		No. of Specimens
Ccde	Config. (a)	Interface/Lay	Type	Type	Load	End Fitting Cable
<u>End Fitting Development &amp; Static Strength Tests</u>						
A	Fitting	Coupling and Adapter	Swaged-Shank	Tensile	To Ultimate	6 3
Aa		Coupling and Adapter	Eye	Tensile	To Ultimate	2 -
B	Fitting	Load Beam	Eye-Splice	Tensile	To Ultimate	6 3
C	Fitting	Hoist Drum (Left & Right)	Swage Button	Tensile	To Ultimate	6 3
<u>End Fitting/Cable--Static Strength Tests</u>						
D-1	Cable and Fittings	301-11149 Right	Eye/Swaged Shank	Tension/Torsion,	To 67% Design	6 3
D-2		301-11170 Left	Shank	Tension/Elongtn;	Ultimate, then	
D-3		301-11170 Right	(E/SS)	Tension-Over-Drum (TOD)	To Failure	
<u>End Fitting and Cable Fatigue (b) Tests</u>						
E-1	Cable and Fittings	301-11149 Right	E/SS	BOD/Cyclic Tension, TOD	Spectrum-10,800 cycles; Ultimate	8 4
E-2		301-11170 Right	E/SS			
E-3		301-10271 Left	Eye-Splice			
E-4		301-11170 Left	E/SS			

TABLE 44. CONTINUED.						
Specimen		End Fitting		Test Conditions		No. of Specimens
Code	Config. (a)	Interface/Lay	Type	Type	Load	End Fitting Cable
F-1 F-2 F-3 F-4	Cable and Fittings	301-11170 Right 301-10271 Right 301-11170 Left 301-11149 Left	E/SS Eye-Splice E/SS E/SS	BOD/Cyclic Tension, Tension, TOD	Spectrum- 21,600 Cycles, Pull LL, 50,000 Cycles; Pull to Failure	8 4
G-1 G-2	Cable and Fittings	301-11149 Right 301-11149 Right	E/SS E/SS	Corrosion/ BOD/Cyclic Tension, TOD	Spectrum- 3,600 Cyc./Salt-Fog, 7,200 Cyc, then Ult.	4 2
TOTAL-FITTINGS & CABLES:					46	22
(a) All fittings included pin bushings per Drawing 301-10253, except eye-splices. (b) Proof-load (50,000 lb) Fatigue Specimens before test. (c) A hoist drum simulation used on all static TOD and fatigue (BOD) tests.						

Design Considerations - ATC Development Cable - The margin provided by the 0.78-inch-diameter 36 X 7 electro-galvanized cable led to the analysis and development of a higher strength-to-weight ratio cable design.

Driving factors in the development of an ATC cable design were:

1. A smaller cable diameter that would make hoist weight savings possible through reduction of drum length and diameter.
2. The 0.78-inch cable weight was 1.219 lb/ft. A cable weight saving of 196.5 lb per aircraft could be realized if the cable weight goal of 0.85 lb/ft could be reached.
3. The 0.78-inch cable used millrun wire with an average tensile strength of 320,000 psi. Wire with 350,000-psi tensile strength and adequate ductility could be produced and used to achieve goals mentioned above.

Based on the design support test results and these design considerations, a 36x7 cable with a 0.70-inch diameter was selected for development. The following design tasks were identified in choosing this approach to find out:

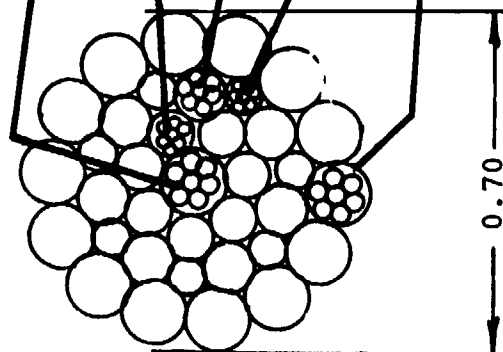
1. Whether, in fact, wire of good quality, with the desired strength/ductility characteristics, could be produced.
2. Whether the 350,000-psi wire produced would be compatible with present stranding, swaging, and cabling tools and manufacturing techniques.

Development Cable Design - 0.70-Inch Diameter Cable  
Description - Construction characteristics of the 36x7 cable are presented in Table 45, which lists the strand and wire characteristics of both right- and left-hand cables. Computed "aggregate breaking strength" (ABS) for the right-lay cable was 95,744 lb, and the left-lay was 91,978 lb. These strengths were based on average measured wire strengths of 363,000 and 348,000 psi for right- and left-lay respectively. Examination of Table 45 shows that the 4,266-lb difference between cable strengths was due to the use of lower strength wires in the outer strands of the left-lay cable.



TABLE 45. DEVELOPMENT CABLE - 0.70-INCH-DIAMETER 36X7 CONSTRUCTION CHARACTERISTICS  
(RIGHT AND LEFT LAY)

Strands		Cable Lay			
		Right	Wire		Left
No.	Location	Diam. (In.)	Total No. Used	Measured Strength psi (10 <sup>-3</sup> )	Aggregate Strength (Pounds)
1	Core	.053	1	331,342	731
7	1st Inner	.051	6	339,726	4,163
7	2nd Inner	.036	7	345,817	2,463
7	2nd Inner	.034	42	367,874	14,028
7	2nd Inner	.036	7	345,817	2,463
7	2nd Inner	.034	42	367,874	14,028
7	2nd Inner	.028	7	365,408	1,575
7	2nd Inner	.026	42	382,348	8,525
14	Outer	.044	14	341,986	7,378
14	Outer	.041	84	365,092	36,120



Calculated aggregate breaking strength, lb: 95,744 91,478

NOTES:

Total metallic area: 0.264 sq.in.  
Average wire stress: 362,942 psi (right lay)  
346,770 psi (left lay)  
Measured weight: 0.948 lb/ft (right lay)  
0.960 lb/ft (left lay)

The right-lay was fabricated completely from one wire source, with a minimum strength of 30,000 psi over the catalog strength value for each wire size used. The outer layer of the left-lay cable, a total of 14 strands, was supplied by a second source, whose strength level goal was 20,000 psi over catalog minimums. Strand designs for left- and right-lay cables were the same. The pattern of wire lay lengths (pitch of twist within strands) and L/d ratios in the 0.70-inch cable were slightly larger than those used in the 0.78-inch-diameter cable. From cable fabricating experience, a lower efficiency was anticipated from use of the high strength wire. To compensate for this, the new cable was fabricated with an increased strand lay length.

Since multi-point and single-point cable applications were relatively close in strength requirements (i.e., 75,000 and 61,300 lb (UTS), respectively), the same cable design was used for both.

Cable Physical Characteristics - The development cable size and weight design estimates were based on  $\pm .001$  tolerance on each wire used. Final characteristics were also subject to the influence of strand compacting. The cables, as delivered, were as follows:

	<u>Actual</u>		<u>Calculated</u>
	<u>Right</u>	<u>Left</u>	
Diameter, in.	.695	.695	.695 to .710
Weight, lb/ft	.948	.960	.982

With the 0.70 cable, the weight reduction over the 0.78 inch cable was 140.5 lb/cargo system.

Cable Construction - A problem of wire damage occurring in the swaging of the outer strands (365,092 psi wire strength, see Table 45), necessitated the use of the lower strength wire in the left-lay cable. The pre-test estimate of minimum breaking strength (MBS) for each cable construction, based on projections of construction losses, was 79,000 and 77,000 lb for right and left lay, respectively.

## END FITTING DEVELOPMENT

### General Objectives

The tension member design objectives were to develop 100%-efficient end fittings for cable interfaces where needed to allow adequate development of full cable strength and provide compatibility in both static and fatigue tests with the 0.70-inch cable design. (A 100% efficient fitting is one whose mechanical gripping strength is greater than the minimum breaking strength of the cable.)

### Approach

Design development cable fitting development was started with the 0.78-inch-diameter 36x7 design support test cables. The swaged type end fitting was selected for this application because of the experience gained during design support tests. (These tests demonstrated that cable ultimate strength could not be achieved with fiece type and spelter sockets.)

Preliminary tests starting with state-of-the-art techniques were used to define the significant swaging parameters involved. The most difficult requirement to meet was the manufacturing of a 100%-efficient fitting for the equalizer bar attachment. Since flexibility in test sample configuration was required, fitting specimens were individually made in the laboratory for use with the 0.78-inch cable. The eye portion of this "laboratory" fitting was machined over-sized for high load carrying capacity and remained the same for all tests. The shank end of the fitting was altered for each fitting test. Alterations included changes in the outside diameter, length, and shape of the cable entry to determine their influence on specimen failure load.

Once the basic guidelines for achieving an adequate mechanical grip were established, tests with the 0.78-inch cable were discontinued, and the final shank configuration was designed for the 0.70-inch development cable. The three eye designs, required as parts of the swaged shank fittings, were validated in separate tests. After each was defined separately, the swaged shank and eye design portions of the fittings were combined into single component designs, as shown in drawing SK301-11561-1. These components were then fabricated as individual test samples and evaluated in the static and fatigue portions of the development test program, which follows. The same procedure was also applied to the development and validation of the eye-splice configuration.

In the drum button development, however, static testing was used alone, since these terminations are only subjected to pure tensile loading.

All tension member end fitting interface types and configurations are given in Table 46, along with the design criteria. During development, the specimens were coded A, Aa, B, C, for swaged shank, eye, eye-splice, and drum button, as called out in Table 44.

Swaged Shank End Fitting Development - "A" Specimens - Development Tests With 0.78-Inch-Diameter Cable -

Development of the 100% efficiency end fitting was initiated with the 0.78-inch-diameter cable during the period when the high strength 0.70-inch-diameter cable was being fabricated. The justification for proceeding with these tests was that the construction of the cable was identical (both were 36x7 although wire diameters varied slightly and that the development with the 0.78-inch cable would proceed on the basis of its ultimate breaking strength (achieving a cable "center break").

End Fitting Type and Material Selection - The cable design support tests utilized commercial swaged and open spelter zinc sockets. Damage resulting from the heat in the application of these fittings precluded development of the full strength of the 0.78-inch cable.

The mechanically swaged fitting was selected for use since it was lighter and less bulky than a "fieke" (a trapped wedge) or the spelter type with low temperature matrix (epoxy) sockets. Therefore, test efforts were confined to the swaged retention. Due to the lack of specific design information for the 36x7 cable, a program was established to define the parameters involved in producing a swaged sleeve of adequate mechanical grip that would not degrade the cable strength. AISI 1035 steel was used for the two initial tests and to investigate swaging efforts with the commercial shank configurations. All additional tests were conducted with AISI 4130, a hardenable material which could be produced with a heat treated "eye" section to reduce weight.

Specimen Design - Each specimen length, eye-to-nose, was 7.25 inches. The swaged length was approximately six inches. The eye section used for applying the load was made over-sized for convenient mounting in the tensile test machine.

This shank specimen configuration, as shown in Figure 99 was used to represent both the equalizer bar and adapter shank applications.

TABLE 46. TENSION MEMBER END FITTING CONFIGURATIONS AND DESIGN CRITERIA.					
End Fitting (Interface)	Fitting Type	Interface Drawing	Design Configuration	Design Loads* (Pounds)	
				Limit	Ultimate
Coupling Equalizer Bar	Eye & Swaged Shank	301-111149	Same for Left- and Right-lay cable	50,000	75,000
Adapter (Single-point)	Eye & Swaged Shank	301-111170	Two eye designs for mating adapter	41,000	61,300
Coupling Load Beam	Eye-splice	301-10271	Same for Left-and Right-lay cable	41,000	61,300
Hoist Drum	Button-Swaged Shank	301-10322	Two shank designs for mating hoist drums	20,000	30,000
*Limit Load - no yield Ultimate Load - no rupture					



Figure 99. Typical AISI 4130 Fitting After Being Swaged onto a 36x7 Cable

Cable assembly specimens used for static strength tests were identified by the letter "A". Each was 5 feet long from eye-to-eye, and included two swaged end fittings. Fitting design varied within and between test specimens depending on results of the previous pull test.

Test Method and Procedure - Tests were conducted on fixed length shank specimens of varying pre-swaged shank diameters and, in some instances, nose (taper) configurations. In each test the final swaged shank diameter was the same.

These tests were to define the range of gripping conditions (amount of swaging pressure applied) between the fitting shank and the cable that would result in a cable pull-out (slip) or a cable rupture within the fitting. The parameter controlling the residual pressure between two parts after swaging was the amount of shank cross-sectional area reduction ( $R_A$ ) which took place by pressing the shank in an under-sized die. Systematically spaced values of  $R_A$  were used to define the swaging pressure (min.-max.) range to arrive at a configuration that would consistently produce a cable "center break" (100% efficient fitting design).

The swaged shank fitting development program was conducted in series of three tests.

Series 1) Tests with 0.78-inch-diameter 36x7 cable  
These tests were a continuation of the design support tests ("F" shank specimens) to achieve a center break of the 0.78-inch cable with standard, commercially available mild steel fittings. These tests resulted in excessive cable damage in the nose of the fitting.

Succeeding tests during this portion of the program achieved the definition of cable slipping loads and a higher cable rupture load using AISI 4130.

Series 2) Tests of 0.70 inch cable 36x7  
Shank area reductions were increased from a slipping configuration, based on 0.78-inch cable tests, to the achievement of a center break. Subsequent tests introduced shank diameter variations to investigate the effect of dimensional tolerances and also reduce the fitting length. Achievement of center breaks during these tests terminated this series with a design configuration.

Series 3) Retest of 0.70-inch 36x7 cable

Additional tests were undertaken to extend the swaged shank investigation to determine the onset of cable rupture in the fitting as a result of encountering cable slippage on one specimen during tension-over-drum tests. These tests maintained the same (design) fitting length and established a shank reduction value which identified the onset of cable degradation from swaging. This third series of tests was supplemented by extensive examination of the physical aspects of the fitting shank, the influence of hardness on swaging, and an x-ray examination of all swaged specimens.

Test Results - Since over-swaging occurred in the design support test sample, F-19, the swaged sleeve cross-sectional area in specimen F-29 was reduced. This was to compensate for the increased cable density that existed between a 36x7 cable and the 6x36 type cable for which the fitting was originally intended. Succeeding tests were directed towards lightening the swaging penetration into the 36x7 cable and shifting the load transfer point further into the fitting until slippage occurred between fitting and cable.

Table 47 displays the shank configuration, the swaging variables evaluated, and the failure loads achieved. Results shown indicate that cable failing load was increased from 83,400 lb to 90,100 lb as the cross-sectional area,  $R_A$ , was reduced from 19% to a value of 10.1% (specimen F-32). While cable breaking loads increased, failure still occurred within the first two inches of the fitting nose (6° taper). Further reduction in swaging pressure and use of a more gradual nose taper eliminated cable damage (failure in the fitting) and produced slippage at 75,800 lb and 74,900 lb with an  $R_A$  of 7.5% in specimens F-33 and F-34.

A comparison of the swaging penetration within the cable strands is seen from the initial test section, specimen F-19, and specimen F-32/VI, shown in Figure 100. The reduced cable damage from the lighter swage on sample F-32 resulted in a 5,000-lb increase in the failing load.

The F-34 specimen included two different end fittings:

1. A constant 7.5% reduction in area ( $R_A$ ) over its length, and
2. An  $R_A$  which varied from 7.1% to 7.5% over its length.



TABLE 47. SWAGED SHANK END FITTING DEVELOPMENT - TESTS WITH 0.78-INCH-DIAMETER DESIGN SUPPORT TEST CABLE (a).							
Swaged length = 6 in. Overall length of fittings = 9-15/16 in. Bore diameter = 0.797 in. Material = AISI 4130 (b)							
Specimen Number	Fitting Number	Nose Taper	Initial O.D., in.	Final O.D., in.	Percent Reduction (c)	$\Delta L$ , in. (d)	Breaking Load, lbs
F-19 (b)	I & II	6° - 1" O.D.	1.545	1.39	19.1	--	83,400
F-29 (b)	I & II	6° - 1" O.D.	1.520	1.39	16.4	--	89,600
F-30	I	6° - 1" O.D. 6° - 1/2" I.D.	1.515	1.385	16.4	0.60	89,700
F-30	II	6° - 1" O.D. 6° - 1/2" I.D.	1.490	1.390	13.0	0.42	--
F-31	III	6° - 1" O.D. 6° - 1/2" I.D.	1.490	1.390	13.0	0.29	89,700
F-31	IV	6° - 1" O.D. 6° - 1/2" I.D.	1.470	1.390	10.6	0.26	--
F-32	V	6° - 1/2" O.D. 1°8' - 1-1/2" I.D.	1.466	1.385	10.7	0.28	--
F-32	VI	6° - 1/2" O.D. 1°8' - 1-1/2" I.D.	1.455	1.380	10.1	0.26	90,100
F-33	VII	1° - 2" O.D.	1.455	1.380	8.8	0.198	--
F-33	VIII	1° - 1.7" O.D.	1.435	1.380	7.5	0.201	75,800 (e)
F-34	IX	1° - 1.7" O.D.	1.435	1.380	7.5	0.152	74,900 (e)

TABLE 47. CONTINUED.							
Specimen Number	Fitting Number	Nose Taper	Initial O.D., in.	Final O.D., in.	Percent Reduction (c)	$\Delta L$ , in. (d)	Breaking Load, lbs
F-34	X (f)	1° - 1.7" O.D.	1.388- 1.438 (g)	1.380	1.2-7.9	0.082	33,500 (h)
F-34	XI (f)	1° - 1.7" O.D.	1.437- 1.440 (g)	1.385	7.1-7.5	0.187	--
F-35	XII	1° - 1.7" O.D.	1.451 (Avg.)	1.380	9.37 (Avg.)	0.240	--
F-35	XIII	1° - 1.7" O.D.	1.461 (Avg.)	1.380	11.23 (Avg.)	0.290	81,000 (i)

(a) Specimen numbers continued from design support test series using 0.78 dia.cable.

(b) AISI 4130 used in all fittings except F-19 and F-29 which used AISI 1035.

(c) 
$$\frac{(\text{Initial O.D.})^2 - (\text{Final O.D.})^2}{(\text{Initial O.D.})^2}$$

(d) Increase in shank length due to swaging.

(e) Cable slipped 1-1/4 inches in fitting.

(f) All cable/fittings assembled with cable lubricant except F-34 which was assembled dry.

(g) Fitting shank tapered over entire length.

(h) Machining error in forming tapered shank resulted in insufficient swage penetration.

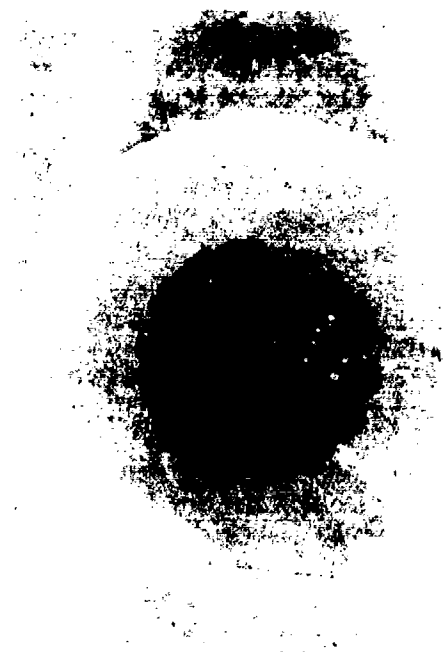
(i) Fitting slip - no cable break.



Specimen F-19 (1035,  $R_A = 19\%$ )



Specimen F-32/VI (AISI 4130 -  
 $R_A = 10.1\%$ )



Specimen F-19: Deep Swaging Penetration - Sleeve Reduction in Area,  $R_A = 19\%$



Specimen F-32/VI: Shallow Swage Penetration - Sleeve Reduction in Area,  $R_A = 10.1\%$

Figure 100. Comparison of Swaging Penetration.

Prior to assembly, the ends of the cable specimen were cleaned with trichlorethylene to remove the surface and interstrand cable lubrication. The specimen was pulled, and it slipped at 74,900 lb (no failing load was obtained). The 7.1%/7.5% RA fitting did not slip at the peak load.

The load achieved in this test was within 1.2% of the yielding load achieved with an identical assembly, F-33, except for presence of the cable lubricant interface. The swaged shank grip test demonstrated that the lubricant in the cable/fitting junction did not reduce its strength. The cable lubricant, therefore, need not be removed before fitting installation, thereby enhancing the corrosion resistance of the joint.

Specimen F-35 was run with tapered shanks to investigate an alternate means of reducing cable damage at the nose of the fitting. The increased slipping load achieved with an RA of 11.3%, however, could not be interpreted fully, compared with other cylindrically shaped specimens without additional work. The tests with the 0.78-inch cable were halted, however, when the initial samples of the 0.70-inch cable became available for development.

While end fitting development with the 0.78-inch cable was discontinued, additional tests were carried on to determine the ultimate strength of the 0.78-inch cable in straight tension and by bending-over-a-drum. This was accomplished subsequent to the completion of the 0.70-inch-diameter cable development to provide essential data for design projections.

The swaged shank grip design for the 0.70-inch cable started with the 0.78-inch test results as a basis. The 0.78-inch-diameter, 36x7 specimens established that acceptable swage type grips could be achieved with the 0.70-inch-diameter development cable with shank area reductions of 9% to 10.6% for a constant cross-section. Specific end fitting development for the 0.70-inch cable was carried on using the 7.5% RA as a starting point.

Only two test specimens were required to achieve a configuration that exceeded the cable breaking strength. Sample fittings on Specimen A-1 were prepared with a long, shallow nose taper of 1° and a cross-section providing an area reduction (RA) of 8.4%, estimated to be part way between a "slippage" and "cable damage" condition.

Results of Straight Tensile Tests to Ultimate - Results of this test were encouraging in that a cable slippage occurred at 66,800 lbs, indicating that cable damage within the nose of the fitting had been avoided although swaging pressure had increased. By further increasing the reduction in area to 10%, the next sample, A-2, (5.88 inch grip length) resulted in a true cable failure or "center break", establishing the cable breaking strength at 78,300 lb for the right-lay construction. Specimen A-3 was prepared to validate the 10% RA configuration and establish whether the difference in swaging pressures resulting from +0.005-inch shank tolerance would influence the mechanical grip. This provided specimen A-3 with a pair of end fittings with an RA range of 9.3 to 10.5%. To further encourage a slippage and to simultaneously evaluate a reduced gripping length, both the fittings used on specimen A-3 were made 1/2 inch shorter (length of 5.38 inches) than in A-2. This, however, was done without reducing the effective gripping length, since the nose taper was changed to 2°. Both fittings on the A-3 specimen survived the cable failure at 78,000 lbs. From this test the shank design (for the equalizer bar and the single point adapters) was fixed with a 5.38-inch swaged length and an RA of 10.0%. The shank geometries used for specimens A-1, A-2, and A-3 are shown in Figure 101. Swaging parameter variations and results of the three tests are given in Table 48.

0.70-Inch Cable Strength Determination - The pure tensile strength of the right-lay 0.70-inch cable was established at a minimum value of 78,000 lb for specimens A-2 and A-3. Subsequent tests of the left-lay cable, specimen A-5, established the strength by center break at 75,100 lb, also in pure tension. Specimen A-5 "center break" is shown in Figure 102.

During these tests, wire breakage was noted (audible "pinging") in the right-lay cable starting at 68,000 lb and in the left-lay cable, starting at 65,000 lb. It was also noted that at rupture almost all inner cable strands were broken, whereas a high percentage of outer strands had not failed. This is illustrated in Table 49, which describes the failure modes of some early tensile samples.

The apparent 10,000-lb spread between the first wire breaks and ultimate cable failure, and similar strand failure characteristics were noted for all 0.70-inch specimens. Both of the above conditions were characteristic of below optimum loading distribution between strands, similar to other constructions (i.e., 6x36 and 6x19) but apparently unlike the 0.78-inch design-support test cable where relatively sudden rupture occurred.

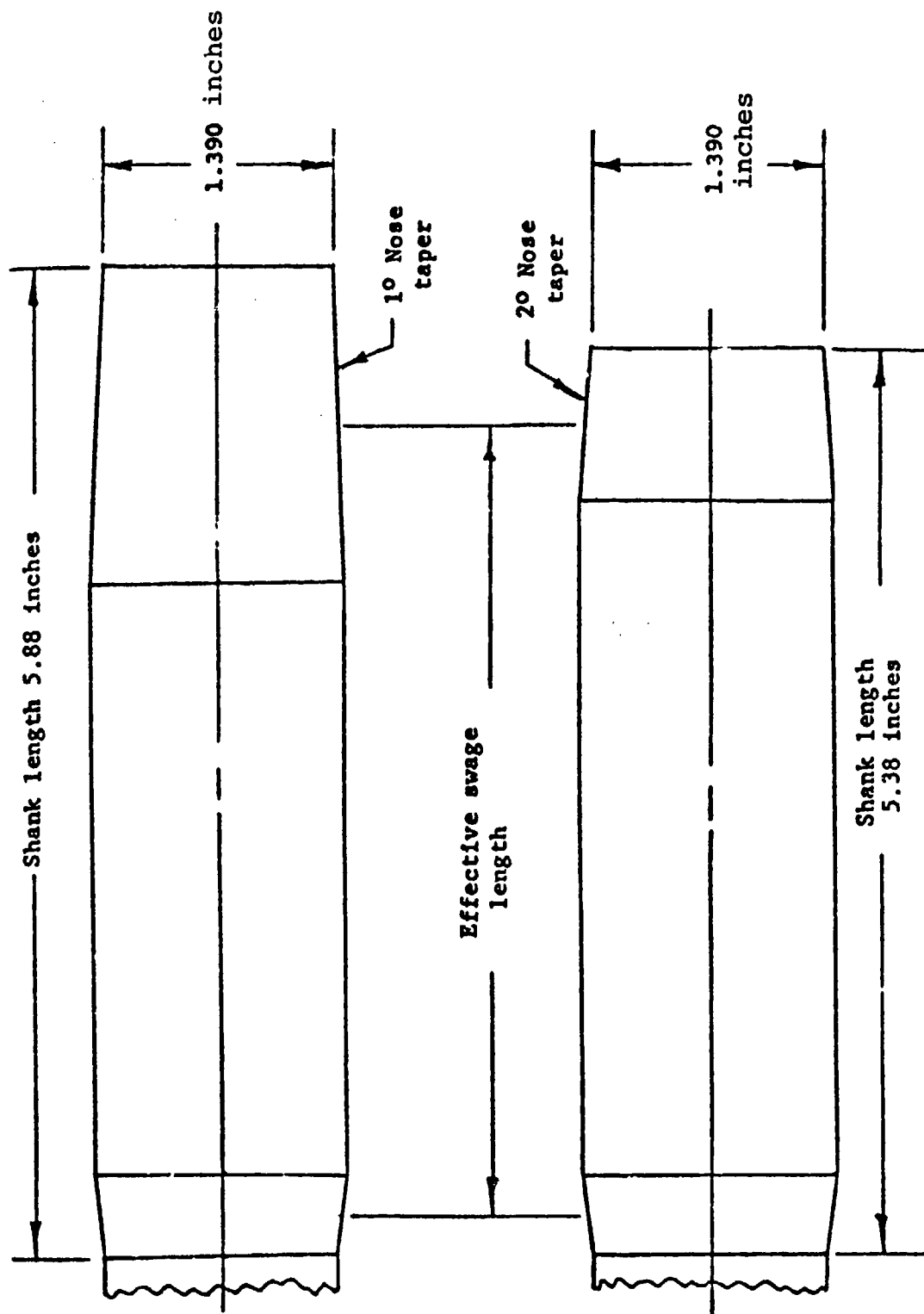


Figure 101. Shank Geometries Showing How Change in Nose Taper Allowed for Shorter Shank Length While Maintaining the Same Effective Swage Length.

TABLE 48. SWAGED SHANK FITTING DEVELOPMENT FOR 0.70-INCH-DIAMETER CABLE. (All specimens proof-loaded to 50,000 lb in straight tension prior to final tensile test. Specimen length: 54 in., eye-to-eye)						
Specimen No. Cable Lay	Fitting Number	Nose Taper on O.D., Degrees	Percent Reduction(a)	Shank Length, Inches	$\Delta L$ in. (b)	Failure Load, lbs.
A-1 Right	I	1	8.4	5.88	0.219	66,800 (c)
	II	1	8.4	5.88	0.235	--
A-2 Right	III	1	10.0	5.88	0.264	78,300 (d)
	IV	1	10.0	5.88	0.251	--
A-3 Right	V	2	9.3	5.38	0.216	78,000 (d)
	VI	2	10.5	5.38	0.274	--
A-4 Left	A-4-1	2	10.0	5.38	0.295	66,900 (e)
	A-4-2	2	10.0	5.38	0.257	--
A-5 Left	A-5-1	2	10.0	5.38	--	75,100 (d)
	A-5-2	2	10.0	5.38	0.305	--
(a) $\frac{(\text{Initial O.D.})^2 - (\text{Final O.D.})^2}{(\text{Initial O.D.})^2}$						
(b) Increase in shank length resulting from swaging.						
(c) Cable slipped two inches in fitting. When specimen was reloaded, the cable slipped out completely at 46,500 pounds.						
(d) Neither fitting failed, a cable "center break" was achieved (cable failure away from an end fitting).						
(e) Cable slipped in fitting. When reloaded, the cable failed inside the same fitting at 65,100-lb tension.						

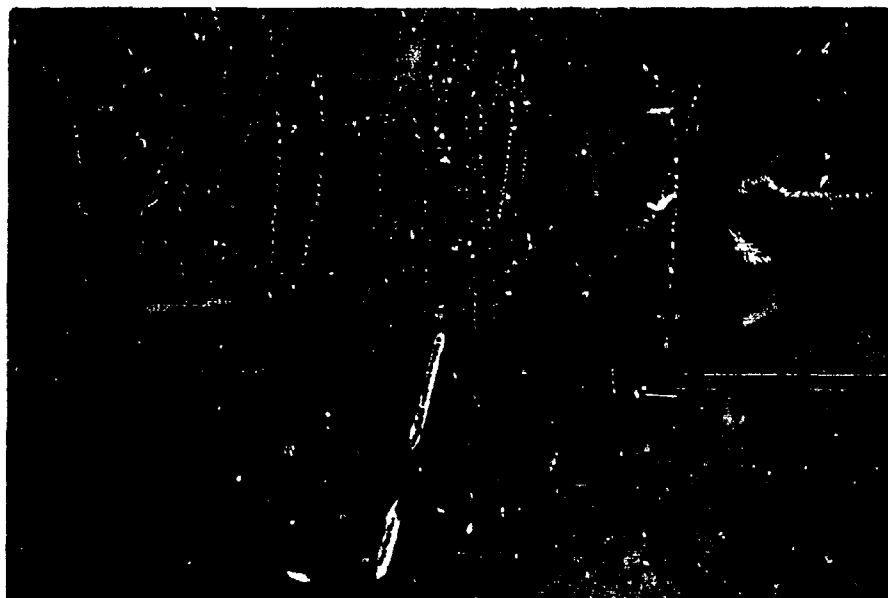


Figure 102, Left-Lay Specimen Showing Cable "Center Break".



TABLE 49. 0.70-INCH CABLE FAILURE CHARACTERISTICS.				
Specimen Number	Cable Lay	Ultimate Breaking Strength	Load at Time of First Wire Breaks	Failure Location
A-2	Right	78,300 lb	68,000 lb	Simultaneous failure of 19 inner & 9 outer strands 2" from fitting #3.
A-3	Right	78,000 lb	-	15 inner strands & 6 outer strands failed approx. 18" from fitting #5.
A-5	Left	75,100 lb	65,000 lb	-
A-6	Right	76,100 lb	-	Tension-over-drum tests failure at drum tangent point.

(Ultimate cable strength was never reached in these tests because of tempering of the wire in the spelter sockets.) This difference in failure characteristic between the 0.70- and 0.78-inch cables was later positively established by legitimate failure tests of the 0.78-inch cable, as explained in the paragraph entitled "Supplemental Tests of 0.78-Inch-Diameter, 36x7 Cable".

In the first left-lay cable strength test, specimen A-4 included two fittings identical to the A-3 design. ( $R_A = 10\%$ , swage length - 5.38 inches). When pulled, one of the fittings slipped at 66,900 lbs. A second load application to this cable assembly resulted in a cable failure inside the shank of the slipped fitting at a load of 65,100 lbs when 11 of the outer strands failed simultaneously. None of the inner strands failed. (The high load value of the second pull after the initial slip was probably due to the load buildup from wedging of the unswaged portion of the cable into the swaged (reduced diameter) hole, as when pulling a cork into a bottle neck.)

A repeat test with specimen A-5, in which two identical fittings were used ( $R_A = 10\%$  and shank hardness  $R_B$  83-87), held intact and the first left-lay cable center break was achieved at 75,100 lbs. Results of these two tests are also included in Table 49.

Typical "laboratory" type end fittings (AISI 4130 material) used for the 0.70-inch-diameter cable tests are shown in Figure 103. A cross-section of specimen A-3/VI ( $R_A = 10.5\%$ ) in Figure 104 shows the swaging penetration of the shank and reduction of cable diameter achieved. See Figure 100 for a comparison with the 0.78-inch cable.

Test Results with Design Development Swaged Shank Configurations - Twenty-two of the twenty-six end fittings subjected to tensile, fatigue and combined fatigue and corrosion tests had swaged shank configurations with  $R_A = 10\%$ . None of these fittings failed in fatigue. One specimen, D-2, slipped at a load of 55,200 lbs during tension-over-drum tests.

Table 50 displays physical characteristics of each of the development specimens and lists their test failing loads.



Figure 103. Typical Swage Fittings and 0.70-Inch-Diameter Cable After Cable Center Breaks

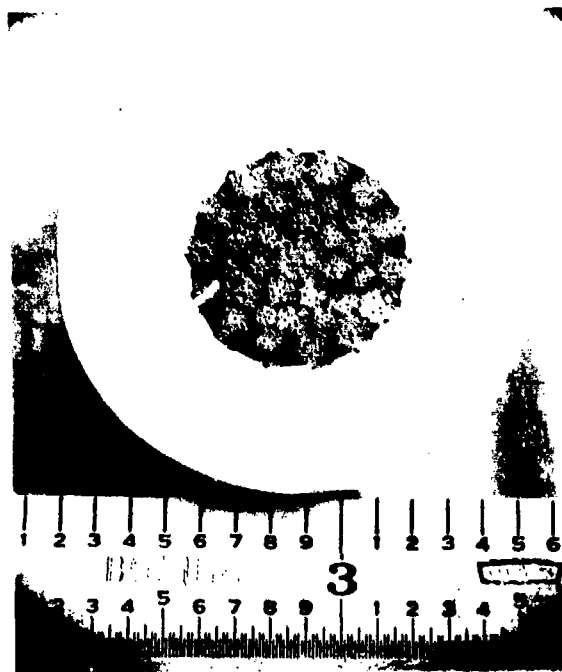


Figure 104. Cut Through Swaged Shank Specimen:  
A-3/VI - 0.70-inch Cable,  $R_A = 10.5\%$

TABLE 50. TEST RESULTS - SWAGED SHANK END FITTING USED IN DEVELOPMENT TESTS.							
Specimen No. and Lay	Fitting Number	Fitting Type	% Reduction (a), RA	$\Delta L$ in. (b)	Specimen Accumulated Cycles	Specimen Breaking Load, lb (d)	Remarks
D-1 Right	D-1-1 D-1-2	EQ-BAR	10 10	0.288 0.310	10 (c)	75,400	Fittings Satisfactory
D-2 Left	D-2-1 D-2-2	SPA-LH	10 10	0.305 0.305	10 (c)	55,200	Fitting Slip-Cable Failure at 65,900 with New Fitting.
D-3 Right	D-3-1 D-3-2	SPA-RH	10 10	0.305 0.282	10 (c)	73,700	Fittings Satisfactory
E-1 Right	E-1-1 E-1-2	SPA-RH	10 10	0.301 0.295	10,800 (e)	73,650	Fittings Satisfactory
E-2 Right	E-2-1 E-2-2	EQ-BAR	10 10	0.299 0.305	10,800 (e)	70,200	Fittings Satisfactory
E-4 Left	E-4-1 E-4-2	SPA-LH	10 10	0.287 0.273	10,800 (e)	69,900	Fittings Satisfactory
F-1 Right	F-1-1 F-1-2	SPA-RH	10 10	0.305 0.318	32,406 (e) (f)	--	Fittings Satisfactory
F-3 Left	F-3-1 F-3-2	EQ-BAR	10 10	0.300 0.293	21,600 (e)	35,000 (f) to 40,000	Fittings Satisfactory
F-4 Left	F-4-1 F-4-2	SPA-LH	10 10	0.293 0.287	50,000 (e)	38,900 (d)	Fittings Satisfactory

TABLE 50. CONTINUED.						
Specimen No. and Lay	Fitting Number	Fitting Type	% Reduction (a), RA	$\Delta L$ in. (b)	Specimen Accumulated Cycles	Specimen Breaking Load, lb (d) TOD
G-1 Right	G-1-1	EQ-BAR	10	0.293	10,800 (e)	62,000 (d)
	G-1-2		10	0.293		Fittings Satisfactory
G-2 Right	G-2-1	EQ-BAR	10	0.295	10,800 (e)	67,500 (d)
	G-2-2		10	0.282		Fittings Satisfactory (Cable Failed Between Drum & Fitting.)
<p>(a) <math>\frac{(\text{Initial O.D.})^2 - (\text{Final O.D.})^2}{(\text{Initial O.D.})^2}</math></p> <p>(b) Increase in shank length due to swaging.</p> <p>(c) 10 Cycles, 0 to 52,000 lbs. (limit load = 50,000 lb.)</p> <p>(d) TOD = Tension-Over-Drum Ultimate Test. Cable failure at sheave tangent point unless otherwise noted.</p> <p>(e) Load Spectrum Cycling with zero-load condition between cycles.</p> <p>(f) Cable strand failure during fatigue testing.</p> <p>(g) Failed in straight tension during limit load test.</p>						

Investigation of Failure of Specimen D-2 - The failure of specimen D-2 to meet strength criteria while meeting all fabrication and inspection requirements resulted in a review of all fittings fabricated and tested. An investigation was made to identify the reasons for the reduced gripping pressure. The investigation included the following:

1. Physical dimensions
2. Hole freedom from scale or foreign matter
3. Shank hardness survey
4. Swaging and heat treating processes, and
5. X-ray to check cable length in fitting and swaging uniformity.

No anomalies were found in examining Specimen D-2-1 except that the x-ray revealed a change in density (dark pattern) for 3/8 inch in the center of the fitting; this was coincident with a 1/8-inch-wide circumferential mark around the fitting shank C.D. made by the end of the swaging die. Subsequent longitudinal sectioning of the fitting visually showed this area with a reduced swaging penetration of the fitting material into the grooves between the cable wires and strands. (See Figure 105.)

Since no direct cause was found for the fitting slip, two additional areas of investigation were undertaken:

1. A comparison was made with the fittings that passed the pure tension and TOD ultimate load tests, and
2. Additional tests were run to define the cable sensitivity to damage by swaging. (Values of RA sufficient to cause cable rupture in the fitting.)

The physical inspection of all shank specimens revealed no relationship between cable diameter, hole size, cleanliness, or hardness and the failure. In fact, review of hardness data showed that good fitting performance could be achieved over a relatively wide range of hardnesses and that additional quality control procedures were needed to assure holding the hardness range specified.

Swaging Process - Swaging of all the test fittings was done in a similar manner. Each fitting was swaged 15 to 20 times in a hydraulic swaging press while being rotated about 45 degrees between presses to achieve a

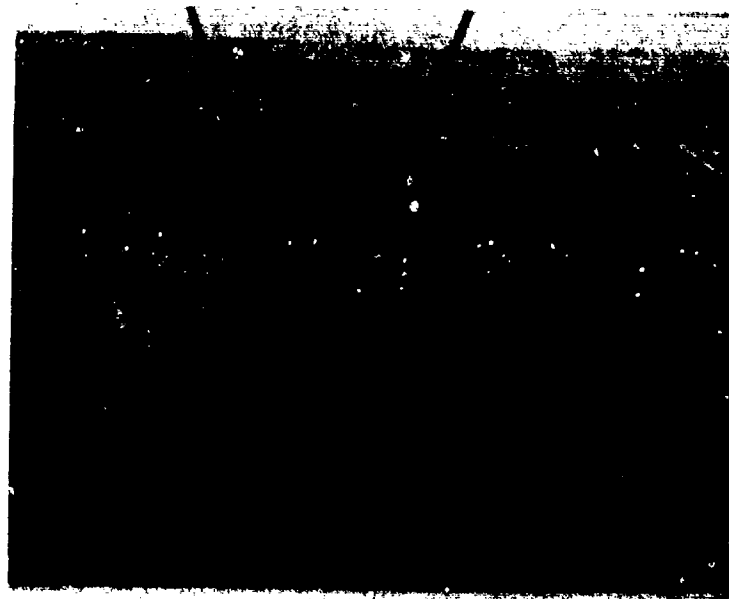


Figure105. Sectioned Swage - End Fitting Showing  
Reduced Swaging Penetration

circular cross-section that conformed to the closed inside diameter of the swaging dies. All swage fittings were installed in the same manner and inspected with a dial caliper to insure that a final outside diameter of 1.380 inches was achieved. Since the dies were not long enough to swage the full length of the shank in one operation, swaging began at the nose end and finished near the eye. The nose portion was completely swaged before moving on toward the eye portion, to force most of the fitting material to flow in the direction of the eye.

After swaging it was noted that an external impression (stretch mark) was left at the edge of the initial swage die location. (See Figure 106) Although visible on most fittings, it was hardly measurable.

X-Ray Inspection - A comparison of x-rays of 22 fittings associated with the die markings, however, revealed variations in swaging effects which were not apparent from watching the process or subsequent dimensional checks. The differences seen were subtle and appeared as slight variations in swaging penetration (near the shank center) where overlapping of the reduction process occurred. The internal "bulges" seen in the films varied in width ( $1/2$  to  $7/8$  inches) and location ( $2-1/8$  to  $3-7/16$  inches from the nose of the fitting). Since the bulged areas represent a reduction in grip length, it was concluded that slippage of the D-2 specimen (shortened length) occurred due to non-uniform swaging, and in the shorter fitting length (5.38 inches), the grip became marginal if the bulge was present. Figures 107 and 108 are photographs produced from the x-rays. Figure 107 is an overall view of specimen F-4 showing the effects of taper at the nose and eye ends with the reduced density (bulge) near the center of the fitting shank. Figure 108 is an enlarged view of the center portion of specimen D-1.

Swaging Sensitivity Tests - Action was then taken to define an adequate grip that could be used confidently with the existing shank and that would be tolerant of the bulges. (Examination of the x-rays showed that only one completely uniform [perfect] swage was achieved in the 22 samples surveyed.) A secondary objective of these tests was to explore swaging procedures to eliminate the bulge.

The test with specimen A-6 proved that swaging penetration could be increased from the design level,  $R_A$  of 10.0%, to 11.9% without cable damage. Tests were



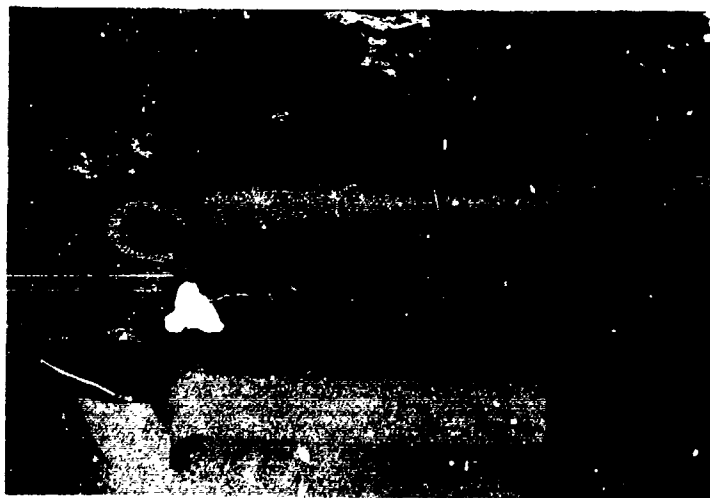


Figure 106. Equalizer-Bar Fittings Before and After Swaging  
on 0.70-Inch, Right-Lay, 36 x 7 Cable  
(P/N SK301-11561-1)



Figure 107. X-Ray of End Fitting Specimen F-4 After Swaging

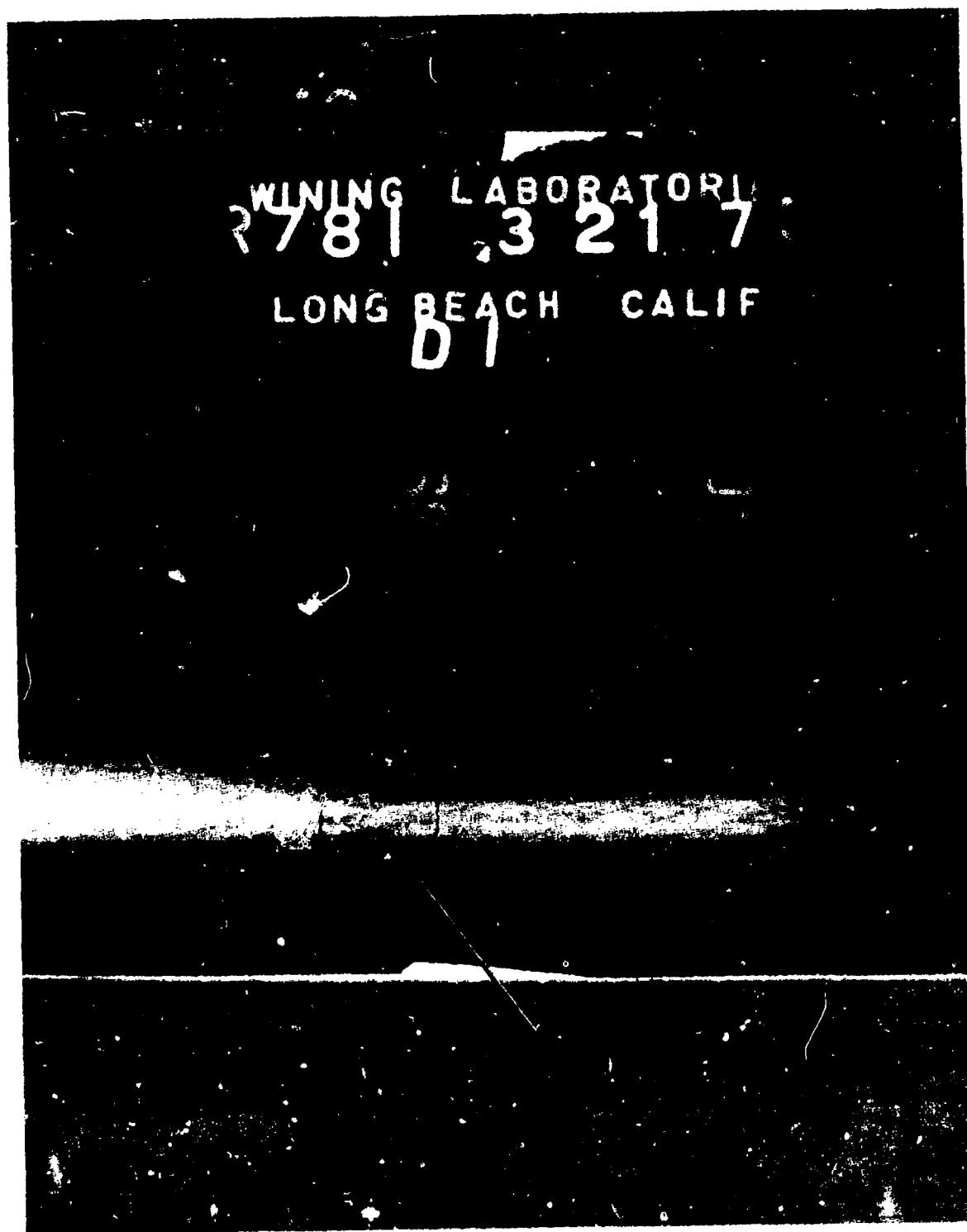


Figure 108. X-Ray of End Fitting Specimen D-1 Showing Reduced Swage Penetration (Bulge) at Center Location

continued with higher  $R_A$ s to define the upper limit of swaging pressure that would not induce cable failure in the fitting. In the procedure used for A-6 and the earlier tests, approximately one-half of the fitting shank (nose) was to the desired final diameter; then the fitting was repositioned in the dies so that the remaining portion of the shank could be swaged. During the second swaging operation, the dies overlapped the initially reduced shank section by at least one-half inch.

In the next test, specimen A-7 with fitting  $R_A$ s of 13.1 and 15.4 percent were evaluated. Both fittings were swaged in a slightly different manner. Swaging was begun at the nose of the fitting by swaging the first two inches of the shank to the desired final diameter. Then, the fitting was moved an additional inch into the swaging dies and swaged down completely. This procedure was continued inch-by-inch until the full length of the shank was completely swaged. X-rays taken after tensile testing revealed many small bulges as opposed to one buldge obtained with the earlier (conventional) method (see Figure 109). The A-7 specimen cable failed in the center at 76,600 lbs with fittings holding satisfactorily.

Since tensile testing of specimen A-7 did not result in cable failure in the fitting, specimen A-8 was prepared with  $R_A$ s of 20.6 and 25.4 percent. The swaging of these fittings was again changed to try to eliminate the bulging. The entire shank length was swaged lightly at one time rather than starting at the nose of the fitting and working toward the eye. Swaging then proceeded with small reductions in diameter over the entire shank length. Axial elongation of these fittings and stretching of the cable within the fitting was approximately double the growth found in the A-7 sample.

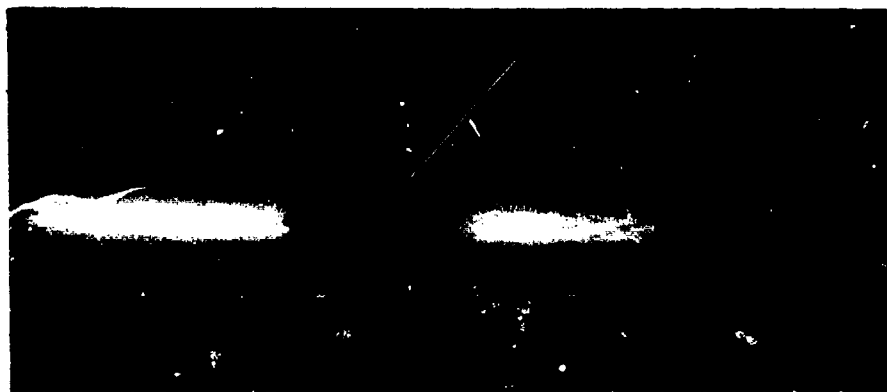
Specimen A-8 failed at 50,000 pounds. While this cable ruptured within fitting A-8-1, strand failures also occurred within the -2 fitting. These simultaneous strand failures (see Figure 110) and the low rupture load were indications of severe cable damage within the fittings.

Validation Tests of the Swaged Shank Design - 0.70-Inch Cable - These tests, identifying the upper limit of acceptable reduction in area, together with the previous occasional pull-out failure at 10% reduction, indicated a rather broad range of swaging limits available. Since severe cable damage was found at 20.6%  $R_A$ , a 13%  $R_A$  was chosen for the design validation tests.



Figure 109. X-Ray of End Fitting Specimen A-7 After Progressive Swaging

A-8-1



A-8-2

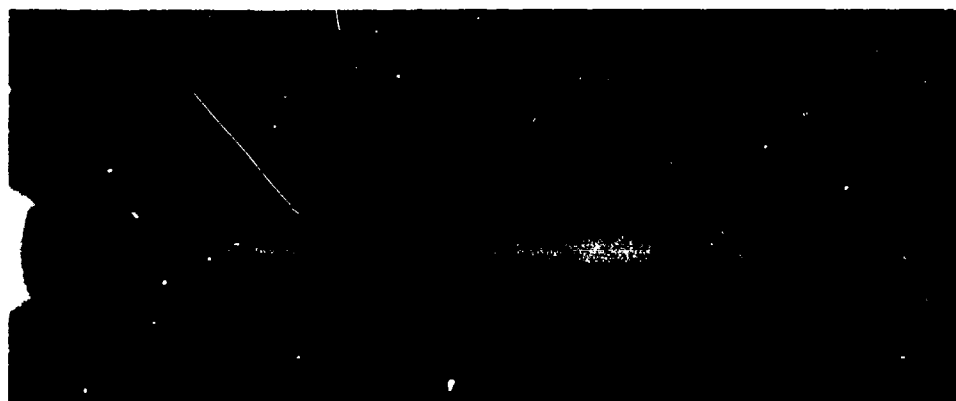


Figure 110. X-Ray of End Fitting Specimen A-8-1 and -2  
After Swaging with  $R_A$ 's = 20.6 and 25.4%

Specimens A-9, A-10, and A-11, which included both right- and left-lay cables, were assembled with six fittings of the same area reductions. Two samples of right-lay cable were used to develop higher test loads. Swaging was done with the original procedure used in the development tests. Cable center breaks were achieved in all cases. However, specimens A-9 and A-11 also incurred broken strands (seen only by x-ray, Figure 111) in one fitting of each sample indicating a near threshold value for cable damage.

The results of these tests, as well as those of specimens A-7 and A-8, are shown in Table 51. These tests verified that higher swaging pressures than originally used in development tests (10%  $R_A$ ) were acceptable for the 5.38-inch swage length and should eliminate any future slip-out failures such as that experienced with Specimen D-2, although swaging penetration may vary along the length of the fitting.

On the basis of the above tests, an  $R_A$  of 12 percent was used for the final design end fitting.

Eye-Section Development Tests - "Aa" Specimens - Static straight tension tests were run to determine the required eye wall shank transition sections. They were evaluated independently of the shank design. The eye section samples used represented the basic geometry configurations for both the equalizer bar and single-point adapter applications. A 75,000-lb ultimate load criteria was used for both designs.

Specimen Design - The "Aa" specimen for the "eye" tensile tests incorporated a threaded end adapter for the tensile machine loading head. The specimen design for the equalizer bar is shown in Figure 112. Figure 113 illustrates the design used for the general shape of the single-point adapter to prove out the minimum cross-section required. Subsequent static and fatigue tests included more material in the eye cross-section to allow assembly in "pairs" (left and right) for the two single-point adapter fittings. The material added for these features is shown in dotted lines for both the right- and left-hand fittings.

To achieve a minimum weight cross-section, these parts were differentially heat treated as would be required by the final eye/swage shank end fitting (the shank required a normalized condition to permit swaging, whereas the eye section required a 150,000-psi heat treat to minimize its size.) These specimens were first annealed to produce an  $R_B$  88-89 hardness in the neck



Figure 111. X-Ray of Overswaged End Fittings with Cable Failure at Fitting Nose



TABLE 51. SUPPLEMENTARY SWAGED SHANK DEVELOPMENT TESTS - 0.70-inch, 36x7 CABLE. (SWAGED LENGTH = 5.38 INCHES; NOSE TAPER = 2°)						
Specimen Number And Lay	Fitting Number	Percent Reduc- tion(a)	Initial Hole I.D., In.	L, Inches(b)	Shank Hardness, RB	Failure Load, Lbs (c)
A-6 Right	A-6-1	11.9	---	0.440	--	76,100 (g)
	A-6-2	11.4	---	0.365	--	
A-7 Right	A-7-1	13.1	0.722	0.473	85	76,600 (d)(e)
	A-7-2	15.4	0.724	0.582	85	
A-8 Right	A-8-1	20.6	0.723	0.743	86	50,000 (f)
	A-8-2	25.4	0.722	0.910	87	
A-9 Right	A-9-1	13.2	0.721	0.443	86	77,200 (d)
	A-9-2	12.7	0.722	0.388	87	
A-10 Left	A-10-1	13.2	0.721	0.452	84	75,300 (d)
	A-10-2	13.1	0.722	0.460	84	
A-11 Right	A-11-1	13.1	0.721	0.441	84	78,300 (d)
	A-11-2	12.7	0.721	0.410	83	78,300 (d)
$\frac{(\text{Initial O.D.})^2 - (\text{Final O.D.})^2}{(\text{Initial O.D.})^2}$						
(a)						
(b) Increased shank length resulting from swaging.						
(c) All specimens were proof-loaded to 50,000 lb prior to ultimate testing. All specimen lengths were 54 inches eye-to-eye, except A-6 which was 144 inches eye-to-eye.						
(d) Cable center break achieved. Also strand failures in fittings A-9-1 & A-11-1 noted by x-ray.						
(e) Machine malfunction occurred - loading rate interrupted at high load level.						
(f) Cable failure occurred in fitting A-8-1, and strands failed in fitting A-8-2.						
(g) Cable failed at drum tangent point during tension-over-drum test.						

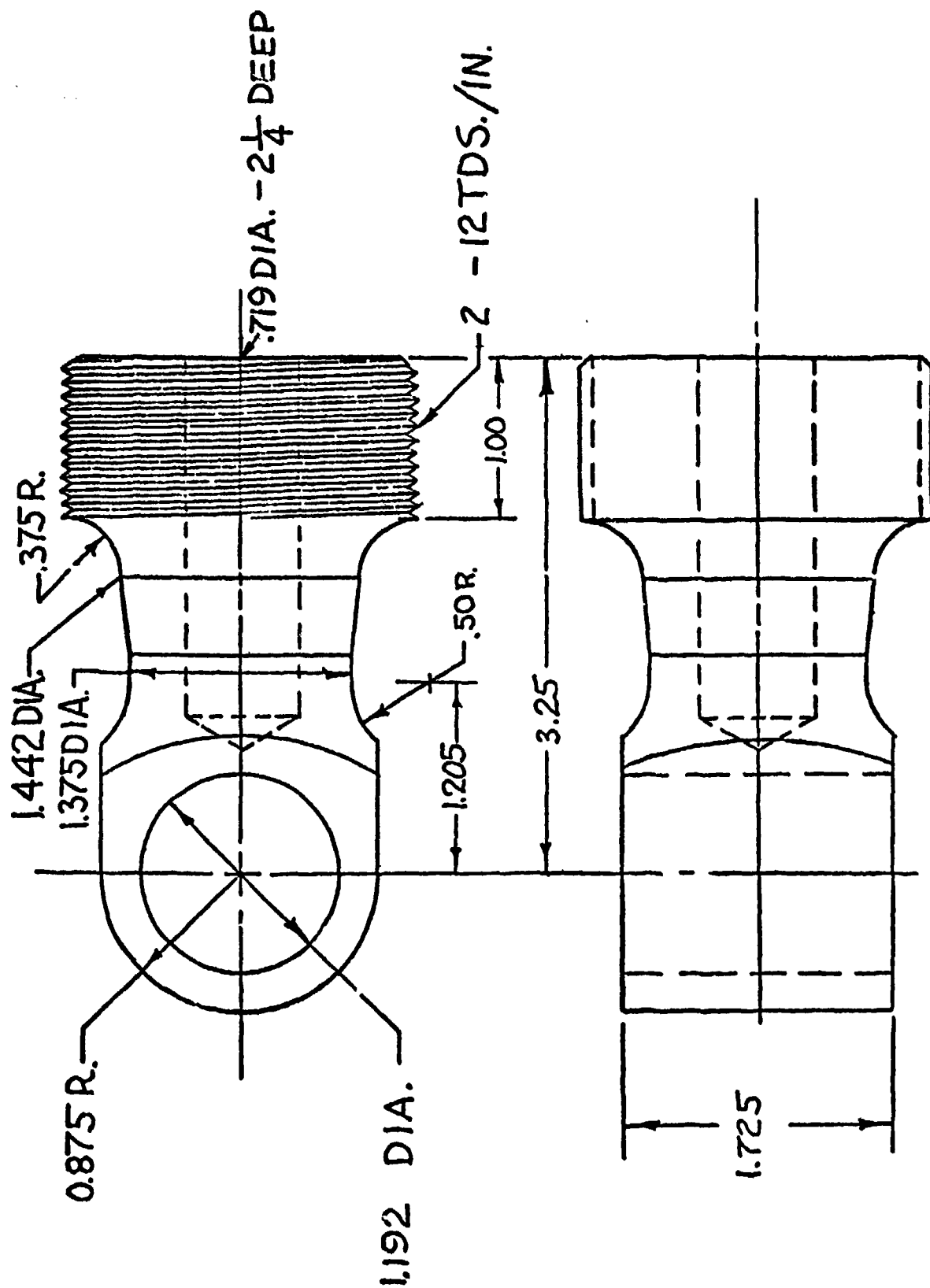


Figure 112. Sketch of Equalizer-Bar Threaded-Eye Configuration



down area (in the threaded section); then the eye portion of the specimen was suspended in a neutral salt bath at a temperature of 1575°F for 15 minutes. This heating was immediately followed by quenching in water and tempering at 850°F for three hours. The eye section hardness produced was Rc 42; subsequent retempering at 950° for three hours yielded an acceptable hardness of Rc 38-39, as required for the desired strength. This heat treating setup is illustrated in Figure 114.

Test Method and Procedure - Each eye section specimen was loaded in tension to 50,000 lb (limit load), removed and inspected for permanent elongation, then reinstalled in the machine and pulled to failure.

Test Results - Tensile tests of eye section samples representing both end fitting terminations were satisfactory. No yield was noted at 50,000 lb, and failures to achieve ultimate loads were classic modes of failure, shown in Figure 115.

The test failing loads were higher than required for the final hardware. Hardness and failing loads for the test specimens, and projected minimum strength for the development hardware are shown for each configuration in Table 52, along with expected margins of safety.

The failure of the single-point adapter fitting eye was influenced by a machining error that resulted in excessive material removal in the location of the failure. However, the single-point adapter fitting eye configurations required by the design were each to be enlarged to prevent interchanging the right- and left-lay, single-point adapter cables. This modification resulted in two eye configurations, each with more material in the eye portion (see Figure 113). Although these new configurations were not retested, calculations indicated that the eye portion is no longer the weakest area. The weakest area on all fittings is the shank at the location of the equalizer bar fitting failure (Figure 115). Based on the minimum metallic area of 1.079 square inches, and minimum hardness of RB 83 (76,000 psi ultimate tensile strength), a minimum ultimate strength of 82,000 lbs is expected for all fittings.

Since the results indicated that the tested eye sections adequately met design requirements, all specimens prepared for cable and end fitting evaluations incorporated the configurations described above.

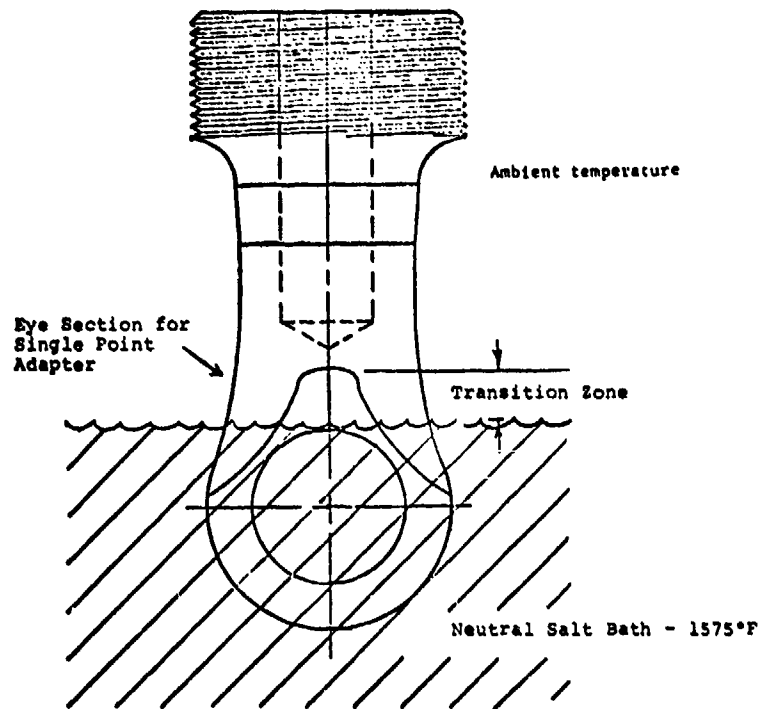


Figure 114. Differential Heat-Treatment Setup



Figure 115. Eye Section - Failure Modes

TABLE 52. TEST SPECIMEN FAILING LOADS AND CALCULATIONS OF STRENGTHS OF SIMILAR FITTINGS WITH MINIMUM HARDNESS.					
Fitting	Actual Rupture Load, Lbs	Estimated Hardness In Failure Zone	Minimum Hardness	Predicted Rupture Load, Lbs	Margin of Safety
Single Point	96,000	RC 39	RC 34	81,800 (a)	+0.09
Equalizer Bar	108,750	RB 89	RB 83	97,235 (b)	+0.30
(a) Based on ratio using appropriate tensile strengths of 176,000- and 150,000-psi for RC 39 and RC 34, respectively, for heat treated section material.					
(b) Based on ratio using appropriate tensile strengths of 85,000 and 76,000 psi for RB 89 and RB 83, respectively, for normalized section material					

(Note: The separately developed shank grip and eye configurations, described in the preceding two sections of this document, were combined into an equalizer bar and single-point adapter end fitting, as a single specimen, for design development and evaluation under all subsequent tests conducted on E, F, and G specimens.)

#### Eye-Splice Development - "B" Specimens

The single-point adapter tension members support a pair of coaxial sheaves between an adapter fitting and coupling load beam. The load beam maximum cross-section is three inches in diameter, requiring a large opening, light weight end termination for both left and right-hand cables.

The design to be developed was to use commercial swaged sleeves to form a common eye-splice with the cable loop radius supported by a thimble.

The 75,000-lb ultimate load criterion was selected instead of the actual requirement (61,300 lb) (see Table 44) to make more cable failure load data available for this evaluation program.

#### Specimen Design

Each eye-splice "B" specimen was 5 feet long. The assemblies fabricated for initial tests used commercial parts to form a 3x10-inch loop, as shown in Figure 116. Final test specimens for the eye-splice used a single dual-hole swaged sleeve in place of the multiple swaged sleeve shown, forming a 3x7-inch loop.

#### Test Method and Procedure

Two test specimens were needed to define the development configuration. A third specimen was used to investigate size reduction. Each specimen was mounted on the 3-inch loading pins to simulate the coupling load beam attachment and pulled to failure. Each of the specimens was different. They were built in sequence and are described below.

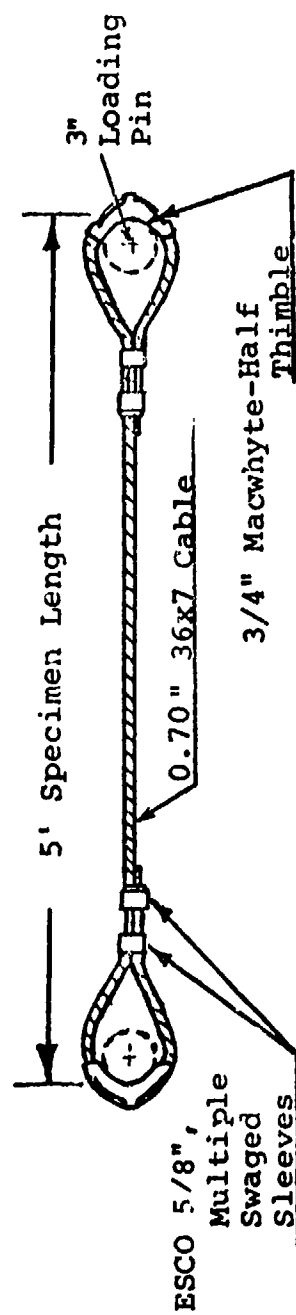


Figure 116. Typical Eye-Splice Test Specimen.



### Test Results

Development of the eye-splice configuration to be used on the coupling load beam required three iterations of testing. First, available commercial hardware (Figure 116) was evaluated and found marginal. Then, a special swaged sleeve made of cold drawn mild steel was designed and proved satisfactory. A failure during tension-over-drum tests, resulting from material imperfections, dictated that repeat tests be conducted to validate the use of a new material (AISI 4130).

Results of all tests in the eye-splice development are described below:

Commercial Hardware Tests on 36x7 Cable - In the first eye-splice test, specimen B-1 was assembled using commercial ESCO 5/8-inch duplex sleeves and MacWhyte 3/4-inch crescent thimbles. Splice I was fastened with two sleeves and one cap, Splice II with one sleeve and one cap (see Figures 117 and 118). These sleeves were pressed on with the standard dies used for fabrication of wire rope slings.

After pressing, it was observed that the cable had been severely distorted (see Figure 119), due to the swaging pressure (ropes side-by-side in a circular die). This rope distortion is normally not so severe with a six-strand rope due to nesting of the large strands and, therefore, is tolerable in that application. However, for the 36x7 wire rope, the distortion had a severely degrading effect. When specimen B-1 was loaded, all 36 strands failed simultaneously within the nose of the capped sleeve on Splice II, at a load of 61,700 lbs. Figure 120 is a photograph of this failure.

While the failing load achieved with the B-1 specimen, using commercial components, was 400 lb higher than required, it was not considered an adequate margin due to uncertainty in controlling the cable damage created by swaging the duplex sleeves. (Commercial hardware does not exist for the 36x7 cable.)

To provide minimum cable distortion and more uniform pressure on the cable during swaging, a cylindrical sleeve containing two parallel holes for the cable loop and a separating web to support the cable were designed as shown in Figure 121. Figure 122 shows a schematic comparison of the commercial and new sleeve configurations before and after swaging.

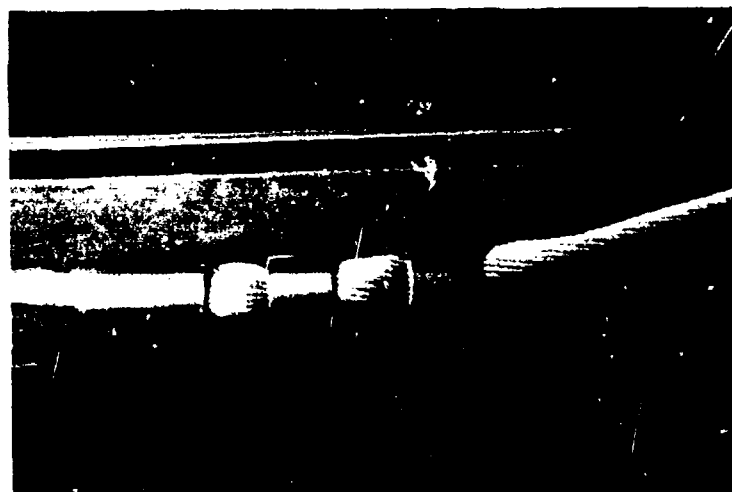


Figure 117. Splice I Using Two Sleeves and a Cap



Figure 118. Splice II Using One Sleeve and a Cap

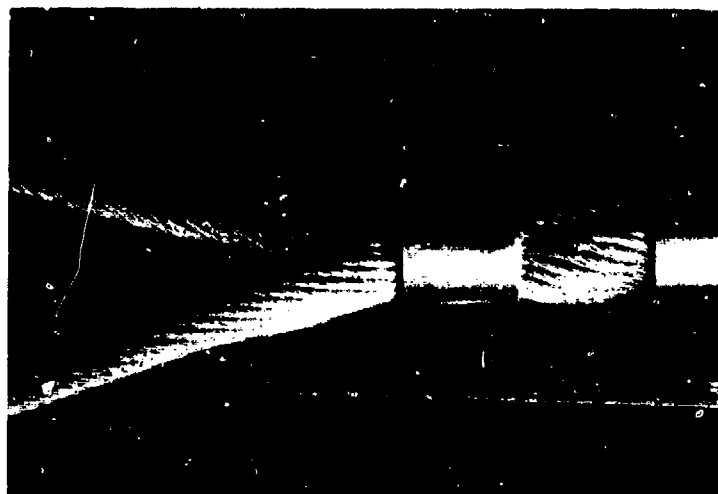


Figure 119. Distortion of Cable After Swaging of Sleeves.



Figure 120. Failure of Eye Splice Using Standard Sleeves.

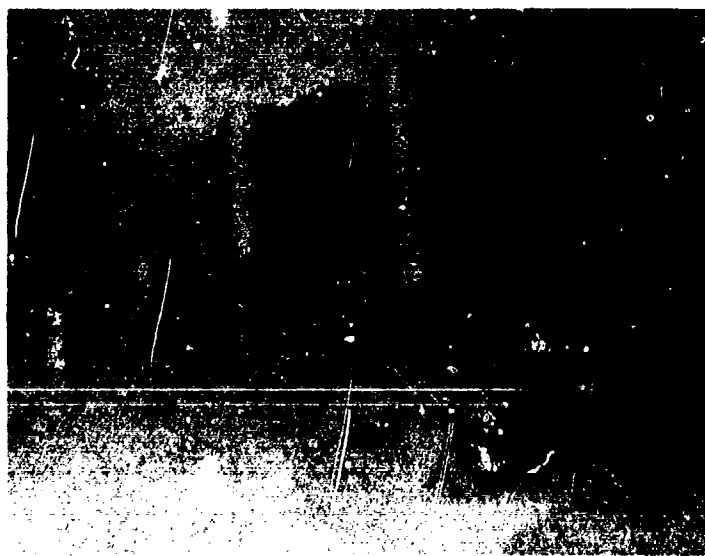
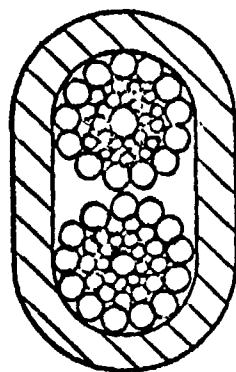
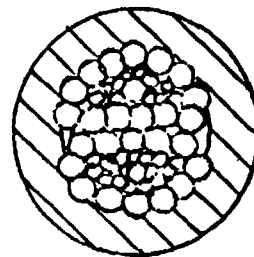


Figure 121. Eye-Splice Sleeves Designed to Prevent Cable Distortion Upon Swaging.

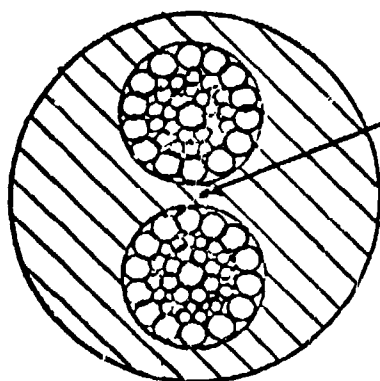


Before Swaging



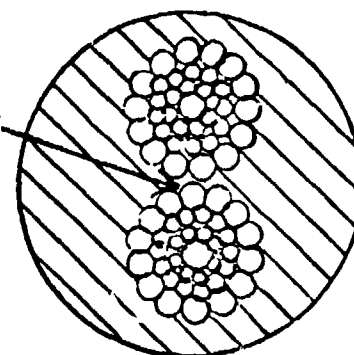
After Swaging

Approximate Configuration of Esco Duplex Sleeve Before and After Swaging



Before Swaging

WEB  
SEPARATING  
CABLES



After Swaging

Approximate Configuration of Dual Hole Sleeve Before and After Swaging

Figure 122. Comparison of Commercial and New Sleeve Configuration.

Dual Hole Swaged Sleeve - AISI 1018 Material - Specimen B-2 (Figure 123), using 4- and 6-inch sleeve lengths and a 10-inch loop, proved to be 100% efficient since a cable center break was obtained at 80,000 lbs. The B-2 test specimen after failure is shown in Figure 124. A cross-section of the parallel cable swage is shown in Figure 125. Subsequent tests with specimen B-3 having 2-1/2- and 3-inch sleeves and a 5-1/2-inch loop failed by slippage of the 2-1/2 inch sleeve at 74,900 lbs. This showed that the shorter length was marginal for demonstration of cable strength.

The 3-inch grip length was calculated as adequate up to loads of approximately 90,000 lbs. Examination of the specimen at 50,000 lbs (limit load) showed no yielding. Particular attention was paid to the end of the sleeve where the two cables entered the fitting.

Based on these tests, the eye-splice configuration selected for the specimens E-3 and F-2 of the development fatigue and tension-over-drum program consisted of a dual hole sleeve, 3 inches long with a 7-inch loop, as described by drawings 301-11561/5 and 301-10253-3 and -4. The material used was AISI 1018.

Dual Hole Swaged Sleeve Tension-Over-Drum Tests - AISI 1018 Material - During tension-over-drum tests, specimen E-3 failed. While failure occurred above its design ultimate requirements, it did not allow determination of the cable failing load, as was intended. The fitting failed through one of two thin wall sections reduced by swaging. An investigation was made which included sectioning, hardness checks, and macro and micro examination of the material. Metallurgical tests showed that material defects (inclusions) were present in the surfaces of the cracked outer wall and the inner web (separated during examination, not broken during test). The sleeve half-section shown in Figure 126 shows both inclusion locations, and an enlargement (24X) shows the foreign material found in the web between the cables. The earlier, successful tests apparently did not have material discontinuities in the thin area of the swage. This examination confirmed the desirability of using a more uniform, swageable material, such as AISI 4130, for this sleeve application where size and material cleanliness are important.

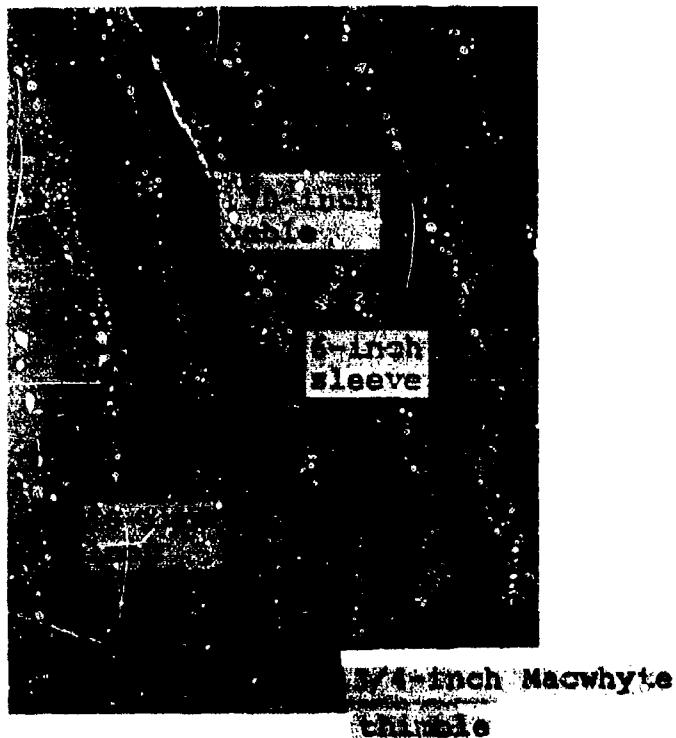


Figure 123 Eye-Splice Specimen B-2 Using Cylindrical Sleeves (cold rolled steel), 4 and 6-Inch Sleeve Lengths, 10-Inch Loop Length, and 3/4-Inch Macwhyte Thimble.



Figure 124. Center Break of Eye-Splice Specimen B-2,  
2 Inches From the 6-Inch Sleeve.



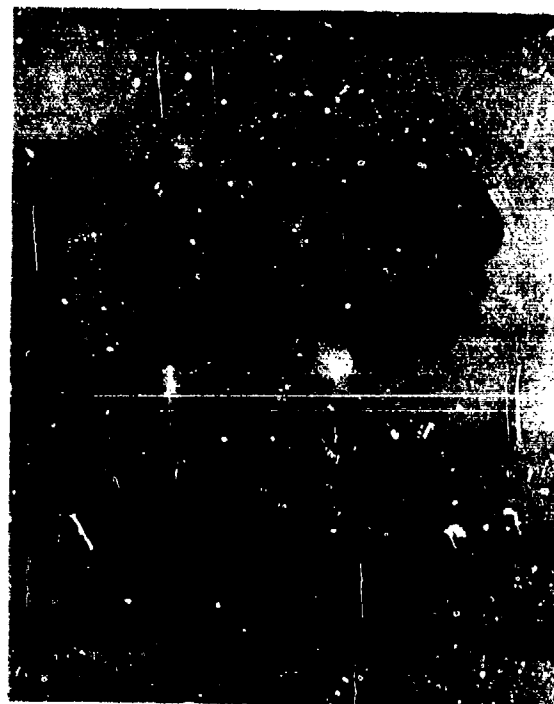
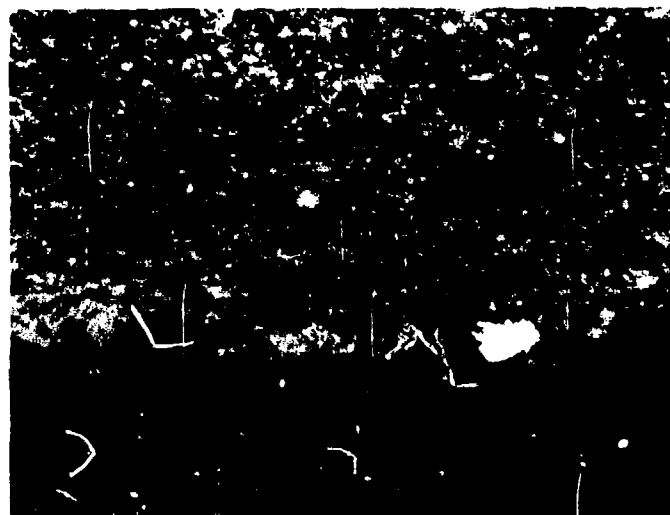


Figure 125. Center Section of Eye-Splice Specimen,  
B-2/IV, Two 0.70-inch Cables,  
 $R_A = 11.9\%$



1/2 Section of Specimen E-3 - Top Arrow, Origin Revealed  
By Sectioning, Bottom, OD Origin Caused Rupture.



Outline of Discolored Area, ID Origin

Figure 126. Section Views of Specimen E-3, Which Ruptured  
at 62,300 lb (Eye-Splice, Swaged Dual Hole  
Sleeve, P/N SK301-11561-6)

Validation Tests - AISI 4130 Eye-Splices - Six additional sleeve tests were conducted to establish the reduction in area required for the 4130 sleeve. Duplicating the sleeve dimensions with 4130 ( $R_A = 11.9\%$ ) resulted in a slip at 62,200 lbs. This failure indicated that the 4130 required more reduction to obtain the same gripping force (swage penetration) provided by the cold drawn lower grade steel. An increase in  $R_A$  to 13.7% with specimen B-6 produced cable rupture within the fitting at 73,000 lbs. An  $R_A$  of 12.8% in specimen B-5 produced a threshold value (onset of cable rupture) sufficiently above the 61,300-lb requirement to remove the assembly from a slip condition tendency. To maintain the same fitting length (3 inches) with the 4130 material, an  $R_A = 12.8\%$ , as a maximum, was used for the demonstration hardware. Table 53 lists dimensional data and breaking loads developed with all of the eye-splice end fitting specimens tested.

#### Hoist Drum Button Development - "C" Specimens

The "C" specimens were used to develop the cable retention for the hoist drum. The end fittings were developed using the same material, and a swaging technique was established for the swaged shank, "A" specimens. A different diameter and length was used for left- and right-lay cable to provide mutually exclusive installations. The ultimate load criteria used for the test was 30,000 lbs.

#### Specimen Design

Two 5-foot-long drum button specimens, C-1 and C-2, were prepared using left-lay cable. Each specimen had one drum button representing the left- and one representing the right-lay installation. The material used was AISI 4130, zinc coated per QQZ325 Class 1. Each drum button was a cylindrical section with a 27/32-inch-diameter hole along its axis. After swaging, the buttons were trimmed to 3 inches for the right-lay and 2-1/2 inches for the left-lay. This evaluation was being made with button lengths 1/2-inch shorter than the interface requirement, to allow for a 1/2-inch shim in each drum button cavity. This adjustment was to compensate for any tolerance build-up between drum and cable.

#### Test Method and Procedure

The test specimens were pulled in straight tension to failure by loading the inboard shoulders in compression. This provided loading in a similar manner to that experienced in the actual hoist drum. A uniform loading rate was used.

TABLE 53. EYE-SPLICE DEVELOPMENT TESTS FOR 0.70-INCH-DIAMETER CABLE.					
*All specimens were right-lay cable and proof-loaded to 50,000 lb straight tension, except B-2. *MacWhyte 3/4-inch crescent thimbles used on all eye-splices.					
Specimen Number	Sleeve Number	Sleeves/Material	Percent Reduction(a)	Total Swage Length, in.	Failure Load, lbs.
B-1 Right	I	2 ESCO SS duplex plus duplex cap	--	4.38	--
	II	1 ESCO SS duplex plus duplex cap	--	3.38	61,700
B-2 Right	III	2-hole, AISI 1018	11.9	3.95	80,000 (b)
	IV	2-hole, AISI 1018	11.9	5.99	--
B-3 Right	V	2-hole, AISI 1018	11.9	3.0	--
	VI	2-hole, AISI 1018	11.9	2.5	74,900 (c)
B-4 Left	B-4-1	2-hole, AISI 4130	11.9	3.0	--
	B-4-2	2-hole, AISI 4130	11.9	3.0	62,200 (d)
B-5 Right	B-5-1	2-hole, AISI 4130	12.8	3.0	--
	B-5-2	2-hole, AISI 4130	12.8	3.0	71,000 (e)
B-6 Right	B-6-1	2-hole, AISI 4130	13.7	3.0	--
	B-6-2	2-hole, AISI 4130	13.7	3.0	73,000 (f)
(a) $(\text{Initial O.D.})^2 - (\text{Final O.D.})^2$ (Initial O.D.) <sup>2</sup>					
(b) Neither splice failed; a cable center break was achieved. Specimen was not proof-loaded before test.					
(c) Rope slipped in the sleeve. A subsequent loading resulted in a complete pull-out at a load of 50,600 lbs.					
(d) Cable pulled-out of sleeve.					
(e) Two outer strands failed at nose of sleeve B-5-2. A second pull resulted in failure of numerous other strands at 76,000 lbs at the same location.					
(f) Twenty-four strands failed at nose of sleeve B-6-2.					

### Test Results

Two test configurations were needed to establish that the ultimate strength requirement was met with the shortened drum button length. This was accomplished by increasing the area of reduction,  $R_A$  from 7.4% to approximately 17%. The final specimen, C-2-1, failed (by pull-out) at 45,600 lbs, 150% of the design ultimate requirement. The dimensional configuration of the two specimens used and the test results are given in Table 54. A photograph of the C-2-1 specimen after pull-out is given in Figure 127.

Three observations were made during these drum button tests:

1. At 36,400 lbs (above design ultimate), the torque developed by the cable caused rotation of the fitting in the test fixture, which resulted in unlaying of the cable and an immediate drop in load. On load relaxation, the cable lay was restored to normal. After this occurrence, the fitting was restrained from rotation, reloaded, and experienced a pull-out (45,600 lbs); see Figure 114.
2. In the loading of this C-2 specimen to 36,400 lbs, two distinct "pops" were heard and thought to be seating of the cable in the test fixture. Examination of the fitting remaining after pull-out showed, however, that a slippage on the order of 1/16 inch had occurred between the outer and inner strands (the two "pops" apparently indicated that both fittings had slipped). At this time, the slip was not identified with any load below 30,000 lbs. (Although slipped, the second fitting survived the 45,600-lb load.)
3. It was observed that the drum button outer diameter, after swaging, was not uniformly circular and that the final outside diameter varied beyond the dimensional limits that were obtained with the longer swaged shank sections.

### Assembly of Drum Buttons - Demonstration Components

Subsequent to these observations, assembly of the full-length cable for demonstration units and hoist development tests, 123 and 160 feet respectively, drum buttons of 3 of the 13 cable assemblies fabricated were found to have slippage of between .008 and .020 inch. These slippages occurred in the range of 17,300 to 19,300 lbs with a requirement of no yield below 20,000 lbs.

TABLE 54. RESULTS OF HOIST DRUM-BUTTON DEVELOPMENT TESTS.

All Specimens Left-lay Cable  
Button Material - AISI 4130 Steel

Specimen Number	Button Number & Type	Initial O.D., in.	Final O.D., in.	Percent Reduction (a)	Effective Length, in.	Failure Load, Pounds
C-1	C-1-1 Left	1.320	1.270	7.4	2-1/2	18,400
	C-1-2 Right	1.205	1.140	10.5	3	
C-2	C-2-1 Left	1.385	1.265	16.6	2-1/2	45,600
	C-2-2 Right	1.275	1.160	17.2	3	
$(a) \frac{(\text{Initial O.D.})^2 - (\text{Final O.D.})^2}{(\text{Initial O.D.})^2}$						



Figure 127. End of Drum Button After Cable Pull Out

Observations 2 and 3 above, and the final assembly experience suggest that the design be modified to use the original fitting length (1/2-inch longer than test specimen).

### Assembly Fatigue and Validation Tests

#### End Fitting Preparation

Eye/Swaged Shank Preparation - The eye/swaged shank end fittings fabricated for the fatigue and validation tests were composites of the empirical designs established by the preceding tests. The finished fittings, shown in Figure 128, had a swaged length of 5.38 inches and an  $R_A$  of 10.0%. They are dimensionally in accordance with drawing SK301-11561 as described under "Tension Member Drawings". The equalizer bar interface fitting, -1, is exactly as tested. The single-point adapter fittings, -2 and -3, are structurally the same except that material was added to the eye sections to make them sufficiently different to assure that only a pair, one right- and one left-hand cable, could be assembled in the adapter/sheave assembly.

(The right-hand, -2 fitting eye wall thickness was increased 0.250 inch over a  $200^\circ$  arc. The left-hand, -3 fitting maintained the original eye wall thickness, but was increased in width by 0.060 inch.)

The end fitting preparation included:

1. Normalizing for maximum ductility to  $R_B$  83-87.
2. Heat treatment of eye in a neutral salt bath to obtain a hardness of RC 34-38 (hardness tested and certified), and
3. Zinc plate, 0.0002 (without post bake, since RC 40) per QQZ325, Class 1.

Swaging the end fitting to the cable was performed as previously described. The SK301-11561-1 end fittings are shown, before and after swaging, in Figure 106.



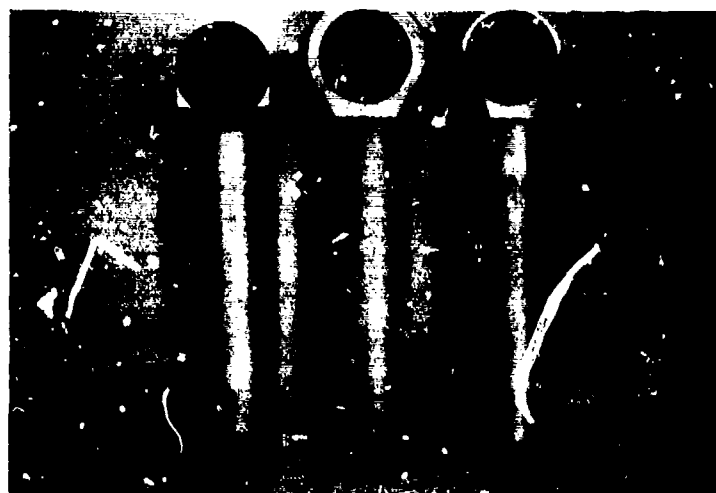


Figure 128. Edge and Face Views of SK301-11561 End Fittings and Bushings for Tension Members. (From Left to Right (SK301-11561): -1 Equalizer Bar, -2 R.H. Single Point Adapter, and -3 L.H. Single Point Adapter Fittings)

Eye-Splice Preparation - The two-hole, eye-splice sleeves, fabricated for the "E" and "F" specimen tests, were made from cold-drawn mild steel (AISI 1018) and coated with a minimum 0.0002-inch-thick zinc plate, per Specification QQZ325, Class 1.

The MacWhyte 3/4-inch crescent thimbles required grinding on the inner radius, to remove excess material remaining from the casting process. This surface was smoothed to conform to a 3-inch-diameter pin. These thimbles were also zinc plated prior to installation.

The technique for forming an eye-splice using the two-hole sleeve was as follows: The cable was passed through one of the holes, then doubled back and forced through to the end of the outer hole. By gripping the sleeve and the cable, the loop was tightened until the desired 7-inch loop was formed. The sleeve was then pressed in a split die, whose inside diameter was 1-3/4 inches (when closed). The sleeve holes were aligned relative to the split die, so that on the first press the cables were pressed together. The sleeve was then rotated 90° for the second and succeeding presses. This technique minimized distortion along the thinnest sections of the sleeve. However, it was noted that the edge of the center web between the two holes was fractured during swaging.

(NOTE: The dual hole sleeve design included an .080-inch [non-structural] web separating the cables. In theory, this was to avoid direct contact and distortion during swaging by maintaining uniform swaging pressure around each cable. Figure 125 shows that the cables were not distorted from swaging. It was noted, however, that compression of the cables caused small splits to occur in the ends of the web, due to the reduction in section and penetration of the cable strands. This occurred with both the AISI 1018 and the 4130 materials. Since this web was non-structural, all tests were conducted with this condition, without change or effect on test results. The specimen E-3 failure was not influenced by the web cracks.)

After swaging the sleeve, the MacWhyte thimble was slipped into the cable loop and centered. The ears of the thimble were peened over by gripping the thimble in a vice and striking the ears with a hammer until they are forced firmly against the cable. The completed assembly after test is shown in Figure 129 .

After cable tests were completed, two of the sleeves were examined by x-ray, magnetic particle, and liquid penetrant inspection. None of these methods revealed any flaws in the sleeves.

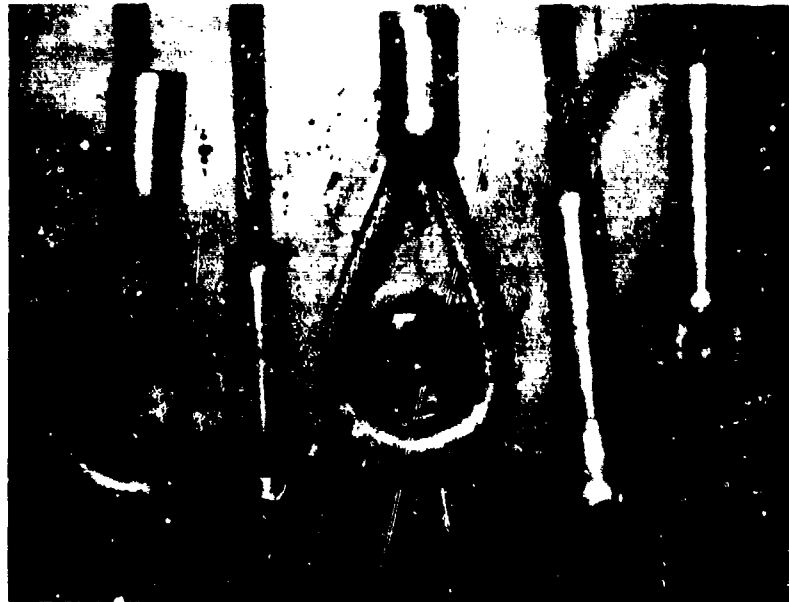


Figure 129. Array of Fittings After Test



Figure 130. Extensometer Attached to Cable During Tension/Elongation Measurements

End Fitting/Cable Assembly Static Strength Tests  
(Tension, Elongation, and Torsion) - "D" Specimens

Objective - Tensile tests were conducted to determine the elongation and torsional characteristics of both left- and right-lay cables at loadings up to and including limit load (50,000 lbs).

Specimen Design - Three cable samples (Group D) were tested. Each specimen was 12 feet long and was terminated with specimens of eye/swaged shank end fittings, representative of those developed for the equalizer bar and single-point adapter. Two of the cable samples were right-lay and one left-lay.

Test Method and Procedure - The test fixture consisted of an in-line load frame and hydraulic cylinder, which applied a pure tensile load to the specimen as shown in Figure 130. A tension/torque load cell and SR-4 strain indicators were used to read cable tension and torque simultaneously. Strain was monitored with an extensometer consisting of a pair of parallel dial indicators and fastened to the cable over a 100-inch gage length. The dial gages provided a precision within .00001 inch of strain per inch of gage length.

Each of the three specimens was loaded in turn. Elongation and torsion data were collected under both increasing and decreasing tensile loads at intervals of 5,000 lbs. The maximum load applied to each specimen was to be the design limit load. A total of 10 loading cycles were applied to establish the stable load elongation curve after removal of the cable constructional stretch. The test data was collected during the first and tenth loading cycles.

Test Results - Load/Elongation Characteristics - Load/elongation curves for the RH and LH cables are presented in Figures 131 and 132. These plots show the individual cable characteristics, such as the removal of constructional stretch (permanent elongation between the initial and final runs), and load/unload and linearity characteristics.

Data recorded for the first and tenth loading cycles shows that there was little permanent elongation noted after the original loading cycle. From the data taken on the tenth run, the right-lay sample exhibited proportional characteristics between 10,000 lbs (50% design

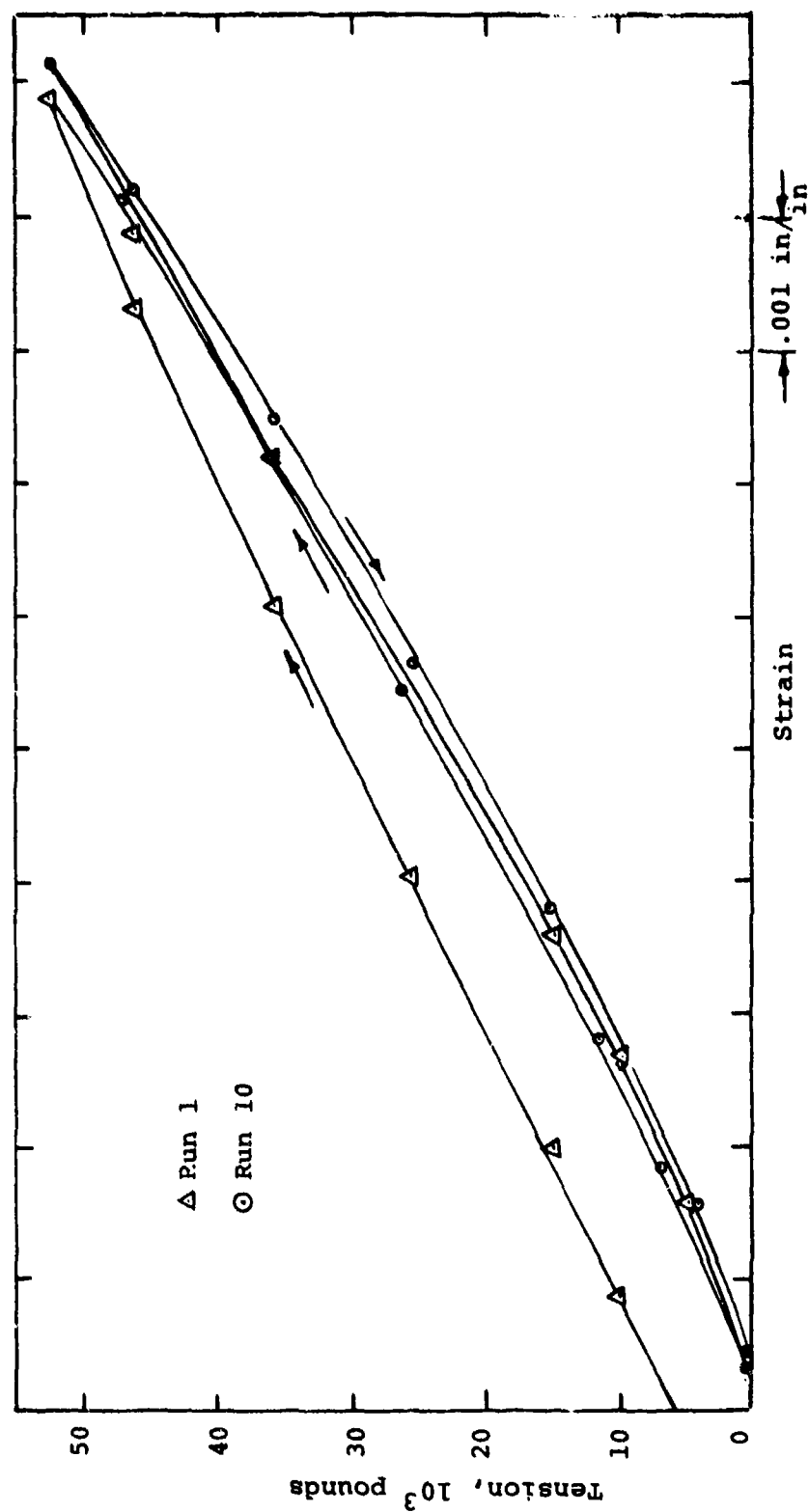


Figure 131, Tension/Elongation Characteristics of Right-Lay, 36x7 Cable (Specimen D-1).

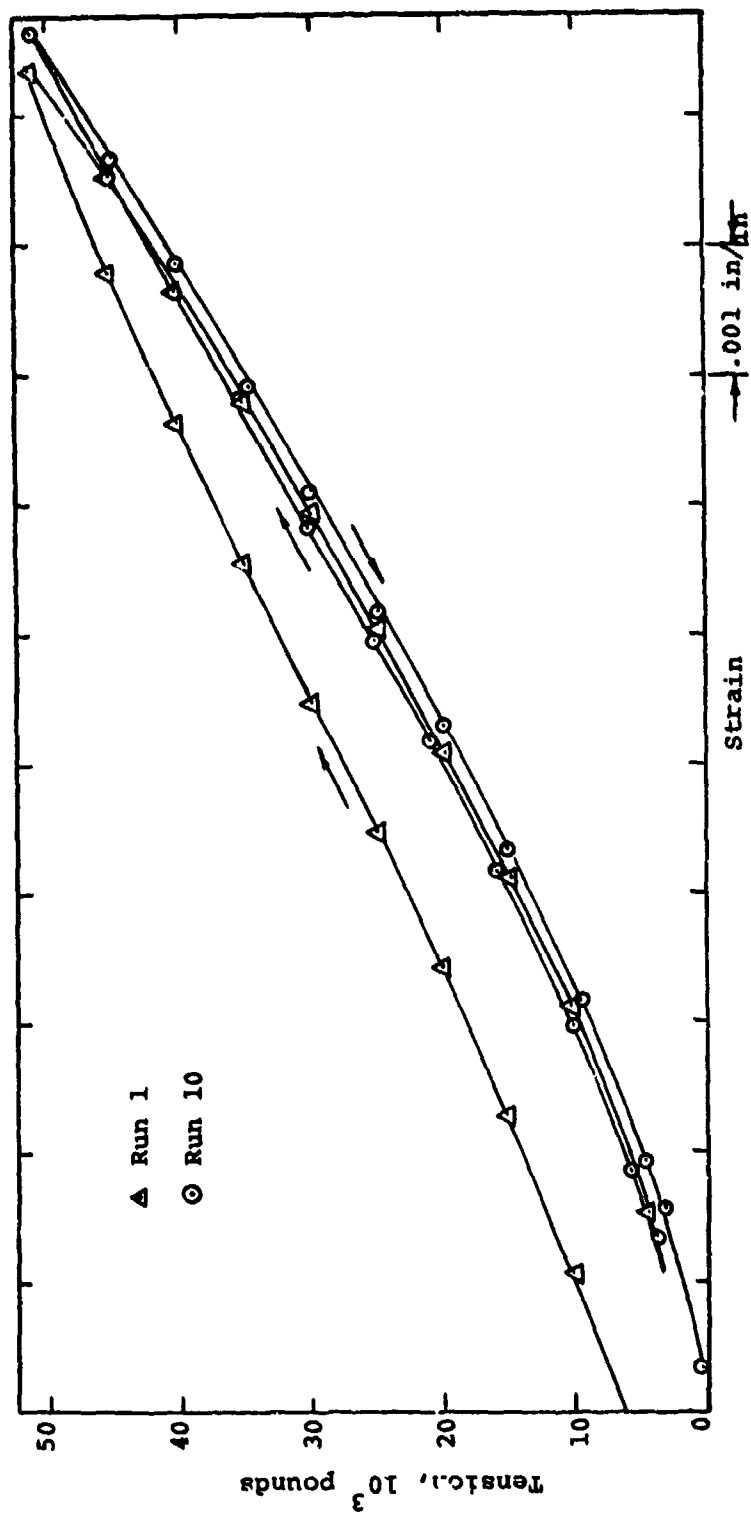


Figure 132 . Tension/Elongation Characteristics of Left-Lay, 36x7 Cable (Specimen D-2).

load) and 52,000 lbs (the maximum test load, which exceeded the design limit load of 50,000 lbs). The left-lay cable sample showed linearity from 20,000 lbs (design load) to 52,000 lbs. Based on a metallic area for each cable of 0.264 sq inch, Young's Modulus, E, for left- and right-lay cable samples was calculated at  $20.9 \times 10^6$  psi.

Torsional Characteristics - Removal of constructional stretch was also apparent in comparing torque curves of the initial and final runs for both left- and right-lay cables. These characteristics are shown with specimens D-1 and D-2 in Figures 133 through 135. Figure 136 shows only the final run torque data from specimen D-3 (right-lay). The right-lay cable displayed a slightly non-linear tension-torsion relationship (Figure 136) below approximately 10,000 lbs, but the left-lay cable (Figure 137) appeared nonlinear in torque behavior to 15,000 lbs. These characteristics were not evident during design support test evaluation of the 0.78-inch-diameter cable of the same 36x7 construction and suggests that all the strands in the 0.70-inch-diameter cables did not share the tension proportionally in the 10,000- to 15,000-lb range. These low initial torque characteristics will result if the inner strands carried the greater part of the load. With subsequent loading, stretch of the inner strands allowed the other strands to assume more load, thereby increasing the output torque of the assembly. This unequal load sharing could be the result of increased looseness in the construction from insufficient preforming of the cable strands. (Additional evidence of less than optimum strand load distribution was apparent by wire breakage below ultimate load, noted in both straight tensile and tension-over-drum tests.)

In the "paired cable" system, the torque mismatch demonstrated between left and right cables, rather than the individual absolute cable torque, determines the balance within each hoist suspension system. The maximum torque differential observed between left and right cable specimens, D-2 and D-3 (from Figures 136 and 137), was 40 in-lb at design tensile load (20,000 lbs). The maximum rotation of the equalizer bar resulting is calculated at  $4.9^\circ$  when the cable payout is 100 feet. Elongation and torque data taken from the three "D" specimens is summarized in Table 55.

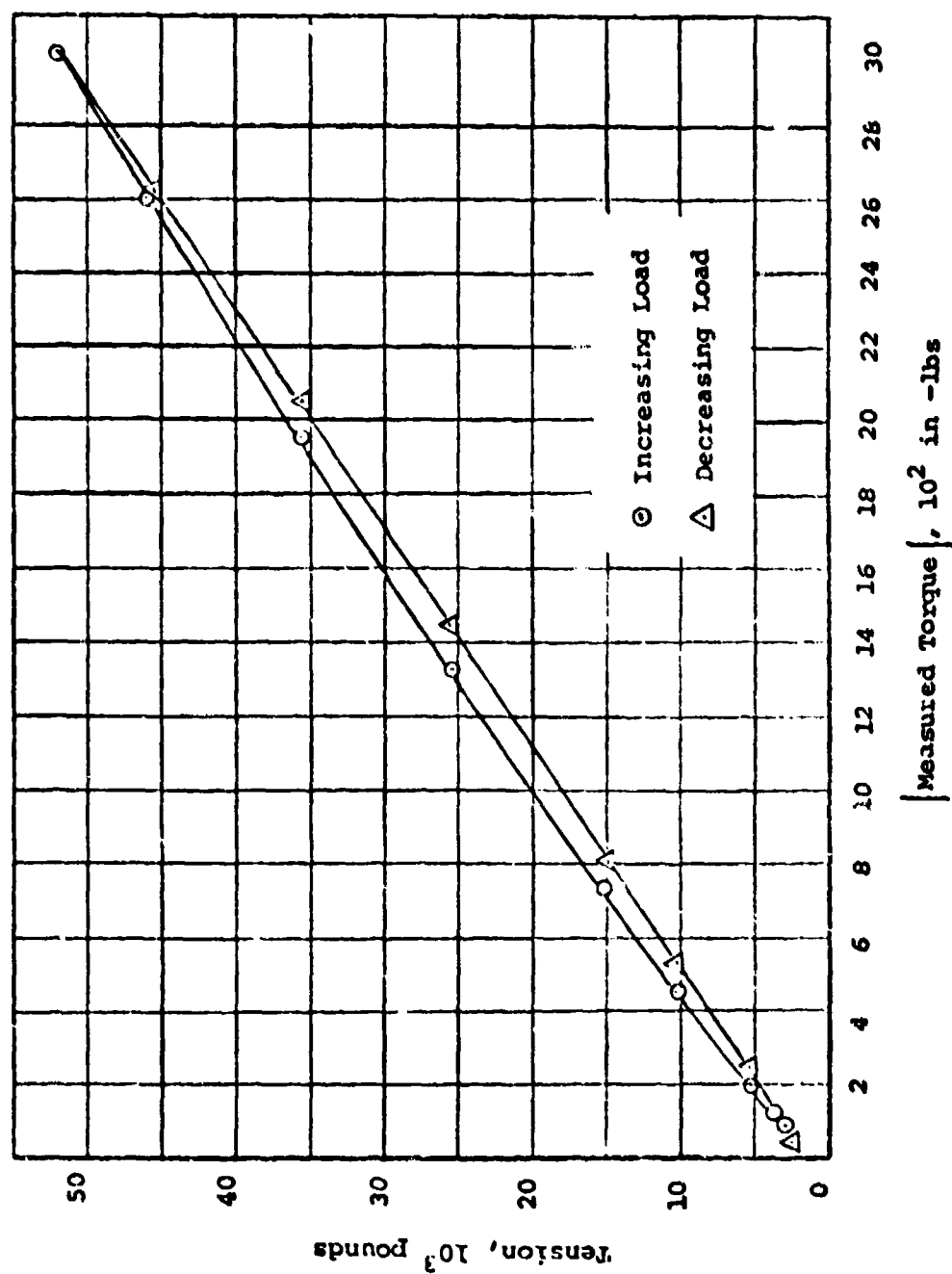


Figure 133 . Tension/Torque Characteristics of Right-Lay, 36x7 Cable  
(Specimen D-1, Run 1).



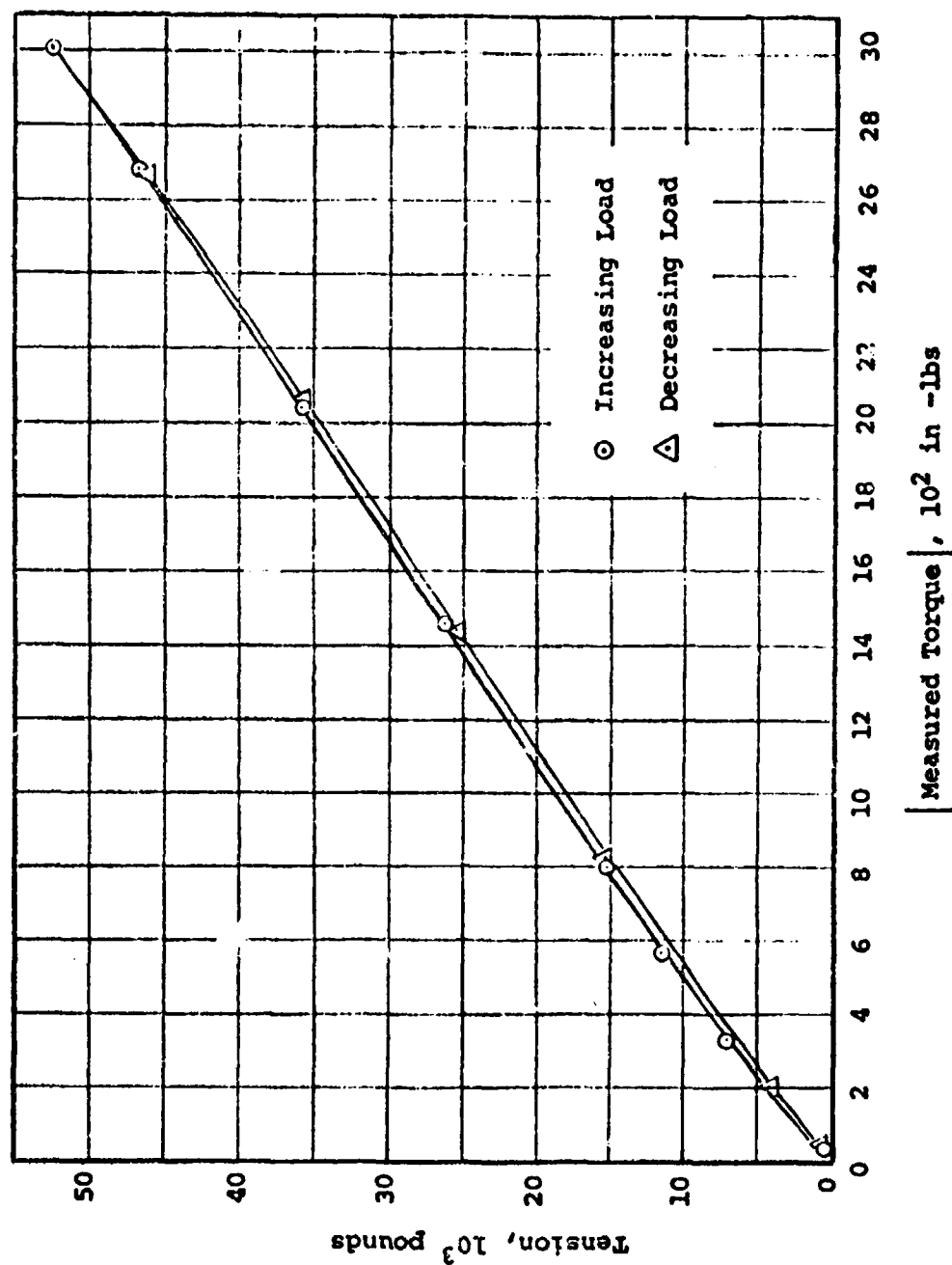


Figure 134 . Tension/Torque Characteristics of Right-Lay, 36x7 Cable (Specimen D-1, Run 10).

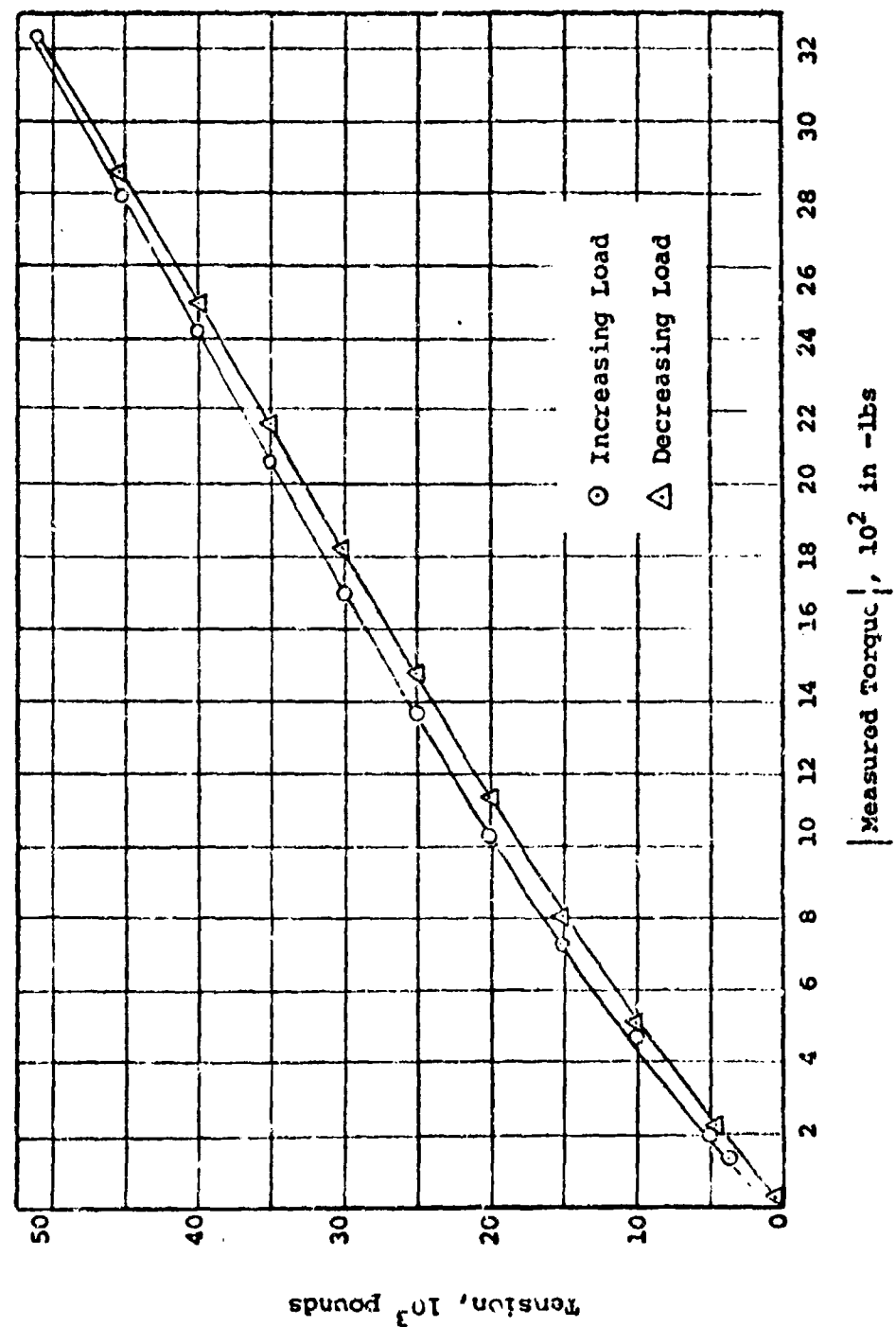


Figure 135 - Tension/Torque Characteristics of Left-Lay, 36x7 Cable  
(Specimen D-2, Run 1).

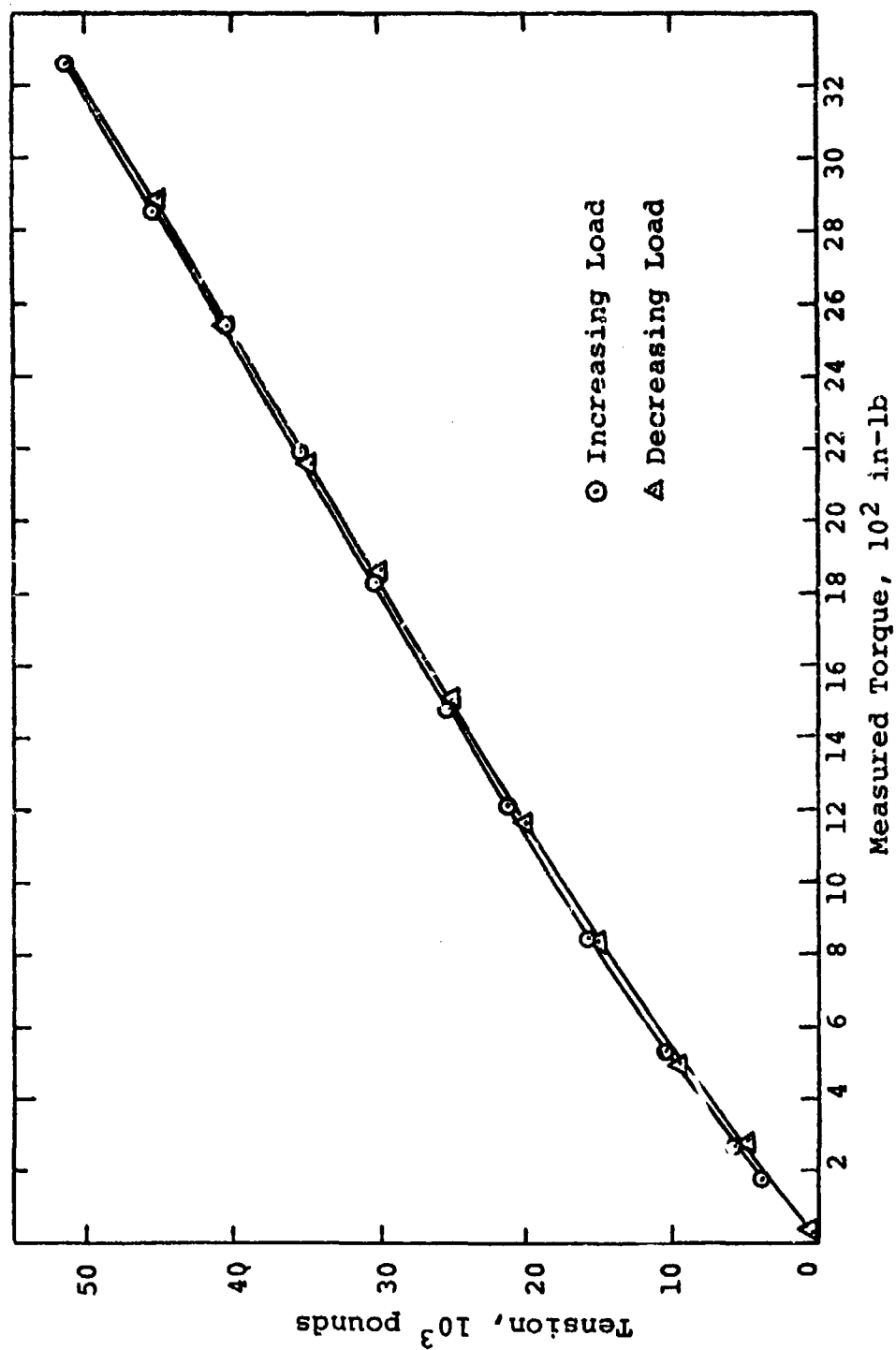


Figure 136. Tension/Torque Characteristics of Left-Lay, 36x7 Cable (Specimen D-2, Run 10).

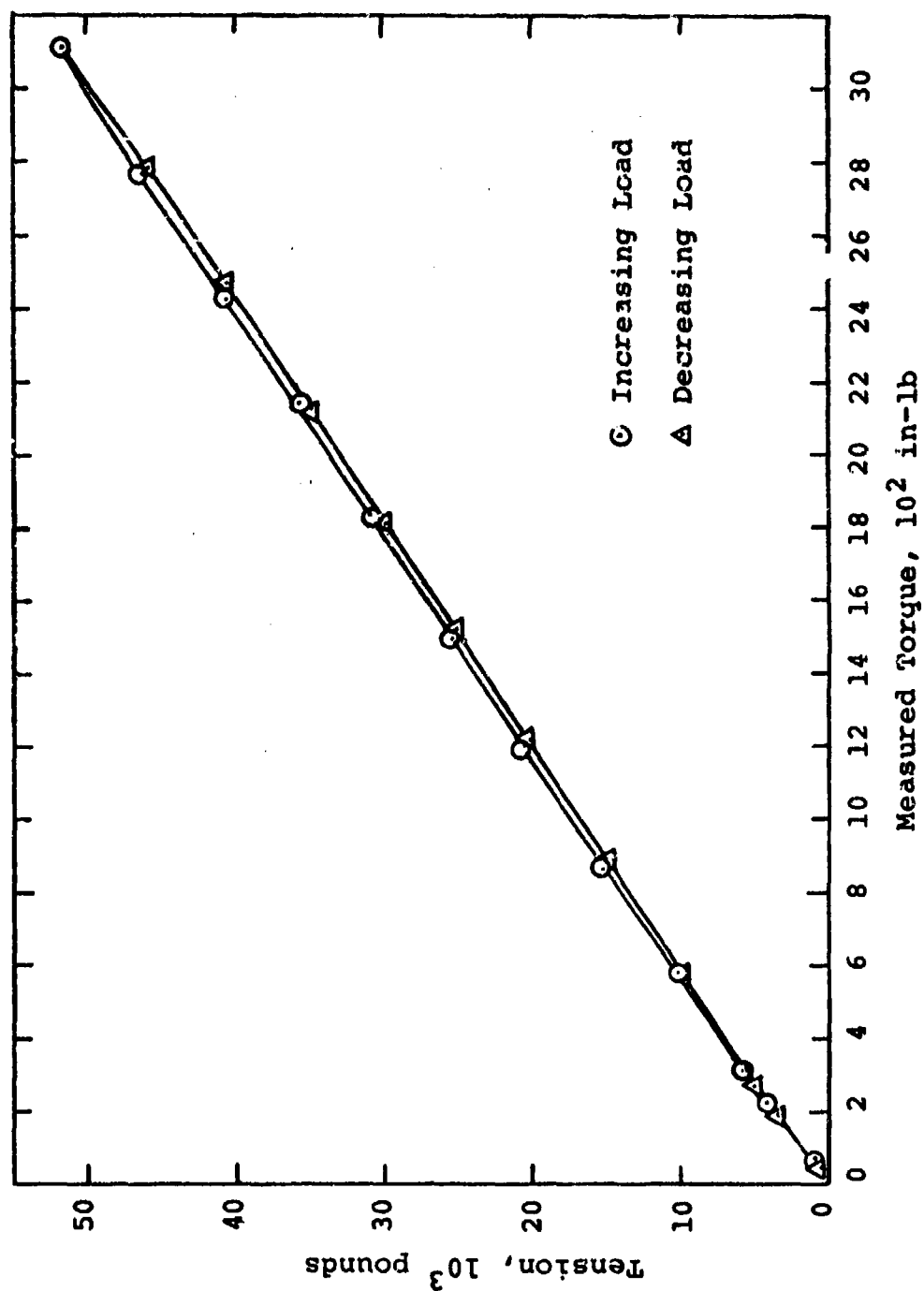


Figure 137. Tension/Torque Characteristics of Right-Lay, 36x7 Cable (Specimen D-3, Run 10).

TABLE 55. RESULTS OF TENSION/ELONGATION AND TENSION/  
TORQUE TESTS.

Cable - 0.70-Inch-Diameter, 25x7 Construction  
Metallic Area = .264 Sq.In.

Specimen Number and Lay	Modulus of Elasticity, E. PSI	Torque at 20,000 Lbs. In-Lbs.
D-1 Right	$20.9 \times 10^6$	1,090
D-2 Left	$20.9 \times 10^6$	1,120
D-3 Right	$20.9 \times 10^6$	1,160

### Fatigue Tests - End Fittings and Cables

Objectives - Fatigue tests of end fittings and cable specimens under cyclic tension, bending and wrap pressure loading were conducted. The tests simulated the load lifting and lowering cycles experienced by a cable wrapped on a hoist drum in a helicopter. The objectives of these tests were to:

1. Demonstrate that the tension member cable assemblies, when subjected to alternating loads, will endure 10,800 cycles under design spectrum loading,
2. Establish the cable assembly fatigue life, and
3. Evaluate the effect of corrosion resulting from 240 hours of salt-fog exposure under test conditions of (1) above.

Specimen Design - Ten cable specimens were tested. Each consisted of a 12-foot length of cable terminated with end fittings developed and discussed earlier in the text. Specimens were tested in sets of two, each set consisting of a pair of left- or right-lay cables as defined in Table 44. Six of the specimens were made of right-lay cable, four of left-lay cable. Of the 20 end fittings subjected to fatigue tests, eight were of the equalizer bar design, eight were of the single-point adapter design, and four were configured as eye-splices.

Specimen preparation included proof-loading to 50,000 lbs to verify the static adequacy of the fitting installations before testing.

Test Fixture and Instrumentation - A layout of the test machine, with typical cable specimens, is shown in Figures 138 and 139. In this machine, two specimens were tested simultaneously, with each specimen wrapped around a simulated single groove drum. The cable specimens were connected end-to-end through the individual end fittings to form an endless loop. Unlaying of the cable was prevented by using two specimens of the same lay direction in a single test setup. A hydraulic cylinder provided the cyclic tensile loads, and a mechanical drive system caused the specimens to reciprocate back and forth, resulting in bending of each cable specimen as it wrapped around its drum. A reciprocating stroke of 19 inches was used, providing each specimen of cable with two 19 inch test sections in which the bending was concentrated. The drum pitch diameter to cable diameter ratio was 26.7:1. The configuration of the drum groove shown in Figure 140 conformed closely to the cable radius and duplicated the ATC hoist design. The drum material was AISI 9310, hardened to Rockwell C32-42 and was surfaced with 0.0005 to 0.0010 inch of electroless nickel. The cable drums were offset to provide a fleet angle of  $0^{\circ} 45'$  to simulate cable wear conditions. The instrumentation used for the bend-over-drum/cyclic tension fatigue tests consisted of a load cell and strain indicators used initially to calibrate the load pressure indicators on the machine. Fatigue cycles accumulated were recorded by electronic counter with an automatic shut-off of the cycling mechanism after the desired number of cycles were completed. This feature was employed for making scheduled visual examinations of the specimens and for changing cable tension in accordance with design load spectrum schedule.

Test Method and Procedure - General Procedure - The cable/fitting fatigue tests were conducted under ambient laboratory conditions. The cable of each specimen was subjected to the two types of cyclic loading:

1. Bending off-and-on the simulated hoist drum,
2. Cyclic variations of tension, from 0 to design spectrum load levels.

The cable test sections were subjected to both types of loading, whereas the end fitting/cable junction endured only the cyclic tensile loading. The loading schedule

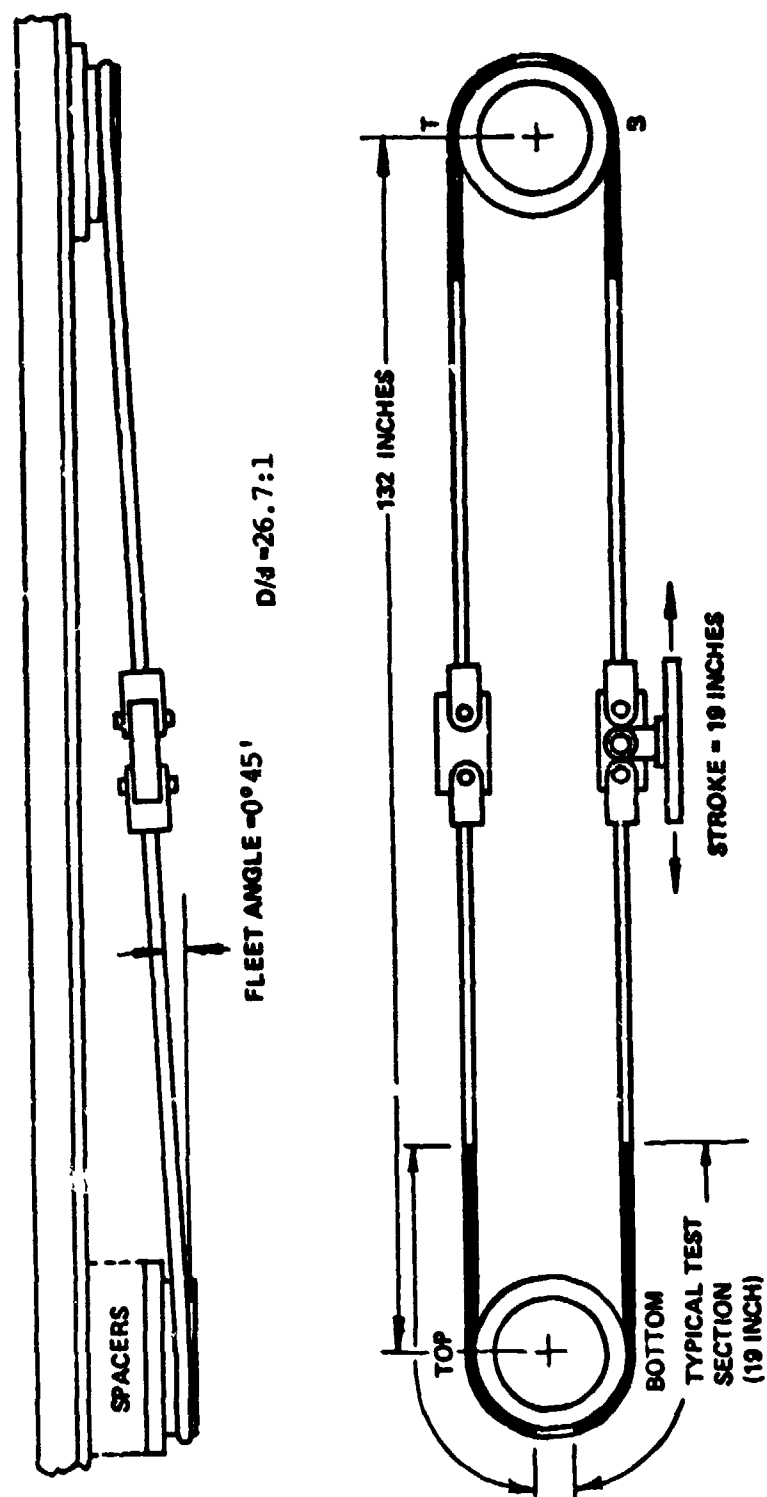


Figure 138 . Layout of Tension/Bending Fatigue Machine and a Typical Specimen.



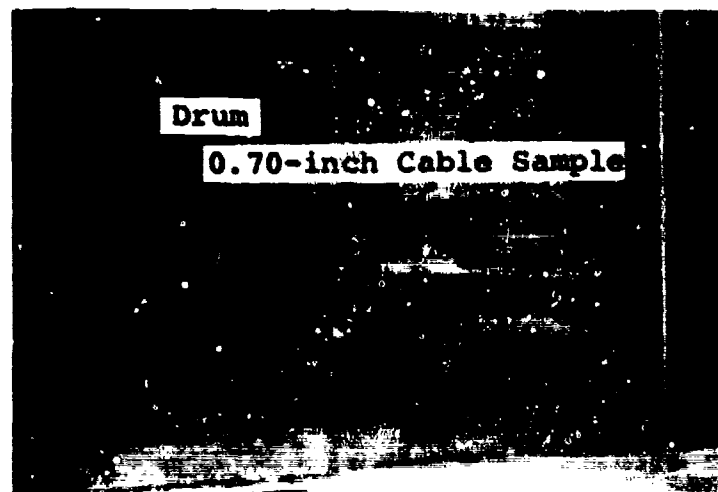
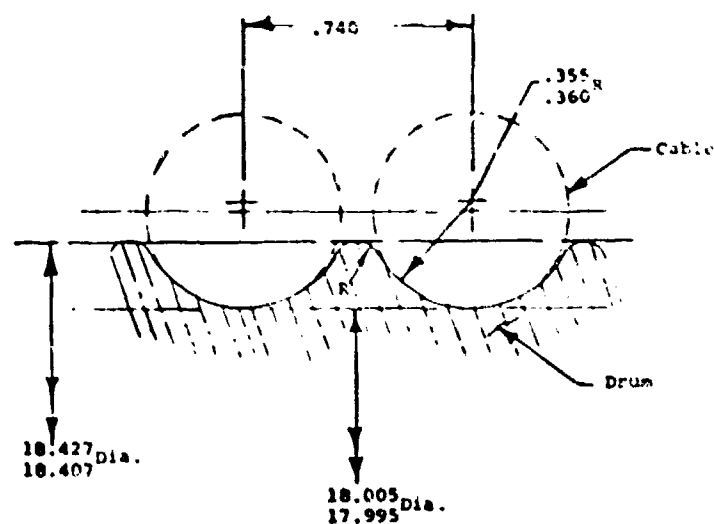


Figure 139. Machine Used For Tension and Bend-Over-Drum Fatigue Tests



DRUM DATA:

MATERIAL - 9310 AIR MELT STEEL PER AMS 6260F  
 HEAT TREAT  $R_c$  32-42 PER MIL-H-6875F  
 SURFACE FINISH  $6\frac{3}{4}$ /  
 ELECTROLESS NICKEL PER MIL-C-26074B  
 .0005 - .0010 THICK  
 H.T.  $325^\circ\text{F} \pm 25^\circ\text{F}$  FOR 1-3 HOURS

Figure 140. Hoist Drum Groove Configuration Using 0.70-Inch-Diameter, 36x7 Cable

was conducted in accordance with the HLH ATC cargo system design spectrum loading, shown in Table 56. During these tests, the spectrum was divided into ten equal blocks of cycles. Each pair of specimens first received 108 cycles at a load of 25,000 lbs, then 810 cycles at 20,000 lbs, then 108 cycles at 10,000 lbs, and finally 54 cycles at 5,000 lbs. The tensile load was dropped to 0 after each bending cycle and then reapplied before the next bending cycle. This pattern of cycles and loads was repeated nine times for a total of 10,800 fatigue cycles, as a simulation of the load acquisition, lifting, lowering, and release sequence expected during normal service of the HLH Cargo System. The cycling rate used varied during the period of test from an initial two cycles per minute during the early portions of the test to 13 cycles per minute later in the test program, as machine cycling capability (hydraulic capacity) was increased.

TABLE 56. CARGO SYSTEM/TENSION MEMBER DESIGN SPECTRUM LOADING.				
Fatigue Life Cycles		Percent Design Load	Test Load, lbs	Percent Design Ultimate
Percent Of Life	Number of Cycles			
10	1,080	125	25,000	33.3
75	8,100	100	20,000	26.7
10	1,080	50	10,000	13.3
<u>5</u>	<u>540</u>	25	5,000	6.7
100	10,800			

Specific Fatigue Tests - The fatigue test program was conducted with ten specimens divided into three groups, designated "E", "F" and "G".

Single Life Cycle Tests - Four E specimens were configured with samples of each eye type end fitting according to Table 44. Each specimen was subjected to 10,800 cycles of bending and tension as described above.

Fatigue Life Tests - The purpose of the Group F specimens was to establish:

1. The life cycle margin available beyond the 10,800-cycle requirement,
2. The "g" loading capability that existed after completion of two life cycle periods (21,600 load cycles),
3. The cable/end fitting failure modes, and
4. Data "scatter" under extended cycling conditions.

The four specimens were configured with three end fitting designs, as defined in Table 44. Each specimen was cycled 21,600 times and then pull tested at a 2.5 g load level (50,000 lbs). Surviving samples were subjected to additional cycles for a total of 50,000 or failure, whichever occurred first.

Corrosion/Fatigue Tests - The two G specimens prepared with equalizer bar end fittings were first subjected to 3,600 cycles of spectrum loading, followed by an accelerated, 240-hour corrosion test in a salt-fog atmosphere (five times the requirement of MIL-STD-810B). This was followed by an additional 7,200 cycles of spectrum loading after exposure, for a total of 10,800 fatigue cycles.

Determination of Cable Degradation - Each of the E, F and G specimens surviving the fatigue tests, and not segregated for internal examination, was subjected to a tension-over-drum (TOD) ultimate test to determine the remaining tensile strength (RTS), or strength loss resulting from fatigue or fatigue and corrosion. Two of the samples in the fatigue life program were taken apart to determine the extent and mode of wire or strand failures due to cyclic loading.

Results of all specimens tested by TOD are reported later in this section in the paragraph entitled "Tension-Over-Drum Cable Strength Tests:."

Test Results - During the cable assembly fatigue tests, the cable samples, end fittings, and bearings of all specimens were physically inspected after each block of 1800 cycles, to check for failures. These examinations were for wire breakage, excessive temperature build-up, wear of the cable or drum surfaces, condition of the cable lubrication, or any other factor that would constitute a failure. Dimensional checks were also made of several

specimens to relate these characteristics, if possible, to cable failure. Following completion of their designated test periods, seven of the samples were subjected to tension-over-drum tests to evaluate their ultimate tensile strength following endurance. Of the remaining three samples, two were dissected to investigate the condition of internal wires, and the third sample was failed in pure tension. Following are comments on the endurance capability of each test specimen and observations made during testing.

Single Life Cycle Fatigue Tests - E Specimens - Two pairs of E cable assembly specimens (two right-lay and two left-lay cables) successfully completed 10,800 tension/bending fatigue cycles without any visible wire breakage (see Table 57) and were pulled to failure during tension-over-drum (TOD) tests. Lubricant migration from the cable was noted during these tests. It is discussed in paragraph entitled "Cable Lubricant Migration".

Corrosion/Fatigue Tests - G Specimens - The two G cable assembly specimens were also tested for 10,800 load cycles, as the E specimens were, except that the complete specimens were subjected to corrosion for 10 days. Corrosion was introduced after having first completed 1/3 of the fatigue cycle schedule under the rationale that some coating wear had taken place and that considerable cable lubricant had been removed by the flexing and bending action of the cable. The test specimens were wiped to remove excess lubricant before being suspended in the corrosion chamber. Care was taken to insure that all portions of the cable and the cable end fitting were fully exposed for maximum effect of the corrosive salt-fog medium. Following this exposure and without removal of the products of corrosion, the test samples were reinstalled in the test machine and the remaining 2/3 of the fatigue cycles scheduled were completed. A visual examination after completion of tests revealed no wire breakage (see Table 57) at that point nor any significant lubricant migration through the corroded coating.

Figure 141 shows the two cables and fittings, specimens G-1 and G-2, before exposure to salt-fog, and Figure 142 shows their condition after 120 hours of exposure. Note that the fittings alone show considerable corrosion, whereas the cable has just a few spots indicating rust. Figure 143 shows the cables and fittings at the conclusion of the 240 hours salt-fog exposure.

TABLE 57. RESULTS OF FATIGUE TESTS - CYCLIC TENSION AND BEND-OVER-DRUM.						
E Specimens - Laboratory Environment G Specimens - Corrosion Samples						
Specimen Number and Lay	End Fitting		Fatigue History		Comments	
	Type	% Area Reduction	Accumulated Cycles	Observable Wire Strand Breaks		
E-1 Right	(2)SPA-	10	10,800	0		
E-2 Right	(2)EQ-BAR	10	10,800	0		
E-3 Left	(2)EYE-SPLICE	11.9	10,800	0	All specimens to TOD	
E-4 Left	(2)SPA-	10	10,800	0	Test for RTS Evaluation	
G-1 Right	(2)EQ-BAR	10	10,800	0		
G-2 Right	(2)EQ-BAR	10	10,800	0		
<p>Notes: 1) All specimens proof-loaded in straight tension to 50,000 lb (limit load) before test.</p> <p>2) Load spectrum cycling over 18.7-inch pitch-diameter drum with a zero-load condition between bending cycles.</p> <p>3) G Specimens: 10 days of accelerated salt-fog corrosion exposure applied after 3600 cycles. Remaining 7200 load cycles completed after salt-fog exposure.</p>						

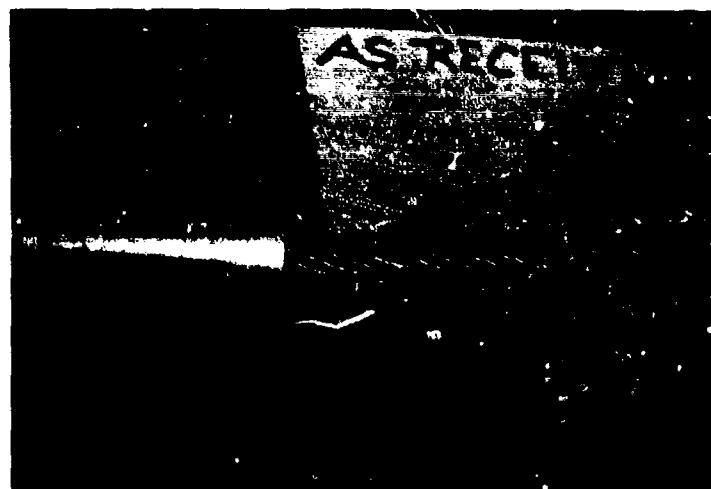
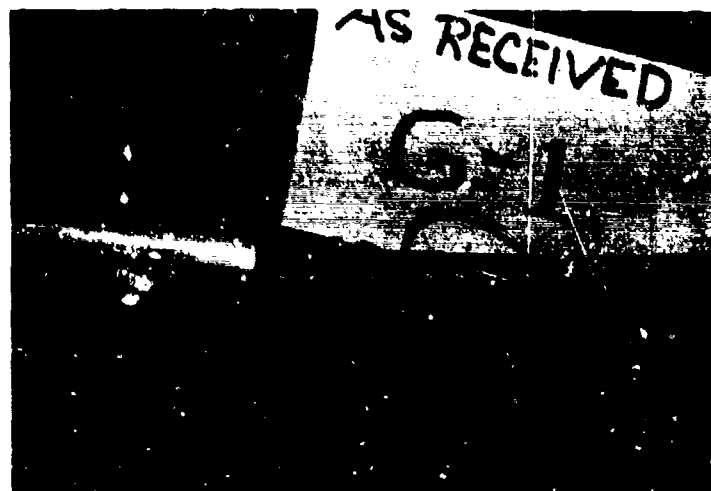


Figure 141. Specimens G-1 and G-2 After 3200 Fatigue Cycles But Before Salt-Fog Exposure

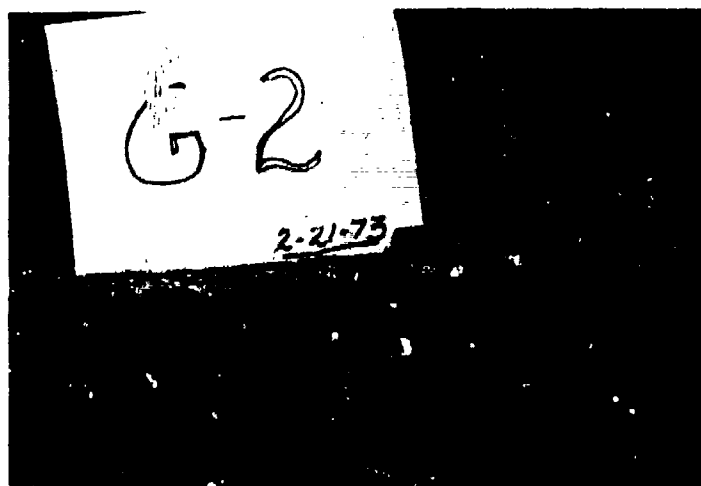


Figure 142. Salt-Fog Exposure Specimens After 120 Hours

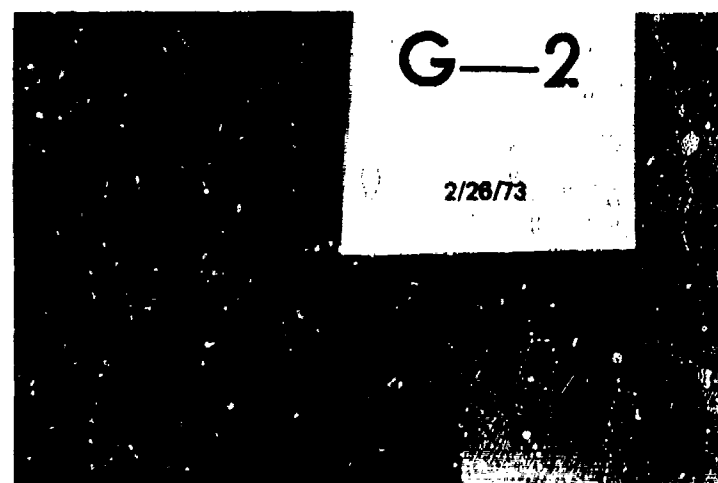
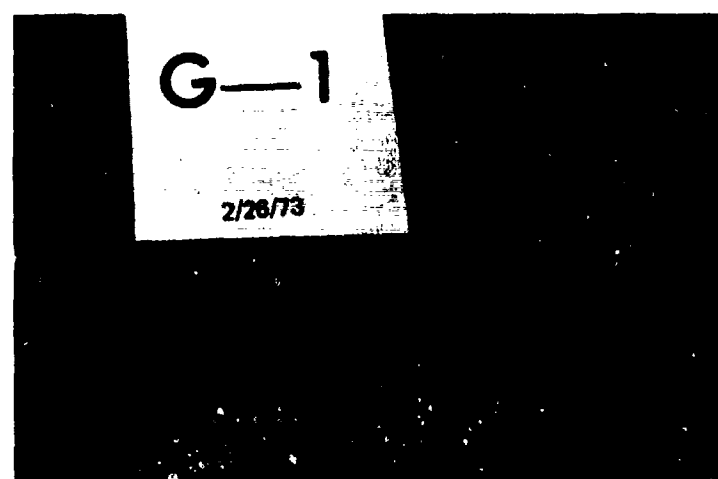


Figure 143. Salt-Fog Exposure Specimens After 240 Hours



The cable had many visible rust spots and in appearance was approximately the same as the 0.78-inch-diameter cable previously tested under the same conditions. However, the fittings originally coated with a 0.0002-inch-thick zinc plate had rusted badly at this point.

The results of subsequent tension-over-drum tests of these specimens are shown below.

With respect to the corrosion testing completed, the following comments are relevant.

1. A 240-hour accelerated salt-fog corrosion test was selected to go beyond MIL-STD-810B requirements (48 hours) in order to determine the effects of severe corrosion on the cable and cable/end fitting junctions.

This extended corrosion test was imposed on the galvanized carbon steel to afford a direct as possible comparison with the results of the design support tests.

In these tests there was no discernable influence of corrosion on the cable strength; end fitting failures made it impossible to determine actual cable strength at that time. The severity of the tests imposed on the 0.70-inch development samples, however, was undoubtedly increased greatly by the application of corrosion during, rather than after the endurance cycling, as was done in the 0.78-inch cable.

2. The condition of the cable samples when the test was resumed, following the application of corrosion, was believed to be poorer than would be tolerated in field-use.
3. The results of the coating test on the end fittings indicated the need for an increase in coating thickness.

Fatigue Life Tests - F Specimens - All four F specimens completed 21,600 cycles satisfactorily without wire breaks. Three specimens survived the 50,000-lb static load after the two life cycle periods, specimen F-3 did not; it failed at a load between 35,000 and 40,000 lbs.

The fourth specimen, F-4, completed the 50,000-cycle program, although it sustained seven wire breaks (internal-audibly noted) under the 2.5 g load application. On subsequent TOD tests its tensile strength was 38,900 lbs.

Specimen F-1 and F-2 (both right-lay) went on to complete 32,406 and 38,895 cycles after the limit load application. Their tests were terminated by the occurrence of strand failures during the 25,000-lb loading portion of the spectrum load schedule, immediately after an inspection. Catastrophic failure was not involved, rather, the tests were discontinued to perform an internal examination on the specimens. A section of F-3 was also examined.

Of the four specimens, the right-lays (F-1 and F-2) were the more consistent, completing an average of 3.3 life cycles; the left-lays (F-3 and F-4) were more variable, completing 2 and 4.6 life cycles. The life and wire break history of the F specimens is given in Table 58.

Cable failure modes are defined in Tables 59 and 60 from the internal examinations of F-1, F-2 and F-3 specimens. Note the vast difference in degradation of the two test sections of F-2 even though only five outer wire breaks were identified just 15 cycles prior to test cessation (when one outer strand failed). Macroscopic examination of the broken core wires reveal that fatigue cracks were noted to be present in the wire surface farthest from the center of curvature of the drum, propagating toward the drum center. The dissections performed on these test specimens indicated that the extent of wire breakage in the cable due to fatigue damage was not apparent by external examination.

Estimating Cable Degradation - Where visible wire breaks in a cable are not an indication of cable damage, a possible alternative method for recognizing cable degradation appears possible from cable length measurement. Data taken during the course of the endurance limit test for samples F-2, F-3, and F-4 showed measurable changes in length of a significant amount;  $3/4$  of an inch in the worst case (F-3) from a baseline measurement taken after initial proof-loading (initial proof-loading itself results in approximately  $1/2$  inch of permanent elongation in removal of constructional stretch). Measurements recorded are shown in Table 61. In specimen F-4, the increase in length appears relatable to the remaining tensile strength rather than the number of cycles accumulated.

TABLE 58. RESULTS OF ENDURANCE LIMIT FATIGUE TESTS FOR F SPECIMENS.						
Specimen Number and Lay	End Fitting		Fatigue History		Comments	
	Type	% Area Reduction	Accumulated Cycles	Observable Wire/Strand Breaks		
F-1 Right	(2)SPA-RH	10	32,400 32,406	4 Wires Many Strands	.Test Cont'd. .Test Term., Specimen Disected	
F-2 Right	(2)EYE-SPLICE	11.9	32,400 38,880 38,895	1 Wire 5 Wires 1 Strand	.Test Cont'd. .Test Cont'd. .Test Term., Specimen Disected	
F-3 Left	(2)EQ-BAR	10	21,500	Cable Rupture	.Failed during limit load (straight) tensile test at 35,000 to 40,000	
F-4 Left	(2)SPA-LH	10	50,000	1 Strand	.Specimen to TOD Test for RTS-38,900	
Dummy Right	(2)"LAB."	--	6,489	-0-	.No tensile tests	
Dummy Left	(2)"LAB."	--	28,400	-0-	.No tensile tests	
Notes: 1) All specimens proof-loaded, 50,000 lbs. straight tension before test.						
2) Load spectrum cycling over 18.7-inch pitch-diameter drum with a zero loaded condition between bending cycles. One HLH/ATC Life Cycle = 10,800 Spectrum Loading Cycles.						
3) Limit load, 50,000 lbs. reapplied to each specimen after completion of 21,600 spectrum loading cycles.						
4) Dummies were used to replace specimens F-1 and F-3 in order to continue tests of specimens F-2 and F-4.						

TABLE 59. RESULTS OF INTERNAL EXAMINATION OF TENSION/  
BEND-OVER-DRUM FATIGUE SPECIMENS.  
(Tests Sections Which Did Not Fail)

Specimen Number	Wire Breaks	Location
F-1	1	Second Layer (large strand)
	7	Core Strand
F-2	7	Core Strand
F-3	12	Core Strand

TABLE 60. RESULTS OF INTERNAL EXAMINATION OF TENSION/BEND-OVER-DRUM FATIGUE SPECIMEN F-2										
Strand Layer & No.	Wire Breaks	Strand Layer & No.	Wire Breaks	Second Layer		Third Layer		Strand Layer & No.	Wire Breaks	Wire Breaks
				Second Layer		Third Layer				
Outer										
1	1	1 Large (b)	6	1	4 + F	--	20 + 2 F			
2	3	2 Small	6	2	1 + F					
3	1	3 Large	9	3	4 + F					
4	5	4 Small	7	4	4 + F					
5	3	5 Large	7	5	0 + F					
6	1	6 Small	6	6	1 + F					
7	3	7 Large	1 + F	7	0 + F					
8	2	8 Small	7							
9	0	9 Large	0 + F							
10	7	10 Small	0 + F							
11	8	11 Large	0 + F							
12	8 + F(a)	12 Small	0 + F							
13	1	13 Large	0 + F							
14	1	14 Small	0 + F							

(a) "F" indicates a total failure of the strand at one or more locations, in addition to wire breaks at other locations.

(b) The second strand layer contains two strand sizes - "large" or "small" indicates the size.

(a) "F" indicates a total failure of the strand at one or more locations, in addition to wire breaks at other locations.

(b) The second strand layer contains two strand sizes - "large" or "small" indicates the size.

TABLE 61. CABLE ELONGATION DUE TO FATIGUE TESTING.			
Specimen Number and Lay	Accumulated Cycles	Changes in Specimen Length, in.	Comments
F-2	32,406	1/2	End of Test
F-3	21,600	3/4	Failed on Proof-Loading 40,000 lb.
F-4	21,600	0	Test Continued
	50,000	5/8	Test Terminated Failed; TOD @ 38,900 lb.

In the actual paired cable installation, damage to one cable would be apparent in tilting of the equalizer bar. However, similar damage existing in both cables would not be discernable in this manner. Therefore, a measurement of physical dimensions of the cable under a reference load and temperature could be used (with proper background data) to estimate cable damage due to fatigue.

#### Tension-Over-Drum Cable Strength Tests - A, B, D, E, F, and G Specimens

Objective - Tension-over-drum (TOD) tests were conducted to determine cable ultimate strength when bent over a drum as the basic validation criteria for the cargo system tension member. TOD tests of new cable served to determine wrap pressure losses by comparison with results of "pure" or straight tensile tests. TOD tests were also used to evaluate performance degradation of specimens subjected to spectrum loading fatigue and specimens combining corrosion and fatigue. The performance degradation was measured by determining the tensile strength remaining (RTS) in each cable.

Specimen Design - A total of twelve end fitting/cable specimens were tested by TOD; ten had previous test histories. Three D specimens were new, except for 10 cycles to limit load during tension/elongation tests; seven were E, F, and G specimens which were fatigue tested; and two were new specimens added to the program. The A-6 specimen was added to the program to evaluate the bending loss of new (proof-loaded) cable and specimen B-4 was used to evaluate AISI 4130 as a material for the eye-splice swaged sleeve as a replacement for the AISI 1018 used in specimen E-3.

Test Method and Procedure - Tension-over-drum tests were performed on a horizontal, hydraulically loaded tensile machine of 600,000-lb capacity. The test setup is shown in Figure 144. Each specimen was attached through one end fitting to a load-equalizer plate, looped around the simulated hoist drum for 180°, and attached through its remaining end fitting and a load cell to the load equalizer plate. Load was applied by a hydraulic cylinder attached to the drum. The load equalizer plate was restrained at a point midway between the end fittings (18.7-inch separation). A uniform loading rate was maintained during each test and was approximately the same for all specimens. The loading rate was 1 inch per minute.

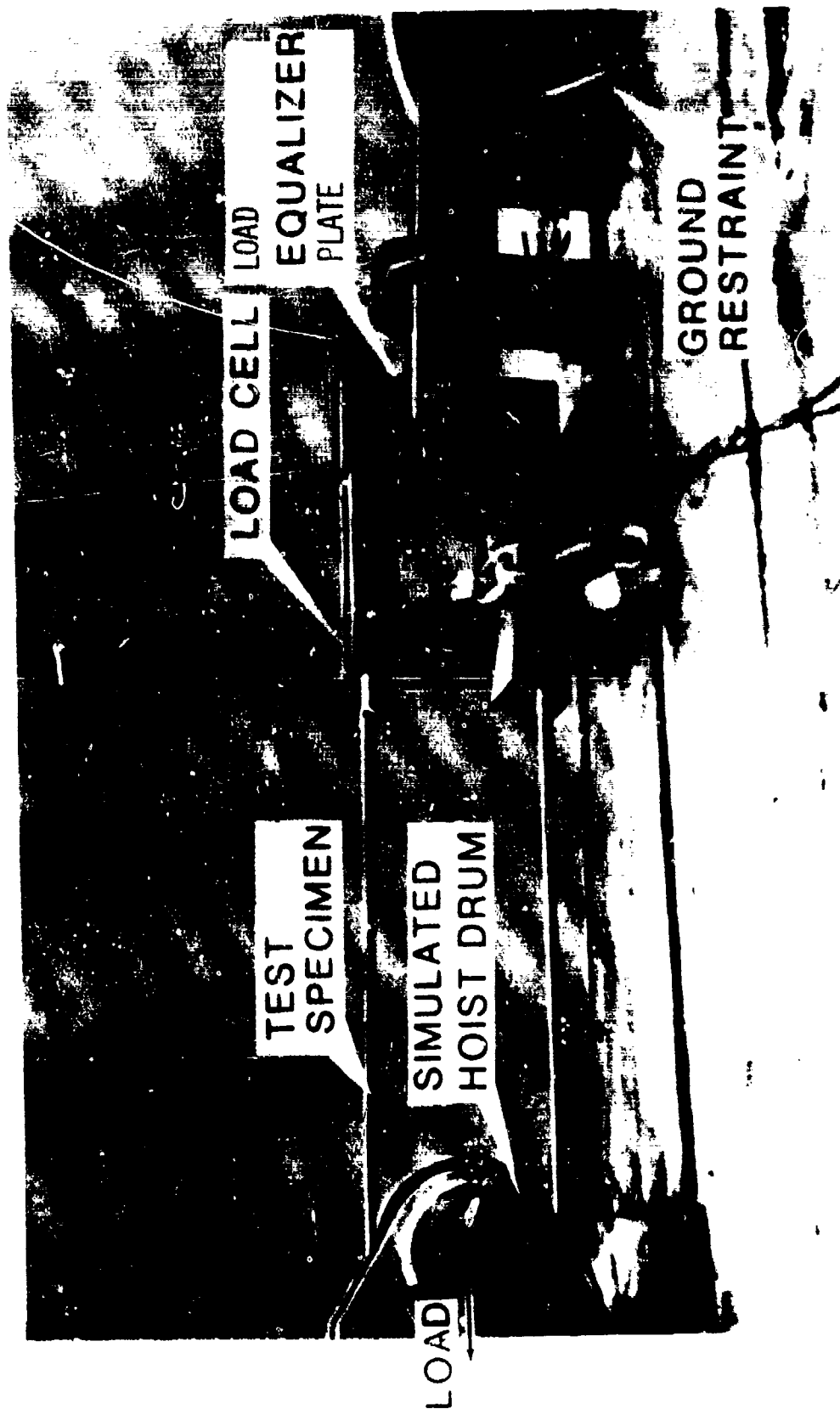


Figure 144. Tension-Over-Drum Ultimate Test Rig - 0.70-Inch, 36x7 Cable and ATC Fittings



Acceptance criteria for the 0.70-inch-diameter development cable and end fittings for the HLH/ATC design are stipulated in Table 62. They are a measure of the acceptability of the development design configuration with respect to the TOD test results. These criteria were applicable to all TOD test specimens, with two exceptions:

1. Except for the drum button designs, cable criteria were used as a test requirement for all swaged end fittings.
2. Group F Specimens which were "run-out" samples to define the tension member fatigue life.

Cable Strength Tests - Results - The resulting TOD breaking loads are summarized in Table 63. Only two specimens, A-6 and D-1, reached or exceeded the required minimum breaking strength of 75,000 lbs.

Cable tensile strengths demonstrated by TOD tests of E fatigue and G corrosion/fatigue samples did not meet strength criteria (refer to "Hoist"- Table 62). Based on these criteria, the tension member cable was unacceptable for unrestricted aircraft use on an operational cargo handling system subject to 2.5-g loading. All specimens of groups A, D, and E met the limit load criteria of 50,000 lbs without yield. The G specimens did not. Individual wire failures were noted to begin at 46,500 lbs (G-1) and 49,200 lbs (G-2) during TOD tests.

The development designs, however, demonstrated RTS load levels sufficiently close to requirements to be acceptable for use on the HLH ATC Demonstration Tests.

Cable Strength Losses - Cable strength losses due to fatigue and combined fatigue and corrosion damage were demonstrated by TOD tests. The TOD criteria, although more severe, was selected over straight tensile criteria as being more realistic for a drum-mounted cable. The TOD criteria includes losses due to cable bending and wrap pressure.

Using right-lay cable data, the maximum losses were calculated from the TOD test results and displayed in Table 64. Future cable design in the 36x7 construction should consider the losses incurred by the E samples and the 2.4% bending/wrap pressure loss (TOD) incurred by the A-6 sample with respect to the cable manufacturers straight tensile criteria.

TABLE 62. TENSION-OVER-DRUM TEST CRITERIA		
Cable and Interface	Design Loads, Lb	
	Limit	Ultimate
	(No Yield)	(Min. Breaking) Strength
<u>HOIST</u>		
Cable and Equalizer Bar (Eye/Swaged Shank)	50,000	75,000
<u>SINGLE POINT ADAPTER</u>		
Cable/Adapter (Eye/Swaged Shank and Eye-Splice)	41,000	61,300

TABLE 63. SUMMARY OF TENSION-OVER-DRUM TEST RESULTS.		
Specimen Number/Lay	Prior Test History	TOD(a) Breaking Load, Pounds
A-6	K One Limit Load Cycle (Proof Load)	76,100
D-1	R Tension/Elongation (b)	75,400
D-2	L Tension/Elongation (b)	65,900 (c)
D-3	R Tension/Elongation (b)	73,700
E-1	R BOD/T(d) -10,800 Cycles	73,700
E-2	R BOD/T(d) -10,800 Cycles	70,200
E-3	L BOD/T(d) -10,800 Cycles	62,300 (e)
E-4	L BOD/T(d) -10,800 Cycles	69,900
F-4	L BOD/T(d) 50,000 Cycles (Endurance Limit Test)	38,900
G-1	R BOD/T Corrosion (f) -10,800 Cycles	62,000
G-2	R BOD/T Corrosion (f) -10,800 Cycles	67,500
<p>(a) TOD - Tension Over Drum. Failure at drum tangent point, unless otherwise noted.</p> <p>(b) D specimens were subjected to 10 tensile load cycles from 0 to 52,000 lbs prior to ultimate TOD test.</p> <p>(c) One of the original left-hand single-point adapter fittings slipped at a load of 55,200 lbs. This fitting was replaced and the subsequent pull resulted in cable failure at 65,900-lb tension. (Slip and resulting shock may have damaged cable).</p> <p>(d) BOD/T - Bend-Over-Drum/Tension Fatigue Test using spectrum loading and a zero-load condition between bending cycles. Drum pitch diameter = 18.7 inches. Cycling stroke = 19 inches. A set of 10,800 load cycles is equivalent to A/C life criteria</p> <p>(e) Eye splice sleeve failed by splitting. (Material defect found)</p> <p>(f) G specimens completed 3600 fatigue cycles, then were exposed to salt-fog for 240 hours followed by 7200 additional fatigue cycles.</p>		

TABLE 64. TENSION-OVER-DRUM CABLE STRENGTH LOSSES. (Baseline-Right-Lay Cable Straight Tensile Strength)			
Specimen Group	Prior Test History (a)		Maximum Strength Loss, %
	Test	Cycles or Hours*	
A	None	None	2.4
D	Tension - 0 to 52,000 lbs.	10	5.5
E	BOD/T(d) Fatigue, Spectrum Loading	10,800	9.8
G	BOD/T(d) Fatigue and Corrosion Spectrum Loading Salt-Fog Exposure	10,800 240*	20.3 (E)
F	BCD/T(d) Fatigue, Life Test	50,000	48 (c)
<p>(a) All specimens proof-loaded to 50,000 lbs before test history.</p> <p>(b) Results not applicable to field test use - refer to paragraph entitled "Corrosion/Fatigue Tests".</p> <p>(c) Test terminated at 50,000 cycles by test plan. Left-lay specimen - no right-lay specimen (F group) available for TOD test.</p> <p>(d) BOD/T - Bend-Over-Drum/Tension Fatigue Test using spectrum loading and a zero-load condition between bending cycles. Drum pitch diameter = 18.7 inches. Cycling stroke = 19 inches. A set of 10,800 load cycles is equivalent to A/C life criteria</p>			

The 240-hour exposure period used for the G (combined fatigue and corrosion) specimens was selected to be severe. In future tests, an exposure criterion that is more representative of field usage should be selected in order to determine the magnitude of strength losses under more realistic circumstances.

The only F sample in the TOD test group, F-4, when adjusted for left-lay strength, showed an approximate loss of 47% after the completion of 4.63 life cycles. This, however, was the longest lived sample in the group. F-3, was at the other extreme, incurring about the same loss after completion of 2 life cycles of fatigue spectrum loading.

The strength loss experienced by the D samples, while of no significance in terms of an operational "g" loading simulation at 5.5%, introduced the same order of loss due to the high load level cycles as the pure bending loss found with specimen A-6.

End Fittings - Test Results - During initial tension-over-drum tests involving nine specimens from groups D, E, and G, two fitting failures were experienced. The first failure was specimen D-2, which slipped at 55,200 lbs. This was an equalizer bar fitting (swaged shank) with a minimum requirement of 75,000 lbs. The D-2 specimen swaging was based on a reduction of area of 10%. On investigation, it was found that the fitting had been inadequately swaged in its center section. A replacement fitting was immediately applied and the D-2 cable specimen was pulled to failure. Although a center break of the cable was achieved, the low strength value of 65,900 lb was suspect, indicating that the cable specimen could have been damaged by the shock load encountered when the fitting slipped (it did not pull off cable). After extensive examination of the swaging process used, the development design was reconfigured to an  $R_A$  of 11.9% to eliminate slippage. This new swaged shank configuration was represented by specimen A-6. As recorded in Table 63, A-6 broke in the center of the cable without sign of any slippage or wire damage within the fitting.

The second fitting failure encountered in the TOD tests was specimen E-3, which used an eye-splice configuration with a dual hole AISI 1018 sleeve. The fitting failed by splitting as shown in Figure 145. This was subsequently attributed to inclusions in the AISI 1018 material. In view of the cable damage encountered by the D-2 specimen as result of the sudden load change,

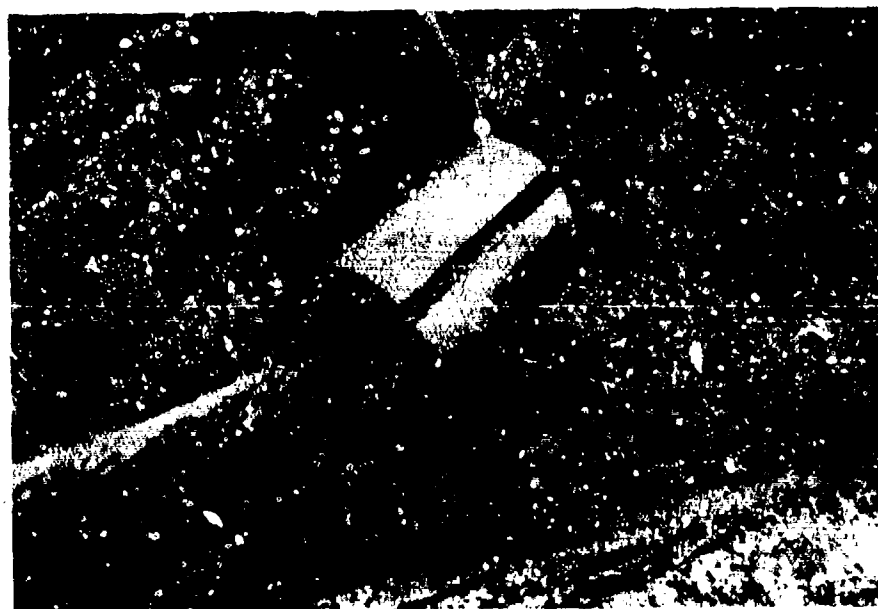


Figure 145. Eye-Splice Sleeve Failure of Specimen E-3  
at 62,300 lb.

the testing of the E-3 specimen was terminated. New fitting configuration tests, however, were undertaken. It should be noted that although the E-3 fitting failed, it had actually marginally exceeded the requirements for the single-point adapter listed in Table 62. A material change was nevertheless undertaken to achieve higher strength capability for the termination in order to use all test specimens for gathering cable data in the ultimate strength region.

#### Cable Lubricant Migration

During the initial fatigue tests, it was noted that the initial cable lubricant appeared on the surface along the entire length of cable, both on the straight and bend portions. This was first observed at approximately 900 cycles. After 1,080 cycles, the lubricant was removed with a cloth and solvent from a portion of the cable, but was observed to return to the surface with continued cycling. This lubricant continued to migrate to the surface in a bubbly state on all cable samples throughout this and other tests. No dripping of lubricant was noted. This migration was believed to be from the pumping action created by the relative motion between the strands under the combined tensile and bending cyclic loading. Figure 146 shows the lubricant bubbles found between the strands after 5,400 cycles of testing. This lubricant migration continued throughout the entire fatigue test program on all ten specimens, and was notably different from that experienced during design support testing of the 0.78-inch, 36x7 cable. During design support tests, the lubricant merely wet the cable surface in the sections of the specimens bent over the drum, since cyclic tension was not included.

#### Drum Wear

During the TOD tests, seven cables failed in the section bending over the drum. Figure 147 shows the drum groove after the tension-over-drum tests. Most of the electroless nickel was removed by cable breaks; however, the base material was only slightly marred. Cross marks are from left- and right-lay cables used on the same drum. This drum was also used for approximately 103,000 fatigue cycles with left- and right-lay cables before TOD tests.

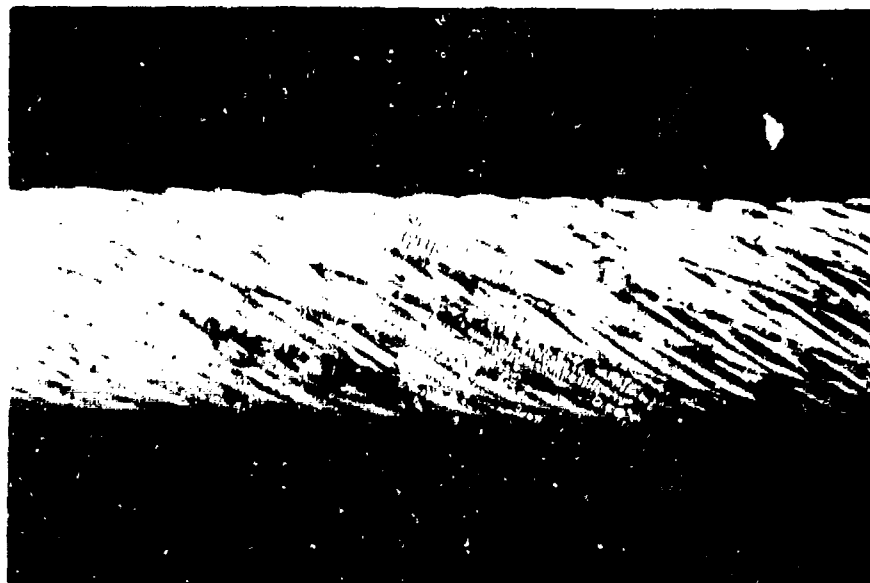


Figure 146. Cable Lubricant Migration After 5400 Load Cycles. (Cable was cleaned after 4320 cycles.)

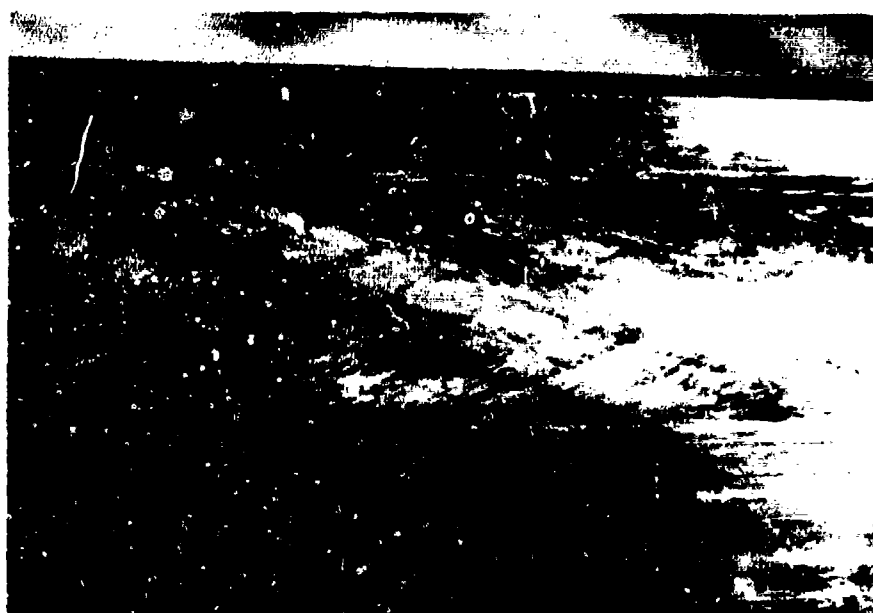


Figure 147. Sheave Groove After Tension-Over-Drum Testing.



### Bearings and Pins

Bearings - The bearings used in the eyes of the equalizer bar and single-point adapter fittings were selected from Military Standard MS 21241. They were Teflon-lined stainless steel flanged sleeves with a basic bore diameter of 1.0 inch. Bearings with 3/4-inch sleeve lengths were used in the equalizer bar fittings; 1/2-inch sleeves were used in both left- and right-hand single-point adapter fittings. These fittings were made with an eye inside diameter sufficiently large to allow easy removal of the bearings after each test so that the same set of bearings could be used repeatedly. Figure 148 shows two bearings after many fatigue tests.

Pins - The fitting pins to be used in HX ATC designs were required to have a diameter of 0.996-0.997 inch, a surface finish of 32, and an ultimate tensile strength of 180,000 psi. The actual material tensile strength of the pins used during design development tests was 168,500 psi. Pin diameter and surface finish were as indicated above.

The pins were not damaged during any of the testing until the final tension-over-drum ultimate tests. At that time, some of the pins were slightly bent.

### Supplemental Tests of 0.78-Inch-Diameter, 36x7 Cable

The development and evaluation tests conducted on the 0.70-inch cable established that both gains and losses in performance had occurred in the 36 x 7 with the use of the high strength wire. Improvements were made in strength-to-weight ratio and reduced cable size, but deficiencies were encountered in achieving balanced load distribution between strands and maintaining efficiency. Both factors contributed to an inability to completely meet all strength criteria following fatigue test, although life-cycle requirements were met. As a result, investigation of the design support test cable, the 0.78-inch, 36x7 construction using mill run wire, was resumed to provide more design data on its strength characteristics.

Three tests were conducted using two 5-foot and one 12-foot cable specimens. Full cable strength was developed with failure at a load of 93,490 lbs in straight tension. The tension-over-drum test developed a "center break" at 92,300 lbs, demonstrating a bending loss of 1.25% at a 24.1 D/d.

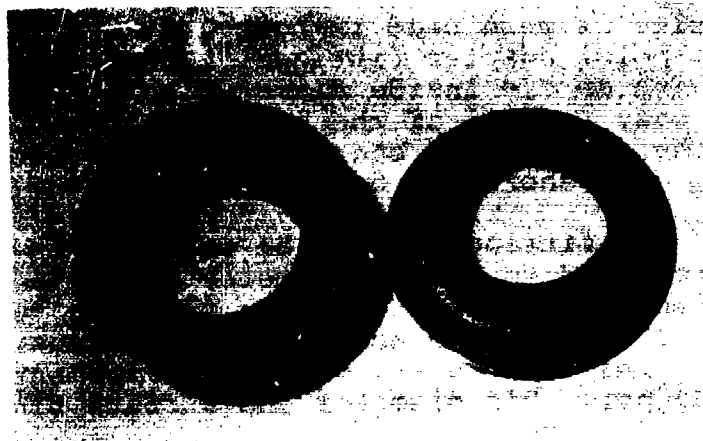


Figure 148. Photographs of MS 21241 Bearings  
After Repeated Testing

The test demonstrated an 88.5% efficiency for the 0.78-inch construction, compared to a 82% efficiency for the 0.70-inch cable, and gave significant evidence of better load distribution between strands. In the larger cable, all wires were broken nearly simultaneously, compared to the 0.70-inch cable, in which wire breakage occurred over a 10,000-lb range preceding failure. Table 65 provides significant details of the end fittings and test conditions used to establish the basic characteristics of the 0.78-inch cable.

These tests established the superiority of the 0.78-inch cable over the 0.70-inch cable and provided a good data base in terms of cable strength for using a 0.72-inch diameter cable as a production design tension member. The 0.72-inch cable fabricated from electro-galvanized carbon steel "millrun" music wire with an average wire tensile strength of 315,000 psi will meet HLH ATC criteria.

TABLE 65. SUMMARY - NEW 0.78-INCH, 36 X 7 TEST DATA. (SHEAVE PD-18.72 IN. D/d = 24.1)				
Test	% Area Reduction	Swaged Length, In	Failing Load, lb	Comment
Tensile	9	8	92,800	Slip
Tensile	9	13.90	93,490	Cable center-break
Tension-over-drum	11.7	8	92,300	Cable center-break

## CONCLUSIONS

The design development tests of the tension member with the 0.70-inch-diameter, 36x7 cable using high strength (363,000 psi, average) galvanized carbon steel music wire and end fittings, demonstrated the following:

1. The cable and eye-type end fittings (as modified after failure) met all static criteria.
2. The cable (E specimens) did not meet the 75,000-lb bend-over-drum ultimate strength requirement following completion of 10,800 bending and tensile fatigue cycles under spectrum loading. The deviation from the ultimate tensile strength (UTS) requirement was 5,100 lbs. In view of the small (6.8%) strength delta, the cable can be considered acceptable for use on the HLH ATC Demonstration Program, and conditional use in future applications on the HLH prototype.
3. The eye-type end fittings satisfactorily met fatigue criteria. The drum button end fittings (shortened length) demonstrated an ultimate (45,600 lb strength of 150% of the requirement, although minute slippage occurred slightly below the limit load level (20,000 lbs). The 1/2-inch longer drum buttons allowed by the interface design are expected to meet all static requirements.
4. The cable tensile strength remaining after combined fatigue and 240-hour corrosion (G specimens) test did not meet either limit load or ultimate requirements. However, the corrosion criterion used is considered unrelateable to field use. This test program determined cable strength degradation for a specific test duration, whereas actual degradation due to corrosion that may be experienced in service should be determined by appropriate tests.
5. Tests to determine fatigue life (F specimens) demonstrated good consistency and life margin with the right-lay configuration and wider scatter with the left-lay cable. While remaining tensile strength criteria following completion of one life cycle (10,800 load cycles) were not met (see 2 above) the life-cycle tests show that catastrophic failure of the cable is beyond the number of cycles conducted under this program.

## CARGO COUPLING

### DESIGN SUPPORT TESTS

Photoelastic models of two-load beam configurations were fabricated and tested to determine the most efficient geometry and to minimize the weight of the coupling load beam. Stress intensities across critical sections were evaluated for both specimens. A study of these intensities, in conjunction with an analysis, resulted in the conclusion that an "L" shape is more efficient than a "C" shape, and that 250,000-psi heat treated steel is more efficient than 6Al-4V titanium for this particular application. Complete details of this test and the supporting analysis are contained in Reference 1.

A series of subsystem hardware tests were conducted to evaluate and substantiate the overall design and new concepts of the coupling system. These included the following:

1. Push rod test
2. Load beam
  - a. Ultimate test
  - b. Coating test
  - c. Sealing test, including sand and dust
  - d. Latch test
3. Pivot bearing test
4. Pulley coating test

#### Push rod Test

The signal mechanism is actuated through a new push rod system which eliminates the normal slip rings used in all previous designs where continuous rotation is required. Tests were conducted to prove the system and confirm the microswitch mounting positions for optimum lever actuation.

The push-rod system was actuated vertically for 10,600 cycles. The rotating portion was rotated 1,400,000 times to correspond to the 3600-flight hour life span of the aircraft. Results of the tests indicated little or no wear on this portion of the electrical system and actuating mechanism.

#### Load Beam

Load Beam Ultimate Test - The load beam ultimate test was conducted to confirm both the design and strength of the material. Only ninety percent of

the ultimate was realized due to the material being improperly forged. As a result, a number of changes were implemented in the load beam configuration:

1. The load beam shaft is now a separate part.
  - a. This allows a smaller forging billet.
  - b. This decreases the stress concentration at the billet juncture of the load beam shaft and hub.
2. A straight billet is used instead of a bent billet, which would normally be necessary for the grain flow to follow the load beam tongue curve.
  - a. A straight billet is more economical and requires less time to forge. The cost order-of-magnitude is approximately 4:1.
  - b. Vendor facilities for supplying the bent billet were restricted to only one company, which had the tooling to accomplish the bending operation.
  - c. The straight billet can be oriented to provide proper grain to conform to major stress distribution.

Although one completed load beam was improperly forged, some of its properties were improved through solution heat treatment for use in the first completed coupling assembly. This treatment had been recommended by one material manufacturer in order to regain some of the material properties lost because of the improper forging technique used in the first five delivered load beam billets. This beam was used for the complete coupling assembly limit load test and for environmental testing in order that the development test schedule would not be compromised. This unit was replaced prior to final delivery of the coupling to the ATC program.

A further ultimate test was conducted on the new load beam design with satisfactory results. The new beam failed at 243,500 pounds with no yielding at the limit load of 140,000 pounds.

Coating Test - Tests were conducted on the load beam to evaluate the ability of nedox and nickel boron coatings to reduce the coefficient of friction between the load beam and the sling. Although good results were obtained with both coatings, the bare beam did not impose any restraint on sling release.

Sealing Test - Tests were conducted to check the ability of the coupling assembly seal to prevent leakage of water during short-time immersions. Additional tests included sand and dust. The 3/16x3/16 square configuration of foam rubber seals adds little in weight but is expected to increase the operational life of the coupling through the exclusion of dirt. It effectively prevented foreign matter from entering the coupling around the load beam interface area.

Latch Test - A load beam latch mechanism test was conducted which established the reliability of the latch mechanism repeatedly released with approximately a 1000-pound load. Initial cycle tests were run to establish the configuration of a Belleville washer stack which is compressed when a load is applied to the load beam.

As the load is applied and the stack of washers, mounted within the load latch bar, is compressed, the push-rod system electrically deactivates the power to the solenoid, thus electrically rendering the system inoperative above the 1000-pound load requirement. As the load is removed from the load beam, the stack expands and reactivates the electrical system for a release signal. An additional over-center lock is established at loads above 1000 pounds to lock the mechanical release system, should the electrical interlock fail. Five-hundred load cycles were run to verify the 1000-pound load release limit.

#### Pivot Bearing Tests

A series of tests were conducted to determine the adequacy of the non-lubricated, teflon-lined bearing shells in various design positions of the coupling assembly.

Areas of application include:

1. Equalizer bar
  - a. Tension member end
  - b. Coupling quick-release pin
2. Load beam pivot point
3. Load latch pivot point
4. Sheave assembly pulley

Tests were conducted on the most representative units through the load design spectrum in cycling the rotation points in the bearing shells. At the conclusion of the tests, the teflon bearing lining was examined for signs of wear. The conclusion was that each design position of a bearing would meet the design requirements of minimum maintenance and attention throughout the design life of the total coupling design.

#### Pulley Coating Test

A series of tests were conducted to determine what effect the application of a coating to the aluminum single-point sheave assembly pulley grooves would have on minimizing the wear in the grooves by the load cables. Four different coatings were compared:

1. Hard anodizing
2. Tufam - a product of the General Magnaplate Corp.
3. Sermatell - a product of the Teleflex Company
4. Nicket-Boron - a product of the DuPont Company

Tests were conducted by cycling the pulley back and forth under its normal operating load of 56,000 pounds for some 3600 cycles. At the conclusion of the cycling operation, the grooves were examined for wear of the cable against the groove surface. It was concluded that, although all of the coatings gave adequate protection against wear, the hard anodizing was the best of four tested.



## DESIGN DEVELOPMENT TESTS

### Test Specimen Design

The test specimen is shown in Figures 149 and 150.

### Coupling (Cargo Hook) Assembly Tests

The following tests were conducted:

- Functional tests
- Static loads - one specimen tested to design limit load
- Endurance test - one specimen subjected to an endurance test of 500 cycles

The endurance test was conducted under simulated operating conditions. Design limit load was applied continuously over all cycles. Environmental conditions of sand, oil, dust, humidity, salt spray, and temperature were also evaluated.

### Release System Endurance Test

One release system, including primary and secondary release systems, was subjected to an endurance test of 500 actuation cycles, with releases (openings) made with loads ranging from 40 pounds to the 1,000-pound design limit load.

### Coupling Endurance Test

Test Conditions - A load cycle consisted of the following steps:

1. Close load beam and latch
2. Apply 56,000 lb to load beam
3. Reduce load to specified value and release.

The following load cycles were performed:

<u>Number</u>	<u>Specified Release Value</u>
350	40 lb
55	500 lb
100	1,000 lb

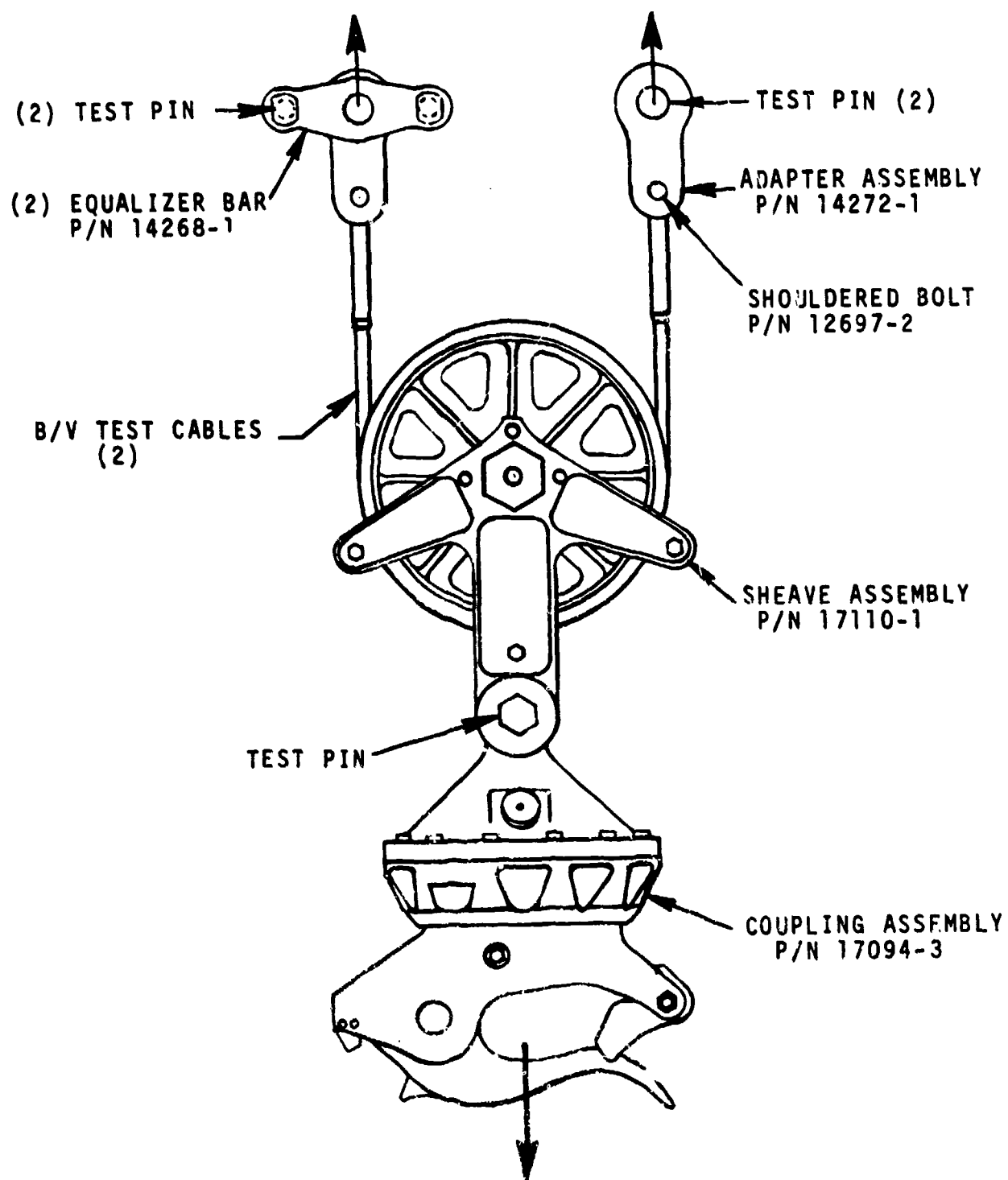


Figure 149. Coupling Device Test Specimen.

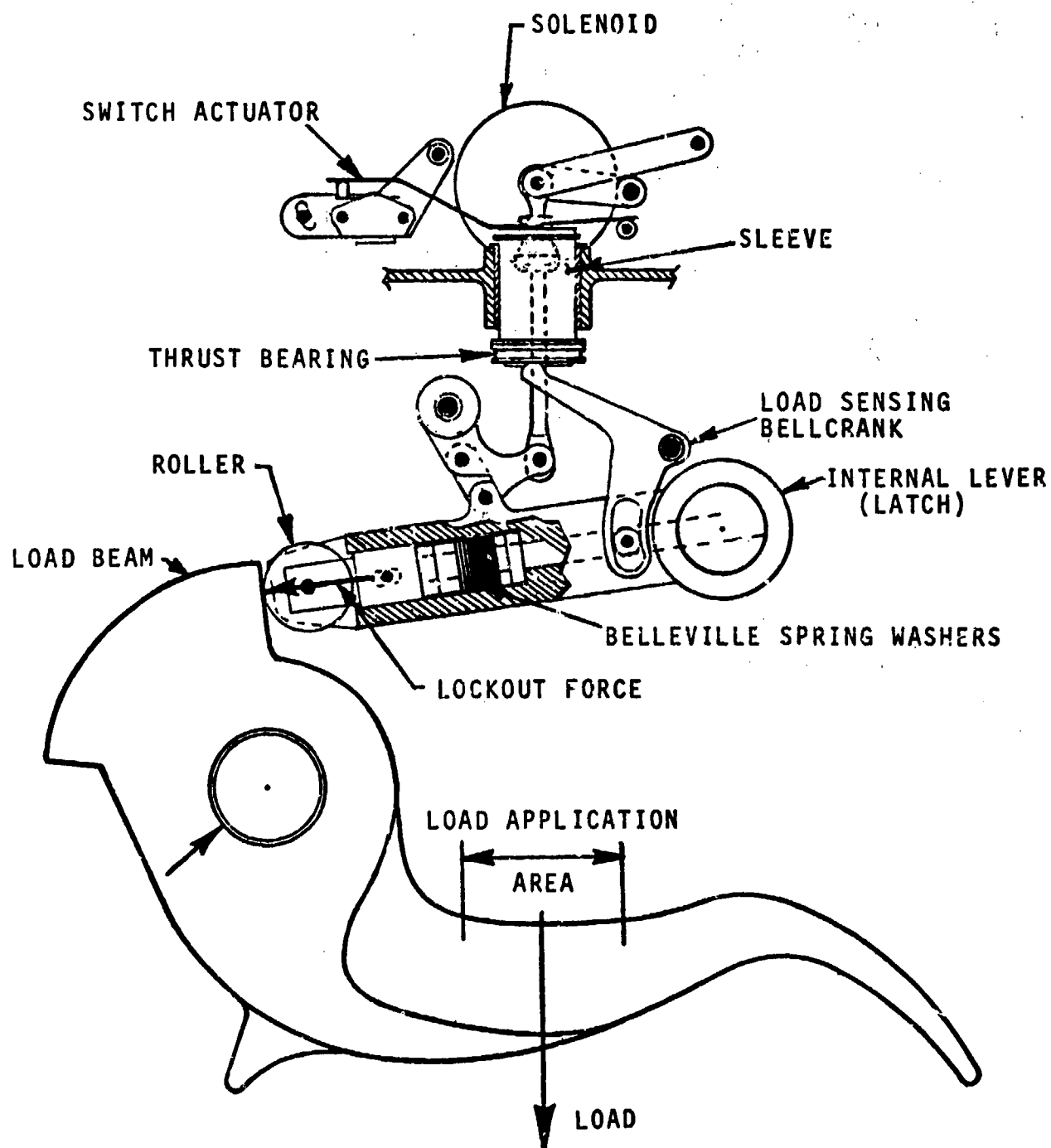


Figure 150. Schematic of Load Beam Latch Sensing Mechanism.

Initial Release - The first functional checks indicated that the mechanism would not electrically release a load on the load beam greater than 450 lb. This meant that the angle at which the face of the load beam was machined had to be changed slightly to decrease the "ramp" effect of this face.

Since prior experience indicated that releasability was greatly dependent on small variations in the ramp angle, considerable effort was directed toward developing a ramp/roller relationship which would be satisfactory for release of loads up to 1000 lb. Tests were conducted starting with a ramp angle at 90° to the centerline of the latch; i.e., a line drawn between the roller contact point on the ramp through the latch pivot was at 90° to the ramp surface.

Rework of the ramp angle was accomplished in 15' steps until an angle which allowed satisfactory release at all specified loads was provided. The relationship of load beam ramp angle to the latch roller is such that for each 0° 15' angular change to the face of the load beam, 0.0036 inch must be machined from the tip of the load beam. The ramp angle was machined in the face of the load beam over a width of 0.562 inch to accommodate the roller. When the face of the load beam (on each side of this recess) contacts the face of the internal lever during the "locked-out" mode, the line of action of the reaction on the load beam face passes below the fulcrum of the internal lever, keeping the mechanism in the locked condition.

#### Loading and Release Cycles

Loading and Release at 40 Pounds - A 2-1/2-inch-wide, three-ply, nylon sling was used for load application. The "lockout switch" was adjusted so that the solenoid was re-energized at approximately 1,000-lb decreasing load. Loads were applied to 56,000 lb and then reduced to an approximate 5,000-lb load level, at which point the scale reading was changed to the 0 to 6,000-lb scale to provide greater reading accuracy. The lockout switch was wired to a battery and lamp and the load was recorded when the light went out under increasing load (de-energizing solenoid) and again when the lights came on (energizing solenoid) under decreasing load. A relay limited the current through the switch to 0.25 amp. Sixty-four releases were made during this initial run with the load differential between 400 lb and 700 lb, depending on the sling position within the load beam throat.

Before continuing the test, the switch was readjusted to approximately the 1,000-lb reading. A total of 350 releases at 40 lb were completed as specified. On several of these releases, the load beam would not manually relatch. Disassembly and inspection of the mechanism indicated high friction between the clevis pin and the curved slot in the bellcrank lever, which sometimes prevented the internal lever dropping down to latch the load beam. This bellcrank lever (P/N 13382-1) was redesigned with a curved slot wide enough to accept a small ball bearing to minimize the friction.

Loading and Releases at 1,000 Pounds - Once again the switch was adjusted after reassembly of the test model to approximately the 1,000-pound load limit. A total of 100 releases was then completed. With the switch set at the desired release load, the switch was kept depressed when decreasing the load from 56,000 lb and the mechanism released the moment the solenoid circuit was closed. The load differential was 600 lb to 300 lb and, of course, was sensitive to the position of the sling.

Loading and Release at 500 Pounds - A total of 37 loading and release cycles had been completed when it was decided to replace the badly worn nylon sling used to apply the load. The test was continued to 55 releases with a new nylon sling. The release loading differential was approximately 600 lb to 800 lb.

#### Analysis of Coupling Endurance Test Results

Release Loads - The tests show that the coupling assembly will release loads of between 40 lb and 1,000 lb. It is necessary to adjust and set the redundant lockout switches to the proper position to achieve this, and it is recommended that the switches be set to release at 1,000 lb decreasing load.

Lockout Mechanism - It was shown that a system of Belleville springs performs satisfactorily as a lockout mechanism and that a spring stack of three discs in parallel and seven such sets in series provide the necessary load/deflection characteristics to permit the lockout mechanism to function within the prescribed load range.

Lockout Load Tolerance - The applied load at which the lockout mechanism de-energized the solenoid is never precisely the same for repeated loadings. This is because the location of the sling is never precisely the same within the load application area for repeated loadings. This tolerance is approximately +350 lb.

Due to the hysteresis of the Belleville springs and the movement differential of the lockout switches, and other mechanism frictions, the decreasing load at which the solenoid is again energized differs from the increasing load at which the solenoid is de-energized. If the switches are set for the solenoid circuit to become energized at 1,000 lb decreasing load, then the solenoid circuit will become de-energized at approximately 1,750 lb increasing load. In order to minimize the mechanism frictions, all moving steel parts which contribute to these frictions have been coated with general Magnaplate Nedox SF-2 electroless nickel coating, which is impregnated with teflon.

Setting of Mechanical Cable Release Assembly - Before the coupling assembly was fully assembled, the mechanical cable release assembly was mounted on a fixture in a Tinius Olsen test machine and the Belleville spring discs preloaded to provide the appropriate force range for a remote mechanical release. The nut, P/N 12724-1, was adjusted so that it required a cable force of 250 lb to 300 lb to pull the release arm out of its cam detent. This ensures that there will be no inadvertent manual cable release due to air load. Once out of the detent, the cable force falls off to approximately 170 lb and then further rotation of the release arm allows the cam to increase the cable force to 320 lb to 400 lb when a mechanical cable release takes place.

Subsequently, Boeing Vertol requested that the mechanical release force be reduced so that it did not exceed 290 lb. The assembly was adjusted so that the force to overcome the detent was 130 lb to 140 lb and the force increases to 220 lb to 240 lb with full rotation of the cam. When this release assembly was installed in the coupling assembly, the mechanical force to release at ambient temperature was 190 lb to 210 lb when the sling was centered on the load beam with a 1,000-lb weight. It has been noted that this force increases to 265 lb when the sling is placed close to the keeper.

Setting of Switches - During assembly of the coupling (P/N 17094-3), before the attachment of the upper conical housing, the unit was bolted to a fixture and mounted in the Tinius-Olsen test machine.

The lockout switches were adjusted to cut power to the solenoids at 1,660 lb increasing load and to reactivate the electrical circuit at 970 lb decreasing load. Due to the hysteresis of the Belleville springs in the internal lever and the movement differential of the switches, these loads can have a range of 1,400 lb to 1,700 lb for the increasing load and 1,100 lb to 800 lb for the decreasing load.

The "hook open" switches were adjusted to be actuated by their cam, and the "mode switches" were set to a position which located the top of the actuator (P/N 13428-1) a distance of 3.86 inches above the diaphragm (P/N 17117-1).

Acceptance Load Test - The coupling assembly was mounted in the structural test frame with the sheave assembly and test cables. An acceptance load of 56,000 lb was applied to the system and held for 30 seconds. A subsequent revision of this test procedure increased this load to 112,000 lb. The developmental test unit was subjected to this 112,000-lb load during refurbishment.

#### Release System Endurance Test

General - The test specimen was subjected to a series of normal and trail angle releases with 40-lb, 500 lb and a 1,000-lb weights suspended from the load beam, and these releases were conducted in the dual solenoid, single solenoid, or remote mechanical mode of release. To determine the time lapsed between the actuating of the release switch and the dropping of the weight, the release cycle was filmed using 8mm film at 32 frames per second.

Testing was performed according to this schedule:

<u>Release Load</u>	<u>Configuration</u>	<u>No. of Releases</u>
40	Normal	370
40	Trail Angle	23
500	Normal	20
500	Trail Angle	11
1,000	Normal	96
1,000	Trail Angle	13

Normal Releases With 40-Pound Weight - The coupling device (N 17094-1) was mounted in a jib frame. With a 40-lb weight suspended vertically from the load beam, the coupling assembly was subjected to 370 normal releases in the following modes:

- 123 releases - dual solenoids
- 123 releases - single solenoid
- 124 releases - ground release knob

At every tenth release during this sequence, the torque required to rotate the swivel was measured. This was found to be a constant 54 in-lb.

To determine the time lapsed between actuating the release switch and dropping the weight, the cycle was filmed using 8mm film at 32 frames per second. Pressing the release switch also lit a lamp which showed on the film. The number of frames required to show that the weight was clear of the load beam and also to show that the load beam was relatched, were counted to determine the lapsed time.

For both dual and single solenoid releases, it was found that for a 40-lb weight on the load beam, the elapsed time for weight to clear load beam was:

$$\frac{12 \text{ Frames}}{32 \text{ Frames/sec}} = 0.40 \text{ sec}$$

and lapsed time for load beam to relatch was:

$$\frac{18 \text{ Frames}}{32 \text{ Frames/sec}} = 0.60 \text{ sec}$$

This is the slowest time for a load release, since it was later observed that heavier weights resulted in shorter release times.

Trail Angle Releases - 40-Pound Weight - To conduct releases with the coupling device in a trail angle configuration, the unit was pulled to one side by a hand hoist until the sideplate of the sheave assembly was inclined at the required angle to the vertical. The angle was measured by means of a universal protractor. To incline the unit to the vertical, a side force was applied to the shackle. This resulted in the coupling assembly being inclined at 44° to the vertical when the sheave assembly was at 33° to the vertical.



A total of five releases were performed initially, in the following manner:

- 2 releases - dual solenoid
- 2 releases - single solenoid
- 1 release - ground release knob

After these five releases were completed, the trail angle was increased in an attempt to determine the maximum trail angle for a 40-pound weight release.

The results achieved using the dual solenoid node are shown in Table 66.

Table 67 shows the results obtained for the single solenoid release mode.

Releases in the ground release knob mode with a 40-lb shackle on the load beam were as shown in Table 68.

Normal Releases - 500-Pound Weight - With a 500-lb weight on the load beam, a total of 20 normal releases were imposed on the coupling device.

- 7 releases - dual solenoids
- 6 releases - single solenoid
- 6 releases - remote mechanical release

TABLE 66. MAXIMUM TRAIL ANGLE FOR 40-LB WEIGHT RELEASE.				
Release No.	Mode	Vertical Angle of Sheave	Vertical Angle of Coupling	Remarks
1	Dual Solenoid	33°	44°	Weight towards fulcrum.
2	Dual Solenoid	33°	44°	Weight towards keeper.
3	Dual Solenoid	33°	44°	Weight pulling sideways on shackle.
4	Dual Solenoid	35°	45°	-
5	Dual Solenoid	40°	46°	-
6	Dual Solenoid	45°	50°	-
7	Dual Solenoid	50°	55°	-
A trail angle of 50° was the maximum achievable angle due to the cable fitting touching the pulley.				

TABLE 67. RESULTS FOR SINGLE SOLENOID RELEASE MODE.				
Release No.	Mode	Vertical Angle of Sheave	Vertical Angle of Coupling	Remarks
1	Single Solenoid	33°	40°	-
2	Single Solenoid	33°	40°	-
3	Single Solenoid	35°	42°	-
4	Single Solenoid	40°	46°	-
5	Single Solenoid	45°	51°	-
6	Single Solenoid	50°	56°	-
Each of the releases performed satisfactorily. The maximum trail angle achieved was 50° due to the cable fitting touching the pulley.				

TABLE 68. GROUND RELEASE KNOB MODE WITH 40-LB SHACKLE  
ON LOAD BEAM.

Release No.	Mode	Vertical Angle of Sheave	Vertical Angle of Coupling	Remarks
1	Ground Rel. Knob	33°	39°	-
2	Ground Rel. Knob	35°	41°	-
3	Ground Rel. Knob	40°	47°	-
4	Ground Rel. Knob	45°	50°	-
5	Ground Rel. Knob	50°	55°	-
As before, the maximum trail angle achieved was 50° due to the test cable fitting touching the pulley.				

All releases were performed satisfactorily. On two occasions during each mode of release, the torque required to rotate the swivel was measured and found to be 47 in-lb. Room ambient temperature was approximately 70 degrees Fahrenheit.

The cable force for the six remote mechanical releases ranged from 370 lb to 390 lb, which was consistent with original setting of the spring discs within the remote mechanical cable release assembly, P/N 13417-1.

With the 500-lb weight, the lapsed time for the weight to clear the load beam for both dual and single solenoid releases was:

$$\frac{8 \text{ Frames}}{32 \text{ Frames/sec}} = 0.25 \text{ sec}$$

and the lapsed time for the load beam to relatch was:

$$\frac{14 \text{ Frames}}{32 \text{ Frames/sec}} = 0.45 \text{ sec}$$

#### Trail Angle Releases - 500-Pound Weight

A total of eleven trail angle releases were conducted:

- 4 Releases - Dual solenoid
- 4 Releases - Single solenoid
- 3 Releases - Remote mechanical

The maximum trail angle attained was 45° and was limited because the fitting at one end of the test cable was very close to the pulley. The results are tabulated in Table 69.

#### Normal Releases - 1,000-Pound Weight

The following releases were conducted:

- 32 Releases - Dual solenoids
- 32 Releases - Single solenoid
- 32 Releases - Remote mechanical

At every tenth release, the torque required to rotate the swivel was measured and found to be a fairly constant 54 in-lb.

The thirty-one remote mechanical releases required cable forces ranging from 375 lb to 470 lb for release.

TABLE 69. RESULTS OF 45° TRAIL ANGLE RELEASE.				
Release No.	Mode	Vertical Angle of Sheave	Vertical Angle of Coupling	Release Force
1	Dual Solenoids	33°	35°	-
2	Dual Solenoids	33°	35°	-
3	Dual Solenoids	40°	43°	-
4	Dual Solenoids	45°	49°	-
5	Single Solenoid	33°	35°	-
6	Single Solenoid	33°	35°	-
7	Single Solenoid	40°	43°	-
8	Single Solenoid	45°	49°	-
9	Remote Mechanical	33°	35°	380 lb
10	Remote Mechanical	40°	42°	370 lb
11	Remote Mechanical	45°	48°	370 lb

From the 8mm movie film for both dual and single solenoid releases, the lapsed time for the 1,000-lb weight to clear the load beam was:

$$\frac{8 \text{ Frames}}{32 \text{ Frames/sec}} = 0.25 \text{ sec}$$

and the lapsed time for the load beam to relatch was:

$$\frac{14 \text{ Frames}}{32 \text{ Frames/sec}} = 0.45 \text{ sec}$$

#### Trail Angle Releases - 1,000-Pound Weight

Releases were conducted at the 33°, 40°, and 45° trail angles. These angles, shown in Table 70, were measured with a universal protractor.

#### Vertical Load Threshold Test

The coupling assembly (P/N 17094-3) was mounted in the Tinius-Olsen test machine and subjected to a series of load releases in an attempt to determine the threshold load at which the coupling would not release under the dual solenoid, single solenoid, or remote mechanical release mode.

It was found that the threshold for the electrical releases was predetermined by the "lockout" system. The system would release loads with either the dual or single solenoid operation until approximately 1,600 lb increasing load was reached, when the solenoid circuit was de-energized and no electrical release was possible. With the decreasing load, an electrical release was possible when the load was reduced to approximately 1,000 lb, when the solenoid circuit was again energized.

#### Limit Load Test

##### Functional Check

The coupling device was installed in a structural test frame. The 40-lb weight was suspended from the load beam and it was verified that the lower part of the coupling assembly had a 360° freedom of swivel capability. In checking the torque required to rotate the swivel, it was found that on a 7.5-ft arm the forces required were barely measurable. The 40-lb weight was then released electrically.

TABLE 70. RESULTS OF 33°, 40°, AND 45° TRAIL ANGLE RELEASES

Release No.	Mode	Vertical Angle of Sheave	Vertical Angle of Coupling	Remarks
1	Dual Solenoid	33°	36°	-
2	Dual Solenoid	33°	36°	-
3	Dual Solenoid	40°	40°	-
4	Dual Solenoid	45°	45°	-
5	Single Solenoid	33°	35°	-
6	Single Solenoid	33°	36°	-
7	Single Solenoid	40°	40°	-
8	Single Solenoid	45°	45°	Did not release
9	Dual Solenoid	45°	45°	O K
10	Single Solenoid	0°	0°	O K
11	Remote Mechanical	33°	35°	P-410 lb
12	Remote Mechanical	40°	40°	P-500 lb
13	Remote Mechanical	45°	45°	P-455 lb
The trail angle could not be increased beyond 45° due to the cable end fitting touching the pulley.				

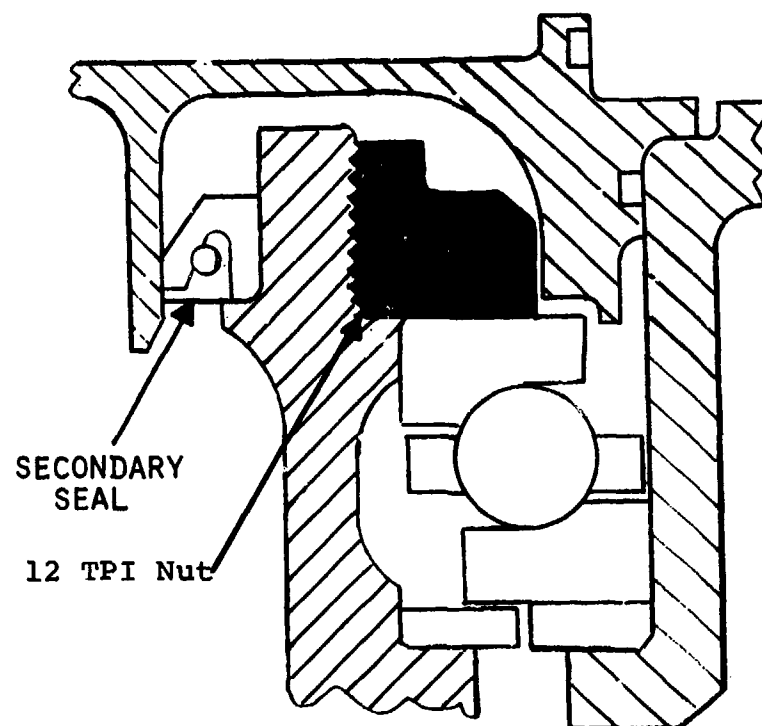


Limit Load Application - A test swivel and loading links were added to the test installation. It was again verified that the swivels were free to rotate 360°. Load was applied gradually and it was noted that the "lockout" light on the control box went off at 1,800-lb load. The load was held at the 10,000-lb level for a torque measurement and a load beam deflection reading. A mechanical force gauge was used at each end of a 7.5-ft length of wood to apply a "couple" which just overcame the frictional torque of the two swivels. This procedure was repeated for each 10,000-lb increment of applied load. Load was applied incrementally until a 110,000-lb load was reached. At this point, it was found that the oil was overheating in the hydraulic pump that supplied loading pressure, causing it to become less viscous. As a consequence, the oil was being forced past the pump seals, limiting the output of the pump. The load was removed in increments, and the test links and swivel were removed from the test frame so that another hole could be drilled in the hinged beam, 3 inches closer to the fulcrum. This gave the hydraulic cylinder a greater leverage for attainment of the required 140,000-lb load. Resuming the test, the 130,000-lb load was reached without incident. As the final increment of loading was being applied, a failure occurred when the dial read 11,500 lbs, which was equivalent to a 138,000-lb applied load. The coupling assembly was removed from the test rig and disassembled for inspection.

The investigation revealed that under load the swivel bearing retaining nut had rolled outward, reducing the number of threads in engagement with the housing assembly (see Figure 151). The remaining threads failed under the 138,000-pound load.

The nut was redesigned to Revision F of the drawing. The length of thread was increased to extend the nut inside the bearing to minimize any rolling action under load. A flange was provided across the top of the housing to increase the moment of inertia of the nut, and a lip was added to the nut inside the housing to support a seal and also to prevent any tendency for the sideplates to separate at the manufacturing split.

Original  
Configuration



Redesigned  
Configuration

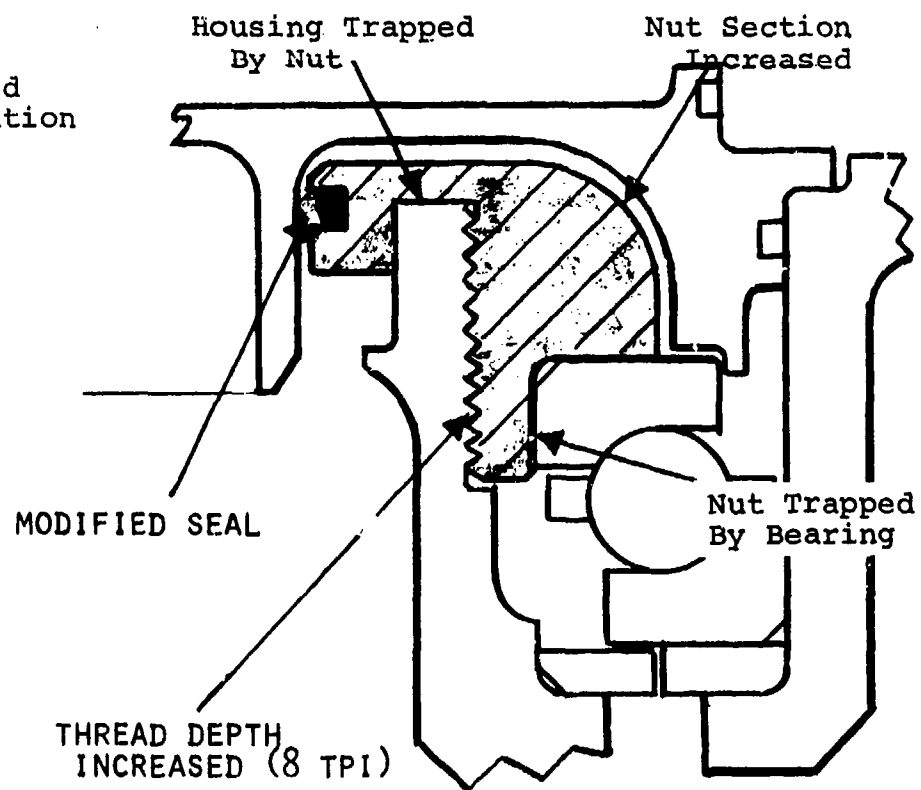


Figure 151. Coupling Retaining Nut Redesign.

The 8.625-12-3A left-hand thread on the housing was removed, and the housing was remachined to include a longer, coarser thread (8.4375-8N-3A) to match the new nut.

It was also found that the face of the internal lever (P/N 14267-1 Rev. 'E'), which was in contact with the face of the load beam, had deformed permanently.

To prevent a recurrence of the yielding of this face, the lever was redesigned. The angle of the face was changed from 2°5' to 1°45' to raise the theoretical line of reaction (at the interface of the lever and load beam) closer to the fulcrum of the internal lever, thus reducing the downward locking of the internal lever.

#### Limit Load Retest

The coupling device was reinstalled in the structural test frame ready for the retest. The redesigned housing, nut, and internal lever were incorporated in the coupling assembly.

Once again, load was applied in 10,000-lb increments up to the limit load of 140,000 lb. This limit load was held for 60 seconds. Load was then reduced in similar increments back to zero. As the load was reduced from the 140,000 lb to the 130,000- and 120,000-lb levels, a difficulty was encountered in measuring the torque with the 7.5-ft arm, and the torque readings at these two values were considered unreliable. The limit load test was then repeated using a 10-ft arm for measuring the torques.

At each loading increment, deflection readings were taken at a point on the load beam. Load deflection data and the torque on two swivels are shown in Figures 152 and 153.

It was also observed during this limit load test that, at the 70,000-lb load level, the "mode light" on the control box went out and remained out until the load was reduced to below 70,000 lb. Examination later showed the setting of the mode switch to be marginal. These two switches were readjusted and performed satisfactorily during subsequent acceptance load tests at 112,000 lb.

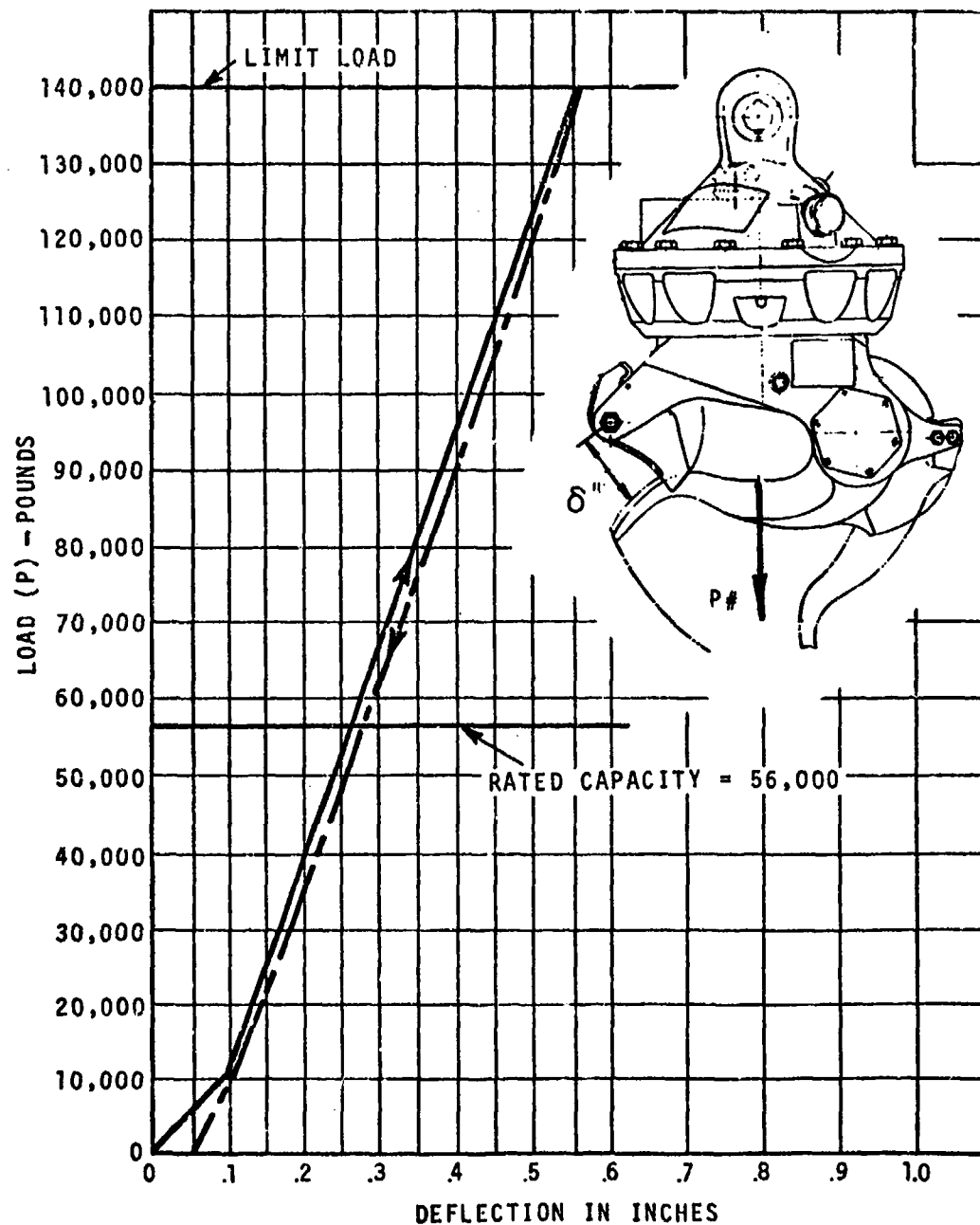


Figure 152. Load Deflection Curve.

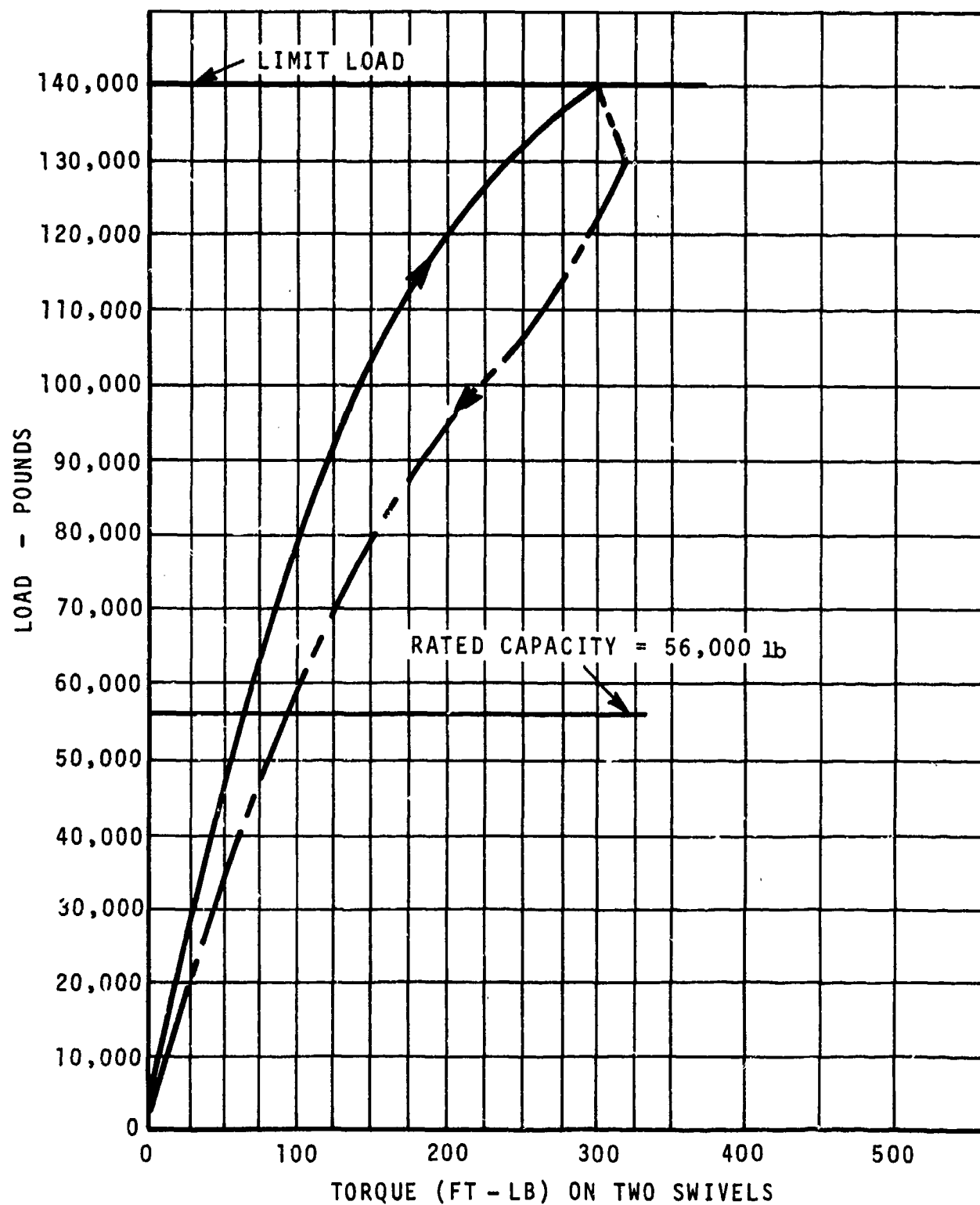


Figure 153. Torque on Two Swivels.

Functional Test - Immediately after the limit load test, the test coupling assembly (which was later designated S/N 4 after refurbishment) was subjected to a functional test. The coupling performed satisfactorily under both 56,000-pound and 112,000-pound acceptance loads.

Inspection After Limit Load Retest - After the functional test, the coupling device was disassembled and subjected to an inspection. The only visible signs of deformation were on the faces of the load beam and internal lever in the area of their contact. This deformation was so slight that it was considered to be acceptable.

### Environmental Tests

General - The coupling performance was evaluated by performing a series of normal operating functions during or after exposure to each of the categories of environment listed below. A total of approximately 500 coupling operations were performed during the course of the environmental tests.

- High temperature
- Low temperature
- Humidity
- Vibration
- Salt-fog
- Oil spray
- Dust
- Mechanical shock

### High Temperature Test

Procedure - The coupling was placed in a test chamber at room temperature long enough to check operations of the load beam at the 40-lb and 1,000-lb loads and to perform a visual examination. The chamber temperature was raised to 71°C (160°F) over a period of one hour and was maintained in this condition for 48 hours. While maintaining this condition, the coupling assembly was operated for the number of cycles shown below using the specified loads and release modes:

Load	40 lb		250 lb	1,000 lb	
Release Mode	Prim.	Sec.	Mech.	Prim.	Sec.
No. of Operations	50	20	5	15	10

After completing the required operations, the chamber temperature was adjusted to room ambient and maintained until the coupling temperature approached stabilization. Operation of the load beam was then checked using each release mode with 40-lb and 1,000-lb loads.

Results - The electrically operated release mode performed as required. A mechanical release force of 400 pounds was measured with the 250-pound load. A lockout load of 1,530 pounds was measured with an unlock load of 932 pounds. A visual examination of the coupling, made for deterioration of parts, uncovered no discrepancies.

#### Low Temperature Test

Procedure - The coupling remained in the same test setup as used for the high temperature test. The chamber was lowered to -54°C (-65°F) and maintained at that temperature until the test specimen approached stabilization. The coupling was then operated as shown below:

Load	40 lb		250 lb	1,000 lb	
Release Mode	Prim.	Sec.	Mech.	Prim.	Sec.
No. of Operations	50	20	5	15	10

After completing the required number of release attempts, the chamber temperature was returned to room ambient over a period of one hour. This condition was maintained until the test specimen approached stabilization. Operation of the load beam was next checked for each load and release mode indicated above. A visual examination of the coupling assembly was then made for deterioration of parts.

Results - The primary and secondary release modes operated satisfactorily under the 40-lb load, as did the primary release mode at a 1,000-lb load. However, the secondary release, single solenoid, would not completely release the load beam until the 1,000-lb load had been reduced to approximately 400 lb. During the ten operations required for the secondary release, the 400-lb load was substituted for the 1,000-lb load.

It was observed that if the load would not release, a second actuation of the solenoid would release the load.

At -65°F, the lockout mechanism was verified by using the mechanical release. With 2,000 lbs on the load beam, the hook would not release with a pull of over 700 lbs, as intended by the design.

Mechanical release of the 250-lb load required a cable force of approximately 640-lbs.

Visual examination of the assembly revealed that paint was peeling on the latching unit.

#### Special Low Temperature Test

Procedure - After modifications were made to lower the mechanical release force requirements, the unit was placed in the test chamber and subjected to a cold test of all release modes at -25°F.

Results - After stabilizing at -25°F, all release modes were checked and found to function properly. Also, the mechanical release force for a 500-lb load was determined to be 300 lb cable pull.

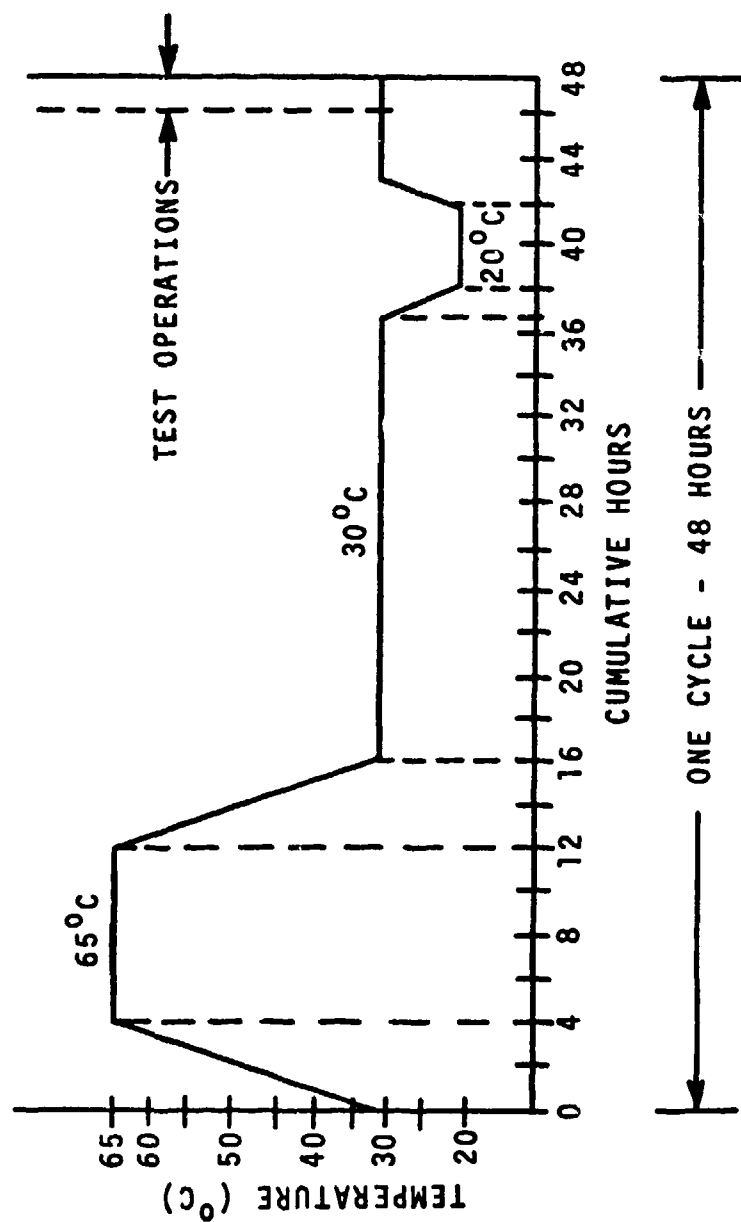
#### Humidity Test

Procedure - The test setup used for the high and low temperature testing was also used for humidity testing. Initially, the chamber was maintained at room temperature, with uncontrolled humidity, long enough to check operation of the load beam at the 40-lb and 1,000-lb loads for each release mode. The coupling was next conditioned at +54°C (149°F) for 24 hours, followed by another 24 hours at +23°C (73°F) and 50 percent relative humidity.

After completing the conditioning periods, the chamber temperature was raised to +30°C (86°F). A total of five 48-hour temperature and humidity cycles were then performed in accordance with Figure 154. During the last two hours of each humidity cycle, the following coupling releases were performed:

Load	40 lb			1000 lb	
Release Mode	Prim.	Sec.	Mech.	Prim.	Sec.
No. of Operations (per cycle)	13	6	1	3	2





- NOTES:
1. RELATIVE HUMIDITY SHALL REMAIN AT  $94 \pm 4\%$  AT ALL TIMES.
  2. RATE OF TEMPERATURE CHANGE BETWEEN  $30^{\circ}\text{C}$  AND  $65^{\circ}\text{C}$  SHALL NOT BE LESS THAN  $8^{\circ}\text{C}$  PER HOUR.
  3. TOLERANCE DURING TEMPERATURE CHANGE SHALL NOT BE GREATER THAN  $\pm 3^{\circ}\text{C}$ .

Figure 154. 48-Hour Humidity Cycle.

After completion of the fifth cycle, the chamber was adjusted to 23°C (73°F) and 50 percent relative humidity, and maintained for a period of 24 hours. Operation of the load beam was then checked for each load and release mode indicated above. A visual examination was then made of the coupling.

Results - After the second 48-hour humidity cycle, the coupling assembly electrical release would not function. The manual and mechanical releases were satisfactory. The test was stopped and the assembly analyzed. The cause of failure was a loose wire on the terminal strip inside the bell housing. Lock washers were added to all terminals. When released under a 1000-lb load in the fixture, the coupling assembly was exposed to hammer-type shocks which apparently tended to loosen the screw-type terminals. The problem was not related to humidity exposure. The remaining portion of the test was performed satisfactorily. The post-test inspection did not reveal any discrepancies.

#### Vibration Tests

Procedure - The coupling assembly was subjected to vibration testing with the vibratory force applied through the equalizer bar assembly. The coupling was unloaded throughout the test. Sinusoidal vibration sweeps were conducted at the input levels shown below in the vertical, horizontal, and transverse directions, to search for resonances using a strobe light. Each sweep was logarithmic from 5 Hz to 500 Hz and back to 5 Hz over a period of 5 minutes.

<u>Frequency Hz</u>	<u>Vibration Level</u>
5 to 20	0.10-inch double amplitude
20 to 33	+2g
33 to 52	0.036-inch double amplitude
52 to 500	+5g

The coupling was monitored electrically during the tests for analysis information in the event the release mechanism activated without an intentional signal. No unintentional releases occurred.

Three-hour dwell tests were performed in each of the three axes following the resonance searches. Since no resonances were observed, the entire three hours was sinusoidal cycling.

After completion of the vibration testing in all three axes, the coupling was submitted to the following operations:

Load	40 lb			1000 lb	
Release Mode	Prim.	Sec.	Mech.	Prim.	Sec.
No. of Operations	30	10	5	10	5

Results - During the first axis (vertical input), two of the three green lights on the coupling failed. Shortly after that, the third warning light also failed. No other evidence of damage was observed, and all release mode operations were performed satisfactorily.

The light failures were traced to an unsupported bulb filament in the original C-2R type bulbs and a supply voltage during the environment tests which exceeded the bulb design voltage. Lamp life is a function of the voltage to the tenth power. Bulbs of the C-2V type, which have supported filaments and a higher design voltage, were substituted to provide a greater tolerance to vibration and overvoltage conditions.

#### Salt Fog Tests

Procedure - The test consisted of 48 hours of exposure to a 5% salt fog in accordance with the requirements of MIL-STD-810B, Method 509, Procedure I. After completion of the test the coupling was removed from the chamber and submitted to the following release mode operations:

Load	40 lb			1000 lb	
Release Mode	Prim.	Sec.	Mech.	Prim.	Sec.
No. of Operations	13	6	1	3	2

Results - There was no evidence of corrosion on the unit following this test. The assembly was placed in the test fixture for application of the required release modes and loads; all operations were completed satisfactorily.

#### Oil Spray Tests

Procedure This test was performed immediately following the salt fog test. The coupling was cleaned externally to make certain that any salt residue had been removed. The unit was next sprayed with a fine mist of oil conforming to MIL-L-7808, covering the entire surface. The assembly then remained at laboratory conditions for 48 hours. After this period the following release mode operations were performed:

Load	40 lb			1000 lb	
Release Mode	Prim.	Sec.	Mech.	Prim.	Sec.
No. of Operations	1	1	1	1	1

Results - The required operations were satisfactorily performed using the various release modes.

#### Dust Test

Procedure - The dust test was performed immediately following completion of the oil spray test with no intermediate cleaning. The assembly was placed in the dust chamber where the temperature was then set at +23°C (73°F) with a relative humidity just under 22%. The air velocity was adjusted to 1750 fpm and the dust feeder was set at 0.3 grams per cubic foot. These conditions were maintained for a period of six hours. The coupling was then removed from the chamber and submitted to the following release mode operations:

Load	40 lb			1000 lb	
Release Mode	Prim.	Sec.	Mech.	Prim.	Sec.
No. of Operations	19	10	1	10	5

Immediately after completing the required operations, the coupling assembly was replaced in the dust chamber. With the dust feed "off" and the air velocity controlled at 300 fpm, the chamber temperature was raised to +63°C (145°F) with a relative humidity maintained at just under 10%. This condition was maintained for approximately 16 hours.

After the 16 hour period, the above release mode operations were repeated.

Results - All release operations after the six-hour period and after the sixteen-hour period were performed satisfactorily.

#### Mechanical Shock Test

Procedure - The mechanical shock test was performed by physically dropping the coupling assembly from the required height onto a 2-inch-thick plywood sheet resting on a concrete floor in accordance with MIL-STD-810B, Method 516.1, Procedure II. The assembly was subjected to two drops in each of the five orientations listed in Table 71. Following each pair of drops, the specified release mode operations were performed.

TABLE 71. MECHANICAL SHOCK TEST.						
	Load Beam Weight (lb)	40	40	40	1,000	1,000
	Mode of Release	Mech.	Prim.	Sec.	Prim.	Sec.
Drop						
Coupling Orientation	Front	1	1	1	1	1
	Left Side	1	1	1	1	1
	Right Side	1	1	1	1	1
	Back Side	1	1	1	1	1
	Bottom of Load Beam	1	1	1	1	1
TOTAL		5	5	5	5	5 25

Results - All operations were performed satisfactorily. Post-test inspection of the coupling revealed that the manual release knob was bent slightly, however, functioning of the knob was not impaired.

#### Maximum Static Load Test

A failure of coupling serial number 1 occurred following completion of maximum static load testing on the integrated test rig. The suspension was in the single-point configuration with the lower coupling attached to a hard-point set in the concrete rig base. The coupling housing side-plate lugs failed at an indicated tension of 146,000 lb, which was 6,000 lb over the maximum required load. Figure 155 shows the failed coupling.

Failure occurred at the tension critical section of the load beam pivot lugs extending from the lower housing, which is fabricated from 7075-T651 aluminum alloy plate. It was found that the heat treat cycle for the failed parts did not include a solution treat after rough machining and prior to aging to the -T73 condition. However, in addition, the investigation uncovered an unconservative assumption in the stress analysis of the lug area and a lack of sufficient latitude in the positioning of the load shackle or donut on the load beam.



Figure 155 Failed Cargo Coupling.



Figure 155 Failed Cargo Coupling.

The coupling design has been modified to increase the ultimate load capability of the pivot lugs as shown in Figure 156 with the drawing call-out for the heat treat clarified to prevent misinterpretation. The load beam shape was revised as shown in Figure 156 to provide more positive positioning of the shackle or donut.



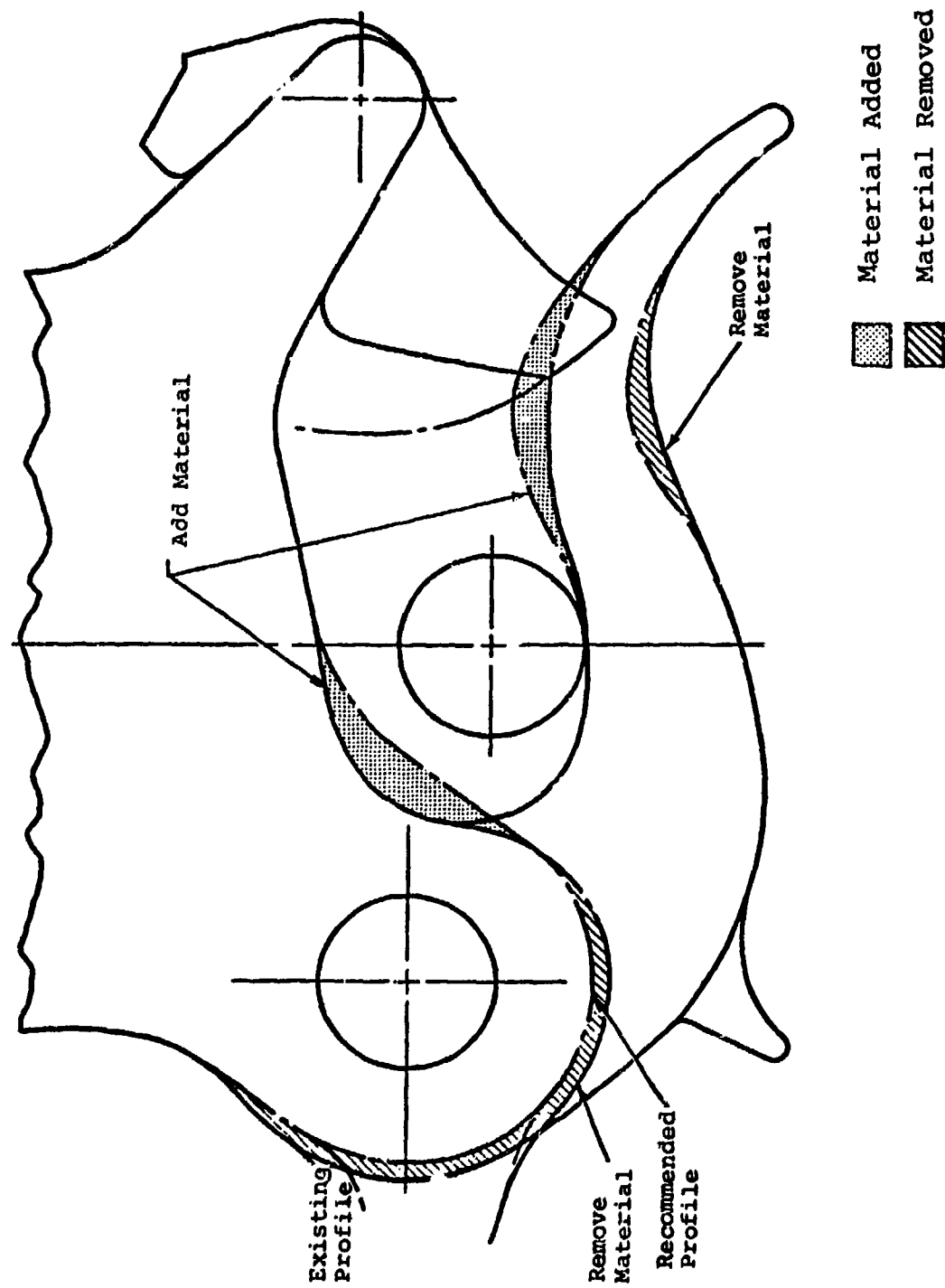


Figure 156. Coupling Modifications.

## SIGNAL CONDUCTOR REELING MECHANISM

### DESIGN SUPPORT TESTS

The reeling mechanism was simulated by a 4.4-inch-diameter turbine wheel. A simple 8-inch-diameter take-up drum was fabricated and driven through a gear ratio of 16.3:1. A length of quarter-inch cable (approximately 100 feet) was wound on the drum. The test setup is shown in Figure 157.

For the first test, the cable was run through an overhead pulley. The turbine inlet air pressure was then set at a given value and measurements of cable tension were taken for three modes of operation:

1. Reeling in at 120 ft/min
2. Static conditions
3. Reeling out at 120 ft/min

This was done for a variety of inlet air pressures. The results of this test are shown in Figure 158.

For the second test, the overhead pulley was removed and the cable was pulled in the horizontal direction. The same data was taken as in the previous test. Figure 159 shows the results of this test.

In the third test, the gearbox was drained of all excess oil and the same tests were performed. The results of this test are plotted in Figure 160.

The relatively wide variation in force between forward and reverse at a given air pressure was due in part to the friction of the lower head pulley. The amount of energy required to bend the cable around this pulley also contributed to the nonuniform cable tension. These two factors were responsible for over half the "dead band" at stable conditions.

The test unit has a high coefficient of static friction. The unit employed two face-type seals, one on the output shaft and one on the high-speed shaft. The friction caused by these two seals was also responsible for part of the "dead band." Figure 161 shows the data corrected for this friction.

Draining the oil from the gearbox helped to decrease the variation in force during dynamic operation.

The results show the availability of a fairly constant torque over the range of operation.

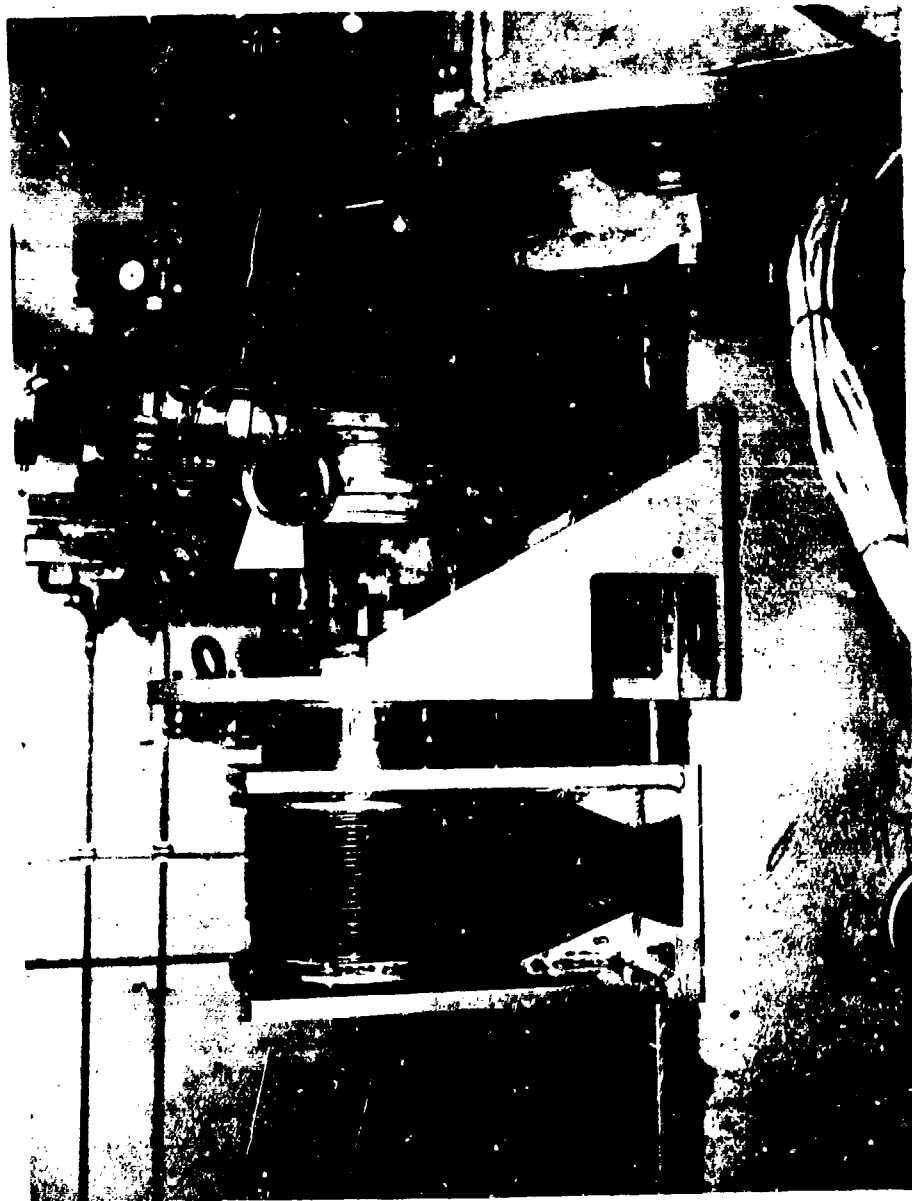


Figure 157. Reeling Mechanism Test Stand.

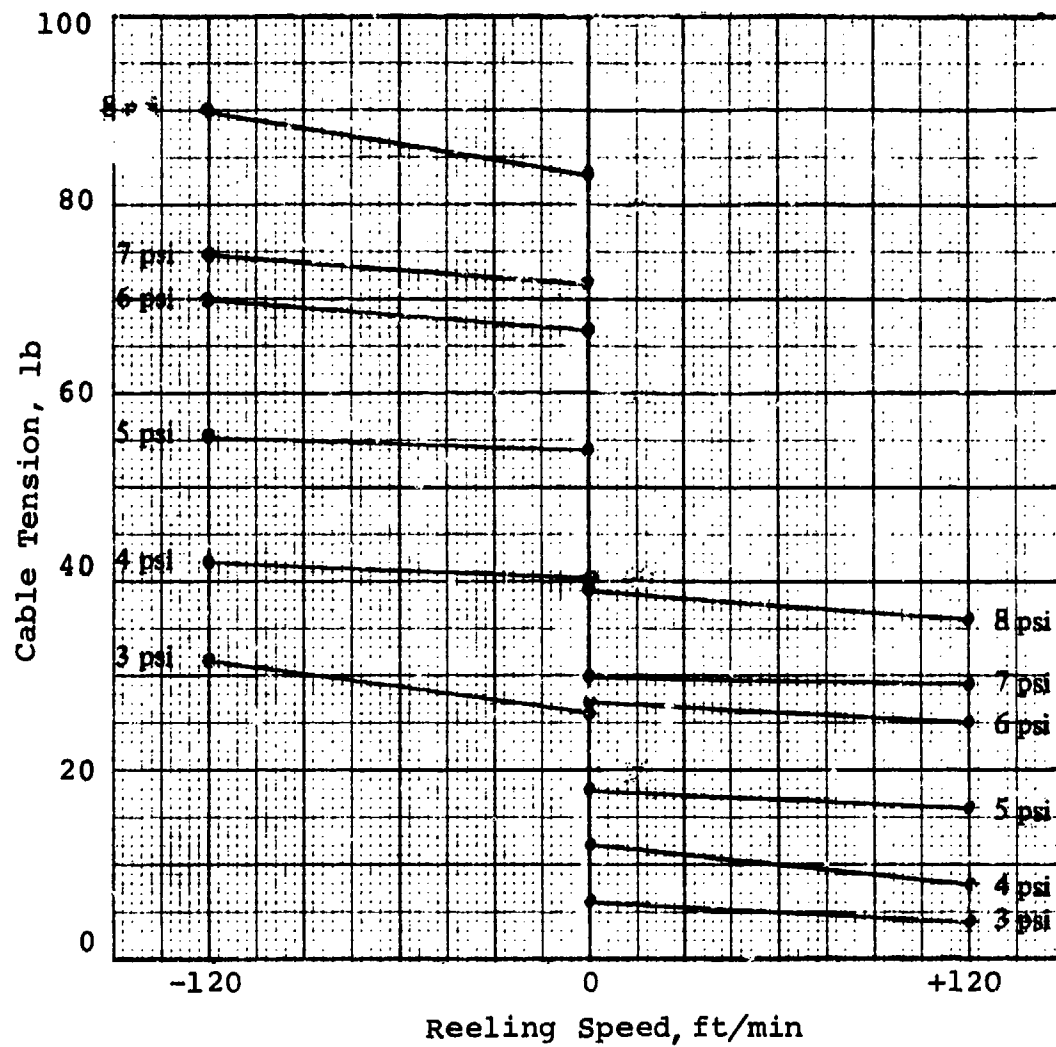


Figure 158. Reeling Mechanism Response with Overhead Pulley.

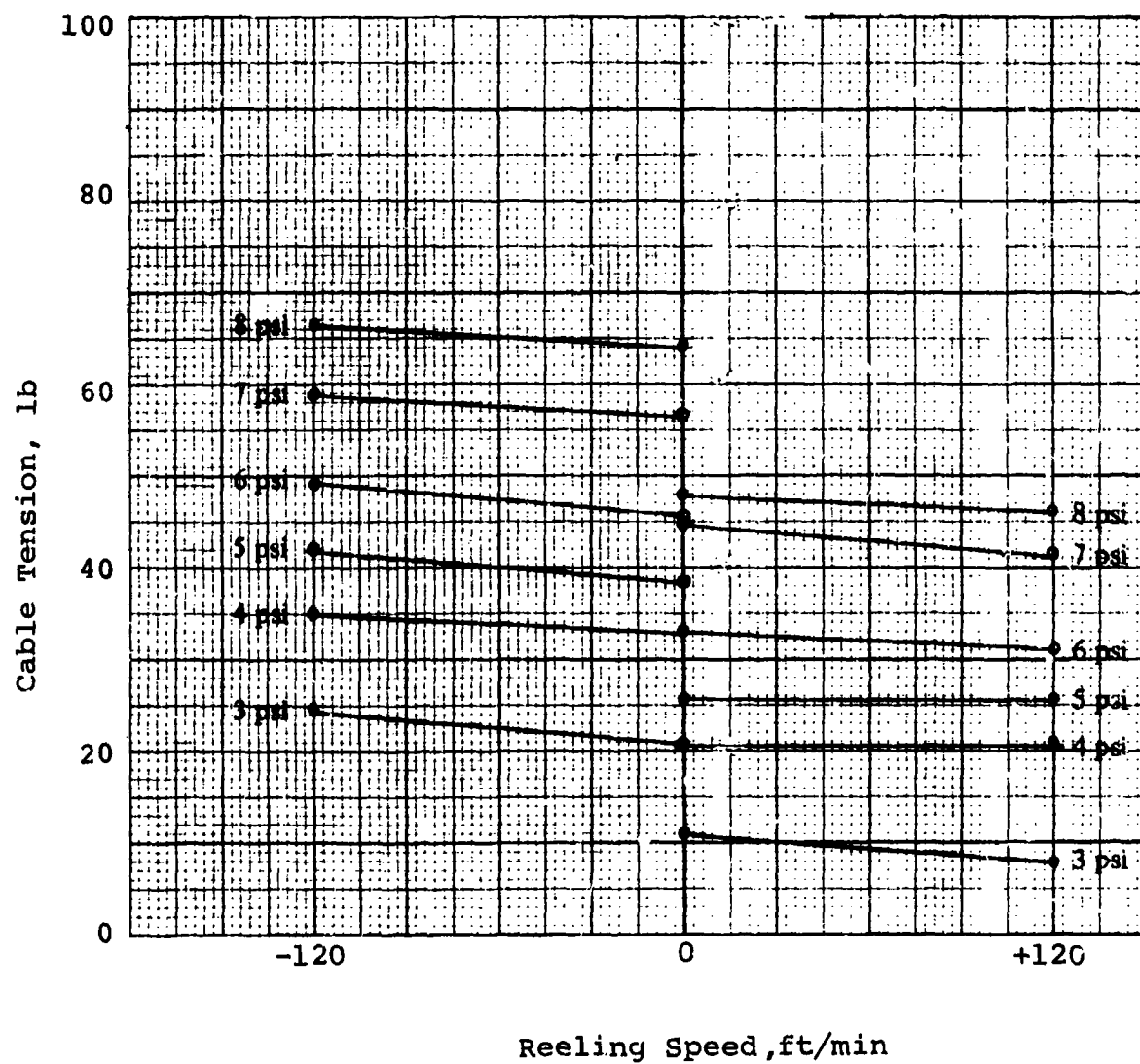


Figure 159. Reeling Mechanism Response without Overhead Pulley.

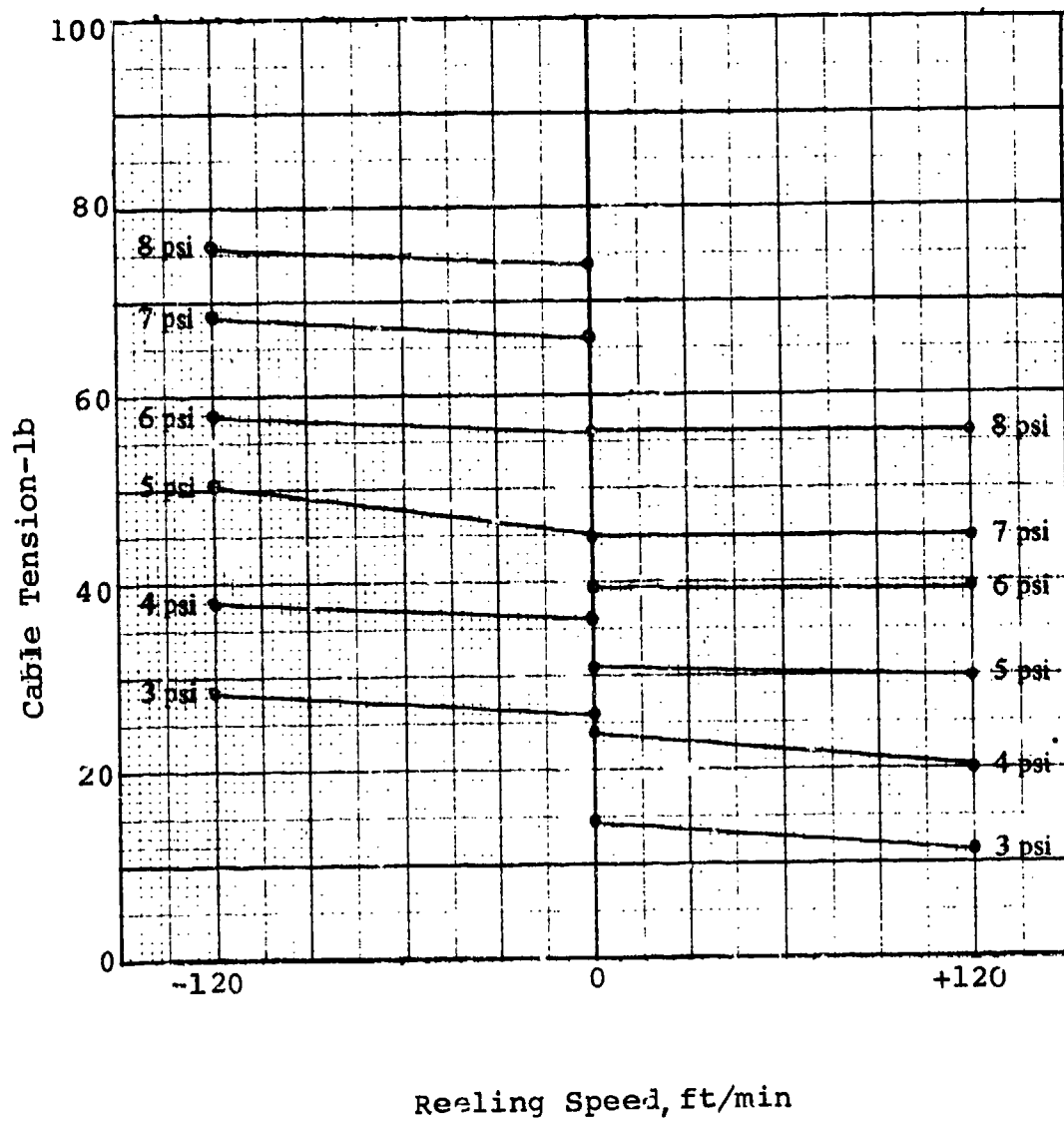


Figure 160. Reeling Mechanism Response without Excess Oil.

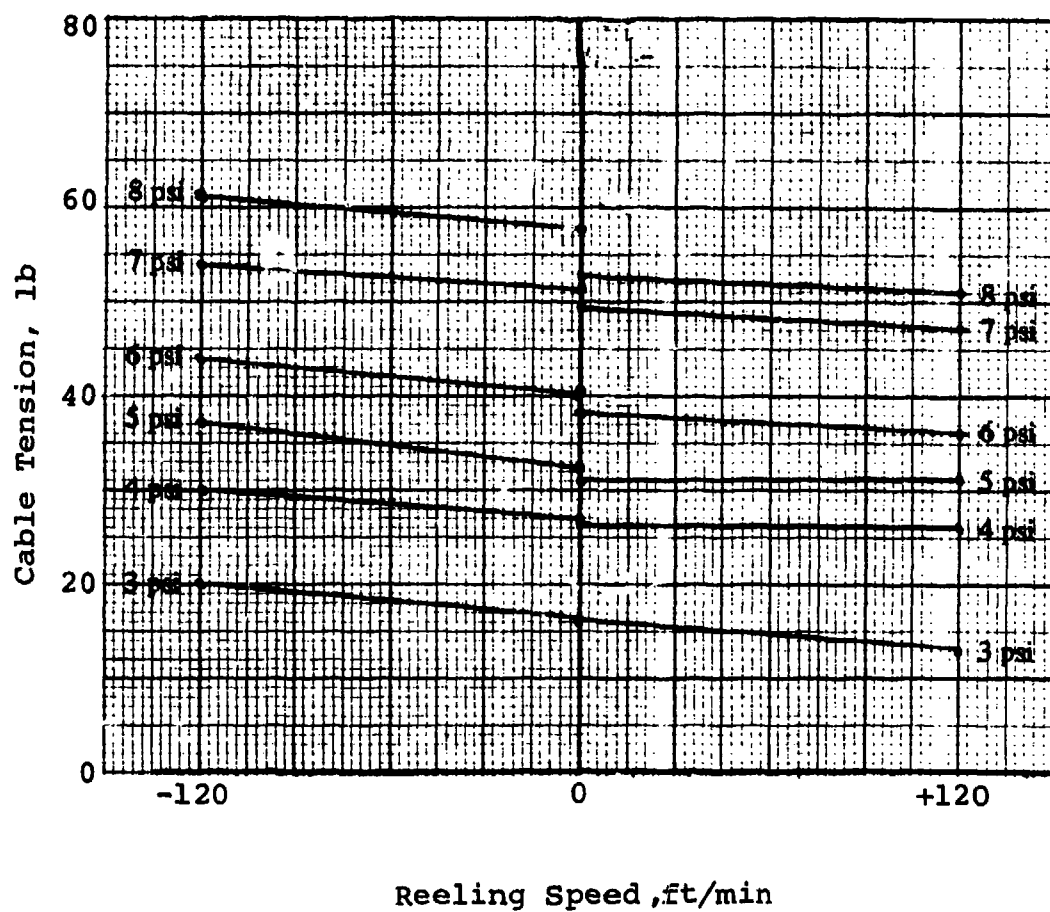


Figure 161. Reeling Mechanism Response Corrected for Static Friction.

## DESIGN DEVELOPMENT TESTS

### Test Item

The HLH signal conductor reeling mechanism consists of a turbine wheel driving a takeup drum through a 3-mesh, spur gear train with a reduction ratio of 63.4:1. The turbine is equipped with three nozzles. One nozzle is active at all times (the constant tension nozzle), while the other two can be activated with a solenoid on-off valve. The activation of the two additional nozzles roughly triples the flow of air to the turbine to increase the cable tension for mechanical hook release.

The mechanism is equipped with a splined shaft between the gearbox and takeup drum which is designed to shear during cargo jettison. Thus, a free-falling load will not accelerate the turbine wheel, gears, and bearings to a destructive speed. The turbine is aerodynamically limited to a safe runaway speed in the event that the main cables are cut and the spline is sheared while the airflow to the turbine continues.

### Shear Section Test

Objective - The purpose of this test was to demonstrate the operation of the splined shaft between the gearbox and takeup drum which is designed to shear during cargo jettison.

Test Procedure - The shaft was placed in a Tinius-Olsen torsion testing machine and a load was applied until the shaft sheared.

Results - The splined shaft tested in the Tinius-Olsen torsion tester sheared at 2050 in-lbs, which is equal to 565 lbs of tension on the external conductor (middle cable layer). This is approximately 1.6 times the tension necessary for hook release (350 lb in steady state condition), and above the 1.5 times margin-of-safety factor recommended in the design specification. In the three tests where shear occurred (510, 550 and 550 lb), the tension level of the cable was near or above the margin-of-safety factor.

No damage was suffered by the unit, and the operation of the mechanism was not impaired.



### Runaway Speed Test

Objective - The purpose of this test was to insure that, in the event the signal conductor is severed, the runaway speed of the turbine wheel, the input shaft, and the gearing will be low enough so as not to cause damage to the reeling drum, the gearing, and the turbine wheel.

Test Procedure - The reeling mechanism was placed in the test stand, and the spline shaft was removed to disconnect the reeling drum from the turbine wheel.

Air was supplied to the tension air duct at various temperatures and pressures. At each pressure difference, the turbine was allowed to accelerate to runaway speed.

Results - The entire test was run without any throttling orifice in the turbine nozzle air supply line. This represents a 15% increase in the air pressure at the nozzle. Therefore the test was run in increments up to a limit of 40 psig, which is equivalent to 46 psig with the orifice installed. The turbine runaway speed for all conditions was well below the design burst speed of 100,000 rpm, as shown in Table 72.

### Stalled Operation Test

Objective - The purpose of this test was to establish that the external conductor tension was within the 65- to 95-lb range with the turbine stalled using one nozzle. Additionally, the lubricating oil and tape cavity temperatures were measured to insure that no damage would be incurred as a result of stalled operation.

Test Procedure - The reeling mechanism was placed on the test stand, and the takeup drum of the test stand was secured to maintain zero speed during testing.

During the test, the inlet air pressure was set at either 37 or 45 psig. The cable was varied from one to three layers on the reel. The inlet air temperatures were varied as follows: 200°F, 260°F, 330°F, 414°F, and 460°F. All combinations of the above temperatures, layers, and pressures were run.

Results - During the entire test, the oil temperature in the gearbox and the air temperature in the tape cavity remained within the specified limits. Cable tensions measured at the various temperatures, cable layers, and pressures are shown in Table 73.

TABLE 72. SIGNAL CONDUCTOR REEL RUNAWAY SPEEDS.				
System Pressure (PSIG) (Without Orifice)	Turbine Inlet Temp (°F)	Turbine Runaway Speed (RPM)	Calculated Values	
			Turbine Inlet Temp (°R)	Runaway Speed at 874°R
10	78	4,500	538	5,735
14	78	15,000	538	19,118
20	78	22,400	538	28,550
25	78	28,300	538	36,070
30	78	30,800	538	39,256
11	257	2,000	717	2,208
14	259	4,000	719	4,410
19.5	261	24,000	721	26,424
25	265	28,900	725	31,731
29	268	31,600	728	34,623
35.5	276	37,000	736	40,319
39	276	38,200	736	41,627

TABLE 73. MEASURED CABLE TENSIONS - STALLED OPERATION.								
Inlet Air Temp °F	Actual Temp	Inlet Air Press. PSIG	No. Layers on SCRM	Cable Tension (lb)				Corrected Cable Tension* (lb)
				Data Pt 1	Data Pt 2	Data Pt 3	Ave	
200	-	37	3	-	-	-	-	-
	186		2	70	67	-	68.5	68.50
	196		1	80	80	-	80.	77.36
	196	45	1	90	100	-	95.	91.87
	186		2	85	83	-	84.	84.
	-		3	-	-	-	-	-
260	276	37	3	70	70	63	67.67	70.06
	246		2	73	70	70	71.	71.
	276		1	80	80	85	81.67	78.97
	276	45	1	103	90	100	97.67	94.44
	246		2	83	90	90	87.67	87.67
	276		3	80	85	87	84.	86.97
330	339	37	3	80	70	-	75.	76.65
	333		2	70	70	73	71.	71.
	322		1	75	75	75	75.	72.53
	322	45	1	97	95	100	97.33	94.12
	333		2	87	83	85	85.	85.
	339		3	80	85	90	85.	88.
414	408	37	3	60	75	75	70	72.47
	403		2	75	80	78	77.67	77.67
	414		1	88	90	83	87.	84.13
	414	45	1	97	99	102	99.3	96.
	403		2	90	90	90	90.	90.
	408		3	80	80	90	83.33	86.27
460	460	37	3	65	65	68	66.	68.33
	470		2	80	80	80	80.	80.
	455		1	83	78	85	82.	79.29
	455	45	1	100	95	90	95.	91.87
	470		2	90	88	90	89.33	89.33
	460		3	85	85	85	85.	88.
*One- and three-layer tension values are adjusted to produce a two-layer average tension value.								

### Normal Duty Cycle Test

Objective - To demonstrate the proper operation of the reeling mechanism and the maintenance of positive cable tensions, using several inlet temperature conditions and two inlet air pressures during cable speed and reel direction cycles, simulating normal load acquisition and deposition.

Test Procedure - The unit was setup on the test stand and run according to the requirements listed below:

1. The auxiliary takeup drum was to be driven so as to maintain the cable speeds shown in Table 74.
2. The test was to be run for each pressure and temperature condition shown in Table 75.
3. The cable acceleration was to be less than 1 ft/sec<sup>2</sup> in either direction.

TABLE 74. DRIVING CONDITIONS - NORMAL DUTY CYCLE TEST.		
Conductor Cable Speed (ft/min)	Hoisting/Reversing	Time
120	R	50 seconds
60	H	100 seconds
60	R	100 seconds
120	H	50 seconds
0	-	10.0 minutes

TABLE 75. PRESSURE AND TEMPERATURE CONDITIONS -NORMAL DUTY CYCLE TEST.	
Inlet Air Pressure (psig)	Inlet Air Temperature (°F)
37	200
45	200
37	260
45	260
37	330
45	330
37	414
45	414
37	460
45	460

## Results

The test was run without incident, and no situations occurred to adversely affect the unit or its operation. Cable tension was maintained on the external conductor throughout the sequences as shown in Table 76.

Both the temperature in the gearbox and the air temperature in the tape cavity remained within the specified limits.

TABLE 76. NORMAL DUTY CYCLES.

Inlet Air Temp °F	Actual Temp	Inlet Air Press. PSIG	Cable Speed ft/min	Hoisting/Reversing	Cable* Tension lb
200	186	45	120	R	110
	192		60	H	70
	204		60	R	110
	186		120	H	60
260	262	37	120	R	90
	251		60	H	55
	246		60	R	85
	262		120	H	50
	235	45	120	R	110
	229		60	H	70
	240		60	R	110
	229		120	H	65
330	344	37	120	R	90
	344		60	H	60
	344		60	R	90
	344		120	H	50
	333	45	120	R	110
	333		60	H	70
	338		60	R	107
	333		120	H	65
414	383	37	120	R	95
	380		60	H	60
	377		60	R	90
	385		120	H	55
	366	45	120	R	110
	376		60	H	75
	387		60	R	110
	372		120	H	70

TABLE 76. Continued					
Inlet Air Temp °F	Actual Temp	Inlet Air Press. PSIG	Cable Speed ft/min	Hoisting/ Reversing	Cable* Tension lb
460	425	37	120	R	95
	425		60	H	60
	418		60	R	93
	425		120	H	57
	438	45	120	R	110
	436		60	H	75
	431		60	R	110
	445		120	H	70
*2nd layer average.					

#### Fleet Angle Test

##### Objective

To demonstrate that reeling mechanism performance was not significantly affected by a 30° fleet angle.

##### Test Procedure

The normal duty cycle test, discussed previously, was repeated with the reeling mechanism rotated 30° from the direction of pu l of the test drum. The mechanism and conductor cable were then subjected to the speeds, temperatures, and pressures specified in Table 76.

##### Results

No malfunctions occurred during the fleet angle test nor was the operation of the reeling mechanism impaired.

#### Transient Operation Test

##### Objective

To evaluate the capability of the reeling mechanism to maintain tension on the signal conductor during load accelerations from zero to 120 feet per minute in both the hoisting and lowering directions.

### Test Procedure

The test unit was mounted on the test stand. Air at a temperature of 414°F and a pressure of 45 psig was applied to the normal tension inlet duct of the unit. The external conductor was then accelerated to a speed of 120 fpm in times varying between 0.6 second and 2.0 seconds. Cable tensions were measured during the acceleration and deceleration in both the hoisting and lowering directions.

### Results

During the transient operation test no damage was suffered by the reeling mechanism nor was the operation impaired. For all rates of acceleration, cable tension was maintained to eliminate slack. Maximum tension observed was 277 lb, as shown in Table 77.

### Hook Release Test

#### Objective

The purpose of this test was to demonstrate that the reeling mechanism would impart an adequate pull in the conductor to release the hook (the alternate mode of hook release).

#### Test Procedure

The reeling mechanism was mounted on the test stand and the test drum was locked in position for zero speed during the test.

Two air pressures (37 and 45 psig) were supplied to the inlets of the one main nozzle and the two auxiliary nozzles. Temperatures used were 200°, 260°, 330°, 414°, and 460°F. The above pressures and temperatures were applied in all combinations and the number of layers of cable on the reeling mechanism drum was varied between one and three. Each test run was for a duration of five seconds.

#### Results

Table 78 shows the tension produced when the hook release tension duct valve was opened. The values for one and three layers of cable were corrected to an average of two layers. The tests showed that the average cable tension was 333.2 lb as calculated during steady-state conditions. Spiking, which occurred at the beginning of each five-second run, was sufficient in some cases to



TABLE 77. TEST DATA FOR TRANSIENT OPERATION.

Inlet Air Temp (°F)	Actual Temp (°F)	Actual Press (PSIG)	Speed (ft/min)	Hoisting/ Reversing	Accel Time (sec)	Cable Tension (lb)		Decel Time (sec)
						Accel	Decel	
414	398	45	120	R	.6	277	148	.8
414	398	45	120	R	.6	268	155	.7
414	398	45	120	R	.7	265	150	.7
414	398	45	120	H	.8	155	243	.7
414	398	45	120	H	.9	163	243	.7
414	398	45	120	H	.9	165	232	.8
414	398	45	120	H	.8	100	155	.8
414	401	45	120	H	.7	95	160	.8
414	403	45	120	R	.9	200	95	.9
414	403	45	120	R	.9	200	108	.9
414	403	45	120	R	.8	218	105	1.0
414	403	45	120	H	.8	95	150	.9
414	403	45	120	H	.8	103	150	.9
414	405	45	120	H	.7	95	145	1.0
414	406	45	120	R	1.2	148	88	1.2
414	406	45	120	R	1.2	167	85	1.3
414	408	45	120	R	1.2	165	88	1.3
414	408	45	120	R	1.2	182	92	1.3
414	408	45	120	H	1.1	75	123	1.3
414	408	45	120	H	1.1	78	113	1.2
414	408	45	120	H	1.1	72	118	1.2
414	408	45	120	R	1.6	138	84	1.6
414	408	45	120	R	1.6	145	82	1.6
414	408	45	120	R	1.6	170	90	1.7
414	408	45	120	H	1.5	75	110	1.6
414	408	45	120	H	1.6	80	105	1.5
414	408	45	120	H	1.4	72	98	1.4
414	408	45	120	R	1.8	127	82	1.9
414	408	45	120	R	1.9	137	96	2.0
414	408	45	120	R	1.9	145	88	1.9
414	408	45	120	H	1.8	75	103	1.9
414	408	45	120	H	1.9	75	98	2.0
414	408	45	120	H	1.9	73	90	2.1
414	408	45	120	R	.7	228	148	.8
414	408	45	120	R	.7	250	145	.7
414	408	45	120	R	.6	250	153	.7
414	408	45	120	R	.6	266	153	.7
414	408	45	120	H	.6	170	225	.7
414	408	45	120	H	.8	150	228	.8
414	408	45	120	H	.8	155	207	.7
414	408	45	120	H	.7	138	208	.7

TABLE 78. RESULTS OF HOOK RELEASE TEST.								
Inlet Air Temp °F	Actual Temp	Inlet Air Press PSIG	No. Layers on SCRM	Cable Tension (lb)				Corrected Cable Tension* (lb)
				Data Pt 1	Data Pt 2	Data Pt 3	Avg.	
200	192	37	3	280	280	270	276.66	286.43
	210		2	310	310	330	316.66	316.66
	229		1	380	360	330	356.67	344.90
	192	45	3	325	325	325	325.00	336.47
	216		2	352	350	330	344.00	344.00
	229		1	350	390	380	373.33	361.01
260	298	37	3	290	280	275	281.66	291.60
	251		2	335	310	325	323.33	323.33
	287		1	385	370	350	368.33	356.20
	287	45	3	340	360	340	346.66	358.90
	251		2	340	400	375	371.66	371.66
	276		1	390	400	400	396.67	383.58
330	355	37	3	280	280	275	278.33	288.66
	344		2	255	280	-	267.50	267.50
	344		1	350	355	375	360.00	348.12
	344	5	3	353	370	350	358.33	370.98
	-		2	-	-	-	-	-
	344		1	390	390	387	389.00	376.16
414	418	37	3	280	275	275	277.00	286.78
	408		2	310	310	310	310.00	310.00
	418		1	330	325	380	345.00	333.60
	428	45	3	320	300	315	311.67	322.67
	418		2	340	335	335	336.67	336.67
	430		1	360	420	410	396.60	383.50
460	490	37	3	265	275	275	272.00	281.60
	480		2	270	330	305	301.67	301.67
	470		1	305	350	340	331.60	320.08
	500	45	3	330	350	340	340.00	352.00
	480		2	350	370	360	360.00	350.00
	485		1	370	370	375	371.67	359.40
*One and three layer tension values are adjusted to produce a two layer average tension value.								

have the hook release tension approach that of spline shear. This was attributed to the rate at which the hook release duct valve was opened. This rate should be reduced to decrease the spike to a point where the spline shear margin-of-safety approaches 1.5. Maximum hook release tension, transient or steady state, should be approximately 400 lb.

### Endurance Test

#### Objective

The purpose of this test was to establish that the unit would operate satisfactorily during a series of one hour tests under specified operating conditions.

#### Test Procedure

The operating cycle was as shown in Table 79.

TABLE 79. ENDURANCE TEST OPERATING CYCLE.		
Conductor Cable Speed (ft/min)	Time (sec)	Hoisting/Reversing
120	50	R
60	100	H
60	100	R
120	50	H

Distribution of time during the one-hour test was as shown in Table 80.

TABLE 80. TIME ALLOCATION - ENDURANCE TEST.	
Activity	Time (minutes)
Operating Cycle (per Table 79)	5
Stalled Operation	10
Operating Cycle	5
Stalled Operation	10
Operating Cycle	5
Stalled Operation	25

The applied air pressure was 45 psig, and the applied air temperature was between 300° and 400°F. The one hour test was repeated five times.

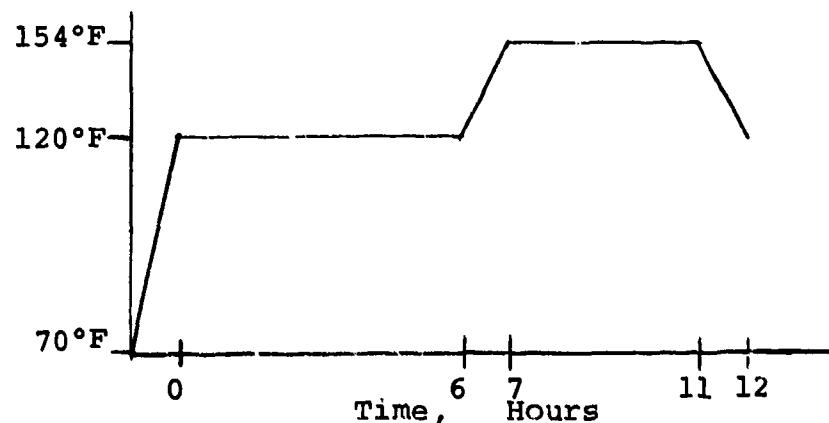
### Results

During testing no malfunctions occurred that were detrimental to the operation of the unit. Temperatures remained normal for the test and were within specifications.

## Environmental Tests

### High Temperature Test

Test Procedure - The test item was placed in a test chamber in accordance with MIL-STD-810B, Section 3, Paragraph 3.2.2, and subjected to the temperature/time cycle shown below:

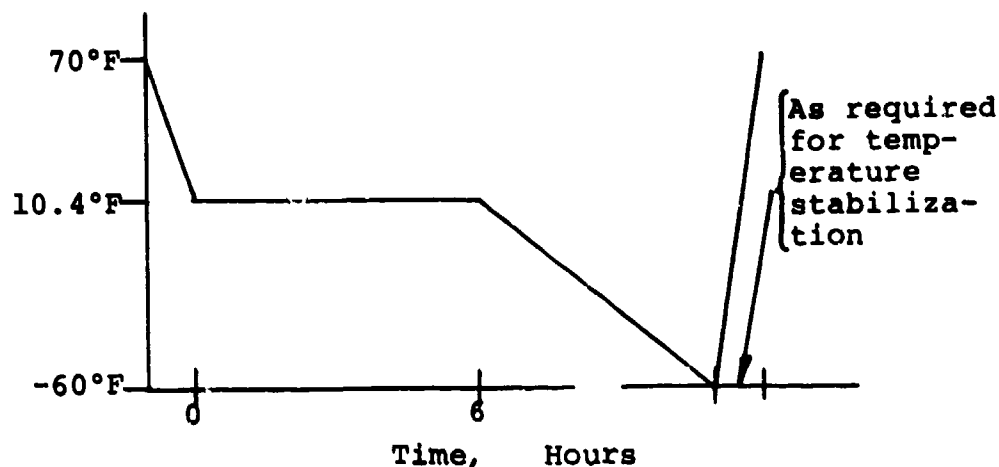


The cycle from time zero to 12 hours was then repeated two additional times. The unit was then cooled to laboratory ambient conditions and run through an operational test.

Results - The reeling mechanism was not damaged and no adverse conditions resulted from the high temperature test.

### Cold Temperature Test

Test Procedure - The test item was placed in a test chamber in accordance with MIL-STD-810B, Section 3, Paragraph 3.2.2, and subjected to the temperature/time cycle shown below:



Results - The reeling mechanism was not damaged and no adverse conditions resulted from the low temperature test.

#### Salt Fog Test

Test Procedure - The test item was cleaned and prepared in accordance with MIL-STD-810B, Section 509, Paragraph 3.1.5, and placed in the test chamber in accordance with Paragraph 3.2.2 of Section 3 of the same document. The test item was then exposed to salt fog for a period of 48 hours with the salt solution and internal chamber temperature maintained as specified in MIL-STD-810B, Method 509. The unit was removed, visually inspected and subjected to an operational test.

Results - Upon examination of the unit, it was noted that the two level wind drive sprockets had started to rust as a result of the test. These two items are off-the-shelf items that had no protective coating. Due to this rusting, a change was made for both sprockets, and they will be supplied with a dry film lubricant. Corrosion was also noted on the cable drum in an area where the anodizing had been worn by the braided cable. No other visible damage was sustained by the unit, and its operation was not impaired by the test.

#### Humidity Test

##### Test Procedure

1. The test item was placed in the test chamber in accordance with MIL-STD-810B, Section 3, Paragraph 3.2.2. Prior to starting the test, the internal chamber was at standard ambient temperature with uncontrolled humidity.

2. The internal chamber temperature was then gradually raised to 71°C (160°F), and the relative humidity was raised to 95% over a period of 2 hours.
3. A temperature of 71°C (160°F) was maintained for 6 hours.
4. Maintaining 85-percent relative humidity, the internal chamber temperature was reduced in 16 hours to 28°C.
5. Steps 1, 2, and 3 were repeated for 10 cycles.
6. The test item was then removed from the chamber and allowed to return to ambient conditions and stabilize.
7. The test item was then subjected to an operational test.

Results - Since the humidity test was run subsequent to the salt fog test, the sprockets were coated with dry lubricant and consequently showed no rusting as a result of the test. No other parts of the unit showed signs of damage, and the operation of the unit was not impaired.

#### Low Temperature Functional Test

Objective - To demonstrate release system functional operation and to determine steady-state pull on the signal conductor.

#### Test Procedure

1. The reeling mechanism was placed in the test stand/chamber, and the temperature was reduced to -25°F.
2. When the unit internal temperature reached -25°F, this temperature was stabilized and maintained for two hours.
3. Pneumatic air supply temperature was adjusted to approximately 300°F, simulating the estimated air supply temperature at an ambient temperature of -25°F.
4. Steady-state pull and release operations were then performed at simulated hoisting velocities of 0, 30, 60, 90, and 120 feet per minute. At each condition, electrical circuit continuity

was checked to insure functional adequacy of the primary release modes.

5. The procedure of 4 above was repeated two additional times.

Results - During the low temperature functional test, there were no malfunctions that occurred which were detrimental to the operation of the unit, and no parts were damaged due to cold temperatures.

#### High Temperature Functional Tests

Objective - To demonstrate release system functional operation at elevated temperatures and to determine the steady-state pull on the signal conductor.

#### Test Procedure

1. The reeling mechanism was placed in the test stand/chamber, and the temperature was increased to +125°F and maintained for one hour.
2. Pneumatic air supply temperature was adjusted to 450°F with the modulating valve closed to maintain the test unit temperature at +125°F.
3. Steady state pull and release operations were then performed at simulated hoisting velocities of 0, 30, 60, 90, and 120 feet per minute. At each condition, electrical circuit continuity was checked to insure functional adequacy of the primary release modes.
4. The procedure of 3 above was repeated two additional times.

Results - During the high temperature functional test, there were no malfunctions that occurred which were detrimental to the operation of the unit, and no parts were damaged due to high temperatures.

#### Sand and Dust Test

#### Test Procedure

1. The signal conductor reel mechanism was placed in the test chamber in accordance with MIL-STD-810B, Section 3, Paragraph 3.2.2.

2. An internal chamber temperature of 73°F was then established with a relative humidity of approximately 10 percent.
3. Air velocity was adjusted to 1,750 feet per minute with a dust concentration of 0.3 gram per cubic foot. These conditions were maintained for 6 hours.
4. Next, dust feed was stopped, and air velocity reduced to 300 feet per minute with an air temperature of 145°F and a relative humidity of 10 percent. These conditions were maintained for 16 hours.

Test Results - Visual examination of the test specimen revealed no evidence of physical damage. Neither the unit nor its operation, subsequent to the test, were impaired due to the sand and dust exposure.

#### Teardown and Inspection

Following the environmental tests, there was a final teardown and inspection of the signal conductor reeling mechanism. The results of this inspection are as follows. All items were visually inspected with the following defects noted:

1. Bearing, P/N EP6003-3204, located on the hot air inlet end of the level wind shaft, was seized. Cause of the seizure was sand and dust within the shielding of the grease packed bearing. A better sand and dust seal must be provided. This seizure did not hinder the operation of the unit because the spanner nut, P/N MS172239, was loose on the shaft and the level wind shaft rotated the bearing bore. The nut was still retained by the washer, key retaining, P/N MS19070-33.
2. Cable guide roller, P/N EP6003-3249, was not rotating and indicated chafing on one surface from the cable passing against that surface. The roller was not rotating because the shoulder bolt supporting the roller in the bracket was not long enough to tighten the nut without clamping the bracket to the roller. The tolerance buildup is such that the next length bolt or a shim will be used to prevent clamping.



3. Some corrosion was noted on the cable drum, P/N EP6003-3130, as a result of the salt fog test. As previously stated, this was due to abrasion between the shielded cable and the drum surface. Originally, MIL-A-8625 Type II, Class I, anodizing was called out. This was changed to a MIL-A-8625 Type III anodizing to increase surface durability.
4. Gearshaft, P/N EP6003-3106, had a .0003-.0004" lead error on the small gear section and was worn at the high point. Had the gear teeth been machined to tolerance, tooth contact would have been continuous across the entire surface and not concentrated at one point. This caused excessive wear until the high point was worn evenly across the teeth.
5. The signal conductor cable and tape were checked and passed the continuity inspection.
6. All remaining hardware in the unit showed normal wear patterns.

Following teardown and inspection, the unit was reassembled for a final acceptance test.

#### Final Acceptance Test

##### Objective

To insure that the combined effect of all environmental tests did not deteriorate the performance of the reeling mechanism.

##### Test Procedure

The normal duty cycle and hook release tests discussed previously were repeated.

##### Results

The final acceptance test was run without incident and no situation occurred to adversely affect the reeling mechanism or its operation.

## CONTROLS AND DISPLAY SYSTEM

### DESIGN SUPPORT TESTS

Tests conducted to demonstrate feasibility and to establish design criteria for the hoist control system are covered in the hoist drive system section of this document.

### DESIGN DEVELOPMENT TESTS

Controls and display components that were tested are:

1. Cable length indicator
2. Cable tension indicator
3. Cable length and cable tension interface electronics unit
4. The cathode ray tube (CRT) monitor of the VAS system

### Cable Length Indicator

Tests conducted on the cable length indicator confirmed the correct functioning of the hoist position indicators and power-off flag display. Leakage current was measured to be 11 $\mu$ A, well within the acceptance limit of 50 $\mu$ A. A lighting test confirmed that the indicator met the following criteria:

1. All symbols to be visible to the eye at a viewing distance of 28 inches.
2. The counter wheels and legends to be evenly illuminated.
3. The viewing angle to be greater than 25° at the 3:00 and 9:00 o'clock positions.
4. The brightness of the lighted white portion of the indicator to be  $1.0 \pm 0.5$  foot-lambert.
5. The brightness of the black portions of the instrument to be  $0.06 \pm 0.04$  foot-lambert.
6. There is to be no stray light leaking from the instrument, and the lamp filaments to be shielded from direct view.

Accuracy tests confirmed that the length indications were proportional to the input signal within 0.5% of the indicator reading.

### Cable Tension Indicator

Tests conducted on the cable tension indicator were similar to the tests conducted on the cable length indicator.

Testing confirmed the correct functioning of the hook status legend, load range status flag, and power-off flag. Insulation resistance was tested and the leakage current was measured to be 1  $\mu$ A, well within the acceptance limit of 50  $\mu$ A. A lighting test confirmed that the indicator successfully met the same criteria as detailed in the cable length indication test. Accuracy tests confirmed that the tension and weight displays were proportional to the input signals within the required 0.25% of full-scale reading.

### Cable Length and Cable Tension Interface Electronics Unit

Tests conducted on the interface electronics unit confirmed the correct functioning of the unit and that all output values were within the required tolerance.

### Ten-Inch Cathode Ray Tube (CTR) Monitor

The test information for this item is presented in greater detail than that for the previously discussed display hardware, as the testing went beyond functional tests and included qualification testing. The monitor, used in the electro-optical viewing system, operates on a standard television display format. It is capable of displaying video with separate synchronization pulses (real time display) or with synchronization pulses included in composite video (recorder playback). Environmental performance capabilities of the monitor were verified by the following tests:

- Temperature shock
- High temperature
- Humidity
- Low temperature
- Shock
- Sand and dust
- Salt atmosphere
- Temperature-altitude
- Insulation and dielectric

### Temperature Shock Test

Specification Requirement - The monitor shall comply with the thermal requirements of MIL-E-5400, Section 3.2.24.1, Class 1. Compliance shall be demonstrated by successful completion of the temperature shock test of MIL-STD-810B, Procedure 1, Method 503. The monitor shall function within the acceptance test requirements subsequent to this environment.

Test Procedure - Two temperature chambers were used for this test. One chamber was adjusted to  $+71 \pm 1.4^{\circ}\text{C}$  ( $+160 \pm 2.5^{\circ}\text{F}$ ) and the other,  $-54 \pm 1.4^{\circ}\text{C}$  ( $-65 \pm 2.5^{\circ}\text{F}$ ).

Power was applied to the monitor to verify proper operation. The monitor, without cables or external connection, was subjected to the following temperature cycles:

1. The monitor was placed in the  $+71^{\circ}\text{C}$  ( $+165^{\circ}\text{F}$ ) chamber for a period of 4 hours.
2. The monitor was transferred to the  $-54^{\circ}\text{C}$  ( $-65^{\circ}\text{F}$ ) chamber for a period of 4 hours. This transfer was accomplished in less than 5 minutes.
3. The monitor was transferred to the  $+71^{\circ}\text{C}$  ( $+165^{\circ}\text{F}$ ) chamber for a period of 4 hours. This transfer was accomplished in less than 5 minutes.

The test was, for convenience, interrupted during this cycle by returning the monitor to room ambient after the 1-hour minimum exposure to  $+71^{\circ}\text{C}$  ( $+165^{\circ}\text{F}$ ). The next step started at the beginning of  $+71^{\circ}\text{C}$  (Step 3).

4. Repeat 2.
5. Repeat 3.
6. Repeat 2.

After completing all three cycles, the monitor was allowed 2 hours to return to room ambient prior to conducting the post test acceptance checks.

Test Results - The monitor complied with the requirements of temperature shock testing.

#### High Temperature

Requirement - The monitor shall comply with the thermal requirements of MIL-E-5400, Section 3.2.24.1, Class 1. Compliance shall be demonstrated by successful completion of the high temperature test of MIL-STD-810B, Procedure 1, Method 501.

Test Procedure - The temperature chamber and monitor were stabilized at room ambient conditions prior to this test. The following procedure was used to complete this requirement.

1. The monitor was placed in the temperature chamber. The power and video cables were connected through the access port of the chamber.
2. Power was applied to the monitor and its operation verified. Power was then removed.
3. The temperature of the chamber was increased to +71°C (+160°F) and the monitor temperature allowed to stabilize.
4. This temperature was maintained for a period of 48 hours with the relative humidity at a maximum of 15%.
5. The temperature of the chamber was decreased to +55°C (+130°F) and the monitor allowed to stabilize.
6. Power was applied to the monitor and correct operation verified while maintaining the +55°C environment. Power was then removed.
7. The monitor was then allowed to return to room temperature.
8. The monitor was removed from the chamber and visually examined for damage or deterioration that would impair future operation.

A post-test acceptance check was conducted.

Test Results - The monitor complied with the requirements of high temperature testing.

#### Humidity

Requirement - The monitors shall withstand exposure to relative humidities from zero to 100%. Compliance shall be demonstrated by successful completion of the humidity test MIL-STD-810, Procedure 1, Method 507, except that no moisture may be removed by any means other than normal run-off or drainage.

Test Procedure - The humidity chamber and monitor were stabilized at room ambient conditions prior to this test.

The following procedure was used to complete this requirement:

1. The performance of the monitor was verified prior to initiating this test.
2. The power and video cables were removed and the dust covers installed over all external connectors.
3. The temperature of the chamber was progressively increased to  $+71^{\circ}\text{C}$  ( $+160^{\circ}\text{F}$ ) and the humidity to 95%, over a period of 2 hours.
4. The conditions of Step 3 were maintained for 6 hours.
5. The temperature of the chamber was gradually reduced to  $+28^{\circ}\text{C} \pm 10^{\circ}\text{C}$  ( $+82^{\circ}\text{F} \pm 18^{\circ}\text{F}$ ) over the next 16 hours. The humidity was maintained in excess of 85%.
6. Steps 3, 4, 5, were repeated for a total of 10 cycles (240 hours total exposure time).
7. The monitor was removed from the chamber and visually examined for physical deterioration that would impair future operation. Moisture was not removed by artificial means.
8. A post-test acceptance check was conducted.

Test Results - The monitor complied with the requirements of humidity testing.

#### Low Temperature Test

Requirement - The monitors shall meet the thermal requirements of MIL-E-5400, Section 3.2.24.1, Class 1. Compliance shall be demonstrated by successful completion of the low temperature test in accordance with MIL-STD-810, Procedure 1, Method 502. This test shall be performed within one hour of completion of the humidity test of the previous paragraph. The temperature shall be reduced to  $-62^{\circ}\text{C}$  and maintained for 24 hours and then raised to  $-54^{\circ}\text{C}$  for operational tests.

Test Procedure - The temperature chamber was stabilized at room temperature prior to this test. The following procedure was used in this test:

1. The monitor was placed in the temperature chamber and the power and video cables connected.
2. Power was applied to the monitor to verify operation. Power was then removed.
3. The temperature of the chamber was reduced to  $-62^{\circ}\text{C}$  ( $-80^{\circ}\text{F}$ ) and maintained for 24 hours.
4. The monitor was examined for damage or deterioration that would impair future operation (cracked knobs, glass, etc.).
5. The temperature of the chamber was increased to  $-54^{\circ}\text{C}$  ( $-65^{\circ}\text{F}$ ) and allowed to stabilize.
6. Power was applied to the monitor and the operation verified while maintaining the  $-54^{\circ}\text{C}$  ( $-65^{\circ}\text{F}$ ) environment. Power was then removed.
7. The monitor was then allowed to return to room temperature.
8. After removal from the chamber, the monitor was examined for damage or deterioration that would impair future operation.

Test Results - The monitor complied with the requirements of low temperature testing.

## Shock Test

Requirements - Compliance shall be demonstrated by successful completion of the shock test in accordance with MIL-STD-810, Procedure V, Method 516.

Test Procedure - The monitor, without external connections, was placed on a solid wooden bench top that was 1-5/8 inches thick.

The following procedure was used to complete this test:

1. The monitor was placed on the bench, base down (refer to Figure 162).
2. The rear of the chassis was raised 4 inches above the bench and allowed to drop freely back to the bench.
3. The left side of the chassis was raised 4 inches above the bench and allowed to drop freely back to the bench.
4. The procedure of step 3 was repeated 3 times using the right side and again using the front.
5. The monitor was placed on its left side (refer to Figure 162).
6. One edge of the monitor was raised 4 inches above the bench and allowed to drop freely back to the bench. This procedure was repeated for each of the other edges.
7. The monitor was placed on its right side (refer to Figure 162).
8. One edge of the monitor was raised 4 inches above the bench and allowed to drop freely back to the bench. This procedure was repeated for each of the other edges.
9. The monitor was placed on its top (refer to Figure 162).
10. One edge of the monitor was raised 4 inches above the bench and allowed to drop freely back to the bench. This procedure was repeated for each of the other edges.



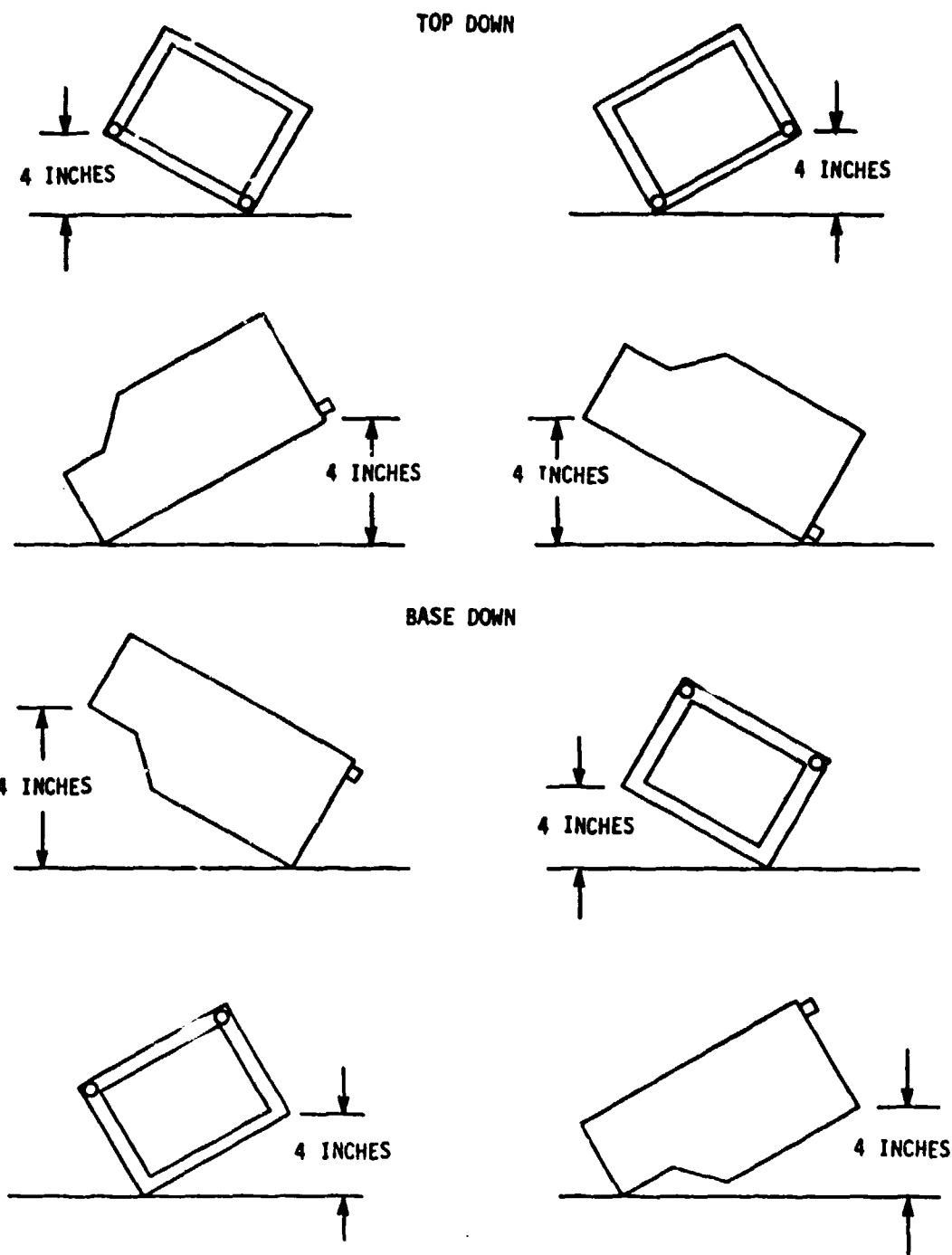


Figure 162. Shock Test Position.

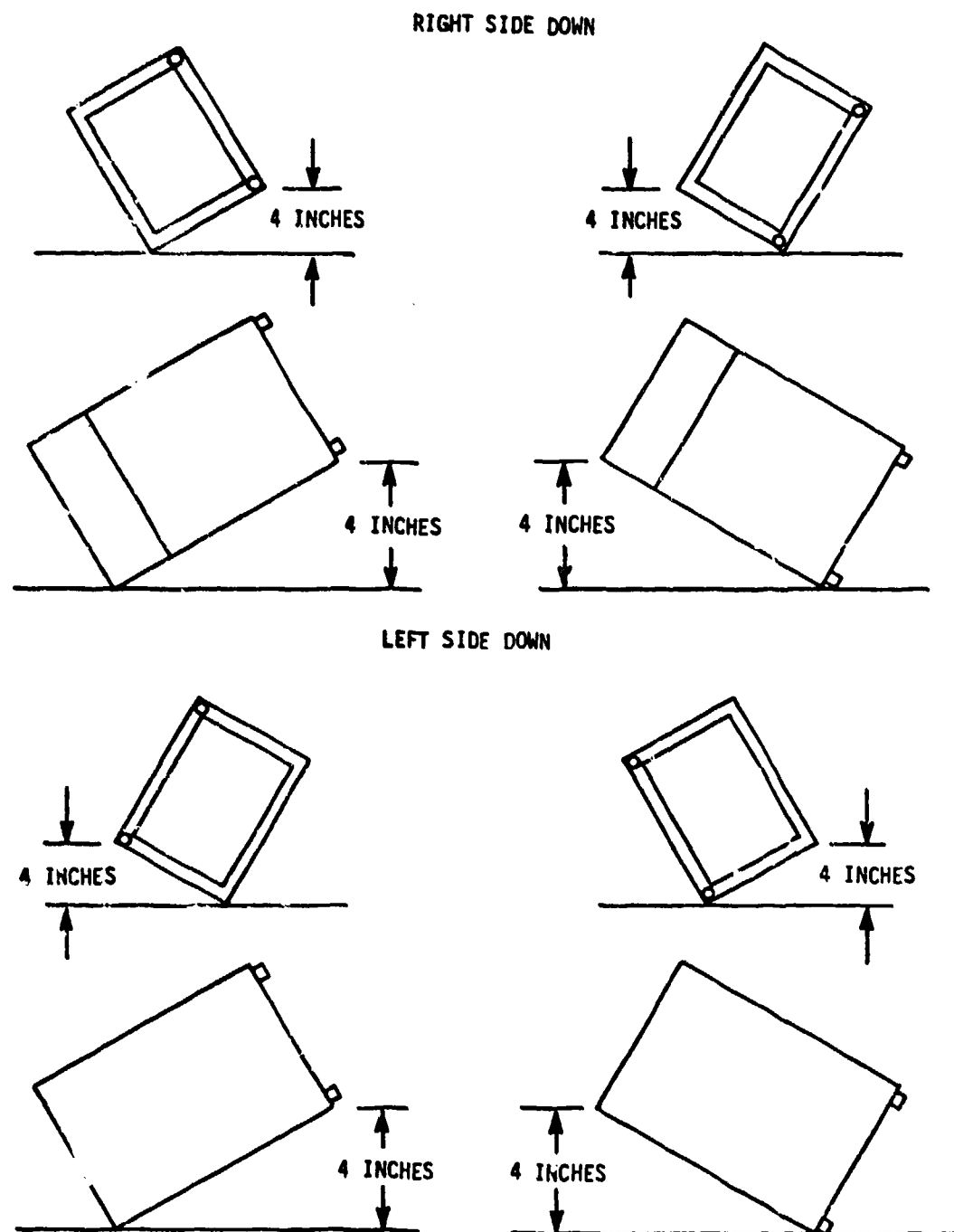


Figure 162. Shock Test Position Concluded.

11. The monitor was visually examined for damage or deterioration that would impair future operation.
12. Power was applied to the monitor and a post-test acceptance check completed.

Test Results - The monitor complied with the requirements of the shock test.

#### Sand and Dust

Requirement - Compliance shall be demonstrated by successful completion of the sand and dust test of MIL-STD-810B, Procedure 1, Method 510. Exposed glass surfaces shall be protected from this environment.

Test Procedure - The test chamber and monitor were stabilized at room conditions prior to this test.

The following procedure was used to complete this requirement:

1. The monitor was placed in the sand and dust chamber. A minimum of 4 inches clearance was maintained from other objects and the chamber walls. The monitor was oriented in the chamber such that the rear of the monitor was exposed to the dust stream.
2. Proper operation was verified prior to the start of this test. The dust covers were installed over all external connectors. Heavy kraft paper was placed over the exposed section of the CRT and taped in place with masking tape, leaving the knobs and lamp exposed.
3. The chamber conditions were adjusted to +23°C (+73°F) and a relative humidity of less than 22%. The air flow velocity was adjusted to 1750 ±250 feet per minute and the dust concentration to 0.3 ±0.2 gram per cubic foot.
4. These conditions were maintained for 6 hours.
5. The dust feed was stopped and the air velocity reduced to 300 ±200 feet per minute.

6. The chamber temperature was increased to +63°C (+145°F), while the relative humidity was reduced to less than 10%.
7. These conditions were maintained for 16 hours.
8. The air velocity was adjusted to 1750 ±250 feet per minute while maintaining the temperature at +63°C (+145°F). The dust concentration was adjusted to 0.3±0.2 gram per cubic foot.
9. These conditions were maintained for 6 hours.
10. All chamber controls were turned off and the monitor was allowed to return to room conditions.
11. The accumulated dust was removed from the monitor by brushing, wiping or shaking.
12. The monitor was removed from the chamber and visually examined for physical deterioration that would impair future operation.
13. The monitor was returned to Conrac and post test acceptance checks were initiated within one hour.

Test Results - The monitor complied with the requirements of sand and dust testing.

#### Salt Atmosphere

Requirement - Compliance shall be demonstrated by successful completion of the salt atmosphere test of MIL-STD-810B, Procedure 1, Method 509. Exposed glass surfaces may be wiped clean prior to performance tests.

Test Procedure - The test chamber and monitor were stabilized at room ambient conditions prior to this test.

The following procedure was used to complete this requirement:

1. Proper operation was confirmed prior to the start of this test. The dust covers were installed over all external connectors.
2. The monitor was placed in the salt atmosphere chamber.

3. Immediately before exposure, all outer surfaces of the monitor and chamber rack were cleaned with clean tap water.
4. The chamber temperature was increased to +35°C (+95°F) and the required salt atmosphere injected.
5. These conditions were maintained for 48 hours.
6. The monitor was removed from the chamber and salt deposits were removed from the case and CRT face with warm tap water.
7. The monitor was visually examined for physical deterioration that would impair future operation.
8. The monitor was returned to Conrac and post-test acceptance checks were indicated within one hour.
9. The monitor was stored at room conditions for 48 hours and the post-test acceptance checks were repeated.
10. The monitor was again inspected for physical deterioration that would impair future operation.

Test Results - The monitor complied with the requirements of salt atmosphere testing.

#### Temperature-Altitude

Requirement - The monitor shall meet the requirements of MIL-E-5400, Section 3.2.24.1, Class 1. The monitor shall withstand pressure altitudes from sea level to 50,000 feet and shall withstand a pressure change of 32 psi per second over a range of 8 psi.

Compliance shall be demonstrated by successful completion of the temperature-altitude test of MIL-STD-810B, Procedure 1, Method 504, Class 1 equipment.

Test Procedure - The chambers and monitor were stabilized at room ambient prior to this test.

The following procedure was used to complete this test:

1. The altitude chamber was placed inside the temperature chamber with the view-port towards the front. The monitor was placed inside the altitude chamber so the face of the CRT could be viewed during test. Provisions were made to periodically monitor the thermocouple connected to the monitor.

The power and video was connected to the monitor through the connectors on the front wall of the altitude chamber.

2. Power was applied to the monitor to verify operation. The power was then removed.
3. The chamber temperature was adjusted to  $-62^{\circ}\text{C}$  ( $-80^{\circ}\text{F}$ ) and ambient altitude. These conditions were maintained for two hours after the thermocouple on the chassis indicated stabilization.
4. The temperature was adjusted to  $-54^{\circ}\text{C}$  ( $-65^{\circ}\text{F}$ ) and ambient altitude. After temperature stabilization, 23 VDC and 111 VAC input power was applied and operation verified. Power was removed and the monitor allowed to restabilize.
5. Step 4 was repeated.
6. Step 4 was again repeated, but this time the altitude in the chamber was increased to 50,000 feet and the input power adjusted to 31 VDC and 121 VAC. Correct operation was verified and the power then removed.
7. The environmental conditions were adjusted to  $-10^{\circ}\text{C}$  ( $-14^{\circ}\text{F}$ ) at ambient altitude. After stabilization, the door was opened and frost allowed to form and melt but not evaporate. The door was closed and 31 VDC and 121 VAC input power applied to verify proper operation.

The power was turned off and on at least three times, and proper operation verified each time.

8. The chamber conditions were returned to room ambient and the monitor was removed. 31 VDC power was applied and post-test acceptance checks were conducted. Power was removed and the monitor returned to the chamber.
9. The chamber temperature was adjusted to +85°C (+185°F) and maintained for 16 hours after stabilization.
10. The chamber temperature was reduced to +55°C (+131°F) and 31 VDC and 121 VAC input power applied to verify proper operation. The power remained on for 4 hours, and the thermocouples were recorded every 30 minutes. Proper operation was verified during and after the 4 hours. Power was then removed.
11. The chamber temperature was adjusted to +71°C (+160°F). After stabilization, 31 VDC and 121 VAC input power was applied for 30 minutes and then removed for 15 minutes.
12. The power on/off cycle of step 11 was repeated for a total of 4 cycles. Proper operation was verified during each on-period. Power was then removed. Thermocouples were monitored every 10 minutes.
13. The chamber temperature was adjusted to +30°C (+86°F) and after temperature stabilization, 31 VDC and 121 VAC input power was applied. The altitude was adjusted to 40,000 feet. These conditions were maintained for 4 hours. Proper operation was verified throughout the 4-hour period. Power was then removed and the altitude returned to ambient. Thermocouples were monitored every 30 minutes.
14. The chamber temperature was adjusted to +47°C (116°F) and after stabilization, the altitude was increased to 40,000 feet. 31 VDC and 121 VAC input power was applied to verify proper operation. The power remained on for 30 minutes followed by a 15-minute off period. This power-on and power-off cycle was repeated for a total of four times. Thermocouple readings were repeated every 10 minutes.

15. The chamber temperature was adjusted to +20°C (68°F) and after temperature stabilization, 31 VDC and 121 VAC power was applied and the altitude increased to 50,000 feet. After stabilization of temperature and altitude, the input power was readjusted to 31 VDC.

These conditions were maintained for 4 hours, the thermocouple readings being recorded every 30 minutes. Proper operation was verified continuously.

16. The chamber temperature was adjusted to +35°C (+95°F) and after temperature stabilization, the altitude increased to 50,000 feet. After stabilization of temperature and altitude, 31 VDC and 121 VAC input power was applied.

The power was allowed to remain on for 30 minutes followed by a 15-minute off period. This power-on and power-off cycle was repeated for a total of four times. Thermocouple readings were recorded every 10 minutes. Proper operation was verified continuously. The chamber was returned to ambient conditions and monitor power removed. The monitor was removed from the chamber.

Test Results - The monitor complied with the requirements of temperature-altitude testing.

#### Insulation and Dielectric

Requirements - The insulation resistance shall be measured at 500 volts DC  $\pm 10\%$  for equipment rated up to 250 volts rms operating. After a maximum one-minute electrification time, the insulation resistance shall be not less than 75 megohms.

A potential of 1500 volts rms, 60 Hz shall be applied for one minute between the chassis and all terminals tied together. Radio noise filters, if connected to the chassis, may be disconnected during this test. The voltage shall be applied at a uniform rate of 250 to 500 volts per second. During the test, any arcing, sparkover, or breakdown shall constitute failure.



Test Equipment - The following equipment was used to perform this test:

1. Dielectric Tester
2. Hi-Pot Tester

Test Procedure - The following plug-in assemblies and sub-assemblies were removed or disconnected from the monitor prior to this test:

<u>Name</u>	<u>Model No.</u>
Vertical and Sync	3002013
Video	3062015
Horizontal	3062017
Low Voltage	3062019
High Voltage	3062124
CRT	3062005
Yoke	3062067
Horizontal #2	3062026
Horizontal #3	3062028
Low Voltage #2	3062024
T1	3062081
Rear Panel	3062088

A single wire was attached to points 1 through 7 of TB1 on the interconnect assembly 3062052. The specified voltage was applied between the wire and case ground for the specified time.

Test Results - The monitor complied with the requirements of Insulation and Dielectric Testing.

## VISUAL AUGMENTATION SYSTEM

### DESIGN SUPPORT TESTS

Laboratory tests were conducted to demonstrate the visual augmentation system with simulated inputs. The laboratory test specimen was composed of an electro-optic sensor, electronic drive, character generator, display programmer, and display.

The concept selected for the HLH application is a low light level closed-circuit TV system. It has a wide field of view and is operable over a very wide dynamic range of scene illumination.

Hardware consists of a U.S. Army Cobra Night Fire Control System (CNFCS) modified to:

1. eliminate the azimuth gimbal
2. change and add lens elements
3. change from a 525-line scan to an 875-line scan
4. add a new 875-line TV display monitor

The CNFCS illuminator has been changed from a rectangular uniform field to a circular uniform field. A new control panel has been provided, and a unit called an Electronic Interface Unit (EIU) is included to generate and position cargo coupling symbology on the display.

Categories of tests and demonstrations performed on the VAS, and a summary of the test results, are provided in the following paragraphs. The reader is directed to Reference 2 for a complete description of the laboratory tests and results.

### Tests and Demonstrations

1. Optical tests to verify and calibrate the field of view, aperture, zoom range, distortion, filter characteristics, and mechanical function of zoom control, iris control, and filter insertion.
2. Sensor and display component tests of physical characteristics (size, weight, etc.) and operational parameters (band width, resolution, sensitivity, etc.).
3. Symbology generation, positional accuracy, and calibration.

4. System operation demonstrations.
5. Environmental tests on fabricated components.

### Results

Optical Tests - Image motion effects did not appear visually objectionable unless small and relatively very bright objects (relative to the surround) were in view. These led to very noticeable lag or tailing

Geometric distortion of the optics due to the orthographic projection OP-fish-eye format ( $y = 10 M \sin \phi$ ) and the ISIT camera tube (pincushion distortion) was such that, for a minimum field of view ( $32^\circ \times 32^\circ$ ), noticeable pincushion was evident on the display. For the maximum field of view as seen on the display, the full 180-degree field of the OP-fish-eye lens could not be displayed. This was due to some misalignment in the optical chain, which caused some vignetting.

Five bright specks were visible on the right side of the display.

Uniformity in the display will be degraded somewhat by the central hot spot of the illuminator beam.

Component Tests - The visual physical-inspection of the components uncovered several workmanship discrepancies. These were recorded, and corrective measures were completed and inspected prior to delivery.

Symbology Tests - Initially, there were some instabilities and positional inaccuracy in some of the six symbols, caused by wiring errors and malfunctioning circuit components. Before acceptance, these discrepancies were corrected.

System Operation Tests - All the control functions were exercised for the camera, display, symbology, and turret; and satisfactory functioning was obtained. The three prime lens assemblies were utilized and adjudged to perform essentially as expected. The system sensitivity was very good both with ambient light and with the illuminator. Two items that were considered before flight testing were elimination of blanking during lens zoom and control panel illumination reduction; however, these items were not considered part of the acceptability criteria.

## STATIC ELECTRICITY DISCHARGE SYSTEM

### INTRODUCTION

The most troublesome static electricity problem affecting a large helicopter, such as the HLH is the equalization of potential between the hovering vehicle and the ground during external cargo hookup operations.

The initial HLH/ATC design objective was to provide a system which would limit the energy transfer on ground contact to 1 millijoule. For a heavy lift helicopter of approximately 120,000 pounds gross weight and an electrical capacitance on the order of 2000 picofarads, this is equivalent to no more than about 1000 volts potential. All previous tests have indicated that maximal charging rates are in the order of 300 microamperes for a 40,000-pound helicopter gross weight. For the 120,000-pound HLH, an estimated charging rate of 600 microamperes was set as the objective for dissipating capability.

The design objective for an active automatic static electricity discharge system for the HLH can be stated as: Not more than 1 millijoule of discharge energy under a 600 microampere natural charging rate.

There are two fundamental approaches to the solution of the hovering helicopter problem:

1. Active Discharge System. Sensing and actively dissipating the proper magnitude and polarity of charges into the surrounding atmosphere to counteract the natural charging of the helicopter. The word "active" results from the use of a very high-voltage power supply to produce the discharge.
2. Passive Discharge System. Reducing the helicopter voltage by means of unpowered rotor blade corona dischargers and contact grounding by means of a dropline (or grounding rope).

The HLH/ATC program began with an experimental investigation aimed at development of an active discharge system. Following laboratory, ground, and full-scale flight tests on a CH-47 helicopter, it was discovered that a fundamental problem exists which prevents correct sensing of the static charge on the helicopter by electric field mills. The program was then re-oriented to passive dissipation and grounding procedures.

The following sections describe the types of testing conducted under the active and passive discharge programs and summarize the results and conclusions. The reader is directed to Reference 3 for complete descriptions of the: tests, instrumentation, data reduction, and analysis techniques.

#### DESIGN SUPPORT TESTS

##### Active Discharge System

Sensing and discharge techniques selected for the HLH were:

1. To sense the potential between the winch-mounted cargo hook and the ground by locating an electric field mill on the hook and evaluating accuracy (fidelity) as a function of the height of this field mill above the ground.
2. To dissipate currents up to 600 microamperes into the exhaust plumes of the helicopter turbo-shaft engines, thereby taking advantage of the high flow velocities in this region to overcome space charge limitations close to the active dissipator electrodes and to provide a mechanism for blowing the free ions away from the helicopter.

##### Test Sequence and Procedure

The test program was divided into three phases:

1. Laboratory dissipator configuration tests using a low-speed wind tunnel and a full-scale mockup of an engine exhaust and aft helicopter fuselage.
2. Helicopter ground tests of selected active dissipator configurations to evaluate the thermal, acoustic, soot, and flow field effects of an actual engine exhaust plume.
3. Full-scale flight tests on a CH-47 helicopter at the U. S. Army Yuma Proving Ground to evaluate active dissipators and remote sensors under conditions of actual helicopter triboelectric charging while hovering in a dust cloud.

### Test Data Collection, Processing, and Analysis

Success or failure of the active dissipation system was predicated on solution of two basic problems:

1. Dissipation of a continuous charging current of 600 microamperes into the air surrounding the hovering helicopter.
2. Correct sensing of the potential difference between the helicopter and the ground while actively dissipating high charging currents.

It was anticipated by Boeing Vertol that the dissipation problem could be solved, but that the question of correct sensing might encounter basic limitations from the physics of ion clouds and from remote sensor concepts, since potentials are inferred rather than actually measured directly. For this reason, Boeing Vertol went to the technical community for expertise in static electricity dissipation in the form of a request for quote (RFQ).

Bids were received from two technically qualified organizations: Dynasciences Corporation and Stanford Research Institute. The sensing problem dictated emphasis on basic electrostatic physics rather than on hardware. Stanford Research Institute (SRI) was selected to perform the program and prepare a final report.

### Task Conclusions

1. Sensing Accuracy. Under heavy triboelectric charging conditions, the ion cloud, which surrounds a large helicopter as a result of natural charging, active dissipation, and electrification of the ground surface, can falsify readings from sensors located on the helicopter fuselage and on a simulated cargo hook lowered to within 5 feet of the ground. The residual discharge energy on the helicopter resulting from these sensor errors can reach 10 joules on the fuselage and 1.0 joule on the cargo hook. This lack of sensor accuracy at high helicopter charging levels prevents any active dissipation system from meeting the system safety objective of the heavy lift helicopter.
2. Dissipation. It will be feasible to actively dissipate 200 microamperes into each turbine exhaust of the HLH for a combined total of 600 microamperes using a bipolar power supply of 200,000 to 250,000 volts potential. Dissipation from corona points extending from the fuselage into the rotor downwash could also

provide currents in excess of 600 microamperes but would require approximately 8 corona points located a minimum of 6 feet away from any conductive surface of the helicopter.

3. Resistance of the Ground. Prior to the June 1972 Yuma desert tests, the resistance of a dry desert was considered to be in the order of  $10^9$  ohms. Measurements at Yuma in May and June 1972, near the end of a 159-day dry spell, have shown that desert resistance is seldom higher than  $10^6$  ohms and never exceeds  $10^7$  ohms. This threw new light on the feasibility of passive dropline discharging techniques in lieu of active dissipation, as shown below:

<u>Ground Resistance</u>	<u>Charging Current</u>	<u>Residual Helicopter Voltage</u>
$10^9$ ohms	600 $\mu$ A	600,000 volts
$10^7$ ohms	600 $\mu$ A	6,000 volts
$10^6$ ohms	600 $\mu$ A	600 volts

#### Recommendations

1. Based on the findings of the active discharge program, it was recommended that the Heavy Lift Helicopter Advanced Technology Component static electricity dissipation program be reoriented from active dissipation to passive dissipation and ground techniques.
2. Primary objective of a passive grounding system should be protection of the ground handler during cargo hookup operations. A reasonable amount of sparking should be accepted upon grounding.
3. Cargo unloading should be protected by contact grounding directly through the cargo itself.
4. For the special case of dry snow, where high surface resistance could prevent successful ground, a winterization kit approach should be used consisting of a projectile and trailing wire to pierce the insulating layer.

#### Passive Discharge System

The primary objective of the passive system is the protection of the cargo handler during cargo hookup operations. This objective presents a design compromise:

1. A highly conductive grounding link (such as a low-resistance wire) between the helicopter and the ground surface will leave the minimum residual voltage on the helicopter. However, in case of inadvertent contact with the cargo handler (prior to contact with the ground surface), it will expose the cargo handler to the full discharge energy stored by the helicopter.
2. If a resistor of several megohms is inserted in the grounding line, it will protect the cargo handler against very high voltages on the helicopter (e.g., 10 Mohms will allow a contact up to 120,000 volts, 20 Mohms over 200,000 volts, etc.), but will leave a residual voltage under heavy charging conditions due to the ohmic voltage drop. At the HLH design maximum charging current of 600 microamperes, a total resistance between the helicopter and ground of 10 Mohms will leave a residual voltage of 6,000 volts on the helicopter and 20 Mohms will leave a residual voltage of 12,000 volts.

#### Design Approach

Two pieces of grounding hardware were considered for the HLH. The first is a resistive grounding link, commonly called a grounding line, which is attached to one cargo coupling and dangles approximately 7 feet below it. As the HLH winches are used to lower the cargo coupling for load hookup, the grounding line contacts the cargo or the ground and thereby discharges the helicopter prior to any handling of the cargo coupling by ground hookup personnel. The second hardware item is a resistive grounding pole intended to be used under the special circumstances of a depot location and a requirement to handle or guide cargo before it touches the ground. In this situation, the grounding pole, which is a loose piece of ground handling equipment, is used to contact the cargo and to thereby discharge the cargo and the helicopter, making it safe for ground handler manipulation.

#### Flight Test Evaluation Program

The static electricity hardware was evaluated under simulated operational conditions during a series of U. S. Army flight tests at Yuma Proving Ground, using a CH-47 Chinook helicopter.

The helicopter hovered over typical surfaces such as macadam, concrete, hard-packed desert, and plowed-up desert and the contact was established by the grounding line, lowered on a simulated cargo hook (aluminum block) or by the grounding pole. Different grounding electrodes (chain) and resistive elements were tested under actual service conditions (whipping



in the helicopter downwash, deployment by dropping the line, and manhandling by grounding pole). In addition, the resistance between the grounding electrode and a good ground was measured and plotted as a function of applied voltage. It soon became obvious that the grounding resistance is sufficiently low to insure acceptable residual voltage after ground contact was made, but that the grounding line and the grounding pole hardware as supplied by The Truax Company are unsuitable for reasons outlined below:

1. Grounding Line

- a) The steel cable of the damage resistive leader corroded. The cable should be encased in vulcanized rubber to exclude water.
- b) The MS connectors were damaged during the test. The connectors should be replaced by a more rugged and more permanent design incorporating a yield feature to fail at 500  $\pm$  100 pounds.
- c) The flexible resistive element failed under test conditions. Being subject to strain during deployment from the helicopter (whipping in the helicopter downwash or being hooked accidentally by the grounding pole), its resistance would leave a residual 18 to 24 volts under 600 microamperes charging and is therefore unacceptable. The transition from resistive coating to the connector was by means of a copper wire, which was failing under normal handling. For this reason, the tests were completed using a rigid ceramic resistor with good resistance stability, but unsuitable for the incorporation in the actual design.
- d) The grounding chain was too short to allow for the vertical motion of the hovering helicopter. The length should be increased by 12 inches.
- e) The contribution of the corona discharge elements to RFI cannot be detected in the presence of other RFI generated under triboelectric charging conditions. These elements should be deleted.

## 2. Grounding Pole

- a) The contact hook did not ensure positive contact with the load or suspension system. In the event that contact is broken, the helicopter regains full voltage in 1 to 2 seconds. A clip-on device should be incorporated in the design.
- b) The 1.0 Mohm resistor does not reduce the sparking of the grounding chain significantly. To limit the danger of spilled fuel ignition, a much higher resistance would be required, which would defeat the voltage lowering process.
- c) The water droplet collar is too heavy.
- d) The pole grip is too small in diameter and length, making it difficult to hold with both hands.

### Task Conclusions

The following conclusions have been drawn from the flight evaluation of passive static electricity hardware:

- 1. The concept of a resistive grounding link between a hovering heavy lift helicopter and the ground for static electricity potential equalization is viable for typical moderate climate surfaces.
- 2. A passive grounding line with a 10-Mohm series resistance should be employed on the HLH to protect ground handlers from static electricity during cargo hookup operations. The design of the grounding line should be revised to provide 10 Mohm resistance stable within  $\pm 1$  Mohm under temperature, voltage, and strain variations, to retain its flexibility, and to provide good protection against service abuse.
- 3. A grounding pole should not be used with the HLH, since ground personnel could receive severe shocks if contact were inadvertently lost with the cargo.

# INTEGRATED TEST RIG DEMONSTRATION

## OBJECTIVES

Cargo handling system components were tested as an integrated system to demonstrate achievement of design and to evaluate functional, performance, and reliability characteristics.

## FACILITY

A 70-foot clear-height twin-tower test fixture, called the integrated test rig, was designed and fabricated for this program. Figure 163 shows the rig, which was located at the Contractor's facility in Ridley Park, Pennsylvania, on a site adjacent and to the west of the Engineering Laboratory, Building 3-31.

The integrated test rig is designed to allow the cycling of a load through approximately 50 feet of cable deployment in either the normal two-point mode or in a single-point mode. The rig is designed to be dismantled and re-erected at another site if required. Major elements of the integrated test rig are:

1. A twin tower structural steel framework with a 70-ft vertical clearance.
2. A pneumatic air supply and distribution system providing air at a 4.3 to 1 pressure ratio to the hoist interfaces and to the signal conductor reeling mechanism.
3. Electrical power supplies of:

120/80V	3-phase	60 Hz
115V	1-phase	60 Hz
120/208V	3-phase	400 Hz
28 VDC		
4. Instrumentation and displays.
5. Operating control station simulating the rear-facing, load-controlling crewman station in the heavy lift helicopter.

The structural steel framework consists of two steel I beam towers, 14 x 14 square feet, supporting a pair of horizontal, internally braced, 30-inch deep, wide flange I beams with

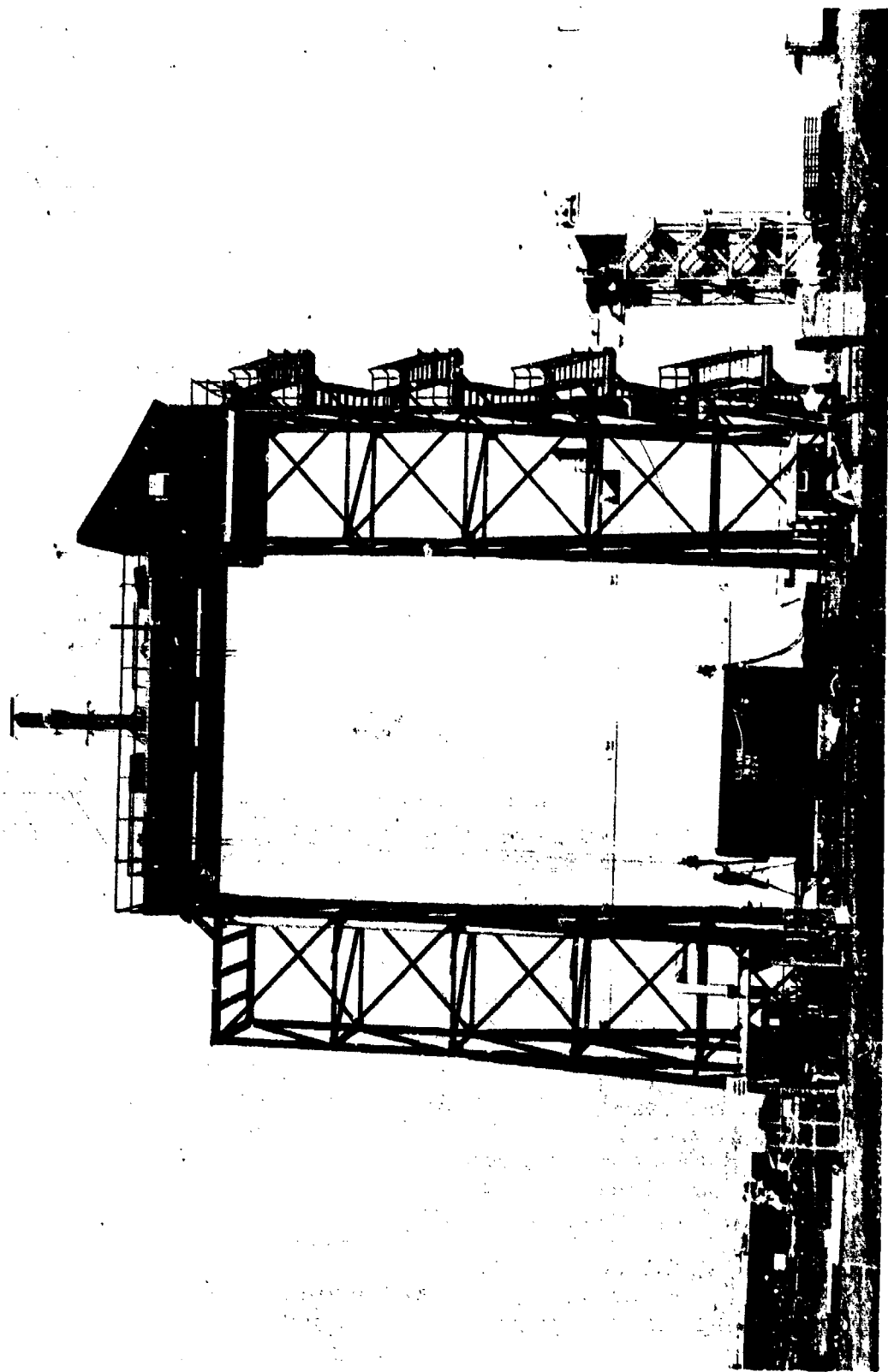


Figure 163. Integrated Test Rig.

40-foot spans. Lateral outriggers buttress the towers. The helicopter hoist assemblies are housed in ground assembled modules which are raised and installed between the horizontal I beams.

The test rig simulates a full-scale installation of the cargo handling system in the Heavy Lift Helicopter in the following respects:

1. Compatibility with full-scale cargo handling components.
2. Power, control, geometry, and physical spacing of hoist assemblies.
3. Level fuselage attitude.
4. Relative location, type of hoist controls, and layout of load-controlling crewman (LCC) station.

In addition, the test rig incorporates a longitudinal hoist span positioning system capable of providing hoist separations of 16, 22, and 26 feet.

#### SPECIMEN

The test specimen consisted of components and assemblies in sufficient quantities to provide one complete helicopter cargo handling system (excluding the visual augmentation system).

The components and assemblies that were included in this test are listed here.

1. Pneumatic hoist drive unit
2. Hoist assembly
3. Tension member
4. Cargo coupling
5. Cable cutter
6. Load isolator
7. Signal transfer system
8. Span positioning system
9. Control and display systems
10. Hoist drive modulating valve assembly
11. Hoist drive controller
12. Pneumatic supply articulating ducts
13. Single-point adapter

Each component was designed and fabricated as part of the HLH/ATC Program and has undergone specialized design development testing to verify its particular unique functions. Physical and functional compatibility of the individual components and total system operational performance were demonstrated as part of this test program.

#### TEST METHOD AND RESULTS

##### DEMONSTRATION OBJECTIVES

This program was a system demonstration of individual components which had previously undergone development testing. Feasibility and achievement of design and functional and performance characteristics of the cargo handling system were to be demonstrated by performance of the following without failure, yielding, abnormal wear, or damage to any major component:

1. Hoisting a 58,520-lb load, single and dual point, at speeds from 0 to 60 ft/min.
2. Lowering a 58,520-lb load, single and dual point, at speeds from 0 to 60 ft/min.
3. High speed payout of the cargo coupling at speeds of up to 120 ft/min.
4. Pneumatically braking a 58,520-lb load to a stop from a speed of 60 ft/min during both hoisting and lowering.
5. Holding a 58,520-lb load for 5 minutes.
6. Releasing 1,000-lb loads from one cargo coupling by commanding the normal (electrical) mode and the alternate (mechanical) release mode.
7. With no load on the cargo coupling, a change of hoist position will be commanded by selection of the appropriate electrical switch positions. The hoists shall unlock, move to their alternate locations, relock, and reactivate all normal hoisting systems.

## TEST SEGMENTS

The program was divided into a series of activities which grouped similar types of buildup and evaluation testing into increments which could be tracked and identified as each task was completed. Table 81 shows the list of activities, the associated span times for accomplishment, and the calendar month in which each task was completed.

### Functional Tests

#### Lifting Capacity

Test loads consisted of stacked kirksite blocks, and empty and ballasted U.S. Army MILVAN 8x8x20-foot containers (see Figures 164 and 165). Nylon slings and a container handling device, Boeing Vertol P/N SK24955 (see Figure 166) were also utilized. Initially, using supply air of 55 psia at temperatures of up to 360°F; zero load and individual loads of 4,000, 6,800, and 17,100 lb, and multi-point loads of up to 32,000 lb were hoisted 50 ft. Hoist-drive units, S/N 3 and 4, were used throughout this load buildup. Hoist drive units, S/N 1 and 2 (redesigned to improve performance) were tested with zero and 17,100-lb individual loads and the 32,000-lb multi-point load. The latter tests were conducted with the air turbine motor (ATM), test controller (preselect speed), and the hoist control grip. All loads were operated individually and in synchronous control modes.

Hoisting and reversing speeds were increased progressively until maximum speeds were attained. Each load weight was stopped at approximately mid-height to evaluate smoothness of deceleration, braking, and starting.

A change was made in the pneumatic power generator (PPG) for the test rig to permit operation at higher supply air pressures. With supply air of 55, 58, and 63 psia; individual loads of 12 tons and 16.8 tons on each hoist; separate loads of 16.8 tons on the aft hoist and 12 tons on the forward hoist (a 40/60 design load distribution); and separate loads of 12 tons on the aft hoist and 16.8 tons on the forward hoist were hoisted through a 50-foot distance. Maximum hoisting and reversing speeds were attained and smoothness of deceleration, braking, and starting were evaluated. These tests were repeated for evaluation with a MILVAN container both empty and ballasted to a gross weight of 58,544 pounds.

TABLE 81. MATRIX OF CARGO HANDLING SYSTEM, INTEGRATED-TEST-RIG TEST REQUIREMENTS AND PERIODS OF TESTING											
ACTIVITY	1973		1974								
	NOV	DEC	JAN	FEB	MAR	APR	MAY	JUN			
Lifting Capacity Tests											
Static Capacity Tests											
Normal Braking											
Static and Dynamic Hook Releases											
Control Function Tests											
Max. Cable Angle Tests											
Sensor Function Tests											
Tension Member Velocity											
900 Two-Pt. Cycles											
900 Single-Pt. Cycles											
Max. Static Load Demo											
Tear-down Inspections											



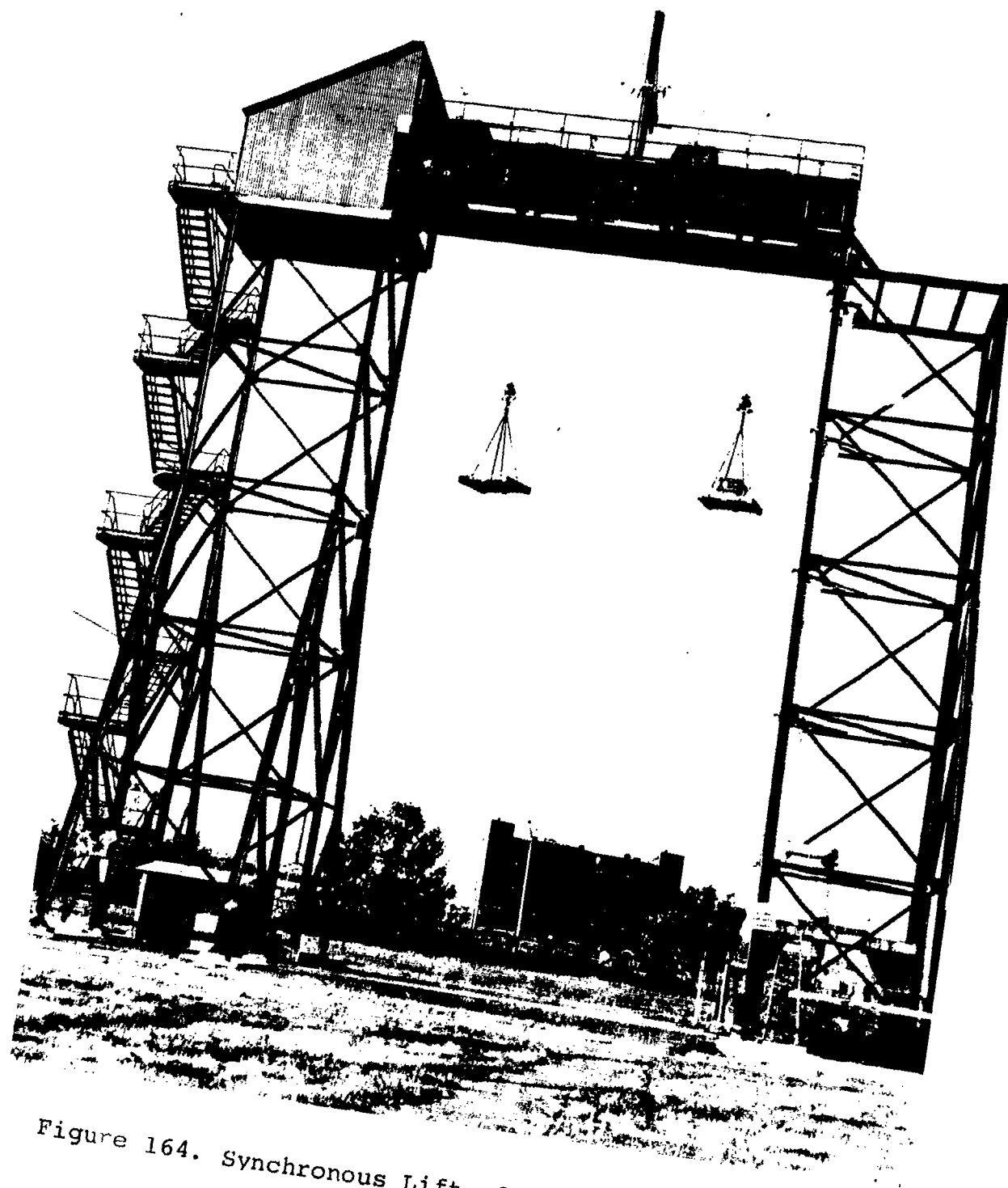


Figure 164. Synchronous Lift of 4,000- and 6,800-Lb Loads.

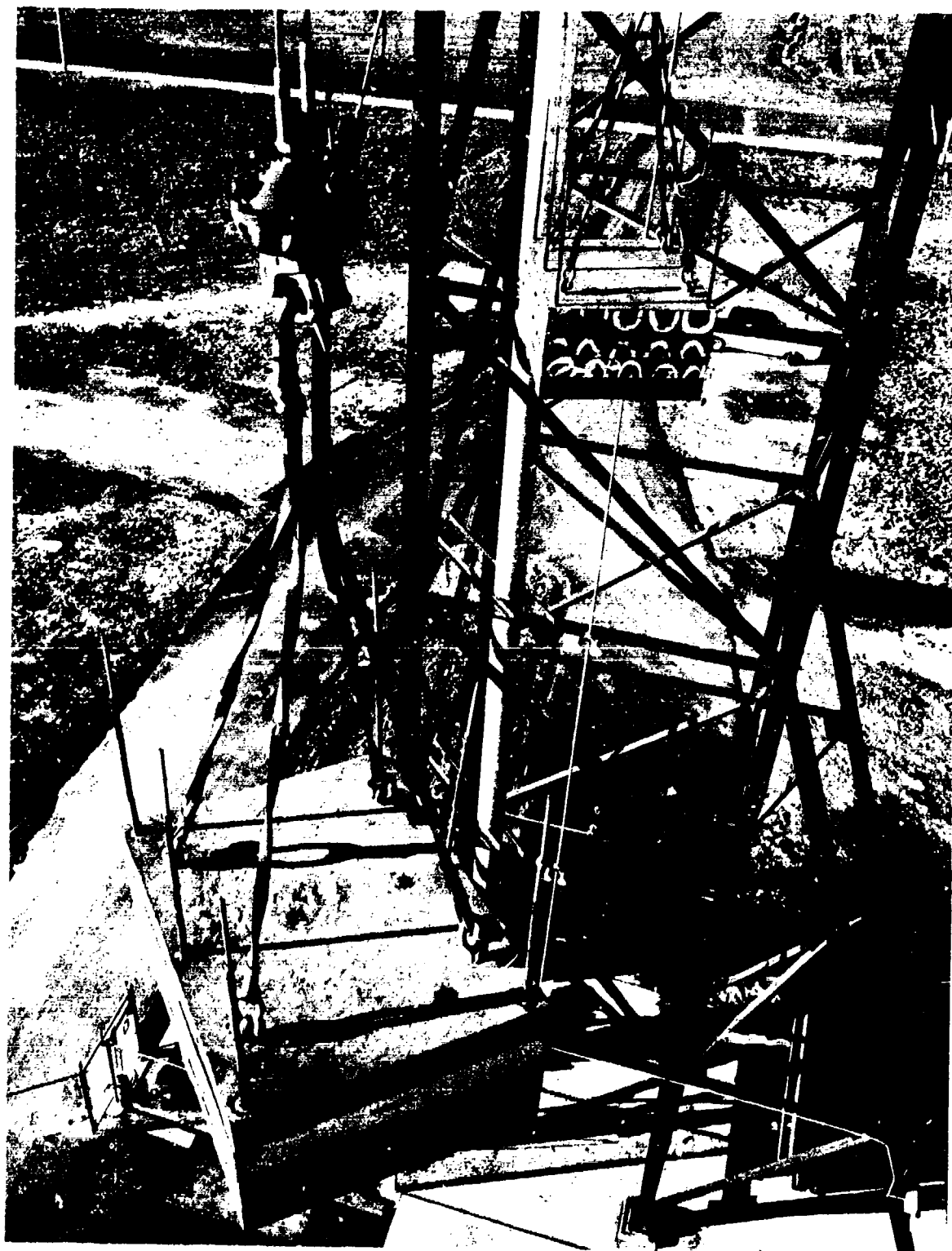


Figure 165. Control Room View of 32,000-Lb Load Used In Synchronous Hoisting Tests

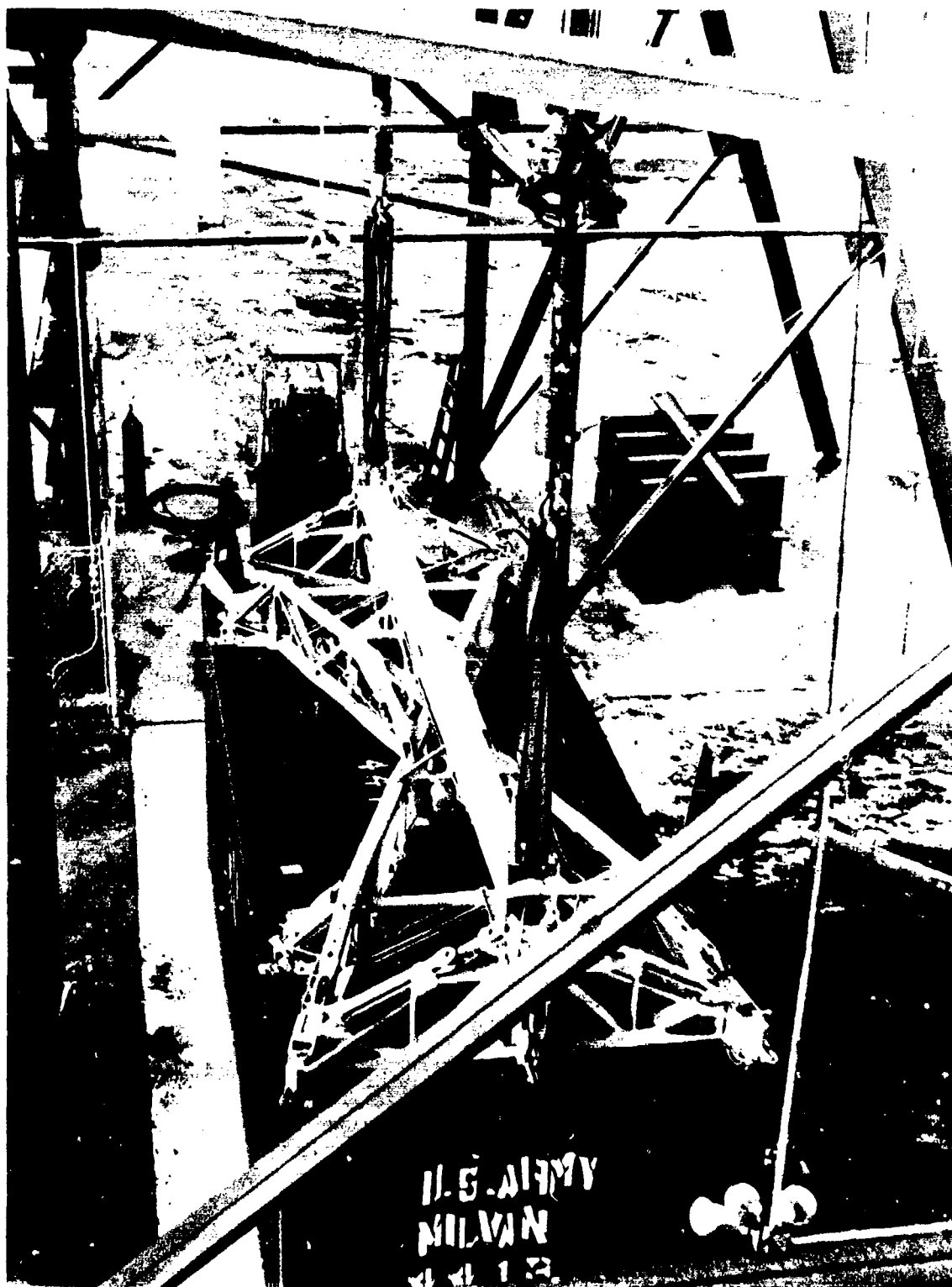


Figure 166. Container Handling Device SK24955.

### Static Capacity

The test loads described above under Lifting Capacity were held suspended for periods exceeding 5 minutes in the normal course of testing. In many cases, loads were held statically with the pneumatic power generator at idle or completely shut down. During these static checks, loads were monitored on the digital display unit.

### Cable Angle

Maximum design cable angles were verified in the pitch direction with an inclinometer (Engis Equipment Company, Vernier Angle Gage Model A) and in the roll direction by measuring the linear and vertical displacement of the top of the cable end swage fitting at the coupling connection and calculating the angle. The couplings were positioned so that there was a dimension of 60 inches between the cable guide of the angle sensor mechanism and the top of the cable end swage fitting. The couplings were then manually displaced with a manila line attached to the coupling/cable assembly connection in the four mutually perpendicular directions corresponding to the fore, aft, left, and right directions of helicopter flight. The cable angle sensors confirmed that the following angles could be attained without the cable contacting any structure, and that the automatic hoist shutdown system operated correctly.

<u>Direction</u>	<u>Design Max. Angle</u>
Forward	30°
Aft	40°
Left	30°
Right	30°

### Tension Member Velocity

Loaded tension member velocities were measured during the testing outlined under Lifting Capacity. Unloaded tension member maximum payout speeds were recorded on each hoist while lowering the empty cargo couplings and signal conductor. The speeds were observed on speed indicators. Table 82 provides a list of maximum measured tension member velocities at various times during the program.

TABLE 82. MAXIMUM MEASURED TENSION MEMBER VELOCITIES - FPM										
2-pt. Test Cycles*	Mode **	UNLOADED				2-pt Test Cycles*	LOADED(29-TON 2-PT.SUSPENDED LOAD)			
		Fwd Hoist		Aft Hoist			Fwd Hoist		Aft Hoist	
		Up	Down	Up	Down		Up	Down	Up	Down
83	Sync	100	--	102	--	158	51	69	53	70
385	Sync	109	--	110	--	238	55	70	56	70
385	SH	115	54	--	--	360	54	65	55	65
385	SH	--	--	119	74	462	54	70	55	71
424	SH	118	54	--	--	488	52	64	54	65
424	SH	--	--	118	79	599	57	62	58	62
424	Sync	112	--	112	--	633	55	60	57	60
572	SH	117	54	--	--	725	53	62	55	62
572	SH	--	--	124	71	765	52	61	54	61
782	Sync	100	--	100	--	799	55	60	57	60
910	SH	--	--	123	75	855	51	61	53	61
910	Sync	100	50	100	51	896	52	65	52	65
912	SH	--	--	115	70	911	50	65	50	65
912	Sync	110	50	110	50					
* Number of 29-ton 2-point test cycles completed prior to velocity check. ** Sync - Both hoists operated simultaneously. SH - Single-hoist operation.										

\* Number of 29-ton 2-point test cycles completed prior to velocity check.  
 \*\* Sync - Both hoists operated simultaneously. SH - Single-hoist operation.

### Braking

Normal braking was demonstrated in conjunction with the test outlined in the lifting capacity section of this report. In addition, test loads were stopped clear of the ground and the pneumatic power supply was shut down to verify the static holding capability of the hoist drive integral brake system. The brake was used to hold the various loads for a minimum of 5 minutes without any inputs by the load controlling crewman.

### Static and Dynamic Hook Releases

Normal release of each cargo coupling was verified with hook loads of 40, 201, and 1,000 pounds. With the load just clear of the ground, the normal hook release was actuated once. Complete separation of the load from the cargo coupling was confirmed visually. Closure of the hook load beam was confirmed by indicators at the LCC station and by manual confirmation at each cargo coupling. Figure 167 shows the release of the 1,000-pound load.

Mechanical alternate release was verified at each cargo coupling using the same hook loads. With the load just clear of the ground, the mechanical release was actuated. Complete separation of the load from the cargo coupling was confirmed visually.

Overload release prevention was verified at each cargo coupling using a 2,100-pound load. With the load just clear of the ground, the normal (electrical) and the alternate (mechanical) release modes were actuated individually. Retention of the load was confirmed visually.

### Control Functions

Each of the normal and emergency cargo handling system control functions listed below was cycled through its full range of operation, and the actual system responses were observed and documented. Succeeding paragraphs provide descriptions of the findings of each of these tests.

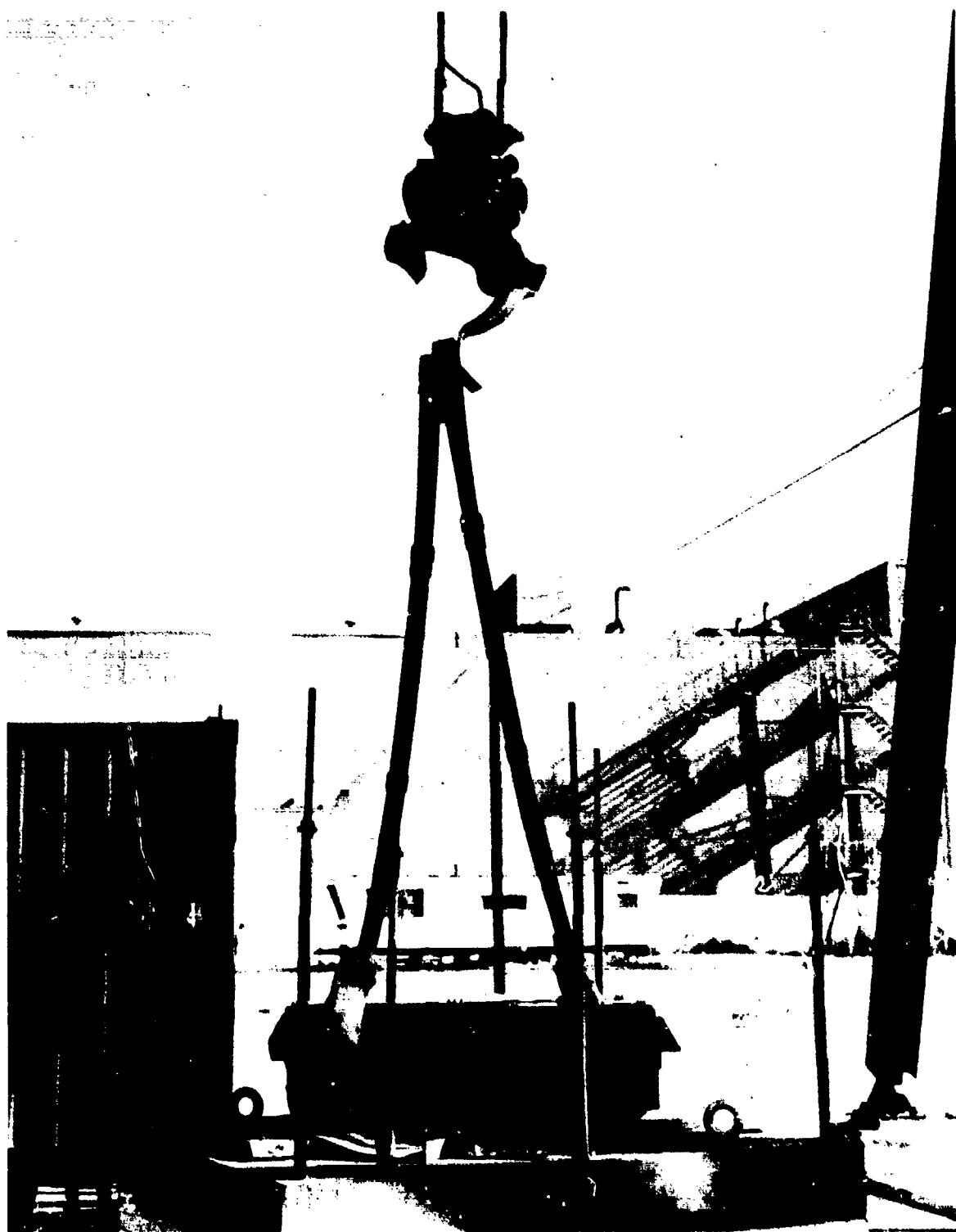


Figure 167. Release of the 1,000-Lb Load From 301-10231 Coupling Assembly.

1. Forward hoist command
2. Aft hoist command
3. Sync control
4. Forward hoist span position control
5. Aft hoist span position control
6. Forward coupling operate/stow limit
7. Aft coupling operate/stow limit
8. Forward hoist speed limiting
9. Aft hoist speed limiting
10. Cable cut shut down
11. Forward hoist cable pitch angle shut down
12. Aft hoist cable pitch angle shut down
13. Forward normal release safe/arm switch
14. Aft normal release safe/arm switch
15. Normal release switch
16. Mechanical release switch
17. Control panel power switch
18. Control station transfer

Forward hoist command was designed to provide control of the hoisting or reversing speed of the cable drum of the forward hoist. The control is activated by a pressure sensitive thumb switch mounted forward (in reference to the aircraft installation) on a hand grip. The design of the control was such that pressure resulted in a cubical parabola-shaped signal to provide increased sensitivity at slow speeds. During the testing, the control performed essentially as intended except that the signal shaping did not provide the optimum control in the high-speed range. The signal shaping format was changed to provide a constant command signal at any thumb pressure above that required for maximum speed while maintaining the increased sensitivity at slow speeds. With the revised shaping, the control operated as desired.

Aft hoist command - This command was modified in the same manner as the forward hoist system and resulted in improved control at maximum speed while maintaining high sensitivity in the low-speed range.

Sync Control was designed to provide synchronous operation of the forward and aft hoists and was activated by a push button switch located next to the control grip. Activation of the synchronized mode was indicated by a red lamp located on the grip. Activation resulted in the forward hoist command switch becoming the synchronous hoist command. When the sync control was operated, it performed as



designed, with less than a 1 $\frac{1}{2}$  (1 foot) difference in cable payout after three 50-foot lift cycles of the 29-ton demonstration load.

Forward hoist span control was designed to position the forward hoist at either a forward or aft position. The positioning mechanism was activated by a pushbutton switch. When the hoist was locked in position, the hoist positioning switch was illuminated indicating the position the hoist was in (i.e., FWD or AFT). The operation/stow switch was also illuminated to indicate operation. Activation of the control with no load on the hoist resulted in locking pins being withdrawn and the extinguishing of both switch lights and it would not be possible to operate the hoists. When the pins were fully withdrawn, the span position motor/mechanism would move the hoist to the desired position, at which point the wheels of the hoist module would position in detents of the traversing tracks and the locking pins would automatically move to the locked position. When fully locked, the traversing control switch and operate/stow switch illuminated, indicating the new position of the hoist module and allowing operation of the hoist. The movement of a hoist could be reversed anywhere in the cycle by the control switch. To stop the move anywhere in the cycle other than in the locked position, control panel power had to be shut off. The duration of the forward hoist moving cycle from one position to another was 55 seconds, which met the goal of one minute or less.

Aft hoist span control operated the same as the forward span control. The duration of the aft hoist moving cycle was also 55 seconds.

Forward coupling operate/stow limit control was designed to limit hoist operation between maximum 'up' and 'down' coupling positions. The design provided a push-button switch which allowed overriding the 'up' operation stop limit so that the coupling could be hoisted to the 'stow' position. Stopping of the hoist in the 'up' position was accomplished automatically by proximity switches. It was found during the initial functional check of the system that the target located on the hoist drum and designed to activate the proximity switch did not remain in contact with the switch for a long enough duration. A redesigned target in the form of a plate increased the proximity duration sufficiently to stop the hoist. With the redesigned target, the control operated as intended.

The 'up' limit proximity switches were located and adjusted on the ITR to stop the coupling approximately 5 feet below the hoist at the operational limit and 4-1/2 feet below the hoist at the stow limit.

When the operation 'up' limit is reached, an 'up' limit condition lamp lights and further hoisting is not possible; however, reversing (operating hoist down) is possible and is indicated by the switch remaining illuminated OPR (operate). At this point, pressing the operate/stow switch allows hoisting to the 'stow' position. This condition is indicated by a 'stow' command light. When the 'stow' position is reached, the switch indicates 'stow'; then the 'stow' command light extinguishes and it is not possible to operate the hoist up or down. Pressing the OPR/STO switch results in the switch indicating OPR, the stow command lamp lighting, and the allowing of operation of the hoist down only. Throughout these sequences, the lamp indicating that the operation 'up' limit has been reached, remains on and only operating the hoist down is possible even below the operation up limit. When in this condition, in order to hoist, it is necessary to turn control power off and then on to reset the control for normal operation, up and down. This reset also extinguishes the operation 'up' limit indicating lamp and lights the operation command light.

The operating 'down' limit was designed to be activated at a cable payout of 100 feet by an indicator signal. Since it was not practical to pay out 100 feet of cable from the ITR, which has a working height of approximately 65 feet, attenuation of the signal by the addition of gain controls allows the selection of a down limit of 100, 70, or 50 feet. When the 70- or 50-foot limit is selected, the hoist stops at the appropriate cable payout lengths programmed into the system. The 'down' limit condition light comes on, and operation is possible only in the up direction. When above the 'down' limit again, resetting the control for normal up and down operation is necessary and is done by turning control power off and then on. At this time, the down limit condition light extinguishes.

The design provides an additional hoist 'down' limit beyond the operation 'down' limit and is activated by a micro-switch. This function was operated when the cables were changed at the completion of the demonstration tests. All control functions operated as intended.

Aft coupling operate/stow limit operated the same as the forward control.

Forward hoist speed limiting is an automatic control designed to provide a proportional slow down in hoist speed between a designated cable length and the stow limit when hoisting and another cable pay-out length and 'down' operating limit when reeling out. The control is initiated by the cable payout signal. See Table 83 for the nominal cable lengths and operating and stow limits. This control operated as intended.

Aft hoist speed limiting operated the same as the forward hoist speed limiting. Table 83 shows the nominal cable lengths and operating and stow limits.

Cable cut shutdown is designed to stop hoist operation when the cable cut switch is activated. The switch was activated without explosive squibs installed and the hoists stopped and could not be operated, as designed.

Forward hoist cable pitch angle shutdown is designed to automatically shut down hoist operation when the cable forward or aft pitch angle is 30° or greater. This control was checked manually as described previously under the cable angle functional check and also while operating using the single-point adapter. The angles causing shutdown indications were measured during the manual check, and were 30°9' forward pitch and 31°50' aft pitch. During single-point operation of both hoists, the load was hoisted until the angles of the cables were great enough to reach an automatic shutdown.

TABLE 83. Cable Payout Limits.						
Hoist	Control Gain Setting	'Up' Slow Speed Initiation	'Up' Operation Limit	'Up' Stow Limit	'Down' Slow Speed Initiation	'Down' Operation Limit
Fwd	100'	22'	5'	4½'	*	*
Fwd	70'	14'	5'	4½'		50' **
Fwd	50'	10'	5'	4½'		38'
Aft	100'	20'	5'	4½'	*	*
Aft	75'	14'	5'	4½'		50' **
Aft	50'	10'	5'	4½'		38'

\*Not practical to obtain on integrated test rig, which has working height of 65 feet.

\*\*Control was set to stop at the 38-and 50-foot lengths, respectively to allow for sling and MILVAN container height.

Aft hoist cable pitch angle shutdown operated the same as the forward hoist shut down. The measured aft pitch angle, which initiated a shut-down signal, was  $29^{\circ} 12'$ . The forward pitch angle was limited to approximately  $26^{\circ}$  due to a cotter key that was used to replace a pin in the cable angle sensing mechanism. This interference was corrected and the shut down was checked; however, the angle at shutdown was not measured. The angle was estimated to be approximately  $30^{\circ}$ .

Forward normal release safe/arm switch was designed to provide a safety for the normal release of the coupling. When this push-button switch is illuminated 'SAFE', pressing the normal release will not open the coupling. It is necessary to activate the switch so that it is illuminated 'ARM' before a normal release of the forward coupling can be made. This control operated as designed.

Aft normal release safe/arm switch operates the same as the forward switch and controls the release of the aft coupling. This control operated as designed.

Normal release switch electrically opens either the forward or aft coupling, or both couplings simultaneously, depending on which coupling or couplings are armed, providing that the coupling loads are less than the 1,000 to 2,000 pounds mechanical lockout level within the coupling itself. This control operated as designed.

Mechanical release was designed to be a backup mode of opening the couplings in case the normal electrical release is not operational. Activating the push button for this control in the dual hook mode opens air supply valves momentarily to each of the signal reel turbines which induces sudden jerks in the signal conductor cables releasing loads less than 1,000 pounds from each of the couplings. In the single-point mode, an electrical lockout system prevents the mechanical jerk from being applied to the upper coupling. These controls operated as designed.

Control panel power switch is used to turn on power, to reset the hoist command controls after operation limits are activated, to reset the logic control after any other automatic shut down and to stop the hoists in emergencies. This switch operated satisfactorily.

Control station transfer was designed to transfer control of the system to either the cockpit or the LCC station. The push-button switch illuminates to indicate which station is selected, "LCC" or "CKPT". This control was not used on the ITR, which only had an LCC station.

Sensor Function - Each of the sensors for cable angle, cable length and cable tension was checked for its ability to follow the required function, the smooth operation of the pickup devices, and the correct response of the indicators. Each sensor was moved through its full range of design maximum angles and performed as designed.

#### Demonstration Program

The demonstration program consisted of the following test:

1. 904 two-point hoisting cycles of a 29-ton load.
2. 904 single-point hoisting cycles of a 29-ton load.
3. Maximum static load tests in both the single- and two-point suspension configurations.

#### Two-Point Suspension Demonstration

The test load for the two-point demonstration cycling was configured to an actual gross weight of 58,544 lb, based on the design load of 56,000 lb, a 60/40 load distribution, a 2520-lb aerodynamic down load (50/50 split), and available ballast increments.

Design Load Distribution - (60% of load on forward hoist selected arbitrarily since the design covers any load arrangement within the 60/40 to 40/60 limits.)

Forward hoist	=	33,600	+	1,260	=	34,860	lb
Aft hoist	=	22,400	+	1,260	=	23,660	lb
Total, Design Load					=	58,520	lb

### Test Load Configuration

MILVAN S/N 4413	=	4,630 lb
SK24955 Container Handling Device S/N 2	=	1,200 lb
1/2" Steel Plate covering MILVAN floor	=	<u>3,060 lb</u>
Tare Weight, Total	=	8,890 lb

KirkSITE ballast	=	48,594 lb
Lead ballast	=	<u>1,060 lb</u>
Ballast, Total	=	49,654 lb

Total Test Load Wt. (MILVAN + Ballast + Tare)	=	58,544 lb
---	---	-----------

### Weight and Balance Measurements

Final load distribution measurements were made using two 50,000-lb load cells and a Baldwin-Lima-Hamilton Percent Load Indicator.

Forward hoist load	59.2%
Aft hoist load	40.8%

Figure 168 shows the ballasted MILVAN and the container handling device. Figure 169 shows the load measurement configuration with the container load lifted off the ground.

A complete description of the test fixture (Integrated Test Rig) used for all three parts of the demonstration program is contained in Volume II of this document.

A total of 904 two-point hoisting and lowering cycles were performed using the load weight of 58,544 pounds. Testing consisted of 113 sets of the basic eight endurance cycle elements (113 x 8 = 904) shown in Table 84. Test conditions for this demonstration included:

1. External load type: 8x8x20-foot MILVAN container
2. Center of gravity: 60/40 split
3. Suspension: Tandem dual hook
4. Longitudinal hoist span (traverse) setting: 16 feet (except where noted)
5. Container lifting device: U.S. Army Helicopter Transported Container Handling Device

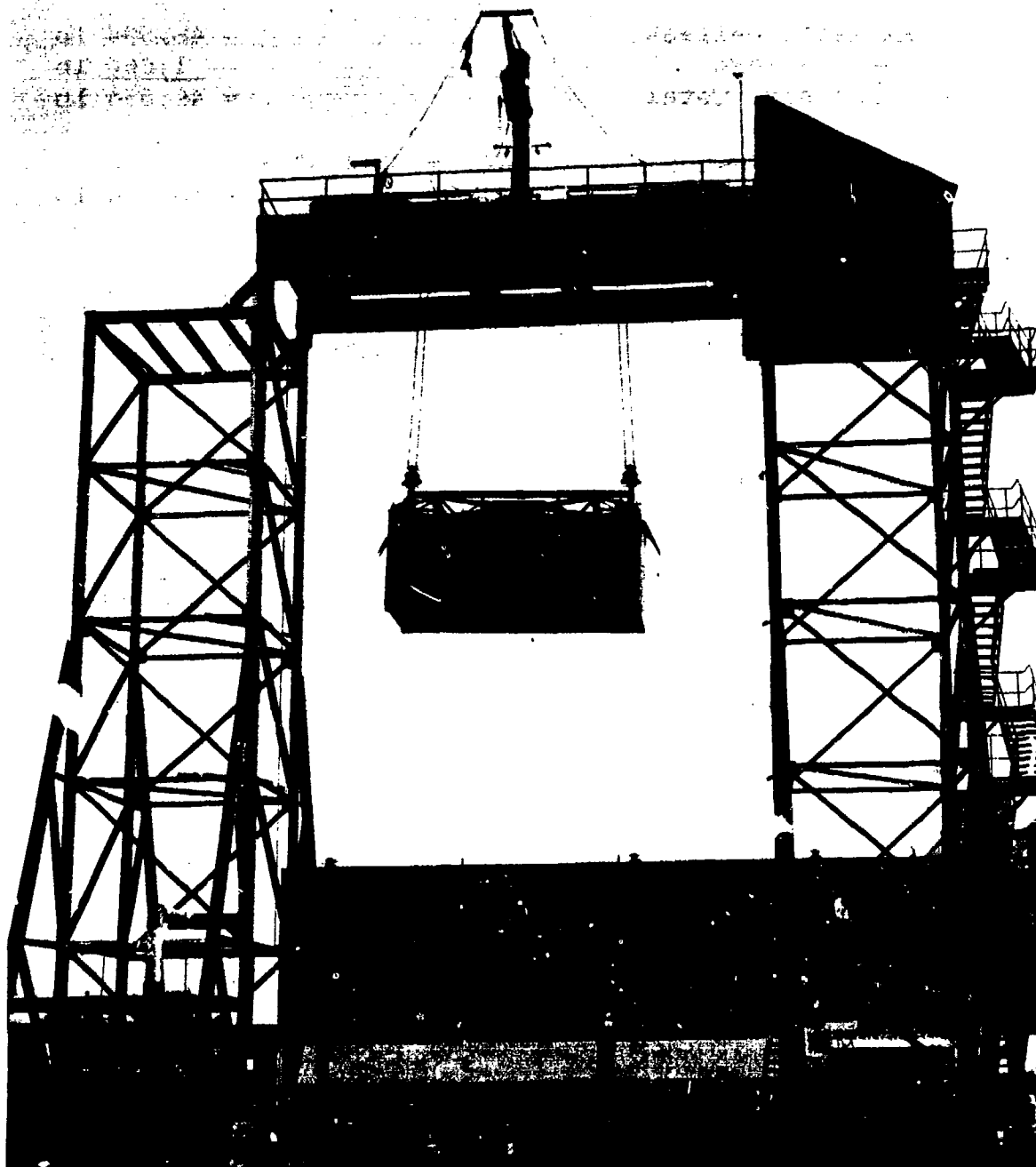


Figure 168. Demonstration Test of HLH/ATC Two-Point Suspension with MILVAN and Container Handling Device - Test Load 58,544 Pounds.

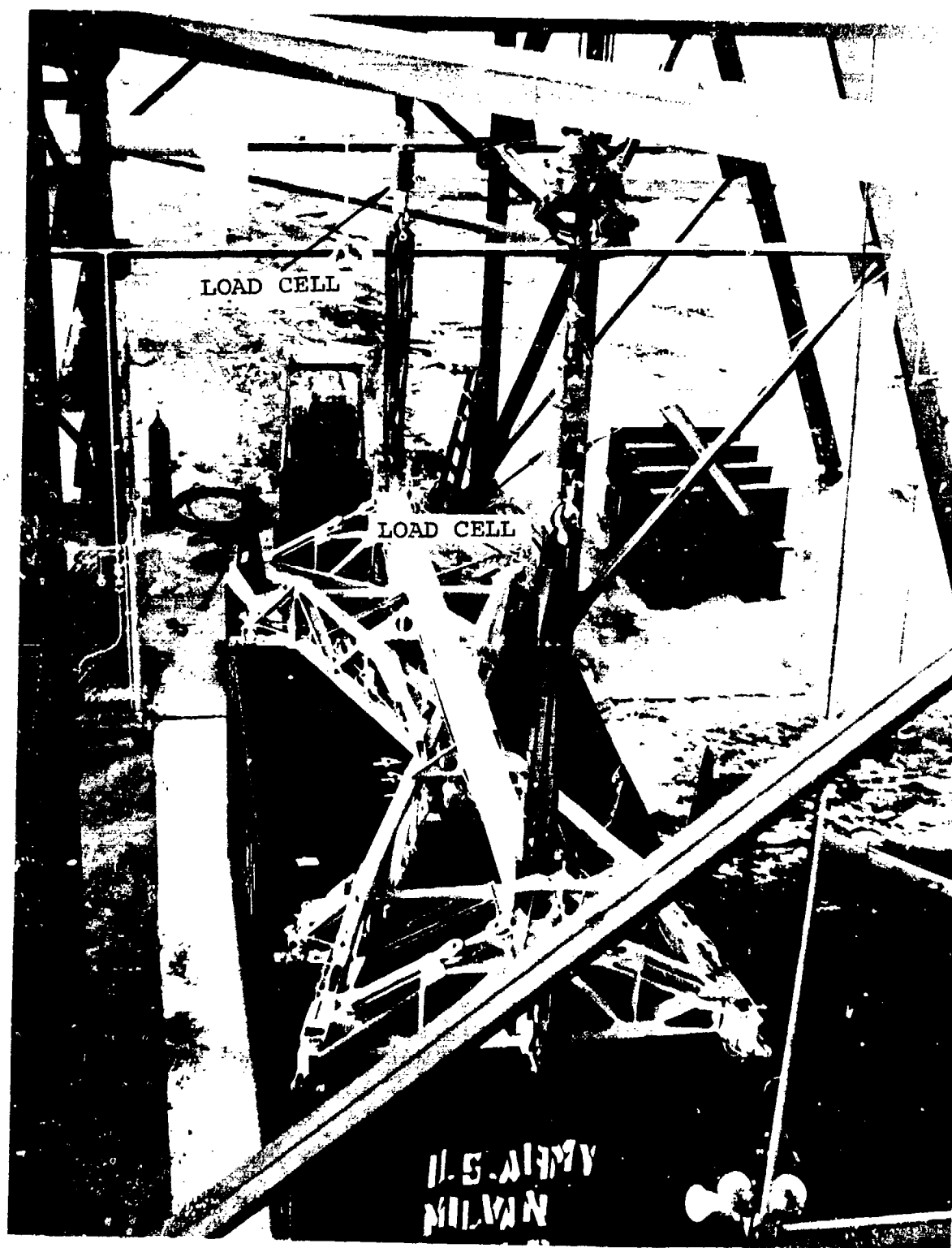


Figure 169. Instrumentation and Rigging Used for Weighing Ballasted MILVAN.



Table 84. Two-Point Suspension Demonstration Consisting of Eight Basic Endurance Cycle Elements.

Sequence Item	Activity	Special Considerations
1	Load	
2	Lift Load (50')	Attain Design Hoist Speed (60'/min)
3	Lower Load (50')	"
4	Lift Load (50')	"
5	Lower Load (50')	"
6	Hook Release	Normal Mode
7	Load Hookup	
8	Lift Load (50')	Attain Design Hoist Speed (60'/min)
9	Lower Load (50')	"
10	Lift Load (50')	"
11	Lower Load (50')	"
12	Hook Release	Normal Mode
13	Cycle Traversing	16' to 26' to 16'
14	Load Hookup	
15	Lift Load (50')	Attain Design Hoist Speed (60'/min)
16	Lower Load (50')	"
17	Lift Load (50')	"
18	Lower Load (50')	"
19	Hook Release	Normal Mode
20	Load Hookup	
21	Lift Load (50')	Attain Design Hoist Speed (60'/min)
22	Lower Load (50')	"
23	Lift Load (50')	"
24	Lower Load (50')	"
25	Hook Release	Backup Mode (Mechanical)
26	Cycle Traversing	16' to 26' to 16'

All load hookups were performed by ground handling personnel who engaged the cargo couplings with the lifting fittings of the container device. The Integrated Test Rig operator, in the simulated helicopter load controlling crewman station, then took over and performed the load lifts and descents, hook releases, and span positioning traverse cycles.

No periodic maintenance was scheduled or performed on the cargo handling system components during the demonstration. Malfunctions which occurred during this test are presented in a separate section, following the three demonstration test sections.

### Single-Point Suspension Demonstration

The test load for the single-point demonstration was configured to an actual gross weight of 58,559 pounds. The load consisted of two stacks of seven nominal 4000-pound kirksite blocks, each with a top mounted ballast box to bring the combined weight over the minimum required level of 58,520 pounds.

The suspension configuration utilized the single-point adapter assembly attached to the basic cargo handling system. Load attachment was via two 100,000-pound ultimate tensile strength (UTS), Aeroquip nylon donuts and a series of U.S. Army Aerial Delivery, 12-foot, six-ply nylon slings, FSN 1670-823-5041, as shown in Figures 170 and 171.

A total of 904 single-point hoisting and lowering cycles were performed consisting of 113 sets of the basic eight endurance cycle elements shown in Table 85. Test Conditions for this demonstration included:

1. External load type: Dual stacks of kirksite blocks
2. Suspension: Single-point adapter
3. Longitudinal hoist span (traverse) setting: 16 feet

All load hookups were performed manually by ground handling personnel who engaged the nylon donuts with the cargo coupling. The integrated test rig operator then took over and performed the load lifts and descents, and hook releases.

No periodic maintenance was scheduled or performed on the cargo handling system components during the demonstration. Malfunctions which occurred during this test are presented in a separate section following the three demonstration tests.

### Maximum Static Load Demonstration

#### Single Hoist

The aft hoist assembly was used for this test in conjunction with hook serial number 2. The setup is shown in Figure 172.

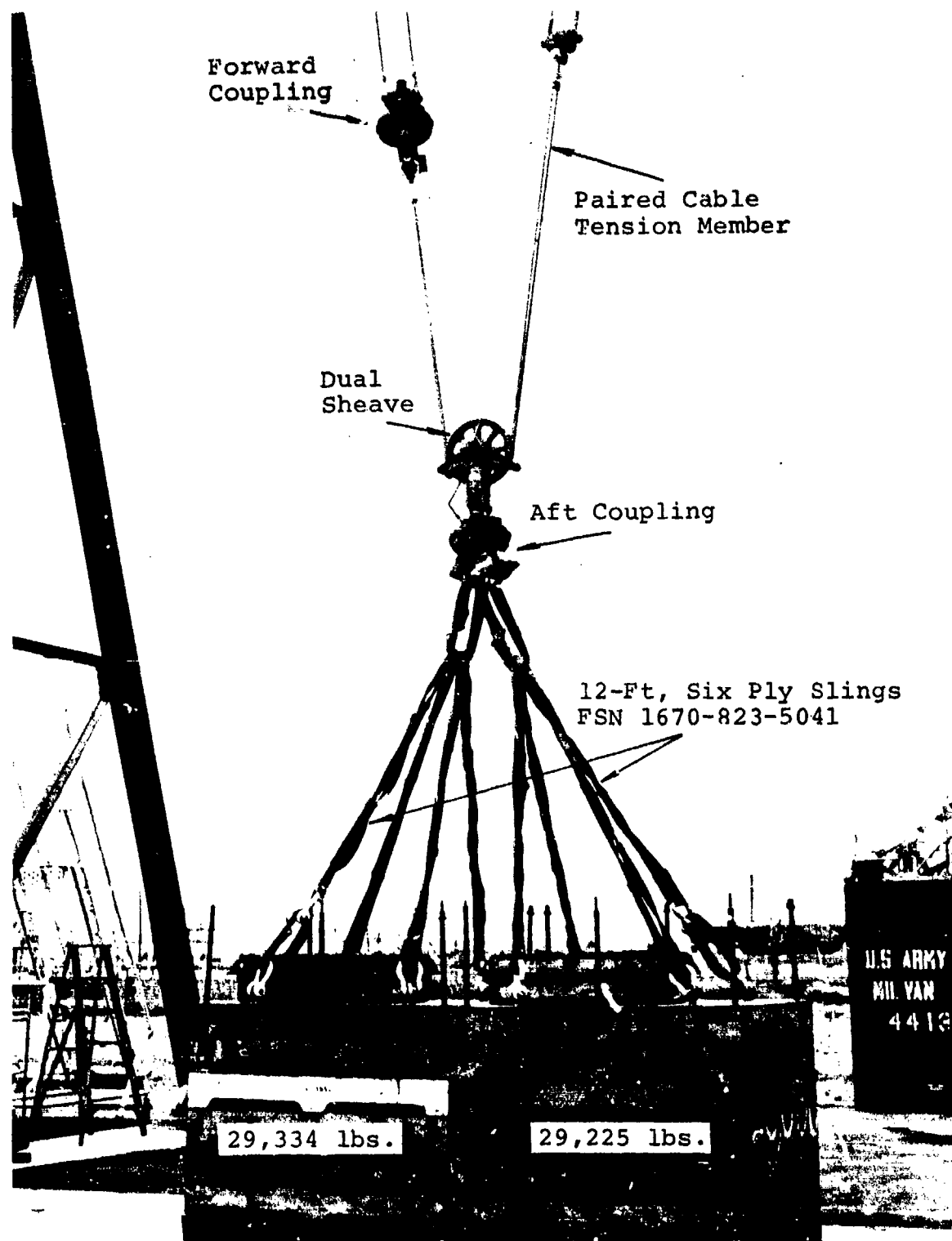


Figure 170. Single-Point Adapter and 58,559-lb Test Load (58,520 Design).

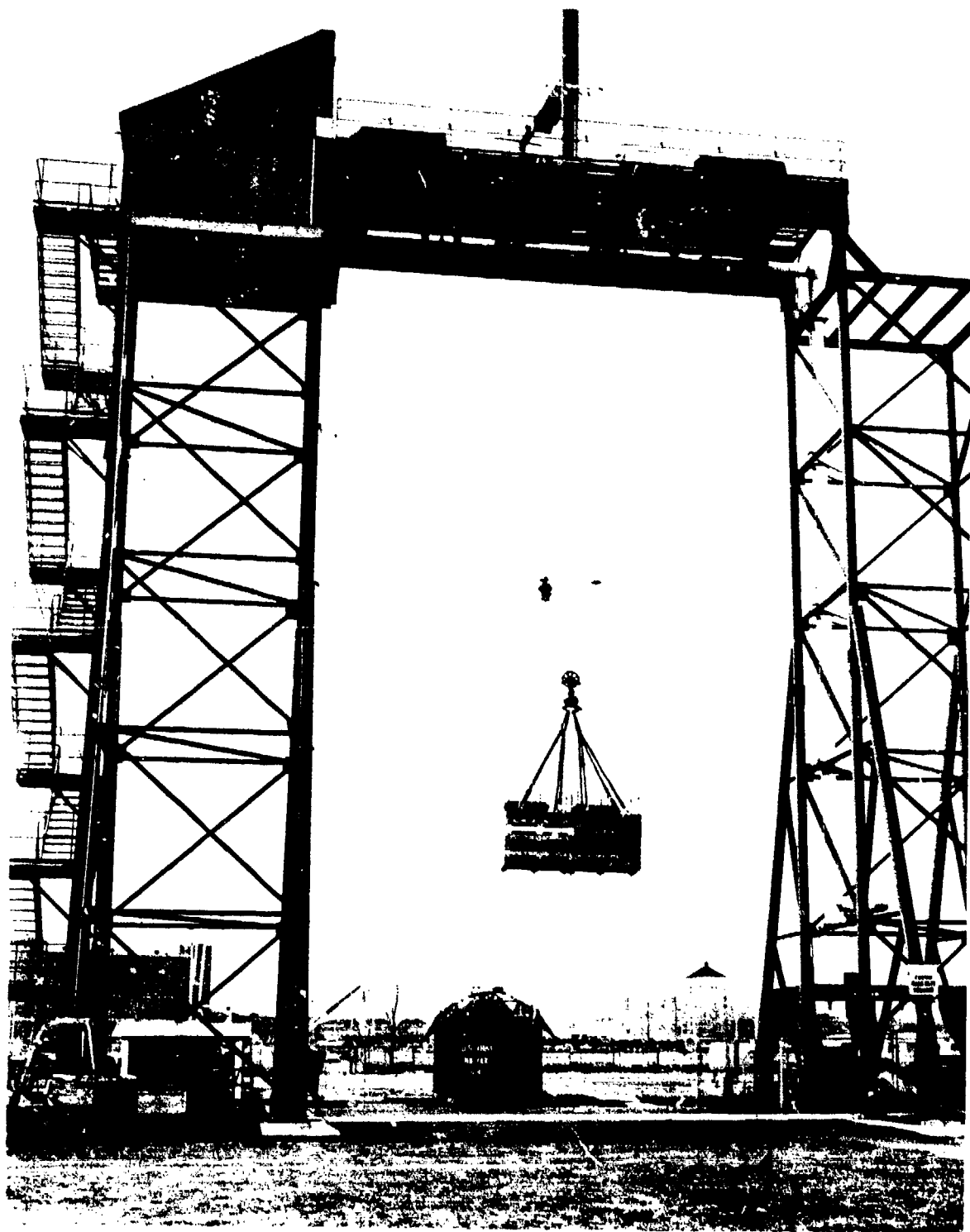


Figure 171. Hoisting the 58,559-lb Test Load Used For Single-Point Demonstration Cycles.

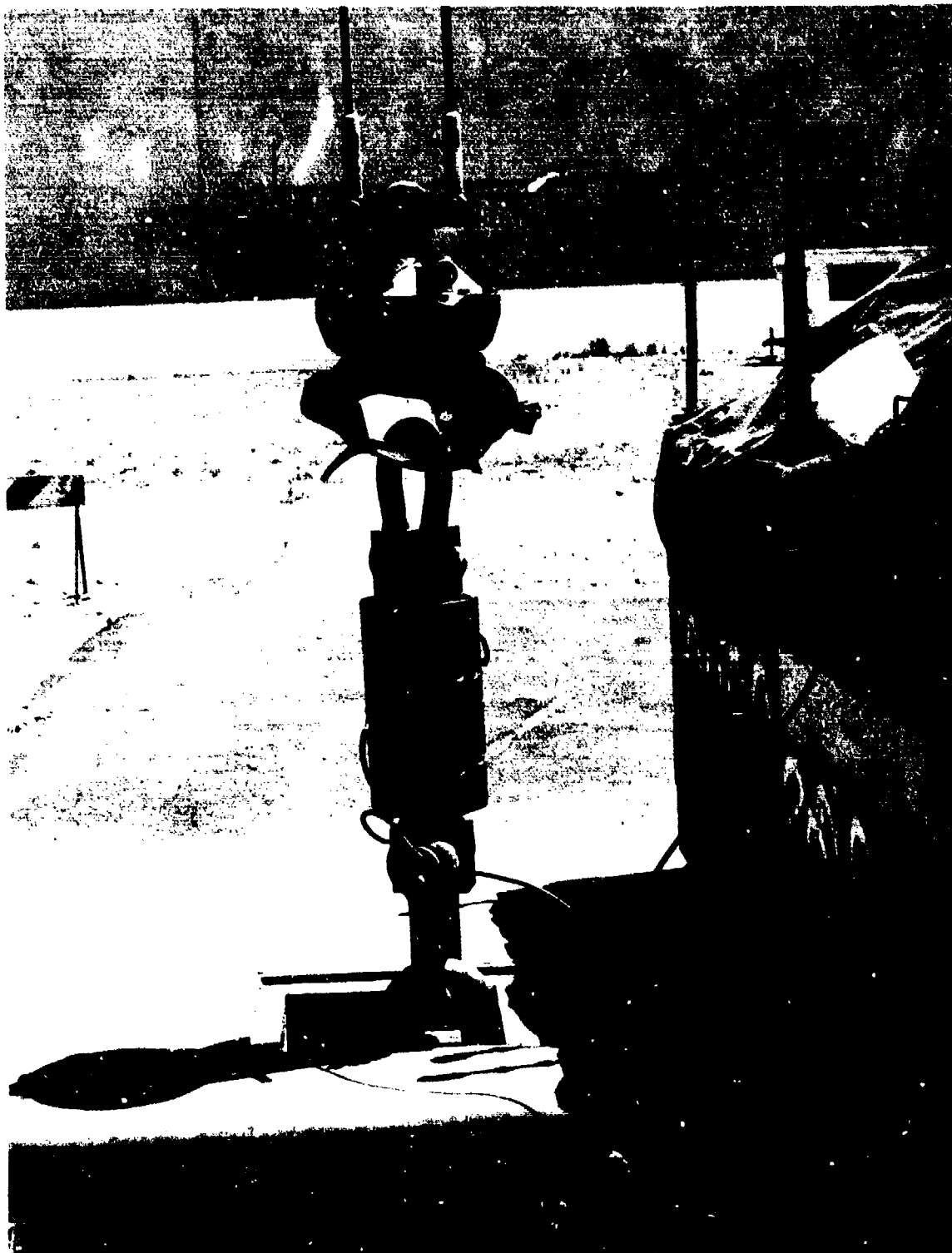


Figure 172. Maximum Static Load Demonstration.

TABLE 85. Single-Point Suspension Demonstration Consisting of Eight Basic Endurance Cycle Elements		
Sequence Item	Activity	Special Considerations
1	Load Hookup	
2	Load Hoist	Attain Design Hoist Speed (60'/min)
3	Load Lower	"
4	Load Hoist	"
5	Load Lower	"
6	Hook Release	Normal Mode
7	Load Hookup	
8	Load Hoist	Attain Design Hoist Speed (60'/min)
9	Load Lower	"
10	Load Hoist	"
11	Load Lower	"
12	Hook Release	Normal Mode
13	Load Hookup	
14	Load Hoist	Attain Design Hoist Speed (60'/min)
15	Load Lower	"
16	Load Hoist	"
17	Load Lower	"
18	Hook Release	Normal Mode
19	Load Hookup	
20	Load Hoist	Attain Design Hoist Speed (60'/min)
21	Load Lower	"
22	Load Hoist	"
23	Load Lower	"
24	Hook Release	Backup Mode (Mechanical)

A checkout run was made with the PPG operating at 100% rpm and 63 psia supply pressure. This run used an 8-ply nylon donut between the hook and the "dead man" load shackle. A light load of 13,000 pounds was applied for system checkout and was satisfactory.

The nylon doughnut was removed and the hook was then coupled directly to the "DEAD MAN" load. Loads of 28,000 lb to 40,000 lb were applied as buildup increments, and it was found that the characteristics of the hoist and the control system made loading and unloading quite sensitive.

It was anticipated that the loading and sudden release of tension might cause the load isolators to bottom out

at both ends of their stroke, subjecting the torque reaction arms to abnormal loads. To eliminate this possibility, both load isolators were bled of pressure. Loads were then applied up to 83,000 pounds for brief periods of time to evaluate system reactions, which proved to be satisfactory.

Final test loads of 88,000 lb were accomplished in two runs. Inspection of the hook and hoist assembly during and after the test showed no apparent deformation, deterioration, or damage resulting from this test.

#### Dual Hoist (Single-Point Mode)

Equipment for this test included: both forward and aft hoists, their cable assemblies, the single-point adapter, and hooks (serial numbers 1 and 4). Cargo hook S/N 1 was used at the load lifting point and S/N 4 cargo hook at the location above the single-point sheave.

Loading was accomplished by pulsing the hoists individually with the controller in the single-hoist operating mode. The first run was made over a fifteen second period in three successive load increments until a 70-ton (140,000-lb) load was obtained. The load was then dropped back to 54 tons (108,000 lb) and held there for 19 seconds. The second run was made, and with hoisting command nulled at 70 tons (140,000 lb), the loading continued to 74 tons (148,000 lb). At that load, after a period of 1/2 second, the hook S/N 1 failed.

#### Demonstration Program Malfunctions

The following malfunctions occurred during the demonstration tests. Each is presented with the number of reoccurrences, the lift cycle or cycles at which it occurred (Cycles 1 to 904 are two-point; 905 to 1808 are single point), and the cause.

1. Unable to open hook using normal mode.

Number of Occurrences: 11

Lift Cycles at which Malfunctions Occurred: 8, 16, 460, 540, 824, 856, 1306, 1442, 1488, 1616, and 1632. (Cycles 1 to 904, 2-point mode; 905 to 1808, single-point mode.)

Cause

Throughout the test program, the signal conductor cable failed in various modes, being open and/or shorted. This is primarily due to the use of the hook mechanical release method, where the outer shell of the signal conductor cable becomes the mechanical member of the release method. This outer shell elongates when pulled for the mechanical release, thereby pinching or breaking the internal signal wires of the cable.

2. "Hook Open" indication under load.

Number of Occurrences: 10

Lift Cycles at which Malfunctions Occurred: 128, 332, 361, 395, 1112, 1124, 1130, 1143, 1175, 1600.

Cause

Open and/or shorted signal conductor wires.

3. Forward hoist creeps up upon shutdown with or without a load.

Number of Occurrences: 6

Lift Cycles at which Malfunctions Occurred: 339, 357, 363, 368, 450, 456.

Cause

Inherent design feature in the hoist controller. Efforts to install limited changes in component values result in improved operation in the shutdown mode, but affected the stability of the hoisting and lowering modulating valves.



4. Articulating ducts worn (air supply).

Number of Occurrences: 5

Lift Cycles at which Malfunctions Occurred: 140,  
369, 776, 1410.

Cause

Duct-shaping wire coil perforates outer duct surface, which allows air leak path between layers and causes outer rubber coating to peel off and work out from under band clamp.

Note: Prototype and production aircraft will have fixed hoists, which will not require the use of these ducts.

5. Aft hoist out of sync during maximum up operation (with cold hoists).

Number of Occurrences: 4

Lift Cycles at which Malfunctions Occurred:  
41, 44, 123, 146.

Cause

In the sync mode during this abnormal operation, one hoist would start while the other would not, or in some cases, would start later.

6. Forward hoist would not respond at all times to a command in the sync mode.

Number of Occurrences: 4

Lift Cycles at which Malfunctions Occurred:  
79, 131, 155, 163.

Cause

Original sync mode logic allowed individual hoist operation as soon as the hoist brake switches were closed. Since this did not always occur simultaneously, one hoist would start to move before the

other. A change in logic, requiring closure of both hoist brake switches before either hoist could move, corrected the condition.

7. Aft hoist emitting light smoke from exhaust duct.

Number of Occurrences: 4

Lift Cycles at which Malfunctions Occurred:  
503, 516, 688, 733.

Excessive clearance in air turbine labyrinth seal.

8. Aft-hoist main-bevel-gear chip warning light on.

Number of Occurrences: 4

Lift Cycles at which Malfunctions Occurred:  
555, 628, 1007, 1719.

Cause

Three instances were caused by metallic fuzz and the fourth by conductive grease from another part of the system.

9. Span positioning motor shorted out.

Number of Occurrences: 3

Lift Cycles at which Malfunctions Occurred:  
12, 816, 1808.

Cause

Water penetrated into the motor causing heavy corrosion of the starter and rotor assembly, which resulted in a breakdown of insulation on the rotor, causing electrical failure.

Note: The intended location of this assembly in the aircraft will not be exposed to the elements; the installation on the test rig provided no protection whatsoever, and each time it rained, water collected in this assembly.

10. Digital total load indicator readout periodically erroneous and intermittent.

Number of Occurrences: 3

Lift Cycles at which Malfunctions Occurred:  
163, 337, 1113.

Cause

Digital indicator was reading signals generated by the load isolator load cells and associated circuits which, from time to time, open circuited, shorted out, and became out of balance.

11. Modulating valve oscillates after stopping.

Number of Occurrences: 2

Lift Cycles at which Malfunctions Occurred:  
1266, 1343.

Cause

Spurious signals influenced the hoist controller.

12. Cable reeling mechanism jammed during hoisting.

Number of Occurrences: 1

Lift Cycles at which Malfunctions Occurred: 211

Cause

This condition only occurred on the forward system, primarily caused by the cable piling up on the reel due to the adverse angle of the cable because of the incorrect positioning of the reeling mechanism relative to the centerline of the hook. This condition also occurred during rig checkout when a reduced air supply orifice was used in an attempt to reduce the signal conductor cable tension. The reel was too slow for fast hoisting.

13. Hook disengaged from cargo handling device when engaging load at a high rate of speed.

Number of Occurrences: 1

Lift Cycles at which Malfunctions Occurred: 376

Cause

By design, the hook has a mechanical release feature actuated by a sudden increase in tension of the signal conductor cable from a steady 50-70 lb to over 250 lb -- in short, an inertial actuation release system. By driving the hook and the container handling device onto the load at speeds of over 40 ft/min, the required inertia is generated and the hook releases.

14. Aft hoist ceased operation abruptly while hoisting.

Number of Occurrences: 1

Lift Cycles at which Malfunctions Occurred: 451

Cause

The jackshaft in the ATM shifted position (weld failed), subsequently, the supporting bearing failed, allowing the turbine to run free and the brake to come on. One-piece jackshaft designed and retrofitted in all ATMs.

15. Aft hoist jammed in spanning track.

Number of Occurrences: 1

Lift Cycles at which Malfunctions Occurred: 472

Cause

Excessive side play between the wheels and the side rail in the area of the hard point recess.

16. Aft hoist stopped during descent with load and would not restart.

Number of Occurrences: 1

Lift Cycles at which Malfunctions Occurred: 532

Cause

Butt splice in the brake switch circuit loosened and open-circuited, causing the shut down.

17. Forward signal reel conductor chafing on side of level wind mechanism.

Number of Occurrences: 1

Lift Cycles at which Malfunctions Occurred: 540

Cause

Under certain conditions, the cable angle is such that the cable does not ride on the guide pulleys of the level wind mechanism.

18. After one successful mechanical coupling release, the coupling would not mechanically release.

Number of Occurrences: 1

Lift Cycles at which Malfunctions Occurred: 1058

Cause

This malfunction occurs when the signal conductor reel does not achieve the required inertia to release the hook. (This happens only when consecutive pulls are made.)

19. Forward cable tension indicator very erratic.

Number of Occurrences: 1

Lift Cycles at which Malfunctions Occurred: 1089

Cause

The tape indicator became detached from its drive mechanism.

- 20 Hoist down speed limited to 45 ft/min maximum.

Number of Occurrences: 1

Lift Cycles at which Malfunctions Occurred: 1122

Cause

Short circuit in the power circuits to the load isolators caused the voltage level available to the down command function circuits to be lower than required.

21. Cargo coupling assembly failed.

Number of Occurrences: 1

Lift Cycles at which Malfunctions Occurred:  
After 1808

Cause

This failure occurred during the last test of the program on the single-point dual hoist maximum static load (140,000 lbs). The first attempt to obtain 140,000 lbs was made momentarily but dropped back to 108,000 lbs, the second attempt did reach 140,000 lbs and was increased to 148,000 lbs. After 1/2 second at that load, the hook failed at the coupling side-plate lugs.

The design analysis and fabrication cycle for these parts was examined in detail. The analysis of the lug area included an assumption that results in a positive stress margin, however, a more vigorous analysis showed the lug to be approximately 11% below required strength.

In addition, the heat treat cycle for the parts did not include a solution treat after rough machining and before aging to the -T73 condition. This resulted in the material properties being those of six-inch plate rather

than the 2-to 3-inch section. Metallurgical examination of the failed parts confirms that the tensile properties were 61,000 psi UTS rather than the 63,000 psi UTS of the smaller section.

#### CONCLUSION

The Integrated Test Rig Demonstration Program confirmed the functioning of the ATC hardware as a cargo handling system. All functional requirements were achieved. Performance of the system for payout of an empty coupling did not meet the demonstration objective of 120 ft/min. The reduced performance in this mode is due to the excessive windage loss when running the hoisting turbine in reverse and is discussed in those sections of this report concerned with the hoist drive. The hardware is suitable for use in the prototype aircraft.

## TEARDOWN INSPECTION AND RESULTS

### OBJECTIVE

At the conclusion of the demonstration tests, the following subsystems were removed from the ITR, disassembled and visually inspected to evaluate their condition and assess their suitability for further use:

1. Hoist drive units - S/N 001 and 002
  - a. Hoist pneumatic control valves - forward units
  - b. Articulated duct - forward assembly
2. Hoist assemblies - S/N 103 and 104
3. Load isolators - S/N DRG-2267-73 and DRG-2269-73
4. Tension members - Fwd S/N RH-3 and LH-3  
Aft S/N RH-1 and LH-1  
SPA S/N RH-1 and LH-3
5. Couplings - S/N 2 and 4
6. Signal conductor reels - S/N 001 and 002
7. Single-point adapter - S/N 1
8. Span actuator - S/N 4
9. Displays - cable payout and cable tension units
  - a. Hoist grip (speed controller)

In addition to the visual inspection, the following component inspections were performed:

1. Hoist drums - magnetic particle, NDT
2. Tension members - dimensional checks, Eddy current NDT, and x-ray

Results of the teardown inspection are discussed under individual subsystem sections which follow.

### INSPECTION FINDINGS

#### HOIST DRIV

#### TEM

#### Operational Histories

The operational histories of the inspected hoist drive units are as follows:



Two-Point Hoisting Mode (58,544 lb Total)

S/N 001 (Aft hoist loaded at 12 tons) = 470 cycles  
S/N 002 (Fwd hoist loaded at 17 tons) = 904 cycles

Single-Point Hoisting Mode (58,559 lb Total)

S/N 001\* (Aft hoist loaded at 14.7 tons) = 904 cycles  
S/N 002 (Fwd hoist loaded at 14.7 tons) = 904 cycles

(\*Note: The jackshaft failure occurred in this unit during the two-point demonstration. A two-piece jackshaft replacement was installed prior to the single-point demonstration.)

Maximum Static Load Demonstration

S/N 001 Multi-point mode stall torque = 88,000 lb  
S/N 001 (Aft hoist) single-point mode = 74,000 lb  
S/N 002 (Fwd hoist) single-point mode = 74,000 lb

Findings

Inspection results of the disassembled units are as follows. An overall view of the parts from S/N 001 is shown in Figure 173. Significant comments on the components are as follows:

Gearbox and Turbine S/N 001

1. A small amount of fretting found on the jackshaft pinion end, P/N EP6003-35, bearing support O.D., and the P/N EP6003-109 bearing inner race I.D. (gear to bearing interface). Two cracks radiating from electron beam weld from shaft to lightening hole (see Figure 174).
2. Lube pump shaft, P/N EP6003-53: wear at scavenge pump journal bearing and at associated P/N EP6003-43 pump housing journal bearing.
3. The reversing turbine shroud of P/N EP6003-4513 turbine wheel assembly had minor shroud damage (nicks and rubbing) on the nozzle side from some foreign object.
4. A piece of the outer edge of one reversing turbine nozzle guide vane was broken off. This may have been the foreign object that caused the shroud damage noted in Item 3 above.
5. All other hardware in normal condition.

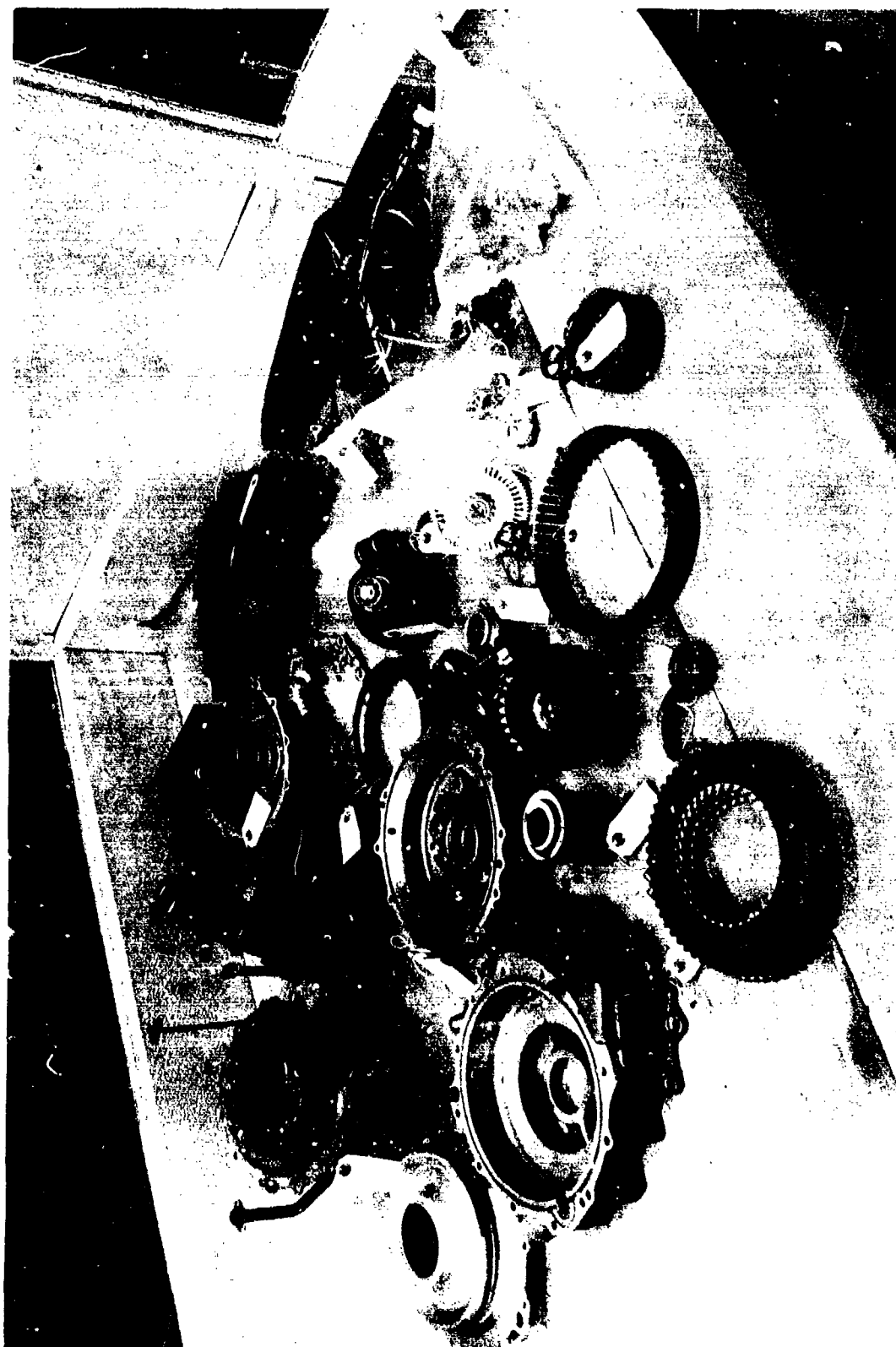


Figure 173. Hoist Drive Unit, S/N 001.

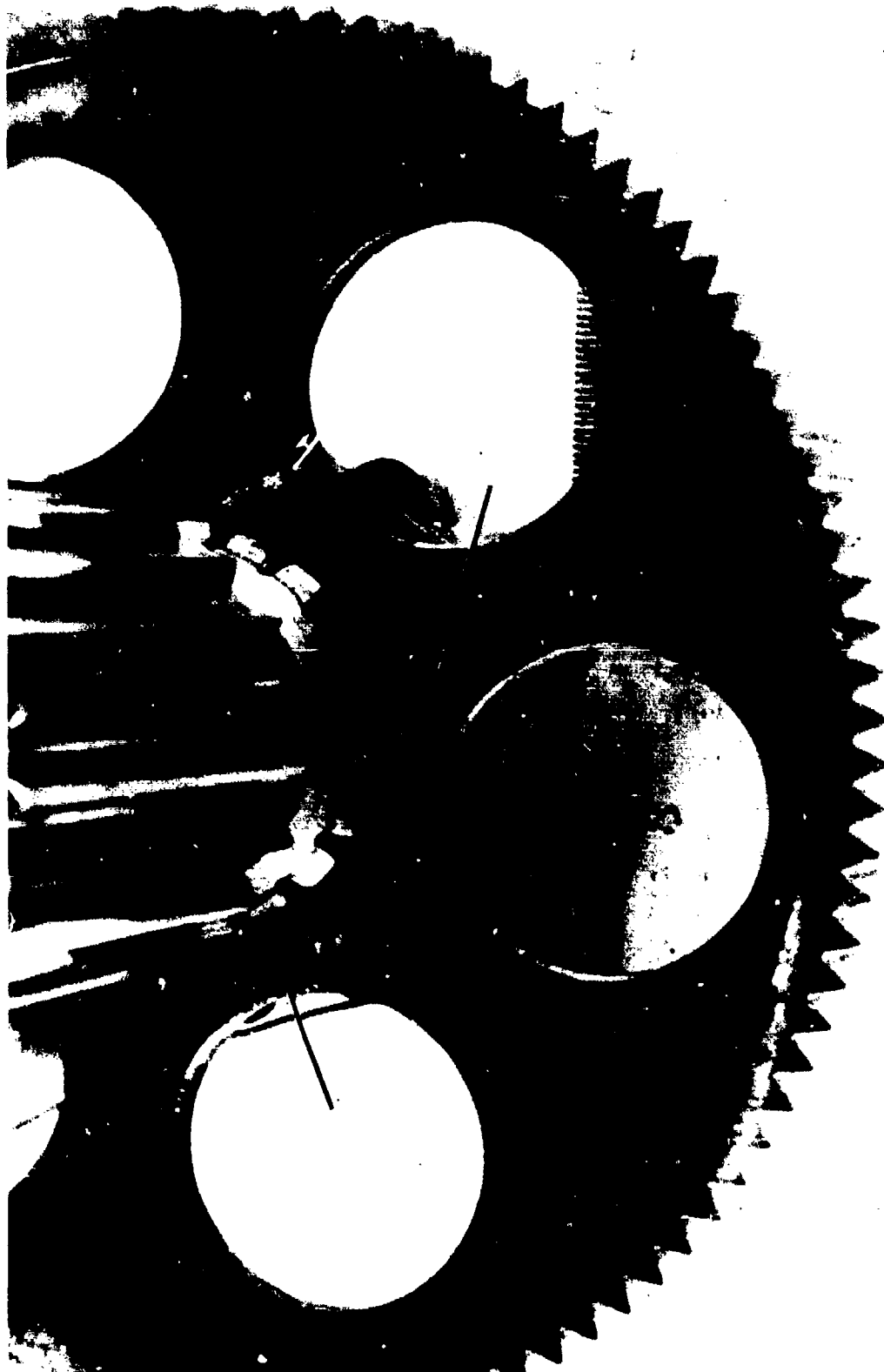


Figure 174. Two Cracks Radiating From Electron Beam Weld  
From Shaft to Lightening Hole.

#### Brake Assembly S/N 001

1. Transfer of a small amount of aluminum material from P/N EP6003-73 housing to the brake disc that rotates relative to the housing during each ATM start.
2. All other brake hardware in normal condition.

#### Gearbox and Turbine S/N 002

1. Reversing turbine buckets of P/N EP6003-4513 turbine wheel assembly were damaged over about 1/2 of their length on the nozzle side, apparently from a foreign object. The bucket is nearly swaged closed. The shroud has a raised lip on the damaged side O.D., but is otherwise undamaged. (See Figure 175).
2. The reversing turbine nozzles in P/N EP6003-4511 housing are swaged nearly closed from the foreign object noted in Item 1 above (see Figure 176).
3. P/N EP6003-35, one crack in gear, EB weld to lightening hole similar to that shown in Figure 174.
4. All other hardware in normal condition.

#### Brake Assembly S/N 002

1. Transfer of a small amount of aluminum material from P/N EP6003-73 housing to brake disk, which rotates relative to the housing during each ATM start.
2. All other brake hardware in normal condition.

#### Pneumatic Valves

The on-off, modulating (ATM) and brake control valve assemblies used with drive assembly S/N 002 were in good condition.

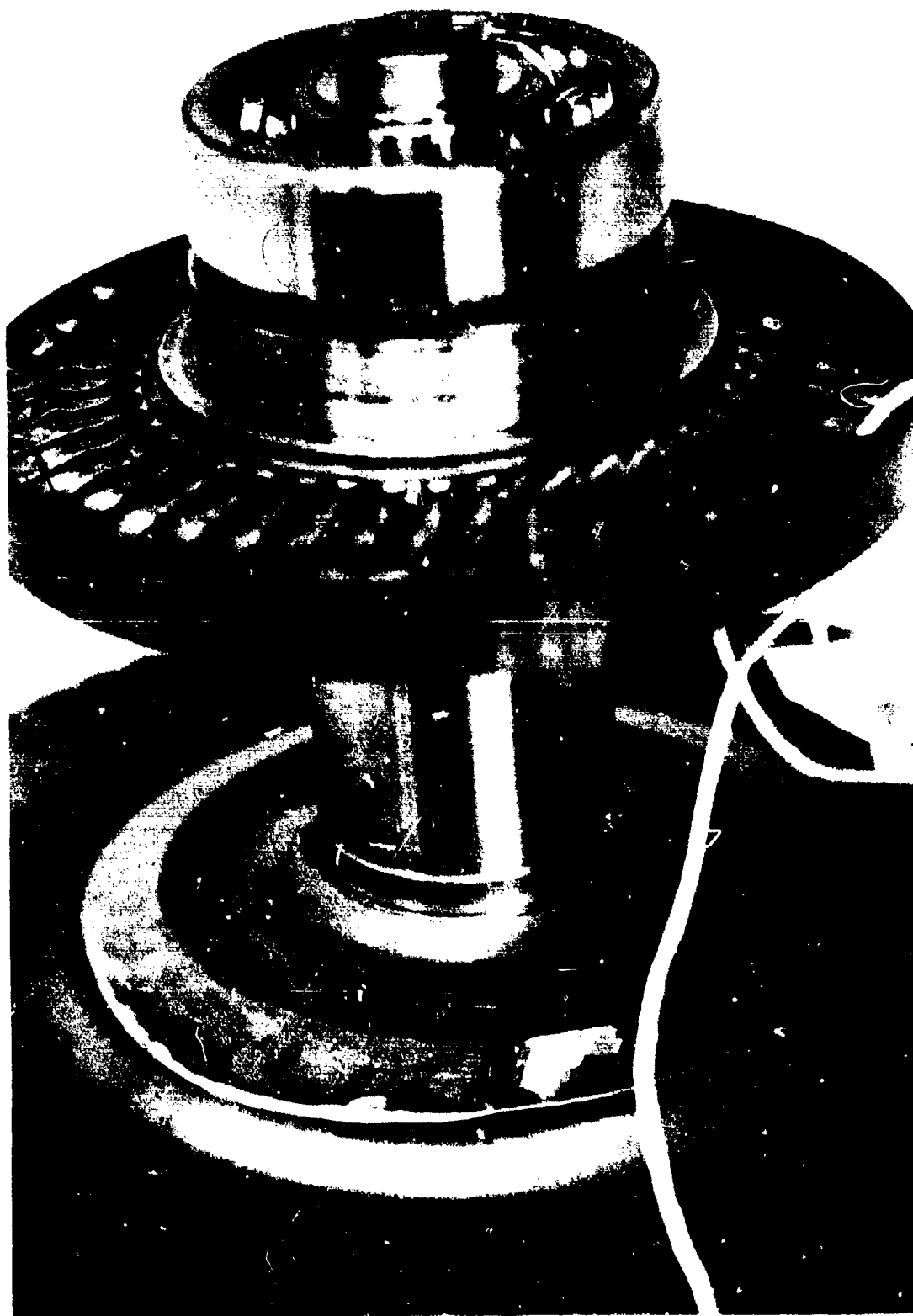


Figure 175. Hoist Drive S/N 2 Turbine Wheel.

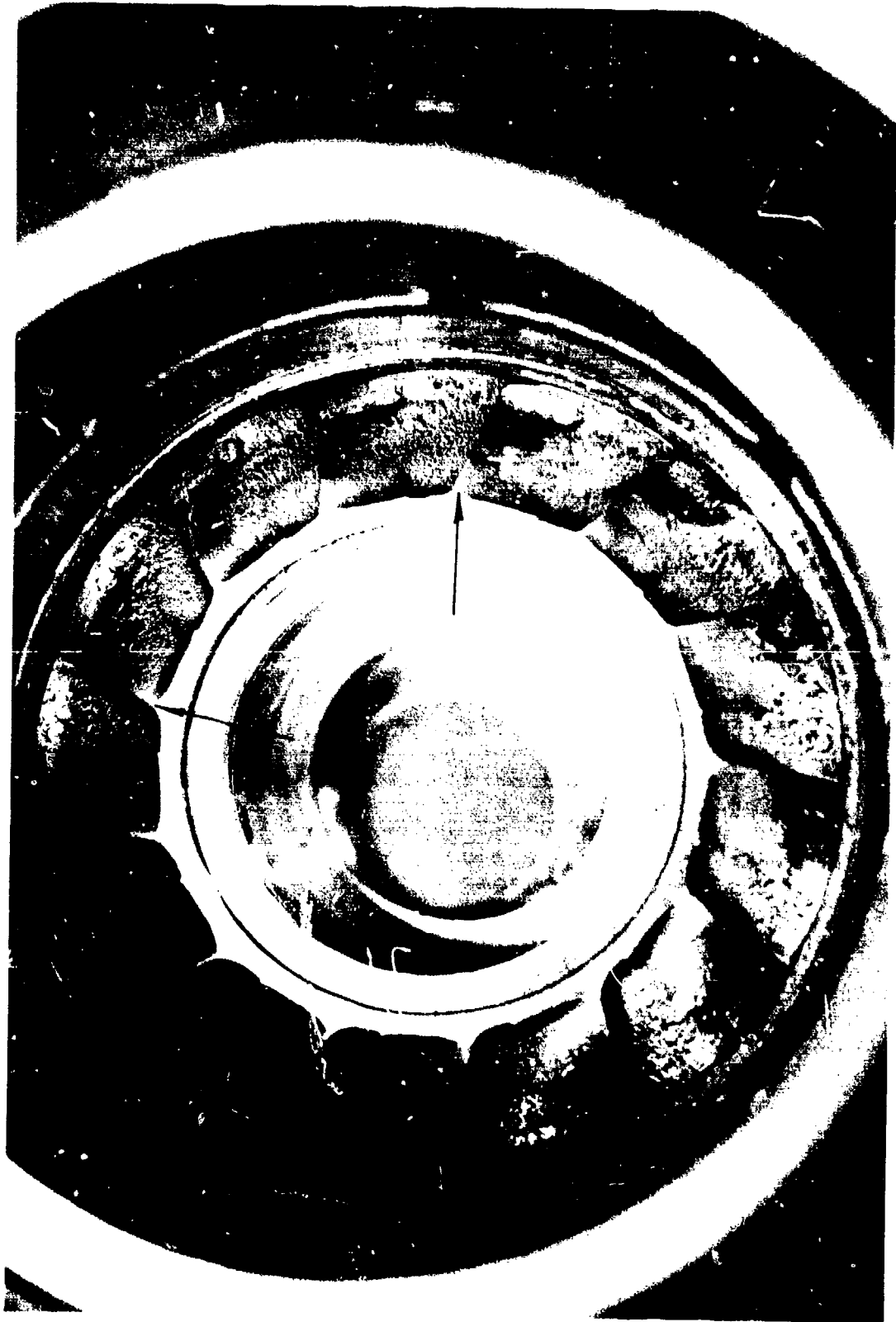


Figure 176. Hoist Drive S/N 2 Reversing Turbine Nozzle.

### ARTICULATING DUCT

The articulating air supply duct configuration used for the final 153 lift cycles (of a total of 226) was satisfactory and is shown in Figure 177.

### HOIST ASSEMBLY

The two hoist assemblies were installed in the rig in October, 1973. Hoist S/N 104 was removed in April, 1974, and S/N 103 was removed in March, 1975.

The operational history of the two assemblies is as follows:

<u>Test</u>	<u>Load</u>	<u>Cycles</u>
Functional	Zero to 16.8 tons ea.	200 Est.
Multi-point	29 tons	904
Single-point	29 tons	904
Static load	37 tons ea.	1

The forward hoist (S/N 104) was subjected to 60% of the multi-point load and the aft hoist (S/N 103) to 40 percent load to simulate the design maximum cargo center of gravity offset. The hoists were examined on teardown and the following observations were made:

1. Lockpin support block P/N 301-11515-6 corroded. Electroless nickel flaking off.
2. Light corrosion on LH and RH drum support structure and drum end plates.
3. LH drum-gear-housing support-bearing inboard-retainer 'O'-ring seal broken in two places. (Hoist S/N 104)
4. LH drum (Hoist S/N 104) end plate button P/N 42198D128 worn by contact with first-stage sun gear shaft. Sun gear shaft end also worn and discolored.
5. RH drum (Hoist S/N 103) end plate button P/N 42198D128 worn by contact with first-stage sun gear shaft. The thrust washer in the axial stackup was broken in three pieces and was found off the sun gear shaft, embedded in the packing grease. Figure 178 shows the RH drum part stackup with the broken washer. Figure 179 is a closeup of the RH and LH sun gears showing the wear and discoloration of the LH gear.
6. RH drum (Hoist S/N 104) third stage planet shafts P/N 42198E112, retaining nuts were finger tight. (LH unit nuts had very low torque.)



Figure 177. Articulating Duct.





Figure 178. Hoist S/N 103 - Right Hand Drum Parts Stackup with  
Broken Thrust Washer.



Figure 179. Hoist S/N 103-Left and Right Sun Gears With Wear and Discoloration on LH Part.

7. LH and RH drums - drum support ball splines - ball return tubes corroded on the outside.
8. RH ball splines (Hoist S/N 104) - one ball missing (total of 123 instead of 124).
9. The electroless nickel plating on some linear ball race support tracks had worn through.
10. Planetary ring gear/housing has a black coating on faying surface of support structure.
11. LH drum (Hoist S/N 104) thrust washer between 2nd and 3rd stage planetary has grooves on thrust face. (Mating surface has slight indentation similar to a hardness test mark.)
12. Hoist support fittings (P/N 301-11514-1 and -3) have some corrosion on the inside surfaces. (Opposite fittings of similar configuration have no signs of corrosion.)
13. LH and RH isolator arm support bearings (Hoist S/N 104): Taper roller bearing closest to isolator arm has debris rolled into ourter race. LH and RH inner races have large craters.
14. Valve package support structure attachment bolts have corroded.

Generally, all gears were in good condition, reflecting satisfactory contact patterns. All bearings with the exception of the outboard third stage planet carrier support bearing (Hoist S/N 104) were also satisfactory.

Of the above observations, Items 1, 2, 7, 12, and 14 relate to corrosion. While the integrated test rig installation was more exposed than the aircraft installation, the surface protection of the hoist elements will be improved for the prototype.

The failed "O" ring, Item 3, appeared to have been mispositioned on assembly so that clamping of the bearing retainer resulted in shearing the "O" ring.

Items 4, 5, and 11 indicate that two of the four planetary assemblies had axial preload. Since straight spur gears, which have no tendency to induce axial loads, are used, it is recommended that the design requirement for axial clearance be increased to eliminate the need for adjustment shims for the production design. Currently, several dimensions must be measured, and added to or subtracted from to establish the shimming

requirements. Errors in this procedure can result in the preloads experienced with the ATC units.

The third stage planet shaft retaining nuts, Item 5, have a low torque requirement since the shafts are installed through an open "C" section of the planet carrier; high torques would cause distortion of the carrier. The retaining nuts have a positive lock feature which prevents them from backing off.

The wear of the nickel plating on the ball spline is not detrimental to the ball spline function. The plating is required for corrosion protection of the drum surface and some wear in the grooves can be expected.

The location of the outboard third stage planet carrier support bearing may be seen on Figure 180. On disassembly, the outer race showed signs of metal particles having been rolled into the bearing surface. The inner race had a spall at one location and the initiation of spalls at one location on the LH drum bearing and two locations on the RH drum bearing. Figure 181 illustrates the damaged inner races.

The inner race of the third stage planet carrier support bearing is semi-static; i.e., rotation is limited by the deflection of the load isolator. Hence, for a constant load, the isolator will deflect to a specific length, and the load reacting force on the bearing is always in the same location.

As all the demonstration cycles in the single-point mode were conducted with a constant load, the reaction was always at the same location on this bearing. Normal aircraft service with a spectrum of loads would result in the reaction being distributed over a 60° segment of the bearing, reducing the possibility of this spalled condition.

Discussions with the bearing manufacturer established recommendations to improve the capacity of this bearing as follows:

1. Increase the preload on the bearing. As the bearing installation is relatively flexible, a higher preload will help maintain full roller contact under load.
2. Crown the rollers at the small diameter end. Crowning will help eliminate concentrated loading at the small diameter end of the roller.
3. Increase the number of rollers in the bearing. A change in roller cage configuration would allow approximately 30% more rollers. New tooling would be required to implement this change.

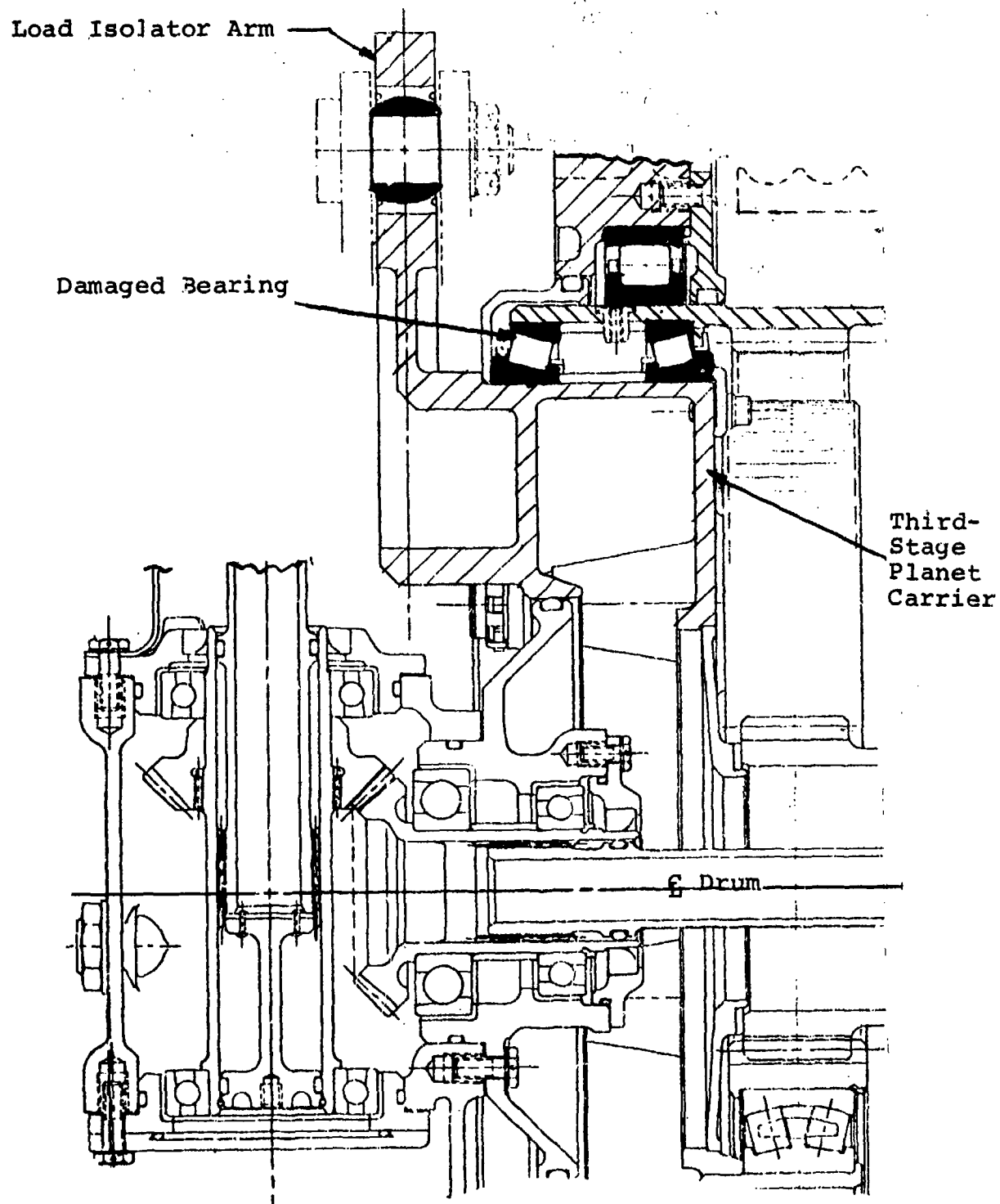


Figure 180. Location of Damaged Bearing.

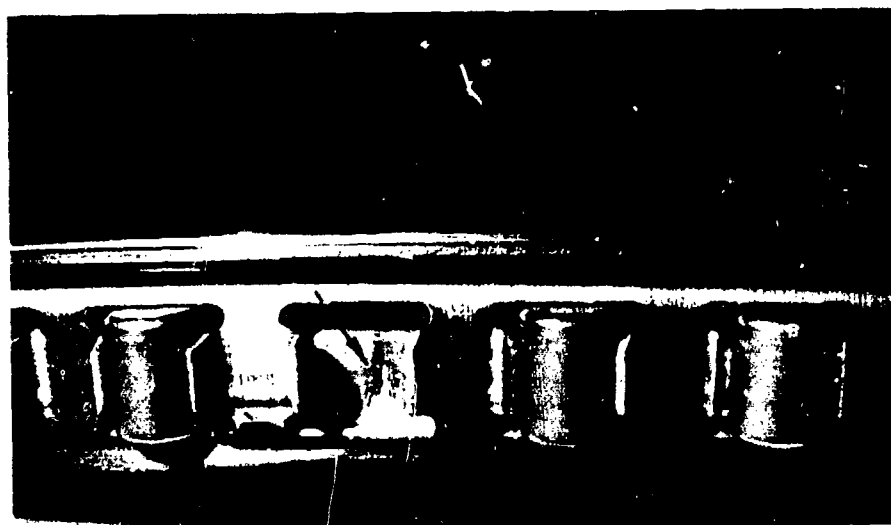
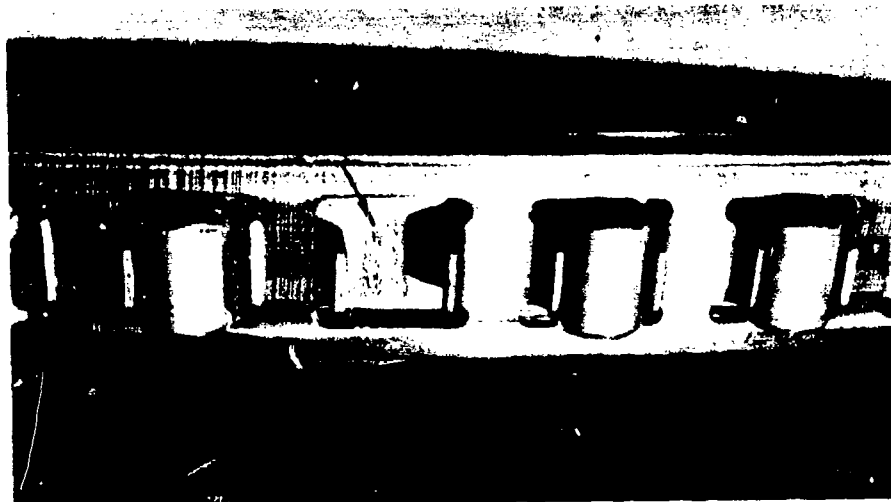


Figure 181. Spalled Bearing - Damaged Inner Races.

Magnetic particle inspection of the drum revealed a series of cracks in the drum ball grooves. The cracks are located in the base of the ball grooves on the inner surface of the drum, randomly dispersed as listed in Figure 182. There does not appear to be any relationship between loading and these cracks, as many cracks are in areas not loaded by the limited hoisting distance used on the ITR.

Discussion with the hoist vendor, Western Gear Corporation, and their subcontractor, Beaver Precision Products, concluded that the cracks were due to a straightening operation conducted on the drums after the ball grooves had been carburized and hardened. The following recommendations are made to ensure that future drums will not exhibit similar characteristics:

1. An improved quenching tool should be designed to limit distortion.
2. Prohibit straightening of the drum after the grooves have been hardened.
3. Shot-peen the groove area prior to nickel plating.
4. A final magnetic particle inspection should be conducted after nickel plating.

The general external condition of the drums is shown in Figure 183.

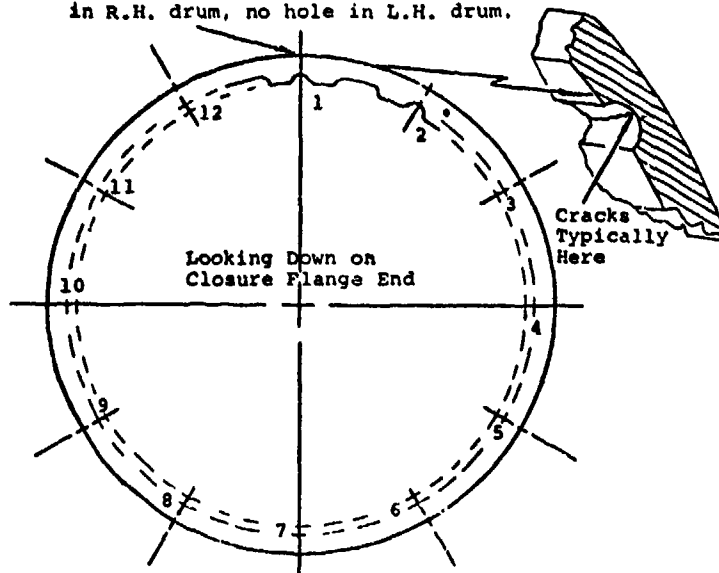
#### FIRST-STAGE BEVEL GEAR ASSEMBLIES

The first-stage bevel gear assembly from hoist S/N 104 was disassembled and found in satisfactory condition. The first stage bevel gear assembly from the aft hoist, S/N 103, was also removed and disassembled to investigate the chip detector warning signals that occurred during the demonstration cycles on the ITR. At the time of the first warning signal, the gearbox was drained and the magnetic plug had collected a quantity of fine steel slivers. Subsequent warnings were caused by individual slivers. Teardown did not reveal any obvious cause of these slivers. Gear teeth show good wear patterns and the bearings appear to be satisfactory. There was no evidence of further slivers within the housing.

#### LOAD ISOLATOR

The load isolators used with the hoist S/N 104 experienced the same load operational history except that they were used in a bottomed-out condition (zero air pressure) for the one-time maximum static load test. This was done to avoid damage to the hoist in case of a sudden load release which was

No. 1 Position located by blind hole  
in R.H. drum, no hole in L.H. drum.



HOIST S/N 104

	GROOVE	POSITION OF CRACKS - INCHES (FLANGE END IS 0)
L.H. DRUM 42193-R51	1	11 to 13, 14 to 19
	3	7 to 9
	4	0 to 8 1/2
	8	18 to 20 1/4 (end)
	9	16 to 20 1/4 (end)
	10	0 to 4
R.H. DRUM 42198-R50	2	1/2 to 1, 1 1/2 to 2 1/2, 5 to 6 3/8
	4	12 to 12 1/4
	5	4 1/2 to 4 3/4
	7	4 to 4 1/2, 12 to 12 1/2
	9	7 to 7 1/4

HOIST S/N 103

	GROOVE	POSITION OF CRACKS - INCHES (FLANGE END IS 0)
L.H. DRUM 42198-R51	1	1/2 to 7 3/4 (intermittent) 15 to 20 1/4 (end)
	2	15 to 20 1/4 (end)
	3	17 to 20 1/4 (end)
	4	0 to 5 3/4, 17 to 20 1/4 (end)
	5	19 3/4 to 20 1/4
	6	0 to 20 1/4 (end)
	8	18 to 19 3/4
	9	0 to 8, 8 1/2 to 12
	10	16 1/2 to 17 1/2
	11	1 1/4 to 2, 6 1/2 to 10 1/2, 12 to 12 1/2
	12	1/2 to 3 1/4, 8 1/2 to 20 1/4 (end)
R.H. DRUM 42198-R51	2	0 to 1 1/2, 2 to 20 (numerous small cracks)
	3	1 to 3 3/4, 5 to 6 3/4, 8 to 20 1/4 end
	5	1 to 9 1/2, 10 to 20 1/4 (end)
	6	1 to 19
	7	3 to 13 1/2, 19 3/4 to 20 1/4 (end)
	8	0 to 20 (numerous cracks)
	9	3 1/2 to 16, 17 to 17 1/4, 17 3/4 to 18 1/2
	10	4 3/4 to 17, 19 to 20 1/4
	11	1 to 20 1/4
	12	2 to 8 1/2, 9 1/2 to 14 1/2, 16 1/2 to 18
		(visible gouge through plating 12 to 12 1/2)

Figure 182. Location of Cracks in Ball Grooves.



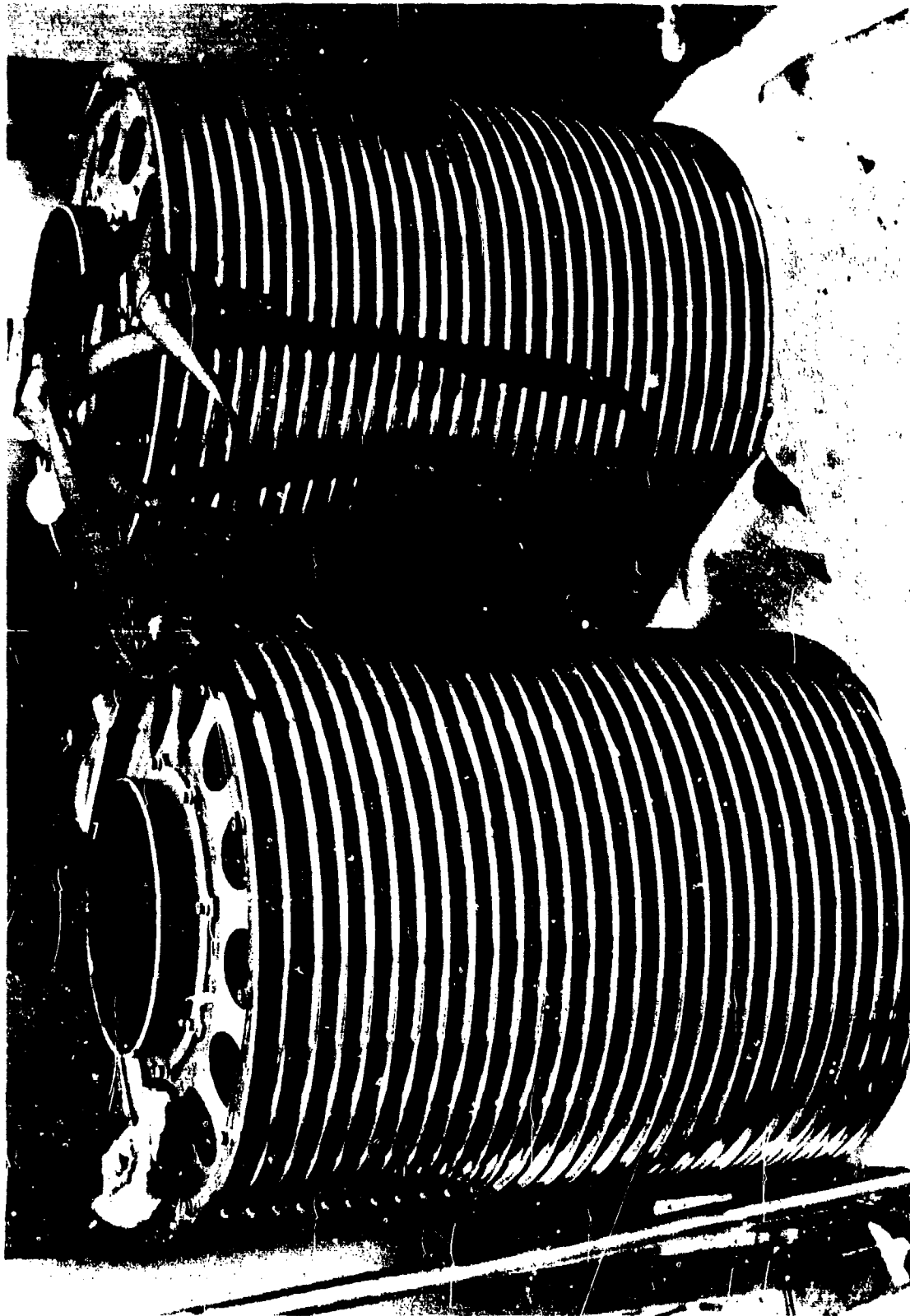


Figure 183. Hoist Drums, S/N 104.

possible with the operating procedure used.

The following observations were made during the inspection:

1. The gland assembly of S/N DRG2269-73 had a sliver of brass embedded in the gland backup ring.
2. The gland assembly of S/N DRG2267-73 had wire strands from the gauze separation extruding into the gland area.
3. The three-piece bearing on each isolator showed signs of wear towards one end only.

There was no oil in the recuperator section of the unit although an oil mist had accumulated on the chamber walls.

#### TENSION MEMBER

Both sets of hoist cables on the ITR were used for the entirety of the 1,808 hoisting cycle program. The single-point adapter cables were used for 904 cycles. The principle loads during the cycles were at design level: 17 tons on the forward hoist and 12 tons on the aft hoist (60/40 split) during multi-point cycles and 29 tons evenly split during the single-point tests. Many additional cycles were accumulated during systems checkout, and functional and performance tests. On the aft hoist (individually operated) stall torque single cable tensions of 44,000 lb (88,000 lb total load in the paired cable) were developed during repeated tests. In addition, stall torque single cable tensions of 37,000 lb were developed using both hoists in the single-point mode (37,000 x 4 = 148,000 lb total load).

During the maximum load portion of the single-point test, all cables in the set were kinked as a result of the coupling failure. All cables and end fittings were x-rayed to check for internal failure. Special attention was paid to areas subject to high tensile and bending loads during overall test program, as well as the kinked locations. An eddy current NDT device was also used, but without conclusive results.

Upon removal from the hoists, the tension members were found to be heavily coated with lubricant (primarily from inside the cable) and an accumulation of particles (fine grit and fibers) from their outside use and semi-protected storage over a seven-month period. This condition was also noted on the single-point adapter cables, but to a lesser degree (single-point adapter exposure approximately 3-1/2 months).

After hand cleaning with a solvent, the cables and end fittings appeared bright and free of corrosion. Scratches were perceptible on some portions of the strand surfaces, but no signs of coating removal or wear were noted. An analysis of debris cleaned from the cable showed it to contain the following types of material:

Fibers	- vegetable cellulose
Grit	- fine silicone particles
Metallics	- magnetic and non-magnetic (extremely fine sizes)
Colored particles	- zinc chromate primer, white and green paint (all used in area of cable)
Plastic particles	- typical of bagging material

Except for damage incurred as a result of the coupling failure, the cables were in good condition. Figure 184 shows the single-point adapter cables. Results of the cable dimensional checks are shown in Table 86.

#### COUPLING

Three couplings, S/N 1, 2, and 4, were used during the ITR tests. Unit S/N 1 failed during the maximum static load test. Testing accumulated on these units was as follows:

<u>Unit</u>	<u>Cycling Tests</u>		<u>Static Load</u>
	<u>Multi-Point (MP)</u>	<u>Single-Point (SP)</u>	
S/N 1 (Aft)	904 cycles, 24,000 lb.	167 cycles, 58,000 lb.	SP, 146,000 lb.
S/N 2 (Fwd)	904 cycles, 34,000 lb.	---	---
S/N 4 (Aft)	---	737 cycles, 58,000 lb.	MP, 88,000 lb. Sp, 74,000 lb.

Both S/Ns 2 and 4 were examined after this testing. The following observations were made on inspection:

1. Both couplings showed signs of water having entered through the mechanical release cable entry.



Figure 184. Single-point Adapter Cables.

TABLE 86. CABLE DIAMETER MEASUREMENTS FOLLOWING DEMONSTRATION TESTS AND COUPLING FAILURE.

Hoist S/N 103				Assy. S/N				Hoist S/N 104			
301-10253-1-3 SK301-11561-1-1				301-10253-2-3 SK301-11561-1-11				301-10253-2-1 SK301-11561-1-2			
Dist. From Hook End (Ft)	Wire Dia (Inch)	Dev. From 0.695 Inch (Dia)	Dist. From Hook End (Ft)	Wire Dia (Inch)	Dev. From 0.695 Inch (Dia)	Dist. From Hook End (Ft)	Wire Dia (Inch)	Dev. From 0.695 Inch (Dia)	Dist. From Hook End (Ft)	Wire Dia (Inch)	Dev. From 0.695 Inch (Dia)
3	.694 .692 .695	-.001 -.003 -	3	.689 .690 .691	-.006 -.005 -.004	3	.689 .690 .688	-.006 -.005 -.007	10	.702 .744 .715	+.007 +.049 -
30	.694 .690 .695	-.001 -.005 -	30	.687 .685 .687	-.008 -.010 -.008	30	.683 .689 .685	-.012 -.006 -.010	30	.694 .693 .695	-.001 -.002 -
40	.691 .694 .690	-.004 -.001 -.005	40	.681 .685 .684	-.014 -.010 -.011	40	.684 .684 .684	-.011 -.011 -.011	40	.697 .691 .695	+.002 -.004 -
50	.694 .696 .695	-.001 +.001 -	50	.685 .693 .686	-.010 -.002 -.009	50	.677 .687 .689	-.018 -.008 -.006	50	.691 .691 .693	-.004 -.004 -.002
100	.696 .694 .693	+.001 -.001 -.002	100	.691 .691 .689	-.004 -.004 -.006	100	.684 .687 .685	-.011 -.008 -.010	100	.699 .700 .695	+.004 +.005 -
120	.696 .694 .693	+.001 -.001 -.002	120	.690 .691 .689	-.005 -.004 -.006	120	.684 .683 .683	-.011 -.012 -.012	120	.697 .691 .697	+.002 -.004 +.002

TABLE 86 CONTINUED.

Single-Point Adapter Cable Assembly						
SK301-10253-4-1 S/N SK301-11561-2-1				S/N SK301-10253-3-3		
Dist. From Hook End (Ft)	Wire Dia (Inch)	Dev. From 0.695 Inch (Dia)	Dist. From Hook End (Ft)	Wire Dia (Inch)	Dev. From 0.695 Inch (Dia)	
1	.687 .691 .690	-.008 -.004 -.005	1	.691 .689 .691	-.004 -.006 -.004	
8	.684 .687 .684	-.011 -.008 -.011	7	.691 .683 .687	-.004 -.012 -.008	
10	.685 .688 .687	-.010 -.007 -.008	9	.683 .685 .687	-.012 -.010 -.008	
14.75	.686 .685 .687	-.009 -.010 -.008	14.75	.691 .690 .691	-.004 -.005 -.004	

2. The swivel bearing on S/N 2 was pitted due to moisture accumulation. Swivel bearing on S/N 4 discolored.
  3. Small bearings located in the load-lockout linkage lever at the internal lever were worn on S/N 4. One bearing was cracked across the outer race.
  4. The mechanical release cable fairlead on S/N 4 was not tight. This part cannot seat correctly due to the shape of the dome, requiring a revised chamfer on the fairlead.
  5. The release linkage center pull rod on S/N 4 has excessive free movement in the bearing.
  6. The load beam seals on S/N 2 were breaking apart; these seals will be replaced with the solid-section seal, as fitted to S/N 4.
- All other components were in satisfactory condition.

The water entry, which caused the corroded swivel bearing, is due to moisture passing through the clamped termination of the flexible bellows seal at the mechanical release cable entry. Moisture tracks through the braided conductor cable, eventually draining into the bearing cavity.

#### SIGNAL CONDUCTOR REELING MECHANISM (SCRM)

Disassembly and inspection of the SCRM's followed the functional tests and the 1,808 demonstration cycles on the ITR, which included a seven-month exposure period to the elements.

The following are the results of the inspection of the disassembled units.

#### Level Wind Area, S/N 1

1. P/N EP6003-3204 ball bearing rusted and pitted on the exterior that was exposed toward inside of carriage. The air side bearing exhibited the most rust. Both bearings turned freely.
2. P/N MS51975-5 shoulder bolts need to be longer to prevent clamping of P/N EP6003-3249 cable guide roller. The outboard cable guide roller radius was worn in an axial direction.

#### Cable Drum Area, S/N 1

1. P/N EP6003-3130 cable drum had some surface corrosion on the drum O.D. It had the appearance of an electrolytic reaction between the cable and drum.

2. P/N EP6003-3115 cable drum bearing, on the gearbox end, has a higher drag than the opposite drum bearing, which was removed.
3. The cable dust cover of P/N EP6003-3190 level wind bracket was scuffed by the cable on the inner surface.

Gearbox and Geartrain (See Figure 185)

1. P/N EP6003-3123 splined shaft (drum drive) sheared during hook failure under maximum cable tension (See Figure 186).
2. P/N EP6003-3120 expansion plug came out of P/N EP6003-3109 gear (final drive) when the -3123 spline shaft sheared.
3. P/N EP6003-3107 jackshaft gear had heavy contact and pitchline fatigue on the side of the gear toward the turbine.
4. P/N EP6003-3106 jackshaft pinion has heavy contact on gear side (toward turbine). This matches up with -3107 gear pitchline fatigue.
5. P/N EP6003-3189 tape assembly - two sharp bends midway in tape. Continuity okay.

The SCRM S/N 2 components noted were as follows:

Level Wind Area S/N 2

1. P/N EP6003-3204 ball bearing rusted and fretted on the exposed exterior surface that was on the inside of the carriage. The air side bearing was rusted most severely and was rough when rotated.
2. Snap-rings that hold in cam-lock bearings in level wind assembly P/N EP6003-3240 rusted badly. Nearly missing in one case.
3. Tubular teflon bushing in level wind assembly P/N EP6003-3240 that slides over P/N EP6003-3218 guide spacer was partially extended out of its bore.
4. P/N MS51975-5 shoulder bolt should be longer to prevent clamping of P/N EP6003-3249 cable guide roller. The outboard cable guide roller radius was worn in an axial direction.



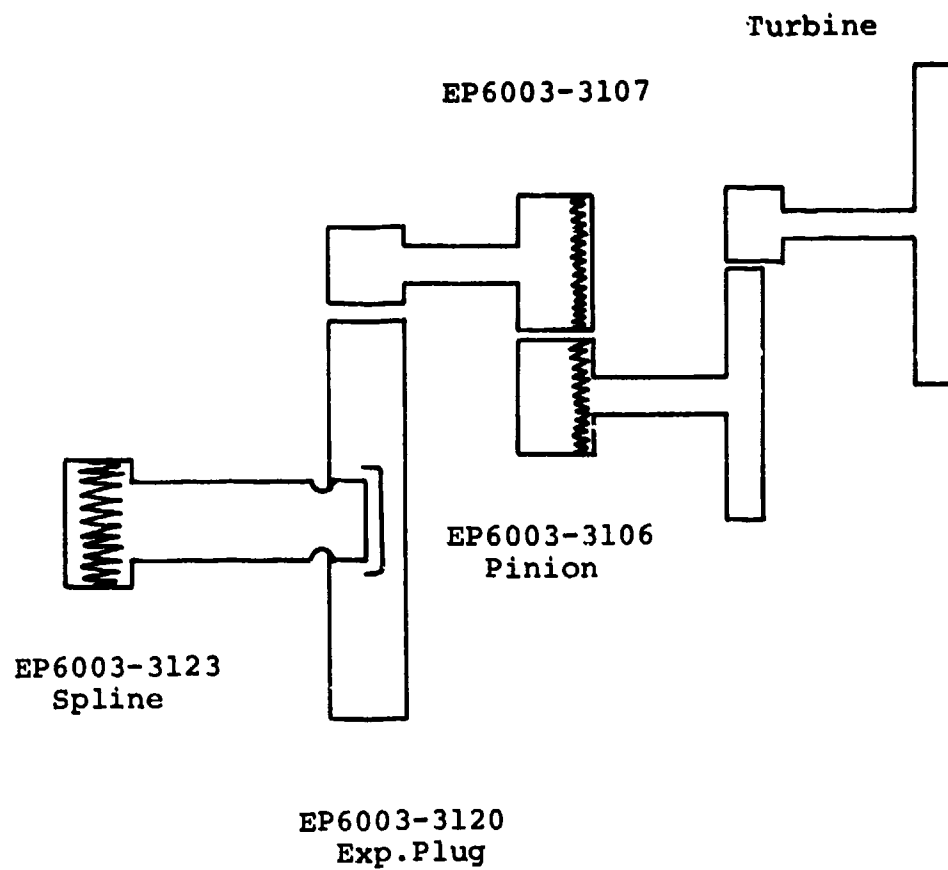


Figure 185. SCRM S/N 1 Gearbox and Geartrain.



Figure 186. Sheared SRM Splined Shaft.

#### Cable Drum Area S/N 2

1. Cable drum P/N EP6003-3130 has a small piece broken out of the cable anchor ball socket. Surface anodize worn through at O.D. step of second layer, first wrap, adjacent to the ball socket anchor.
2. P/N EP6003-3135 retainer bearing insert assembly (teflon) 1-inch length of teflon ring shoulder is missing. Teflon used for support of cable cover.
3. P/N EP6003-3115 cable drum bearing, on gearbox end, has higher drag than opposite drum bearing, which was removed.

#### Gearbox and Geartrain S/N 2 (See Figure 187)

1. P/N EP6003-3123 splined shaft (drum drive) sheared during hook failure under maximum cable tension location was similar to that experienced on the splined shaft of S/N 1, the shear shown in Figure 186.
2. P/N EP6003-3109 gear (final drive) had tip scuffing on four teeth on the final drive spline end. Also, there was heavy contact at the tooth flank on this end of gear.
3. P/N EP6003-3108 jackshaft pinion has surface fatigue in the roots of four teeth. Contact pattern appears uniform. The fatigue matched up with the tip fatigue from the mating - 3109 gear.
4. P/N EP6003-3107 jackshaft gear had very high contact on the end toward the turbine. There was a contact pattern over about one-half of tooth length.
5. P/N EP6003-3106 jackshaft pinion has heavy contact on gear side (toward turbine). This matches up with -3107 gear contact.
6. P/N EP6003-3106 jackshaft gear has heavy contact on end away from turbine.
7. P/N EP6003-3049 turbine gear has heaviest contact on side away from turbine. This matches up with pattern from -3106 jackshaft gear.

#### SPAN POSITIONING ACTUATOR

The span actuator from the forward hoist installation, S/N 4, was examined. This unit was used for 226 span positioning cycles, its exposure time was 7 months, and the unit was non-operational at the time of removal.

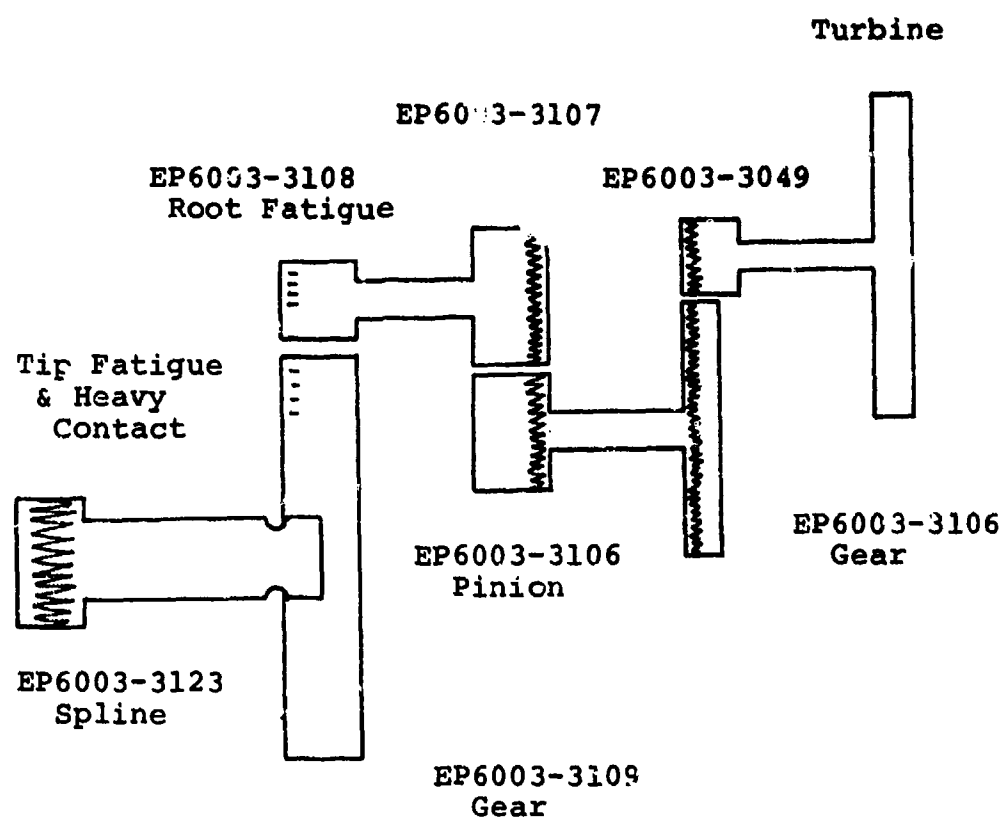


Figure 187. SCRM S/N 2 Gearbox and Geartrain.

Disassembly of the forward span positioning actuator revealed water damage. Water enters the unit through the brake release shaft and causes corrosion of the motor support bearing and motor armature, which prevents rotation. All other gearing and bearings were in good condition.

The design of the actuator has been modified to incorporate a seal on the brake release shaft and to add improved corrosion protection.

#### SINGLE-POINT ADAPTER (SPA)

The SPA, S/N 1, was employed for all the single-point suspension mode tests. This consisted of functional checkout, 904 lift cycles, and static loading. The following items were noted on inspection:

1. The quick release pin P/N 14271-1 has light corrosion on the visible portion of the internal surface.
2. Side plates - Flanges of the teflon faced bearings have the teflon scored and torn. This could be the result of the coupling failure at limit load.
3. Sheave bearing - The inner surface of the teflon-lined bearing is extensively flaked. (See Figure 188).
4. Sheave grooves - The finish has been destroyed and the cables have worn the grooves over the principle load areas.
5. The three spacers separating the side plates and preventing the cable from leaving the sheave groove have worn from cable abrasion.

The assembly was slightly damaged when the coupling failed. The two cable assemblies were kinked (see Figure 184), and there were nicks on the outside diameter of the sheave.

At the maximum wear area in the sheave groove, the hard anodize finish had been worn through, leaving the cable pattern in the aluminum. The uniform loading on the ITR has caused the sheave wear to be concentrated in one segment of the sheave. Aircraft service with drag components and a spectrum of loads will cause the sheave to rotate, distributing the wear over a greater area. This wear does not affect the satisfactory operation of the adapter.

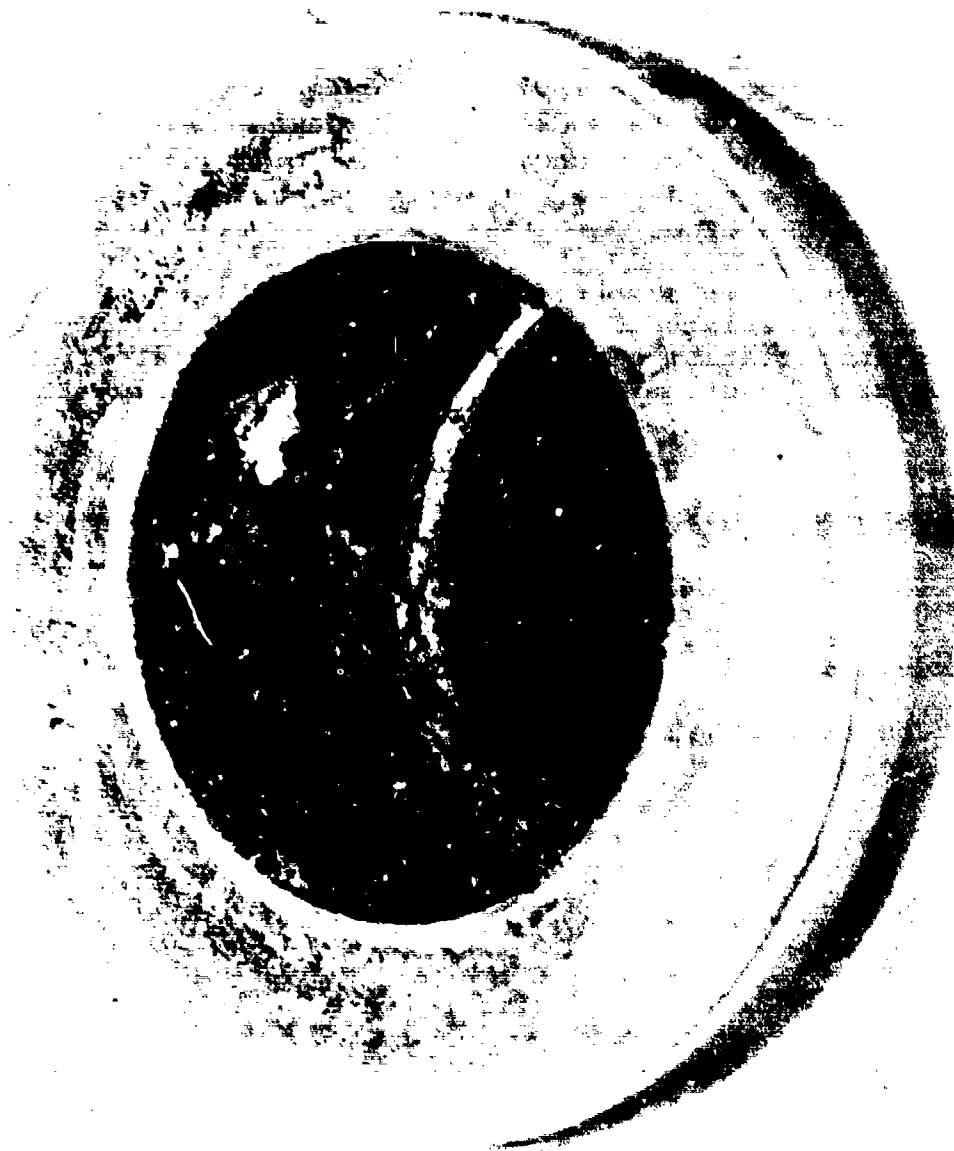


Figure 188. Extensive Flaking of Sheave Bearing Teflon Lining.

## CONTROLS AND DISPLAYS

### Cable Length and Tension Indicators

Both the cable tension and length indicator units were in operational use during the entire eight-month test program. Several instances of erratic indicator tape operation were experienced during the ITR operations. Both the cable tension and cable length indicators exhibited this problem. The primary cause of this discrepancy was determined to be a takeup reel spring deficiency, which allowed the tape to go slack and jump off the reel, thereby requiring disassembly to re-engage the tape.

During the teardown inspection of the cable tension indicator, this condition existed. This discrepancy will be corrected with the installation of an improved take-up reel which has a better spring action and an improved tape groove.

### Cargo System Control Panel

Inspection of the panel revealed no discrepancies.

### Hoist Control Grip

Inspection of the hoist control grip revealed no discrepancies.

## CONCLUSIONS

The HLH cargo handling system developed under the ATC program and demonstrated in the integrated test rig (ITR) has proved the validity of the basic concept of pneumatically powered hoist assemblies.

The control system was developed to provide the precision and synchronization necessary for an airborne lifting system. The program has validated the hardware design and construction, demonstrating adequate strength together with reliable operation and low maintenance requirements.

The concept of using a separate signal conductor system with the ability to provide a remote mechanical pull as a coupling release system was demonstrated as being a practical proposition. The conductor cable design, as used for the ITR demonstrations, requires some changes to improve the reliability of the electrical conductors.

The span positioning system was deleted as a requirement for the HLH prototype during the ATC program. However, the system was included in the ITR and span position changes were demonstrated. The consistent operation of such a system is dependent on the accurate alignment of upper and lower track surfaces, and the development of a track cleaning arrangement.

The static electricity discharge portion of the ATC program established that a passive system consisting of a resistive grounding line hanging below the HLH cargo would provide the required protection for ground personnel during cargo hook-up operations.

With suitable repackaging of the electronic interface unit, the hardware, as developed in this program, is suitable for use in the HLH prototype.



## RECOMMENDATIONS

Resulting from the individual component development tests and demonstrations in the integrated test rig (ITR), the following recommendations are made for further design iterations and studies to improve the overall system effectiveness. The major recommendations are also listed on Page 473 of Volume 1.

### SYSTEM

Introduce a conductor reel air shut-off valve to operate when the coupling approaches the HLH airframe. This valve would prevent the conductor cable from pulling the coupling out of line when bringing the coupling to the stow position. The valve would be controlled to operate automatically when the coupling was approximately 5 feet from the stowed position.

The release criteria for the cargo coupling should be re-evaluated to justify the necessity for the remote mechanical release mode. During the integrated test rig demonstration cycles, the majority of the system malfunctions were due to shorted or broken wires within the conductor. Many of these breaks appear to be due to the high tensile forces induced by the use of the remote mechanical release system. While the conductor cable can be redesigned to improve the conductor reliability retaining the mechanical system, elimination would result in cost savings by eliminating parts within the coupling and simplifying the conductor reel.

### HOIST DRIVE

An additional iteration of the hoist drive nozzle and turbine wheel design should be performed to optimize the efficiency of this unit. Consideration should be given to modifying the high speed drive gear ratio to provide increased hoisting and lowering speeds at design load. This increase would be above the speeds specified for the ATC design, to reduce the operational cycle time.

### HOIST

The hoist design should be reviewed for cost and weight reductions. The review should emphasize design for interchangeability and ease of maintenance.

### TENSION MEMBER

The recommended tension member design for the HLH prototype is a 72-inch-diameter, 36x7 construction, millrun wire cable to provide the ultimate tensile strength after a fatigue life cycle. However, to obtain a better understanding of the effects of a service environment on this type of cable, the existing .70-in-diameter cables from the integrated test rig demonstrations should be evaluated for ultimate and fatigue strength.

A program to determine a form of non-destructive testing applicable to the type of tension member used in this program would enable the useful life of the cables to be optimized. Such a program would consider changes in eddy current and x-ray indications during a fatigue test to establish a relationship between changes in indications and remaining cable life.

The program to evaluate Kevlar 29 fiber tension members, initiated as part of the ATC program, should be continued to provide fatigue data for future consideration.

### SIGNAL CONDUCTOR

The signal conductor cable should be revised to provide greater reliability for the electrical conductors. The design should provide for improved sealing at the point of entry of the mechanical portion of the cable into the coupling housing.

### SINGLE-POINT ADAPTER

Consideration should be given to eliminating the eye-splice ends of the single-point adapter cables. While the operation of the single-point adapter during the integrated test rig demonstrations was satisfactory, it was seen that after a period of continuous operation, the eye-splice ends tended to locate at the load beam keeper of the coupling. A change to terminate both ends of the adapter cables with fittings will require both couplings to be removed for attachment to the hoist cables. However, this arrangement would always ensure correct cable alignment, delete the two mode lockout switches in each coupling and eliminate one conductor from the signal-conductor system.

### COUPLING

The shape of the coupling load beam should be revised to ensure that the load shackle or ring will always locate close to the coupling centerline.

## CONTROLS AND DISPLAYS

The speed command concept of a molded handgrip with thumb-operated transducers has proven to be a viable speed control. The transducers are force sensitive, and the general opinion of operators has been that the force requirement is high, particularly for payout commands. A study should be conducted to optimize the forces needed for control and to investigate alternate configurations, such as a displacement type of control.

The total control system should be reviewed with the objective of integrating the system and simplifying the interface requirements between sensors, control logic, actuators, and displays.

## REFERENCES

1. Nutley, William, TECHNOLOGY DEVELOPMENT REPORT MODEL 301 HLH/ATC CARGO HANDLING SYSTEM COUPLING, Boeing Vertol Company, A Division of the Boeing Company, USAAMRDL Technical Report 73-88, U. S. Army Air Mobility Research and Development Laboratory, Fort Eustis, Virginia 23604, January 1973.
2. Simpson, Louie F., HLH TECHNOLOGY DEVELOPMENT REPORT - VISUAL AUGMENTATION SYSTEM (VAS) LABORATORY DEMONSTRATION AND TEST RESULTS, Boeing Vertol Company, A Division of the Boeing Company, USAAMRDL Technical Report 74-68, U. S. Army Air Mobility Research and Development Laboratory, Fort Eustis, Virginia 23604, October 1974.
3. Solak, B. John, and Wilson, Gregory J., TECHNOLOGY DEVELOPMENT REPORT - RESULTS OF STATIC ELECTRICITY DISCHARGE SYSTEM TESTS (ACTIVE AND PASSIVE) HEAVY LIFT HELICOPTER, Boeing Vertol Company, A Division of the Boeing Company, USAAMRDL Technical Report 74-22, U. S. Army Air Mobility Research and Development Laboratory, Fort Eustis, Virginia 23604, May 1974.